A Study of the Deflection and Strength of Partially Prestressed Concrete Beams with Unbonded Tendons

A thesis presented for the

Degree of Doctor of Philosophy

by

Kwong-Yiu Chu

The Department of Civil Engineering

The University of Leeds

October 1985

SYNOPSIS

Fifteen beams with unbonded tendons consisting of I and rectangular sections with different amounts of prestressed and non-prestressed reinforcement, were tested under short-term and sustained loading and a combination of sustained loading with intermittent short-term cyclic loading(combined loading). Two additional ordinary reinforced concrete beams were tested under combined loading for comparison purposes. Results indicated that a noticeable amount of non-recoverable residual deflection occurred due to the effect of cyclic load. The cause was believed to be non-recoverable creep strain and increased creep rate under cyclic loading.

An analytical method was formulated for calculating the short-term deflection of unbonded partially prestressed beams. The deflection was calculated by integration of curvature based on the recommendations of CP110, Appendix A, with certain modification. The computed results agreed well with the experiments. The experimental deflection was also checked against the computed results according to the Model Code and the ACI Code. The former was found to be unconservative for unbonded I-section beams. The ACI Code I-effective formula might require modification of the power in order to produce consistently conservative results. Moreover, the ACI simplified formula for calculating the long-term deflection was unconservative for unbonded beams both for sustained and combined loading.

The flexural strength of the test beamswas greater than predicted by the CP110, Tam-Pannell and the ACI Code methods mainly due to underestimation of the tendon stress at ultimate moment. The stress in the tendon reached the 0.2% proof stress and the stress in the non-prestressed steel sometimes reached the 2.5% proof stress. The friction between the tendon and the concrete caused localised stress change and hence increased the strength of the unbonded beam significantly.

ACKNOWLEDGEMENTS

I would like to thank Professor A.R.Cusens, Head of Civil Engineering Department of the University of Leeds, for allowing the use of the facilities for this investigation.

I am greatly indebted to Dr.E.W.Bennett for his unfailing help during my study in Leeds University and especially his constructive criticism, constant guidance and encouragement throughout the course of this research.

I would like to extent my appreciation of and thanks to : The technical staff for their assistance in the preparation of test ; my friends Dr.K.H.Lee and Mr.H.S.Lai, my brothers Kwong-Chiu and Kwong-Yan for helping me in the experimental work; Mr.R.Duxbury for taking the photographs and Mrs.C.Duxbury for typing part of this thesis.

I would also like to express my deep gratitude to my wife, Kwai-Ying, for the love, patience and support she gave me during my study.

I am also indebted to my parents, brothers and sisters for their encouragement and support so that I have the opportunity to study in this country.

The Studentship provided by the Leeds University during the period of this investigation is gratefully acknowledged.

TABLE OF CONTENTS

Notation

a	Maximum deflection at midspan at ultimate moment
A	Area of concrete section
A_p	Area of prestressing steel
A_{ps}	Equivalent area of prestressed steel having strength equal to the combined strength of the prestressing tendons and non-prestressed steel.
A_s	Area of non-prestressed steel
b_b	Breadth of bottom flange
b_t	Breadth of top flange
b_w	Breadth of web
d	Effective depth of total steel
d_p	Effective depth of tendons
d_s	Effective depth of non-prestressed steel
e	Eccentricity of tendons
E_c	Modulus of elasticity of concrete
E_s	Modulus of elasticity of steel
f_c	Concrete stress at the top fibre generally
f_c'	Concrete compressive strength-cylinder
f_{co}	Concrete stress at the top fibre under M_o
f_{ct}	Modulus of rupture
f_{cu}	Concrete compressive strength-cube
f_p	Stress in tendons
f_{pb}	Stress in tendon at ultimate moment
f_{pe} , f_{se}	Effective prestress in tendons
f_{pu}	Ultimate strength of tendon
f_{py}	Yield stress of tendon
f_s	Stress in non-prestressed steel
f_{sav}	Average steel stress in non-prestressed steel
f_t	Average tensile stress of concrete between cracks

f_{scr}	Non-prestressed steel stress at the appearance of the first flexural crack
f_y	Yield stress of non-prestressed steel
F_o	Total steel forces under M_o
Δf_{pb}	Increase in tendon stress due to friction
h	Total depth of section
h_b	Thickness of bottom flange
h_f	Thickness of top flange
I_{cr}	Second moment of area of cracked section
I_e	Effective second moment of area
I_g	Second moment of area of gross section
I_{rep}	Effective second moment of area under repeated loads
L, L_t	Span length
M	External applied moment
M_{cr}	Cracking moment
M_{max}	Maximum applied moment
M_o	Decompression moment
M_{ser}	Service moment
M_u	Ultimate moment of resistance
M_{ud}	Design ultimate moment of resistance
P	Force in tendons under M
P_{cr}	Cracking load
P_e	Effective prestressing force
P_o	Force in tendons under M_o
P_{rep}	Repeated load
P_{ult}	Ultimate load
R_e	Effective force in non-prestressed steel due to P_e
R	Force in non-prestressed steel under M
R_o	Force in non-prestressed steel under M_o
$1/r_{av}$	Average curvature

$1/r_{cr}$ Curvature at cracked section

$1/r_{uc}$ Curvature at midway between adjacent cracks

x Depth of neutral axis

α Modular ratio of steel to concrete

β Distribution coefficient

C_t Creep coefficient

ε_{cav} Average concrete strain between cracks

ε_{cp} Virtual concrete strain at tendon level under M

ε_{cpe} Concrete strain at tendon level due to P_e, R_e

ε_{cpo} Concrete strain at tendon level under M_o

ε_{cre} Concrete strain at non-prestressed steel level due to P_e, R_e

ε_{cro} Concrete strain at non-prestressed steel level under M_o

ε_{cu} Concrete strain at the top at failure

ε_{se} Initial prestrain in the tendon

$\Delta\varepsilon_c$ Change in concrete strain

$\Delta\varepsilon_p$ Change in tendon strain

λ x/d

μ Coefficient of friction

ϕ_u Strain factor in uncracked stage generally

ϕ_c Strain factor in cracked stage generally

ρ' $A_s'/b\ d$

ρ_p $A_p/b\ d$

ρ_s $A_s/b\ d$

θ Angle of deviation

Abbreviations

ACI	American Concrete Institute
ASCE	American Society of Civil Engineers
BS	British Standard
CEB	Comité Euro-Internationale du Betoń
CP	Code of Practice
FIP	Federation Internationale de la Precontrainte
IABSE	International Association of Bridge and Structural Engineers
ICE	Institution of Civil Engineers
PCI	Prestressed Concrete Institute

List of Tables

CHAPTER ONE

INTRODUCTION

1.1 Object of Present Investigation

A programme of research was carried out on partially prestressed concrete beams with unbonded tendons with the following objectives :-

(1) To develop an analytical method for calculating the short-term deflection.

(2) To investigate the experimental deflection including the effect of tension — stiffening, under a combination of permanent sustained load with intermittent short-term cyclic loading.

(3) To appraise the recommendations of present Codes, especially ACI-318 , concerning the calculation of short-term and long-term deflection.

(4) To consider the ultimate moment developed in the tests, with particular reference to the stress in the unbonded tendons.

In the design of a partially prestressed concrete member, deflection is one of the main criteria to be considered by the designers, in view of the reduced stiffness after cracking.

Current methods[1] of deflection computation have been largely based on empirical formulae derived from tests. Analytical study is now necessary, however, to establish a rational framework for the calculation of a wide range of types of member.

A combination of permanent sustained load with short-term cyclic load is more representative of the loading encountered by a structure in practice than either monotonic static loading, cyclic loading or sustained loading alone. This type of loading has been neglected by other researchers until the recent work of Bennett and Lee[2] on concrete beams partially prestressed with pretensioned strands.

Very little research[3.4] has been reported on partially prestressed beams with unbonded tendons, particularly when cracked under service load conditions. The latter is particularly important as a promising application of partial prestressing is in flat slabs for which unbonded tendons are often used.

1.2 Brief Notes on Partial Prestressing

In 1940, Abeles[5] proposed the concept of partial prestressing as a development of an earlier suggestion of Emperger[6]. In a partially prestressed structure, tensile stresses in the concrete or even hair cracks are permitted under working load, and although much criticism had been levelled at this type of structure, it was nevertheless accepted by the Chief Engineers' Department, British Railways, Eastern Region[7], in 1948. Nowadays, partial prestressing has gained worldwide

acceptance and has become increasingly importance as an efficient form of material utilization.

Partial prestressing can be achieved by either stressing the tendon to a lesser degree than normally done in full prestressing or combining non-prestressed steel with a small number of tendons which are stressed to the usual allowable value. However, the latter is usually preferred in view of structural performance and economic considerations.

Partial prestressing has the advantages of better control of deflection (i.e. reduction of the camber compared with a fully prestressed structure and of the deflection under service load compared with reinforced concrete) and increase of ductility over a fully prestressed member. The latter is of particular value in design for impact or seismic loading. In addition, catastrophic failure can be avoided. The addition of non-prestressed steel can improve the structural performance (i.e. crack and deflection control and increase of ultimate moment) of a member and is essential for members with unbonded tendons.

On the other hand, partial prestressing has the disadvantages of the possibility of corrosion of the highly stressed tendons through the cracks and higher loss of prestress due to the presence of a larger steel area.

1.3 Classification of Prestressed Concrete

Partial prestressing provides an intermediate solution

between a fully prestressed and a reinforced concrete member. In CP110[8], cl.4.3.3.2.2 , a comprehensive classification of prestressed concrete is given on the basis of the degree of flexural tensile stress or cracking permissible under working load. The classification is as follows :-

Class 1 members : No tensile stress is permitted.

Class 2 members : Tensile stresses are permitted but should be less than the limiting flexural tensile stresses so that cracking is restricted.

Class 3 members : Cracks of limited width are allowed.

Both Class 2 and Class 3 members are referred to as partially prestressed. However, in this thesis, the term partially prestressed is generally applied to Class 3 members.

1.4 Construction of Prestressed Members with Unbonded Tendons

Since their introduction, unbonded tendons have been a rather controversial subject amongst designers. A major step in reconciliation has been the issuing of "Tentative Recommendation for Members Prestressed with Unbonded Tendons" [9] in 1969 by the ACI-ASCE Committee 423. Thereafter, more authoritative documents [10,11,12] have been published in the U.S.A. and the U.K. to provide guidance for the appropriate use of this form of construction.

Nevertheless, arguments continue as to the merits of bonded versus unbonded tendons. In general, the latter would lead to significant economies due to simplicity of construction and the shortening of construction time. In addition, unbonded tendons can be replaced, restressed or destressed when required in the life-time of a structure. On the other hand, there are the disadvantages of the corrosion problem, poorer structural performance and lower strength as compared with bonded tendons.

A survey on unbonded tendons carried out by Schupack [13] has indicated that the number of corrosion incidents reported in completed permanent structures represent an extremely small percentage and no case of catastrophic failure of this type of structure has been reported. Research has indicated that serviceability performance, including cracking and deflection control, and the ultimate capacity can be improved by the use of additional non-prestressed bonded reinforcement.

Unbonded tendons are widely used for floor and roof slabs in buildings. In the U.S.A. , almost 99 % of the total area of post-tensioned floor-slabs is constructed with unbonded rather than bonded tendons. Economy is the obvious reason. In addition, in view of the undulating tendon profile through the floor span, unbonded tendons, being greased and wrapped in plastic tubes, will have less friction loss than bonded tendons. The problems of grouting tendons in ducts of minimum size do not of course occur.

The other field in which unbonded tendons are used extensively is that of nuclear reactor pressure vessels. This is

because in the case of settlement or undesirable structural conditions, the tendons can be re-stressed or replaced to retrive the situation. Additional bonded non-prestressed steel is usually provided.

The application of unbonded tendons for beams and girders are less frequent than for slabs and pressure vessels. However, if there are not many beams in a building , it may be more economical to use unbonded con-struction and to add non-prestressed bonded steel at critical points where needed.

1.5 Outline of Thesis

The thesis consists of seven chapters as follows :-

Following the general introduction in the present chapter, Chapter Two gives a brief definition of the three most common design parameters for partial prestressing. This is followed by a detailed survey of research both on unbonded tendons and on the deflection of partial prestressed members. Methods currently recommended for the calculation of deflection in several engineering codes are also reviewed.

In Chapter Three, the programme of research with the objective outlined is discussed in detail.

In Chapter Four, a method based on the modified reinforced concrete cracked section theory is adapted for the analysis of an unbonded prestressed cracked section. The

analytical method for calculating the deflection of a cracked prestressed concrete beam by integration of curvature is described, and preceded by a brief review of various proposals for the consideration of the tension stiffening effect.

In Chapter Five, the experimental programme, including the description of test beams and testing procedure, is outlined.

In Chapter Six, the behaviour of the test beams is described and discussed. Comparisons are made and discussed between the experimental and theoretical results.

In Chapter Seven, the conclusions from the investigation are summarised and recommendations for future study are made.

References, tables, figures and appendices are added after the text.

CHAPTER TWO

LITERATURE REVIEW

2.1 Introduction

The concept of partial prestressing was originated by Emperger[6] and developed by Abeles[5,14,15]. Since then, the research has increased gradually and after more than forty years of development, partial prestressing is now probably accepted world wide in engineering codes of practice. However, its full potential has yet to be utilized by designers. It is not surprising to find that the use of unbonded partially prestressed concrete is further restricted because the research information behind design assumptions for this type of member is extremely little when compared with the tests reported on fully bonded members.

In this chapter, some of the design parameters for partially prestressed concrete will be briefly discussed and followed by a detailed survey of literature on unbonded prestressed concrete members. Finally, a review of research on deflection and a summary of code recommendations for calculating deflection will also be given.

2.2 Design Parameters for Partial Prestressing

2.2.1 Hypothetical Tensile Stress

Abeles[16] proposed a design procedure for partially prestressed concrete in terms of permissible nominal concrete tensile stress (hypothetical tensile stress) as an index of degree of cracking of the member. The nominal tensile stress is the stress developed in the tensile face of the member and is calculated on the basis of the uncracked concrete section. This method was adopted in the British Code, CP110[8] in which the permissible values of hypothetical tensile stress depend on the nature of the tendons, permissible crack width, concrete quality, depth of section, and the quantity and the distribution of reinforcement. It is assumed that if the hypothetical tensile stress does not exceed the allowable limit, the crack width will not exceed the specified value. This approach has the advantage of simplicity because it allows partially prestressed concrete to be designed using the linear elastic theory. On the other hand, it has the disadvantage that one set of stresses are imposed over a large variety of Class 3 structures. Furthermore, research has indicated that the crack width is more closely related to the steel stress rather than to the hypothetical tensile stress. Siriaksorn and Naaman[17] further demonstrated that the latter could vary between 3 and 23 N/mm2 to cause the same crack width of 0.2 mm. Moreover, the influence of shape of section and bond efficiency of the non-prestressed steel on the hypothetical tensile stress are not included, both of which Abeles[16] believed to be of greatest importance. No permissible values are given for Class 3 members with unbonded tendons which may restrict the use of this method.

2.2.2 Partial Prestressing Ratio

Naaman[18] advocated another parameter namely the partial prestressing ratio, for the design of partially prestressed concrete. This is based on the ultimate strength requirements and defined as the ratio of the ultimate resisting moment due to the prestressing steel to the ultimate resisting moment due to the total tensile steel. The ratio vary from zero to unity to cover the range of structure between ordinary reinforced concrete to fully prestressed concrete. It serves as an index of the level of prestress of a partially prestressed section and provides an ultimate strength solution which can be checked for serviceability requirements. It should be noted that although the level of prestress of an unbonded partially prestressed member is the same as in the comparable member with bonded tendons, the partial prestressing ratio of the former is lower because the tendon stress developed at the ultimate moment is always lower in the unbonded member.

2.2.3 Degree of Prestress

A different design parameter known as "degree of prestress" has been used extensively in Europe, especially Switzerland. This is based on the service load behaviour of a member and defined as the ratio of the moment at decompression to the full service moment. It is similar to partial prestressing ratio and ranges from zero to about unity in covering the full range of structures between reinforced and fully prestressed concrete, but it provides a smoother transition between these two extremes. For example, if a prestressed member without any non-prestressed steel is designed to develop tensile stress under

service load , it will be partially prestressed and can be defined by a degree of prestress less than unity. On the other hand, it could be classified as fully prestressed according to definition by the partial prestressing ratio. The degree of prestress has another advantage in that the designer can directly see if the degree of prestress chosen will, for instance, be sufficient to cover a certain proportion of the design load.

2.3 Previous Research on Unbonded Prestressed Members

In the development of prestressed concrete, engineers always emphasized the important of establishing bond between the prestressing steel and the concrete in order to provide protection of the former from corrosion, to increase the safety against failure and reduce the crack width and spacing. The use of unbonded tendons was limited because of the resulting undesirable structural behaviour and insufficient knowledge. However, in recent years economic considerations have become increasingly important and unbonded tendon systems have begun to be used where they offer technical advantages.

Members with unbonded post-tensioned tendons behave less satisfactorily than the well-bonded ones with fewer and wider cracks. As the load increases, the cracks increase rapidly in width and depth and the deflection becomes large. Abeles[19] indicated that in partial prestressing with unbonded tendons, the great advantage of good bond can be retained and the above disadvantages avoided by the use of well bonded non-prestressed steel placed close to the tensile face. This has been confirmed in

numerous tests by other researchers [20]. In fact, Mattock et al[21] observed that such partially prestressed beams have serviceability characteristics, ductility and strength, equal to or better than comparable beams with bonded tendons.

There has been a different of opinion between investigators on the best type of non-prestressed steel. Chaikes[22] recommended the use of ordinary grade steel rather the high strength steel advocated by Abeles[23] who considered Chaike's suggestion to be uneconomical and likely to cause further loss of prestress due to the larger amount of steel. Nevertheless, Abeles[19] later admitted that the use of lower strength strands might be preferable from the point of view of rigidity after cracking. Bennett and Chandrasekhar[24] carried out a series of tests on partially prestressed beams of rectangular section and concluded that the beams reinforced with deformed bar gave better performance and no significantly greater loss of prestress as compared with the beams with a smaller percentage of high strength steel. Stevens[25] also found that the beams with strands as reinforcement showed poor recovery compared with conventional reinforcement.

Some designers are reluctant to use unbonded tendons because of the uncertainty of the tendon stress developed at the ultimate moment. This stress and hence the flexure strength of an unbonded beam is lower than in the comparable fully bonded beam. Evans[26] was the first to recognize that the loss of bond in prestressed concrete could lead to a reduction in the strength of the member and Baker[27] later studied this by considering the

strain relationship between the tendon and the adjacent concrete. Baker suggested that at the failure section, the strain in the concrete can be related to the tendon strain by a factor which can be determined from experiment. This strain factor is affected by several variables such as span/depth ratio of the member, cable profile, loading condition and crack distribution. He found that the factor ranged from 0.1 to 0.35 and suggested a safe limiting value of 0.1 for unbonded tendons. According to Baker, the total tendon strain is given by

$$\varepsilon_{su} = \varepsilon_{se} + \phi(1-\lambda)\frac{\varepsilon_{cu}}{\lambda}$$

where ε_{se} = initial prestrain in the tendon.

ε_{cu} = concrete strain at the top at failure.

λ = depth of neutral axis/effective depth.

ϕ = strain factor.

The final steel stress f_{pb} may be obtained from the steel stress-strain curve for a given value of λ which however in turn depends on the f_{pb} with the relationship

$$\lambda = \frac{\rho_p f_{pb}}{\alpha f_{cu}}$$

where $\alpha = C/(f_{cu} b d \lambda)$

C = total compressive force at the ultimate moment.

The values of f_{pb} and λ can be obtained by iterative procedure.

More research has been done in development of Baker's method. Reversz[28] concluded from a study of published test results that $\phi\varepsilon_{cu}$ was equal to 0.05% for unbonded beams and 0.2% for grouted beams. Later, Gifford[29] was convinced that the strain factor bore an approximately linear relation to λ and a value of about 0.2 would provide a satisfactory result. Cowan[30] has shown the effect of the variation of neutral axis depth with strain factor in tabular form.

ϕ	1.0	0.9	0.8	0.6	0.4	0.2	0.1
λ	0.35	0.33	0.30	0.26	0.18	0.10	0.05

Janney et al carried out a series of tests on nineteen beams including eight unbonded beams, three of which had additional deformed bars. For the five purely unbonded beams, the average value of $\phi\varepsilon_{cu}/\lambda$ was equal to 0.0033, but for those beams with additional deformed bars, it was equal to 0.0035. From these findings, they concluded that the presence of deformed bars did not appreciably increase the stress of the unbonded strands in spite of the fact that the crack pattern of the beams was changed. The results obtained agreed quite well with those predicted by Baker's method with Gifford's amendment of $\phi = \lambda$.

All these efforts were however criticised by Pannell[31] for lack of accuracy in failing to consider one important parameter, namely the span/effective depth ratio (l/d) of the member. Pannell conducted a series of tests on thirty-eight beams of rectangular section with l/d ratio and initial prestress as the design parameters. He concluded that Baker's method always gave

conservative results because the use of low stress-block, ultimate concrete strain and strain factor. The method used by Janney et al were only accurate for the beams with an l/d ratio of about 12. The predictions for the other class of beams were extremely optimistic.

This parameter was later adopted in CP110:1972 in which the ratios (f_{pb} /f_{pe}), (l/d) and (A_{ps} f_{pe} /f_{cu} bd) are related in Table 38. The trend is that f_{pb} /f_{pe} decreases sharply as l/d increases. However, the table is only applicable to those members with a l/d ratio between 10 and 30.

Tam and Pannell[32] later further improved the early analysis suggested by Pannell for unbonded partially prestressed members. The following equations for predicting the tendon stress ,f_{pb} , were proposed.

$$f_{pb} = \frac{q_u f_{cu}}{\rho_p}$$

$$q_u = \frac{q_e + \xi}{1+\xi/\alpha} - \frac{q_s \xi}{\alpha+\xi}$$

$$\xi = \psi \rho_p \varepsilon_{cu} E_s \, d/L \, f_{cu}$$

$$q_e = \rho_p \, f_{pe}/f_{cu}$$

$$q_s = \rho_s \, f_y/f_{cu}$$

$$\alpha = C/f_{cu} \, bd\lambda$$

where L = length of prestressing tendon from anchorage to anchorage.

ψ = (plastic hinge length)/ λd , which should be obtained from test and a value of 10.5 was suggested.

$\rho_p = A_p/bd$.

$\rho_s = A_s/bd$.

This method is not simple but it takes many important variables into consideration.

However, the calculation of the tendon stress f_{pb} using any of the above methods was found to be time-consuming and simplified expressions for predicting f_{pb} have therefore been developed. The following early expression was suggested by Warwaruk et al[33] who found that the increase in tendon stress from f_{pe} to f_{pb} i.e. $(f_{pb} - f_{pe})$ decreased as the ratio (ρ_p / f_c') increased :

$$f_{pb} = f_{pe} + 30000 - \frac{\rho_p}{fc'} \times 10^{10} \quad \text{in psi}$$

This expression is not limited to a particular range of the ratio (ρ_p / f_c') but f_{pe} should not be greater than 60% of the tendon tensile strength. It was criticised by Mattock et al[21] for being too conservative, in particular for beams with low (ρ_p / f_c') values, and the alternative expression was proposed :

$$f_{pb} = f_{pe} + 10000 + \frac{1.4f'_c}{100\rho_p} \quad \text{in psi}$$

This equation does reflected the behaviour of the beams for which the parameter (ρ_p / f_c') is small and provides a conservative value of f_{pb} for the data in Reference[21]. A slightly more conservative version of this expression has been adopted in the ACI Code(318-77) [34]:

$$f_{pb} = f_{pe} + 10000 + \frac{f'_c}{100\rho_p} \qquad \text{(psi unit)}$$

where f_{pb} shall not be taken greater than f_{py} nor (f_{pe} +60000) psi.

In a recent publication by Mojtahedi and Gamble[35] , attention has again been drawn to the importance of l/d ratio. It was demonstrated that the ACI Code expression cannot safely and consistently be used to predict the ultimate tendon stress in the unbonded members with high value of the l/d ratio. This is especially true in those cases where strength requirements govern the steel area. This resulted in a further amendment to the expression for f_{pb} in the recent ACI Code (318-83) [1] to cover the influence of the l/d ratio. In accordance with the new code, the ACI(318-77) expression for f_{pb} is now limited to members with a l/d ratio of 35 or less. For members with a l/d ratio of greater than 35, the following equation should be used.

$$f_{pb} = f_{pe} + 10000 + \frac{f'_c}{300\rho_p} \qquad \text{(psi unit)}$$

where f_{pb} shall not be greater than f_{py} nor (f_{pe} +30000) psi.

More recently, Balaguru[36] suggested a semi-empirical

equation to calculate the increase in tendon stress to check serviceability conditions.

$$\Delta f_p = [\alpha_1(\frac{\delta}{e}) - \alpha_2(\frac{\delta}{e})^2]E_s$$

$$\alpha_1 = 0.00923\ (\frac{e}{L}) + 5.11\ (\frac{e}{L})^2 \qquad 0 < \frac{e}{L} < 0.06$$

$$\alpha_2 = \frac{11}{10^7}\ \text{Exp}\ (135\ \frac{e}{L}) \qquad 0 < \frac{e}{L} < 0.04$$

$$\alpha_2 = \frac{\text{Exp}\ (75\ \frac{e}{L})}{10^5} \qquad 0.04 < \frac{e}{L} < 0.06$$

where e = maximum eccentricity of the cable.

L = span of the beam.

δ = maximum deflection calculated by assuming that the beam is a reinforced concrete beam.

Elzanaty and Nilson[4] on the other hand proposed the following method to calculate the increase of tendon stress under service load.

$$\Delta f_p = \frac{E_s}{E_c L} \int_0^L \frac{M_x e}{I}\ dx$$

where M_x = applied moment.

I = moment of inertia.

$I = I_g$ for uncracked section.

$I = I_e$ for cracked section. I_e is calculated on the basis of reinforced concrete section.

The validity of these two methods is questionable because both require the unbonded member to be treated as reinforced concrete in calculating the deflection and effective moment of inertia.

It can be seen from above that various methods have been proposed to predict the tendon stress in unbonded members at service or failure load. In the present investigation, some of these methods will check against the limited number of experimental results. In addition, the influence of friction between the tendon and duct on the ultimate strength of unbonded member will be examined.

2.4 Previous Research on Deflection

After more than four decades of development of partial prestressing, the analytical method of calculating deflection of this type of member has not yet been fully studied although the problem of deflection and the parameters affecting it have been investigated by researchers for some years. Most of the tests reported and here reviewed have been on fully bonded Class 3 members and hardly any attention has been devoted to the deflection of unbonded partially prestressed members.

2.4.1 Bonded Partially Prestressed Concrete Beams

Abeles was responsible for many early tests on partially prestressed beams, a few of which were related to deflection. Abeles, Brown and Woods[37] tested three identical sets of beams

under static, sustained and fatigue loading. Each series consisted of eight beams of rectangular section reinforced with strand , some of which were pretensioned. The beams were made of different types of concrete and five of them were partially prestressed. Observations from the sustained loading test indicated that the long-term deflection was greatly affected by the ambient temperature and humidity conditions. An appreciable amount of non-elastic deformation occurred in the early period of loading and progressed at a reduced rate. After a period of 117 days, the non-elastic deflection increased by 50% of the instantaneous value in the beams maintained at 37% of the static failure load and almost double in the beams loaded to 50%. During the 29 days unloaded period, good recovery of the non-elastic deformation was observed. This temporary removal of load could be beneficial insofar as a further increase in deflection was delayed when the sustained load was reapplied. Moreover, in the beams reloaded for the second time, the deflection increased at a gradient approximately the same as that of the first loading period. The instantaneous deflection was increased by creep deformation to a much greater extent when the load was applied at an early age than when it was applied at an age of about six months.

Extensive research on partially prestressed concrete was carried out at the University of Leeds in the late sixties under the supervision of Bennett. Bennett and Dave[38,39] tested forty rectangular section beams prestressed by pretensioned wires with varying level of prestress and reinforcemnet ratio. Eight beams were tested by sustaining the design load (50% of design ultimate load) for period of between 276 and 600 days. After 500 days, the

ratio of deflection to the initial elastic deflection for the beams was found to vary from 2.12 to 2.64 and it was therefore suggested that the deflection due to sustained load could be considered to be approximately double the instantaneous value.

Bennett and Chandrasekhar[24,40,41] conducted further tests on thirty-six rectangular section beams. The design parameters of the beams were the level of prestress, reinforcement ratio, type of reinforcement and cover to reinforcement. The deflection of the beams in which high-strength wire or strand was used as non-prestressed reinforcement was found to exceed the limit specified in the code ,the reason being that these beams contained a lower total area of steel and thus were less stiff after cracking. Furthermore, it was observed that the deflection was not affected by varying the cover over the reinforcement.

Three beams were tested under sustained loading (50% of design ultimate load) and it was observed that even after 300 days of loading, there was no sign of stabilization of the deflection and after nearly 400 days, the maximum increase in deflection was found to be 150% of the initial elastic value under static load. The greatest increase occurred in all the beams within the first 20 days after loading. The beams did not show a good recovery during a 30 days unloaded period; even in the beam with the highest prestress , only 13% of the total non-elastic deflection was recovered.

Bennett and Veerasubramanian[42,43] carried out tests on thirty-seven beams with the level of prestress, reinforcement

ratio and shape of section as the parameters to be studied. Apart from the results that confirmed previous research, they concluded that the deflection of a cracked prestressed beam was affected by the shape of section. The composite and monolithic T-beams were stiffer than the I- and retangular beams and showed better overall performance.

More recently, Bennett and Lee[2,44] tested nine partially prestressed beams of I-section with pretensioned strands. The level of prestress and reinforcement ratio of the beams were varied. The main parameter to be studied was the effect of a combination of sustained and cyclic short-term loading on deflection. The beams were maintained at half the service load (33% of design ultimate load) for a period of up to 46 days during which time the load was increased to full service load up to 7 times in intermittent short-term cycles. Three companion beams were tested under permanent load alone.

The authors observed that there was an increase in the residual deflection after each intermittent cycles, only part of which was recovered. As a consequence, the deflection under sustained loading was increased by the residual effect of the intermittent cycles of loading. They suggested that the deflection due to the combined loading appeared to be similar to the sum of the deflection due to the permanent and intermittent cyclic load applied separately, and further demonstrated that the ACI Building Code (318-83) recommendations for calculating deflection were only applicable to the first cycle of short-term loading or to the permanent load alone. The latter recommendations were found to be

unconservative for beams tested under the combined type of loading mentioned above.

An analytical method based on the CP110 recommendations was developed for calculating the deflection of a bonded partially prestressed beam.

In the U.S.A. , Branson[45] investigated the problem of deflection as early as 1963, however, most of his studies were related to reinforced concrete. He suggested that the deflection of a cracked reinforced concrete member could be calculated by using an effective moment of inertia (I_e) of the concrete section where I_e was obtained by means of a proposed empirical formula, details of which will be discussed later.

More recently, Branson has extended his work to partially prestressed concrete. Branson and Shaikh[46] tested twelve prestressed beams of rectangular section with pretensioned tendons and found it to be important to use the transformed section properties for calculating deflection.

Branson and Kripanarayanan[47] have studied the influence of load repetitions on the stiffness of cracked prestressed members and proposed the following expression for computing the average effective moment of inertia under repeated loads.

$$I_{rep} = \psi I_e + (1-\psi) I_g$$

where ψ = $(P_{ult} - P_{rep})/(P_{ult} - P_{cr})$.

I_e = effective moment of inertia.

I_g = gross moment of inertia.

P_{ult} = estimated ultimate load based on ACI Code.

P_{rep} = cycling load or maximum load in a given cycle.

P_{cr} = load at initial cracking corresponding to M_{cr}.

It appeared that I_{rep} can be used for calculating the unloading and reloading deflection up to the maximum load P_{rep} in the previous cycle but the cumulative residual deflection due to repetitions of this load has not been considered. It only accounts for the residual deflection due to cracking alone, the effects of creep having been neglected.

By comparing with the tests results on fifteen beams, the predicted values obtained from this expression were found to be within 20% of the actual results for normal working load level.

Recently, Branson and Trost[48] carried out tests on two unbonded prestressed , one bonded prestressed and one reinforced concrete beams. The unbonded beams were tested under two and four cycles of loading of a few hour duration and the remainder were tested under two cycles of short-term loading. In each cycle, the beam was loaded to a maximum load higher than in the previous cycle.

A method for estimating the time-dependent effect on deflection of creep and cracking under a limited number of loading cycles was outlined. For the first loading cycle, the time-

dependent deflection was given by $K_t C_t$ times the instantaneous value where K_t was a reduction factor for the effect of compression steel and downward movement of the neutral axis with time.

For short-term creep : $K_t = 1.0 /(1 + 50 \rho')$.

For long-term creep : $K_t = 0.85/(1 + 50 \rho')$.

C_t was the creep coefficient defined as the ratio of creep strain to initial strain. For a limited number of loading cycles, the time-dependent deflection was given by $(K_t C_t + F_{rep})$ times the instantaneous deflection where F_{rep} was a factor taking into account the increased deflection due to the effect of cracking under repeated loading cycles. It ranged between 0.1 and 0.2 for two to four loading cycles but would be become higher for more cycles of loading.

The deflection computed by means of I-effective expression seemed to agree quite well with the test results for the first cycle of loading but for the unbonded beams it was found that the usual I-effective equation had to be modified by using the power of 4 instead of 3 in order to allow for reduced stiffness compared with a bonded beam.

2.4.2 Unbonded Prestressed Concrete Beams

Early tests by Evans[26] demonstrated that the deflection after cracking was considerably higher in unbonded prestressed beams than in either conventional reinforced concrete or fully-bonded prestressed beams. This was supported by tests from Janney et al[20] who further demonstrated that the addition

of non-prestressed steel reduced the deflection. Further tests by Warwaruk et al[33] confirmed that the phenomenon was more pronounced in beams having a low value of ρ' / f_c'. This was because the tensile force resisted by the concrete before cracking was transferred to the entire length of the tendons in order to maintain equilibrium which was achieved at the expense of greater total elongation of the tendon and relatively larger deflection of the beam. In contrast, the phenomenon was not observed in beams having high values of ρ' / f_c' or with additional bonded reinforcement because the steel in these beams could provide the tensile force lost by the concrete with little increase in strain.

Of the thirty-six partially prestressed beams tested by Chandrasekhar[41], three were unbonded with additional deformed bars. The deflection was generally only slightly greater than that of corresponding bonded beams and confirmed that the deformation could be greatly reduced by the addition of bonded reinforcement. The test carried out by Veerasubramanian[43] also included three unbonded partially prestressed beams of I-shaped section. The unbonded beams were reported to behave similarly to the corresponding bonded ones as long as the strain in the non-prestressed steel was within the elastic range. When the non-prestressed steel strain entered the inelastic range, the beams had a flatter load-deflection curve than the comparable bonded beams. The flexural behaviour was similar to that previously observed in beams of rectangular section.

It is evident from the review and literature search that there has been a number of tests on partially prestressed concrete

beams, but the development of an analytical method of deflection computation is still in its infancy. Bennett and Lee have formulated an analytical procedure for bonded beams but similar approach for unbonded members was not developed. They have also demonstrated the importance of the combined type of loading which seems to be more likely to occur in practice than either short-term cyclic load or permanent load alone.

2.5 Present Code Recommendations on Deflection Computation

2.5.1 General

The result of excessive deflection would be to impair the appearance and efficiency of a structure. Design recommendations and guidance for calculating deflection are therefore suggested for designers in most engineering codes in order to safe-guard the structure in serviceable conditions.

For calculating the short-term deflection of uncracked members, most engineering codes suggested that the linear elastic theory may be used in conjunction with the appropriate concrete section properties. The CEB-FIP Model Code permits the use of the uncracked transformed concrete section, but both the British and ACI Code specify that the gross concrete section should be used.

For calculating the deflection of cracked members, and members under long-term loading, various recommendations have been given in the codes and will be described in the following Sections.

2.5.2 British Standard, CP110:1972

The code[8] suggests that the total long-term deflection due to the prestressing force, dead load and any sustained imposed loading of uncracked members may be estimated by using an effective elastic modulus of concrete which allows for creep.

For calculating the deflection of cracked members, a general method has been outlined in Appendix A. This approach involves assessment the curvature of successive sections of a member and the deflected profile can be obtained by integrating the curvature along the member. In calculating the curvature, the tension stiffening of the concrete between the cracks, allowing for its long-term effect, should be taken into consideration. It is equal to 1.0 N/mm2 for short-term loading and 0.55 N/mm2 for long-term loading. Under long-term loading, an effetive modulus of concrete may also be used for calculating the curvature of the sections.

2.5.3 ACI Building Code (318-83)

When the member is cracked, the effective moment of inertia (I_e) of the member should be used for deflection computation. The I_e formula is given by :

$$I_e = I_g \left(\frac{M_{cr}}{M_{max}}\right)^3 + \left[1 - \left(\frac{M_{cr}}{M_{max}}\right)^3\right] I_{cr}$$

where M_{cr} = cracking moment.

M_{max} = maximum applied moment.

other terms are the same as previously defined.

This expression was originally proposed by Branson and is applicable for cracked reinforced concrete. It has taken account the tension stiffening effect which will be disappear at higher load. No consideration however has been taken of the influence of long-term loading on the tension stiffening effect. Although the above expression was originally derived for reinforced concrete , it can be extended to cracked prestressed members with slightly modifications as recommended by a number of researchers[48,49] recently.

$$I_e = \left(\frac{M_{cr}-Pe}{M_{max}-Pe}\right)^3 I_g - \left[1 - \left(\frac{M_{cr}-Pe}{M_{max}-Pe}\right)^3\right] I_{cr}$$

For calculating the additional long-term deflection, the following expression may be used.

$$\lambda = \frac{\xi}{1 + 50\rho'}$$

where ξ = time-dependent factor for sustained load.

ρ' = percentage of compression steel at mid-span for simple and continuous span and at support for cantilever.

2.5.4 CEB-FIP Model Code

The method recommended in the Model Code[50] for

calculating the deflection of cracked members is somewhat similar to the approach given in CP110, Appendix A. The contribution of tension stiffening of the concrete between the cracks, which reduced the mean tensile strain in the bonded reinforcement, may be taken into account by the following expression.

$$\varepsilon_{sm} = \frac{f_s}{E_s}\left[1 - \beta_1\beta_2\left(\frac{f_{scr}}{f_s}\right)^2\right] + 0.4\,\frac{f_s}{E_s}$$

This expression will be further discussed in Chapter Four.

For calculating the long-term deflection, the code suggests that the total curvature comprising the sum of the elastic curvature and the curvatures due to creep and shrinkage should be used.

$$(1/r)_t = (1/r)_e + (1/r)_{cc} + (1/r)_{cs}$$

where suffix t : total

e : elastic

cc : creep

cs : shrinkage

CHAPTER THREE

PROGRAMME OF RESEARCH

3.1 Development of an Analytical Method on Short-Term Deflection Computation

In considering serviceability, the control of deflection of a structural member is important to a designer . The Codes of Practice do not normally require deflection to be calculated if certain specified span/depth ratios are not exceeded .However ,if the deflection is particularly important or if the specified span/depth ratios are exceeded, a reliable method for calculating the deflection becomes necessary.

The deflection of prestressed concrete members (Class 1 and 2 according to CP110) is not usually large enough to be a problem provided the members remain uncracked for all loads throughout the life of the structure. There have been cases where excessive camber due to prestress has caused serious troubles, but this deflection can be accurately computed by elastic uncracked section analysis without difficulty. In contrast, partially prestressed concrete (Class 3) and ordinary reinforced concrete members do crack under working load, and the estimation of deflection will therefore become more complicated. In practice, the span/depth ratios adopted in reinforced concrete design are rarely beyond the limits specified in the Codes because of the depth required for flexural strength. On the other hand, the

control of deflection will be important in Class 3 members with their reduced depth; particularly so for those with unbonded tendons which undergo a larger deflection than members with fully bonded tendons under similar conditions

The complication of analysing a cracked prestressed concrete section will be increased by the presence of unbonded tendons because of the strains in the tendon and adjacent concrete are not compatible. Furthermore, calculation based on the curvature of a cracked section will over-estimate the actual deflection for two reasons. First, the members are usually only partially cracked, i.e. cracks only occur in the high moment regions while the concrete remains uncracked at the other sections. The second reason is that the tension stiffening contribution of the concrete between the cracked sections will reduce the average curvature. A precise computation of deflection should take account of these factors.

Several empirical formulae[1] have been proposed in recent years to provide an alternatives for calculation of deflection. These formulae are derived from test results on reinforced concrete members, and have been used for prestressed concrete members with results which have been claimed to be satisfactory when compared with tests[45]. Nevertheless, the validity and reliability of these simplified expressions for the prediction of the deflection of partially prestressed concrete members with unbonded tendons, is still uncertain. An analytical method of calculating deflection which can be checked against the limited number of experimental results is therefore necessary for

a full understanding of flexural deformation leading to the improvement of simpler design formulae. Such an improvement would encourage designers to make more use of this type of structure in practice.

A general method of calculating deflection by integrating the curvature of each section along the member has been recommended in CP110. The procedure in the present investigation will be to develop an analytical method on the basis of the CP110 approach for predicting the short-term deflection of Class 3 members with unbonded tendons. The procedures are complicated and a computer program was developed for the study.

3.2 Experimental Programme

3.2.1 Selection of Parameters

There are many factors which may affect the flexural behaviour of unbonded partially prestressed concrete beams. The important parameters are as follows :

(1) Size and shape of section

(2) Level of prestress

(3) Ratio of reinforcement(prestressed and non-prestressed steel)

(4) Position of reinforcement in section

(5) Span/effective depth ratio

(6) Characteristics of material

(7) Friction between tendon and duct

(8) Pattern of loading (eg. uniformly distributed load or

concentrated loads)

(9) Types of loading (eg. short-term or sustained)

The investigation of the above parameters was limited by the time available for the research. It was therefore decided to consider (1), (2), (3) and (9) as the major parameters to be studied with all the other parameters kept constant as far as practicable.

Fifteen beams of effective span 6 metres and overall depth 305 mm were designed varying selected parameters. All the beams were prestressed with post-tensioned high tensile wires left ungrouted, and were tested simply supported under a two point loading arrangement. Two additional reinforced concrete beams were included for comparison purposes. Further details design of the beams will be given in Chapter Five.

3.2.2 Loading Procedures

In early years, the emphasis in research on prestressed concrete members with unbonded tendons was the ultimate behaviour. Therefore, most of the tests by other researchers[20,21,28,31,32] have used either monotonic or short-term cyclic loading up to failure. However, since the present study is also concerned with the flexural behaviour under service loads, other types of loading were considered, namely long-term sustained load and a combination of sustained load with short-term cyclic loading to represent practical loading conditions i.e. a certain proportion of the

design load considered as dead load and the remainder acting as occasional live load. Observation were made of the residual deflection after each load cycle, its recovery and the cumulative residual deflection under cyclic loading, which had been found to be of significance[2].

The experiment were carried out with different loading procedures as follows. All the test commenced with two cycles of short-term loading up to service load. Then :

(1) Eight beams were loaded to failure after 2 or 3 days.

(2) One beam was tested under long-term sustained loading equal to fifty percent of the service load for about a year.

(3) The remainder were tested under a combination of cyclic and sustained loading in which the latter was equal to one half of the service load , and intermittent cycles of load were applied to bring the total load up to the full service load at intervals of about 5 days. The total duration of test was about 30 days.

CHAPTER FOUR

THEORETICAL ANALYSIS

4.1 Analysis of Cracked Section with Unbonded Tendons

4.1.1 Introduction

The calculation of stress in the bonded tensile reinforcement of a cracked member may be necessary for several reasons. It is generally accepted that the computation of deflection should be based on as accurate an assessment as possible of the curvature at the cracked section which in turn is related to the stress or strain in the bonded tensile reinforcement. Furthermore, it is also found that the flexural crack width of a cracked prestressed member is directly influenced by the increase of stress in the bonded tensile steel after the stage of decompression (zero stress in concrete at the tensile face of the member). Bennett et al[51] and Nilson et al[52] demonstrated the importance of this parameter and several crack width formulae have been proposed in which crack width is related to the reinforcement stress. More recently, Nawy and Chiang[3] have also proposed a formula, especially for partially prestressed beams with unbonded tendons, relating crack width to the incremental stress in the non-prestressed steel. Moreover, it may be necessary to consider the stresses in the steel in the cracked section to evaluate the range of stress in the steel to ascertain the degree of safety against fatigue failure.

Partially prestressed concrete members (Class 3) may be expected to crack under working load, and although the stresses in both steel and concrete generally remain within the elastic range, the analysis of the cracked section is still complicated. Linear cracked section analysis is therefore not suitable for design purposes but, nevertheless, since it gives a fairly accurate representation of the flexural behaviour of a cracked member, it is a useful research technique and will be used for the study.

4.1.2 Review of Cracked Section Analysis

No attempts have been made in the past to analyse cracked prestressed concrete section with unbonded tendons although the cracked section theory for fully bonded prestressed concrete section has been developed for some years. Early attempts at the latter by Goschy[53], Birkenmaier[54] and Brettle[55] were not sufficient in some ways, for none had considered non-prestressed steel which is usually present in partially prestressed sections and may be at a different level from the prestressed reinforcement.

The analytical procedure used by Chandrasekhar[41] to determine the reinforcement stresses of prestressed concrete cracked section was formulated on the basis of the linear elastic theory for a reinforced concrete cracked section with suitable modifications to account for the effect of the compressive force used for prestressing. The method, however, was limited to rectangular section and was later improved by Veerasubramanian[43]

to include flanged sections and by Lee[44] to take account of stresses in the bottom flange just before cracking. Results showed the method to give reasonably accurate values of the reinforcement stress in some tests of partially prestressed beams, provided the behaviour of the materials remained elastic. This method will be further explained later in the chapter.

Recently, Nilson[57] has also suggested a method for calculating the flexural stresses in a partially prestressed concrete section after cracking. The idea utilizes the concept of decompression of the concrete section and a fictitious force is introduced in order to bring the overall concrete section to a state of zero stress, so that a prestressed section can be treated as an ordinary reinforced concrete section subject to an eccentric force. The calculation of the fictitious decompression force, however , can be complicated by the presence of time-dependent deformation and prestress losses as pointed out by Tadros[58] . An over-estimation of the force could result in a significant increase in the neutral axis depth and an unconservative estimate of tensile stress and crack width. The formula proposed by Nilson for calculating the decompression force was also criticised by Tadros for neglecting the compressive stress induced in the non-prestressed steel. This stress is significant, particually for partially prestressed concrete sections, in which considerable amounts of non-prestressed steel are usually used. Balaguru[56] has used Nilson's method for calculating the depth of neutral axis of cracked sections with unbonded tendons for design purposes, but this application is not justified because it does not consider the actual change in stress in the unbonded tendons.

4.1.3 Modified Reinforced Concrete Cracked Section Theory

The behaviour of partially prestressed concrete members after cracking may be expected to have a certain similarity to that of ordinary cracked reinforced concrete members. Actually, the former are stiffer than the latter because of the effect of the compressive prestressing force. Moreover, for a reinforced concrete member, the neutral axis of bending coincides with the centroid of the cracked transformed section. However, it is different for a prestressed section in which the neutral axis varies with the applied moment and the compressive prestressing force. This compressive force is not constant after cracking, but depends on the loading and the section properties. In the case of a section having unbonded tendons, the matter is complicated because the stress in the tendons is beam-dependent rather than section-dependent i.e. the change in tendon stress is influenced by the deflected profile of the whole member and is related to the extension of the concrete at the level of tendon. The tendon stress is the same along its entire length between anchorages provided there are no frictional effects between tendons and ducts causing uneven stress distribution. This is an important consideration in the analysis. Nevertheless, the modified reinforced concrete cracked section theory can be adopted with appropriate modifications for this type of prestressed section.

The analysis in the present investigation was based on Chandrasekhar's method and included the improvements by Lee with further modification to allow for the non-compatible strain in the unbonded tendons and the adjacent concrete. This is significant

because an unbonded tendon can move freely inside the duct and consequently the strain will be uniformly distributed throughout its entire length. It therefore follows that for identical conditions, the tendon stress in an unbonded prestressed cracked section has a lower value than in a fully bonded one. On the other hand, the stress in the non-prestressed steel in the former has a higher value than the latter in order for the cracked section to have the same moment of resistance.

The following assumptions are made for the analysis of short-term deflection under service load conditions.

(1) Plane sections remain plane before and after loading.

(2) The concrete strains at any level in the cross section of the beam are proportional to the distance from the neutral axis.

(3) The behaviour of the steel and concrete are perfectly elastic.

(4) The strain between the bonded reinforcement and the adjacent concrete is compatible.

(5) The tensile strength of concrete is ignored after cracking.

(6) The tension stiffening effect of concrete at the point half-way between adjacent cracks is equal to 1 N/mm2 as recommended in CP110 for short-term loading.

(7) Friction between the unbonded tendons and their ducts is negligible.

A partially prestressed concrete member usually exhibits two distinct states of flexural behaviour below service load. In the first stage (uncracked elastic), the concrete section is uncracked or the cracks remain closed. The concrete section is

assumed homogeneous and the deformation is linear; hence the amount of reinforcement has little influence on the deformation. The second stage (cracked elastic) will commence after cracking occurs or the cracks reopen. In the cracked state, the tensile resistance of the concrete is negligible. Moreover, the concrete section is no longer homogeneous, but the section is composed of a compressive zone and disconnected tensile steel. Consequently, the quantity of reinforcement has a much greater influence upon the deformation which is larger than in the previous stage because of the reduced stiffness of the member. There is a transition stage immediately after the occurrence of a microcrack (visible only under microscope) to a visible crack in the virgin load cycle. Microcracks will develop as soon as the concrete stress in the tensile face exceeds the direct tensile strength of the concrete. The stress at which cracking becomes visible corresponding approximately to the modulus of rupture of the concrete.

The cracks will close under the effect of prestressing force after the applied loads are reduced to a certain level and the whole concrete section becomes homogeneous again. On reloading, the cracks reopen at a lower load (about decompression load) because of the loss of the tensile resistance of the concrete after the earlier cracking. It is therefore generally considered that in partially prestressed concrete, the cracked phase commences at the point of decompression of the concrete at the soffit i.e. when the concrete stress ceases to be compressive at the soffit. This assumption is commonly accepted although the cracks may sometimes reopen at a higher load and close at a lower load than the decompression load due to the resistance to slipping

between the concrete and the reinforcement at the cracks.

The Concrete Society Report on Partial Prestressing[59] has shown a simple and convenient method by which the calculated stresses in the cracked section are related to a reference load rather than the decompression load. This reference load is defined as the load causing zero stress in the concrete at the average level of the total reinforcement. However, it was found more convenient in the present work to use the decompression load method for a rigorous analysis taking account of the different levels of the unbonded tendons and the non-prestressed steel.

Fig.4.1(a-f) shows the general stress and strain conditions for a typical partially prestressed beam at different loading stages in which M_o is the decompression moment of the section. To calculate this, it is necessary to know the corresponding forces in both the tendons and the non-prestressed steel, making due allowance for the losses of prestress and the effect of non-prestressed steel on these losses. Referring to the stress and strain distributions under M_o in Fig.4.1(b,e), the forces in the two types of steel are given by:-

$$P_o = P_e + (\varepsilon_{cpe}-\varepsilon_{cpo})\ \phi_u\ A_p\ E_s$$

$$R_o = R_e + (\varepsilon_{cre}-\varepsilon_{cro})\ A_s\ E_s$$

Therefore, the decompression moment is given by:-

$$M_o = F_o\ z_o - P_o\ (h-d_p) - R_o\ (h-d_s)$$

where P_e = effective force in tendon.

R_e = force in non-prestressed steel due to P_e.

ε_{cpe} = effective prestrain at the tendon level.

ε_{cre} = effective prestrain at the non-prestressed steel level.

ε_{cpo} = concrete strain at the tendon level under M_o.

ε_{cro} = concrete strain at the non-prestressed steel level under M_o.

ϕ_u = strain factor in uncracked stage,it is defined as the ratio of the change in tendon strain to the change in concrete strain.

Referring to Fig.4.1(b), by the condition of forces equilibrium , F_o is given by:-

$$F_o = \frac{f_{co}}{2h}\left[b_t h^2 - (b_t - b_w)(h-h_f)^2 + (b_b - b_w)h_b^2\right]$$

from which,

$$f_{co} = \frac{2F_o h}{b_t h^2 - (b_t - b_w)(h-h_f)^2 + (b_b - b_w)h_b^2}$$

but,

$$\varepsilon_{cpo} = \frac{f_{co}(h-d_p)}{E_c h} \quad \text{and} \quad \varepsilon_{cro} = \frac{f_{co}(h-d_s)}{E_c h}$$

therefore,

$$\varepsilon_{cpo} = KF_o(h-d_p) \quad \text{and} \quad \varepsilon_{cro} = KF_o(h-d_s)$$

where,

$$K = \frac{2}{E_c\,[b_t h^2-(b_t-b_w)(h-h_f)^2 + (b_b-b_w)h_b^2]}$$

hence,

$$F_o = P_o + R_o$$

$$= P_e + (\varepsilon_{cpe}-\varepsilon_{cpo})\phi_u A_p E_s + R_e + (\varepsilon_{cre}-\varepsilon_{cro})A_s E_s$$

substitute ε_{cpo} and ε_{cro} into F_o to give,

$$F_o = P_e + [\varepsilon_{cpe}-KF_o(h-d_p)]\phi_u A_p E_s + R_e + [\varepsilon_{cre}-KF_o(h-d_s)]A_s E_s$$

$$= \frac{P_e + R_e + \phi_u \varepsilon_{cpe} A_p E_s + \varepsilon_{cre} A_s E_s}{1 + KE_s[\phi_u(h-d_p)A_p + (h-d_s)A_s]}$$

The decompresssion moment and the strain factor are inter-related, therefore a trial and error procedure is required. The calculation of the strain factor will be further explained in Section 4.1.4 .

With reference to the stress and strain distributions of a cracked section in Fig.4.1(c,f) , the forces in the tendons and the non-prestressed steel are given by :-

$$P = P_o + (\varepsilon_{cpo}+\varepsilon_{cp})\phi_c A_p E_s \qquad \text{.....Eqn.(4.1)}$$

$$R = R_o + (\varepsilon_{cro}+\varepsilon_{cr})A_s E_s \qquad \text{.....Eqn.(4.2)}$$

where ϕ_c is the strain factor in cracked stage.

By equating the conditions of equilibrium of the cracked section the following equations can be obtained :-

(1) From the conditions of strain compatibility,

$$\varepsilon_{cp} = \frac{f_c}{E_c}\left(\frac{d_p - X}{X}\right) \qquad \text{.....Eqn.(4.3)}$$

$$\varepsilon_{cr} = \frac{f_c}{E_c}\left(\frac{d_s - X}{X}\right) \qquad \text{.....Eqn.(4.4)}$$

(2) From the condition of forces equilibrium,

$$P + R = \frac{f_c}{2X}\left[b_t X^2 - (b_t - b_w)(X - h_f)^2 + (b_b - b_w)(X - h + h_b)^2\right]$$

.....Eqn.(4.5)

(3) From the condition of moments equilibrium,

$$M = (P+R)z - p(h - d_p) - R(h - d_s) \qquad \text{.....Eqn.(4.6)}$$

where

$$z = \frac{h[\lambda^2(3-\lambda) - B_1(\lambda - H_1)^2(H_4 - \lambda) + B_2(\lambda - H_3)^2(H_5 - \lambda)]}{3[\lambda^2 - B_1(\lambda - H_1)^2 + B_2(\lambda - H_3)^2]}$$

$\lambda = x/h$

B_1, B_2, H_1, H_3, H_4, H_5 (see next page)

Equating Eqns(4.5) and (4.6) by eliminating f_c and substitute Eqns(4.3) and (4.4) into the new expression. The final equation in terms of the ratio of the depth of the neutral axis (x) to the depth of the section (h) can be expressed in the following form :-

$$W_1\lambda^3 + W_2\lambda^2 + W_3\lambda + W_4 = 0 \qquad \text{.....Eqn.(4.7)}$$

where

$$W_1 = C_3(B_1-1-B_2)$$

$$W_2 = C_3(3-B_1H_4-2B_1H_1+B_2H_5+2B_2H_3) - 3C_5(1-B_1+B_2)$$

$$W_3 = C_3[2B_1H_1H_4+B_1H_1^2-2B_2H_3H_5-B_2H_3^2+pop(1-d_1) +$$

$$pos(1-d_2)] - C_5[6B_1H_1 - 6B_2H_3 + pop + pos]$$

$$W_4 = C_3[B_2H_3^2H_5-B_1H_1^2H_4-d_1pop(1-d_1) - d_2pos(1-d_2)] -$$

$$C_5[3B_2H_3^2-3B_1H_1^2-d_1pop-d_2pos]$$

$$B_1 = 1 - \frac{b_w}{b_t}$$

$$B_2 = \frac{b_b - b_w}{b_t}$$

$$d_1 = \frac{d_p}{h}$$

$$d_2 = \frac{d_s}{h}$$

$$H_1 = \frac{h_f}{h}$$

$$H_2 = \frac{h_b}{h}$$

$$H_3 = 1 - H_2$$

$$H_4 = 3 - 2H_1$$

$$H_5 = 2H_2 + 1$$

$$pop = \frac{6\alpha\ A_p\ \phi_c}{b_t h}$$

$$pos = \frac{6\ A_s \alpha}{b_t h}$$

$$C_3 = F_o + \phi_c\ \varepsilon_{cpo}\ A_p\ E_s + \varepsilon_{cro}\ A_s\ E_s$$

$$C_4 = (P_o + \phi_c\ \varepsilon_{cro}\ A_p\ E_s)(h-d_p) + (R_o+\varepsilon_{cro}\ A_s\ E_s)(h-d_s)$$

$$C_5 = \frac{M + C_4}{h}$$

Eqn(4.7) applies to all practical shapes of section. The terms B_1 and B_2 only apply when the neutral axis is located in the bottom flange of the section. Otherwise, the terms B_2 or both B_1 and B_2 are equal to zero depending on whether the neutral axis is located in the web or top flange respectively. The above cubic equation can be solved with any value of the applied moment (M) if the section and material properties and the initial stresses in steel (tendons and non-prestressed steel) before the application of load are known. In addition, initial values of ϕ_u and ϕ_c are assumed and these are later successively corrected by iterative procedure. Detail of the iteration process will be further explained later.

Once the neutral axis position has been determined, the maximum concrete stress at the top can be obtained from Eqn(4.5). The increase in stress of both the tendons and the non-prestressed steel after the stage of decompression (i.e. from M_o to M) is

given by :-

$$\Delta f_p = (\varepsilon_{cp} + \varepsilon_{cpo})\phi_c E_s$$

and

$$\Delta f_s = (\varepsilon_{cr} + \varepsilon_{cro}) E_s$$

where

$$\varepsilon_{cp} = \frac{f_c(d_p - X)}{E_c X}$$

and

$$\varepsilon_{cr} = \frac{f_c(d_s - X)}{E_c X}$$

4.1.4 Strain Factors

A strain factor was introduced by Baker[27] for the theoretical calculation of the ultimate load of beams with any type of reinforcement and any degree of bond. The strain factor related the strain in the steel and in the adjacent concrete. It was a function of several variables and was equal to unity when the steel was well bonded to the concrete. Baker suggested that this parameter should be determined experimentally and recommended a safe limiting value of 0.1 to be used in the design of unbonded prestressed concrete beam. Janney et al[20] and Pannell et al[31,32] and a good deal of work was carried out on unbonded prestressed beams both theoretically and experimentally to determine the limiting value of the strain factor at the ultimate

state. The results obtained by these researchers are however not suitable for the study of service load conditions. The object of this section is to evaluate the strain factors (ϕ_u and ϕ_c) of an unbonded partially prestressed section up to service load, where ϕ_u and ϕ_c refer to the strain factor in the uncracked and cracked state respectively. The characteristic of an unbonded tendon is that the change in tendon strain is the same over its length and hence the total elongation of the tendon is equal to the total extension of the concrete at the tendon level. The assumption of no friction between the tendons and ducts still applies. The change in tendon strain is therefore a function of the applied moment at all the points along the member depending as it does on the pattern of loading and the profile of the tendons.

When the member in uncracked stage, the change in concrete strain ($\Delta\varepsilon_c$) under moment M_x is given by :-

$$\Delta\varepsilon_c = \frac{1}{E_c}\left[\frac{M_x e}{I_g} - \frac{\delta p}{A}\left(1 + \frac{e^2}{i^2}\right)\right]$$

Hence, the extension of concrete ($\Delta\ell$) and the average change in tendon strain ($\Delta\varepsilon_p$) are given by :-

$$\Delta\ell = \int_0^{L_t} \Delta\varepsilon_c \, dX$$

and

$$\Delta\varepsilon_p = \frac{\Delta\ell}{L_t}$$

$$= \frac{\frac{1}{L_t}\int_0^{L_t} \frac{M_x e}{I_g E_c}\, dX}{\left[1 + \frac{1}{L_t}\int_0^{L_t} \frac{A_p E_s}{A E_c}\left(1 + \frac{e^2}{i^2}\right) dX\right]}$$

therefore,

$$\phi_u = \frac{\Delta\varepsilon_p}{\Delta\varepsilon_c}$$

where $\delta p = A_p E_s \Delta\varepsilon_p$, the additional compressive force in concrete due to the change in tendon strain ($\Delta\varepsilon_p$).

L_t = total length of member.

e = eccentricity of tendons.

M_x = function of applied moment.

The factor ϕ_u can be evaluated provided the function M_x , the section and material properties are known.

In the cracked stage, the member is assumed to be fully cracked over the whole span i.e. the member has a straight tendon

profile and under constant moment, and the tension stiffening of concrete is taken into consideration. The possible strain distribution between adjacent cracks is shown in Fig.4.2 where ε_{cp} is the virtual concrete strain at the tendon level in a cracked section and f_{cts} is the tensile stress in concrete at the same level halfway between cracks regarding as the stiffening effect of concrete. The value of f_{cts} is assumed to be 1 N/mm2 under short-term loading as recommended in CP110. The actual pattern of the longitudinal concrete strain distribution is not known but the average concrete strain can generally be expressed as :-

$$\varepsilon_{cav} = \varepsilon_{cp} - \beta(\varepsilon_{cp} - \varepsilon_{uc})$$

or

$$\varepsilon_{cav} = \varepsilon_{cp} - \beta(\varepsilon_{cp} - \frac{f_{cts}}{E_c}) \qquad \text{.....Eqn.(4.8)}$$

The average concrete strain is thus intermediate between the two value ε_{cp} and ε_{uc} and also depends on the magnitude of β , where β is a strain distribution coefficient and is governed by the tension stiffening effect of concrete. β equal to zero represents the complete loss of tension stiffening thus the average concrete strain is also the virtual concrete strain at the cracks. Bennett[60] has originally proposed a linear distribution which represents β = 0.5 but later investigation by Lee[2] has showed that β = 0.15 was more appropriate for his test results on bonded partially prestressed beams.

From Eqn(4.8), the extension of concrete at the tendon

level after cracking (i.e. from M_o to M) is given by :-

$$\int_0^{L_t} [\varepsilon_{cp} - \beta(\varepsilon_{cp} - \frac{f_{cts}}{E_c})] \, dx$$

Hence,the average change in tendon strain is given by:-

$$\frac{1}{L_t} \int_0^{L_t} [\varepsilon_{cp} - \beta(\varepsilon_{cp} - \frac{f_{cts}}{E_c})] \, dx$$

therefore,

$$\phi_c = \frac{\frac{1}{L_t} \int_0^{L_t} [\varepsilon_{cp} - \beta(\varepsilon_{cp} - \frac{f_{cts}}{E_c})] \, dx}{\varepsilon_{cp}}$$

It should be pointed out that ϕ_c only applies to a member under constant moment along its span. For other types of loading pattern, however, the principle will be the same.

4.1.5 Pattern of Loading

The change in tendon strain depends on the pattern of loading applied to the member. A symmetrical two point loading system is considered for the analysis for comparison with experimental results. Fig.4.3 shows a simply supported beam under

loading. The concrete section is considered to be cracked wherever the applied moment is greater than the decompression moment of the section. The beam is thus partially cracked with concrete sections near the supports remaining uncracked. Referring to Fig.4.3, the beam is divided into 3 regions (L_1 ,L_2 and L_3) where L_1 represents the length of the uncracked region and L_2 and L_3 indicate the length of the cracked region under varying and constant moment respectively. The average change in concrete strain at the tendon level over the entire span can be obtained as follows.

In the uncracked region ,L_1 , the average change in concrete strain is given by :-

$$\Delta\varepsilon_{cpu} = \frac{M_{oj}e}{2E_cI_g\left[1 + \frac{A_p}{A}\alpha\left(1 + \frac{e^2}{i^2}\right)\right]}$$

In the cracked region ,L_2 , the average change in concrete strain before and after cracking is given by :-

Before cracking,

$$\varepsilon_{cpe} - \left(\frac{\varepsilon_{cpom} + \varepsilon_{cpoj}}{2}\right)$$

After cracking,

$$\left(\frac{\varepsilon_{cpom}+\varepsilon_{cpoj}}{2}\right) + \left(\frac{\varepsilon_{cpm}+\varepsilon_{cpoj}}{2}\right) - \beta\left(\frac{\varepsilon_{cpm}+\varepsilon_{cpoj}}{2} - \frac{1}{E_c}\right)$$

Therefore, the total change in concrete strain along L_2 is obtained by adding the two expressions.

$$\Delta\varepsilon_{cpcv} = \varepsilon_{cpe} + \left(\frac{\varepsilon_{cpm}+\varepsilon_{cpoj}}{2}\right) - \beta\left(\frac{\varepsilon_{cpm}+\varepsilon_{cpoj}}{2} - \frac{1}{E_c}\right)$$

where ε_{cpom} = concrete strain at the tendon level in section m-m under M_{om} .

ε_{cpoj} = concrete strain at the tendon level in section j-j under M_{oj} .

ε_{cpm} = virtual concrete strain at the tendon level in section m-m under M_{max} .

In the cracked region ,L_3 , the average changes in concrete strain at the tendon level before and after cracking are given by :-

Before cracking,

$$\varepsilon_{cpe} - \varepsilon_{cpom}$$

After cracking,

$$[\varepsilon_{cpm} - \beta(\varepsilon_{cpm} - \frac{1}{E_c})] + \varepsilon_{cpom}$$

Therefore, the total change in concrete strain along L_3 is given by adding the above expressions.

$$\Delta\varepsilon_{cpcc} = \varepsilon_{cpe} + [\varepsilon_{cpm} - \beta(\varepsilon_{cpm} - \frac{1}{E_c})]$$

Finally, the average change in concrete strain at the tendon level for the entire span ,L_t , is given by :-

$$\Delta\varepsilon_{cav} = \frac{2L_1\Delta\varepsilon_{cpu} + 2L_2\Delta\varepsilon_{cpcv} + L_3\Delta\varepsilon_{cpcc}}{L_t} \qquad \text{.....Eqn.(4.9)}$$

The average change in tendon strain along the beam is,

$$\Delta\varepsilon_p = \Delta\varepsilon_{cav} \qquad \text{.....Eqn.(4.10)}$$

The strain factors at the section m-m and the section j-j are ϕ_{cm} and ϕ_{uj} respectively,

$$\phi_{cm} = \frac{\Delta\varepsilon_p - \Delta\varepsilon_{pom}}{\varepsilon_{cpm} + \varepsilon_{cpom}} \qquad \text{.....Eqn.(4.11)}$$

and

$$\phi_{uj} = \frac{\Delta\varepsilon_p}{\varepsilon_{cpe} - \varepsilon_{cpoj}} \qquad \text{.....Eqn.(4.12)}$$

where $\Delta\varepsilon_{pom}$ is the change in tendon strain while the critical section m-m is at the point of decompression. The term $\Delta\varepsilon_{pom}$ can be derived as follows :-

Referring to Fig.4.4, the function of the linear varying moment is,

$$M_X = \frac{M_{om}\ X}{(L_1 + L_2)}$$

therefore,

$$\Delta\varepsilon_{pom} = \frac{1}{E_c L_t}\left[2\int_0^{L_1+L_2} \frac{M_X e}{I_g}\,dX + \int_0^{L_3} \frac{M_{om} e}{I_g}\,dX - \int_0^{L_t} \left(\frac{A_p E_s \Delta\varepsilon_{pom}}{A}\right)\left(1 + \frac{e^2}{i^2}\right)\,dX\right]$$

hence,

$$\Delta\varepsilon_{pom} = \frac{\frac{M_{om} e}{E_c I_g}\left(\frac{L_3 + L_t}{2L_t}\right)}{1 + \frac{A_p}{A}\alpha\left(1 + \frac{e^2}{i^2}\right)} \qquad \text{.....Eqn.(4.13)}$$

The terms $\Delta\varepsilon_{pom}$ and M_{om} are inter-related by a strain factor ϕ_{um} so that an iterative procedure is required. The expression for the ϕ_{um} is given by :-

$$\phi_{um} = \frac{\Delta\varepsilon_{pom}}{\varepsilon_{cpe} - \varepsilon_{cpom}} \qquad \text{.....Eqn.(4.14)}$$

4.1.6 Summary of Computation Procedures

A summary of the computation procedures involved in the above analysis for unbonded prestressed cracked section is listed below with reference to Fig.4.3. The beam is loaded at two points resulting in a trapesoidal bending moment diagram with a maximum moment M_{max} .

(1) The effective forces (P_e ,R_e) in the two types of steel can be estimated by using the CP110 method or by direct measurement on the beam before testing. From these and the material and section properties of the beam, the effective prestrains in the concrete are calculated.

(2) With an assumed value of the strain factor ϕ_{um} , the decompression moment (M_{om}), the concrete strains (ε_{cpom} , ε_{crom}) at the tendon and non-prestressed steel level and the forces (P_{om} ,R_{om}) in the steel, relating to the decompression moment, are calculated by the general procedures described in Section 4.1.3 . The average tendon

strain ($\Delta\varepsilon_{pom}$) at this stage can be obtained by using Eqn(4.13) and the strain factor can be recalculated by using Eqn(4.14) which is in terms of ε_{cpom} and $\Delta\varepsilon_{pom}$ so that an iterative procedure is necessary.

This step enables the decompression moment (M_{om}) of the critical section to be obtained and compared with the applied moment (M_{max}) to determine whether the beam is cracked. If so, Step(3), i.e. cracked section analysis, follows, otherwise, the uncracked section theory is applied.

(3) The critical section m-m under moment M_{max} is calculated by solving the cubic equation for the depth of the neutral axis with an assumed value of strain factor (ϕ_{cm}). The cubic equation involves the terms ε_{cpom} , ε_{crom} , P_{om} and R_{om} whcih were obtained from Step(2). The concrete stress at the top and the virtual concrete strain (ε_{cpm}) at the level of the tendon can then be evaluated by the procedures described in Section 4.1.3.

(4) The decompression moment (M_{oj}), the concrete strains (ε_{cpoj} , ε_{croj}), and the steel forces (P_{oj} ,R_{oj}) are computed for the section j-j where the concrete stress is zero at the bottom, with an assumed value of strain factor (ϕ_{uj}) and using the procedures in Step(2).

(5) The average change in concrete strains at the tendon level is determined over the entire span by using the procedures described in Section 4.1.5. Referring to Fig.4.3, the beam is divided into 3 regions (L_1 ,L_2 and L_3).

(a) The distance L_1 of the section j-j from the support is found from the the relationship $L_1 = M_{oj} (L_1 + L_2) / M_{max}$.

(b) The average change in concrete strain in each region is determined separately.

(c) Hence the average change in concrete strain over the entire span is obtained.

(6) The average change in tendon strain is equal to the average change in concrete strain obtained in Step(5).

(7) The strain factors (ϕ_{uj} , ϕ_{cm}) are recalculated by using Eqns(4.11) and (4.12), and the new and old values compared, If either has a difference greater than the tolerance (0.0001 in the present application), Steps(3), (4) , (5) and (6) are repeated with the new values of strain factor until the desired accuracy is obtained.

(8) The increase of stress in both types of steel may now be computed.

A computer program has been developed for calculating the deflection of unbonded partially prestressed concrete beams under a symmetrical two-point loading. The program includes the cracked section analysis as described above. The method of calculating the deflection are explained in the next section.

4.2 Analysis of Deflection

4.2.1 Introduction

The need for a rigorous analysis of the deflection of unbonded partially prestressed concrete members has been discussed in Chapter 3. A method will now be presented for the computation of the short-term deflection of this type of member.

The major factors which affect the short-term deflection of a cracked prestressed concrete member under service load are : the modulus of elasticity of concrete; prestressing force; amount of reinforcement; cross section; load distribution and supports conditions; magnitude of load and degree of cracking along the member. The effect of cracking is complicated because cracks appear only in the part of the member under high moment. In addition, the concrete between the cracks still carries some tension. Consequently, the stiffness of the concrete section varies and therefore causes the curvature to vary along the span as indicated in Fig.4.5. The phenomenon of concrete in tension between the cracks is known as the tension stiffening effect and may significantly reduce the average curvature of a cracked section, increasing the effective stiffness above the value calculated by disregrading the tensile strength of the concrete. If the strain at the steel level is considered, rather than the curvature, the average strain in the non-prestressed steel is seem to be less than the strain at the position of the cracks. The mechanism of the tension stiffening effect and its evaluation will be discussed in Section 4.2.2. The determination of the distribution of curvature is an essential step in the analysis of

deflection of cracked prestressed members. Once the distribution is known, the deflected profile of the member can be found using the usual numerical integration technique.

Procedures for determining the average curvatures are given in Section 4.2.3. These are based on the recommendations in CP110, Appendix A. A computer program is developed for the analysis which is applicable for partially prestressed beams with unbonded tendons simply supported and loaded at two points. The program is listed in Appendix .

4.2.2 Tension Stiffening on First Loading

4.2.2.1 General Remarks

Before cracking, the concrete and steel in a partially prestressed concrete member will behave linearly. When the tensile strength of the concrete has been exceeded, flexural cracks will form at the tensile face and extend to a level very close to that of the neutral axis. The tensile resistance of the concrete below the neutral axis is ignored, so that the whole of the tensile force carried by the concrete before cracking must be transferred to the steel which crosses the cracks, in order to satisfy the equilibrium conditions of the section. However, the behaviour in the region between the cracks is not yet fully understood. The tensile stresses are transferred to the concrete by means of bond and evidence from pull-out tests[61] indicates that the bond characteristic are greatly influenced by the type of reinforcing bars; the magnitude of the load and number of load cycles.

When deformed bars are used, the bond between the concrete and steel is effective except in the vicinity of cracks where the bond is destroyed. As the steel stress increases, the local forces induced at the ribs of the reinforcing bars will cause internal cracking thereby decreasing the amount of tension carried by the concrete. At higher loads, the degradation of bond in the concrete becomes continuous until eventually the concrete can provide no tensile resistance at all. At this stage, there is usually longitudinal splitting of the concrete along the line of the bar and the tension stiffening effect contributed by the concrete is completely lost.

4.2.2.2 Methods of Evaluation

Numerous methods[62] have been suggested to allow for the tension stiffening effect in concrete members on the average steel stress for the calculation of crack width, curvature and deflection. This factor is important for calculating the stress in unbonded tendons in the present research.

Basically, the average steel stress is calculated from

$$f_{sav} = f_s - \Delta f_s$$

where f_s = steel stress in a cracked section.

Δf_s = average reduction of steel stress due to tension stiffening effects.

Various expressions have been proposed on the basis of

this principle. Yu and Winter[63] have suggested that the average tensile stress (f_t) of concrete between cracks can be expressed as a fraction of the tensile strength (modulus of rupture, f_{ct}) of plain concrete, i.e. $f_t = K f_{ct}$, where K is a coefficient derived from tests . This tensile stress thus provides a resisting moment and the stress in the reinforcement corresponding to this moment is considered as the average reduction of stress due to the tension stiffening effect. A formula has been proposed in which the tensile strength of concrete is expressed in terms of the compresive strength.

$$\Delta f_s = \frac{0.02(f_c')^{2/3} bh(h - X)}{A_s z} \qquad \text{(in S.I. units)}$$

where f_c' = compression strength of concrete.

b = width of cross-section in tension zone.

z = lever arm of internal forces.

h = depth of section.

x = depth of neutral axis

Rao and Subrahmanyam[64] have found that tension stiffening is reduced when the applied load increases. The following formula has been derived from experimental results :-

$$\varepsilon_{sav} = \frac{f_s}{E_s} - 0.18\left(\frac{f_{scr}}{f_s}\right)\frac{f_{ct}}{\rho_s E_s}$$

where f_{scr} = steel stress at the appearance of the first flexural crack.

The ratio (f_{scr} / f_s) signifies the degree of cracking of the section. The stiffening effect will be vanished as the steel stress (f_s) increases to a higher value.

Rao's expression was further modified as follows for the CEB-FIP Model Code[50] to include the influence of bond, sustained loading and repitition of load, on tension stiffening.

$$\varepsilon_{sav} = \frac{f_s}{E_s}\left[1 - \beta_1\beta_2\left(\frac{f_{scr}}{f_s}\right)^2\right] \not< 0.4\,\frac{f_s}{E_s}$$

where β_1 = a coefficient which characteristics the bond properties of the bars.

β_1 = 1 for high bond bars.

β_1 = 0.5 for plain bars.

β_2 = a coefficient representing the influence of the duration of the application or repitition of the loads.

β_2 = 1 at the first loading.

β_2 = 0.5 for loads applied in a sustained manner or for a large number of load cycles.

In the British Code, CP110, Appendix A[8], two different methods have been adopted to account for the tension stiffening effect in the calculation of crack width and deflection

respectively. According to the Equation 62 in CP110, allowing for the tension stiffening of the concrete in the tensile zone, the average steel strain is given by :-

$$\varepsilon_{sm} = \varepsilon_s - \frac{1.2\ bh(a'- X)}{A_s(h - X)\ f_y} \times 10^{-3}$$

where a' = the distance from the compression face to the point at which the crack width is being calculated.

other terms are the same as defined previously.

On the other hand, according to the recommendation for calculating deflection of a cracked member under short-term loading, the stresses in the concrete in tension may be calculated on the assumption of linear stress distribution and to vary from zero at the neutral axis to a value of 1 N/mm2 at the centroid of the tension steel. However, no further indication is given of the interpretation of this assumption. It is possible that it follows the Yu and Winter proposal in which the tensile stress of concrete (i.e. $K f_{ct}$ = 1 N/mm2) will produce a resisting moment to reduce the average strain of a cracked section. On the other hand, Bennett and Lee in recent work have assumed that the concrete tensile stress is specified at the point halfway between the cracks and further suggested a coefficient (β) to represent the longitudinal curvature distribution between adjacent cracks. This enables the curvature at both the cracked and uncracked section (halfway between cracks) to be calculated. The average curvature can then be obtained by the following expression.

$$\frac{1}{r_{av}} = \frac{1}{r_{cr}} - \beta\left(\frac{1}{r_{cr}} - \frac{1}{r_{uc}}\right)$$

where r_{cr} = radius of curvature at the cracked section.

r_{uc} = radius of curvature at the mid-point between cracks.

β = distribution coefficient.

The interpretation of Bennett and Lee has been adopted for the present investigation but it has been found more convenient to change the definition of β for the strain rather than curvature distribution. This has been discussed in Section 4.1.4. The comparisons of the above methods with test results are discussed in Chapter Six.

4.2.3 Computation of Deflection

The analytical method presented in this section for calculating the deflection of unbonded partially prestressed beams is based on the recommendations in CP110, Appendix A. This is a general method whereby the approach is to assess the curvatures of sections under the appropriate moments and then calculate the deflection by integrating the curvatures over the whole span of the member. It is therefore necessary to calculate the curvatures for a series of sections. The general expression for curvature is given by :-

$$\frac{1}{r} = \frac{\varepsilon_t + \varepsilon_b}{h}$$

where ε_t and ε_b are the concrete strains at the top and bottom of the section respectively and h is the depth of the section. It

is understood that the average concrete strain at the bottom of the cracked section is reduced due to the effect of tension stiffening which is therefore of importance in the analysis. The proposed methods to take this factor into consideration have been discussed in the previous section and in what follows, the recommendation for calculating deflection in CP110 is adopted for the present study. According to this method, the average concrete strain at the tendon level is given by :-

$$\epsilon_{cav} = \epsilon_{cp} - \beta(\epsilon_{cp} - \frac{1}{E_c})$$

where ϵ_{cp} is the virtual concrete strain at the tendon level in the cracked section and β is a distribution coefficient of the longitudinal strain between the cracks. The range of β is between zero and one in which $\beta = 0$ represents the complete loss of tension stiffening. In present investigation, several values of β were studied and compared with test results. The comparisons are discussed in Chapter Six.

Once the average concrete strain is determined, the average curvature of the section is given by :-

$$\frac{1}{r}_{av} = \frac{\frac{f_c}{E_c} + \epsilon_{cav}}{d}_{p} \qquad \text{.....Eqn.(4.15)}$$

where f_c is the concrete stress at the top of the section. It is assumed to be the same over the entire section between the cracks.

The deflected shape of a member is related to the

curvatures by the differential equation,

$$\frac{1}{r_x} = \frac{d^2y}{dx^2}$$

where r_x = radius of curvature at section x along a member.
y = deflection at x.

The deflection may be calculated directly from this equation by integrating the curvatures along the member using the moment-area method. The member is divided into a number of small elements of equal length over each of which, the moment and curvature are assumed to be constant. Before cracking, the curvature of each element can be calculated by using the uncracked section theory. However, after cracking, the cracked section analysis for unbonded member described in Section 4.1.3 should be used for the appropriate sections. While the curvature over the remainder of the beam (i.e. near the supports) can be determined by the uncracked section theory. It should be noted that the average tendon stress over the whole member should be used when analysing these uncracked sections. The computation procedures involved in the analysis are outlined in the next section.

4.2.4 Development of Computer Program for Deflection Computation

A computer program has been developed for calculating the short-term deflection of unbonded partially prestressed concrete beams with straight tendons. The program is applicable to simply supported beams loaded at two symmetrical points. The load

due to the self-weight of the beam , however, is uniformly distributed and will therefore be converted into two point loads such that these loads will cause the same deflection due to the self-weight as calculated by using the linear elastic theory. In the computation, the beam is divided into a number of small elements (81 elements in present study) of equal length and the curvatures of successive elements are determined by the procedures presented below. This should be read in conjunction with the procedures described in Section 4.1.6 .

(1) The section properties based on the transformed concrete section are calculated from the given dimensions and material properties of the beam.

(2) The effective prestrains in the concrete are calculated from the given effective forces in the two types of steel and the section properties obtained in Step(1).

(3) The bending moment in each element is calculated from the given load and the distance of which from the supports.

(4) The decompression moment of the critical section (section under maximum moment) is computed by the procedures described in Step(2) of Section 4.1.6, which is then compared with the applied maximum moment to determine whether the beam is cracked.

(i) If the beam is uncracked, then the curvatures of successive elements along the beam can be determined by

the uncracked section analysis before proceeding to Step(7) for deflection computation.

(ii) Otherwise, the cracked section theory described in Section 4.1.6 (Steps 3 to 7) should be used, thus enabling the average tendon stress to be obtained. In addition, the length of the uncracked region from the support can also be determined.

(5) The respective decompression moment of the elements within the cracked region are calculated and the concrete strains and steel forces relating to this moment are also computed.

(6) Starting from the nearest element to the support, the curvature over each element is calculated using Eqn(4.15) after obtaining the concrete strains at the top and bottom of the element. If the concrete section being considered is within the uncracked region, then the uncracked section theory should be applied. Otherwise, the cracked section theory described in Section 4.1.6 should be used to obtain the depth of the neutral axis of the section. The average concrete strains and the curvature can then be determined. When analysing the elements, the average tendon stress obtained in Step(4) should be used.

(7) The deflected profile of the beam can be obtained by integrating the curvatures of all the elements along the beam using the moment-area method.

In view of the complexity of the computation involved, the procedures have been described above for the second cycle of loading only. In the computation for the first cycle of loading, the decompression moment is replaced by the cracking moment in which the tensile strength of concrete is taken into consideration. The program is listed in Appendix .

CHAPTER FIVE

EXPERIMENTAL PROGRAMME

5.1 Introduction

Seventeen beams, including fifteen unbonded partially prestressed and two reinforced concrete beams, of two different sections (rectangular and I shaped) were tested. The reinforcement used was 7 mm high tensile wire for tendons and 10 mm cold-work deformed bar for non-prestressed steel. The design, material properties and fabrication technique of the test beams will be described in detail in this chapter, and information will be given of the prestressing system, instrumentation and test arrangement and procedure.

5.2 Design Detail of Test Beams

5.2.1 Size and Shape of Sections

The basic consideration for the test beams was that they should fail in flexure and also that they should be as large as practicable so that observations made at the service load might have the maximum degree of relevance to typical structural members. The test beams were therefore designed with an overall depth of 305 mm and total length of 6.3 metres to allow an effective span of 6 metres. Of the seventeen beams tested, fifteen were prestressed with post-tensioned high tensile wire left ungrouted, and the remainder were rectangular reinforced concrete

beams for purposes of comparison. There were nine beams of rectangular section out of the fifteen unbonded prestressed beams and the remaining six were of I-shaped section. The size of the beam is similar to that of some of the small members used in building structures and their proportions are such that they could be regarded as models of bridge beams. The detailed dimensions of the beam are illustrated in Fig.5.1.

5.2.2 Ratio of Reinforcement

The test beams can be divided into three series based on the different ratios of reinforcement so that the design ultimate moment of all the beams in one series is about the same. The three reinforcement ratios for series 1 , 2 and 3 correspond to the tensile resistance provided by respective tendons of 3 , 4 and 5 high tensile wires of 7 mm diameter in a fully prestressed beam without non-prestressed reinforcement. In each series, different number of prestressed wires were used and the corresponding number of non-prestressed reinforcing bars calculated to make up the required ultimate moment, allowing for the fact that there would be a smaller increase of stress in the unbonded tendons then in the bonded tendons used in the previous tests[2]. The design ultimate moment calculated according to CP110, cl.4.3.4 for the three series varies from 36 kNm to 60.1 kNm. Full details of the beams in the three series are given in Tables 5.1 and 5.2 and Fig.5.1 .

5.2.3 Level of Prestress

As mentioned earlier, the 3 series of beams correspond to the tensile resistance provided by 3 , 4 and 5 tendons in fully prestressed beams. However, by replacing some of the prestressing wires by a certain number of bars, it is possible to vary the prestress in the concrete while maintaining about the same design ultimate moment within each series. The level of prestress can be represented by a partial prestressing ratio as advocated by Naaman[18] or by the degree of prestress as used by Bachman[65]. The values of these two parameters together with the main data for the test beams in each series are given in Table 5.1 .

5.2.4 Design Ultimate and Service Moment

Assuming an overall load safety factor of 1.5 for the dead and live load, the design service moment of the beams was taken to be two-thirds of the design ultimate moment. The latter was calculated according to CP110, cl.4.3.4[8] with the material safety factors of 1.5 for concrete and 1.15 for the non-prestressed steel. However, the stress developed in the unbonded tendons at the ultimate moment is governed by the values given in CP110 , Table 38. The design ultimate moment, and hence the service moment, are approximately the same for all the beams in each series. However, the service moment used in the tests is the average in each series. The values of the design ultimate and service moment are given in Table 5.1 .

5.3 Beam Designation

A simple code was use to identify each test beam. Each

reference number consisted of a letter followed by three numerals separated into three parts. The letter refers to the shape of cross section of the beam (eg. I for I-shaped section) and is followed by a number (1,2 or 3) to indicate the reinforcement ratio for the beam series. The second and third number represent the number of tendons and non-prestressed steel bars respectively. Thus, for example, beam R2.3.2 is a rectangular section beam with the second level of total reinforcement, having 3 tendons and 2 non-prestressed steel bars.

5.4 Materials

5.4.1 Concrete

A high strength concrete was chosen to allow the maximum variation of prestress , as described in Section 5.2.3 , without the prestress in the concrete at transfer exceeding the permissible value of half the compressive strength specified in CP110. In addition, it helped to ensure that the beams were under-reinforced for failure. A mix of 1 : 1.5 : 3 by weight with a water/cement ratio of 0.45 was specified so as to comply with the strength requirement for Grade 60 concrete in Table 28 of CP110. The concrete consisted of ordinary Portland cement, natural Nottinghamshire sand and 10 mm crushed quartzite gravel. The concrete was found to develop the required strength of 50 N/mm2 at 7 days. The actual properties of concrete of each beam are given in Table 5.3.

For each mix, all the constituent materials were weighed in the required proportions before being fed into a mixer of 350

kg dry weight capacity. The materials were turned over for about a minute before the addition of the required quantity of water, after which a further two minutes mixing ensured an uniform workable mix. Three batches were necessary for the rectangular beams but only two for the I beams. Slump and compacting factor tests of the fresh concrete were carried out in accordance with BS 1881[66] before the concrete was placed. The compacting factor varied between 0.921 and 0.954 and the values of slump between 30 and 75 mm. Control specimens comprising nine 100 mm cubes, three 150 mm cubes, three 500x100x100 mm prisms and two 300x150 mm diameter cylinders were cast from each mix before the concrete was taken to the casting bed.

5.4.2 Steel

5.4.2.1 Prestressing Steel

The prestressing steel used for all the beams was a 7 mm plain, cold-drawn high tensile wire with a specified characteristic strength of 60.4 kN. The typical stress-strain relationship of the wire obtained from tensile tests is shown in Fig.5.2a and its mechanical properties are given in Table 5.4a.

5.4.2.2 Non-Prestressed Steel

The tensile reinforcement in all the test beams except the fully prestressed beam, consisted of 10 mm cold-work deformed bar with a characteristic strength of 460 N/mm2. The steel is known commercially as "Torbar" . In the fully prestressed beam, R1.3.0, two 6 mm hot-rolled mild steel bars were used to hold the

stirrups.

The results of tensile tests on sample bars are given in Table 5.4b and the typical stress-strain curve is shown in Fig.5.2b .

5.4.2.3 Shear Reinforcement

The shear reinforcement was provided by 6 mm hot-rolled mild steel bar of characteristic strength of 250 N/mm2 bent into closed links as shown in Fig.5.1. Nominal shear reinforcement at a spacing of 150 mm was used throughout the beam except in the support regions where the spacing was reduced to 50 mm. The details of the stirrups are shown in Fig.5.3.

5.4.2.4 Top Reinforcement

Nominal reinforcement was provided at the top along the whole length of the beam to facilitate the formation and location of the reinforcing cage. This consisted of one 6 mm mild steel bar in the I beams and two in the rectangular beams.

5.5 Farbrication of the Test Beams

5.5.1 Formwork

The casting moulds were constructed on a bed consisting of inverted rolled-steel channels and a P.V.C. sheet was screwed to the top of the bed to provide an even, true finish to the soffit of the beams. The sides of the mould were made of steel

channels 305 mm deep, placed back to back. For the I beams, varnished wood pieces shaped to form the webs were fixed to the inside of the channels. The casting bed with the mould for rectangular beams is shown in Fig.5.4.

5.5.2 Casting

The reinforcing cage was prepared as shown in Fig.5.4, placed in position on the casting bed and adjusted in the mould to give the designed cover for the reinforcement. The duct for the tendons was formed by an inflated rubber tube of the required diameter held rigidly in position by locating rings fixed to the sides of the mould at the required level. The sides of the mould were given a coat of mould oil before placing in position and the reinforcing cage was located accurately by means of spacers at regular intervals. A wedge-shaped steel box was fixed to form a void to allow the flaring of the tendons at the anchorages.

The concrete, mixed as described in Section 5.4.1, was placed in layers and compacted by two vibrators bolted loosely on top of the mould. Two G-clamps secured the ends of the mould to prevent distortion during vibration. All precautions were taken to ensure that the concrete flowed freely between reinforcing bars especially in the bottom flange of the I beams. For each batch of concrete, slump and compacting factor tests were carried out and control specimens listed in Section 5.4.1 were cast.

The surface of the beam was later trowelled to ensure a good surface finish and was then covered with wet hessian mats and

polythene sheets, the former of which were watered daily. The mould was stripped and the rubber tube was deflated after 4 days and the beam covered again to prevent possible cracking due to shrinkage whereas the reinforced concrete beams were moved into the curing room at this stage and stored until required for testing. The control specimens were taken into the curing room on the day after casting.

5.5.3 Prestressing

The stressing operation was usually carried out a week after casting. The beam was uncovered on the previous day and allowed to dry. Stainless steel studs for the Demountable mechanical extensometer (Demec gauge) were attached at the specified positions on the beam.

Before stressing, initial readings were taken while the beam was on the casting bed and several cubes were tested to ascertain the compressive strength of the concrete. The required number of wires, lightly greased, were threaded through the duct with care to prevent twisting inside the duct. If the wires had been fitted with electrical strain gauges, particular care was necessary to avoid damage. In spite of these precaution, some gauges became unserviceable during stressing. The end stressing plates were placed over the ends of the wires. This was followed by placing duralumin dynamometer behind the end plate at each end. The wires at the remote end were degreased before locked against a steel cap on the dynamometer by means of anchor grips. At the jacking end, the wires were also degreased before fitting anchor

grips. A force of approximately 2 kN was applied to the first wire by means of a C.C.L. mono-wire jack to secure the end plates and dynamometers in position accurately. The tension in the wire was then increased to 45 kN. This force, infact, corresponded to 75 % of the guaranteed ultimate strength rather than the designed value of 70 % in order to allow for the loss of tendon stress due to slip-in at the anchorage. The apparent extension of the wire was measured and checked against calculated value. The actual force applied by the jack was measured by the jack pressure gauge which had been calibrated previously by the manufacturer. The force was also checked against the readings obtained from the electrical strain gauges on the wire. When the desired force had been attained, the split wedges were hammered into the position and the jack pressure released. The procedure was repeated for other wires. In the beams having more than two wires, the inner wire was tensioned first to minimise transverse bending. The final forces in the wire or wires could be obtained from the dynamometers which had been accurately calibrated. The stressing of the beam is illustrated in Fig.5.5.

When the stressing operation had been completed, the beam was lifted and supported at its ends and the strain readings were taken before moving it into the curing room until required for test.

5.6 Preparation of Beams for Testing

Generally two days before testing, the beam and all the control specimens were taken out of the curing room and the beam

was set up and carefully aligned in the test rig with a clear span of 6 metres. The beam was coated with a thin layer of whitewash to facilitate easy crack detection and measurement of crack width, and dial gauges mounted for deflection measurement. Two rollers were placed on the top of the beam at a distance 2120 mm from either ends to support the load-spreader beam. The loading arrangement is shown in Fig.5.6. The two-point loading arrangement was designed to give almost the same ratio of moment to deflection at the midspan as would be produced by an uniformly distributed load. Strain measurements were taken before the spreader beam was placed in position.

5.7 Instrumentation

5.7.1 Deflection Measurement

Deflection at seven points along the beams, symmetry on either side, was measured by means of Baty dial gauges with a resolution of 0.025 mm or 0.01 mm. The positions of the dial gauges are shown in Fig.5.6.

5.7.2 Strain Measurement

5.7.2.1 Concrete

The longitudinal and transverse strain was measured by a Demountable mechanical extensometer, with a resolution of 10 micro-metre/metre, on a series of 203 mm gauge lengths at the top and bottom of the beam over the whole span and also at five other levels at the five extensometer positions nearest to the midspan. In addition, the local strains in the constant moment region were

also measured by a Demec gauge with a resolution of 24.5 micro-metre/metre over a series of 50 mm gauge lengths. The positions of the Demec points are indicated in Fig.5.6.

5.7.2.2 Steel

The strain in the tendon was measured by three PL-5 electrical strain gauges which were mounted on the prestressing wire, one at the centre and one over each support. The gauge and all the exposed electrical connections were covered with a layer of M-Coat D which provided insulation against any possible electrical leakage. The M-Coat D was in turn covered with a layer of protective coating M-Coat G which sealed the gauge from moisture and contaminants. The treated area was finally enclosed with a heat shrinkageable tube to ensure the coating was well protected from physical damage. The strain gauges were connected to the Peekel strain measuring unit in which could be read to the nearest 5 micro-metre/metre.

5.7.3 Stress

The total forces in the tendons were measured by the duralumin dynamometer at each end of the beam. A full bridge circuit consisted of four PL-10 electrical strain gauges were used for the dynamometer in order to minimize the error due to temperature variation. The dynamometer was precisely calibrated every time before used and it was also wired up to a Peekel.

5.7.4 Crack Detection and Measurement

The formation of cracks were detected with the aid of a hand lamp and magnifying glass. The crack widths were measured with an Ultra Lomara 250b self-illuminated hand microscope with a magnification of 40 and resolution of 0.02 mm.

5.8 Test Arrangement

The general loading arrangement used for the beams under short-term static loading test and combination of sustained loading with intermittent cyclic loading is shown in Fig.5.6. The cyclic loading was applied through a Dennison-Avery 250 kN hydraulic jack and sustained loading was applied to the beam by sets of 100 lbf weights through two sets of lever mechanisms acting at the loading points shown in Fig.5.7. The beams were tested to failure in the same rig. However, the beam under sustained loading alone was transferred to another test rig which consisted of a similar lever mechanism acting at the mid-span of the beam as shown in Fig.5.8. The test rigs have been described in detail by Lee[44].

5.9 Test Procedure

5.9.1 Introduction

Each test commenced with two cycles of short-term loading up to service load. Eight beams were loaded to destruction after 2 or 3 days and one beam was tested under long-term sustained load. The remainder were tested under a combination of sustained and short-term cyclic load. The type of loading of the beams is given in Table 5.5. .

5.9.2 First and Second Cycle of Loading

Testing usually commenced between 3 and 4 weeks after casting and the beam was set up as described in Section 5.6. Before the application of load, the beam was inspected carefully for any cracks due to shrinkage or mis-handling during transportation, after which the initial strain and deflection readings were taken. The electrical strain measuring instrument had been switched on an hour earlier to attain a constant temperature within the apparatus. The spreader beam was then placed in position and then the jack was centred over it. The strain and deflection readings were again taken.

The load was applied in about 12 to 16 increments of between 1 to 3 kN depending on the magnitude of the load required to produce the desired service moment on the beam. The electrical strain gauges and deflection readings were taken at each increment but the concrete strain was measured at larger intervals. The appearance of the first crack was carefully observed and the cracking load was recorded. The widths of cracks at the non-prestressed steel level and the positions of all the cracks within the constant moment zone were measured.

On unloading, only the deflection readings were taken at each load decrement and the load at which complete closure of the largest crack occurred was recorded. The strain readings at half service load and no load were also taken.

In the second cycle of loading, similar testing

procedures were carried out up to the service load. The load at which the cracks reopened was noted.

5.9.3 Combination of Sustained and Short-Term Cyclic Loading

Seven Beams were subjected to combined sustained and short-term cyclic loading. After the first two cycles of loading described above, the strain and deflection readings were taken before the beam was loaded up to half the service load by means of the dead weight and lever mechanisms described in Section 5.8. Deflection readings were taken at each increment and strains were measured at half the service load , full service load and half service load again. The beam would be maintained under this load for about a month before finally loading to failure.

Deflections were recorded daily throughout the sustained loading period. Intermittent cycles of short-term loading up to the full service load were applied through the jack at intervals of about 5 days. Deflection readings were taken throughout these load cycles and strains reading were taken at the half and full service load only.

The total duration of the test was about 30 days and the beam was tested to failure at the end by the procedures described in Section 5.9.5.

5.9.4 Long-Term Sustained Loading

After two cycles of loading as described in Section

5.9.2, the beam R3.3.4 was moved to another rig and tested under sustained loading. Initial strain and deflection readings were taken before the spreader beam and the loading rig assembly was placed in position. The permanent load was then applied by means of dead weights acting upon the beam through a single lever system as shown in Fig.5.8. Deflections were recorded at each increment of load until the total applied load was equal to half the service load. The strain and deflection readings were taken at this load in the usual manner.

The deflections were taken daily for the first month and then twice weekly for the remainder of the test period. The strain readings were taken every 5 days for the first 30 days and at two- or three-week intervals. Throughout this period, a continuous record was maintained of temperature and relative humidity, and control specimens were tested for shrinkage and creep.

The total duration of the test was about eleven months after which the beam was unloaded and left on the rig for about a month to observe the recovery of deformation. Deflections and strains continued to be measured regularly. The beam was finally load to destruction.

5.9.2 Final Loading to Failure

In the final loading, similar procedures were carried out as in the first cycle. Measurements of starin, crack width and deflection were made at each load increment until the condition of the beam was considered unsafe, after which load was

applied steadily until failure occurred. Photographs were taken prior to removal of the beam from the test rig and these are shown in Fig.5.9.

5.10 Control Tests

Control tests on concrete for each beam were carried out according to BS 1881:1983[66] as follows :-

(a) Cubes Test : At the time of stressing, at least three 100 mm cubes were tested and another six were tested on the first day of the test. A further six 100 mm and six 150 mm cubes were tested at the end of testing of the beam.

(b) Split Cylinder Test : At least four cylinders (300x150 mm dia.) were tested on the first day of the test.

(c) Modulus of Rupture : Tests were carried out on at least four prisms (100x100x500 mm) on the first day of the test.

(d) Modulus of Elasticity : Tests were carried out on at least two prisms (100x100x500 mm) on the first day of the test. The strain was measured with a 203 mm Demec extensometer on opposite sides of the prism.

Results obtained from these control tests are given in Table 5.3. In addition, control tests of creep and shrinkage of creep specimens were also performed.

(e) Creep : Creep tests were carried out on four cylindrical specimens (267x76 mm dia.) which were cast from the same concrete mix of the beam R3.3.4 . The test commenced 40 days after casting and continued for about 280 days. The test rig and procedure have been described in detail by Lee[44]. The result of the tests are given in Fig.5.10.

(f) Shrinkage : Shrinkage of the concrete was monitored by measuring the strain with a 203 mm Demec extensometer on an unloaded plain concrete specimen as used for creep test. The result of the test is given in Fig.5.11.

CHAPTER SIX

DISCUSSION OF TEST RESULTS AND COMPARISON WITH THEORETICAL CALCULATIONS

6.1 Introduction

In this chapter, the results of the investigation are discussed in detail. The discussion is divided into three parts, the first dealing with the general behaviour up to service load , the second part dealing with the observations from the beams under combined long-term sustained and short-term cyclic loading and the third dealing with the observations in the final loading especially at the ultimate state. The results of tests are compared with the theoretical results of the analysis described in Chapter Four and some of the methods reviewed in Chapter Two.

6.2 Initial State of Stress Before Testing

The effective prestress in the concrete prior to the application of load is tabulated in Table 6.1. It was calculated on the basis of the uncracked transformed concrete section and the total effective force in the prestressed and non-prestressed steel reinforcement. When computing the loss of prestress in the tendons, all such factors as relaxation of steel, creep and shrinkage of concrete, loss due to slip-in of anchorages at transfer and the effect of non-prestressed steel were taken into consideration. An accurate prediction of these is not easy and the

influence of the non-prestressed steel on the time-dependent stresses caused by shrinkage and creep is particularly complicated. However, it was not necessary to rely on these calculations since the effective stress in the prestressed and non-prestressed steel could be obtained directly from test measurements before the commencement of each test. The effective tendon stress was obtained from the dynamometers as well as the electrical strain gauges on the tendon and the effective compressive stress in the non-prestressed steel was computed by measuring the concrete surface strains at that level.

The initial steel stresses are given in Table 6.2. The losses of prestress in the tendons were generally between 1.2 and 8.9 percent over a period of about 3 weeks. Since the test beams were stored in the curing room until between 12 and 48 hours before testing , the losses due to shrinkage and creep were usually small. The loss due to relaxation and slip-in at the anchorages was about 68 percent of the total loss in most cases.

It is well known that the presence of non-prestressed reinforcement restrains the creep and shrinkage movement of concrete and therefore slightly reduces the loss in the prestressing steel due to contraction, but can, however, significantly reduce the resultant force acting on the concrete and hence cause increase the loss of prestress. This is particularly true in partially prestressed concrete in which the area of the non-prestressed steel is relatively large. Research has confirmed that as the concrete shrinks and creeps under compression there is a consequent increase in the loss of

precompression in concrete. Abeles[67] demonstrated that for beams with about the same ultimate resistance with different amounts of non-prestressed steel , the effective prestress with maximum amount of non-prestressed steel was only 60 percent of that with the minimum amount of non-prestressed steel. In calculating the effective prestress in concrete, Lee[44] demonstrated that by ignoring the compressive force in the non-prestressed steel (as usually done in normal practice), the calculation would give an unconservative result and produce an error of more than 16 percent for the beams with a large amount of prestressed and non-prestressed steel. In present test, the error was found to be varied from 8 percent to as much as 30 percent(I1.1.3).

Referring to Tables 6.1 and 6.2 , the test results confirm that for beams with the same number of prestressing wire but different amounts of non-prestressed steel, there is no significant variation of the loss in the tendons. In contrast, the effective prestress in the concrete is consistently reduced as the amount of non-prestressed steel is increased, eg. the effective prestress in R3.3.4 is only about 86 percent of that in R1.3.0 but the loss in tendons is 3.8 percent in R1.3.0 and 3.7 percent in R3.3.4.

6.3 Behaviour of Test Beams up to the Service Load

6.3.1 Load-Deflection Relationships

6.3.1.1 First Cycle of Loading

The load-deflection curves are useful to indicate the flexural behaviour of the test beams and illustrate the effects of

some of the major parameters. Figs.6.1a to 6.1g show the load-deflection curves of some test beams for the first loading up to the service load. These curves have been grouped in order to study the influence of the level of prestress and the shape of section on the flexural behaviour of the beams.

Generally, the curves exhibit two stages of behaviour. The first stage can be indicated by an approximately straight line and represents the behaviour of the beam before cracking. The extent of this stage depends on the cross section of the beam , the level of prestress and the tensile strength of the concrete. The onset of the second stage can usually be indicated by the deviation of the initially straight portion of the curve and is characterized by a constantly increasing rate of increase of deflection with applied load. This stage signifies the development of cracking, and there is a short transition in which micro-cracks were developed. Figs.6.1a to 6.1c shows the effect of prestress in the beams with about the same design ultimate moment. As would be expected, the effect of increasing the level of prestress is to delay the formation of cracks in the first cycle of loading. Table 6.3 gives the moments at which cracks were first observed and these include the bending moment due to the self-weight of the beam (i.e. 5.1 and 3 kNm for rectangular and I section beam respectively) as well as the weight of the load-spreader beam (2.4 kNm). A study of the table and Figs.6.1a to 6.1c confirms the effect of prestress on the cracking moment.No crack was observed in R1.3.0 at service load although there was a slight change in slope of the load -deflection curve. This may be due to the presence of micro-cracks which were too fine to be detected by

using a hand magnifying glass.

After cracking, the stiffness of the beams is largely a function of the total area of steel and it can be seen that the rate of increase of deflection is greater for the beams with a smaller steel area. For the beams with about the same level of prestress (i.e. same number of tendons) but different amounts of non-prestressed reinforcement, the observed cracking moments were about the same. The slope of the load-deflection curve after the point of cracking was least for the beams with the smallest amount of reinforcement (see Figs.6.1d and 6.1e) but there was no significant difference between the curves before cracking . The results confirm that the increase of deflection before cracking does not depend on the quantity of steel but is mainly related to the modulus of elasticity of concrete.

Figs.6.1f and 6.1g show the load-deflection curves of beams of the same overall dimensions with the same amount of prestressed and non-prestressed steel but different cross section. It was found that the rectangular section beam is stiffer than the I-section although the level of prestress in the latter is higher because of the smaller cross-section area. It may be due to the fact that eventhough they both show a similar rate of increase of deflection after cracking , however, the cracks in the I-section beam developed earlier than in the rectangular section and thus the former has a larger deflection than the latter. Furthermore, more cracks have been found in the I-section beam.

The deflections of all the beams under service load in

the first cycle are summarised in Table 6.4 and were all within the CP110 specified limit (i.e. span/250) which is equivalent to 24 mm for the tests.

On unloading, the load-deflection curve did not retrace the loading path but formed a hysteresis loop. The area of the loop, enclosed by the ascending and descending arms of the load cycle, represents the energy absorbed by the beam during the load cycle. This may occur due to the presence of irreversible phenomena such as breaking of bond and friction between the concrete and steel particularly at the cracks. It is therefore expected that the larger changes in loop area will occur in those beams in which more cracks developed i.e. the reinforced concrete beams and the beams with low prestress and large amount of non-prestressed steel (compare Figs.6.4a , 6.6a and 6.6b). When the applied load was removed, there was a residual deflection in every beam and only part of this recovered in the course of time.

6.3.1.2 Second Cycle of Loading

Figs.6.2a to 6.2d show the load-deflection curves for the second loading omitting the residual deflection. During re-loading, the two-stage behaviour of the load-deflection curves was generally observed but not for the reinforced concrete beams or the beams of low prestress with a large amount of non-prestressed steel (eg. R1.1.3 and R2.1.5) in which the cracks remained open after the first cycle of loading. In general, the beams behaved in a comparable way to the previous cycle but the deviation of the initial straight line occurred at a reduced value of load

corresponding to decompression of the concrete at the soffit. The observed and calculated decompression moments of some test beams are given in Table 6.3. The effect of the level of prestress , amounts of total steel area and the shape of cross-section on the behaviour of the test beams was similar to the observation during the first cycle. The deflections at service load were slightly larger than the value in the first cycle.

When the beams were unloaded, the load-deflection curve again did not retrace the loading path and consequently a further small increase of residual deflection was observed. The area of the hysteresis loop showed a marked reduction when compared to that in the first cycle of loading. The typical curves are illustrated in Figs.6.4b and 6.4c. It should be noted that the loop area in the first cycle seems to be related to the level of prestress i.e. the higher the prestress, the smaller the area. However, the effect of prestress on the loop area were not so pronounced in the second cycle (see Fig.6.5). It may be due to the fact that during the second loading, the bond at the cracks between the concrete and steel has already deterioated and a smaller amount of energy was needed to overcome friction at the steel-concrete interface. The loop area of the beam of low prestress was found to be relatively larger than the one of high prestress because the former has more cracks and hence absorb more energy due to friction.

6.3.1.3 Combined Sustained and Short-term Cyclic Loading

Figs.6.6a to 6.6f show the load-deflection curve of some

test beams throughout the test under combined sustained and short-term intermittent cycles of loading. Referring to Fig.6.6a, the initial deflection at half- and full-service load (i.e. total moment equal to 50 percent and 100 percent of service moment) is indicated by the points marked (1) and (2) respectively. The short-term deflection at the end of the test is represented by point (3) and the long-term deflection at half-service load under the effect of sustained load plus 7 short-term cycles (i.e. 2 initial cycles in the first day of test plus 5 intermittent cycles) up to the service load is indicated by point (4). The increase of deflection at half and full-service load due to the combined loading effects are represented by the horizontal distance between (1) and (4) and between (2) and (3). The deflection of the beams under combined loading test are summarized in Table 6.5.

Generally , the rate of increase of deflection from half- to full-service load is greatest in the first cycle and becomes less in the second and third cycle ;thereafter, the rate becomes approximately constant. This can be seen throught by the slope of the load-deflection curve in Figs.6.6a to 6.6g. The curve also shown that a hysteresis loop was formed during each intermittent load cycle and there was a small amount of residual deflection after removal of the short-term cyclic load. The successive loops were displaced in the deflection direction and the amount of shift was found to be greatest in the first intermittent cycle and to become progressively less in the later cycles. The displacement of the loops is believed to be caused by the increase of deflection over the sustained loading period and

probably some non-recoverable residual deflection after each short-term cyclic loading. These will be discussed in detail in Section 6.4.

6.3.2 Tendon Stress

The tendon stress were measured by the dynamometers and by the electrical strain gauges (E.S.Gs.) fixed on the tendons as already mentioned. It was found that the E.S.Gs. were sensitive to small changes in stress (eg. increase in stress at service load) but some of them, having less protection, were subject to more drift than the dynamometers. On the other hand, the dynamometers were not sensitive to small changes in stress but gave very steady and reliable reading at high load. The results obtained from the E.S.Gs. are therefore used for the first and second cycle of loading while the tendon stresses in final loading are based on the dynamometer readings.

The change in tendon stress of some beams as measured during the first loading is shown in Fig.6.7a. A study of this diagram in conjunction with the load-deflection curve (Fig.6.1c) reveals that the smaller deflection measured in beams with higher prestress was accompanied by a smaller increase of the tendons stress. Similar to the form of the load-deflection curve, the rate of increase of tendon stress was approximately constant up to the flexure cracking load and gradually increased after cracking. The rate at this stage was influenced by the amount of total reinforcement. This can be well illustrated by Fig.6.7c in which the beams (R1.3.0 , R2.3.2 and R3.3.4) have the same number of

tendons but different amounts of non-prestressed steel. The observed cracking load of R2.3.2 and R3.3.4 are 20 kN. The rate of increase of tendon stress after cracking was found to be greater in R2.3.2 than R3.3.4 which has larger steel area. In beams of such as R2.3.2 having a small steel area, in order to maintain the conditions of equilibrium immediately after cracking, when the tensile force carried by the concrete before cracking was transferred to the reinforcement, there was a rapid increase in steel stress and hence a relatively large deflection. This phenomenon was not so obvious in R3.3.4 with a large steel area, since the reinforcement could provide the tensile force lost by the concrete with little increase of strain. Similar observation have been reported in early tests by Warwaruk[33]. The proportion of increase in tendon stress to the effective prestress in tendon ranged from 1.6 percent in R1.3.0 to 8.1 percent in I1.1.3.

At the end of the first cycle, a small increment of tendon stress was observed in some test beams. It is believed to be caused by residual deflection.

In the second cycle of loading, the form of the curves (Fig.6.7b) was again similar to that of the form of the load-deflection curves (see Fig.6.2c). The extent of the initial straight portion was limited by the load at which the cracks reopened. Although the cracks in R3.2.5 remained open at the beginning of the second cycle, there is still a change of slope which may indicate an increased rate of widening of the crack. In general, the amount of prestress significantly affect the rate of increase of the tendon stress, which becomes progressively greater

after reopening of the cracks. There is no sudden increase in stress after decompression of the concrete because the concrete tensile strength at the cracks has already been lost and there is no sudden transfer of tensile stress to the steel.

The tendon stress of R3.3.4 over the sustained loading period is represented in Fig.6.7e. After 336 days, the stress was found to have decreased from 1103 to 1043 N/mm2 amounting to a total loss of about 11 percent of which 5.1 percent occurred during the sustained loading period.

6.3.3 Crack Width

The maximum width of cracks measured at the service load in the first and second cycle are listed in Table 6.4. The limiting crack widths specified in CP110 , cl.2.2.3.2 are 0.1 and 0.2 mm for Class 3 members exposed to a particularly aggressive environment and for normal conditions respectively. Some of the beams have crack width exceeding 0.1 mm but all of them are less than 0.2 mm. Under the effect of cyclic loading, an increase in crack width at service load was generally observed indicating that further slipping of the bonded reinforced bar had occurred. The width of cracks at service load in the last intermittent load cycle were between 0.1 mm and 0.16 mm.

The test results show that the width of cracks observed in the unbonded beams was not excessive for normal atmospheric conditions but may have led to corrosion problems if the beam were under aggressive environmental conditions. However, from an

investigation[68] of unbonded prestressed concrete prisms subjected to one year exposure to either marine atmosphere or normal atmosphere, it was reported that the tendons were perfectly protected from corrosion if they had been suitably coated. These findings may increase the designer's confidence with regard to cracking and hence the resistance of an unbonded member to corrosion, at least under normal atmospheric conditions.

6.3.4 Strain and Curvature Distribution

6.3.4.1 Strain Distribution

The strain distribution over the depth of the beam in the constant moment region during the first and second loading up to the service load is presented in Figs.6.10a to 6.10g. These are elastic (i.e. short-term) values from which the non-elastic strains due to creep and shrinkage at the beginning of test have been deducted. A common feature of the graphs is that all the lines intersect at about the same point initially ,i.e. at the level of the bending axis of the uncracked section. The level of this axis obviously changes at higher loads, hence indicating that the beam has cracked.

In the second loading , it may be seen that the beam of low prestress such as R1.1.3 behaved like an ordinary reinforced concrete beam. Although the applied load had been completely removed, the neutral axis at the beginning of the second cycle of loading remained at a very high level (see Fig.6.10f and 6.11d). This was probably due to the presence of unclosed cracks. In contrast, for the beam with a higher level of prestress such as

I3.3.4, the bending axis of the uncracked section can still be identified in the second loading , but changes at a lower load (15.3 kN) than in the previous cycle (25.3 kN)(compare Figs.6.10e and 6.10g).

The total strain distribution diagrams of R1.3.0 and R1.1.3 without deducting the creep and shrinkage strains are plotted in Figs.6.11a and 6.11b. It can see that the distribution immediately after transfer has changed at the beginning of the test. This has been commonly observed by other investigators on prestressed beams. The cause was due to creep and the biggest difference was observed in R1.3.0 with a high prestress.

The distributions of strain at half-service load before applying the cyclic load are shown in Figs.6.12a to 6.12d. The strains measured at the full-service load are also given in Figs.6.13a to 6.13d. Referring to these figures, there is little change of strain at the level of non-prestressed steel and a progressively lowering of the neutral axis is clearly indicated. From the first two load cycles, it has been observed that the level of neutral axis at service load was not significantly affected by the cyclic load, although the neutral axis in the second cycle was sometimes slightly higher than in the previous cycle. It can therefore be concluded that under the combined loading, the lowering of the neutral axis was mainly due to the effect of creep of concrete under the action of the permanent load rather than the effect of the cyclic load.

The top and bottom surface strains at service load were

measured over the whole span of the beam. It thus enables the curvature of each section along the beam to be calculated by integration the curvatures as recommended in CP110, Appendix A. Referring to Figs.6.14a to 6.14d, it can be seen that the deflection computed by measured strains is in good agreement with the value obtained from the dial gauges.

The strain deformation of R3.3.4, which was maintained at half-service load , is shown in Figs.6.15a and 6.15b. Under the influence of creep of concrete, the top strain increased rapidly in the early stage of loading period and the rate of increase of strain was reduced progressively at the end of the test. No significant change of strain occurred at the bottom because the compressive stress there was small and the presence of non-prestressed steel reinforcement could have restricted the deformation. The minor fluctuation of strain during the course of the test were probably due to the change in ambient temperature.

The longitudinal strain distribution over the constant moment region of some test beams at increasing load in the first cycle is presented in Figs.6.16a to 6.16e. It is generally observed from the top strain distribution that there is no significant variation and therefore it is justifiable to assume that the top concrete strains within the constant moment zone are the same as was done in the earlier theoretical analysis.

Referring to the bottom strain distribution in Fig.6.16a, the occurrence of each peak represents the presence of cracks across the gauge length. The peaks as would be expected,

were found to be more numerous and more closely spaced for a beam with no prestress (compared Figs.6.16a and 6.16b). It is interesting to note that the strains measured about halfway between adjacent cracks were found to be compressive , even in the reinforced concrete beams, although the bottom of the beam might be in tension under bending. This phenomenon may be compared from the observation of a double pull-out test in which a steel bar was embedded in a concrete prism. When the tension in the bar increases, it elongates and so too does the concrete surrounding the bar. The extension of the concrete adjacent to the bar will lead to a contraction of the concrete at the surface of the prism. Consequently, the larger the tension in the bar, the higher the contraction (i.e. compression) at the surface. This pull-out test simulates the tensile region of a cracked beam. It can be seen from the bottom strain distribution diagram in Figs.6.16a to 6.16e that the larger the bending force applied, the larger were the compressive strains measured between the cracks.

At service load, more cracks were developed in the I-section beam than the rectangular one (see Figs.6.16a and 6.16d) although the former had a higher prestress than the latter due to the smaller area of concrete.

6.3.4.2 Curvature Distribution

All the beams, except the reinforced concrete ones, had a negative curvature (convex curvature causing camber) distributed over the constant moment zone before loading indicating that the action of prestress. At service loads, several peaks occurred

which were obviously governed by the bottom strain distribution as shown in Figs.6.16a to 6.16e. The pattern of the distribution agrees with the theory but the curvature distribution between adjacent cracks cannot be concluded unless a more precise measurement of the strain between the cracks is carried out.

It is commonly known that a prestressed beam remains unloaded for a long period of time, the curvature (negative sign) and hence the camber will increase with time over the whole span. However, when the beam is cracked under bending, the concrete sections near midspan usually have positive curvature while the curvature near the supports is negative. When the beam is under sustained load, it may be expected that the curvature will increase in respect to its sign. This was ,however, not the case regarding to the observation from test. In Fig.6.17a , the distribution of curvature of R3.3.4 (maintained under half the service load) along the entire over a period of 336 days clearly show that there was no sign of increase of negative curvature at the sections near supports under long-term loading eventhough the curvature there had a large initial value. Moreover, there is an indication of the curvature in some sections changing from negative into positive during the loading period. This feature is believed to be due to the change of stress and the reversal of the creep strain when the beam was loaded initially. At the beginning of sustained loading test, the bending stress will cause a sudden reduction of the compressive stress at the bottom fibre with the result that some compressive creep strain, which has already occurred since the beam was prestressed , has recovered with time. The strain at the top of the beam was found to be compressive

after loading and hence the strain due to creep will be compressive. Consequently, the change of strain distribution should result in a decrease of negative curvature as observed over the greater part of the span.

The curvature distribution of R1.2.2 and R1.0.5 at half-service load is shown in Figs.6.17b and 6.17c. It appears that the increase of the curvatures, i.e. causing downward deflection, was greatest in the early period of the test. This is because the rate of increase of creep strain, which caused the increase in curvature, was fastest in the early stage of loading.

6.3.5 Residual Deformation

At the end of the first cycle, residual deformations have been observed in all the test beams. These deformations may not fully recover in the course of time and hence become a permanent feature of the beam. Since the residual deformation will affect the behaviour of the test beam in the second and subsequent cycles of loading, a brief discussion of the nature and extent of the residual deformation at the end of the first cycle is considered necessary.

6.3.5.1 Strain

It is believed that the magnitude of residual deflection and residual width of crack at the end of the first cycle are dependent on several factors such as : the level of prestress in the concrete ; the extent of cracking at service load ; the

magnitude of stress in the reinforcement at service load and the residual (inelastic) strain associated with this stress. In addition, the non-elastic strain due to creep of concrete may also be of significance in relating to the residual deflection. An understanding of the cause of the change in strain when unloaded is considered necessary in studying the residual deformations of a member. However, there is very limited experimental information concerning the change in concrete strain (i.e.residual strain) of a structural member particularly if the member is unbonded.

In the present investigation, residual strain has been observed in each test beam at the end of the first cycle. The measured average concrete strain (at zero load, service load and at zero load after unloading) in all the tests is given in Table 6.6. It can be seen that there is a small residual increment of compressive strain or decrement of tensile strain at the top and vice versa at the bottom. This change of strain will result in a change of curvature of the section and a larger deflection than before loading. The residual strain at the top is believed to be caused by the creep of concrete, since the time needed to complete the first cycle of loading was about 3 to 5 hours during which a small amount of creep strain would probably have occurred. On the other hand, the magnitude of the residual top strain does not have a clear relationship with the concrete stress at the top at service load. This may be due to the fact that there are some variable factors, other than concrete stress, which may affect the short-time creep strain, for example the age of the concrete at the time of the test and the exact duration of loading. The creep coefficient of concrete in the beam is approximately represented

by the ratio of the residual top strain (creep strain) to the change in concrete strain (elastic strain) from zero to service load. The ratio for each beam is given in Table 6.6 and has a mean value of 0.19 with a standard deviation of 0.099. A mean value of 0.15 was obtained from Lee's test results on bonded partially prestressed beams.

The residual bottom strain (at level of non-prestressed steel) has generally been observed by many previous investigators[41,43]. The causes and mechanism of formation of this can be explained with respect to the slip of the bars and cracking of the beam. When a beam is loaded after cracking, the non-prestressed steel bars increase in stress in the cracks and slip towards the crack from the adjacent uncracked concrete on each side, so that the crack increase in width. When the load is reduced, the steel bars tend to recover to their original length by slipping in the reverse direction so that the cracks tend to close. However, the cracks will not close completely until a sufficent compressive force has developed in the bars at the crack to reverse the slip. The bigger the prestressing force in the beam, the better the recovery observed. Moreover, the larger the non-prestressed steel area, the greater the compressive force required to reverse the slip in order to close the cracks. This is confirmed in Table 6.6, column 9 where the reinforced concrete beams (R1.0.5 and R2.0.7) and the beams of low prestress with a substantial amount of non-prestressed steel (R1.1.3, R2.1.5 and I1.1.3) are seen to have a larger residual strain than the others.

Fig.6.18a show the relationship between the ratio of the

residual bottom strain to the total change in bottom strain and the non-prestressed steel stress at service load. It is of interest that if the steel stress at service load becomes too high a substantial amount of residual strain may result. According to this diagram, a residual strain ratio of 0.15 will produce a upper bound for all the beams with a steel stress less than 240 N/mm2, but if the steel stress is greater than 240 N/mm2, the ratio may be assumed to be increase linearly with the steel stress as shown. It should be noted that this upper bound envelope of the residual strain ratio is also conservative for the bonded partially prestressed beams tested by Lee. In the draft Swiss Code [69], the maximum allowable bending strain for non-prestressed steel in a partially prestressed member at service load is 0.0012 (equivalent to 240 N/mm2).Referring to Fig.6.18a , it appears that a member designed with this stress limit will not have a large residual deflection.

6.3.5.2 Crack Width

The cracks of some of the test beams (R1.1.3,R1.0.5,R2.1.5,R2.0.7,R3.2.5 and I1.1.3) did not completely close at the end of the first cycle of loading. All these beams had a low prestress with a large non-prestressed steel area so that the behaviour of the cracks conformed to the observations from strain measurements discussed earlier. Beams R2.2.4 and R3.2.5 had the same number of tendons with different amounts of non-prestressed steel. The cracks in the former closed but not those in the latter. This was due to the fact that R3.2.5 had a higher design load and may therefore have been subject to more

cracking than R2.2.4. Moreover, R3.2.5 had a larger area of non-prestressed steel and would therefore have required a greater prestressing force to reverse the slip on unloading. Further evidence is provided by R3.2.5 and I3.2.5, both of which had the same amounts of prestressed and non-prestressed steel and the same design load. I3.2.5 showed a better recovery of crack width because of higher level of prestress in the concrete than R3.2.5. The above observations suggest that a minimum prestressing force should be provided to ensure complete closure of cracks on unloading. This is essential in an unbonded member to avoid the possibility of corrosion of the tendon.

6.3.5.3 Deflection

In the present tests, all the beams had a residual deflection at the end of the first cycle of loading. The magnitude for the unbonded beams varied from 0.78 mm to 3.92 mm and part of this residual deflection recovered after a short period of rest of about 2 to 3 hours but there was never a full recovery, even in the beams with a high degree of prestress (R1.3.0 and R3.4.2). The details of the residual deflections are listed in Table 6.7.

The effect of prestress on the magnitude of residual deflection is significant i.e. the higher the prestress, the better the recovery and hence the smaller the residual deflection. This can be seen in Fig.6.18b. On the other hand, the additional residual deflection at the end of the second cycle of loading ranged between 0.15 mm and 0.56 mm and had no firm relationship with the level of prestress, as shown in Fig.6.18c.

The relationship between the residual deflection and the hypothetical tensile stress in the test beams is illustrated in Fig.6.18d. An approximately linear relationship can be clearly observed provided the level of prestress does not become too small. This is evident since all the beams with a particularly large residual deflection have a low prestress, i.e. only one tendon. The diagram also illustrates that a beam may not necessarily have a large residual deflection, eventhough it has a high hypothetical tensile stress value, provided there is sufficient prestress to reverse the slip and cause the deflection to recover.

It has been reported by other researchers[44,47] that the cause of residual deflection is mainly slip of the bars at the cracks. From this investigation, the above statement was concluded to be generally true for beams with low prestress but with high prestress the effect of short-time creep of the concrete was also thought to be significant. This seemed to be particularly so when the cracks closed on removal of the load, because the effect of slip was then small and the creep strain would be equally important. A comparison of the top and bottom residual strain in Table 6.6 reveals , for example that R3.4.2 with high prestress has approximately equal top and bottom residual strain but R1.1.3 with low prestress has a residual bottom strain almost 3.5 times the value at the top. It therefore appears that Branson's[47] method for the calculation of residual deflection is incorrectly based attributing residual deflection to cracking alone.

In accordance with the findings of the present

investigation, the residual deflection may be calculated as follows :-

(1) The total change in strain at the top and bottom may be computed by using cracked section theory.

(2) The amount of residual top strain(creep strain) can be obtained by multiplying the total change in top strain (elastic strain) by the residual strain ratio (creep coefficient) which is equal to about 0.19 in present tests.

(3) The average residual strain at the bottom may be assumed equal to 0.15 times the average total change in bottom strain provided that the stress in the non-prestressed steel does not exceed 240 N/mm2. If the stress limit is exceeded, a larger ratio should be used.

(4) The curvature at the end of the first cycle of loading may be obtained by knowing the top and bottom prestrain plus the average residual top and bottom strain.

(5) The deflected profile of the beam can now be computed by integration of curvature along the span.

The residual deflection computed on the basis of the Branson's method and the above proposed method are given in Table 6.7. Since the proposed method is partly based on the experimental result, it of course gives a satisfactory result. In contrast, although Branson's method gives a better mean value , it shows a

much poorer correlation than the proposed method. Furthermore, his method gives a reasonable result (in some cases a considerable overestimate) only on the beams of low prestress in which the extent of cracking is large, but for the beams with less cracking, the prediction underestimates the actual value quite significantly. This is mainly due to the fact that the method only takes cracking into consideration and totally ignores the effect of creep.

6.4 Deformation-Time Relationship

6.4.1 Deflection-Time Relationship

The deflection-time relationships of the beam under combined loading are presented in Figs.6.19a to 6.19g. The beams were maintained at 50 percent of the service load throughout the duration of the test and a short-term cyclic load was applied to bring the total load to full-service load. There was a mistake in the test procedure for R2.2.4(see Fig.6.19c) which, after two initial cycles of loading in the first day, was maintained at 75 percent of the service load, but the sustained load was reduced to the desired value two days later.

It can be seen that a residual increment of deflection occurred after each short-term cyclic loading and the total deflection decreased slightly in the next one or two days before continuing to increase under the influence of the sustained load until the next cyclic loading. Some recovery of the residual deflection after the cycle of load can clearly be indicated by the downdard concave slope of the deflection-time curves. It is

interesting to note that the residual deflection after short-term cyclic loading was greatest after the first two cycles but appears to become smaller and to remain constant over the last few cycles. A similar observation has been made by Lee[2] on tests of bonded partially prestressed beams.

The effect of these periodic short-term load cycles on the permanent deformation cannot be observed unless a duplicate beam is tested under sustained load alone for the same period of time. No duplicate beams were included in the test programme due to lack of time. However, the tests by Lee included three companian beams for comparison purposes from which he reported that there was a non-recoverable residual deflection resulting from each cycle of short-term loading which, it appeared, would progressively approach a constant value if the cyclic loading were continued. It was suggested that the deflection under the combined loading was similar to the sum of the deflection due to the two types of loading applied separately and the principle of superposition might be applicable as proposed by McHenry[70] for the superposition of creep strains.

Referring to Table 6.5, column (3), at the end of the combined loading test the deflection of the beams (except R2.0.7) under service load was less than the CP110 limit (i.e. 24 mm), but it appears that the deflection of the reinforced concrete beam R1.0.5 (23.6 mm) would probably have exceeded the limit if a few more load cycles had been applied. This reveals the importance of prestress in deflection control.

Fig.6.19h shows the deflection-time curve of R3.3.4 which was maintained at half the service load for eleven months. The deflection increased rapidly in the early stage of the loading period and then at a progressively lower rate. After eleven months, the deflection (15.1 mm) was found to be 4.3 times the initial instantaneous value (3.53 mm). Dave[38] conducted some sustained loading (at design load) tests on fully bonded partially prestressed beams (with pre-tensioned wires) and reported that the ratio of the final deflection after 500 days to the initial deflection was 2.64. The result therefore illustrates that the rate of increase of deflection under sustained load is greater for unbonded beams. Furthermore, the maximum of 2, recommended in the ACI Code for the ratio of the additional time-dependent deflection to the instantaneous deflection, is unconservative for this test.

After removal of the load the deflection was measured for a further 30 days. A recovery of about 0.89 mm was observed during the first 20 days afterwhich the deflection remained constant for the remainder of the unloaded period.

6.4.2 Concrete Strain-Time Relationship

A study of the strain deformation of the test beams is useful to assist in the analysis of their flexural behaviour under the influence of combined sustained and short-term cyclic loading. The average strains measured over the constant moment region on the concrete surface of the test beam at levels of 5 mm from the top and 23 mm from the soffit (i.e. level of non-prestressed steel) during the test period are presented in Figs.6.20a to

6.20g. During the first 5 days of the sustained loading period, the compressive strain at the top increased rapidly and in contrast, the residual tensile strain at the bottom from first two cycles recovered slightly. As would be expected, the recovery was found to be larger in the prestressed beams. After each short-term load cycle, residual strain deformation was observed at both the top and the bottom of the beam. It is believed that the creep of concrete at the top and further slip of the steel bars at the cracks are the main causes of these residual deformations. From creep tests on plain concrete specimens, it is well-known that if the stress in the concrete is reduced, there is an immediate total recovery of the elastic strain plus a slow recovery of the creep strain over a period of time. By referring to the diagrams in Figs.6.20a to 6.20g, it is not possible to observe whether a creep recovery was taking place at the top since the compressive strain continued to increase over the following sustained loading period. On the other hand, there is a clear indication of recovery of the bottom tensile strain in every beam after the first five days. It is interesting to find that the reinforced concrete beam had about the same amount of recovery as the prestressed beam of the same series, eg. R2.2.4 and R2.0.7 as shown in Figs.6.20c and 6.20d.

At the end of each intermittent load cycle, the amount of residual incremental top strain seemed to be independent of the number of load cycles and in contrast, the residual bottom strain was largest after the first intermittent cycle and became less as the number of load cycles increased. The latter phenomenon may be related to the results obtained by Kankam[61] who carried out double pull-out tests on prisms axially reinforced with a single

bar as a model to simulate the tensile region of a cracked beam. The relationship between the steel stress at the loaded end and the measured end slip is shown in Figs.6.21a and 6.21b in which the curve for each cycle forms a hysteresis loop indicating that there was a variable amount of residual slip in the bar during and after unloading. The loop was widest near the middle part and became narrower at both ends. By the 20th cycle, the total end slip had become larger, showing the basis for the loss of tension stiffening of concrete under the effect of cyclic loading, but, the width of the hysteresis loop was less than in the first cycle as can be seen in Fig.6.21c. It is thus concluded that the additional residual strain after each cycle will be progressively less. Moreover, since the greatest residual end slip was observed when the working stress in the reinforcing bar was between the middle and the maximum, it may be inferred that if a beam, under combined loading, has a reinforcement stress range in the upper half of the loop, it will have a greater residual strain and hence residual deflection than with a greater stress range, eg. between zero and the maximum. It would be interesting to verify this by comparative tests of beams under different ranges of applied load.

The concrete strain at the top of the beam under service load steadily increased at a decreasing rate under the effect of combined loading but, at the bottom, the strain showed only a minor variation in magnitude and there was no indication of a permanent increase in tensile strain under the cyclic load effect after the first cycle. According to the findings of Kankam's tests, there should be an increase in tensile strain at the level of the bonded reinforcement hence indicating a loss of tension

stiffening under cyclic load. The fact that it has not been observed in the present tests may be because the number of load cycles applied to the beam was limited to not more than 8 and was insufficient to cause a significant loss of tension stiffening. In addition, the recovery of the residual strain after each cycle was assisted in most cases by prestress.

In order to study further the effect of the short-term cyclic loading on the residual deformation, it was considered necessary to study some of the test results of Lee. The results of two identical beams subject to sustained loading (50 percent service lod) alone and combined loading respectively are presented in Fig.6.20h. It can be seen that there was little difference of bottom strain between the two beams, except in the first 5 days but in contrast, the magnitude of concrete strain at the top is much larger in the beam under combined loading than the one under sustained load alone. The divergence of the gap between them was found to increase with the number of load cycles. The effect of cyclic loading on the creep deformation is obvious. Research by Whaley and Neville[71] on the creep of concrete concluded that in comparison with a static stress, cyclic loading(585 cycles per minute) accelerated the creep deformation of concrete and moreover, the cyclic creep was largely irrecoverable. Hirst[72] has also shown that the cyclic stress(300 cpm) was to accelerate the process of creep under static stress. These findings may be used to explain the cause of the discrepancy of the top strain-time curve between the two beams. Under the action of each short-term cyclic loading, a small amount of creep strain is observed which may not be fully recovered before the next load cycle and

will therefore remained in the beam, in addition to which the creep rate in the concrete may be increased by the action of short-term cyclic load. This may be seen in Fig.6.20h in which the rate of increase of compressive strain is faster in the beam under combined loading.

From the above discussion, the evidence of the present tests suggests that greater deflection of the beams under combined loading than of the beams under sustained loading alone was mainly influenced by the increase in compressive top strain under the effect of cyclic loading. This increase was thought to be caused by the non-recoverable creep strain and increased creep rate under cyclic load. It would, however, be necessary to verify this conclusion by a greater variety of tests over a longer duration before it may be applied more generally.

6.5 Behaviour of Test Beams in Final Loading

6.5.1 Deflection

Many investigators described the load-deflection curve in the final loading as exhibiting three stages of behaviour. As already explained in Section 6.3.1.1, the first stage can be represented by a virtually straight line indicating that the beam remains uncracked or the cracks remains closed. In the second stage, the curve has a constantly increasing rate of increase of deflection and represents the behaviour of a cracked beam while the reinforcement stress is still within the elastic range. In the third stage, the reinforcement stress is in the inelastic range and the curve is nearly flat, indicating a rapid increase in steel

strain under a small increase of load. However, the third stage will not be observed if the member is over-reinforced because the steel stress will still be within the elastic range when the member fails.

The load-deflection curves of the rectangular section beams for the final loading are shown in Figs.6.3a to 6.3c. The three-stage behaviour can be seen in every beam indicating that the beams are all under-reinforced. The third stage behaviour is rarely observed for completely unbonded beams(i.e. without any additional bonded reinforcement) because the applied load is distributed throughout the entire length and thus the tendon stress at failure seldom reaches the inelastic range. In the present test, R1.3.0 was completely unbonded but shows the third stage behaviour because it has an extremely small steel area (i.e.0.25 percent of the concrete area). The tendon stress reached the inelastic range as is evident from the values measured by the dynamometers. Warwaruk et al[33] carried out tests on unbonded beams, some of which had additional bonded reinforcement. They reported that the third stage behaviour was not observed in any of the beams eventhough one had a steel ratio of as low as 0.184 percent.

A study of the load-deflection curve diagrams reveals that the deflection of the beam at low load was greatly affected by the level of prestress, but as the load increased to about 1.4 times the service load the quantity of total steel appeared to become more influential. Referring to Figs.6.3d and 6.3e, it is surprising to see that the rectangular section beam has a bigger

deflection than the I-section one with the same amounts of prestressed and non-prestressed steel but the opposite is true at service load.

6.5.2 Tendon Stress

The increase of tendon stress was closely related to the deflection of the member. Referring to Figs.6.8a to 6.8c, at low load the effect of prestress on the increase of tendon stress is obvious and the beam with the highest prestress has a relatively small increase of tendon stress compared with the beam with least prestress. However, as the load increase, the tendon stress of the beam with the smallest total steel area increased rapidly indicates that the non-prestressed steel, or possibly the tendon itself, had reached the inelastic range and caused a rapid increase in deflection(Fig.6.8f). This is evident by comparing Fig.6.8a with the corresponding load-deflection curve diagram i.e.Fig.6.3a. It is interesting to see that R3.3.4 has a larger increase in tendon stress than R3.2.5 although the former has a higher level of prestress than the latter. This may be due to the effect of sustained loading. For the beams of different section but with the same amount of prestressed and non-prestressed steel, the increase in tendon stress near ultimate is greater in rectangular section than in I-section beams but vice versa at lower loads (see Figs.6.8d and 6.8e).

The discrepancy of the tendon stress measured at the centre and above the supports by means of electrical strain gauges clearly indicates that the tendon stress was not evenly

distributed along its length. The reason for the discrepancy is friction between the tendons and concrete causing localized stress changes at the contact points. The increase in tendon stress measured at the centre and above the supports for some test beams is presented in Figs.6.9a to 6.9h which may be studied in conjunction with the corresponding load-deflection curves, eg.Figs.6.3a and 6.9a for beam R1.3.0. The higher the applied load on the beam, the larger the deflection and hence the greater the difference in tendon stress between the support and centre, although owing to the high degree of randomness in friction values and in the location of the nearest crack to the centre gauge this is not invariably the case(eg.Fig.6.9b). The biggest difference observed at ultimate load was about 178 N/mm2 in I3.2.5. The increase of tendon stress due to friction will possibly increase the strength of an unbonded member and this will be further discussed in Section 6.5.4 .

6.5.3 Cracking and Mode of Failure

The relationship between maximum crack width at the level of the non-prestressed steel and the applied load of some test beams for the final loading is presented in Fig.6.22. It confirms that the crack width was mainly controlled by the quantity of bonded reinforcement i.e. the greater the non-prestressed steel area, the lower the rate of widening and the width of the cracks. It was observed in the test that the height of the cracks increased rapidly shortly after they reopened; at a higher load the cracks tended to propagated more slowly but widened extensively. This is illustrated approximately in the

average strain distribution over the depth of the beam at increasing load as shown in Figs.6.11e and 6.11f. Oladapo[73] concluded that the shape of section was an important parameter affecting the stability of a crack and that I-section generally had a rapid rate of crack propagation until the depth of crack had penetrated well into the web while rectangular sections showed less tendency to crack instability. This can be confirmed from the observations during the test that cracks in the I-section beams propagated at a faster rate than the rectangular ones at low load, but the difference was not so pronounced at high load. Nevertheness, the widening of cracks found to be more extensive in the rectangular sections than in the I-sections at high load i.e.beyond service load.

Photographs of the crack pattern between the two loaded points of most test beams, taken after destruction, are shown in Fig.5.9. Flexural cracks first occurred within the constant moment region and when the load increased, some of them bifurcated and began to extend at an inclination to the vertical. This was pronounced in beams with a high level of prestress and a small amount of non-prestressed steel such as R1.3.0 and R3.4.2. Furthermore, the bifurcation of the cracks occurred at a lower load in these beams than in the others. The phenomenon of bifurcation has been widely observed by other researchers on purely unbonded beams. It can be seen that R1.3.0 had only two major cracks of considerable width in the constant moment region with marked horizontal extension, and that the width of other cracks was very much less. This is in contrast to the beams with large amounts of bonded reinforcement , in which the crack spacing

became closer and the crack widths smaller. The bifurcation is slight and developed only in the later stages of loading. The addition of bonded reinforcement in an unbonded member thus provided better control of cracking i.e.decreases the width and spacings of the cracks as well as avoiding early crushing of the concrete in the failure section due to propagation of the crack.

It has been observed that for the beams with the same amount of non-prestressed steel but different numbers of tendons eg. R3.4.2, R2.3.2 and R1.2.2,there was no indication of the crack spacing increasing but a reduction in crack width with the increase in the prestressing force. It was felt that the effect of the spacing of the stirrups on the crack spacing was not pronounced and the final crack spacing pattern did not necessarily follow the pattern of the stirrup although the first few cracks may start at the stirrups.

All the beams failed in flexure by crushing of the concrete at the top fibre but usually preceded by yielding of the non-prestressed reinforcement. The latter is indicated by the enormous ductility of the beam before failure. In fact, the yielding of the non-prestressed steel was evident from the examination of it after failure when necking and even fracture were found to have occurred. The failure was initiated by the formation of a large flexural crack which widened and the root of the crack propagated upward with the increase of load up to failure. Shortly before failure, there was a rapid increase of deflection with little increase in loading. The first signs of crushing of the concrete were followed by a sudden increase of deflection and dropping of load. Although the I- and rectangular

section beams failed in flexure and showed an under-reinforced type of failure, there was an distinctive appearance of failure mode in each them after the first visible crushing of concrete. The beams of rectangular section failed with further crushing of concrete at the top. In contrast, soon after the crushing of concrete occurred, the complete section of the I-section beams collapsed violently causing destruction of the concrete surrounding the critical section. This is evident from the photographs in Fig.5.9 taken after destruction while the beam remained in the test rig. The catastrophic failure of a flanged beam was explained by Warwaruk[33] as follows. Up to the first visible crushing of the concrete, the behaviour of beams having flanged sections and a low ratio of reinforcement is very similar to that of rectangular sections as observed in the present tests. Thereafter, the load begins to drop since the internal lever arm is reduced. The position of the neutral axis then moves from the top flange into the web and results in a reduced additional concrete area available for the compression zone. This causes crushing of the entire compressed concrete zone followed by a sudden collapse of the section.

The failure pattern of R2.2.4 clearly indicates that if the beam cover to the main tensile reinforcement is insufficient and there are no stirrups to enclose the bottom reinforcement, there may be a longitudinal splitting failure of the concrete at the soffit.

6.5.4 Flexural Strength

There are many factors which may affect the flexural strength of an unbonded partially prestressed member, such as the stress developed in the tendon and the non-prestressed tensile reinforcement, the strength of concrete, the level of prestress, the nature of loading and the shape of section. Some of these factors will be discussed according to the observations made from the tests but, the prediction of the tendon stress and hence the moment of resistance developed at the ultimate state on the basis of the methods reviewed in Chapter Two willbe discussed in Section 6.6.4 .

When an unbonded partially prestressed beam is designed to fail in flexure, the stress developed in the reinforcement at ultimate moment is the main factor to be considered. The matter is complicated because the strain of the unbonded tendon is not compatible with that of the concrete as usually assumed for the bonded reinforcement. The increase in tendon stress is dependent on geometry of the applied loading or more correctly the deflected profile of the member. The tendon stress is thus distributed throughout the entire length of the beam. In contrast, the additional non-prestressed reinforcement is well bonded to the concrete and the steel stress usually exceeds the yield stress. In the present tests, necking or even fracture of the non-prestressed steel bars was found and it is therefore deduced that the steel stress at failure was within the range between yield stress(497 N/mm2) and fracture(614 N/mm2). With the observed ultimate moment of resistance and the assumed value for the stress in the non-prestressed steel, the stress in the unbonded tendon may be computed by analysing the failure section using a simplified

rectangular stress block(0.6 f_{cu}) for concrete. The computed tendon stresses based on different stress values in the non-prestressed steel are tabulated in Table 6.8 in which are also included the values of the last tendon stress observed from the dynamometers.

Referring to Table 6.8, the computed tendon stress based on the yield stress of the non-prestressed steel was found to be much higher than the observed value except in R2.3.2, and in some instances exceeded the breaking stress of the tendon. Since there was not a case of tendon failure among the tests, it was therefore necessary to assume a higher stress value (eg.0.2% proof stress etc.) in the non-prestressed steel. A close examination of Table 6.8 reveals that the stress developed in the tendon at failure was very high eventhough a high stress value(2.5% proof stress) was assumed in the non-prestressed steel. The tendon stress was probably above the yield point and might have reached the 0.2% proof stress. The stress values measured from the dynamometers were lower than the computed ones. This may be due to the fact that friction existed between the tendon and concrete especially when the beam had a large deflected profile. This friction would cause locally increased stress in the tendon around the centre which would not be detected by the dynamometers at the ends. In addition, the observed tendon stress was low because the readings were not taken at the actual point of failure due to practical difficulty.

In order to study the frictional effect of the stress in the unbonded tendon at ultimate load, the increase in tendon

stress may be computed approximately as follows:-

$$f_{pb} = f'_{pb}\, e^{\mu\theta}$$

$$\Delta f_{pb} = f_{pb} - f'_{pb}$$

$$= f'_{pb}(e^{\mu\theta} - 1)$$

$$= f'_{pb}\, \mu\theta$$

where f_{pb} = tendon stress at the contact point.

f'_{pb} = average tendon stress obtained from dynamometers.

μ = coefficient of friction between concrete and tendon.

θ = angle of deviation between the centre and the end.

Δf_{pb} = increase in tendon stress due to friction.

If the deflected profile is assumed to be parabolic, the angle of deviation can be expressed by $\theta = 4a/L$ where 'a' is the maximum deflection at midspan at ultimate load and 'L' is the span length.

$$\Delta f'_{pb} = \frac{f'_{pb}\, \mu\, 4a}{L}$$

Since the terms f'_{pb} ,'a' and 'L' are known, the increase in tendon stress due to friction can be estimated with an assumed value of the coefficient of friction. In the present investigation, a value of 0.5 was used to calculate Δf_{pb} for each tests. For example, in the beam R1.3.0, it is found that the tendon stress at midspan should be about 1651 N/mm2 rather than 1562 N/mm2 as measured at the end which agrees well with the

calculated value of 1624 N/mm2 in Table 6.8 .

The results for all the tests are given in Table 6.9. A comparison of the computed tendon stress in Table 6.8 with the measured tendon stress corrected to take account of friction reveals that the non-prestressed steel stress in eight test beams must have reached the 2.5% proof stress and in the remainder was not likely to have been less than the 0.5% proof stress.

It has been observed by Burns[74] and Nilson[4] that the effect of increasing the prestressing force is an increase in moment capacity of an unbonded member. In the present tests, for the beams with same amounts of reinforcement but different cross sections, the I-section beam had an ultimate moment slightly higher than the rectangular section and this may be due to higher prestress in the former because of the smaller cross-section area.

It was observed from the rectangular section beams (R1.2.2 and R1.1.3 ; R2.2.4 and R2.1.5) that if one reinforcing bar was replaced by a prestressing wire, the ultimate moment was increased by about 2.6 kNm. A similar difference was therefore expected between R3.3.4 and R3.2.5, but the ultimate moment of R3.3.4 was in fact almost 6.6 kNm less than R3.2.5. This might suggest that the loss in strength of R3.3.4 was due to the effect of sustained loading; however, Chandrasekhar[41] concluded that sustained loading did not adversely affect the static strength of partially prestressed beam although some loss of strength has been reported in cases of sustained over loading. The reason for the loss of strength of R3.3.4 is therefore uncertain.

An examination of the observed ultimate moment in Table 6.18 confirmed that the moment capacity of an unbonded member can be greatly improved by the addition of ordinary high-yield deformed bars, for example the strength of R3.3.4 was almost double the strength of R1.3.0 despite the possibility of loss of strength of the former due to the sustained loading effect.

6.6 Comparison of Theoretical and Experimental Results

6.6.1 Tension Stiffening

It has long been recognized that in a cracked concrete flexural member, the tensile concrete between adjacent cracks assists the tensile reinforcement in carrying the internal tensile force and hence increase the overall bending stiffness of the member. The approach most commonly used is to determine the average steel stress and in fact various empirical expressions based on this approach have been incorporated in design recommendations to allow for the tension stiffening effect. Some of the methods based on this approach have already been described in Section 4.2.2.2. They are namely Yu-Winter's method; CP110,Eq.62 for crack width calculation; Model Code expression; Rao's formula and finally the recommendation in CP110, Appendix A for the deflection calculation with Bennett and Lee's version of interpretation. The last method may be called "β-coefficient method" for convenient.

The experimental and theoretical relationship between applied load and average steel strain for some test beams are shown in Figs.6.23a to 6.23d. The experimental strains are the

average measured concrete surface strains over the constant moment region. The theoretical strains were obtained by the method described in Section 4.2.2.2. Referring to these diagrams, the tension stiffening of a member after cracking may be seen by comparing the experimental curve with the curve totally ignoring the tension stiffening effect i.e.fully cracked section. As the load increased, the rate of increase in experimental steel strain gradually increased and the trend is for the experimental curve to become closer to the curve of no tension stiffening indicating the decay of tension stiffening at high load. This can clearly be seen in Fig.6.23d. Referring to the top diagram of Fig.6.23a, the rate of increase of the average steel strain after cracking of the theoretical curves based on the Yu-Winter method and CP110,Eq.62 is about the same as the one of no tension stiffening. Immediately after cracking, the curve of no tension stiffening has the biggest sudden increase of steel strain, the increase being smaller in the Yu-Winter method and still less according to CP110,Eq.62. This indicates that the allowance for tension stiffening is smaller in the Yu-Winter method than by CP110,Eq.62. Furthermore, since the curves are almost parallel after cracking, neither of the methods allows for the decay of tension stiffening effect under increasing load. On the other hand, referring to the middle diagram of Fig.6.23a, it can be seen that both the Model Code expression and Rao's formula allow for the decay of tension stiffening as the load increases, by including the term (f_{scr} /f_s) to represent the degree of cracking. There is the further advantage of a smoother transition after cracking rather than a suddenly jump of the curve. It will be noted that the slope of the theoretical curves after cracking is approximately the same as that of the

experimental one. The bottom diagram of Fig.6.23a presents the theoretical curve computed by using the β -coefficient method. The β value used was based on the experimental results so as to give a good agreement with the actual deflection. This method also does not allow for the decay of tension stiffening at increasing load, but the gradient of the theoretical curve after cracking can be varied by using a different β value so that a better relation with the experimental curve could be obtained by allowing the β coefficient to decrease at increasing load.

The ratios of the computed results at service load to the experimental values are given for all the test specimens in Table 6.10. A comparison of the mean and standard deviation of the ratios for all the test beams by each method reveals that Rao's expression gave the best mean value of the results but the β -coefficient method had the best correlation. Both CP110,Eq.62 and Yu-Winter method gave a conservative mean value with a relatively poorer correlation. The results also shown that if the tension stiffening effect was ignored, the average steel strain would be over-estimated by almost 60 percent of the measured value. Basically, all the methods produce a conservative result at service load and Rao's and the Model Code expressions showed a better fit to the experimental strain.

The experimental and theoretical load-curvature relationships for some test beams are shown in Figs.6.24a to 6.24d. The experimental curvatures were those obtained from the strain measurements at the top and near bottom level over the constant moment region of the beam. The theoretical curvatures

were obtained by computing the top and bottom strain using cracked section theory but the tension stiffening effect of concrete was taken into consideration according to the methods referred previously. It can be seen that good agreement was obtained from both the Rao's and Model Code expressions. In fact, the form of the load-average curvature curves are similar to the corresponding load-average steel strain curves previously discussed. Although some theoretical curves, computed by expressions other than those of Rao and the Model Code, showed a sudden increase of curvature due to loss of concrete tensile strength shortly after cracking and produced a significant discrepancy between the experimental and theoretical curves, however, the value at service load was the important quantity to be considered. The ratios of the computed increase in curvature at service load to the experimental results for the beams are listed in Table 6.11. The best mean(0.995) of the ratios was obtained from Rao's expression with a good correlation of standard deviation equal to 0.071. The β -coefficient method give a slightly better correlation (S.D.=0.069) than Rao's expression but had a poorer mean value of 1.027. The worst mean was obtained using the Yu-Winter's method with an overestimation of the measured values by 11 percent. It is interesting to note that all the method referred have overestimated the actual average steel strain from 14.9 percent(Rao's formula) to as much as 35.5 percent(Yu-Winter's method) but in contrast, when calculating the average curvature, the discrepancy between the theoretical and experimental result was less than 1 percent with Rao's equation and only 11 percent by the Yu-Winter's method. This may be explained by the fact that although the average steel strain in the test beam was less than

expected, on the other hand, there might be some additional compressive strain at the top fibre due to creep of concrete resulting in a larger curvature.

Based on the above findings on unbonded beams, it may be concluded that when analysing a cracked unbonded beam taking the effect of tension stiffening into consideration, most of the methods gave satisfactory results for predicting the average steel strain and the average curvature. Among the methods used, Rao's and the Model Code expressions are found to be the best in present investigation. The β-coefficient method also produced a very good agreement with the test results but required an accurate β value (i.e. experimental β value). CP110,Eq.62 overestimates the steel strain but it should be noted that this equation is mainly for calculating the width of cracks which is highly variable and for which a conservative estimate will be necessary.

In order to extent the study to fully bonded partially prestressed beams, these methods were used to analyse the test beams of Lee[44]. The ratio of the computed to experimental results for the average steel strain and average curvature at service load are tabulated in Tables 6.12 and 6.13 respectively. It should be noted that the β-coefficient method is now based on the value suggested by Lee of β =0.15. A study of these Tables reveals that the Model Code expression gave excellent results with a good correlation. In contrast, Rao's equation also gave a good mean but a relatively large standard deviation of the results. The β-coefficient method, as would be expected, produced only a fair result because one particular β value was applied to whole set of

beams. The Yu-Winter's method again was the worst of the methods.

From the above observations, it can be concluded that the Model Code will give a very good result for both the bonded and unbonded beams. Furthermore, it is the only one to allow for the loss of tension stiffening under sustained loading or repeated loading.

6.6.2 Deflection

6.6.2.1 Integration of Curvature Based on CP110

An analytical method for calculating the deflection of unbonded partially prestressed beams has been formulated and described in Chapter Four. The method is based on the recommendations in CP110, Appendix A. In addition, a coefficient β is adopted to represent the strain distribution between two cracks, which was devised by Bennett and Lee[2] for curvature distribution where β will range from zero to unity to signify the degree of tension stiffening in the concrete between cracks (β =0 represents the complete loss of tension stiffening).

The theoretical and experimental load-midspan deflection curves of some test beams for the first loading up to the service load are presented in Figs.6.25a to 6.25f and Figs.6.26a to 6.26f for the second loading. It should be noted since there might have been a discrepancy between the measured(from control tests) and the actual modulus of elasticity of the beam, it was considered necessary to adjust the measured modulus value to match the initial slope of the experimental curve in order to obtain a true

comparison, although little or no adjustment was usually needed.

The calculated deflection at service load in the first cycle with varying values of β are compared with the experimental results and given in Table 6.14. It can be seen that the actual deflection was generally underestimated by putting β =0.5. The mean of the ratios of calculated to experimental delection was 0.915. The mean was improved to 0.999 when β =0.33 was used. However, the correlation in either case was only fair. If β =0 was adopted, the method consistently produced conservative results. The correct experimental β value could be obtained by interpolation and is listed in Table 6.14, column(6). The values varies from 0.06 to 0.8 with an average of 0.32. The computed deflection based on β =0.32 was also listed in Table 6.14 and the mean(1.005) obtained is excellent.

Referring to the load-deflection diagrams, the theoretical deflection was computed on the basis of two β values, one of which was used such that it gives a good agreement with the experimental deflection at service load and the other was equal to 0.32 by adopting the average of the experimental β value. In addition, a curve representing total loss of tension stiffening was also included. In the first loading, there is a discontinuity in the theoretical curve immediately after cracking because of the assumption of ignoring the tensile strength of concrete in the cracked section. This would result in a big discrepancy between the theoretical and experimental curve. By comparing the theoretical curve of I1.1.3 and I3.3.4 in Figs.6.25d and 6.25f, the sudden increase of deflection soon after cracking was found to

be smaller in the latter because I3.3.4 has a larger steel area and higher level of prestress than I1.1.3. The tensile force carried by the concrete before cracking was completely tranferred into the steel immediately after cracking and so the smaller the steel area, the bigger increase of steel (mainly non-prestressed steel) strain hence causing a bigger increase of deflection.

In the second cycle of loading, it is clear that the experimental curve was displaced considerably in the deflection direction. The displacement was caused by the residual deflection after the first cycle and led to a significant different between the theory and the experiment especially at lower load because the residual effect had not been considered in the theory. If the permanent deflection at the beginning of the second was omitted, it may be seen that the computed curve follows the trend of the actual one fairly well at lower load. There was no sudden increase of deflection in the theoretical curve after decompression because the concrete tensile strength had been ignored throughout. In general, the experimental deflection of most test beams, except I3.3.4(2nd cycle), at service load in the first and second loading was less than the computed deflection based on the fully cracked section(i.e. $\beta = 0$). Although it appears that a slightly lower β value would be required for the second cycle, it is however difficult to conclude whether the small increase of deflection was due to further loss of tension stiffening or the presence of additional compressive strain due to creep. A study of the measured concrete surface strains would suggest that both of them had happened.

The deflected profile computed on the basis of the corrected β value was also compared with measured value obtained from the dial gauges and was presented in Figs.6.14a to 6.14d. The theoretical and experimental curves agree well.

Bennett and Lee[2] had suggested a β value of 0.15 to cover the whole range of their tests, they however felt that the β value might be related to the degree of cracking at service load. In present investigation, the relationship between the experimental β value and the hypothetical tensile stress is illustrated in Fig.6.27 in which the latter variable is related to the degree of cracking of the test beams. It can be seen that the β value was the highest(1.0) when the hypothetical tensile stress was about 4 N/mm2. As the latter increased to about 10 N/mm2, the β value drop rapidly to about 0.15. Thereafter, the relationship is erratic and a horizontal straight line may be assumed. Nevertheless, it is still difficult to establish a firm relationship between these two parameters.

6.6.2.2 Integration of Curvature Based on Model Code

The method recommended in the CEB-FIP Model Code for calculating the deflection of cracked members is also based on integration of curvature but the tension stiffening effect is considered by a given expression which has already been discussed in Section 4.2.2.2. Since the expression is a function of the term (f_{scr} /f_s) which can be used to signify the degree of cracking, it can account for the fact of decay of tension stiffening at increasing load.

The theoretical and experimental load-deflection curves for some test beams are presented in Figs.6.28a to 6.28j and show a reasonably good agreement. The theoretical curves do not have a sudden increase of deflection immediately after cracking because the term (f_{scr} /f_s) can provide a smooth transition between uncracked and fully cracked stage. Since there is a discrepancy between the computed and observed cracking load, the difference between the theoretical and experimental curves were pronounced around the cracking load. The computed midspan deflection for all test beams at service load in the first cycle is given in Table 6.15,column(1). This method produced a good mean(0.977) of the ratios of calculated to experimental deflection with a reasonably good correlation. A close examination of the results reveals that the deflection of all I-section beams was underestimated by 4 to 15 percent. Lee however found that the Model Code method gave very reliable results on bonded I-section beams(with pretensioned strands). It therefore may be concluded that the deflection of bonded partially prestressed beams as well as unbonded rectangular section beams can be predicted fairly accurately by using the Model Code expression but that the latter is consistently unconservative for unbonded I-sections. This agrees with the results for the computed average curvature in Tables 6.11 and 6.13 for unbonded and bonded beams respectively.

6.6.2.3 ACI Code Simplified Formulae

An alternative method which has been reviewed in Chapter Two, for computing the deflection of cracked member is recommended in the ACI Code[1]. The method is based on an empirical expression

to obtain the effective(i.e.transition between uncracked and fully cracked states) moment of inertia. This expression has also been suggested for use with partially prestressed concrete beams by a number of researchers[49]. Branson and Trost[48] further recommended that the equation would be modified in the case of unbonded members without any non-prestressed reinforcement. They found that the use of power of 4 instead of 3 in the I-effective equation would provide a more rapid transition from I_g to I_{cr} .

In calculating I_{cr} , two procedures had been used. the first one is to treat the cracked section as reinforced concrete, taking the steel stiffness into consideration as usual. This was recommended by Branson and his colleagues. On the other hand, Tadros[58] argued that I_{cr} should be calculated based on the actual behaviour of a prestressed section in which the true bending axis is varied with the applied load under the effect of prestressing force. This is in contrast to reinforced concrete section in which the bending axis is always coincident with the centroid of the section. Lee[44] demonstrated that there was only a minor difference between the results obtained from these approaches. In the present study, the deflection was computed on the basis of the actual transformed section, equivalent reinforced concrete section and actual section again but with a power of 4 in the I-effective equation. The results are tabulated in columns (2), (3) and (4) of Table 6.15. By comparing columns (2) and (3), it is confirmed that the difference between the reinforced concrete section is negligible. The mean of column (2) is 0.975 and indicating that the ACI expression is slightly unconservative for predicting the deflection of unbonded beams but the error is

less than 3 percent. Moreover, the correlation of the results is only fair(i.e.S.D.=0.116). Referring to column (4), the results obtained by using a power of 4 were generally conservative but the deflection of I1.2.2 was underestimated by 23 percent. This is reflected by the fact that the mean of column (4) is 1.08 but with a large standard deviation of 0.148. It may be noted that the deflection of all the beams having a ratio of (M_{cr} /M_{ser}) greater than 0.9 was underestimated even by using the power of 4 in the equation. The theoretical and experimental load-deflection curves of some test beams are presented in Figs.6.29a to 6.29h. Like the Model Code expression, the ACI Code formula provides a smooth transition immediately after cracking. An error in the prediction of the cracking load would cause a significant discrepancy between the theoretical and experimental curves around the cracking load. It can be seen that the rate of increase of deflection after cracking is faster if the power of 4 expression was used. Furthermore, it may be concluded that the power of 4 can be used for calculating the deflection of unbonded prestressed members provided they have a sufficient amount of non-prestressed steel.

When comparing the short-term deflection computed by means of the Model Code and the ACI Code respectively as shown in Table 6.15, the former gives a better mean and standard deviation of the results but required a more complicated computation. In contrast, the ACI method is simple and more suitable for design purposes. Nevertheless, its validity for unbonded beams without bonded reinforcement or only lightly reinforced, needs to be verified.

The ACI building Code recommends a simple method to calculate the additional deflection under long-term loading. This is determined by multiplying the immediate deflection caused by the sustained load by a factor which depends on the time and the area of compression steel. In the present investigation, seven beams were tested under combined loading for about a month and the deflection in the final cycle were computed by adopting the common practice of adding the short-term deflection to the long-term deflection. The results for some test beams are shown in Figs.6.30a to 6.30e. The computed deflection at the half and full service load at the end of the test is tabulated in Table 6.16. It was found that the actual deflection at half service load were underestimated varying from 37 percent(I3.3.4) to as much as 85 percent(R1.0.5). The computed deflections at service load were also smaller than the experimental results by up to 36 percent in I1.2.2. It has been concluded that effect of combined loading would cause non-recoverable residual deflection which was however not taken into consideration in the computation and thus led to a big discrepancy between the calculated and experimental results. Only the predicted deflection of R2.0.7 at service load agrees with the measured value but it may be due to overestimate of the short-term deflection hence compensating for the non-recoverable residual deflection(see Fig.6.30c).

R3.3.4 was tested under sustained load alone for about a year, at the end of which the theoretical deflection was 41 percent less than the experimental value. This indicates that the rate of increase of deflection of unbonded beam under sustained load could be very fast. However, more tests should be carried out

to clarify this.

It may be concluded on the basis of present test results that the ACI method for predicting the long-term deflection of unbonded cracked beam was unconservative in most cases no matter whether the beam was under combined loading or sustained loading alone. The occurrence of intermittent short-term load cycles in the combined loading test could only increase the discrepancy. It was felt that the non-recoverable residual deflection due to combined loading may be represented by a factor as pointed out by Bennett and Lee[2] and should be included in the prediction of long-term deflection. The residual deflection at the end of the first cycle was significant and should also be considered.

6.6.3 Increase in Tendon Stress at Service Loads

Although the increase in tendon stress of unbonded beams at service loads is usually small and does not required checking to satisfy the serviceability limit states, however, it may be interesting to know the tendon stress value. The measured increase of tendon stress under applied load was compared with the computed results obtained by Nilson's and Balaguru's methods reviewed in Section 2.3 as well as from the cracked section analysis described in Chapter Four. The calculated and measured results are listed in Table 6.17 and the curves of increase in tendon stress versus applied load for some test beams are presented in Figs.6.31a to 6.31c. A study of Table 6.17 in conjunction with Figs.6.31a to 6.31c reveals that the results obtained by cracked section analysis based on the correct β value

are consistently conservative. In the analysis, the amount of tensile force carried by the concrete before cracking and transferred to the tendon immediately after cracking was very much overestimated and hence caused a sudden increase in tendon stress after cracking. This would lead to a significant discrepancy between the computed and experimental results. Nilson's and Balaguru's methods show a smoother transition after cracking because both of them rely on the I-effective formula. The former gave a better mean value but the correlation of the results was not good. Balaguru's method generally indicated an under-prediction of the tendon stress. It may be due to the fact that the method was originally derived for beams with a second degree parabolic cable profile under uniformly distributed load, in contrast to the test beams which had straight tendon with two-point loading.

6.6.4 Flexural Strength

There are no specific recommendations in either the British Code CP110, the ACI building Code or the CEB-FIP Model Code for calculating the ultimate strength of unbonded members with additional bonded reinforcement. However, Tam and Pannell[32] has proposed a method for predicting the moment capacity of this type of members, in which several important factors like the span/depth ratio, quantity of non-prestressed steel and the depth of neutral axis at failure were considered in the calculation of the stress in the unbonded tendon. In contrast, the ACI Code and CP110 also provide method to evaluate the tendon stress at ultimate moment but both fail to consider the influencing factors

comprehensively and hence are to some extent limited in application.

In the ACI Code, the tendon stress at failure can be predicted by two given expressions(see Chapter Two) depending on whether the span/depth ratio of the member is above or below the specified value of 35. If the span/depth ratio in not greater than 35 (in the present test l/d = 22 approximately), the code specified that the tendon stress should not be greater than the yield stress or 413 N/mm2(60000 psi) in excess of the effective prestress after all losses have taken place. The expression is a function of the cylinder strength and the ratio of prestressing reinforcement but the influence of the non-prestressed steel on the tendon stress is not considered. Furthermore, the equation was originally adopted from the conservative version of the lower bound empirical equation developed by Mattock[21] based on beams with an l/d ratio of 28. Therefore, the predicted stress may be unconservative if the l/d ratio of the member is larger than 28.

In the British Code CP110, the stress in the unbonded tendon is limited to the value given in cl.4.3.4.3, Table 38 i.e.varying from 1.11 to 1.45 times the effective prestress depending on the ratios of (f_{pe} A_{ps} /f_{cu} bd) and l/d. However, it is limited to members with a l/d ratio between 10 and 30. No comments are made on how to deal with the non-prestressed steel.

In the present investigation, the ultimate moments for the test beams was computed on the basis of the above methods. According to the conclusions in Section 6.5.4, the stress in the

non-prestressed steel at failure was unlikely to be less than the 0.5% proof stress, and sometimes reached the 2.5% proof stress and even fracture of the reinforcement. In working out the ultimate moment of resistance, the 0.5% and 2.5% proof stress have been taken separately as the stress in the non-prestressed steel in the computation. The computed ultimate moments were based on the actual material properties obtained from control specimen tests and unfactored i.e. the material safety factors in CP110 method and the capacity reduction factor in the ACI Code method was removed.

When using the CP110 method, a modification has to be made in order to take the effect of non-prestressed steel into consideration. This modification was used by Veerasubramanian[43] and was done by converting the area of non-prestressed steel into an equivalent area of prestressed steel. The total equivalent steel area is given by $A_{ps} = A_p + A_s f_y / f_{pb}$ where f_{pb} is the breaking stress initially. The ratio of f_{pb} / f_{pe} and the limiting value of x/d may then be obtained from Table 38 in CP110 by interpolation with respect to the l/d ratio and the steel parameter ($A_{ps} f_{pe} / f_{cu}$ bd). The calculated f_{pb} value is checked against the initial value, if the difference between them is greater than 1 percent the procedure will be repeated with the new f_{pb} value until the desired accuracyis achieved. By knowing the stress in the tendon and the non-prestressed steel at failure, the moment of resistance could then be obtained in the usual way. If in case of flanged beams, the moments were obtained in accordance with the assumption specified, nevertheless, all the I-section beams were found to have a neutral axis within the top flange.

The calculated and observed ultimate moments are shown in Table 6.18. It can be seen that all these methods consistently produced conservative results for all test beams even when the stress in the non-prestressed steel was assumed to reach the 2.5% proof stress. The results with the Tam-Pannell and CP110 methods are very similar because the latter was based on results of tests and analysis by Pannell[31]. The slightly modification introduced in using the CP110 method seems reasonable and gives satisfactory results when compared with tests. Since all the beams have about the same 1/d ratio, the Tam-Pannell's method appears to have no advantage over the others. In the present tests, all three methods were found to be safe in predicting the strength of unbonded members with additional bonded reinforcement since the stress in the non-prestressed steel reached so high a value which appears to have influenced the straining capacity of the prestressing steel. The stress in the tendon at failure was much higher than predicted and resulted in underestimation of the ultimate moments. When comparing the observed results with the design ultimate moment which was calculated by the CP110 method with suitable material safety factors, the design value is less than the observed result by between 19 and 38 percent with a mean ratio of 0.68 .

Clear evidence of underestimation of the tendon stress can be found by comparing the predicted and observed tendon stress in Table 6.19. The computed results were obtained by assuming the 0.5% of the proof stress in the non-prestressed steel at failure. According to the ACI method, the maximum amount of tendon stress should not be greater than 413 N/mm2. This is in contrast to present test, in which the value varies from 406 to 535 N/mm2

except R3.3.4 which has a much lower value due to loss strength under the effect of sustained loading. Similarly, the ratio of the tendon stress computed by CP110 at ultimate moment to the effective prestress varies from 1.2 to 1.26 but the ratio for observed value is between 1.24 and 1.5. Generally the predicted tendon stress is largest by the ACI method, and the least valus is obtained by Tam-Pannell's method.

CHAPTER SEVEN

CONCLUSIONS AND SUGGESTIONS FOR FURTHER RESEARCH

7.1 Introduction

The conclusions from present investigation were summarized in this chapter in particular with reference to the objects of the study stated in Chapter One. Suggestions are also made as to those aspects which may be of interest in the light of the findings from present investigation.

7.2 Conclusions

7.2.1 Deformations

7.2.1.1 First and Second Cycle of Loading

Before cracking in the first cycle or decompression in the second cycle, the rate of increase of deflection was mainly related to the modulus of elasticity of concrete and the shape of section but after cracking(or decompression) the rate was largely a function of the quantity of steel, i.e. the larger the steel area, the lower the rate.

The I-section beams had a lower cracking load than beams of rectangular section with the same amounts of prestressed and non-prestressed steel. The rates of increase of deflection after cracking were about the same.

A beam of low prestress with large amount of non-prestressed steel behaves like an ordinary reinforced concrete beam in the second loading.

The deflection of all test beams at service load was less than the CP110 specified limit although the l/d ratio was near the maximum allowable by the code.

Residual strains at the top and bottom were observed at the end of the first cycle. The cause was due to short-term creep of concrete at the top and slip of the bars at the cracks at the bottom.

Beams with a non-prestressed steel stress greater than 240 N/mm2 at service load have developed large residual deflections. The residual deflection of the unbonded beams at the end of the first cycle varied from 0.78 to 3.92 mm. A beam might not necessarily have a large residual deflection, eventhough it had a high hypothetical tensile stress value, provided there was sufficient prestress to recover the deflection. The cause of residual deflection was not only irreversible slip of the bars as usually explained by other researchers but also short-term creep of the concrete. This is especially true for the beams of high prestress in which the cracks closed when unloaded.

Branson's method for calculating residual deflection was not satisfactory because of ignoring the effect of creep.

7.2.1.2 Combined Loading

The rate of increase of deflection from half to full service load was greatest in the first cycle and became less in the second and third cycles. Thereafter, the rate became approximately constant.

The final deflection of the reinforced concrete beams was larger than that of the others and exceeded the CP110 limit. It thus reveals the importance of prestress in deflection control.

Residual increment of deflection occurred after each intermittent short-term load cycle and the increment was greatest after the first two intermittent cycles but became smaller and about constant over the last few cycles. Only part of this increase was recoverable. The common practice of calculating long-term deflection which allows for the effects of creep and shrinkage under the permanent load alone was found to be unconservative.

The lowering of the neutral axis of strain in beams under combined loading was believed to be due to the effect of sustained load.

At the end of each intermittent short-term load cycle, the amount of residual incremental top strain was found to be independent of the number of load cycles and in contrast, the residual bottom strain was largest after the first intermittent cycle and became less as the number of cycles increased.

Recovery of bottom strain was observed during the

sustained loading period indicating a recovery of residual deflection taking place after each intermittent load cycle.

The cause of the non-recoverable residual deflection in present tests was not likely due to loss of tension-stiffening but believed to be the result of non-recoverable creep strain and increased creep rate under the effect of cyclic load.

A increase of crack width was observed at the end of the test but none of the cracks were wider than 0.2 mm. Unbonded members with good protection of the tendons should not have corrosion problems through cracking.

7.2.1.3 Sustained Loading

The top strain increased rapidly in the early stage of the loading period and the rate of increase of strain was reduced progressively at the end. No significant change of strain occurred at the bottom.

The deflection continued to increase although at a progressively reducing rate. After 336 days, the increase in deflection was found to be 3.3 times the initial instantaneous value. The maximum of 2, recommended in the ACI Code for the ratio of the additional time-dependent deflection to the instantaneous deflection, is unconservative for this test.

7.2.2 Tension Stiffening

The effect of tension stiffening will decay as the load increased. When analysing a cracked unbonded beam and taking the effect of tension stiffening into account, the formulae or methods used were found to give satisfactory results for predicting the average steel strain and the average curvature. Among the methods used, Rao's and the Model Code expressions were found to be more accurate in the present tests. The β-coefficient method also produced a very good agreement with the test results but required an accurate β value. The method may be further improved by varying the β value at increasing load. The Yu-Winter's method and the CP110,Eq.62 gave conservative results.

When analysing a cracked bonded beam, the Model Code formula produced the best results with very good correlation with the test results. Rao's formula gave a good mean but poorer consistency.

7.2.3 Calculation of Deflection

7.2.3.1 Integration of Curvature Based on CP110

An analytical method was formulated on the basis of the CP110, Appendix A recommendations for calculating the short-term deflection of unbonded cracked beam. A β coefficient was adopted to signify the degree of tension stiffening in the concrete between cracks where β is between zero and unity.

The deflection computed by ignoring the tension stiffening effect(i.e. β =0) always overestimated the actual value. The experimental β value required to produce a good

agreement between theoretical and experimental deflection varied between 0.06 and 0.8 with an average of 0.32.

The computed deflection after the point of cracking did not agree with the experiments due to totally ignoring the concrete tensile strength in the theory. There was a large discrepancy between the experimental and theoretical load-deflection curve at the beginning of the second cycle due to ignoring the residual deflection in the computation.

The actual deflection at service load in the second cycle was slightly larger than the previous cycle due to additional creep strain at the top and further loss of tension stiffening in the second loading.

The experimental β value at service load was found to be higher for lower values of hypothetical tensile stress. The relationship of the two can be seen in Fig.6.27. More evidence will be needed in order to establish a better relationship between these two parameters. Furthermore, the β value should decrease from unity to the experimental β value as the load increases from cracking load to service load in order to allow for the decay of the tension-stiffening effect at increasing load.

7.2.3.2 Integration of Curvature Based on Model Code

The short-term deflection computed on the basis of the Model Code formula to account for the effect of tension stiffening gave a good agreement with the measured values.

The Model Code expression predicted the trend of the experimental load-deflection curve reasonably well. Better agreement was obtained if the actual cracking load was used.

The Model Code method generally gave reliable and conservative results on bonded I-section beams as well as unbonded partially prestressed beams of rectangular section. However, the latter prediction for unbonded I-section beams was found to be unconservative in most cases.

7.2.3.3 ACI Code Simplified Formulae

The ACI Code I-effective equation was adopted with slight modifications as recommended by other researchers to calculate the short-term deflection of unbonded partially prestressed beams. It was found that the use of the power of 3 in the equation was slightly unconservative with a mean of the computed results 3 percent less than the actual values. The use of the power of 4 provided conservative results for all the test beams except those having a low degree of cracking i.e. M_{cr}/M_{ser} higher than 0.9. The I-effective expression with a power of 4 could be used to predict the deflection of unbonded members with a substantial amount of non-prestressed steel. More tests, however, should be made to justify this. Moreover, a higher power may be required if the unbonded beam is lightly reinforced or without any bonded reinforcement at all.

The difference between the results obtained from the transformed section with or without taking the prestressing effect

into account is not significant.

The ACI method for predicting the long-term deflection of unbonded beams was unconservative no matter whether the beam was under combined loading or sustained loading alone. The non-recoverable residual deflection due to intermittent load cycles should be considered in the computation. In addition, the substantial amount of residual deflection after the first cycle should also be considered.

7.2.4 Increase in Tendon Stress at Service Loads

The increase in tendon stress was governed by the increase in deflection. The amount of increase at service load was small varying from 1.6 to 8.1 percent of the effective prestress.

Elzanaty and Nilson's method for predicting the increase in the tendon stress was satisfactory with a good mean but the consistency was only fair. Balaguru's method always underestimated the tendon stress significantly.

7.2.5 Flexural Strength

The strength of the test beams were higher than that predicted on the basis of the ACI Code, CP110 and Tam-Pannell's method because the actual tendon stress was much higher than that estimated by these methods. The high tendon stress (i.e. probably reached the 0.2% proof stress) at ultimate moment was mainly due to the non-prestressed steel stress reached so high a value(i.e.

sometimes 2.5% proof stress) hence had increased the strain capacity of the tendon. In addition, the friction between the concrete and the tendon caused localized stresses at the contact points which was not allowed for in the computation. An approximate estimation of the increase in tensile stress due to friction indicated that it could be as high as 137 N/mm2. All the methods mentioned gave satisfactory and conservative predictions of the strength of unbonded beams with bonded reinforcement.

The addition of bonded non-prestressed steel greatly improved the strength of an unbonded member.

The effect of sustained loading may adversely affect the strength of an unbonded member.

7.3 Suggestions for Further Research

(1) It has been found that the effect of combined long-term sustained loading and intermittent short-term cyclic loading on the long-term deflection was significant. However,up to the present the test period has been limited to about a month. It will be of interest to extend the duration of test to at least six months to a year time so that the effect of cyclic loading on the loss of tension stiffening may be more pronounced. It is further suggested that the test should consist of sets of three duplicate beams which should be tested under long-term sustained loading alone, combined loading and short-term cyclic loading alone so that the relationship of these three types of loading can be observed.

(2) The residual deflection at the end of the first cycle was found to be significant in affecting the deflection in the subsequent cycles of loading. The existing method for predicting it was however not satisfactory in some ways. More research is needed in this area.

(3) Research on unbonded member under fatigue loading has rarely been carried out. It would be interesting to observed the influence of this on the deflection , non-prestressed steel stress and the strength.

(4) The rate of increase of deflection of unbonded beam was found to be faster than bonded prestressed beam and the suspicion of loss of strength under the effect of sustained loading should be clarified with more tests. A study of this in conjunction with some comparable bonded prestressed beams may find to be useful.

(5) The deflection computation on the basis of CP110 was found quite satisfactory but it can be further improved by producing a simplified expression in relating the β coefficient with the parameter degree of cracking(eg. hypothetical tensile stress) and eventually modify the present theory to a more convenient form to be used for design purposes.

(6) The ACI Code I-effective equation sometimes gave an unconservative prediction of the deflection of beams with unbonded tendons. It may require further verification by tests to ascertain the correct power to be used in the equation.

REFERENCES

[1] ACI Standard 318-83, "Building code requirements for reinforced concrete (ACI 318-83)", American Concrete Institute, Detroit, 1983.

[2] Bennett,E.W. and Lee,K.H., "Deflection of partially prestressed beams under a combination of long-time and short-time loading", ACI Symposium (Deformation of Concrete Structures), sp-86, 1985 .

[3] Nawy,E.G. and Chiang,J.Y., "Serviceability behaviour of post-tensioned beams", PCI Journal, vol.25, No.1, Jan/Feb.1980, pp.74-95 .

[4] Nilson,A.H. and Elzanaty,A., "Flexural behaviour of unbonded post-tensioned partially prestressed concrete beams", Report No.82-15, Nov.1982, Ithaca, New York, Cornell University.

[5] Abeles,P.W., "Saving reinforcement by prestressing", Concrete and Constructional Engineering, vol.35, No.7, July 1940, pp.328-333 . Discussion : vol.36, No.2, Feb.1941, pp.73-96 .

[6] Emperger,H.von, " Stahlbeton mit vorgespannten Zulagen aus hoherwertigen Stahl", Forschungsarbeiton auf dem Gebiete des Eisenbetons, No.47, 1939 .

[7] Abeles,P.W., "Partially prestressed concrete construction built in the Eastern Region of British Railways 1948-1952", Publication of IABSE, 1952, pp.1-13 .

[8] British Standard Code of Practice CP110 : 1972, "The structural use of concrete", British Standard Institution, London, 1972 .

[9] ACI-ASCE Committee 423, "Tentative recommendations for concrete members prestressed with unbonded tendons", ACI Journal, Feb.1969, pp.81-86 .

[10] ACI-ASCE Committee 423, "Tentative recommendations for prestressed concrete flat plates", ACI Journal, vol.71, No.2, Feb.1974 .

[11] Concrete Society, "Flat slabs in post-tensioned concrete with particular regard to the use of unbonded tendon-design recommendations", Concrete Society technical report No.17, 1979 .

[12] Post-tensioning Institute, "Design of post-tensioned slabs", First edition, Glenview, Illinois, U.S.A., 1977 .

[13] Schupack, M., "A survey of the durability performance of post-tensioning tendons", Post-tensioning Institute, Jan.1978 .

[14] Abeles, P.W., "Fully and partly prestressed reinforced concrete", ACI Journal, Proceedings, vol.41, No.3, Jan.1945, pp.181-126 .

[15] Abeles, P.W., "Some new developments in prestressed concrete", Structural Engineer, vol.XXIX, Oct.1951, pp.259-278 .

[16] Abeles, P.W., "Design of partially prestressed concrete beams", ACI Journal, Proceedings, vol.64(11), No.64-58. Oct.1967, pp.669-677 .

[17] Naaman, A.E. and Siriaksorn, A., "Serviceability based design of partially prestressed beams", Discussion paper, PCI Journal, vol.25, No.1, Jan/Feb.1980, pp.146-158 .

[18] Naaman, A.E. and Siriaksorn, A., "Serviceability based design of partailly prestressed beams", Part 1 : Analytic formulation , PCI Journal, vol.24, No.2, March/April 1979, pp.64-89 . Part 2 : Computerized design and evaluation of major parameters, vol.24, No.3, May/June 1979, pp.40-60 .

[19] Abeles, P.W. and Gill, V.L., "The behaviour of partially prestressed beams , containing bonded, non-tensioned strands and curved, non-bonded tendons", IABSE, 8th Congress, New York, 1968, Final report, IVb, pp.918-919.

[20] Janney, J.R., Hognestad, E. and McHenry, D., "Ultimate flexural strength of prestressed and conventionally reinforced concrete beams", ACI Journal, vol.52, No.6, Feb.1956, pp.601-620 .

[21] Mattock, A.H., Yamazaki, J. and Kattula, B.T., "Comparative study of prestressed concrete beams with and without bond", Part 1 , ACI Journal, vol.68, No.2, Feb.1971, pp.116-125 .

[22] Chaikes, S., "Le Beton Precontrainte Arme", Proceeding, FIP, Fourth Congress, Rome, vol.1 , 1962, pp.480-483 .

[23] Abeles, P.W., "Discussion-Theme III", Proceeding, FIP, Fourth Congress, Rome, vol.2, 1962, p.343 .

[24] Bennett, E.W. and Chandrasekhar, C.S., " Supplementary tensile reinforcement in prestressed concrete beams", Concrete, vol.6, Oct.1972, pp.35-39 .

[25] Stevens, R.F., "Tests on prestressed reinforced concrete beams", Concrete, vol.3, No.11, Nov.1969, pp.457-463 .

[26] Evans, R.H., "Relative merits of wire and bar reinforcement in prestressed concrete beams", ICE Journal, vol.17, No.4, Feb.1942, pp.315-329 .

[27] Baker, A.L.L., "A plastic theory of design for ordinary reinforced and prestressed concrete including moment redistribution in continuous members", Magazine of Concrete Research, vol.1, No.2, June 1949, pp.57-66.

[28] Revesz, S., "Factors governing the ultimate bending moment of normal reinforced and prestressed concrete beams, with reference to a proposed plastic theory", Magazine of Concrete Research, vol.5, No.13, Aug.1953, pp.11-26 .

[29] Gifford, F.W., "The design of simply supported prestressed concrete beams for ultimate loads", ICE proceedings, part III, vol.3, No.1, April 1954, pp.125-143 .

[30] Cowan, H.J., "The ultimate strength of prestressed concrete beams", Structural Engineer, vol.33, No.7, July 1955, pp.197-212 .

[31] Pannell, F.N., "The ultimate moment of resistance of unbonded prestressed concrete beams", Magazine of Concrete Research, vol.21, No.66, March 1969, pp.43-54 .

[32] Tam, A. and Pannell, F.N., "The ultimate moment of resistance of unbonded partially prestressed reinforced concrete beams", Magazine of Concrete Research, vol.28, No.97, Dec.1976, pp.203-208 .

[33] Warwaruk, J., Sozen, M.A. and Siess, C.P., "Strength and behaviour in flexure of prestressed concrete beams", Engineering Experiment Station, University of Illinois, Bulletin No.464, 1964 .

[34] ACI Standard 318-77, "Building code requirements for reinforced concrete (ACI 318-77)", American Concrete Institute, Detroit, 1977 .

[35] Mojtahedi, S. and Gamble, W.L., "Ultimate steel stresses in unbonded prestressed concrete", ASCE Journal, vol.104, No.ST7, July 1978, pp.1159-1165 .

[36] Balaguru, P.N., "Increase of stress in unbonded tendons in prestressed concrete beams and slabs", Canadian Journal of Civil Engineering(Ottawa), vol.8, No.2, April/June 1981, pp.262-268 .

[37] Abeles, P.W., Brown, E.I. and Woods, J.O., "Preliminary report on static and sustained loading tests", PCI Journal, vol.13, No.4, Aug.1968, pp.12-32 .

[38] Bennett, E.W. and Dave, N.J., "Test performances and design of concrete beams with limited prestress", Structural Engineer, vol.47, No.12, Dec.1969, pp.487-496 .

[39] Dave, N.J., "Limiting prestressed as a means of economy in structural concrete", Ph.D. thesis, Leeds University, 1967 .

[40] Bennett,E.W. and Chandrasekhar, C.S., "Stresses in the tendons and supplementary reinforcement of class 3 prestressed concrete beams", Building Science, vol.6, No.3, Sept.1971, pp.123-131 .

[41] Chandrasekhar, C.S., "A study of the influence of the properties and distribution of the reinforcement on the behaviour of beams with limited prestress", Ph.D. thesis, Leeds University, 1970 .

[42] Bennett, E.W. and Veerasubramanian, N., "Behaviour of non-rectangular beams with limited prestress after flexural cracking", ACI Journal, Proceedings, vol.69, No.9, Sept.1972, pp.533-542 .

[43] Veerasubramanian, N., "Effect of shape of section on the flexural behaviour of class 3 prestressed concrete beams", Ph.D. thesis, Leeds University , 1971 .

[44] Lee, K.H., "Deformation of partially prestressed concrete beams under service loads", Ph.D. thesis, Leeds University, 1984 .

[45] Branson, D.E., "Instantaneous and time-dependent deflections of simple and continuous reinforced concrete beams, HPR publication 7, part 1, 1-78, Alabama Highway Department, Bureau of Public Roads, Aug.1963 .

[46] Shaikh, A.F. and Branson, D.E., "Non-tensioned steel in prestressed concrete beams", PCI Journal, vol.15, No.1, Feb.1970, pp.14-36 .

[47] Kripanarayanan, K.M. and Branson, D.E., "Short-time deflections of beams under single and repeated load cycles", ACI Journal, vol.69, No.2, pp.110-117 .

[48] Branson, D.E. and Trost, H., "Unified procedures for predicting the deflection and centroidal axis location of partially cracked non-prestressed and prestressed concrete members", ACI Journal, vol.79, No.2, March/April 1982, pp.119-130 .

[49] Moustafa, S.E., "Design of partially prestressed concrete flexural members", Discussion paper, PCI Journal, vol.23, No.3, May/June 16978, pp.72-94 .

[50] CEB-FIP, "Model Code for concrete structures", International System of Unified Standard Codes of Practice for structures, vol.2, London, Comite Euro-international du Beton .

[51] Bennett, E.W. and Chandrasekhar, C.S., "Calculation of the width of cracks in class 3 prestressed beams", ICE Proceedings, vol.49, July 1971, pp.333-346 .

[52] Martino, N.E. and Nilson, A.H., "Crack widths in partially prestressed concrete beams", Ithaca, New York, Cornell University, 1979 .

[53] Goschy, B., "Partially stressed reinforced concrete", Melyepitestud, Szle, vol.14, No.2, 1964, pp.81-83 .

[54] Birkenmaier, M., "Design of partially prestressed concrete units in accordance with the (1966) Standards of the Swiss Association of Engineers and Architects", Annales de L'Institut Technique du Batiment et Travaux Publics, vol.21[241], 1968, pp.57-64 .

[55] Brettle, H.J., "A theory to predict the neutral surface position in rectangular prestressed concrete beams as cracking develops", Constructional Review, Oct.1959, pp.18-23 .

[56] Balaguru, P.N., "Design of partially prestressed post-tensioned beams with unbonded tendons", Concrete International, vol.3, No.11, Nov.1981, pp.30-41 .

[57] Nilson, A.H., "Flexural stresses after cracking in partially prestressed beams", PCI Journal, vol.21, No.4, July/Aug.1976, pp.72-81 .

[58] Tadros, M.K., "Expedient service load analysis of cracked prestressed concrete sections", PCI Journal, vol.27, No.6, Nov/Dec.1982, pp.87-111. Discussion paper, vol.28, No.6, Nov/Dec.1983, pp.137-158 .

[59] The Concrete Society, "Partial prestressing", Report of a Concrete Society working party, 1983, 27pp., Technical report No.23, publication 53.040 .

[60] Bennett, E.W., "Partial prestressing-Developments in prestressed concrete-1", Sawko, F.(Editor), London, Applied Science Publishers, 1978, pp.125-147 .

[61] Kankam, C.K., "Bond characteristics of reinforcing bars with reference to the deformations of concrete structures", Ph.D. thesis, Leeds University, 1983 .

[62] Moosecker, W. and Grasser, E., "Evaluation of tension stiffening effects in reinforced concrete linear members", IABSE (Colloquium on advanced mechanics of reinforced concrete), Delft, June 1981, pp.615-624 .

[63] Yu, W.W. and Winter, G., "Instantaneous and long-time deflections of reinforced concrete beams under working loads", ACI Journal, Proceedings, vol.57, No.1, July 1968, pp.29-50 .

[64] Rao, P.S. and Subrahmanyam, B.V., "Trisegmental moment-curvature relations for reinforced concrete members", ACI Journal, vol.90, No.5, May 1973, pp.346-351 .

[65] Bachmann, H., "Partial prestressing of concrete structures, IABSE Survey" , S-11/79, IABSE, Nov.16979 .

[66] British Standard Institution, "BS1881 : Part 4 and 5, Method of testing concrete", London, 1983 .

[67] Abeles, P.W. and Kung, R., "Prestress losses due to the effect of shrinkage and creep on non-tensioned steel", ACI Journal, vol.70, No.1, Jan.1973, pp.19-27 .

[68] Nagi, H., Masuda, Y., Tanaka, Y. and Kurauchi, M., "Evaluation of corrosion protection of unbonded tendons", Post-tensioning Institute, Pheonix, Arizona, Oct.1978, 36pp.

[69] Bachmann, H., "Partially prestressed concrete. Simplified design based on Swiss Practice since 1968", International Symposium(Nonlinearity and continuity in prestressed concrete), preliminary publication, vol.1, University of Waterloo, Canada, July 1983, pp.29-46 .

[70] McHenry, D., "A new aspect of creep and its application to design", Proceedings of the American Society of Testing Materials, vol.43, 1943, pp.1069-1087 .

[71] Whaley,C.P. and Neville, A.M., "Non-elastic deformation under cyclic compression", Magazine of Concrete Research, vol.25, No.84, Sept.1973, pp.145-154 .

[72] Hirst, G.A., "Mechanisms of deformation of concrete under cyclic uniaxial compression" Ph.D. thesis, Leeds University, 1976 .

[73] Oladapo, I.O., "Stability of tensile cracks in prestressed concrete beams", ASCE Journal, Structural Division, vol.95, st1, Jan.1969, pp.17-31 .

[74] Burns, N.H. and Pierce, D.M., "Strength and behaviour of prestressed concrete members with unbonded tendons", PCI Journal, Oct.1967, pp.15-29 .

TABLE 5.1 INFORMATION OF TEST BEAMS

BEAM REFERENCE	SHAPE OF SECTION *	SERIES NUMBER	NUMBER OF WIRES	NUMBER OF BARS	PARTIAL PRESTRESSING RATIO	DEGREE OF PRESTRESS	DESIGN ULTIMATE MOMENT (kNm)	DESIGN SERVICE MOMENT (kNm)	SERVICE MOMENT IN TEST (kNm)
R1.3.0	R	1	3	0	1.00	1.00	36.2	24.1	25.0
R1.2.2	R	1	2	2	0.55	0.42	38.6	25.7	25.0
R1.1.3	R	1	1	3	0.30	0.20	36.0	24.0	25.0
R1.0.5	R	1	0	5	0.00	0.00	38.2	25.5	25.0
R2.3.2	R	2	3	2	0.64	0.52	47.7	31.8	34.0
R2.2.4	R	2	2	4	0.38	0.29	51.3	34.2	34.0
R2.1.5	R	2	1	5	0.20	0.13	48.9	32.6	34.0
R2.0.7	R	2	0	7	0.00	0.00	50.5	33.7	34.0
R3.4.2	R	3	4	2	0.70	0.59	56.2	37.5	38.5
R3.3.4	R	3	3	4	0.47	0.38	60.1	40.1	38.5
R3.2.5	R	3	2	5	0.33	0.24	57.5	38.3	38.5
I1.2.2	I	1	2	2	0.55	0.48	37.7	25.1	25.0
I1.1.3	I	1	1	3	0.30	0.21	36.5	24.3	25.0
I2.3.2	I	2	3	2	0.64	0.58	46.9	31.3	34.0
I2.2.4	I	2	2	4	0.38	0.31	50.9	33.9	34.0
I3.3.4	I	3	3	4	0.47	0.41	59.2	39.5	38.5
I3.2.5	I	3	2	5	0.32	0.26	57.2	38.1	38.5

* R = Rectangular Section
I = I-Shaped Section

TABLE 5.2 DETAIL OF MAIN REINFORCEMENT

BEAM REFERENCE	PERCENTAGE OF REINFORCEMENT *	AREA OF WIRES (mm^2)	AREA OF BARS (mm^2)	EFFECTIVE DEPTH OF WIRES (mm)	EFFECTIVE DEPTH OF BARS (mm)
R1.3.0	0.25	115.5	------	255	---
R1.2.2	0.51	77.0	157.0	255	282
R1.1.3	0.60	38.5	235.5	255	282
R1.0.5	0.86	------	392.5	---	265
R2.3.2	0.60	115.5	157.0	255	282
R2.2.4	0.85	77.0	314.0	255	282
R2.1.5	0.94	38.5	392.5	255	282
R2.0.7	1.20	------	549.5	---	260
R3.4.2	0.68	154.0	157.0	255	282
R3.3.4	0.94	115.5	314.0	255	282
R3.2.5	1.03	77.0	392.0	255	282
I1.2.2	0.83	77.0	157.0	255	282
I1.1.3	0.97	38.5	235.5	255	282
I2.3.2	0.96	115.5	157.0	255	282
I2.2.4	1.38	77.0	314.0	255	282
I3.3.4	1.52	115.5	314.0	255	282
I3.2.5	1.66	77.0	392.5	255	282

* Total steel area / Nominal concrete area

TABLE 5.3 PROPERTIES OF CONCRETE

BEAM REFERENCE	STRENGTH OF CONCRETE (N/mm²)				MODULUS OF ELASTICITY (kN/mm²)
	COMPRESSIVE		TENSILE		
	100 mm CUBE **	150 mm CUBE *	SPLIT CYLINDER	MODULUS OF RUPTURE	
R1.3.0	66.3	58.8	3.18	4.86	34.3
R1.2.2	61.8-72.4	67.6	3.27	4.36	32.3
R1.1.3	64.0	57.7	3.23	4.32	34.8
R1.0.5	64.9-75.4	69.4	3.75	5.18	32.4
R2.3.2	71.8	69.8	3.95	4.87	32.6
R2.2.4	66.5-77.3	——	3.65	5.48	36.2
R2.1.5	70.9	66.6	3.58	4.42	32.5
R2.0.7	62.3-72.2	66.0	3.40	4.46	34.5
R3.4.2	70.0	62.9	3.56	4.46	35.5
R3.3.4	68.0-79.4	——	3.72	5.10	31.7
R3.2.5	68.7	66.4	3.78	4.58	35.6
I1.2.2	75.1-84.7	77.4	3.66	4.64	35.9
I1.1.3	73.9	73.0	3.71	4.74	34.5
I2.3.2	68.8	63.8	3.12	4.57	35.3
I2.2.4	73.3-80.0	73.4	3.89	4.73	37.9
I3.3.4	78.3-89.5	78.8	3.82	4.62	34.5
I3.2.5	77.4	71.2	3.89	4.59	37.0

** Obtained from the 1st and last days of test
* Obtained from the last day of test
Others were obtained from the 1st day of test

TABLE 5.4a PROPERTIES OF 7 mm HIGH TENSILE WIRE

SAMPLE	YIELD STRESS (N/mm^2)	0.2 % PROOF STRESS (N/mm^2)	ULTIMATE STRESS (N/mm^2)	MODULUS OF ELASTICITY (kN/mm^2)
1	1570	1610	1819	208
2	1570	1610	1783	206
3	1570	1610	1803	205

TABLE 5.4b PROPERTIES OF 10 mm TORBAR

SAMPLE	YIELD STRESS (N/mm^2)	ULTIMATE STRESS (N/mm^2)	MODULUS OF ELASTICITY (kN/mm^2)
1	497	605	198
2	497	614	195

TABLE 5.5 TYPE OF LOADING

BEAM REFERENCE	TYPE OF LOADING
R1.3.0	Short-Term
R1.2.2	Combined Loading
R1.1.3	Short-Term
R1.0.5	Combined Loading
R2.3.2	Short-Term
R2.2.4	Combined Loading
R2.1.5	Short-Term
R2.0.7	Combined Loading
R3.4.2	Short-Term
R3.3.4	Long-Term
R3.2.5	Short-Term
I1.2.2	Combined Loading
I1.1.3	Short-Term
I2.3.2	Short-Term
I2.2.4	Combined Loading
I3.3.4	Combined Loading
I3.2.5	Short-Term

TABLE 6.1 CONCRETE STRESSES IN TEST BEAMS

BEAM REFERENCE	COMPUTED CONCRETE STRESS BASED ON UNCRACKED TRANSFORMED SECTION (N/mm^2)					
	EFFECTIVE PRESTRESS		HALF-SERVICE MOMENT		FULL-SERVICE MOMENT	
	TOP FIBRE	BOTTOM FIBRE	TOP FIBRE	BOTTOM FIBRE	TOP FIBRE	BOTTOM FIRBE
R1.3.0	2.96	-8.78	-2.59	-3.23	-8.14	2.32
R1.2.2	1.65	-5.05	-3.48	-0.28	-8.88	5.12
R1.1.3	0.79	-2.45	-4.44	2.57	-9.85	7.97
R1.0.5	0.00	0.00	-5.33	5.26	-10.66	10.52
R2.3.2	2.66	-8.05	-4.54	-1.24	-12.03	6.25
R2.2.4	1.63	-5.02	-5.38	1.57	-12.71	8.91
R2.1.5	0.68	-2.21	-6.30	4.39	-13.58	11.67
R2.0.7	0.00	0.00	-7.23	7.11	-14.46	14.22
R3.4.2	3.08	-9.48	-4.81	-2.34	-13.27	6.12
R3.3.4	2.46	-7.66	-5.32	-0.72	-13.74	7.70
R3.2.5	1.36	-4.37	-6.35	2.60	-14.63	10.88
I1.2.2	1.09	-6.66	-4.80	-1.31	-10.92	4.80
I1.1.3	0.34	-2.57	-5.43	2.43	-11.51	8.50
I2.3.2	1.60	-9.90	-6.51	-2.82	-15.02	5.69
I2.2.4	0.80	-5.67	-6.89	0.65	-15.12	8.89
I3.3.4	1.36	-8.93	-7.52	-1.67	-17.03	7.85
I3.2.5	0.86	-5.90	-7.85	1.50	-17.08	10.73

Sign Convention : Tension(+ve) , Compression(-ve)

TABLE 6.2 STEEL STRESSES BEFORE TEST

BEAM REFERENCE	TENDON STRESS		NON-PRESTRESSED STEEL STRESS	LOSS IN TENDON
	INITIAL (N/mm^2)	BEFORE TEST (N/mm^2)	(N/mm^2)	(%)
R1.3.0	1143	1099	---	3.8
R1.2.2	1151	1108	-50.4	4.0
R1.1.3	1166	1078	-20.0	7.5
R2.3.2	1172	1113	-54.0	5.0
R2.2.4	1147	1091	-29.0	4.8
R2.1.5	1172	1099	-21.6	6.2
R3.4.2	1118	1018	-104	8.9
R3.3.4	1172	1129	-57.0	3.7
R3.2.5	1172	1069	-41.0	8.8
I1.2.2	1128	1100	-48.2	2.5
I1.1.3	1149	1074	-45.3	6.5
I2.3.2	1127	1087	-86.1	3.5
I2.2.4	1121	1107	-59.2	1.2
I3.3.4	1100	1057	-67.6	3.9
I3.2.5	1131	1107	-45.2	2.1

Sign Convention : Tension (+ve)
Compression (-ve)

TABLE 6.3 OBSERVED AND CALCULATED CRACKING AND DECOMPRESSION MOMENT

BEAM REFERENCE	CRACKING MOMENT (kNm)			DECOMPRESSION MOMENT (kNm)		(2) / (1)	(3) / (1)
	OBSERVED (1)	CALCULATED		OBSERVED	CALCULATED		
		MODULUS OF RUPTURE (2)	SPLIT CYLINDER (3)				
R1.3.0	----	31.5	27.6	----	20.1	----	----
R1.2.2	21.3	23.4	20.7	10.7	12.4	1.10	0.97
R1.1.3	13.9	17.1	14.3	*	6.1	1.23	1.03
R1.0.5	12.3	13.3	9.6	*	0.0	1.08	0.78
R2.3.2	29.8	31.7	29.3	17.0	19.4	1.06	0.98
R2.2.4	24.5	26.7	22.3	12.4	12.7	1.09	0.91
R2.1.5	17.5	16.9	15.4	*	5.7	0.97	0.88
R2.0.7	13.9	11.8	9.0	*	0.0	0.85	0.65
R3.4.2	28.7	34.2	32.0	20.2	23.0	1.19	1.11
R3.3.4	28.7	33.1	29.4	17.0	19.5	1.15	1.02
R3.2.5	23.4	23.6	21.5	*	11.3	1.01	0.92
I1.2.2	21.3	24.8	22.6	13.9	14.4	1.16	1.06
I1.1.3	14.9	16.6	14.2	*	5.7	1.11	0.95
I2.3.2	27.7	30.4	28.1	17.1	21.1	1.10	1.01
I2.2.4	23.4	24.1	22.1	11.8	12.9	1.03	0.94
I3.3.4	28.7	30.2	29.3	19.2	20.1	1.05	1.02
I3.2.5	25.5	25.3	23.5	12.8	13.9	0.99	0.92
					MEAN	1.07	0.95
					S.D.	0.09	0.11

* Cracks did not close at the beginning of the 2nd cycle

TABLE 6.4 DEFORMATIONS AT SERVICE LOADS IN THE 1ST AND 2ND LOADING

BEAM REFERENCE	DEFLECTION (mm)		MAXIMUM CRACK WIDTH (mm)	
	1ST CYCLE	2ND CYCLE	1ST CYCLE	2ND CYCLE
R1.3.0	6.4	6.4	N.C.	H.C.
R1.2.2	8.7	9.3	0.08	0.10
R1.1.3	15.3	15.9	0.12	0.14
R1.0.5	18.7	19.2	0.14	0.16
R2.3.2	12.1	12.7	0.10	0.12
R2.2.4	14.0	15.3	0.10	0.10
R2.1.5	19.8	20.3	0.14	0.14
R2.0.7	23.0	23.7	0.12	0.14
R3.4.2	12.9	13.4	0.06	0.06
R3.3.4	14.6	15.0	0.10	----
R3.2.5	17.5	18.1	0.12	0.12
I1.2.2	9.9	10.3	0.06	0.06
I1.1.3	19.8	20.5	0.14	0.14
I2.3.2	14.9	16.3	0.10	0.12
I2.2.4	17.6	18.2	0.08	0.10
I3.3.4	16.9	17.8	0.06	0.06
I3.2.5	19.7	20.7	0.10	0.10

N.C. Represents Not Cracked
H.C. Represents Hair-Cracks

TABLE 6.5 SUMMARY OF DEFLECTION OF BEAMS UNDER COMBINED LOADING TEST

BEAM REFERENCE	INITIAL DEFLECTION		DURATION OF TEST DAYS (NUMBER OF INTERMITTENT CYCLE)	FINAL DEFLECTION		(2) – (1)	(3) – (4)	(4) – (1)	(4) / (1)
	H.S.L. (1)	S.L. (2)		S.L. (3)	H.S.L. (4)				(5)
R1.2.2	1.6	8.7	25 (5)	13.4	6.3	7.1	7.1	4.7	3.94
R1.0.5	2.0	18.7	25 (5)	23.6	16.0	16.7	7.6	14.0	8.00
R2.2.4	2.6	14.0	30 (6)	19.3	11.2	11.4	8.1	8.6	4.31
R2.0.7	4.8	23.0	25 (5)	28.5	19.3	18.2	9.2	14.5	4.02
I1.2.2	2.3	9.9	25 (5)	13.9	6.4	7.6	7.5	4.1	2.78
I2.2.4	3.7	17.6	25 (5)	22.1	11.3	13.9	10.8	7.6	3.05
I3.3.4	4.5	16.9	30 (6)	23.1	12.1	12.4	11.0	7.6	2.69

All deflection in mm
H.S.L. represents half service load
S.L. represents service load

TABLE 6.6 DATA OF AVERAGE CONCRETE STRAIN IN FIRST CYCLE OF LOADING

BEAM REFERENCE	TOP STRAIN ($\times 10^{-5}$)						BOTTOM STRAIN ($\times 10^{-5}$)					
	Z.L. (1)	S.L. (2)	Z.L. (3)	(3) - (1) (4)	(2) - (3) (5)	(4) / (5)	Z.L. (6)	S.L. (7)	Z.L. (8)	(8) - (6) (9)	(7) - (6) (10)	(9) / (10)
R1.3.0	6	-22	3	-3	-25	0.12	-29	-7	-26	3	22	0.14
R1.2.2	2	-31	-2	-4	-29	0.14	-24	21	-18	6	45	0.13
R1.1.3	-3	-43	-10	-7	-33	0.21	-5	89	19	24	94	0.26
R1.0.5	-7	-48	-20	-13	-28	0.46	1	98	40	39	97	0.40
R2.3.2	3	-39	-2	-5	-37	0.14	-27	22	-22	5	49	0.10
R2.2.4	1	-48	-5	-6	-43	0.14	-12	64	-3	9	76	0.12
R2.1.5	-8	-59	-18	-10	-41	0.24	-9	100	13	22	109	0.20
R2.0.7	-10	-64	-24	-14	-40	0.35	3	132	40	37	129	0.29
R3.4.2	8	-48	2	-6	-50	0.12	-54	-5	-48	6	49	0.12
R3.3.4	3	-48	0	-3	-48	0.06	-24	44	-14	10	68	0.15
R3.2.5	-12	-66	-20	-8	-46	0.17	-22	62	-10	12	84	0.14
I1.2.2	-11	-41	-5	-6	-24	0.25	-27	16	-22	5	43	0.12
I1.1.3	-25	-64	-33	-8	-31	0.26	-19	101	5	14	120	0.12
I2.3.2	0	-52	-6	-6	-46	0.13	-40	39	-32	8	79	0.10
I2.2.4	-11	-62	-17	-6	-45	0.13	-28	67	-18	10	95	0.11
I3.3.4	7	-50	2	-5	-51	0.10	-30	55	-22	8	85	0.09
I3.2.5	0	-53	-6	-6	-47	0.13	-20	87	-9	11	107	0.10

Notes : Top Strain--5mm from the top fibre , Bottom Strain--23mm from soffit
Tension(+ve) , Compression (-ve)
Z.L.--Zero Load , S.L.--Service Load

TABLE 6.7 RESIDUAL DEFLECTION AT THE END OF THE FIRST CYCLE

BEAM REFERENCE	EXPERIMENT (1)	PROPOSED METHOD (2)	BRANSON'S METHOD (3)	(2) / (1)	(3) / (1)
R1.3.0	0.78	1.32	0.00	1.69	0.00
R1.2.2	1.09	1.37	0.14	1.26	0.13
R1.1.3	3.61	3.53	4.98	0.98	1.38
R1.0.5	7.11	5.42	6.78	0.76	0.95
R2.3.2	1.28	1.74	0.18	1.36	0.14
R2.2.4	1.95	2.19	1.89	1.12	0.97
R2.1.5	3.92	2.86	7.89	0.73	2.01
R2.0.7	6.49	6.33	11.1	0.98	1.70
R3.4.2	1.38	1.95	1.01	1.41	0.73
R3.3.4	1.52	2.18	1.17	1.43	0.77
R3.2.5	2.52	2.67	6.26	1.06	2.48
I1.2.2	1.14	1.37	0.00	1.20	0.00
I1.1.3	3.86	3.51	5.15	0.91	1.33
I2.3.2	1.55	2.08	0.69	1.34	0.45
I2.2.4	1.89	2.49	3.31	1.32	1.75
I3.3.4	1.54	2.40	1.64	1.56	1.06
I3.2.5	2.01	2.76	3.83	1.37	0.61
All deflection in mm			MEAN	1.20	0.97
			S.D.	0.26	0.71

TABLE 6.8 EXPERIMENTAL ANALYSIS OF TENDON STRESS AT ULTIMATE MOMENT

BEAM REFERENCE	OBSERVED TENDON STRESS *	COMPUTED TENDON STRESS BASED ON DIFFERENT NON-PRESTRESSED STEEL STRESS							
		YIELD STRESS (497)	0.2% P.S. (516)	0.5% P.S. (532)	1% P.S. (550)	1.5% P.S. (570)	2% P.S. (580)	2.5% P.S. (590)	FRACTURE (614)
R1.3.0+	1562	1624	1624	1624	1624	1624	1624	1624	1624
R1.2.2	1578	1860	1815	1779	1738	1692	1669	1646	1591
R1.1.3	1564	2325	2190	2080	1956	1819	1750	1682	1517
R2.3.2	1648	1651	1621	1597	1569	1539	1523	1508	1471
R2.2.4	1464	2320	2229	2156	2073	1980	1934	1882	1778
R2.1.5	1595	3248	3022	2837	2629	2399	2283	2168	1891
R3.4.2	1443	1607	1585	1566	1545	1522	1511	1499	1472
R3.3.4	1402	1639	1579	1530	1475	1413	1382	1352	1278
R3.2.5	1548	2404	2290	2197	2093	1976	1918	1860	1721
I1.2.2	1571	1995	1950	1914	1872	1827	1804	1781	1726
I1.1.3	1576	2517	2383	2273	2149	2012	1944	1875	1711
I2.3.2	1605	1749	1719	1695	1667	1636	1621	1606	1569
I2.2.4	1558	2238	2148	2074	1991	1899	1853	1807	1697
I3.3.4	1586	1960	1900	1851	1795	1734	1703	1672	1599
I3.2.5	1513	2225	2112	2019	1916	1800	1742	1685	1546

All stresses are in N/mm^2

Breaking stress of tendon = 1800 N/mm^2

* Last reading taken from the dynamometers

P.S. represents proof stress

+ Section without non-prestressed steel

TABLE 6.9 APPROXIMATE ESTIMATION OF THE INCREASE IN TENDON STRESS AT ULTIMATE MOMENT DUE TO FRICTION

BEAM REFERENCE	DEFLECTION AT ULTIMATE LOAD (mm)	OBSERVED f_{pb} (N/mm^2)	INCREASE IN f_{pb} DUE TO FRICTION (N/mm^2)	CORRECTED f_{pb} (N/mm^2)	COMPUTED f_{pb} (FROM TABLE 6.8)	
					0.5% P.S.	2.5% P.S.
R1.3.0+	167	1562	89	1651	1624	1624
R1.2.2	220	1578	120	1698	1779	1646
R1.1.3	161	1564	86	1650	2080	1682
R2.3.2	211	1648	120	1768	1597	1508
R2.2.4	244	1464	124	1588	2156	1882
R2.1.5	254	1595	141	1736	2839	2168
R3.4.2	146	1443	72	1515	1566	1499
R3.3.4	169	1402	81	1483	1530	1352
R3.2.5	252	1548	136	1684	2197	1860
I1.2.2	250	1571	137	1708	1914	1781
I1.1.3	220	1576	120	1696	2273	1875
I2.3.2	194	1605	107	1712	1695	1606
I2.2.4	196	1558	105	1663	2074	1807
I3.3.4	210	1586	115	1701	1851	1672
I3.2.5	160	1513	83	1596	2019	1685

+ Section without non-prestressed steel

TABLE 6.10 AVERAGE NON-PRESTRESSED STEEL STRAIN AT MIDSPAN IN 1ST CYCLE

BEAM REFERENCE	EXPERIMENTAL RESULT ($\times 10^{-6}$)	COMPUTED RESULT / EXPERIMENTAL RESULT					
		YU & WINTER	CP110, EQ. 62	MODEL CODE	RAO	β-COEFFICIENT	NO TENSION STIFFENING
R1.3.0+	-----	-----	-----	-----	-----	-----	-----
R1.2.2	44.31	1.889	1.859	1.295	1.261	0.977	2.369
R1.1.3	94.33	1.225	1.145	1.132	1.162	0.970	1.434
R2.3.2	49.65	1.510	1.566	1.158	1.011	1.173	1.901
R2.2.4	76.58	1.255	1.211	1.083	1.102	0.989	1.431
R2.1.5	108.54	1.096	1.037	1.082	1.105	1.030	1.214
R3.4.2	48.77	2.026	2.088	2.069	1.926	1.749	2.350
R3.3.4	68.34	1.132	1.105	1.085	1.049	1.139	1.299
R3.2.5	84.10	1.330	1.288	1.353	1.356	1.203	1.463
I1.2.2	43.43	1.780	1.689	0.898	0.824	1.260	2.212
I1.1.3	120.29	1.193	1.100	1.045	1.072	1.141	1.326
I2.3.2	79.08	1.234	1.213	1.154	1.068	1.214	1.417
I2.2.4	95.60	1.201	1.146	1.130	1.129	1.207	1.321
I3.3.4	84.75	1.099	1.060	1.079	1.053	1.147	1.214
I3.2.5	107.43	1.001	0.948	0.965	0.967	1.036	1.085
	MEAN	1.355	1.318	1.181	1.149	1.160	1.574
	S.D.	0.309	0.332	0.270	0.247	0.188	0.425

Exp. Results : Changes in strain from zero to service load

\+ Section without non-prestressed steel

TABLE 6.11 AVERAGE CURVATURE AT MIDSPAN IN FIRST CYCLE

BEAM REFERENCE	EXPERIMENTAL RESULT ($\times 10^{-5}$ rad/mm)	COMPUTED RESULT / EXPERIMENTAL RESULT					
		YU & WINTER	CP110, EQ. 62	MODEL CODE	RAO	β-COEFFICIENT	NO TENSION STIFFENING
R1.3.0+	-----	-----	-----	-----	-----	-----	-----
R1.2.2	0.280	1.433	1.416	1.108	1.089	0.980	1.697
R1.1.3	0.481	1.116	1.061	1.053	1.074	1.103	1.260
R2.3.2	0.328	1.259	1.288	1.077	1.000	1.155	1.463
R2.2.4	0.457	1.102	1.076	1.002	1.014	0.964	1.205
R2.1.5	0.578	1.009	0.970	1.000	1.016	0.971	1.088
R3.4.2	0.378	1.137	1.164	1.158	1.096	1.039	1.279
R3.3.4	0.452	1.003	0.988	0.978	0.959	0.986	1.094
R3.2.5	0.502	1.093	1.068	1.107	1.108	1.018	1.170
I1.2.2	0.265	1.451	1.399	0.947	0.904	1.192	1.699
I1.1.3	0.577	1.048	0.980	0.940	0.961	1.016	1.146
I2.3.2	0.471	0.989	0.977	0.944	0.894	0.986	1.095
I2.2.4	0.532	0.985	0.951	0.941	0.940	0.995	1.059
I3.3.4	0.511	0.957	0.934	0.946	0.931	0.988	1.023
I3.2.5	0.583	0.961	0.927	0.938	0.939	0.986	1.015
	MEAN	1.110	1.086	1.006	0.995	1.027	1.235
	S.D.	0.157	0.162	0.076	0.071	0.069	0.221

Exp. Results : Changes in Curvature from zero to service load

+ Section without non-prestressed steel

TABLE 6.12 AVERAGE NON-PRESTRESSED STEEL STRAIN AT MIDSPAN IN 1ST CYCLE (BASED ON LEE'S TESTS)

BEAM REFERENCE	EXPERIMENTAL RESULT ($\times 10^{-5}$)	COMPUTED RESULT / EXPERIMENTAL RESULT					
		YU & WINTER	CP110, EQ. 62	MODEL CODE	RAO	β-COEFFICIENT	NO TENSION STIFFENING
S1.5.2	72.5	1.038	1.034	0.843	0.515	1.135	1.199
S1.4.4	70.8	1.596	1.539	1.301	1.210	1.581	1.714
S1.3.5	99.4	1.202	1.154	1.112	1.105	1.157	1.287
S2.4.2	78.0	1.405	1.389	1.291	1.083	1.468	1.583
S2.3.4	93.5	1.167	1.105	1.022	0.986	1.134	1.263
S2.2.6	96.1	1.140	1.065	1.062	1.066	1.066	1.214
S3.3.2	84.9	1.151	1.119	1.031	0.849	1.221	1.344
S3.2.4	88.2	1.328	1.247	1.097	1.084	1.281	1.456
S3.1.6	108.1	1.004	0.910	0.927	0.944	0.920	1.072
S1.3.5s	105.0	1.156	1.109	1.100	1.088	1.109	1.236
S2.3.4s	100.1	1.078	1.016	0.930	0.900	1.045	1.163
S3.3.2s	93.2	0.896	0.866	0.717	0.519	0.969	1.070
	MEAN	1.180	1.129	1.036	0.946	1.174	1.300
	S.D.	0.181	0.181	0.161	0.214	0.184	0.188

Exp. Results : Changes in strain from zero to service load

TABLE 6.13 AVERAGE CURVATURE AT MIDSPAN IN FIRST CYCLE (BASED ON LEE'S TESTS)

BEAM REFERENCE	EXPERIMENTAL RESULT ($\times 10^{-5}$ rad/mm)	COMPUTED RESULT / EXPERIMENTAL RESULT					
		YU & WINTER	CP110, EQ. 62	MODEL CODE	RAO	β-COEFFICIENT	NO TENSION STIFFENING
S1.5.2	0.439	1.053	1.051	0.938	0.744	1.110	1.148
S1.4.4	0.415	1.240	1.205	1.060	1.004	1.230	1.311
S1.3.5	0.575	1.080	1.051	1.025	1.021	1.053	1.133
S2.4.2	0.445	1.137	1.127	1.065	0.935	1.177	1.249
S2.3.4	0.492	1.193	1.151	1.095	1.070	1.171	1.258
S2.2.6	0.504	1.163	1.113	1.111	1.113	1.113	1.214
S3.3.2	0.448	1.045	1.024	0.964	0.841	1.093	1.176
S3.2.4	0.469	1.270	1.215	1.114	1.106	1.237	1.355
S3.1.6	0.587	1.186	1.116	1.129	1.142	1.124	1.237
S1.3.5e	0.547	1.112	1.080	1.074	1.065	1.080	1.167
S2.3.4e	0.526	1.134	1.092	1.034	1.013	1.112	1.192
S3.3.2e	0.454	0.994	0.972	0.863	0.718	1.047	1.121
	MEAN	1.134	1.100	1.039	0.981	1.129	1.213
	S.D.	0.079	0.068	0.077	0.137	0.060	0.069

Exp. Results : Changes in Curvature from zero to service load

TABLE 6.14 COMPUTED SHORT-TERM DEFLECTION AT SERVICE LOAD IN 1ST CYCLE BASED ON CP110

BEAM REFERENCE	β = 0.5	β = 0.33	β = 0.32	β = 0	EXPERIMENTAL β
R1.3.0	5.6 (0.88)	5.6 (0.88)	5.6 (0.88)	5.6 (0.88)	----
R1.2.2	10.9 (1.25)	11.9 (1.37)	12.0 (1.38)	13.8 (1.59)	0.80
R1.1.3	13.7 (0.90)	16.0 (1.05)	16.1 (1.05)	20.2 (1.32)	0.36
R2.3.2	12.2 (1.01)	13.1 (1.08)	13.2 (1.09)	14.6 (1.21)	0.51
R2.2.4	12.8 (0.91)	14.2 (1.01)	14.2 (1.01)	16.8 (1.20)	0.37
R2.1.5	15.5 (0.78)	17.8 (0.90)	17.9 (0.90)	22.1 (1.12)	0.17
R3.4.2	13.2 (1.02)	13.9 (1.08)	13.9 (1.08)	15.2 (1.18)	0.50
R3.3.4	13.1 (0.90)	14.0 (0.96)	14.4 (0.99)	15.6 (1.07)	0.19
R3.2.5	15.0 (0.86)	16.8 (0.96)	16.9 (0.97)	20.1 (1.15)	0.22
I1.2.2	10.5 (1.06)	11.4 (1.15)	11.4 (1.15)	13.0 (1.31)	0.60
I1.1.3	15.0 (0.76)	17.5 (0.88)	17.6 (0.89)	22.2 (1.12)	0.17
I2.3.2	13.7 (0.92)	14.6 (0.98)	14.7 (0.99)	16.2 (1.09)	0.26
I2.2.4	14.2 (0.81)	15.7 (0.89)	15.8 (0.90)	18.7 (1.06)	0.12
I3.3.4	14.5 (0.86)	15.5 (0.92)	15.6 (0.92)	17.4 (1.03)	0.09
I3.2.5	15.7 (0.80)	17.3 (0.88)	17.4 (0.88)	20.2 (1.03)	0.06
MEAN	(0.915)	(0.999)	(1.005)	(1.157)	0.32
S.D.	(0.123)	(0.129)	(0.130)	(0.158)	0.21

All deflections in mm

Values in brackets are ratios of computed deflection to experimental deflection

TABLE 6.15 COMPUTED SHORT-TERM DEFLECTION BASED ON MODEL CODE AND ACI CODE

BEAM REFERENCE	MODEL CODE (1)	ACI CODE		
		ACTUAL SECTION (2)	R.C. SECTION (3)	ACTUAL SECTION* (4)
R1.3.0	5.7 (0.89)	5.7 (0.89)	5.7 (0.89)	5.7 (0.89)
R1.2.2	9.7 (1.11)	8.0 (0.92)	8.1 (0.93)	8.7 (1.00)
R1.1.3	16.2 (1.06)	15.2 (0.99)	15.2 (0.99)	18.3 (1.20)
R2.3.2	11.5 (0.95)	10.1 (0.84)	10.1 (0.84)	10.7 (0.88)
R2.2.4	14.7 (1.05)	14.6 (1.04)	14.6 (1.04)	16.8 (1.20)
R2.1.5	19.7 (1.00)	21.7 (1.10)	21.7 (1.10)	23.5 (1.19)
R3.4.2	14.0 (1.08)	13.6 (1.06)	13.8 (1.07)	15.1 (1.17)
R3.3.4	14.0 (0.96)	15.0 (1.03)	15.1 (1.04)	16.6 (1.14)
R3.2.5	18.6 (1.06)	21.1 (1.20)	21.1 (1.20)	23.0 (1.31)
I1.2.2	8.4 (0.85)	7.4 (0.75)	7.4 (0.75)	7.6 (0.77)
I1.1.3	17.5 (0.88)	17.0 (0.86)	17.0 (0.86)	20.0 (1.01)
I2.3.2	14.3 (0.96)	13.3 (0.89)	13.4 (0.89)	14.6 (0.98)
I2.2.4	16.3 (0.93)	17.3 (0.98)	17.3 (0.98)	19.7 (1.11)
I3.3.4	16.0 (0.95)	17.4 (1.03)	17.5 (1.04)	19.3 (1.14)
I3.2.5	18.3 (0.93)	20.7 (1.05)	20.7 (1.05)	22.7 (1.15)
MEAN	(0.977)	(0.975)	(0.978)	(1.080)
S.D.	(0.079)	(0.116)	(0.117)	(0.148)

All deflections in mm
+ using power of 4 in the I-effective equation
Values in brackets are ratios of computed to exp. deflection

TABLE 6.16 COMPUTED LONG-TERM DEFLECTION BASDED ON ACI CODE

BEAM REFERENCE	DURATION OF TEST DAYS (NO. OF INTERMITTENT CYCLES)	SERVICE LOAD (mm)	HALF-SERVICE LOAD (mm)
R1.2.2	25 (5)	9.1 (0.68)	2.7 (0.43)
R1.0.5	25 (5)	20.0 (0.85)	2.4 (0.15)
R2.2.4	30 (6)	16.3 (0.84)	4.8 (0.43)
R2.0.7	25 (5)	29.2 (1.02)	11.0 (0.57)
R3.3.4	336 (0)	———	8.9 (0.59)
I1.2.2	25 (5)	8.9 (0.64)	3.9 (0.61)
I2.2.4	25 (5)	19.6 (0.89)	5.9 (0.52)
I3.3.4	30 (6)	20.4 (0.88)	7.6 (0.63)

Values in brackets are (comp./exp. deflection)

TABLE 6.17 INCREASE IN TENDON STRESS AT SERVICE LOADS IN 1ST CYCLE

BEAM REFERENCE	EXPERIMENT (1)	CRACKED SECTION THEORY (2)	NILSON (3)	BALAGURU (4)	(2) / (1)	(3) / (1)	(4) / (1)
R1.3.0	18	19	20	17	1.06	1.11	0.94
R1.2.2	21	35	28	23	1.67	1.33	1.10
R1.1.3	53	73	48	44	1.38	0.91	0.83
R2.3.2	34	51	37	30	1.50	1.09	0.88
R2.2.4	50	63	51	41	1.26	1.02	0.82
R2.1.5	81	97	68	61	1.20	0.84	0.75
R3.4.2	44	53	54	40	1.20	1.23	0.91
R3.3.4	44	62	56	43	1.41	1.27	0.98
R3.2.5	55	80	73	59	1.45	1.33	1.07
I1.2.2	32	41	26	21	1.28	0.81	0.66
I1.1.3	78	97	55	47	1.24	0.71	0.60
I2.3.2	59	64	50	38	1.08	0.85	0.64
I2.2.4	46	80	60	48	1.74	1.30	1.04
I3.3.4	78	72	64	49	0.92	0.82	0.63
I3.2.5	79	88	70	56	1.11	0.89	0.71
				MEAN	1.30	1.03	0.84
				S.D.	0.22	0.21	0.16

All stresses in N/mm^2

TABLE 6.18 COMPUTED AND OBSERVED ULTIMATE MOMENTS OF RESISTANCE

BEAM REFERENCE	EXP. Mu	Mud / EXP. Mu	COMPUTED Mu (UNFACTORED)					
			0.5% PROOF STRESS			2.5% PROOF STRESS		
			TAM & PANNELL	ACI CODE	CP110	TAM & PANNELL	ACI CODE	CP110
R1.3.0	44.89	0.81	37.16 (0.83)	37.37 (0.83)	38.29 (0.85)	37.16 (0.83)	37.37 (0.83)	38.29 (0.85)
R1.2.2	54.75	0.71	46.26 (0.82)	49.17 (0.90)	46.94 (0.86)	48.51 (0.89)	51.47 (0.94)	49.18 (0.90)
R1.1.3	52.09	0.69	45.13 (0.87)	47.15 (0.91)	45.28 (0.87)	48.47 (0.93)	50.56 (0.97)	48.62 (0.93)
R2.3.2	65.03	0.73	57.24 (0.88)	59.50 (0.91)	58.34 (0.90)	59.41 (0.91)	61.75 (0.95)	60.51 (0.93)
R2.2.4	81.46	0.63	67.01 (0.82)	71.38 (0.88)	67.93 (0.83)	71.36 (0.88)	75.85 (0.93)	72.28 (0.89)
R2.1.5	78.81	0.62	65.89 (0.84)	68.47 (0.87)	66.25 (0.84)	71.23 (0.90)	73.96 (0.94)	71.61 (0.91)
R3.4.2	76.69	0.73	64.70 (0.84)	65.68 (0.86)	65.23 (0.85)	66.76 (0.87)	67.85 (0.88)	67.28 (0.88)
R3.3.4	83.90	0.72	78.35 (0.93)	82.31 (0.98)	79.93 (0.95)	82.56 (0.98)	86.68 (1.03)	84.12 (1.00)
R3.2.5	90.47	0.64	75.64 (0.84)	79.45 (0.88)	76.20 (0.84)	80.76 (0.89)	84.77 (0.94)	81.33 (0.90)
I1.2.2	57.63	0.65	46.64 (0.81)	50.47 (0.88)	47.65 (0.83)	48.93 (0.85)	52.80 (0.92)	49.93 (0.87)
I1.1.3	54.24	0.68	45.54 (0.84)	47.69 (0.88)	45.93 (0.85)	48.98 (0.90)	51.20 (0.94)	49.38 (0.91)
I2.3.2	67.17	0.70	56.96 (0.85)	58.69 (0.87)	57.79 (0.86)	59.09 (0.88)	60.92 (0.91)	59.92 (0.89)
I2.2.4	80.42	0.63	66.81 (0.83)	70.85 (0.88)	67.62 (0.84)	71.11 (0.88)	75.28 (0.94)	71.93 (0.89)
I3.3.4	92.61	0.64	76.56 (0.83)	80.40 (0.87)	77.76 (0.84)	80.78 (0.87)	84.78 (0.92)	81.98 (0.89)
I3.2.5	89.01	0.64	76.77 (0.86)	80.98 (0.91)	77.63 (0.87)	81.95 (0.92)	86.34 (0.97)	82.81 (0.93)
MEAN		0.68	(0.85)	(0.89)	(0.86)	(0.89)	(0.93)	(0.90)
S.D.		0.05	(0.028)	(0.032)	(0.030)	(0.034)	(0.042)	(0.033)

All moments in kNm
Values in brackets are (Computed Mu / Observed Mu)
Mud : Calculated design ultimate moment according to CP110

TABLE 6.19 COMPUTED TENDON STRESS AT ULTIMATE MOMENT

BEAM REFERENCE	TAM & PANNELL	ACI CODE	CP110	$f_{pb} - f_{pe}$		f_{pb} / f_{pe}	
				COMPUTED ACI	ACTUAL	COMPUTED CP110	ACTUAL
R1.3.0	1339 (0.86)	1336 (0.86)	1382 (0.88)	237	463	1.26	1.42
R1.2.2	1301 (0.82)	1445 (0.92)	1336 (0.85)	337	470	1.21	1.42
R1.1.3	1302 (0.83)	1491 (0.95)	1316 (0.84)	413	486	1.22	1.45
R2.3.2	1294 (0.79)	1358 (0.82)	1334 (0.81)	245	535	1.20	1.48
R2.2.4	1280 (0.87)	1493 (1.02)	1326 (0.91)	402	373	1.22	1.34
R2.1.5	1289 (0.81)	1503 (0.94)	1316 (0.83)	404	496	1.20	1.45
R3.4.2	1216 (0.84)	1219 (0.84)	1228 (0.85)	201	425	1.21	1.42
R3.3.4	1309 (0.93)	1426 (1.02)	1364 (0.97)	297	273	1.21	1.24
R3.2.5	1259 (0.81)	1426 (0.92)	1282 (0.83)	357	479	1.20	1.45
I1.2.2	1304 (0.83)	1498 (0.95)	1357 (0.86)	398	471	1.23	1.45
I1.1.3	1284 (0.82)	1487 (0.95)	1321 (0.84)	413	502	1.23	1.47
I2.3.2	1299 (0.81)	1341 (0.84)	1329 (0.83)	254	518	1.22	1.48
I2.2.4	1283 (0.82)	1476 (0.95)	1323 (0.85)	369	451	1.20	1.41
I3.3.4	1237 (0.78)	1351 (0.85)	1278 (0.81)	294	529	1.21	1.50
I3.2.5	1306 (0.86)	1497 (0.99)	1346 (0.89)	390	406	1.22	1.37

All stresses in N/mm^2
Results calculated based on 0.5% proof stress in the non-prestressed steel
Values in brackets are ratios of computed result to experimental result

FIG. 4.1 STRESS AND STRAIN DISTRIBUTIONS AT DIFFERENT LOADING STAGES

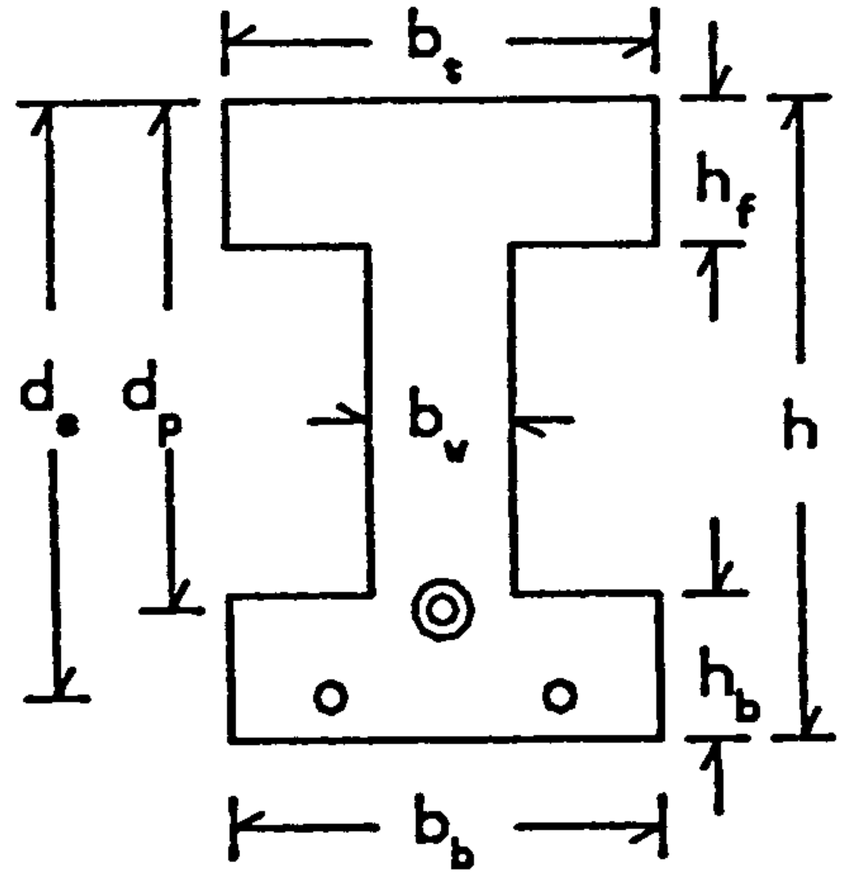

◎ Ap

o As

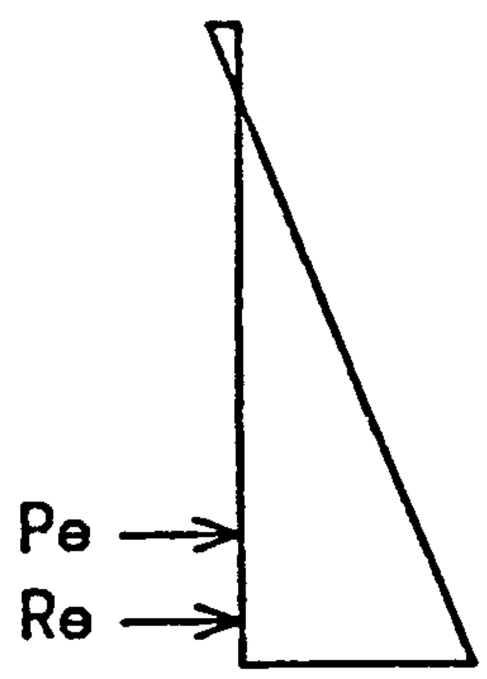

(a)

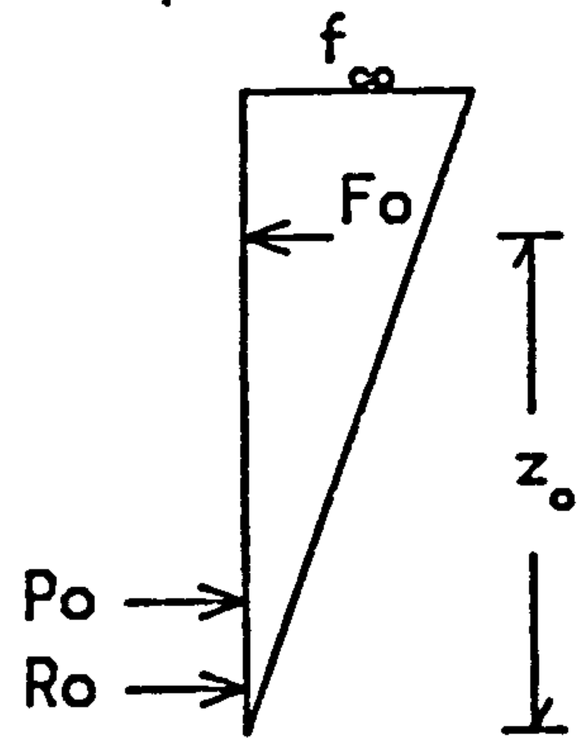

(b)

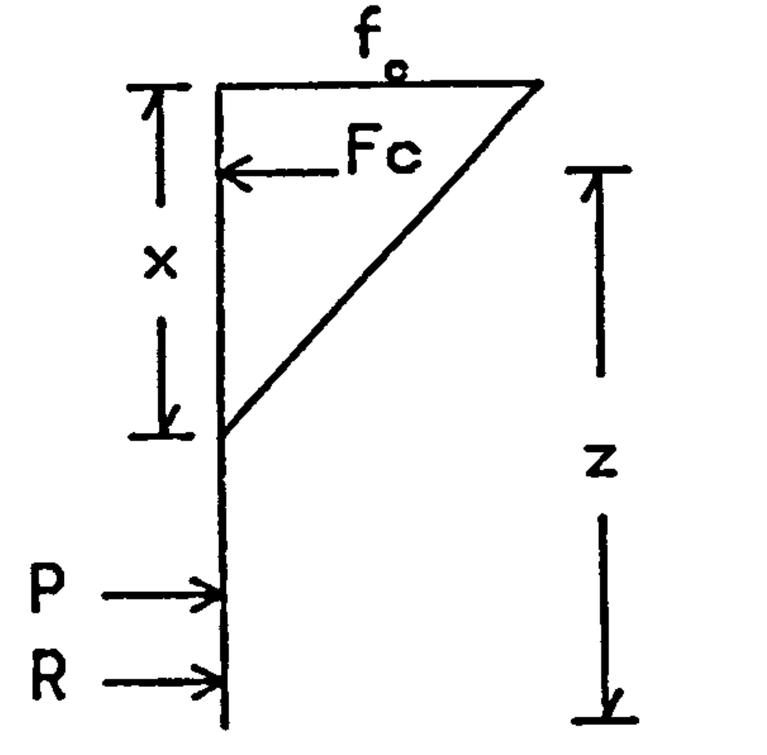

(c)

STRESS DISTRIBUTIONS

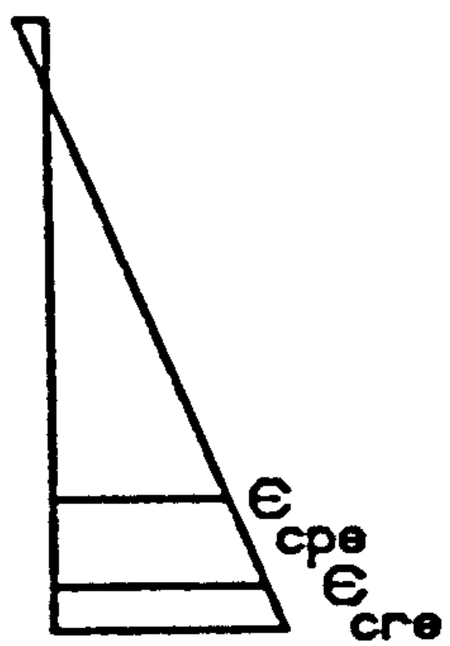

(d)

(e)

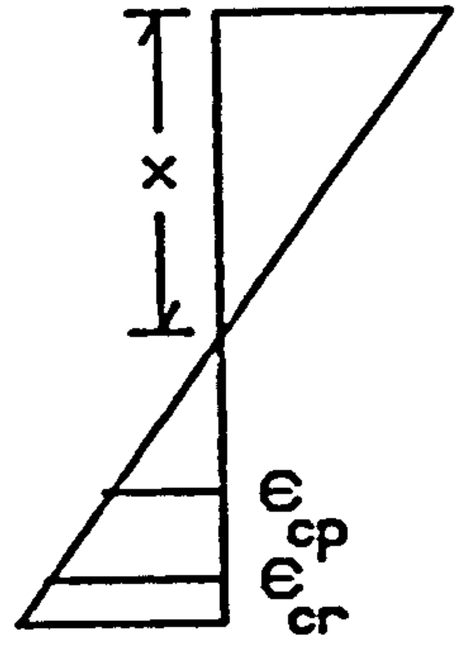

(f)

STRAIN DISTRIBUTIONS

FIG. 4.2 STRAIN DISTRIBUTION BETWEEN CRACKS AT THE TENDON LEVEL

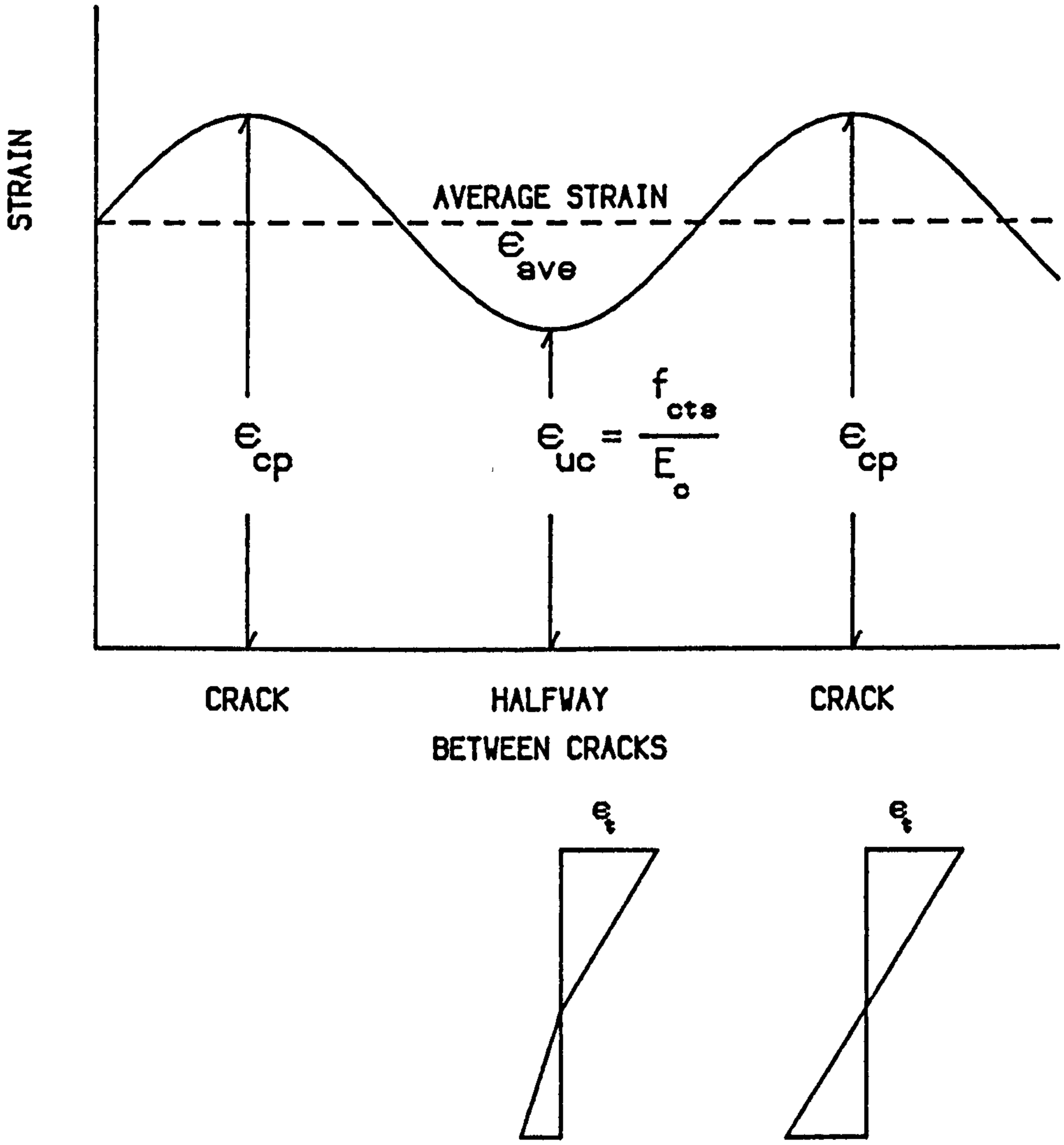

FIG. 4.3 TWO-POINT LOADING SYSTEM

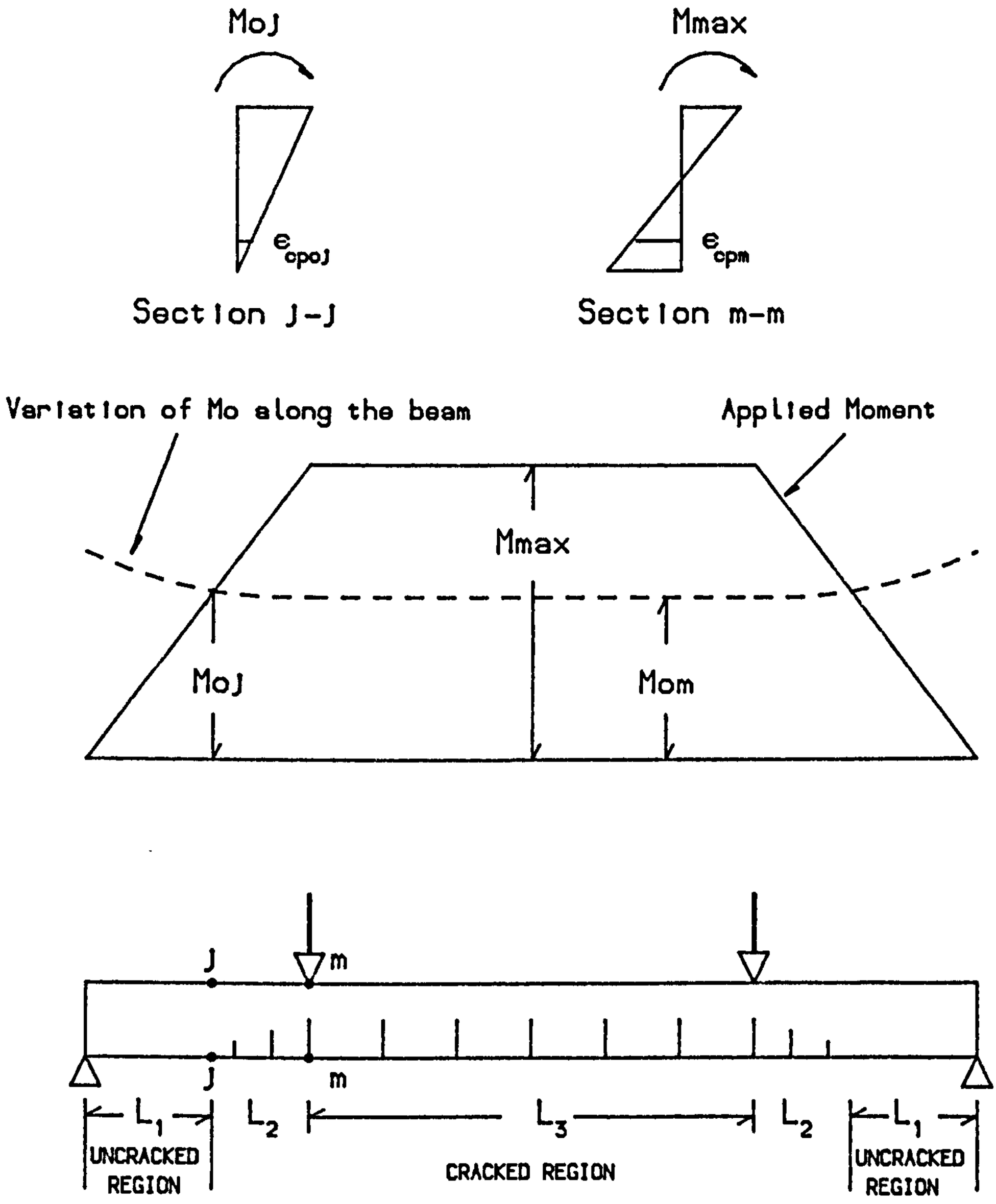

Mom : Decompression Moment of Section m-m
Moj : Decompression Moment of Section J-J

FIG. 4.4 CRITICAL SECTION UNDER DECOMPRESSION MOMENT Mom

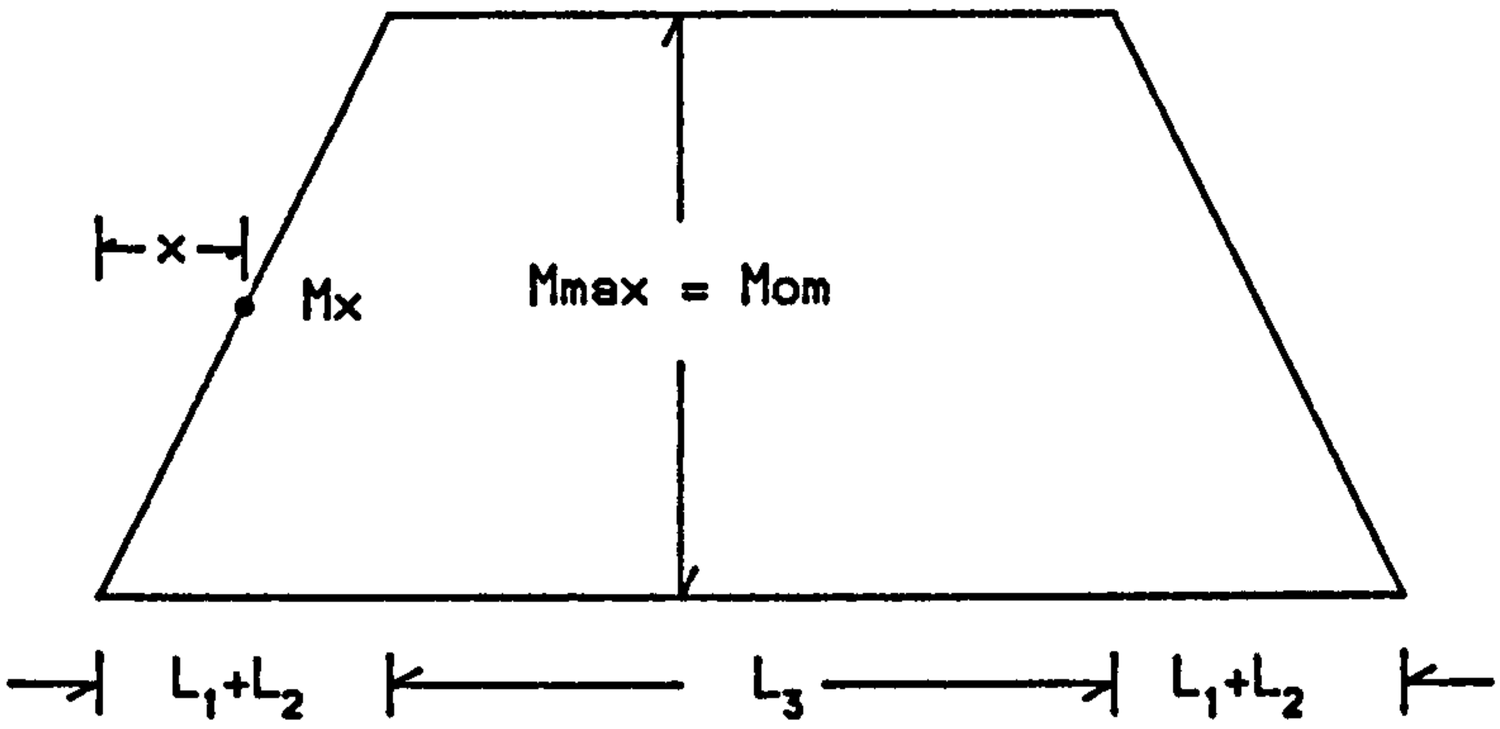

FIG. 4.5 TYPICAL CURVATURE DISTRIBUTION OF A CRACKED PRESTRESSED BEAM

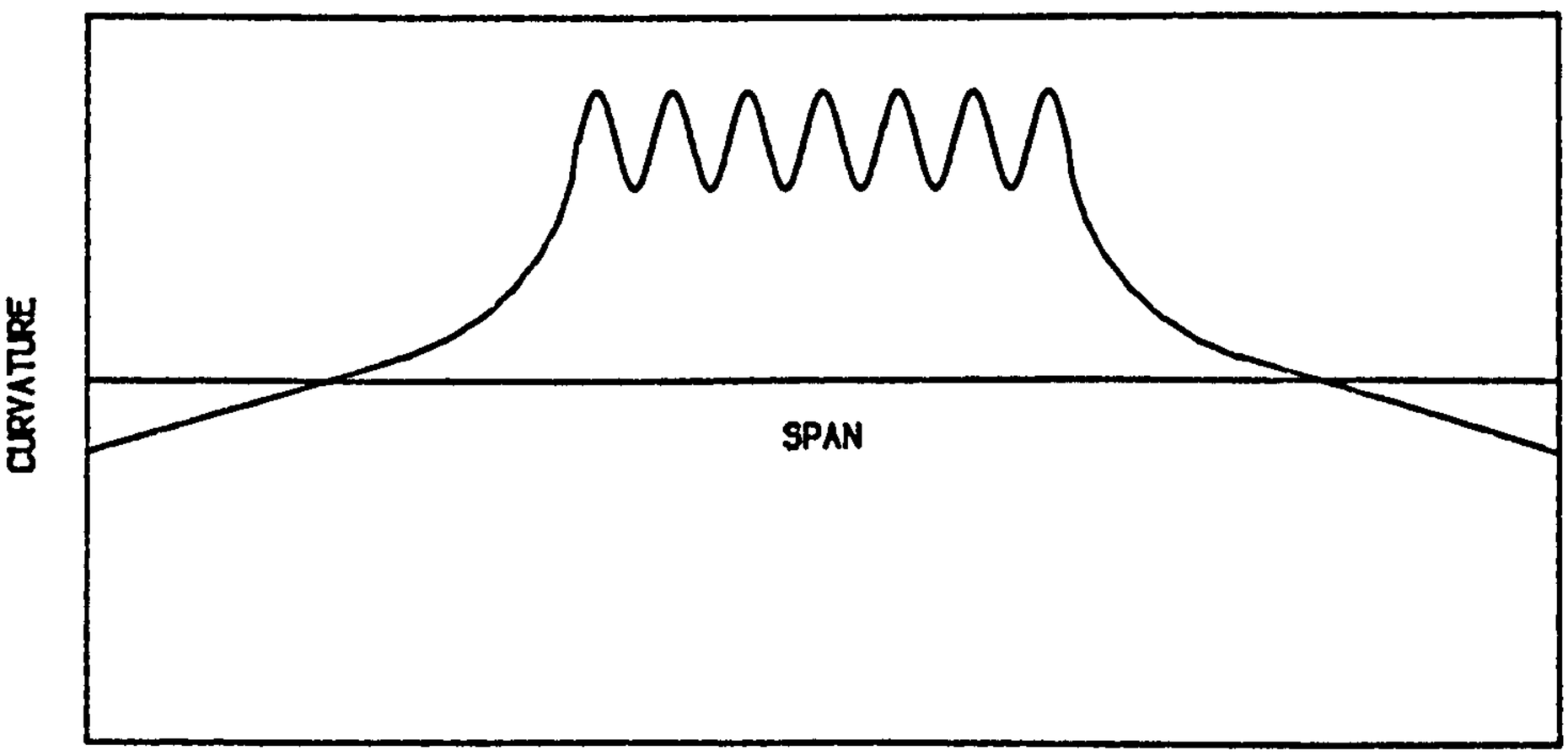

FIG. 5.1 CROSS SECTION OF BEAMS

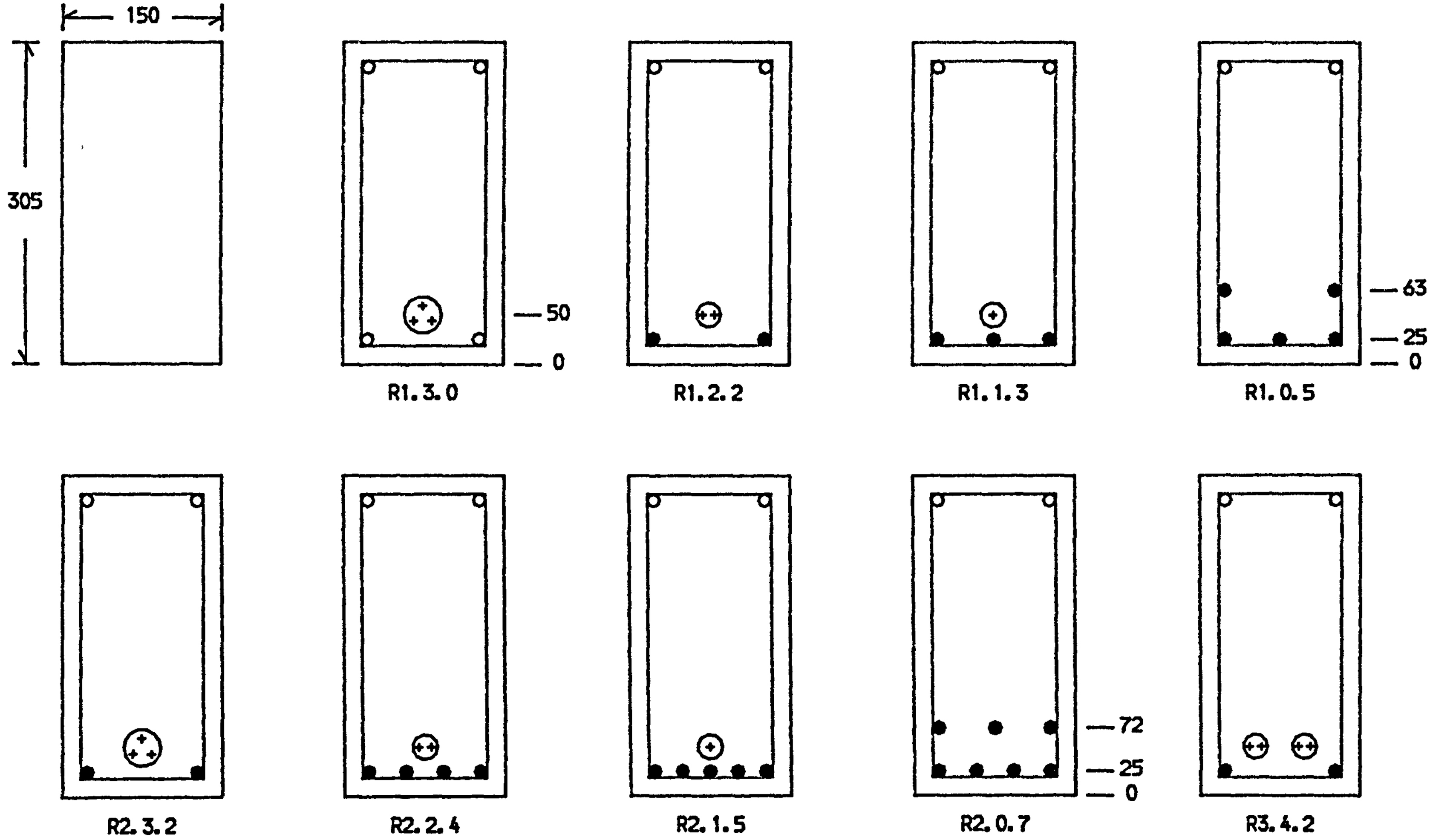

\+ 7 mm high tensile wire
o 6 mm mild steel bar
● 10 mm cold-work deformed bar

Cover to bottom reinforcement (centre) = 23 mm unless otherwise stated
Top and side cover to stirrup = 12 mm
Duct diameter = 20 or 30 mm accordingly

FIG. 5.1 (CONTINUE)

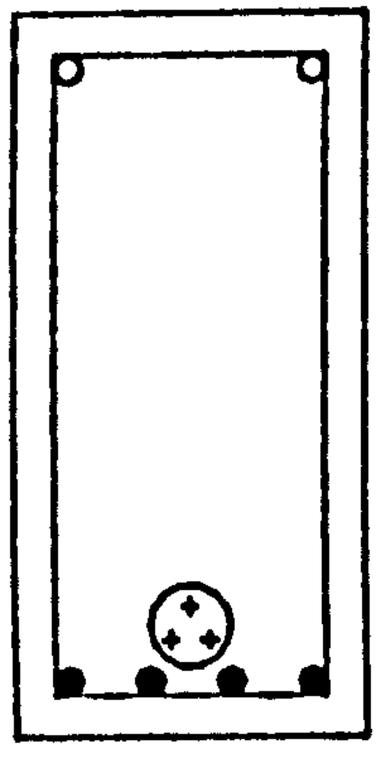

R3.3.4

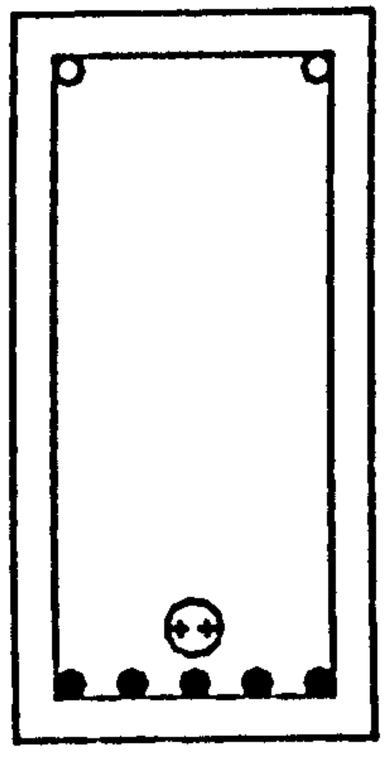

R3.2.5

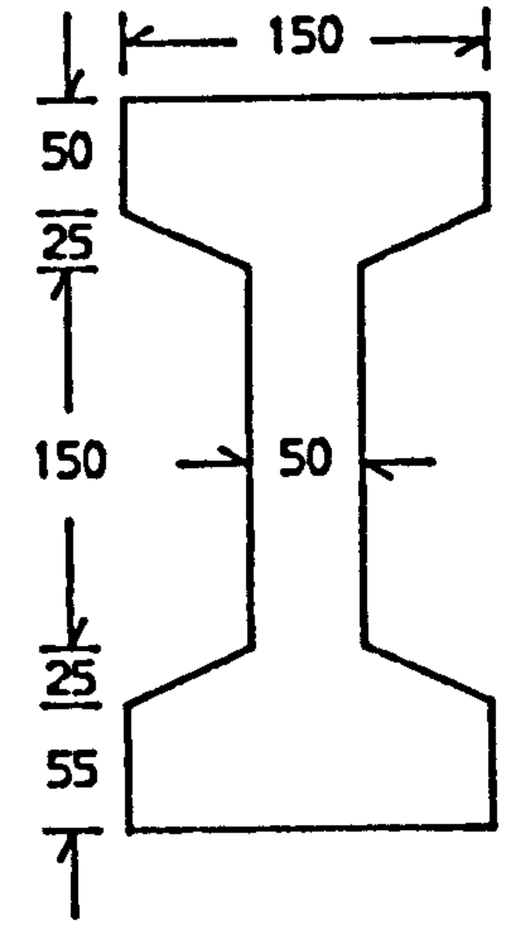

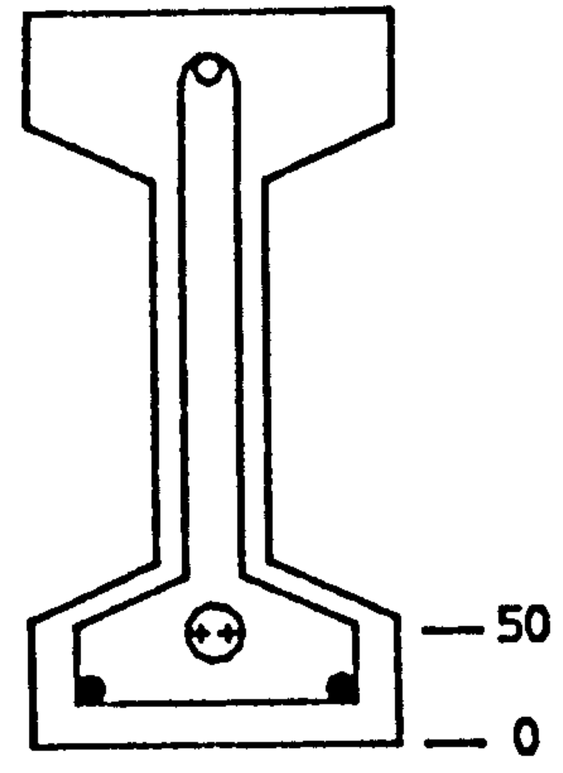

I1.2.2

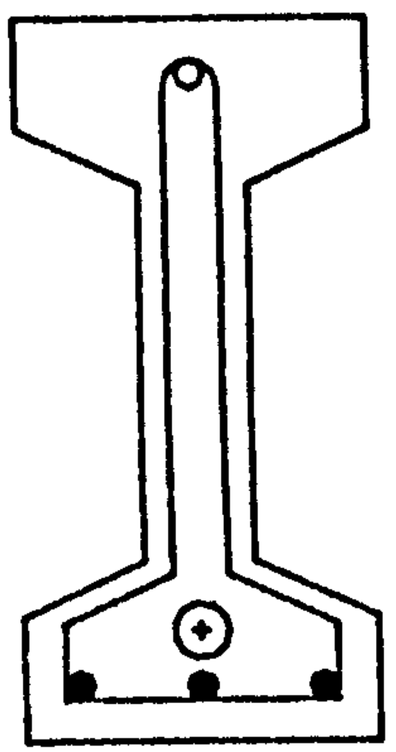

I1.1.3

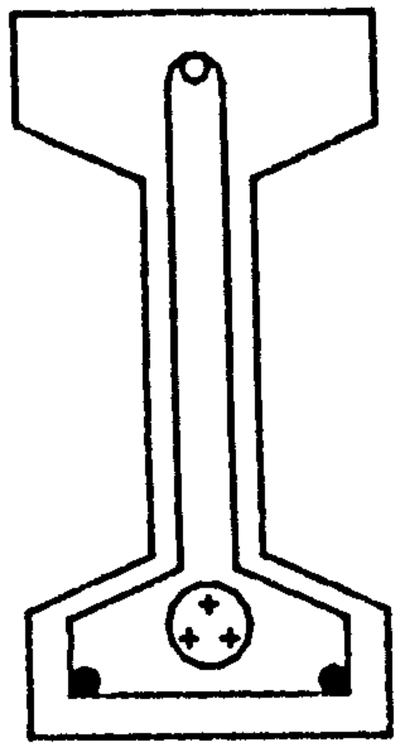

I2.3.2

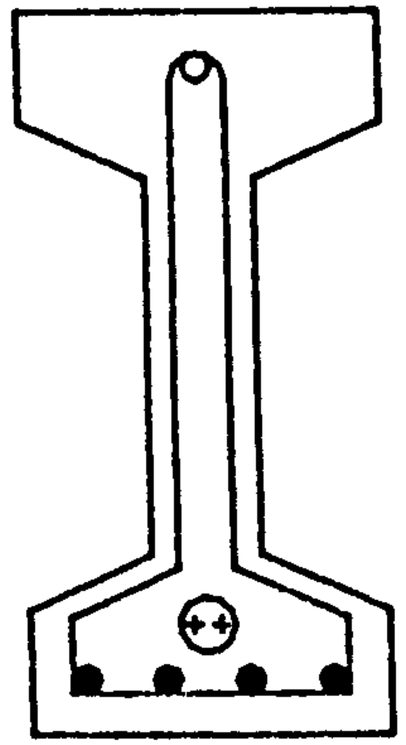

I2.2.4

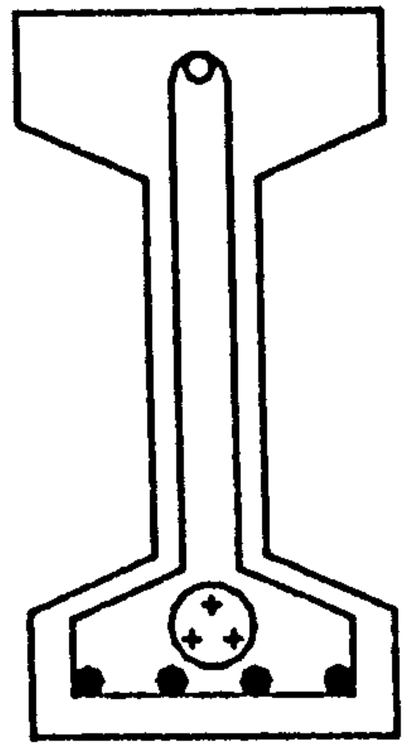

I3.3.4

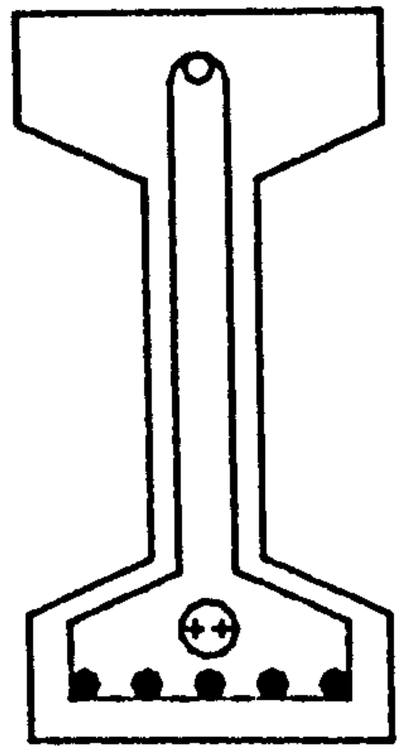

I3.2.5

+ 7 mm high tensile wire
o 6 mm mild steel bar
● 10 mm cold-work deformed bar

Cover to bottom reinforcement (centre) = 23 mm unless otherwise stated
Top and side cover to stirrup = 12 mm
Duct diameter = 20 or 30 mm accordingly
All dimensions in mm

FIG. 5.2a STRESS-STRAIN RELATIONSHIP OF 7 mm HIGH-TENSILE WIRE

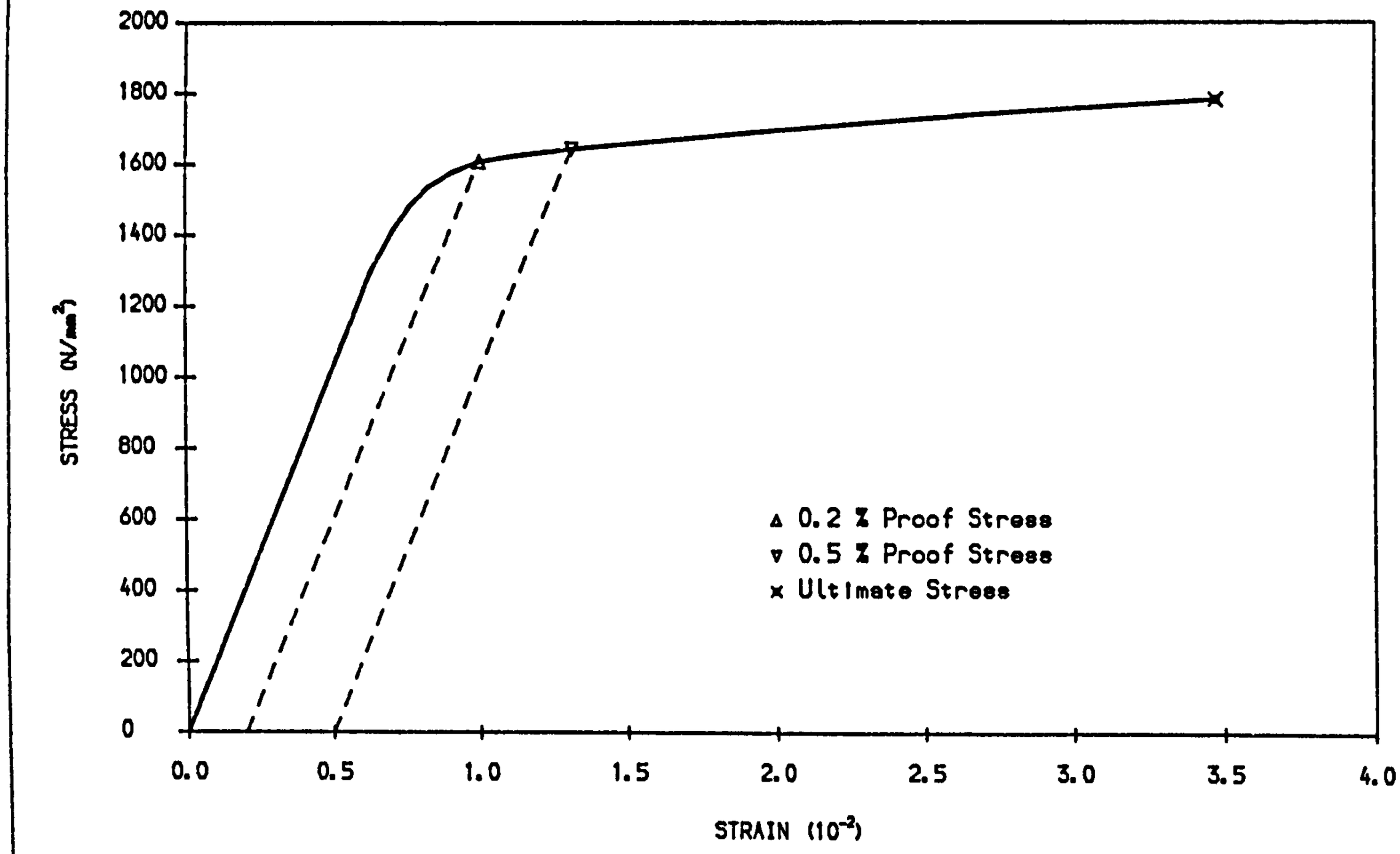

FIG. 5.2b STRESS-STRAIN RELATIONSHIP OF 10 mm COLD-WORK DEFORMED BAR

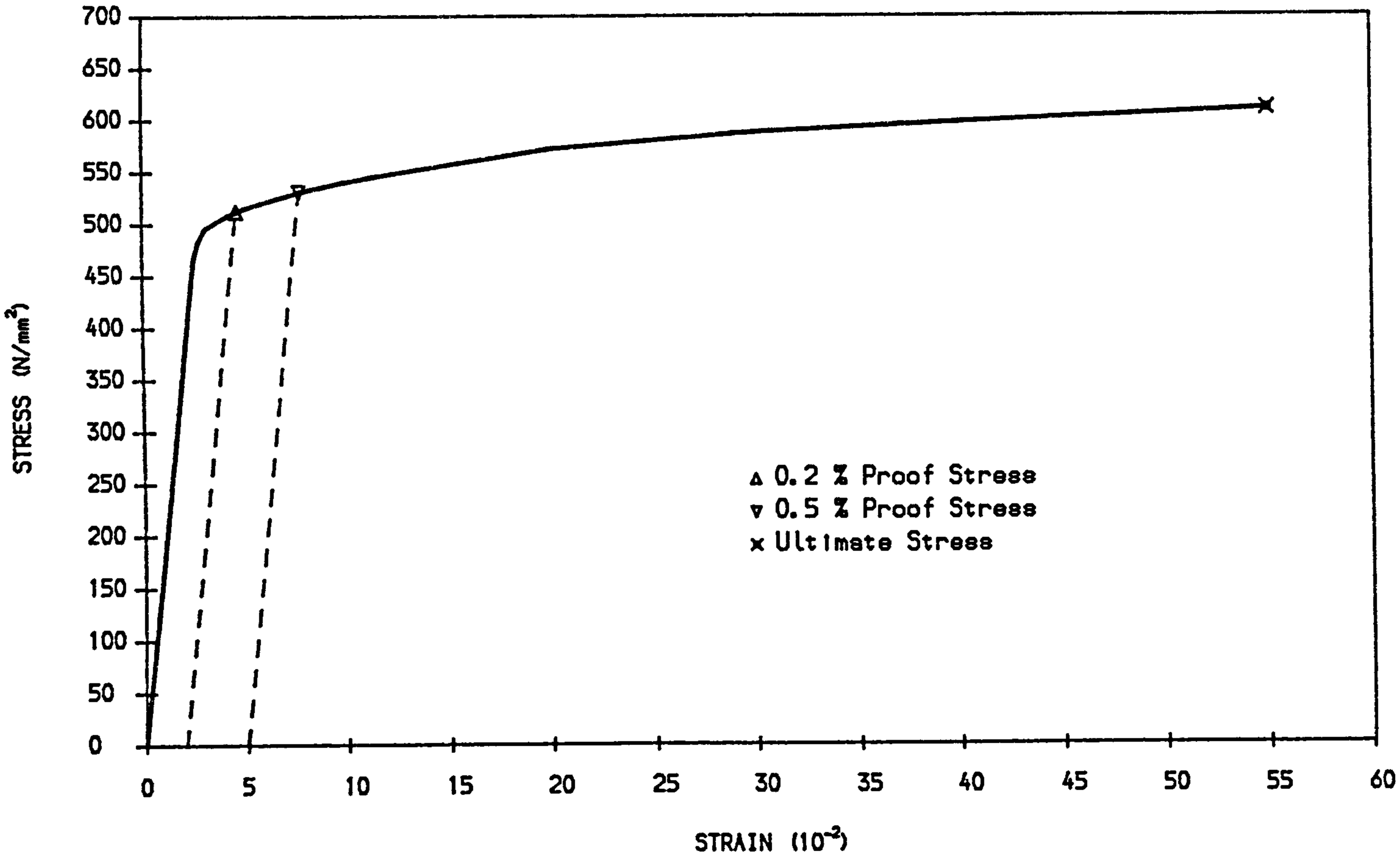

FIG. 5.3 TYPICAL LONGITUDINAL SECTION SHOWING REINFORCEMENT DETAILS

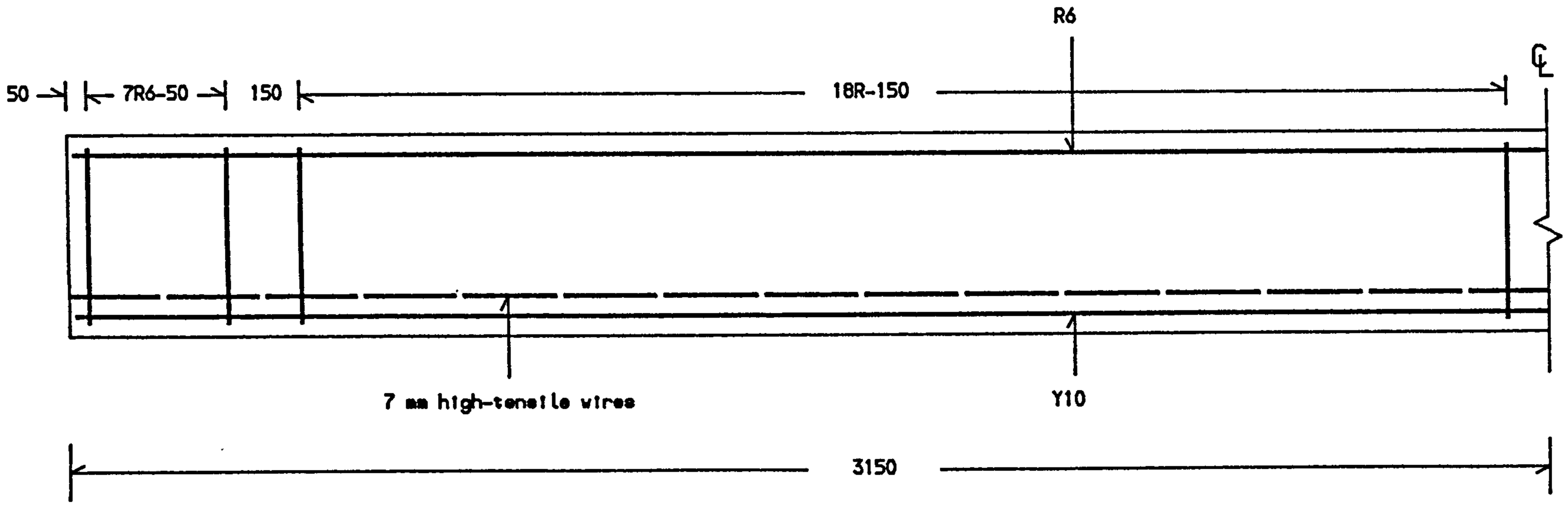

All dimensions in mm
This drawing should be read in conjunction with FIG. 5.1 .

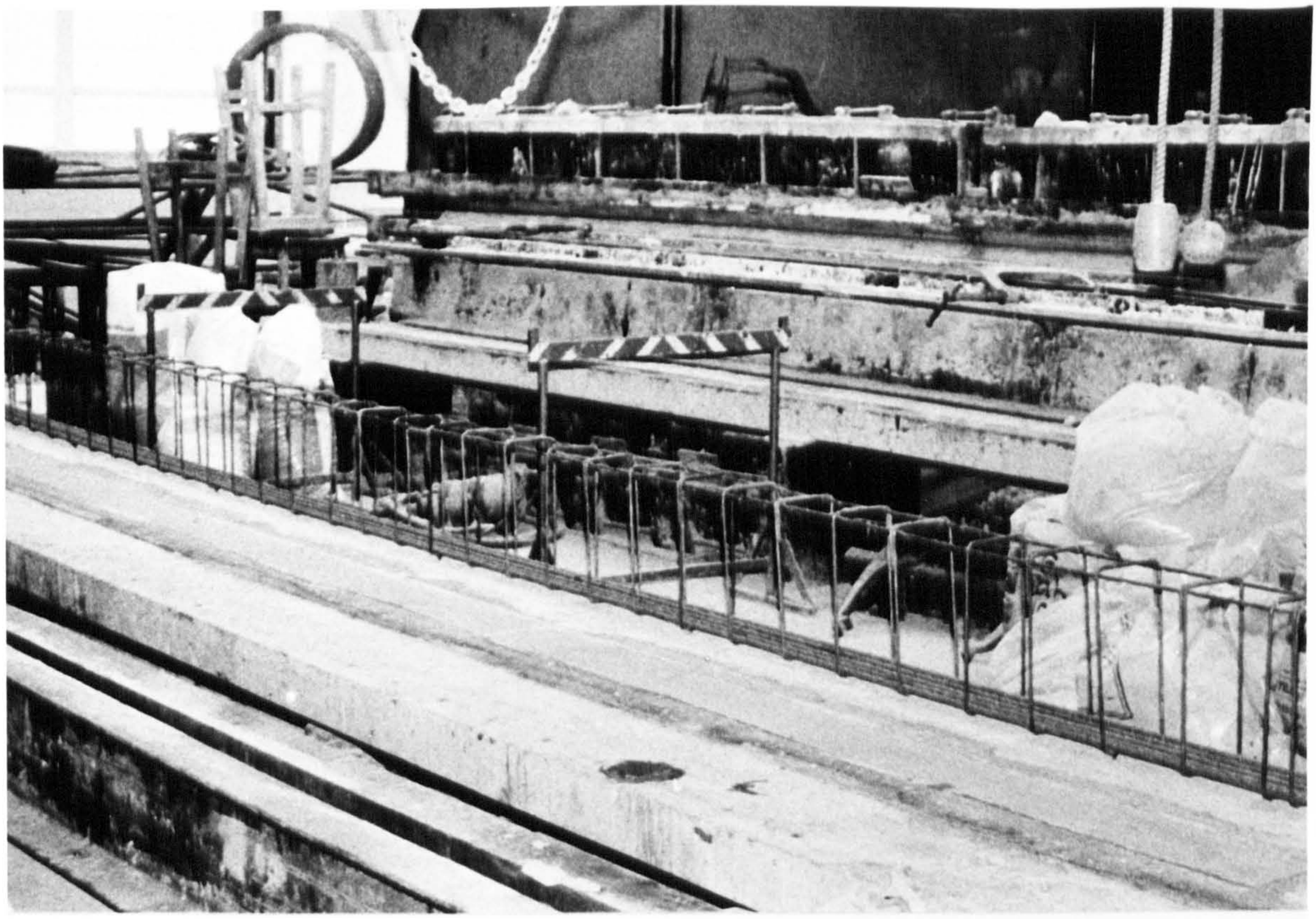

Fig.5.4 Casting bed, mould and reinforcement cage.

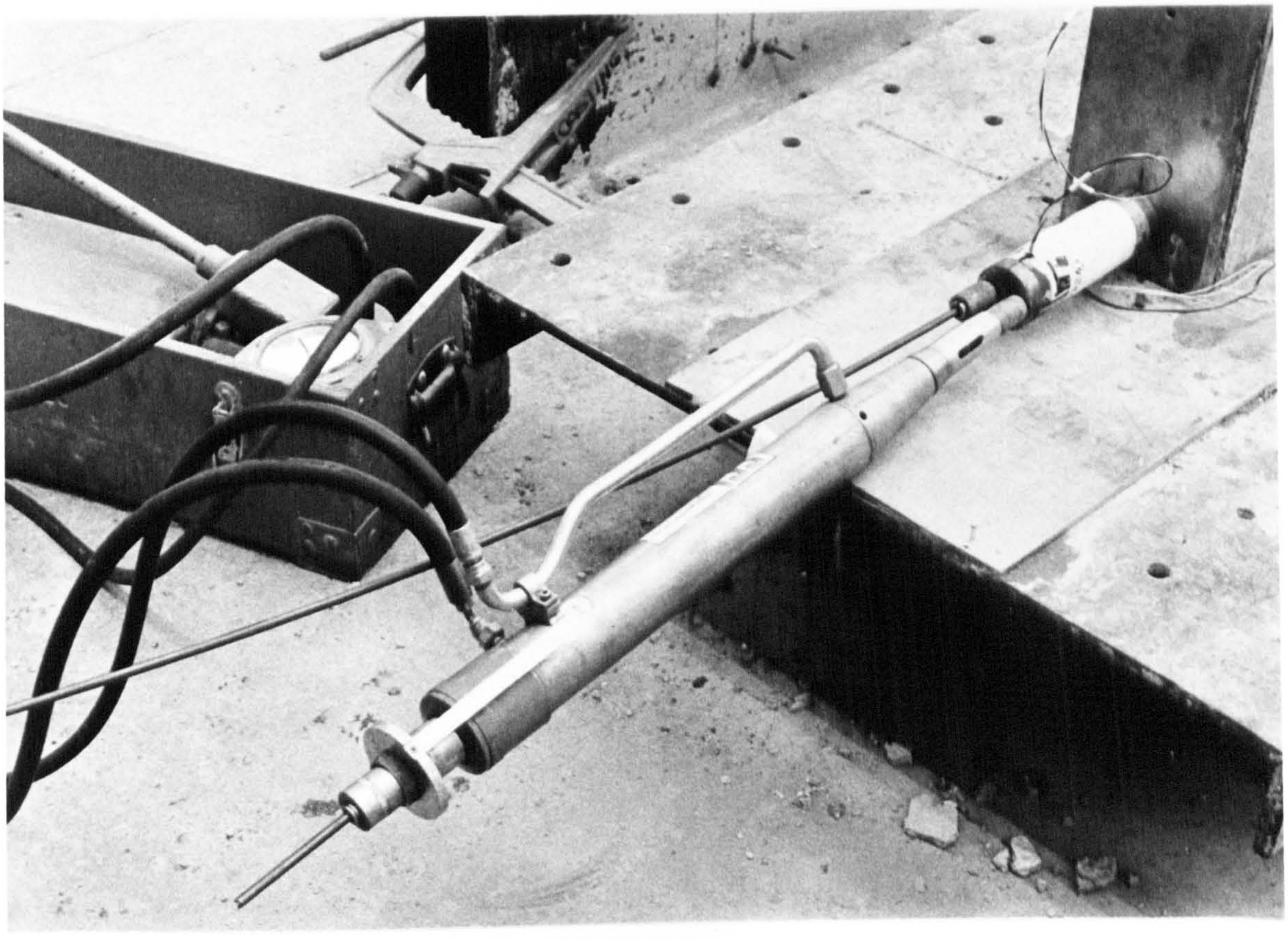

Fig.5.5 Prestressing Apparatus.

FIG.5.6 LOADING ARRANGEMENT, DETAIL POSITIONS OF DEMEC STUDS AND DIAL GAUGES

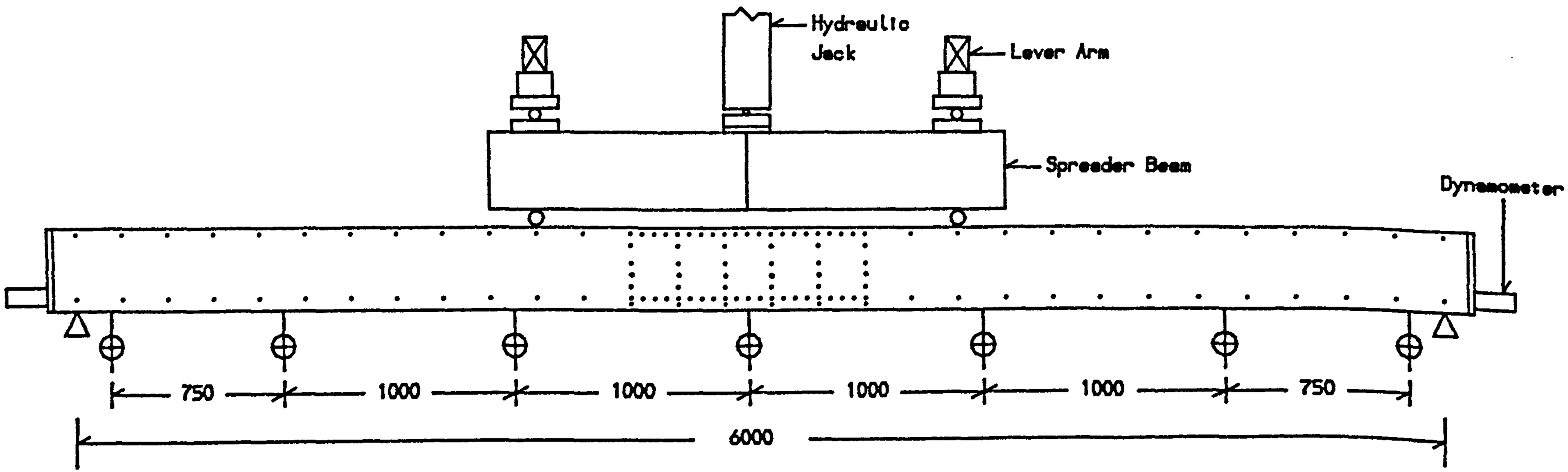

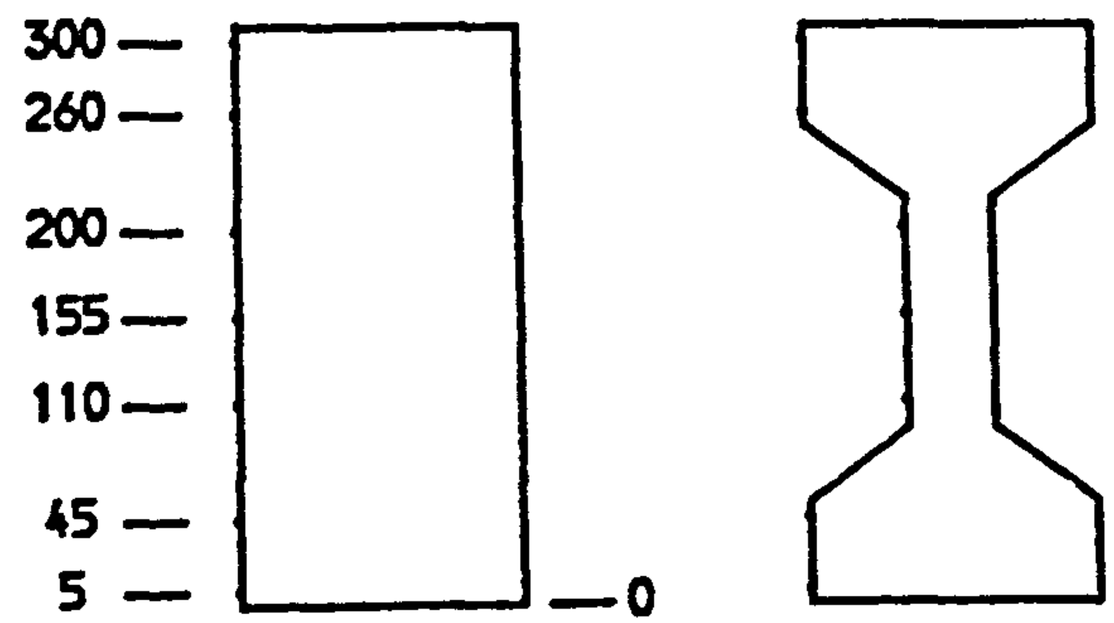

Load Point from support = 2120 mm

All Dimensions in mm

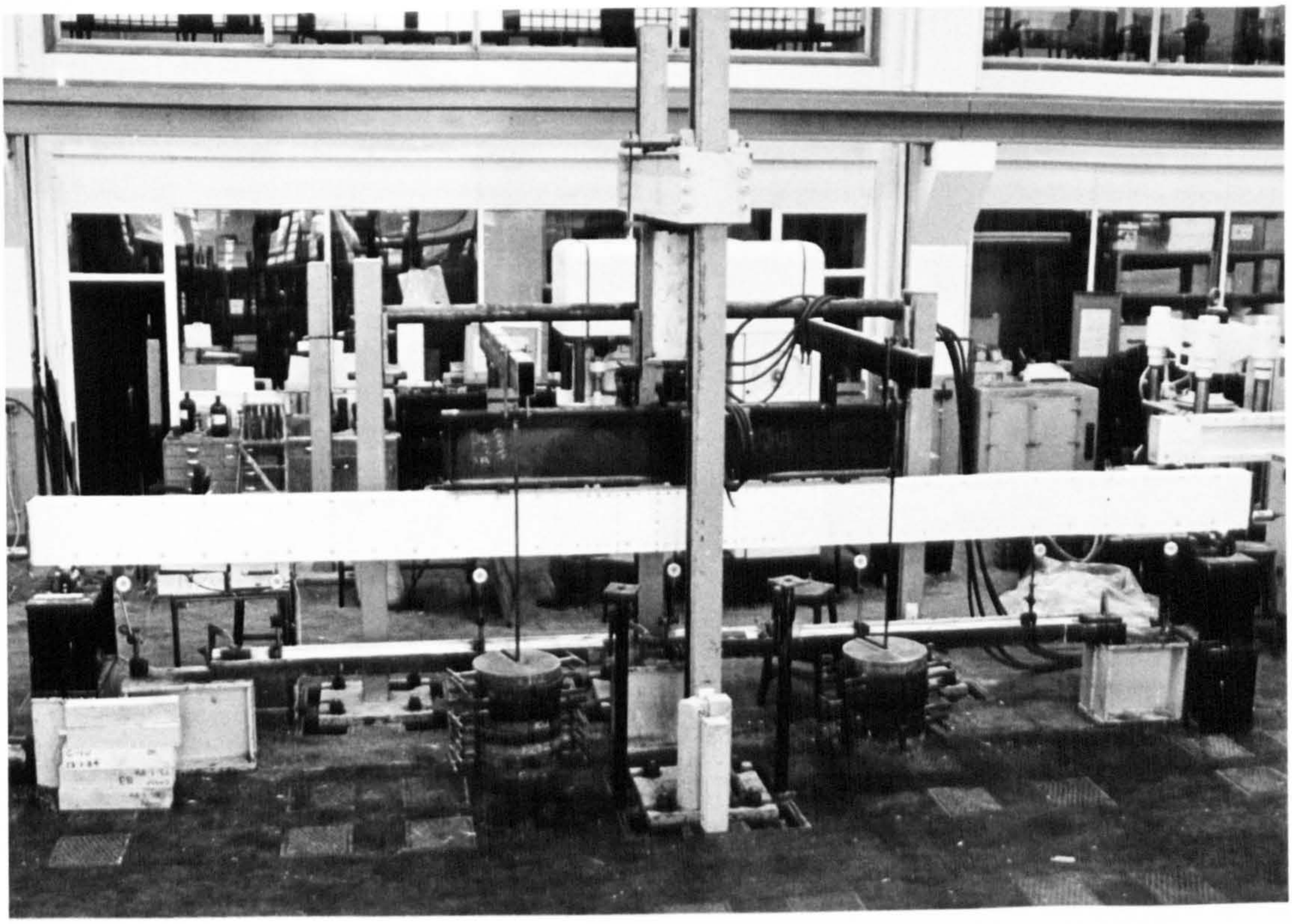

Fig.5.7 Set up for static and combined loading test.

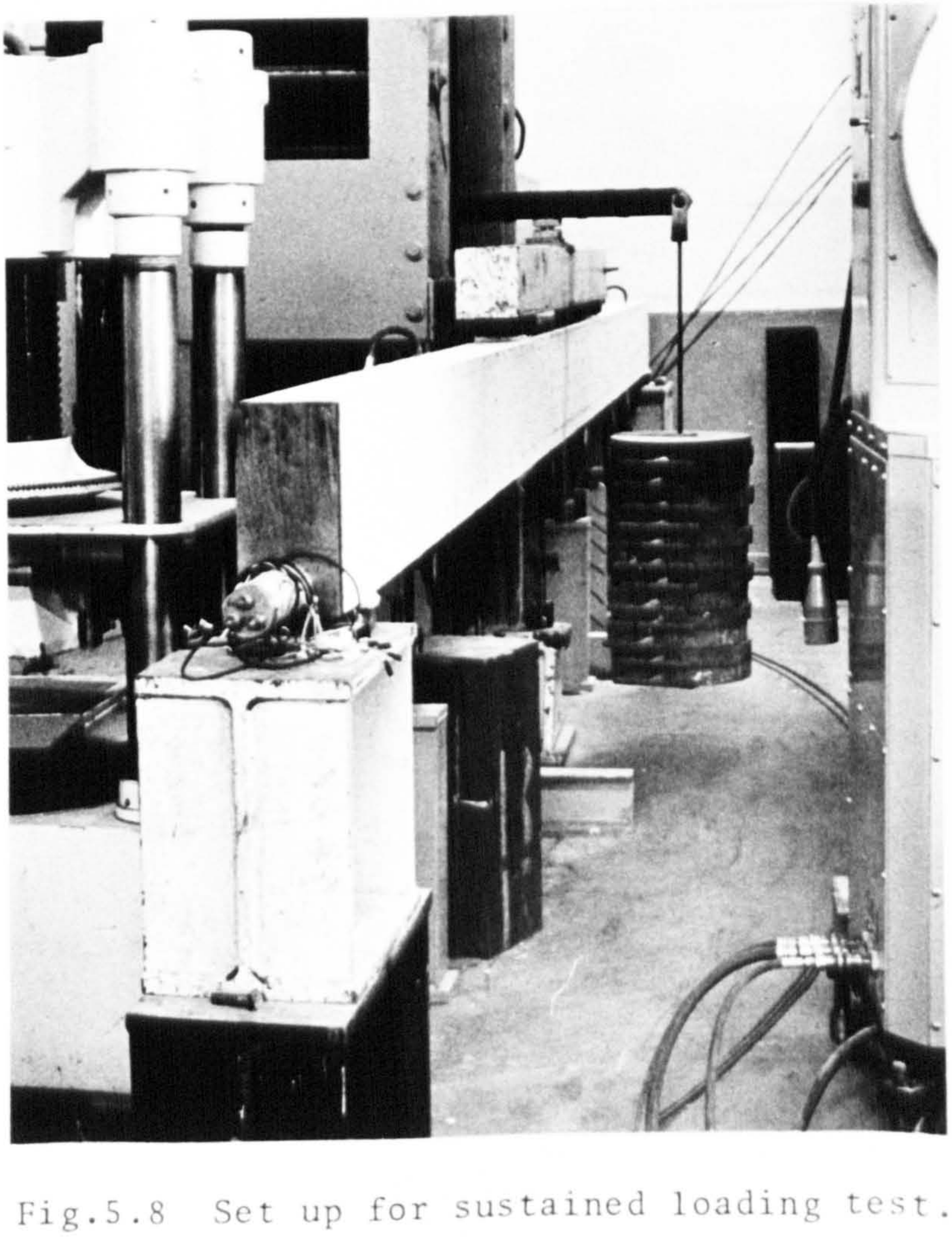

Fig.5.8 Set up for sustained loading test.

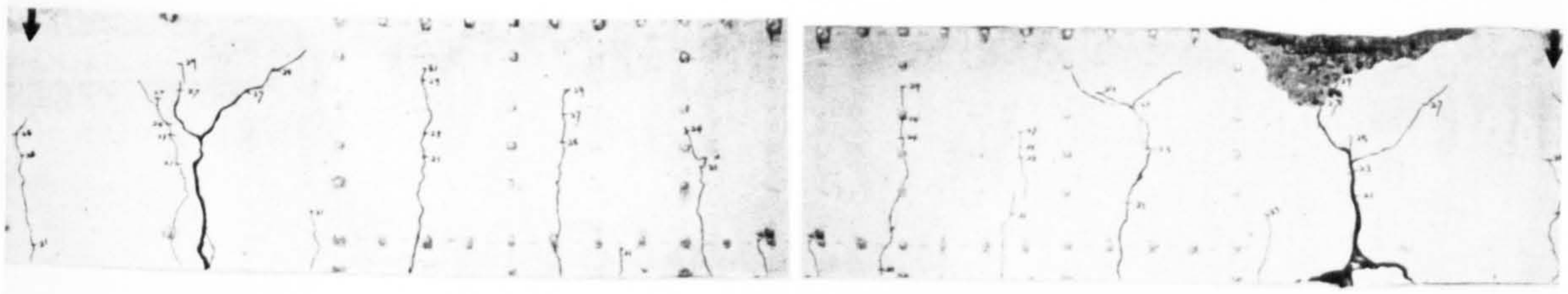

Beam R1.3.0

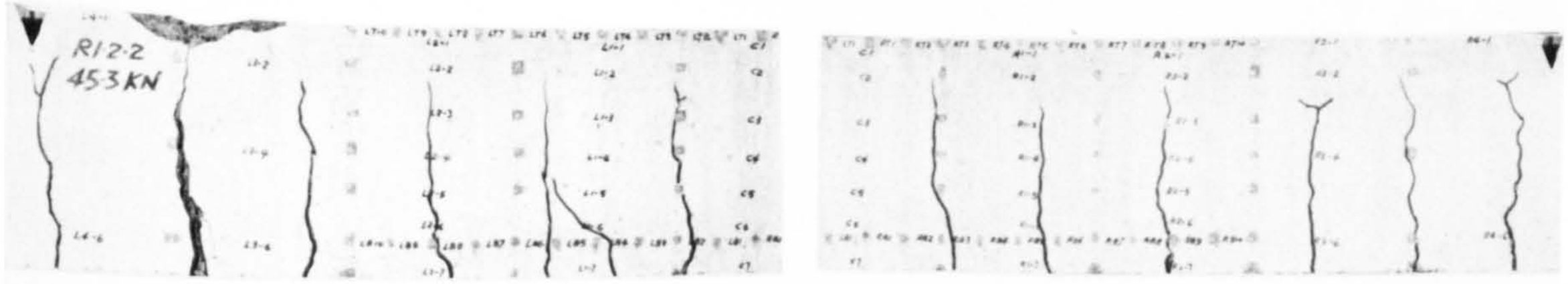

Beam R1.2.2

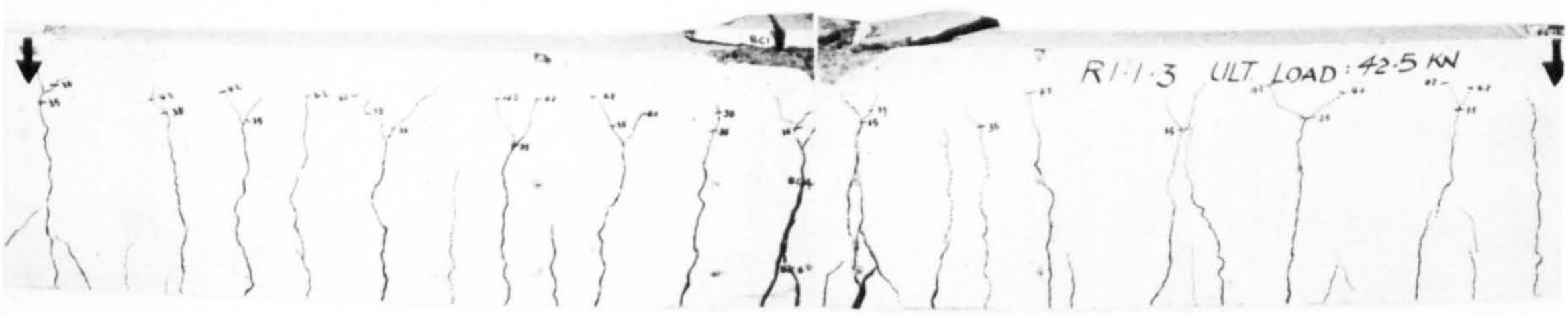

Beam R1.1.3

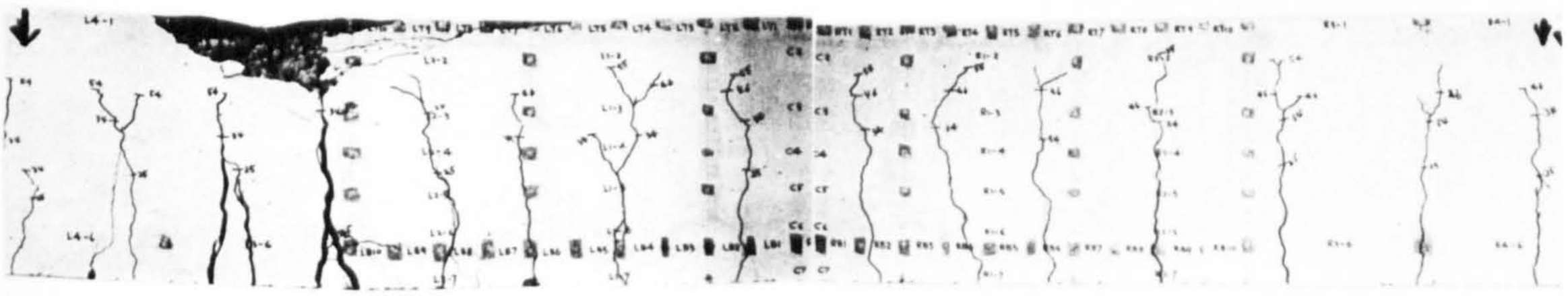

Beam R2.3.2

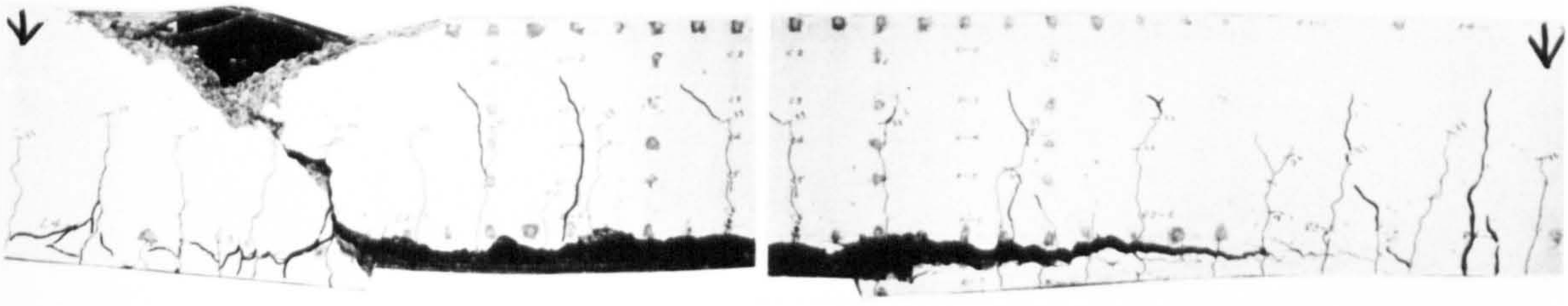

Beam R2.2.4

Fig.5.9 Crack pattern of test beams after destruction.

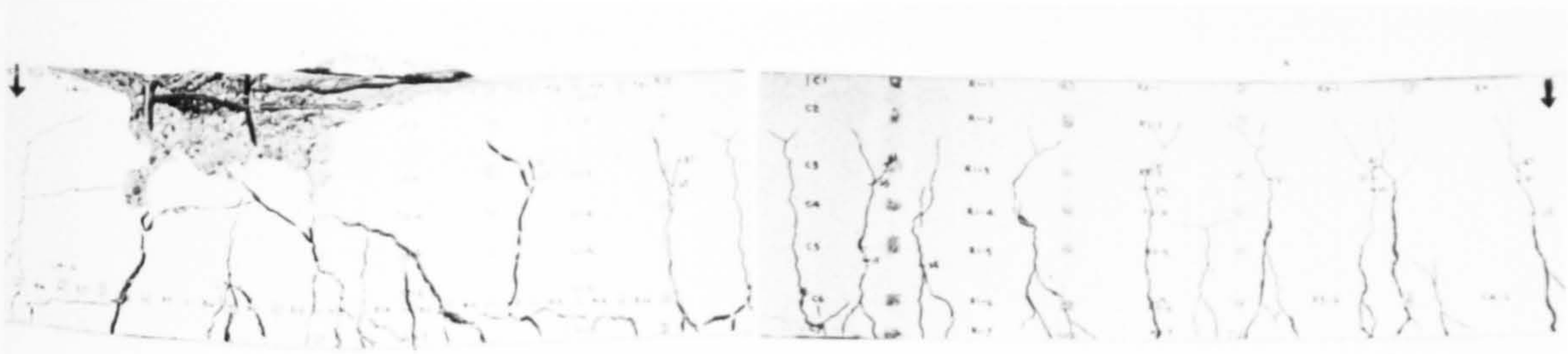

Beam R2.1.5

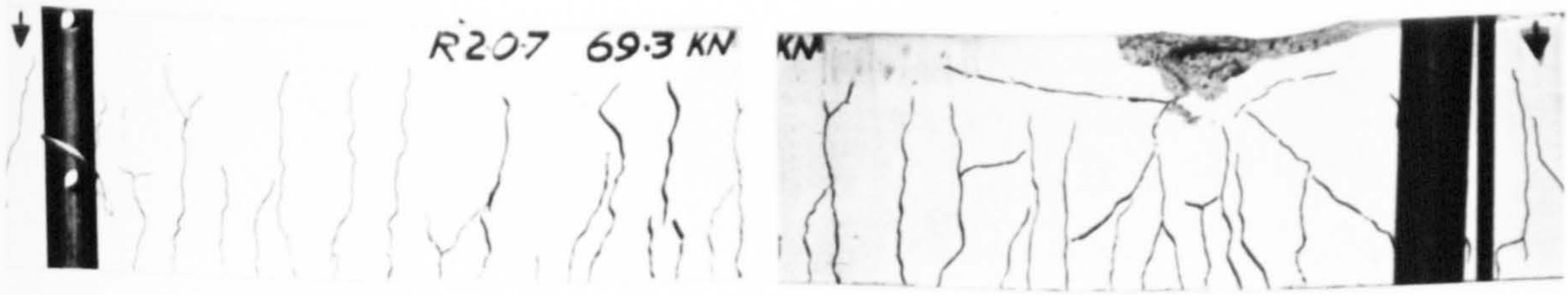

Beam R2.0.7

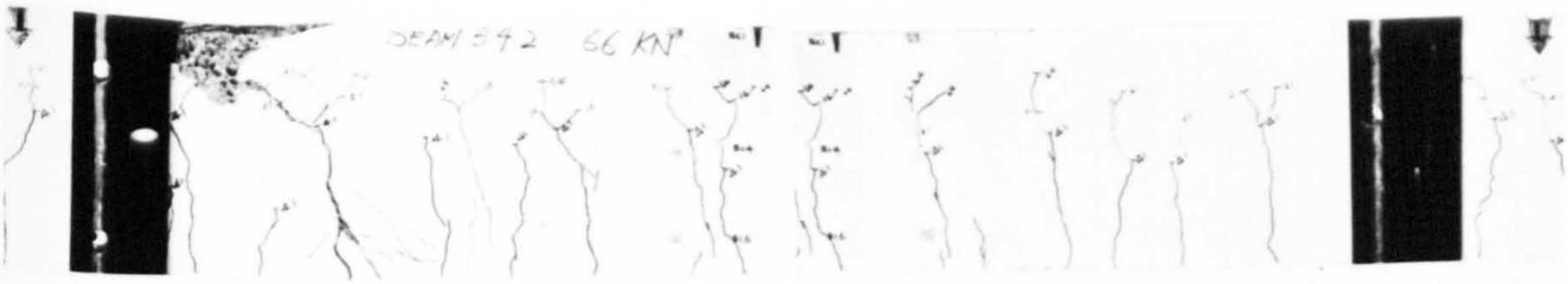

Beam R3.4.2

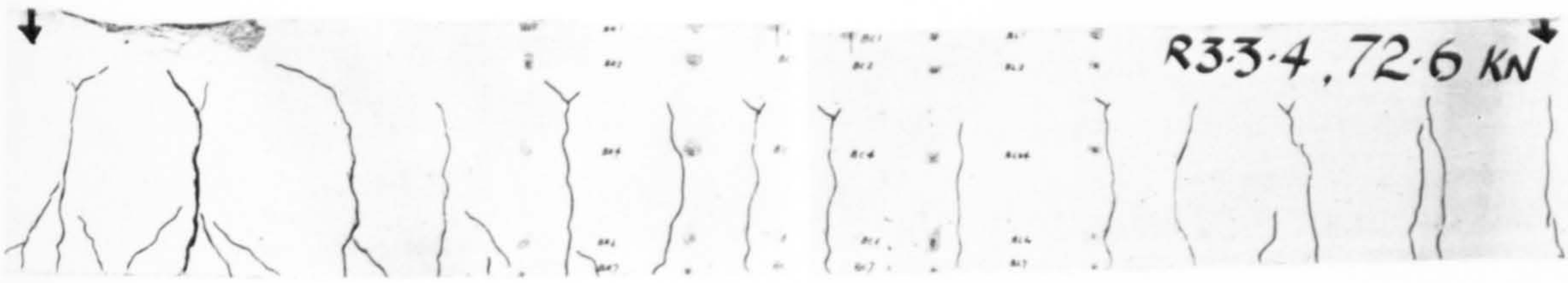

Beam R3.3.4

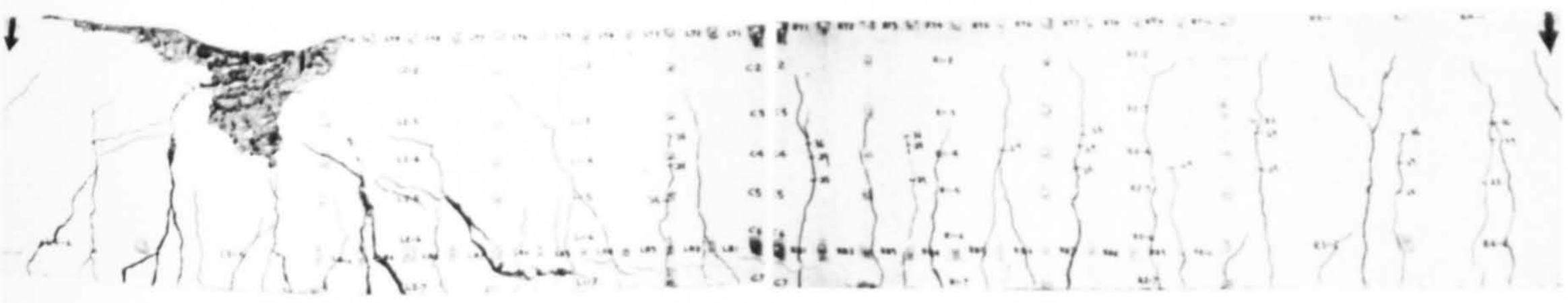

Beam R3.2.5

Fig.5.9 (continued)

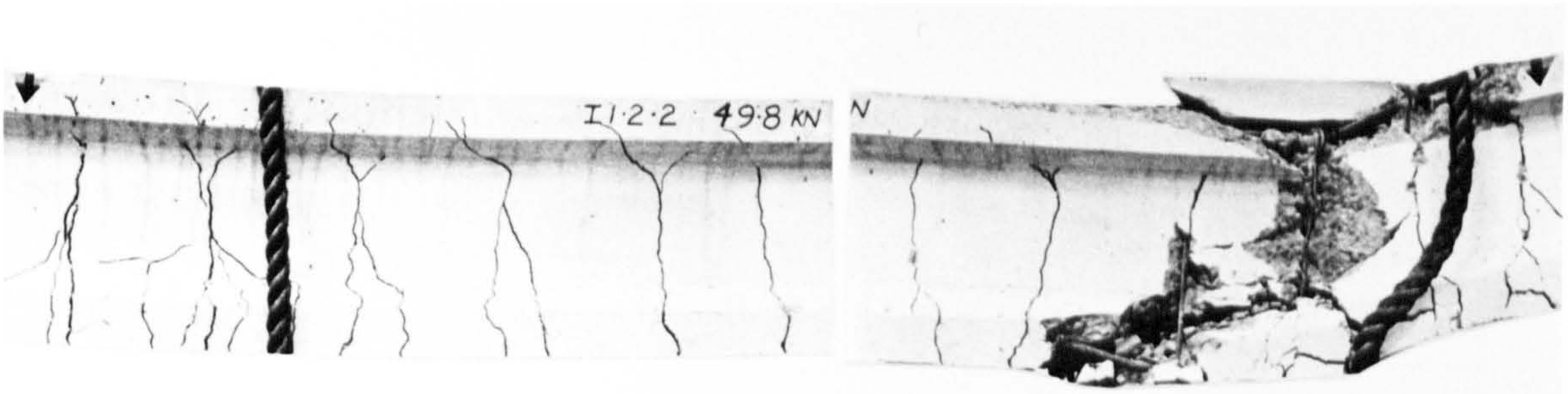

Beam I1.2.2

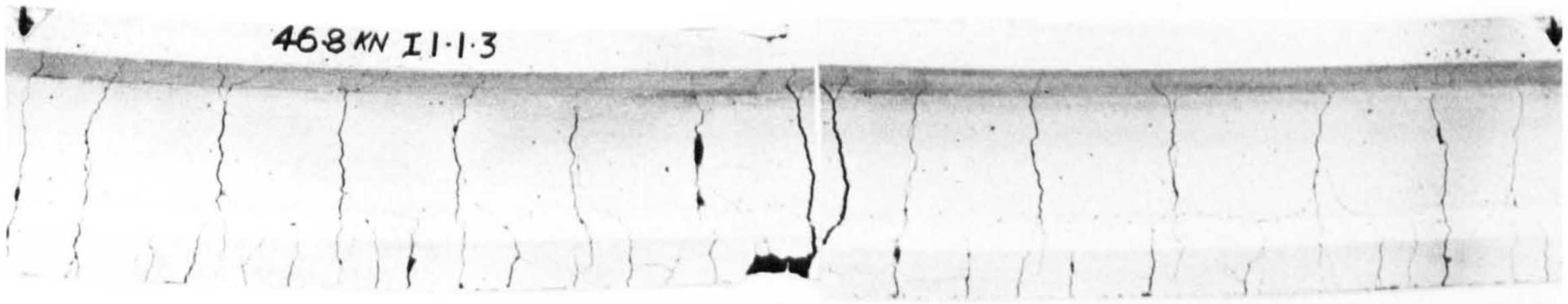

Beam I1.1.3

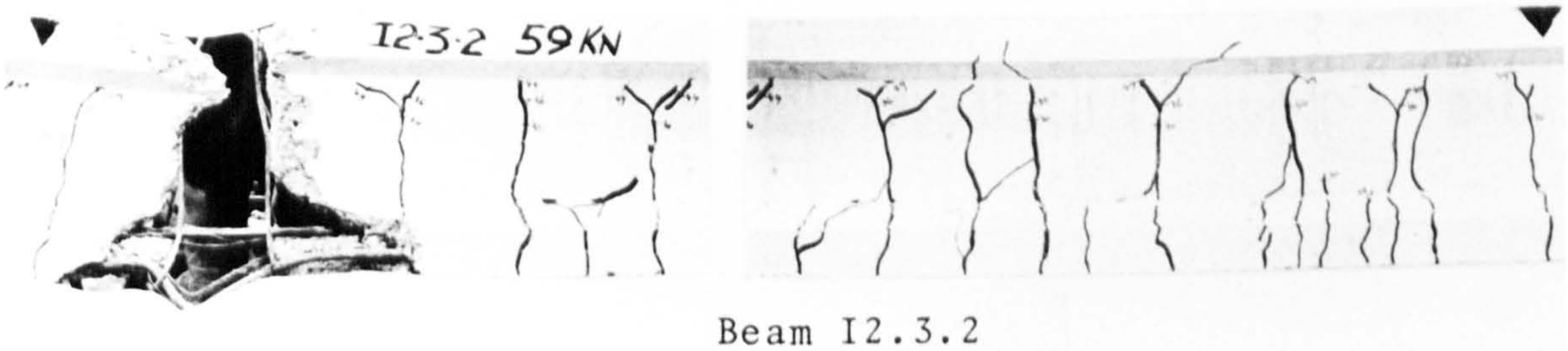

Beam I2.3.2

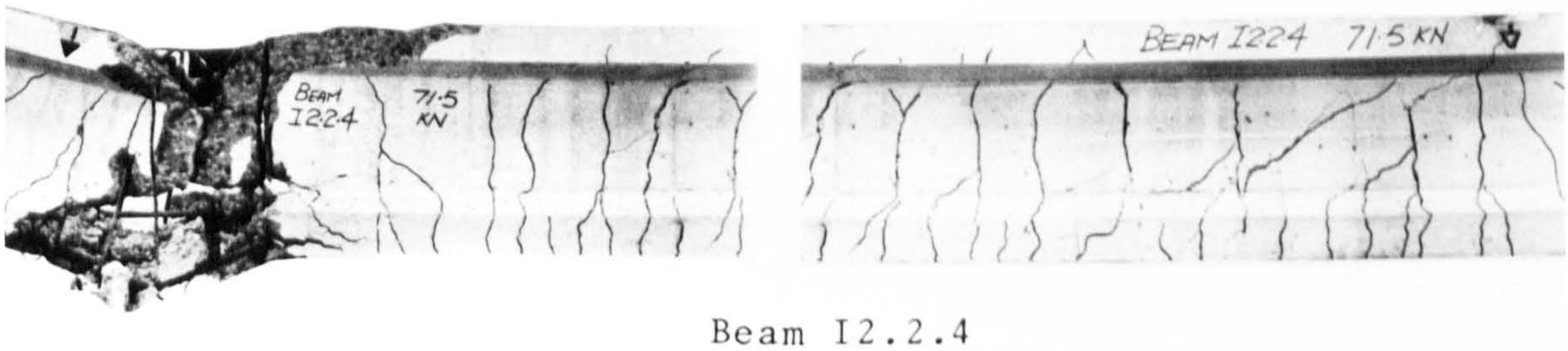

Beam I2.2.4

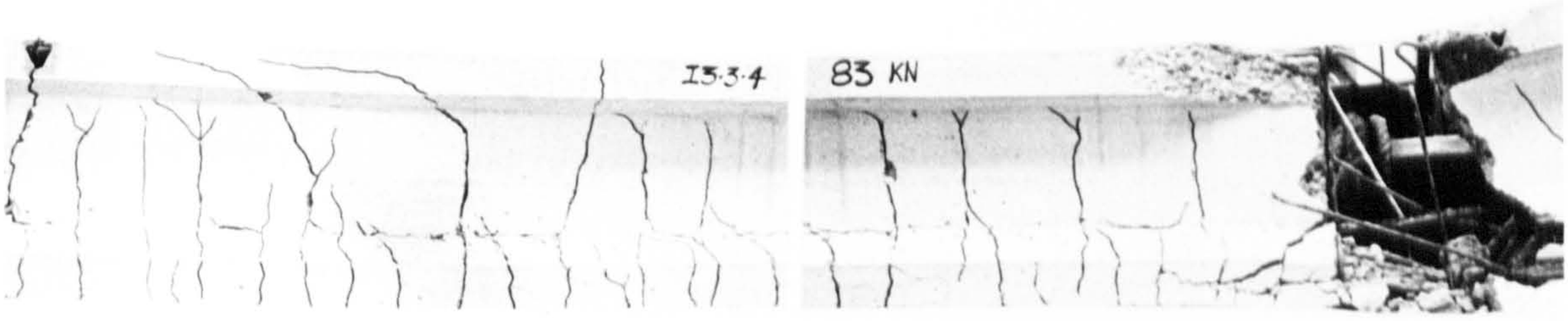

Beam I3.3.4

Fig.5.9 (continued)

FIG.5.10 SPECIFIC CREEP-TIME CURVE OF CREEP SPECIMEN

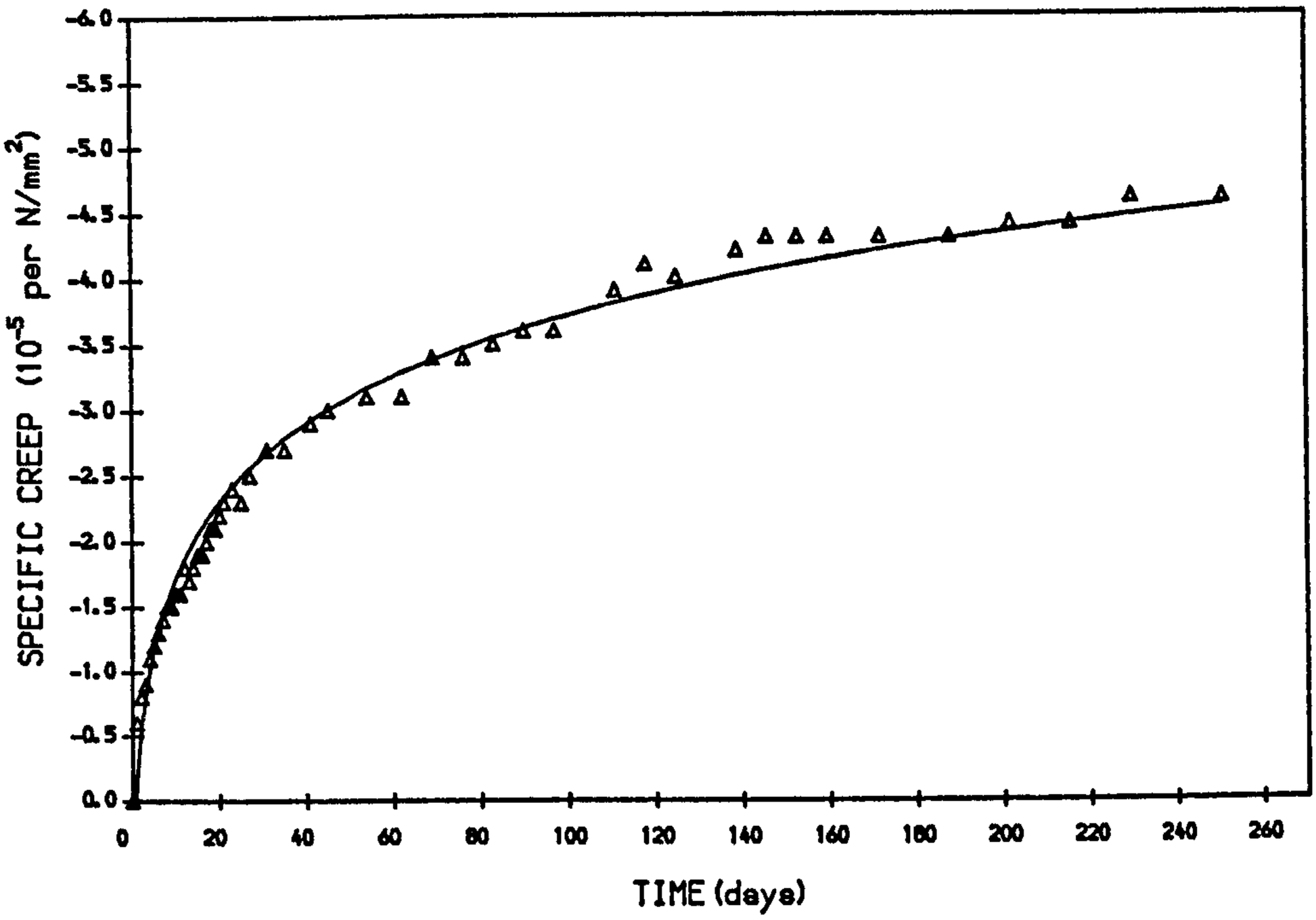

FIG.5.11 SHRINKAGE OF UNLOAD SPECIMEN

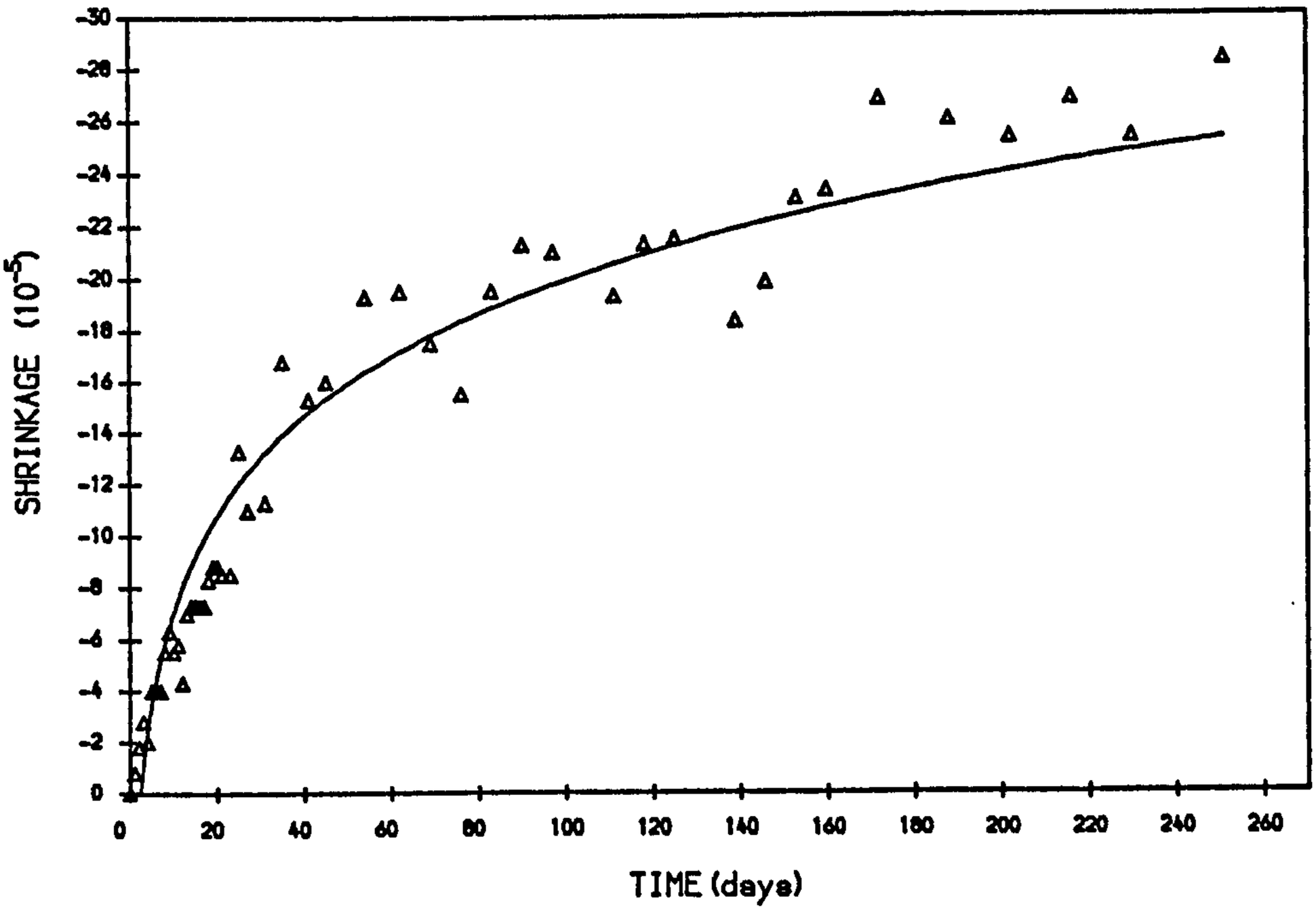

FIG. 6.1a LOAD-DEFLECTION CURVE IN 1ST LOADING (BEAM SERIES 1)

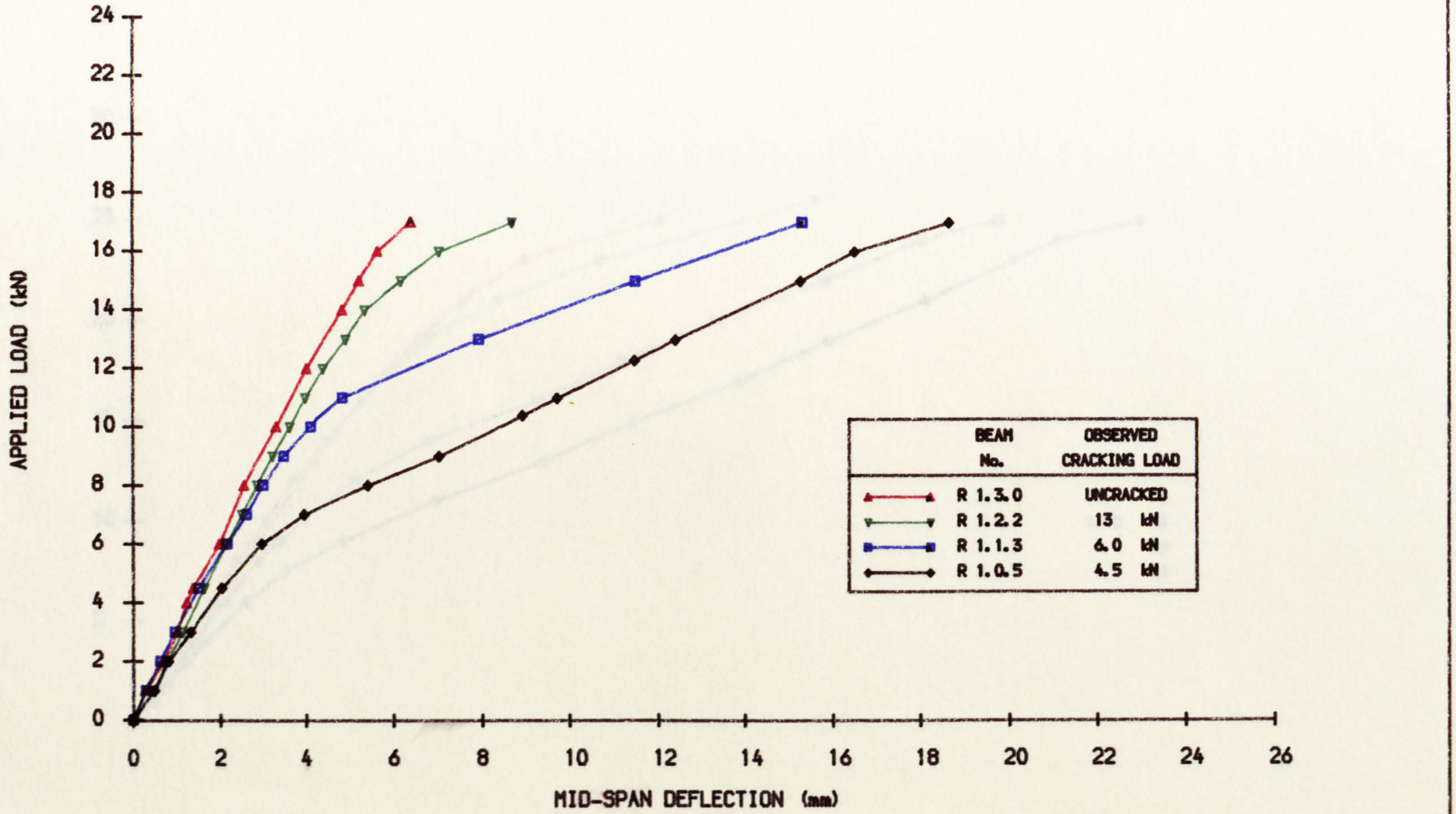

FIG. 6.1b LOAD-DEFLECTION CURVE IN FIRST LOADING (BEAM SERIES 2)

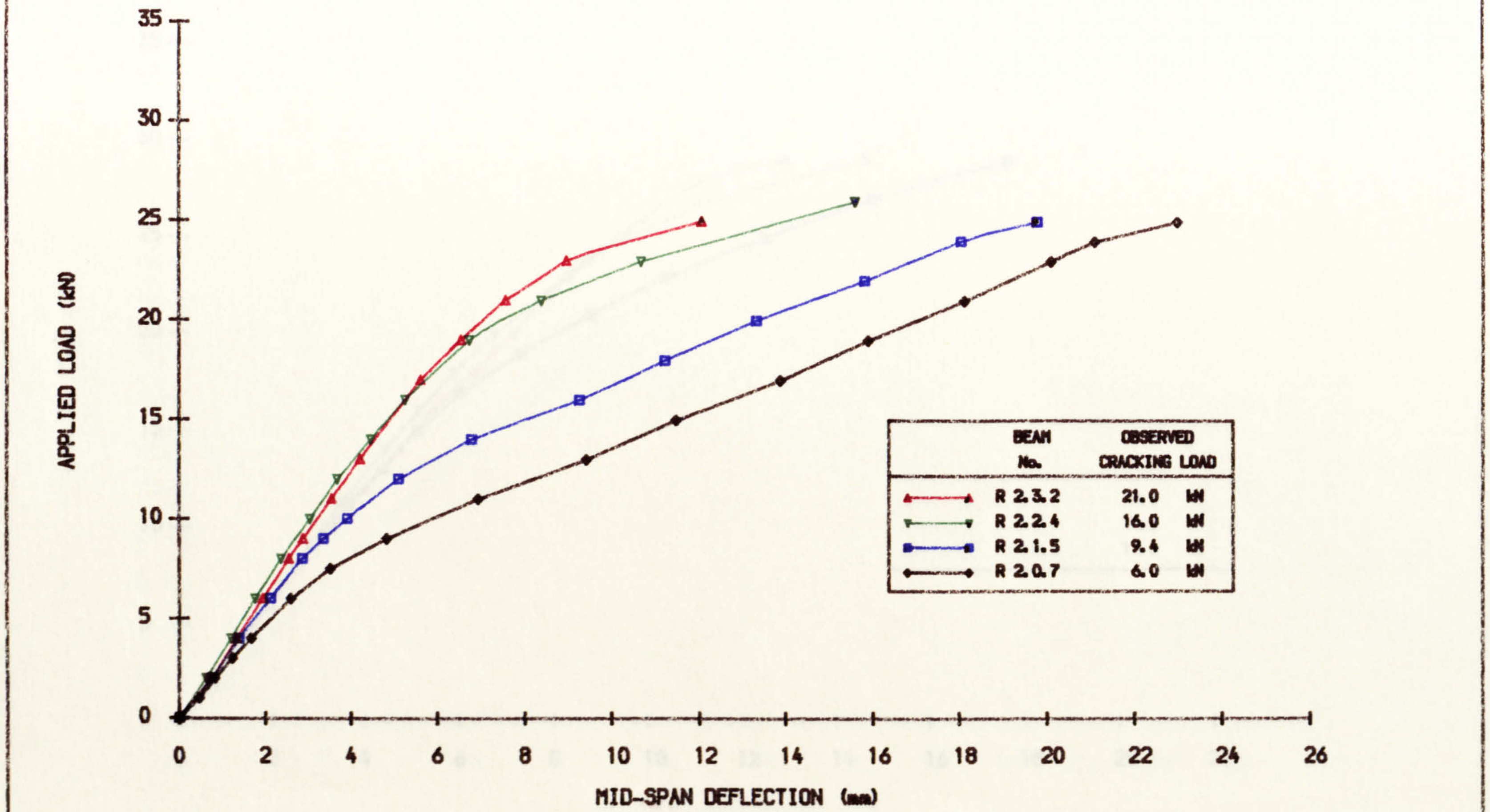

FIG. 6.1c LOAD-DEFLECTION CURVE IN 1ST LOADING (BEAM SERIES 3)

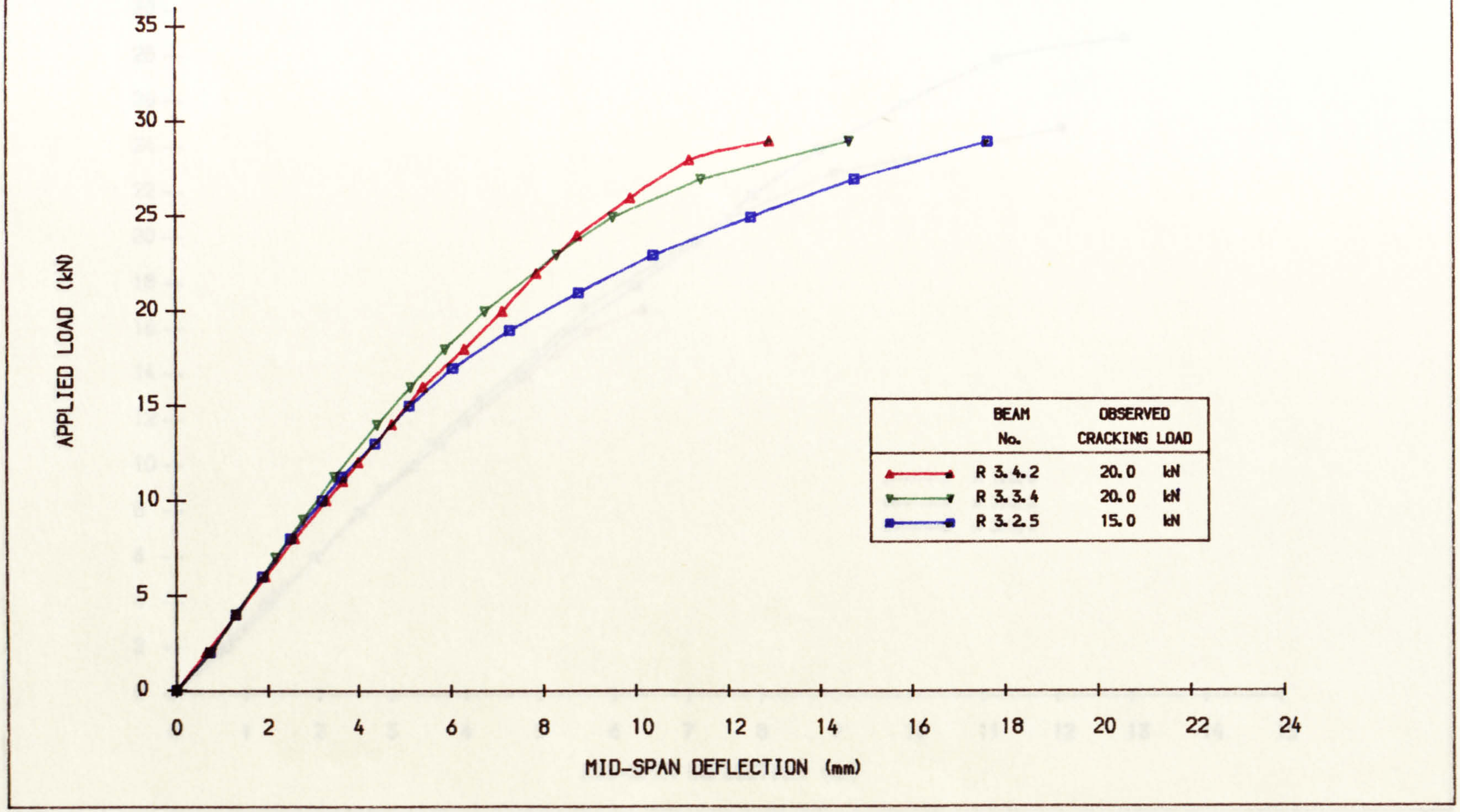

FIG. 6.1d LOAD-DEFLECTION CURVE IN 1ST LOADING (SAME LEVEL OF PRESTRESS)

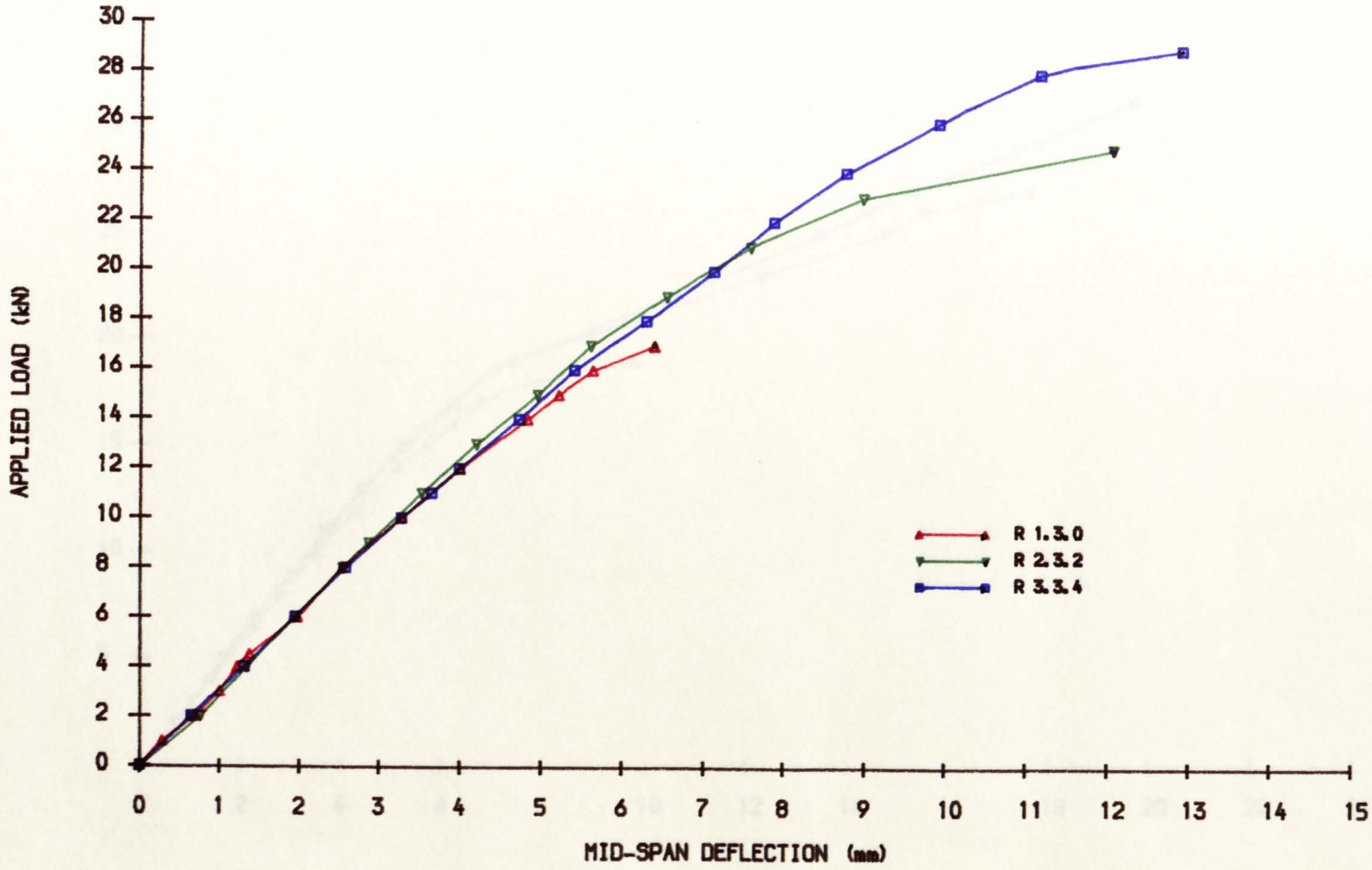

FIG. 6.1e LOAD-DEFLECTION CURVE IN 1ST LOADING (SAME LEVEL OF PRESTRESS)

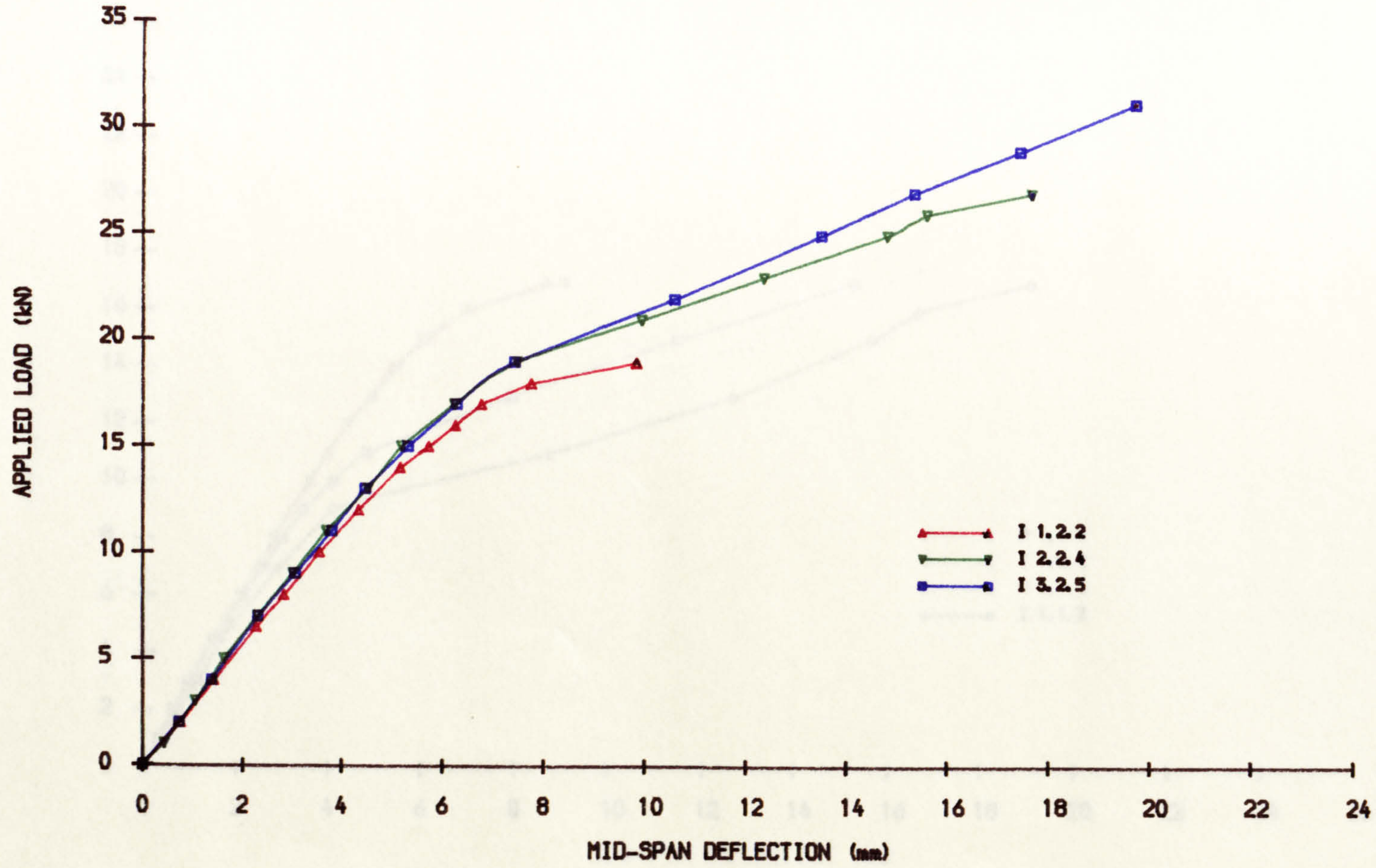

FIG. 6.1f LOAD-DEFLECTION CURVE IN 1ST LOADING (SAME SERIES, DIFFERENT SECTION)

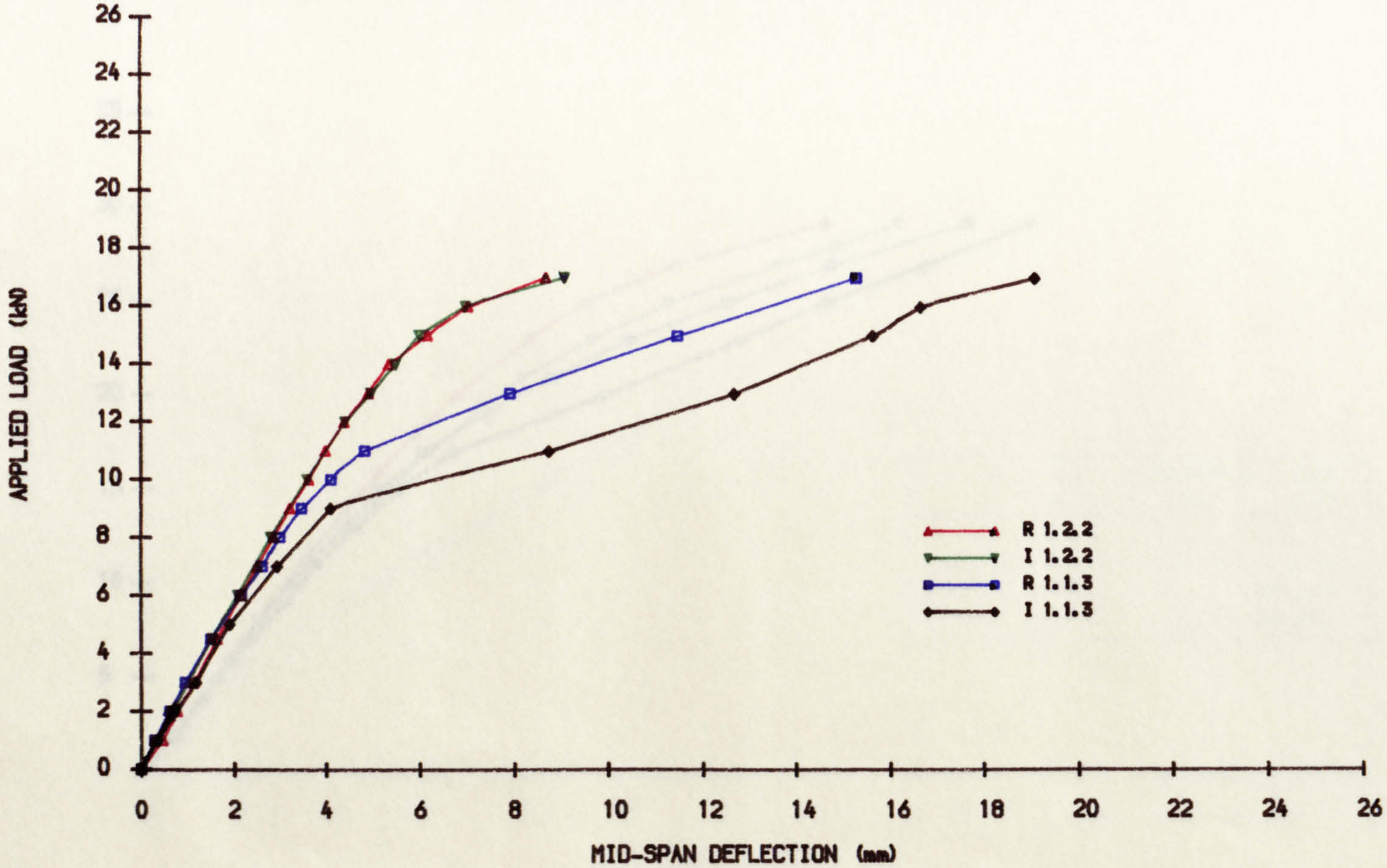

FIG. 6.1g LOAD-DEFLECTION CURVE IN 1ST LOADING (SAME SERIES, DIFFERENT SECTION)

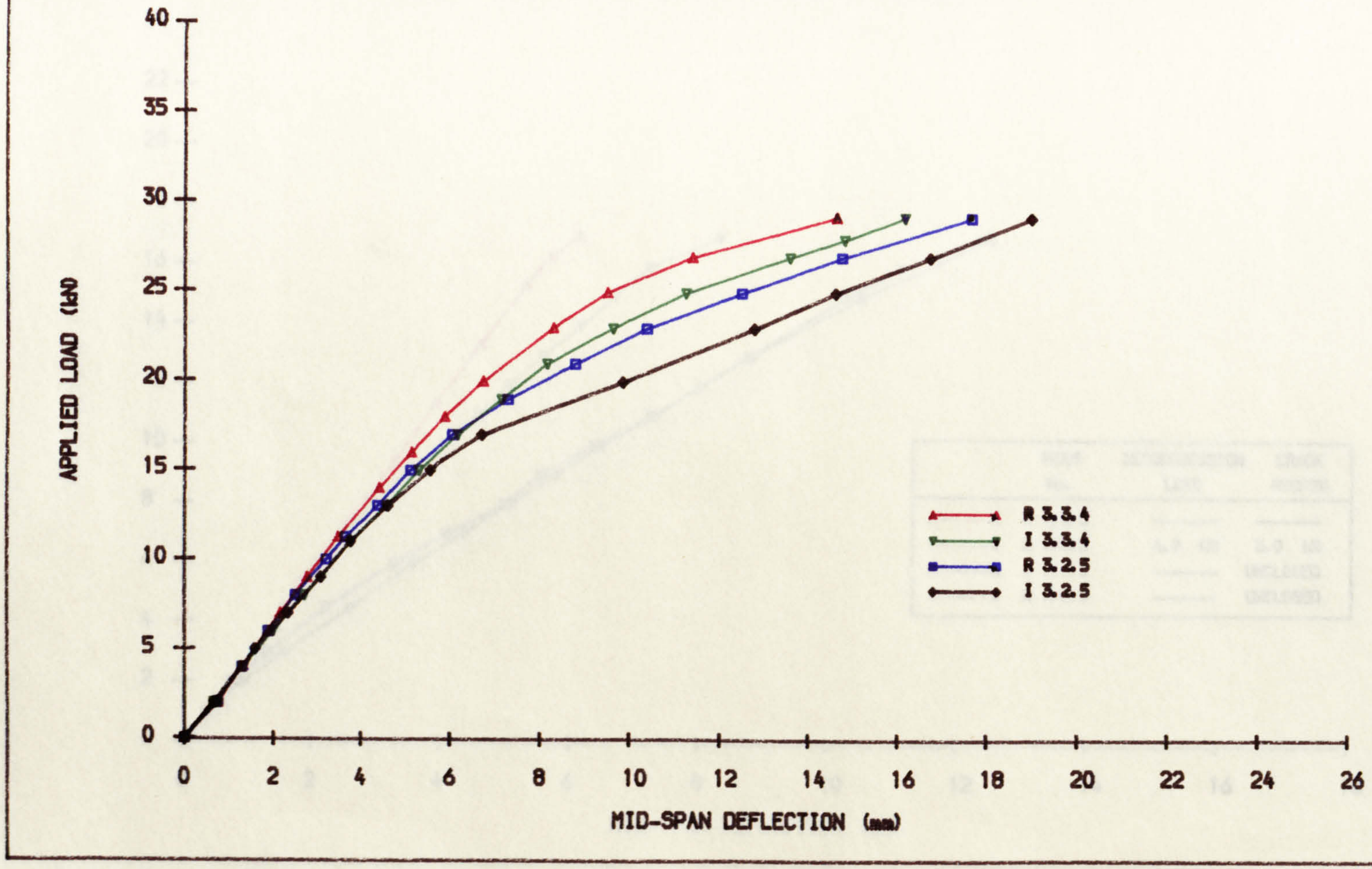

FIG. 6.2a LOAD-DEFLECTION CURVE IN 2ND LOADING (BEAM SERIES 1)

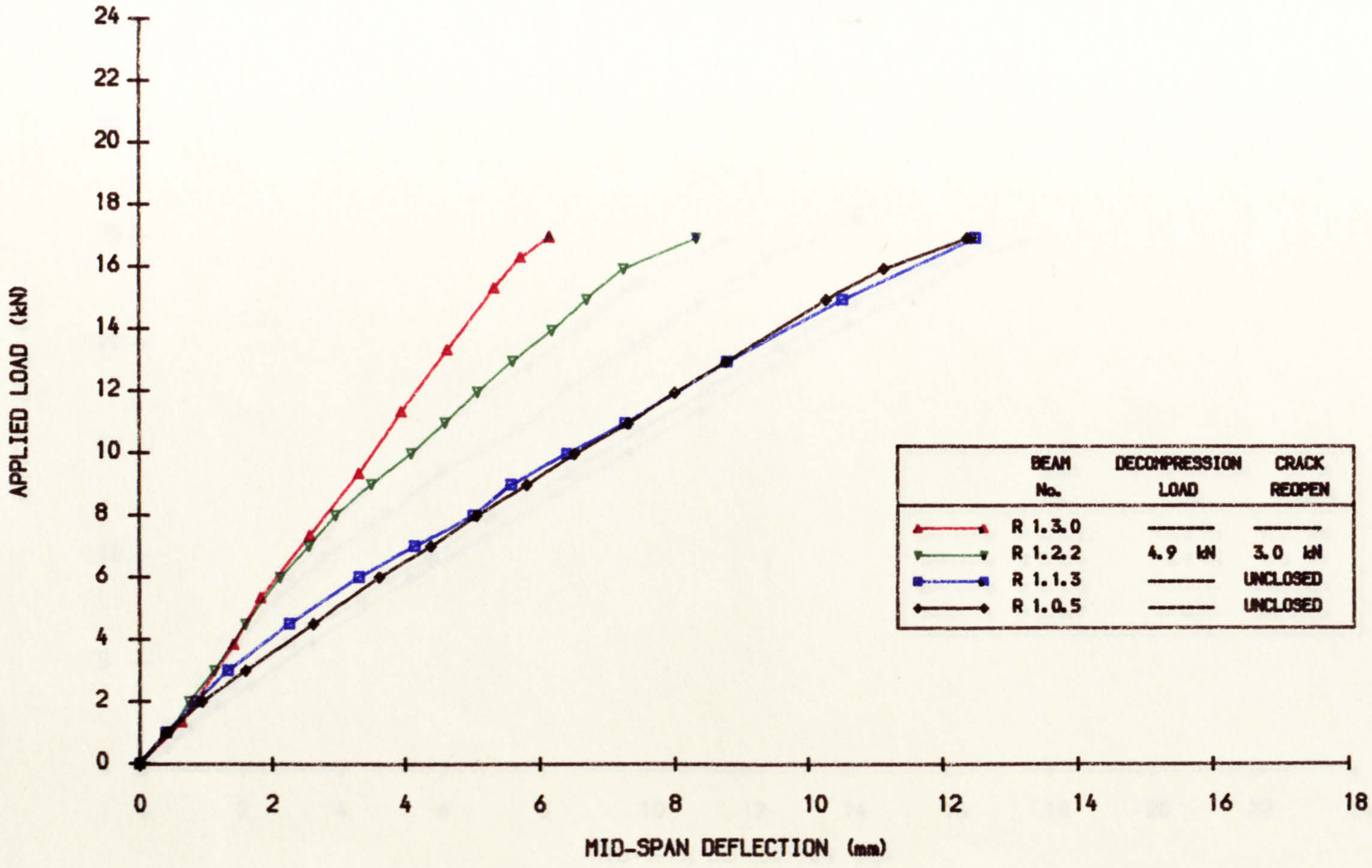

FIG. 6.2b LOAD-DEFLECTION CURVE IN 2ND LOADING (BEAM SERIES 2)

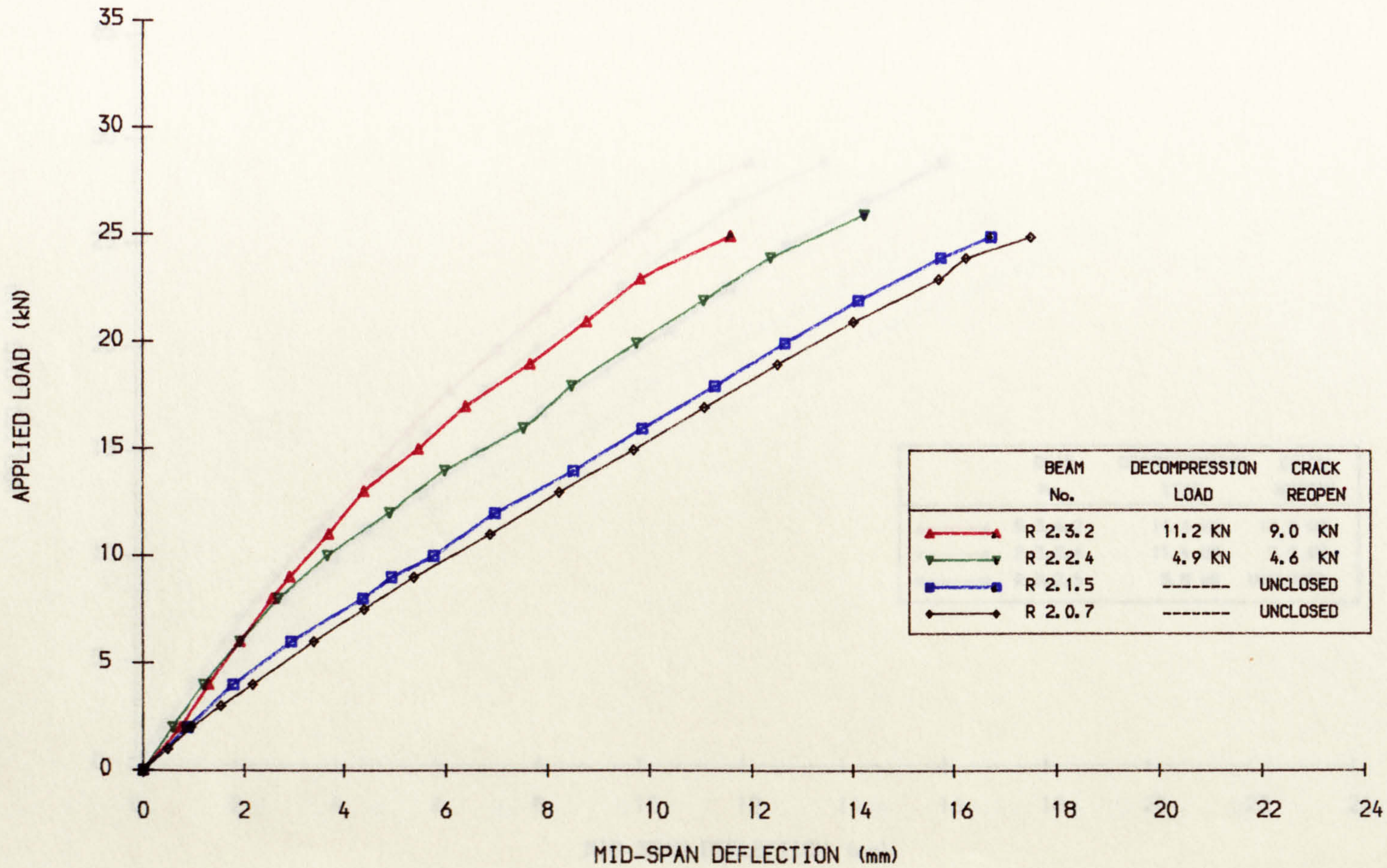

FIG. 6.2c LOAD-DEFLECTION CURVE IN 2ND LOADING (BEAM SERIES 3)

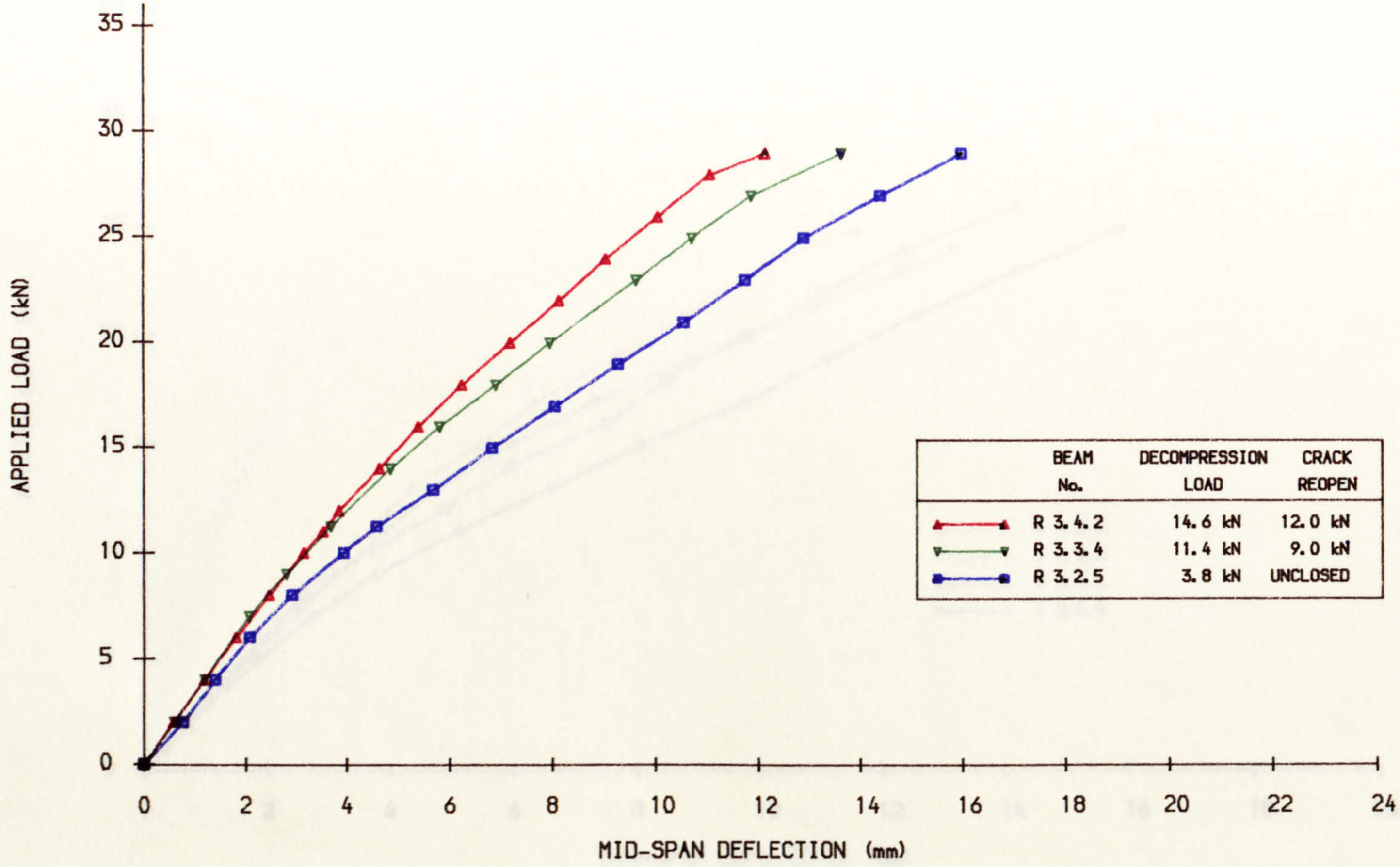

FIG. 6.2d LOAD-DEFLECTION CURVE IN 2ND LOADING (SAME SERIES, DIFFERENT SECTION)

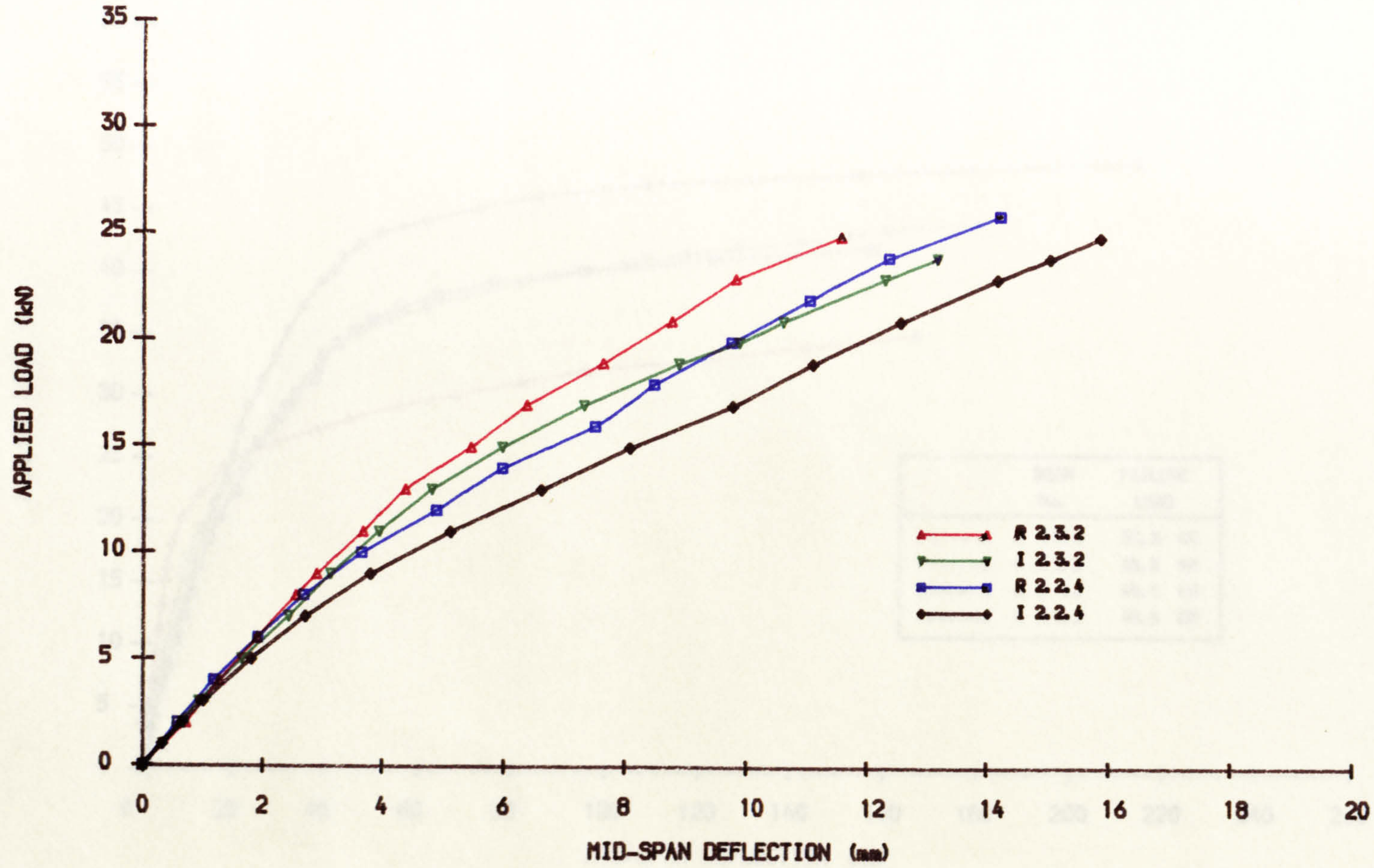

FIG. 6.3a LOAD-DEFLECTION CURVE IN FINAL LOADING (BEAM SERIES 1)

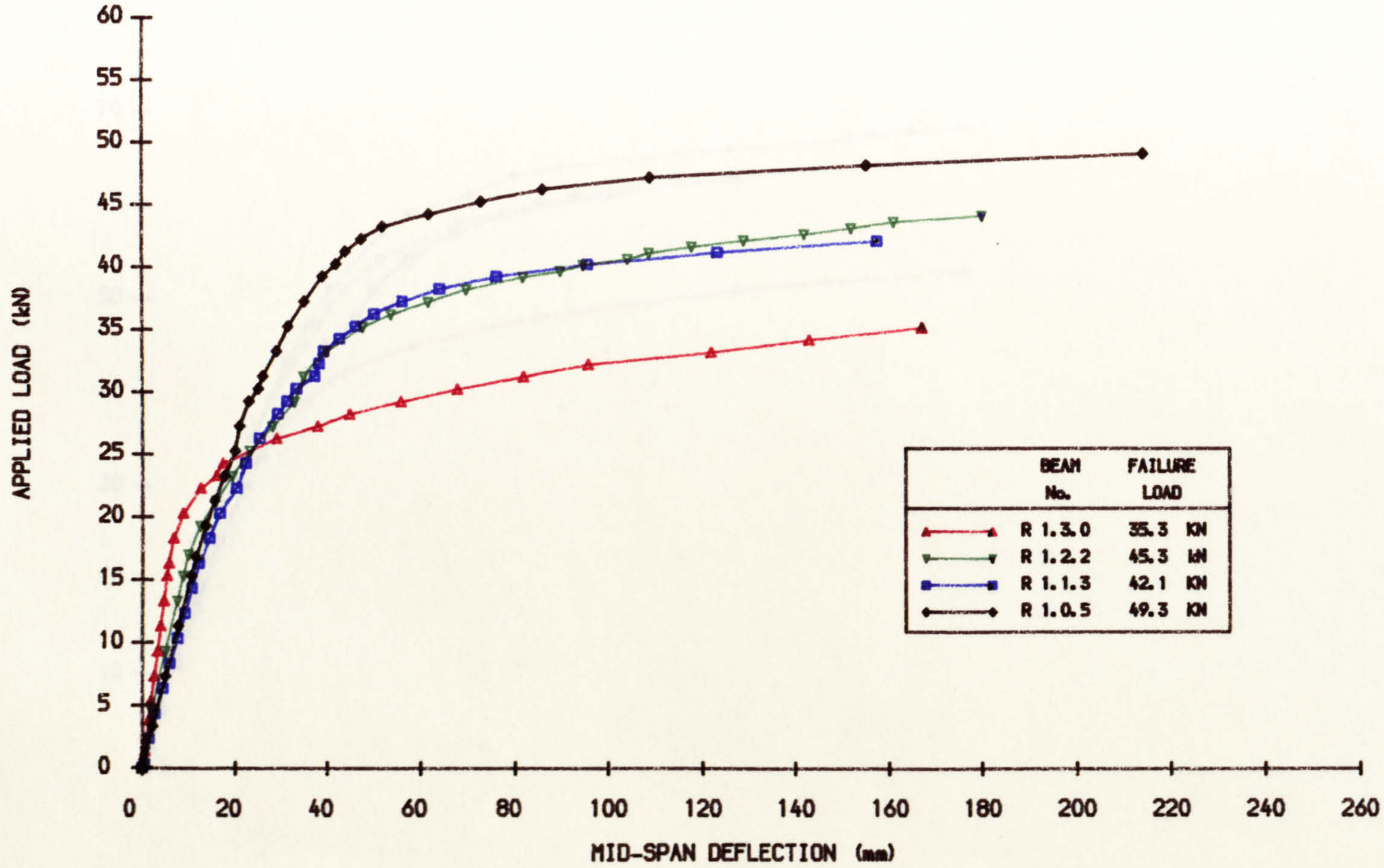

FIG. 6.3b LOAD-DEFLECTION CURVE IN FINAL LOADING (BEAM SERIES 2)

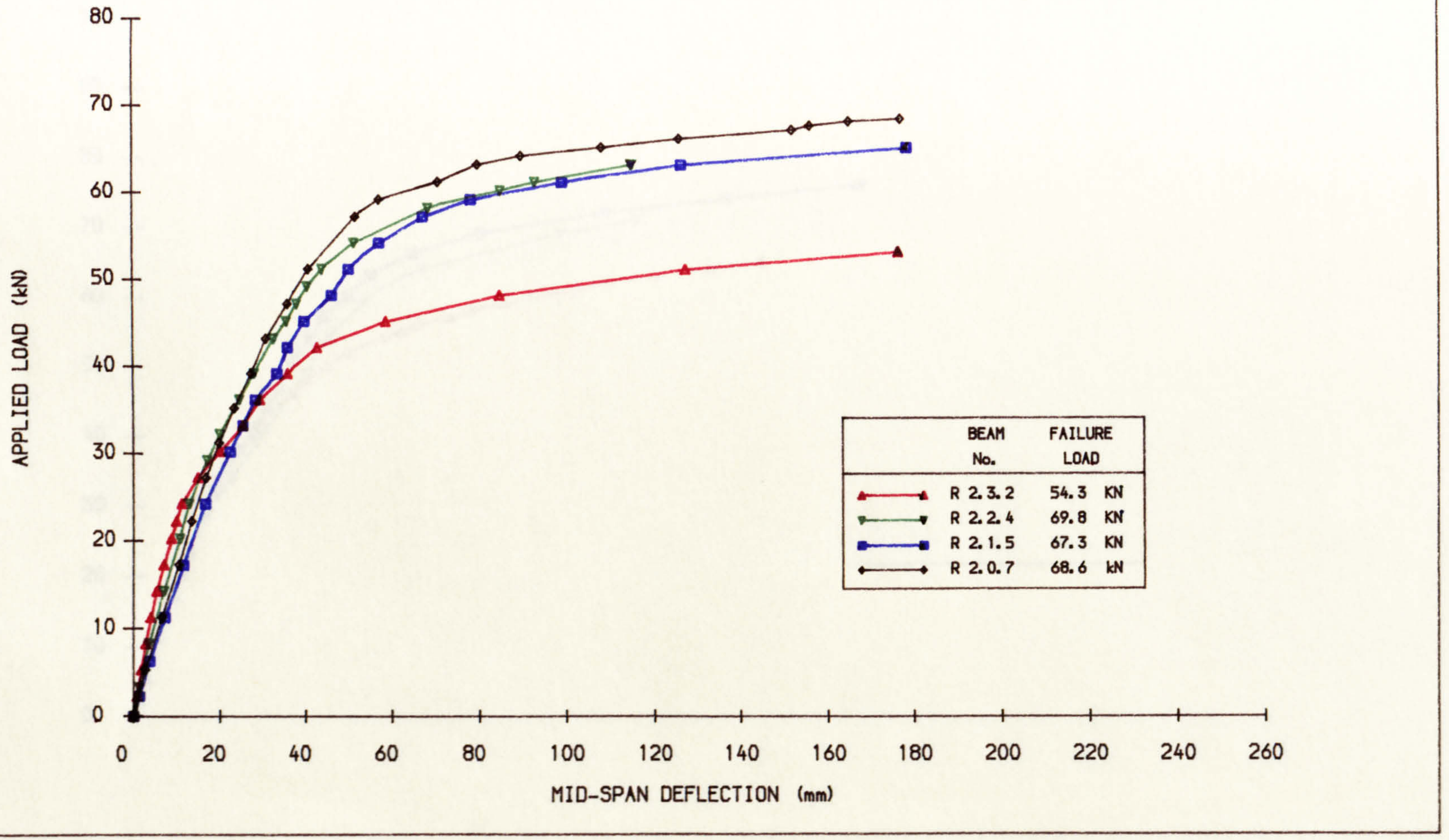

FIG. 6.3c LOAD-DEFLECTION CURVE IN FINAL LOADING (BEAM SERIES 3)

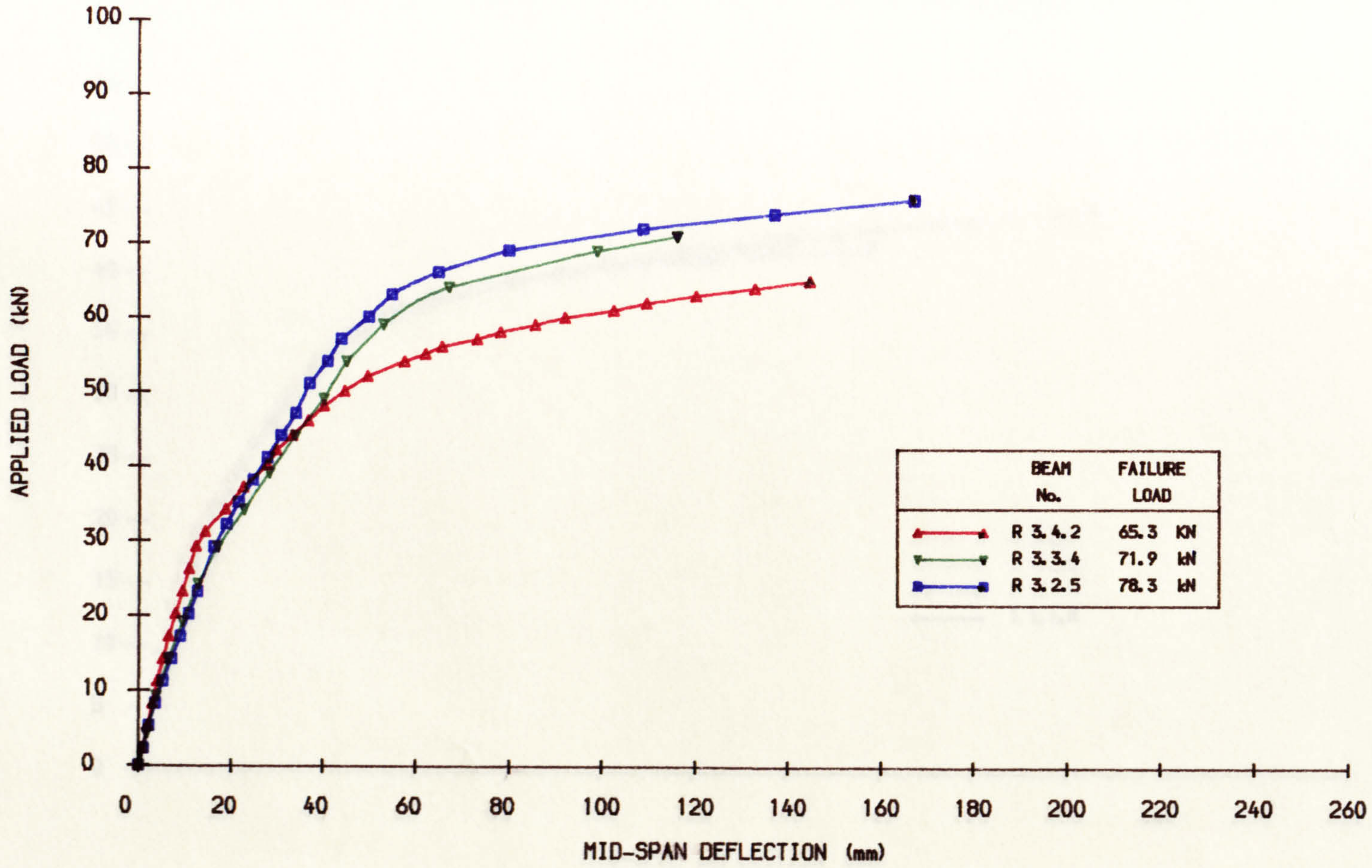

FIG. 6.3d LOAD-DEFLECTION CURVE IN FINAL LOADING (SAME SERIES, DIFFERENT SECTION)

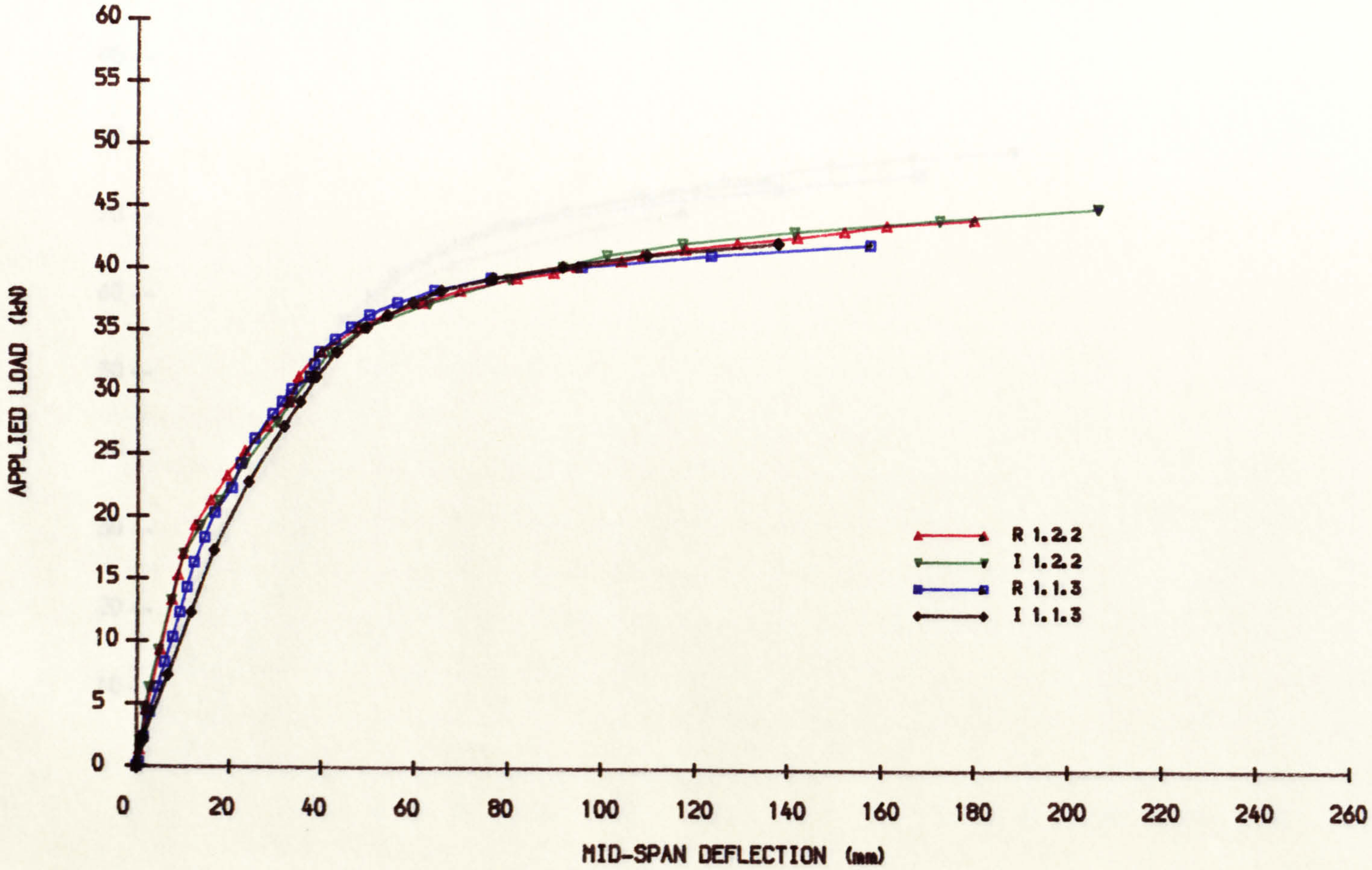

FIG. 6.3e LOAD-DEFLECTION CURVE IN FINAL LOADING (SAME SERIES, DIFFERENT SECTION)

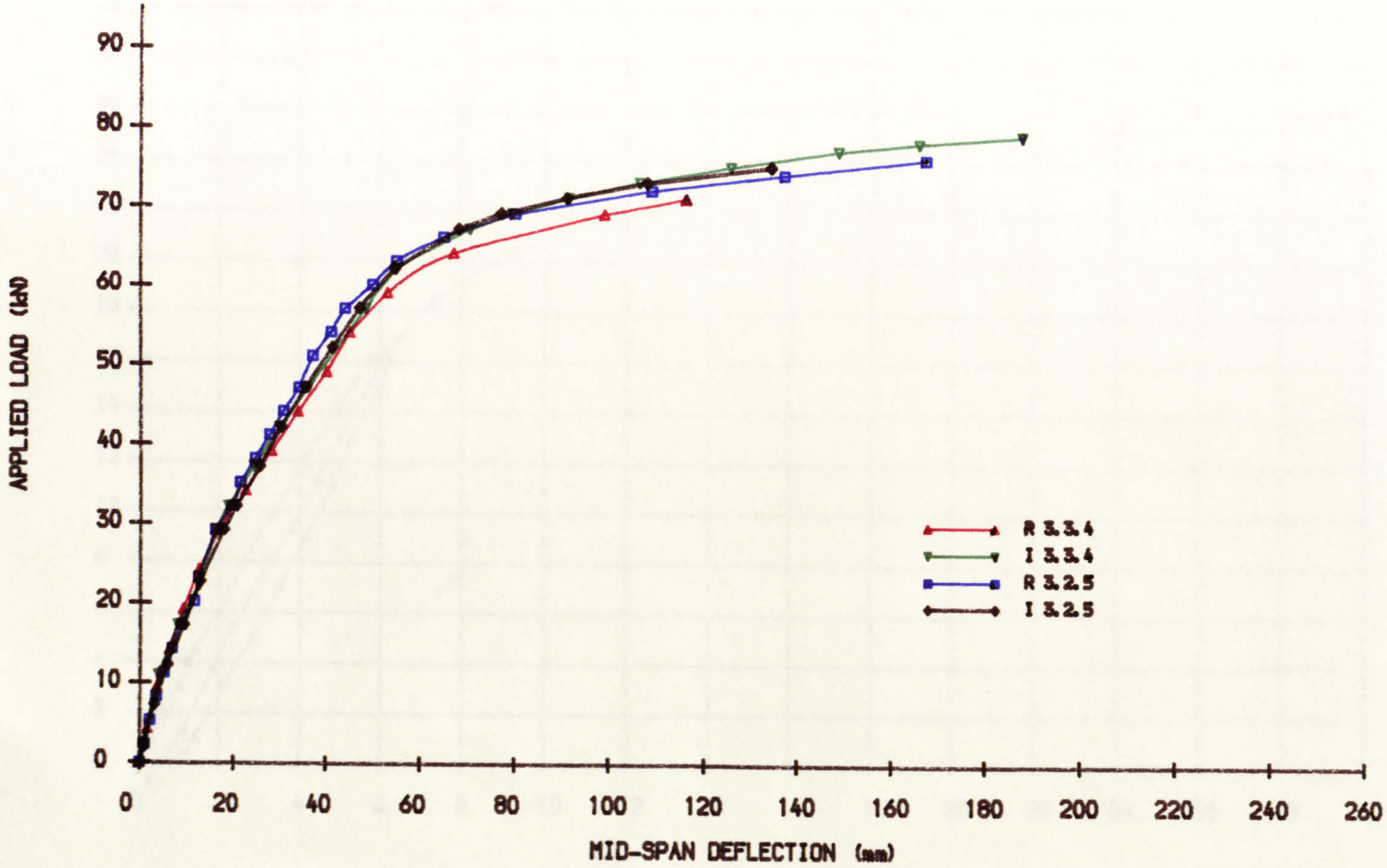

FIG. 6.4a LOAD-DEFLECTION CURVE (BEAM R1.3.0)

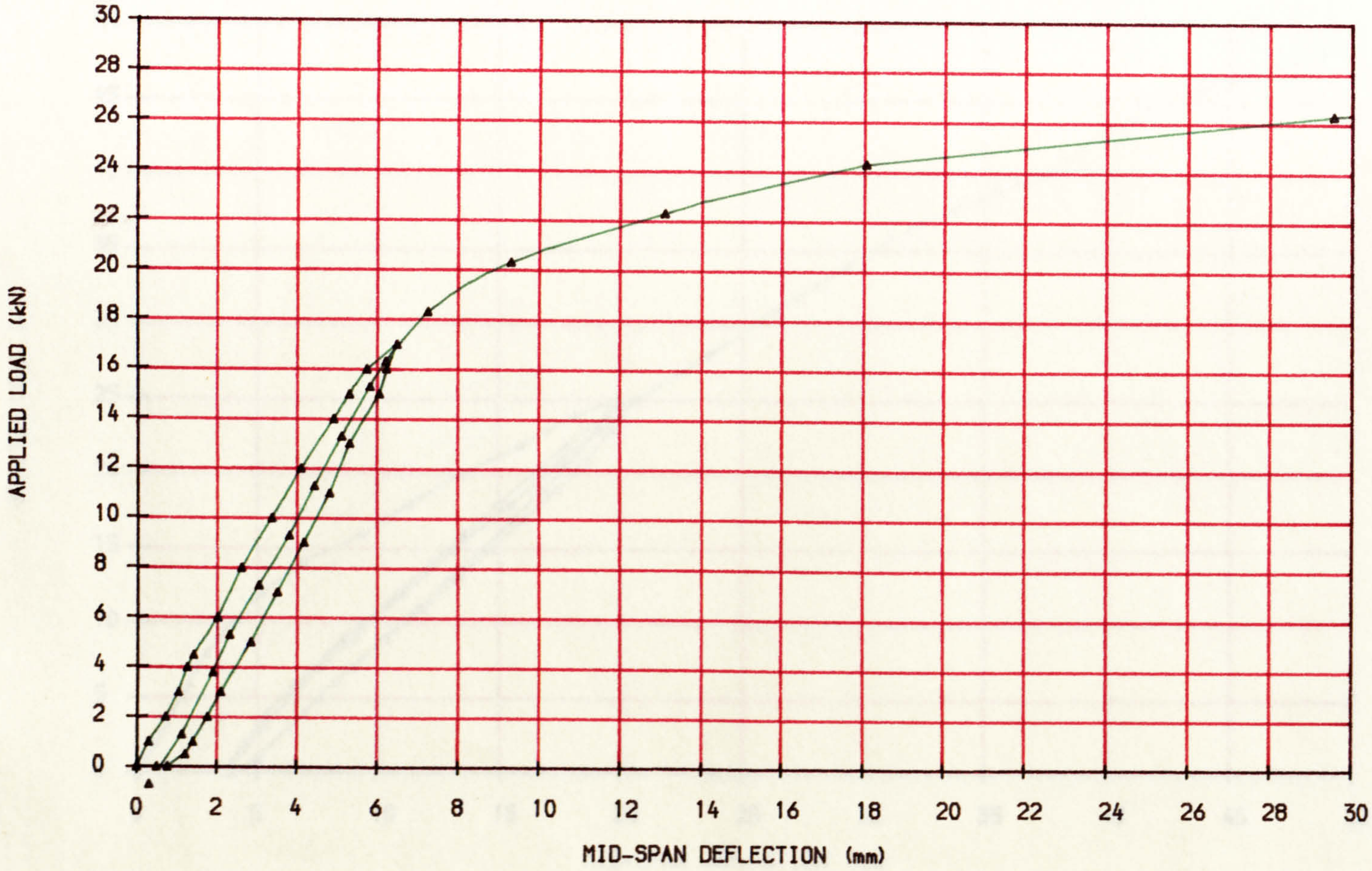

FIG. 6.4b LOAD-DEFLECTION CURVE (BEAM R2.1.5)

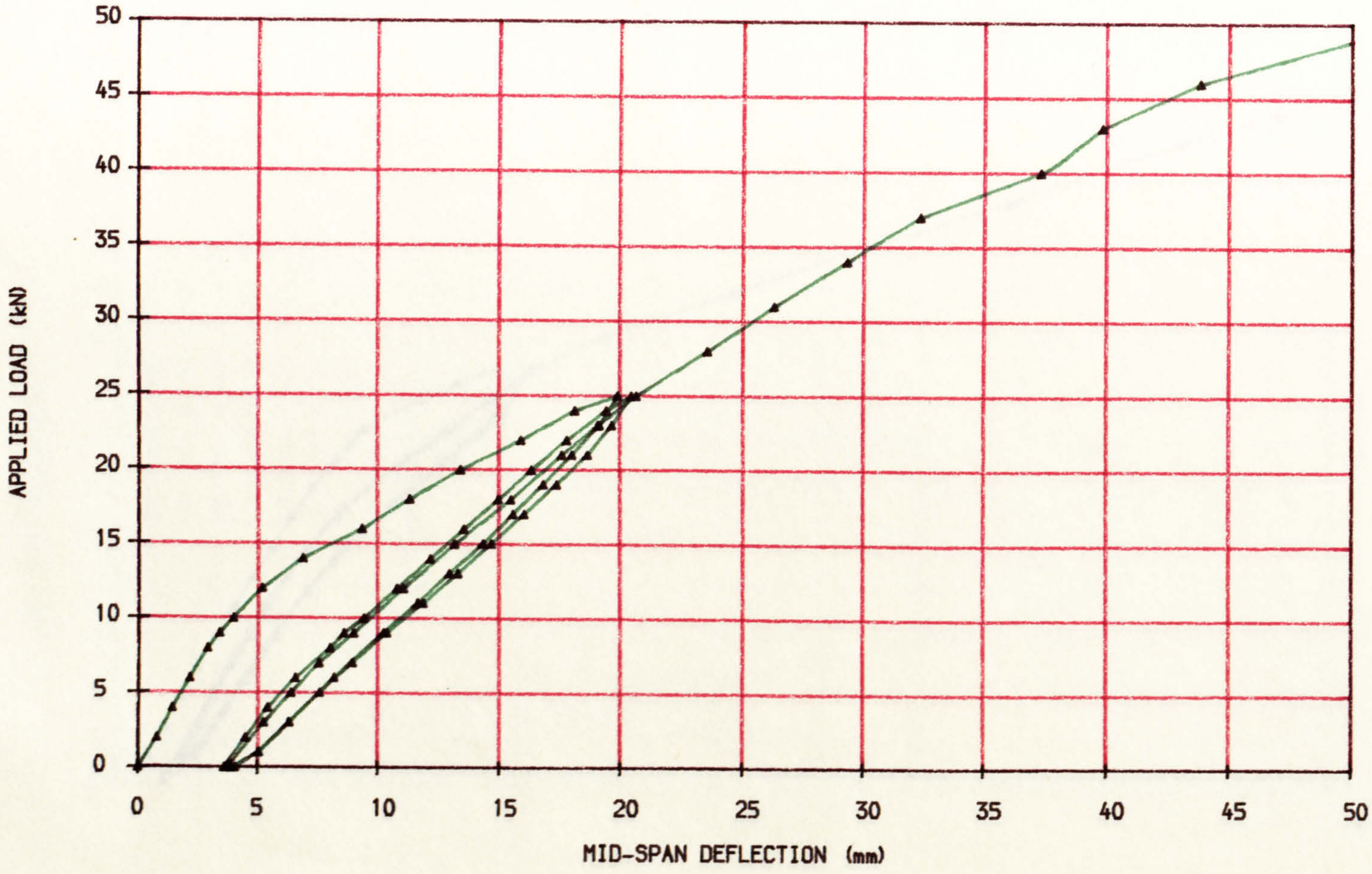

FIG. 6.4c LOAD-DEFLECTION CURVE (BEAM I2.3.2)

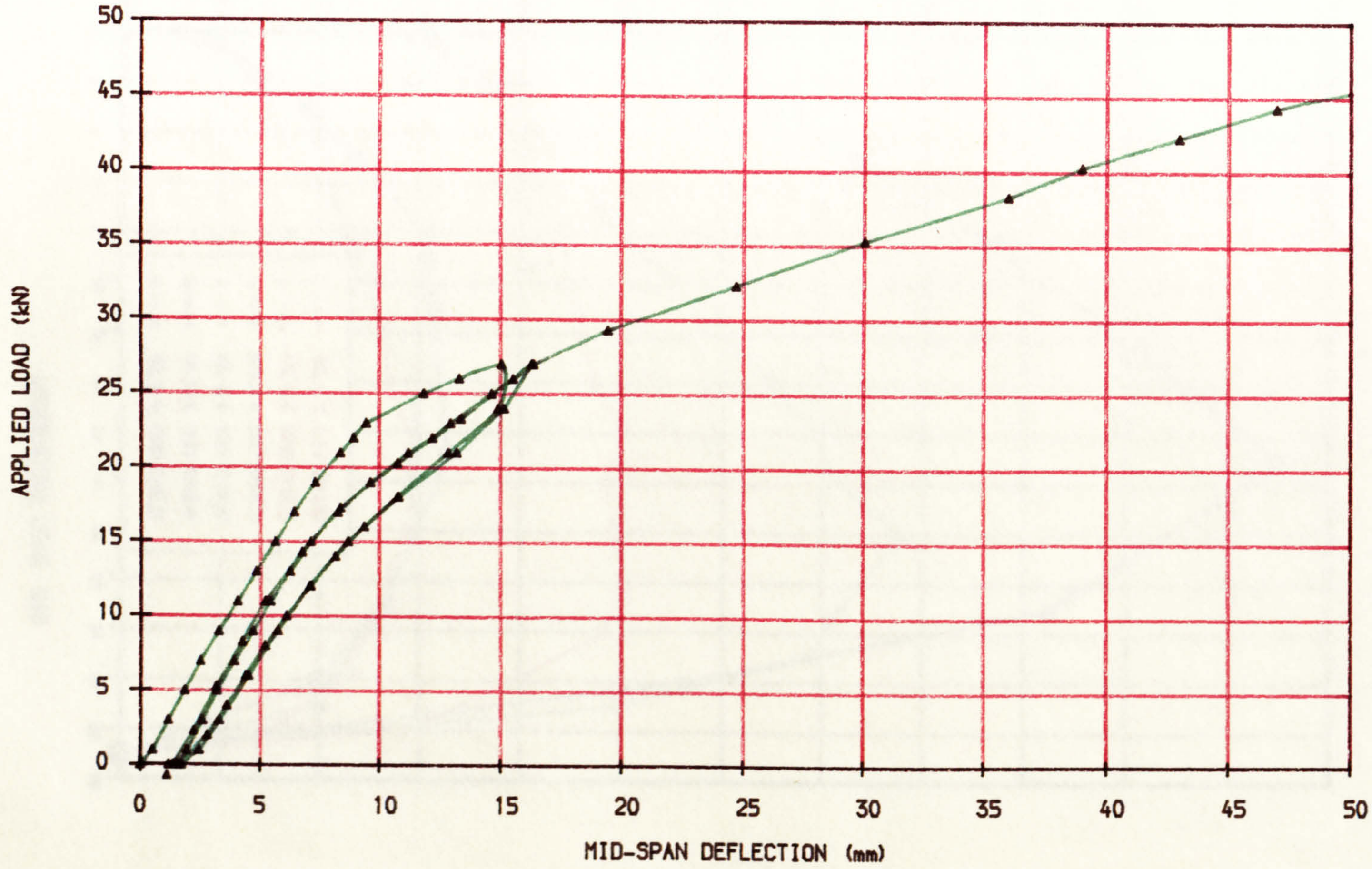

FIG. 6.5 WIDTH OF HYSTERSES LOOP OF LOAD-DEFLECTION CURVE IN DESCENDING LOAD

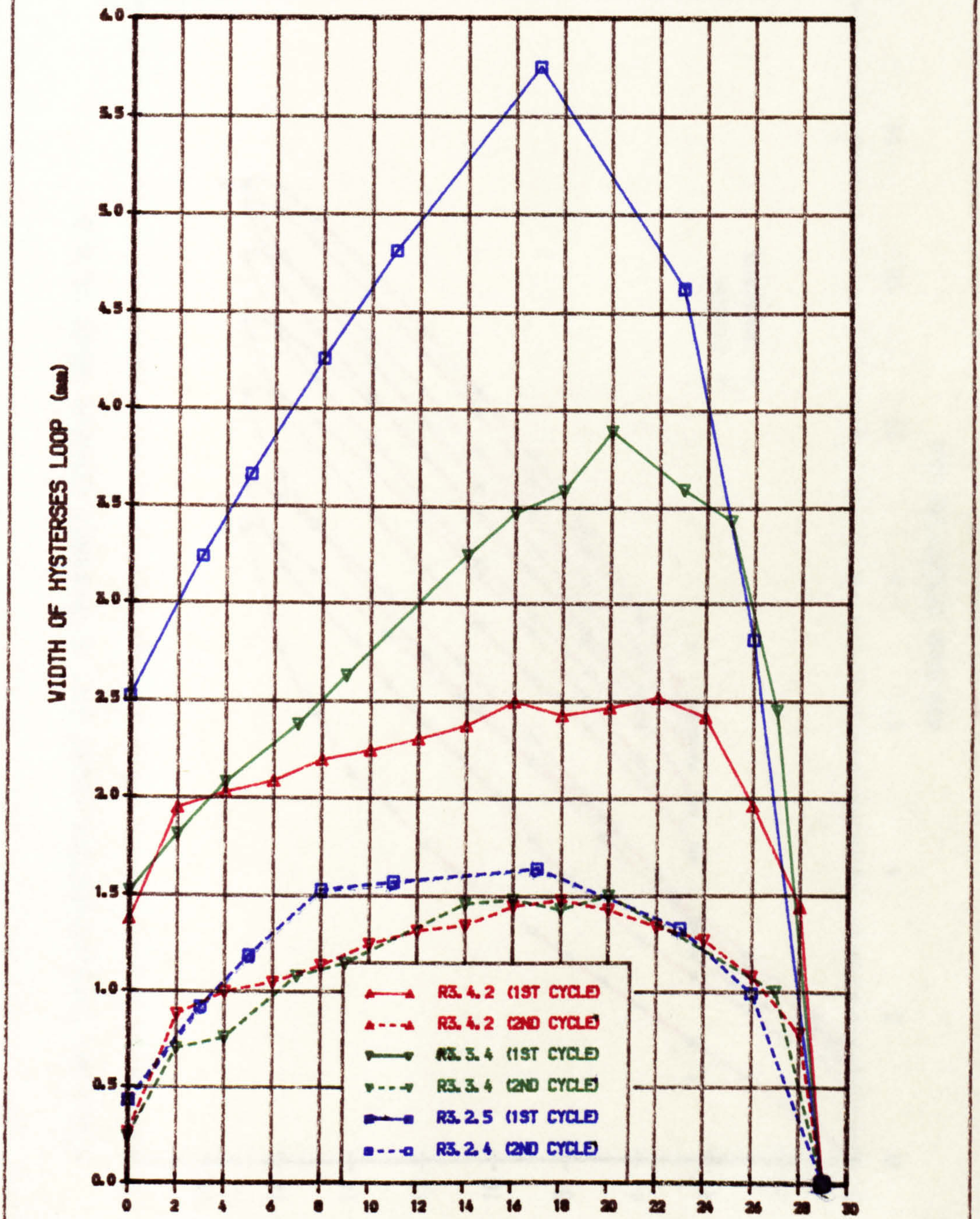

FIG. 6.6a LOAD-DEFLECTION CURVE DUE TO COMBINED LOADING (BEAM R1.2.2)

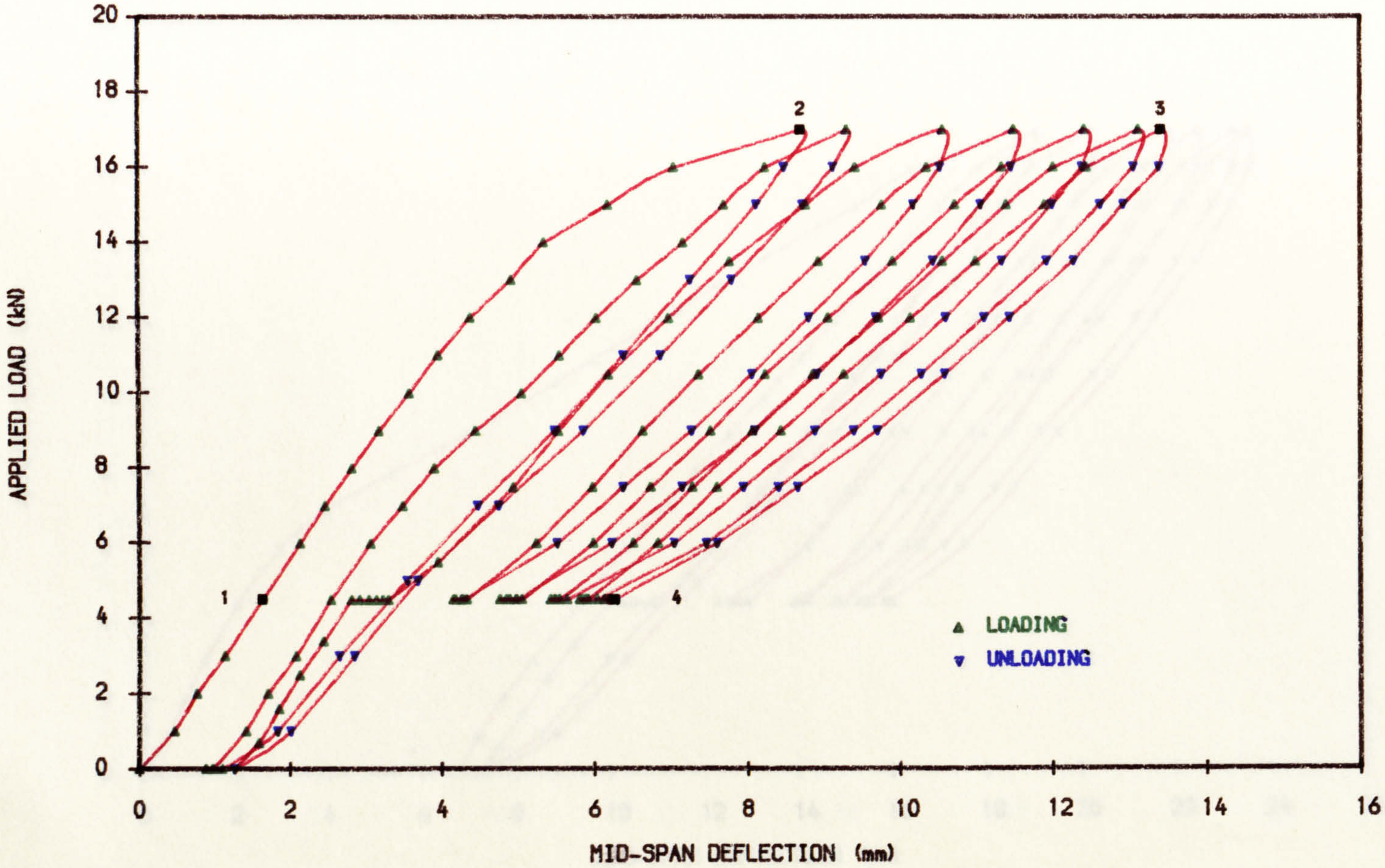

FIG. 6.6b LOAD-DEFLECTION CURVE DUE TO COMBINED LOADING (BEAM R1.0.5)

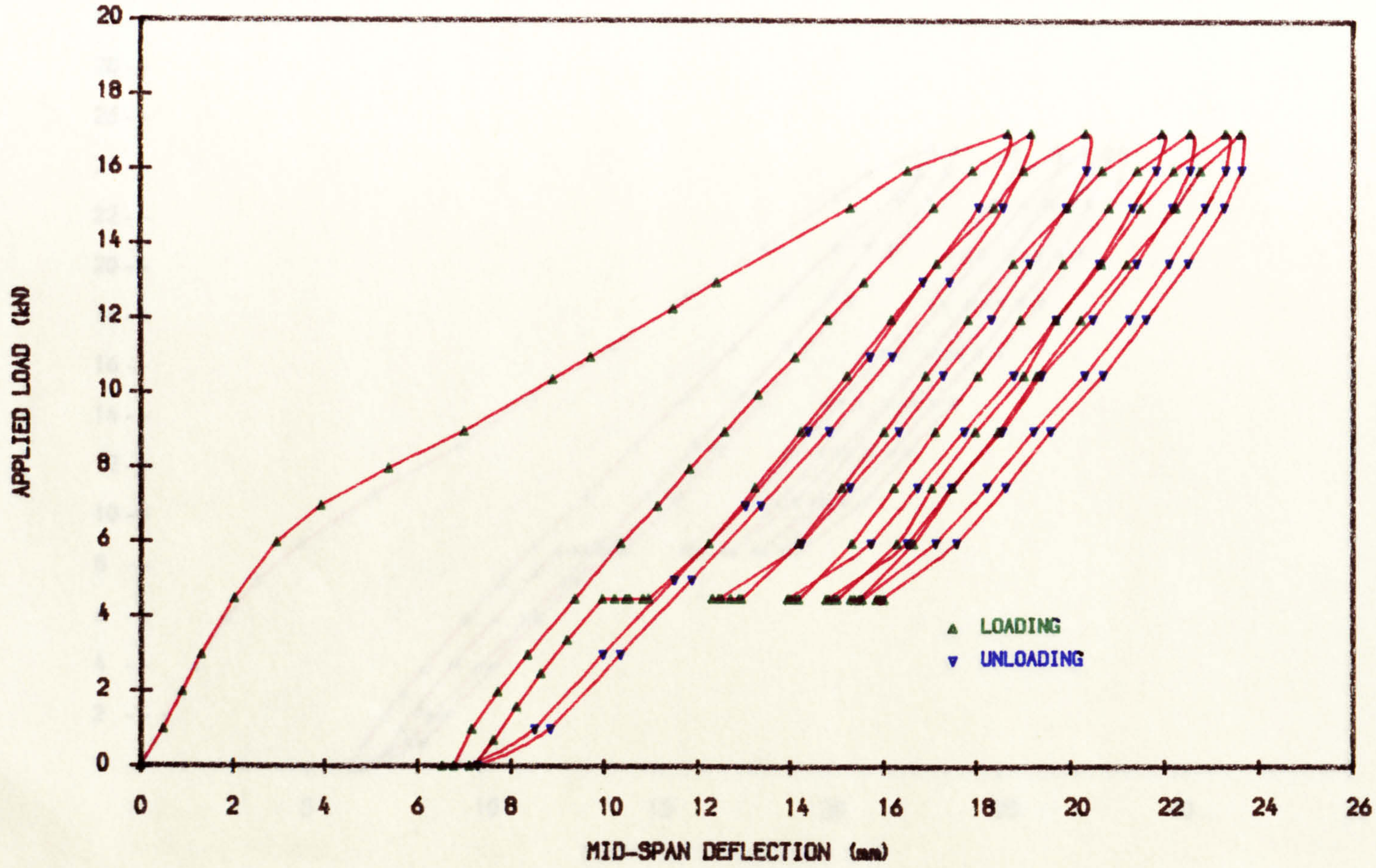

FIG. 6.6c LOAD-DEFLECTION CURVE DUE TO COMBINED LOADING (BEAM R2.0.7)

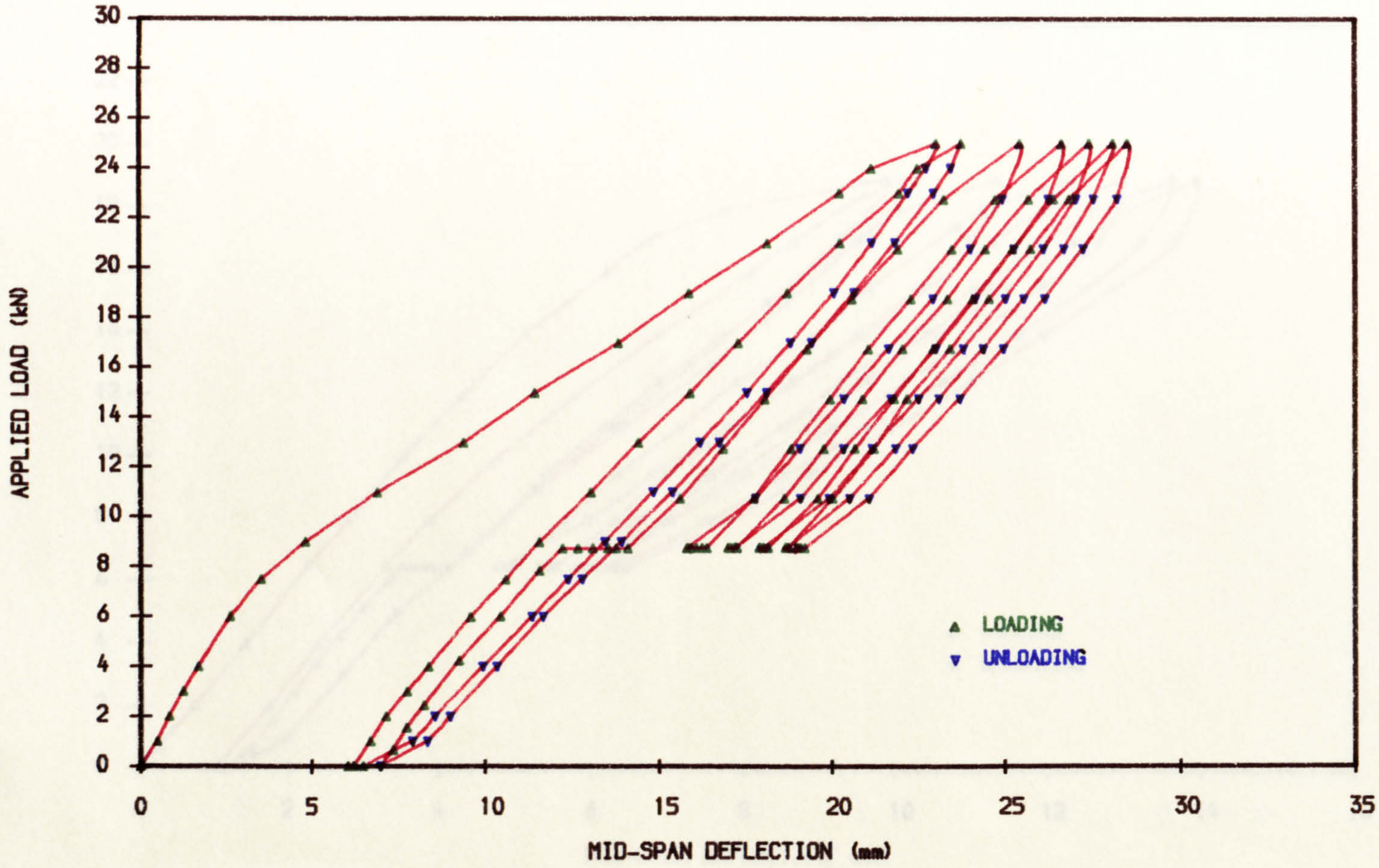

FIG. 6.6d LOAD-DEFLECTION CURVE DUE TO COMBINED LOADING (BEAM I1.2.2)

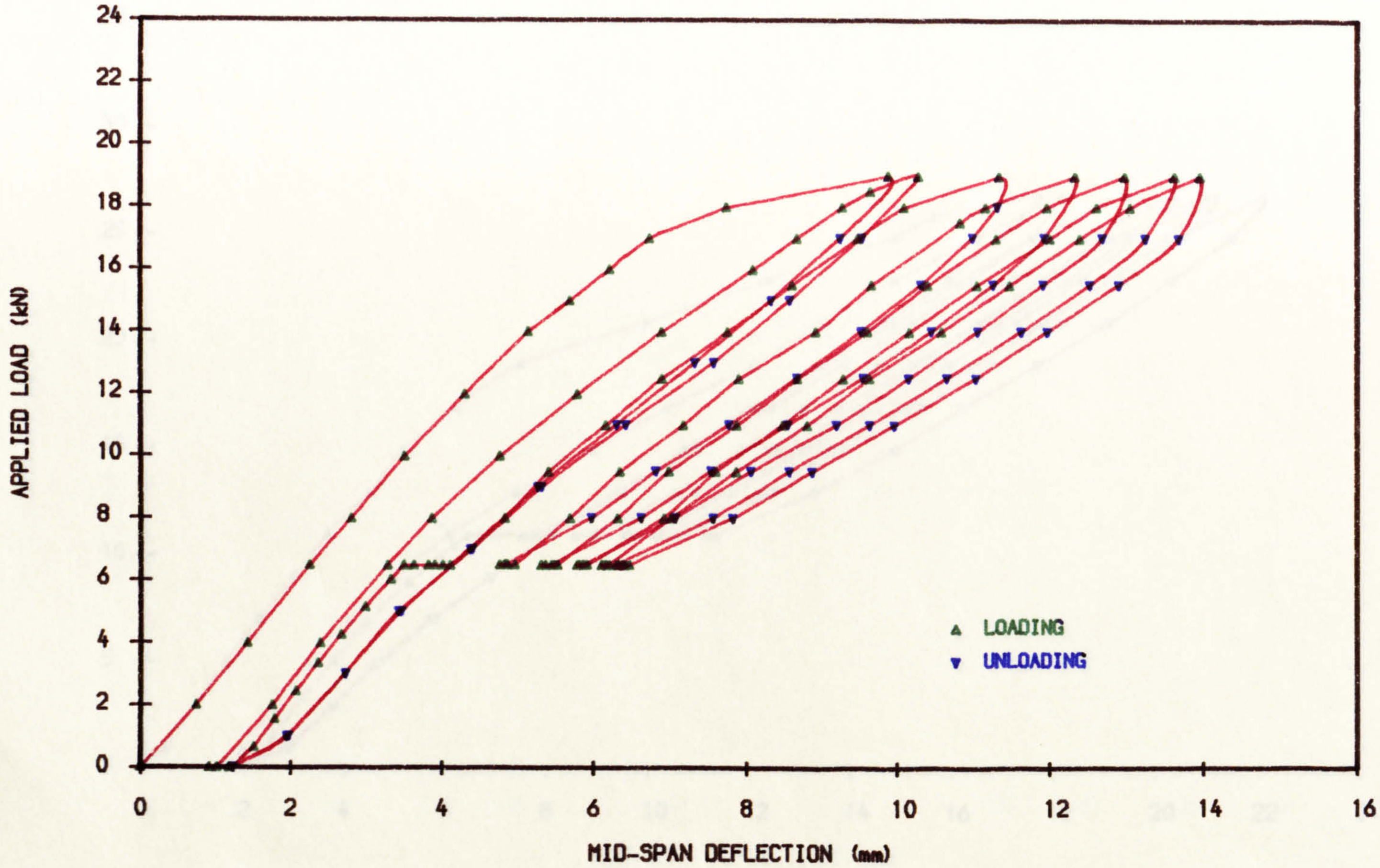

FIG. 6.6e LOAD-DEFLECTION CURVE DUE TO COMBINED LOADING (BEAM I2.2.4)

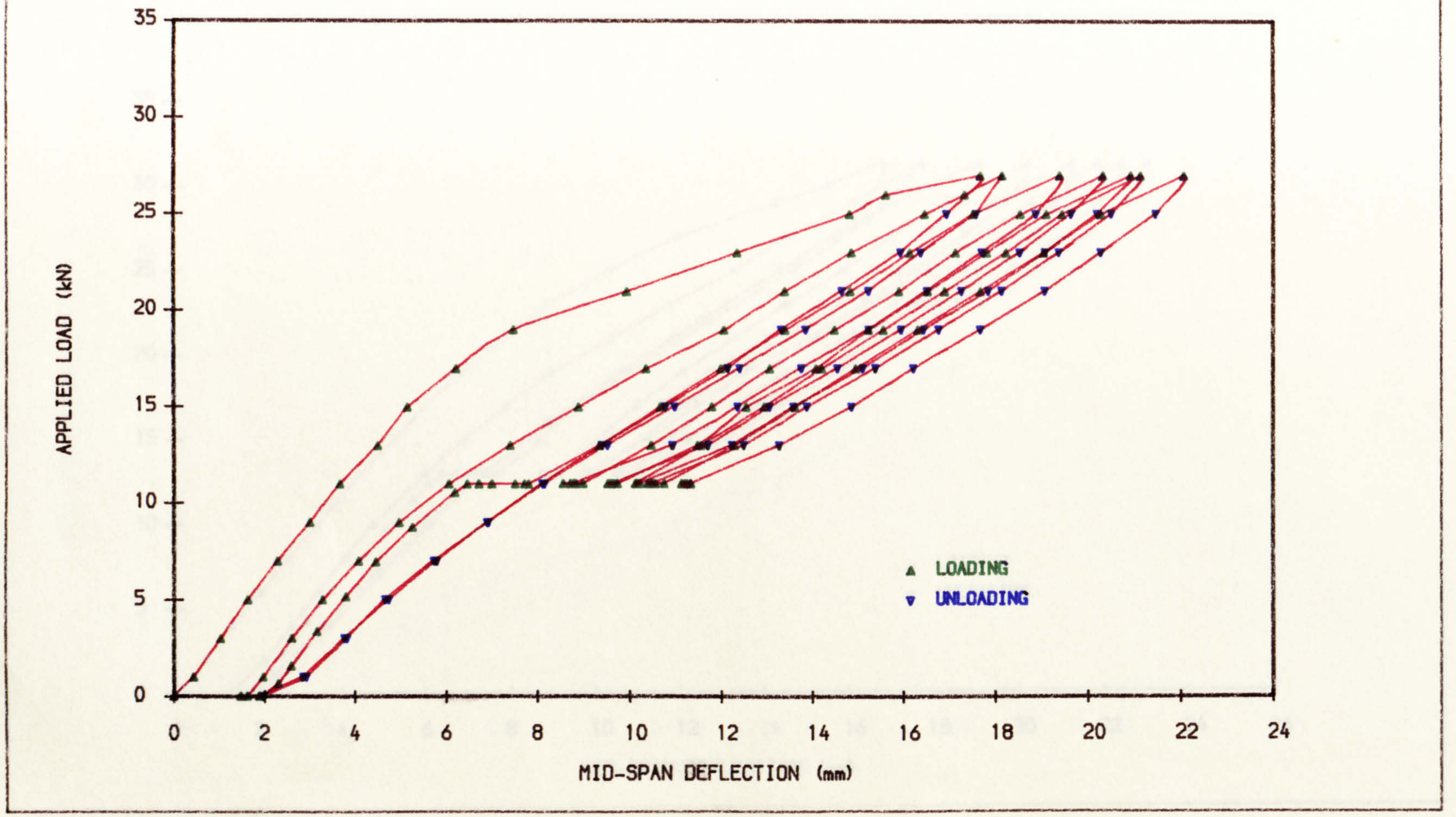

FIG. 6.6f LOAD-DEFLECTION CURVE DUE TO COMBINED LOADING (BEAM I3.3.4)

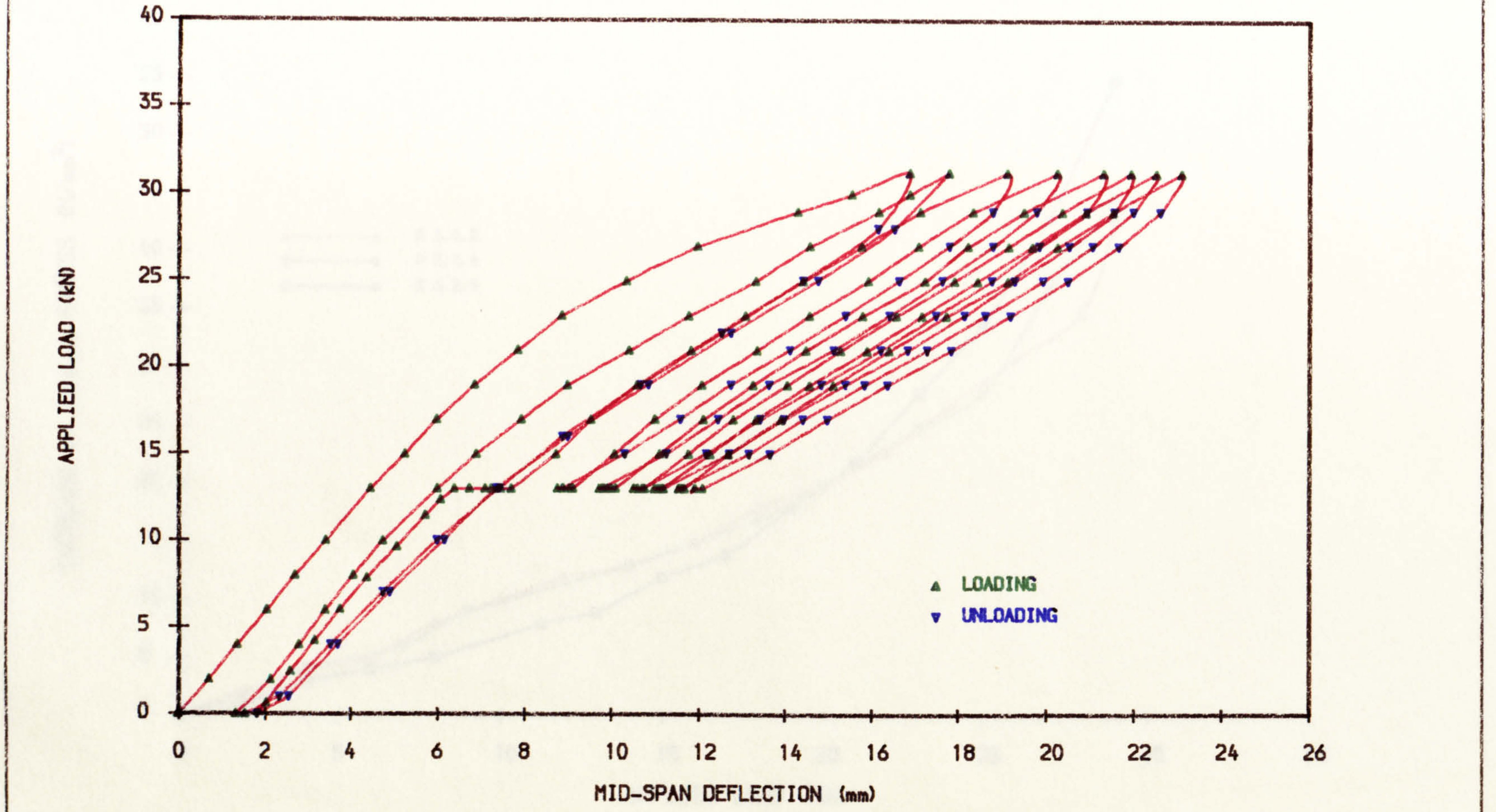

FIG. 6.7a INCREASE IN TENDON STRESS IN 1ST LOADING (BEAM SERIES 3)

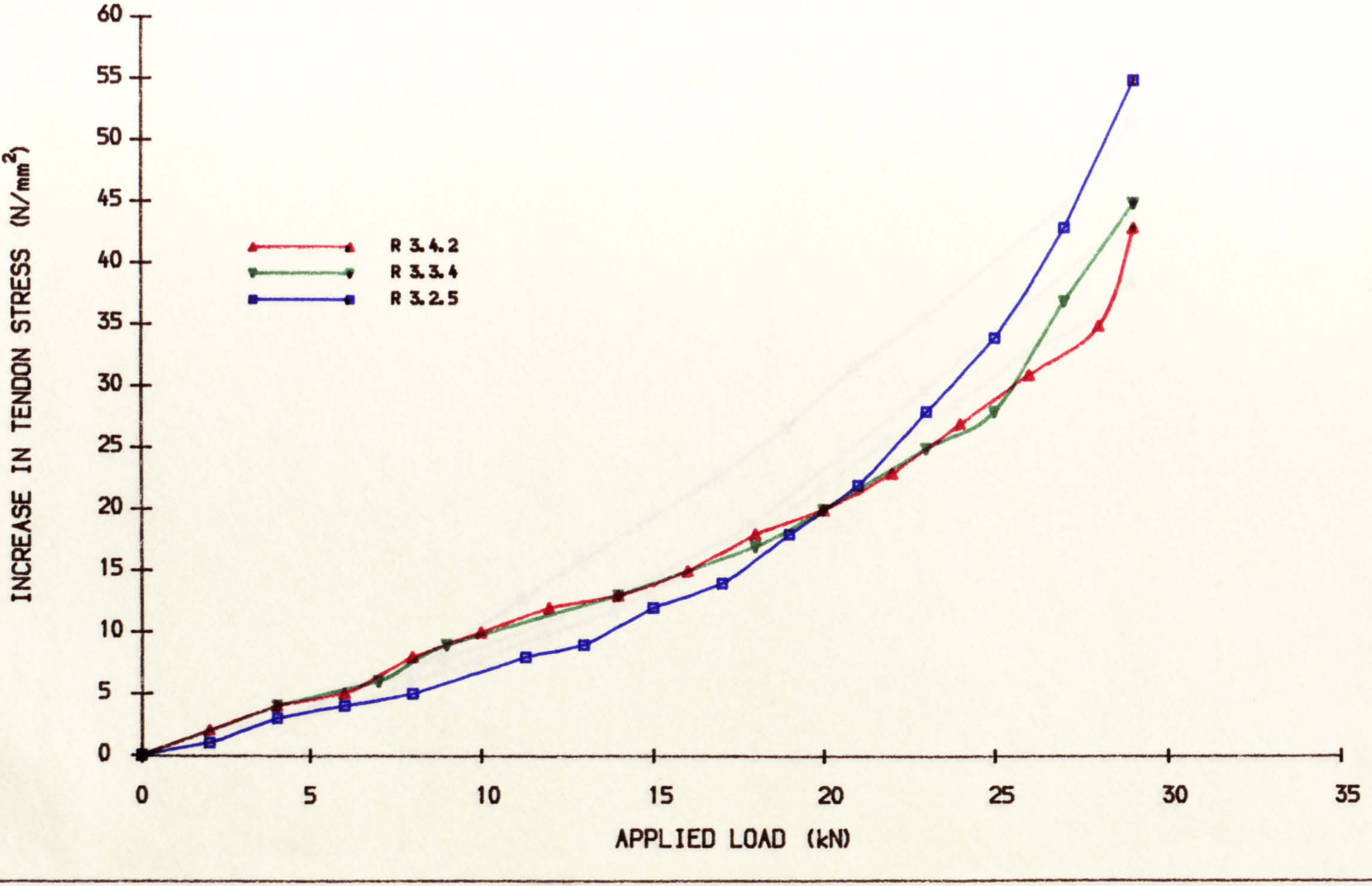

FIG. 6.7b INCREASE IN TENDON STRESS IN 2ND LOADING (BEAM SERIES 3)

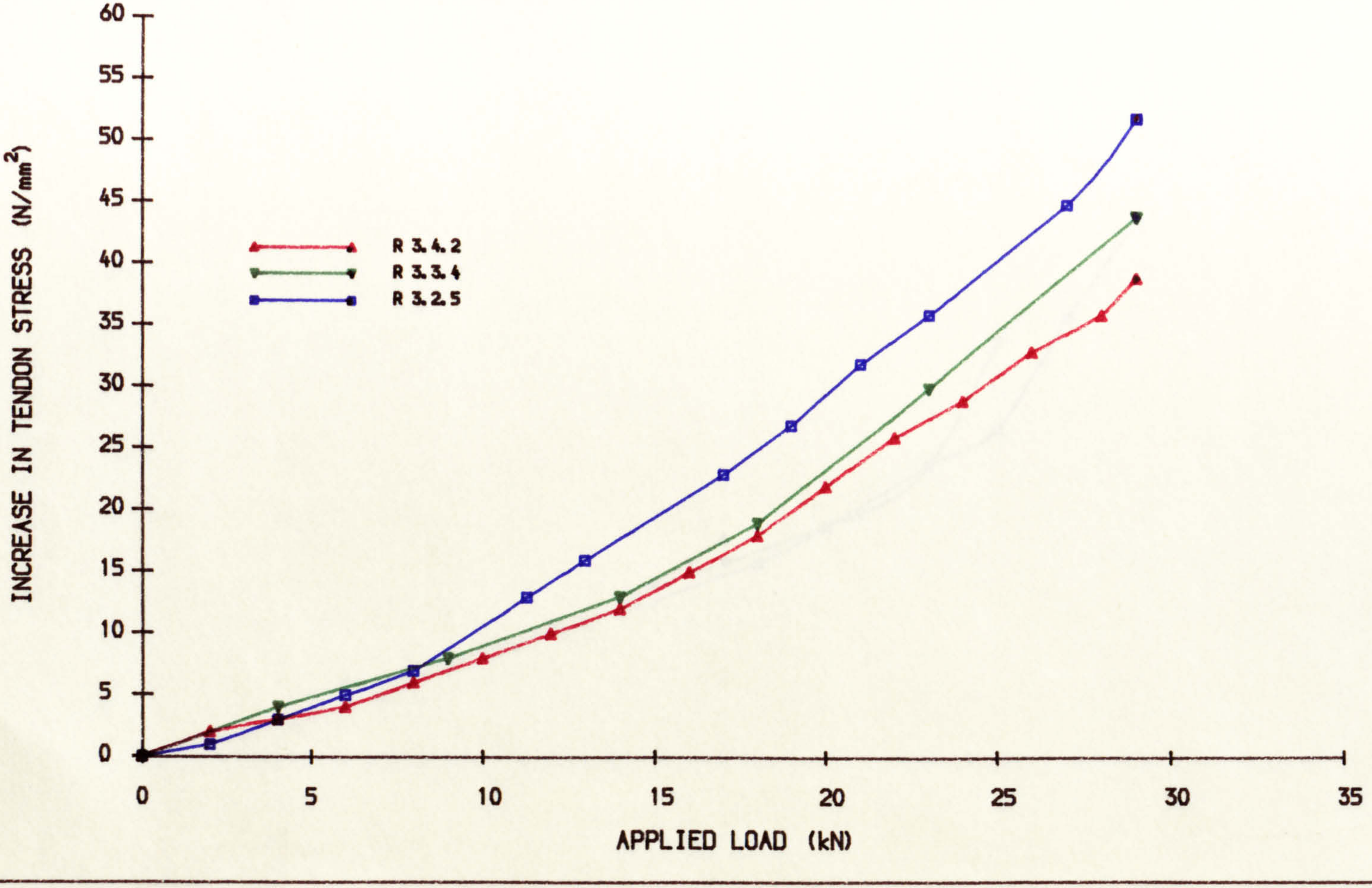

FIG. 6.7c INCREASE IN TENDON STRESS IN 1ST LOADING (SAME LEVEL OF PRESTRESS)

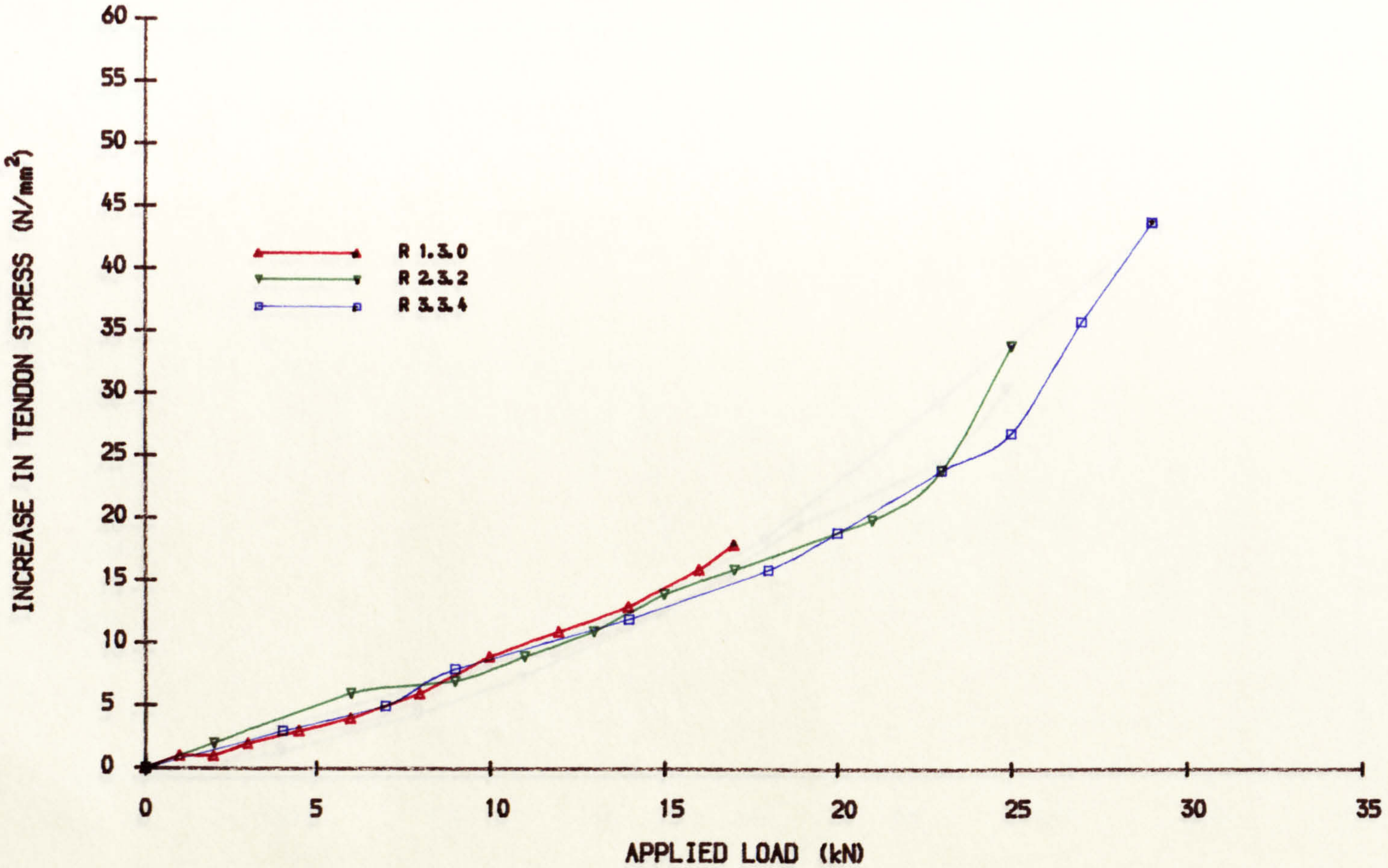

FIG. 6.7d INCREASE IN TENDON STRESS IN 2ND LOADING (SAME LEVEL OF PRESTRESS)

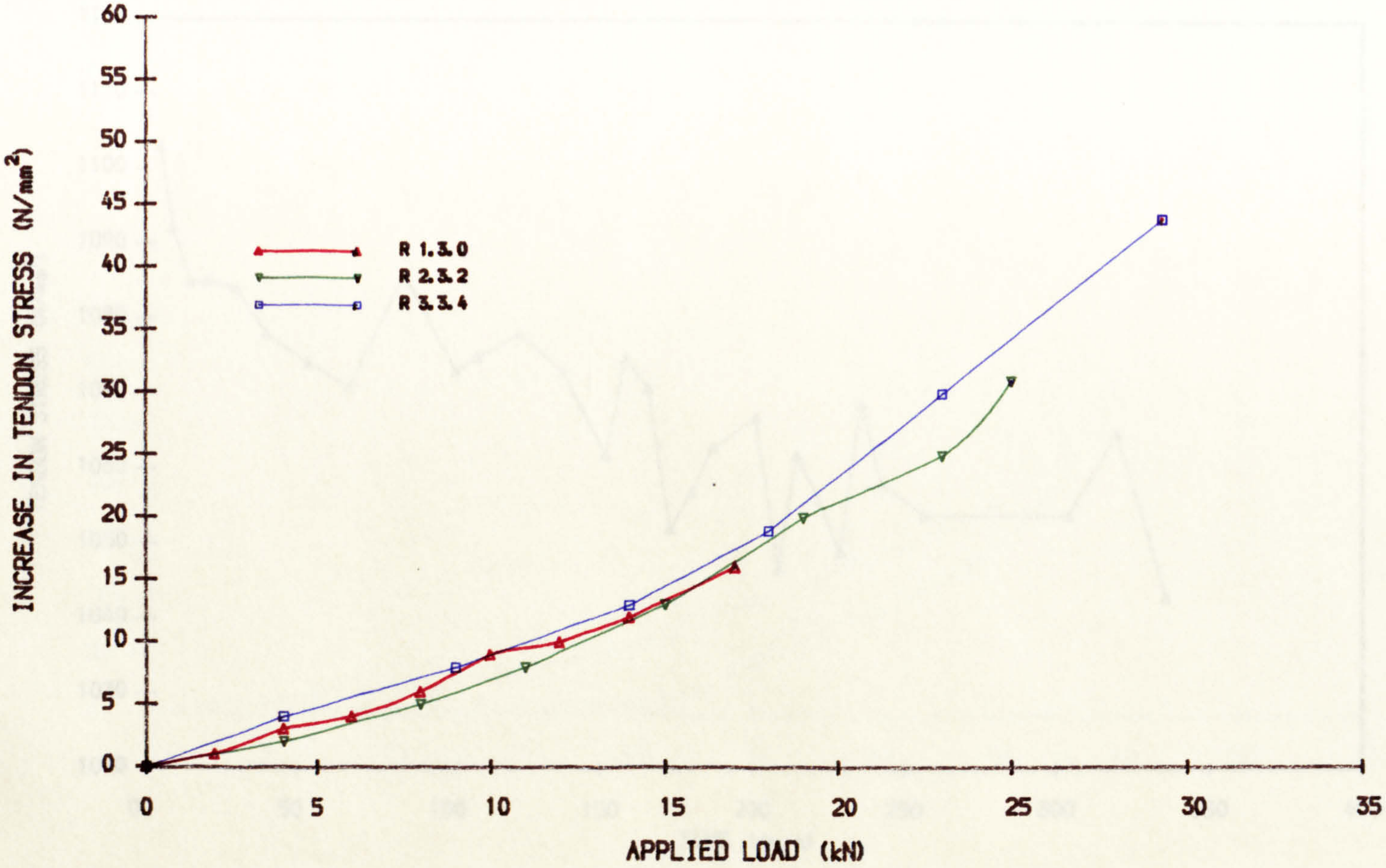

FIG. 6.7e TENDON STRESS UNDER LONG-TERM LOADING (BEAM R3. 3. 4)

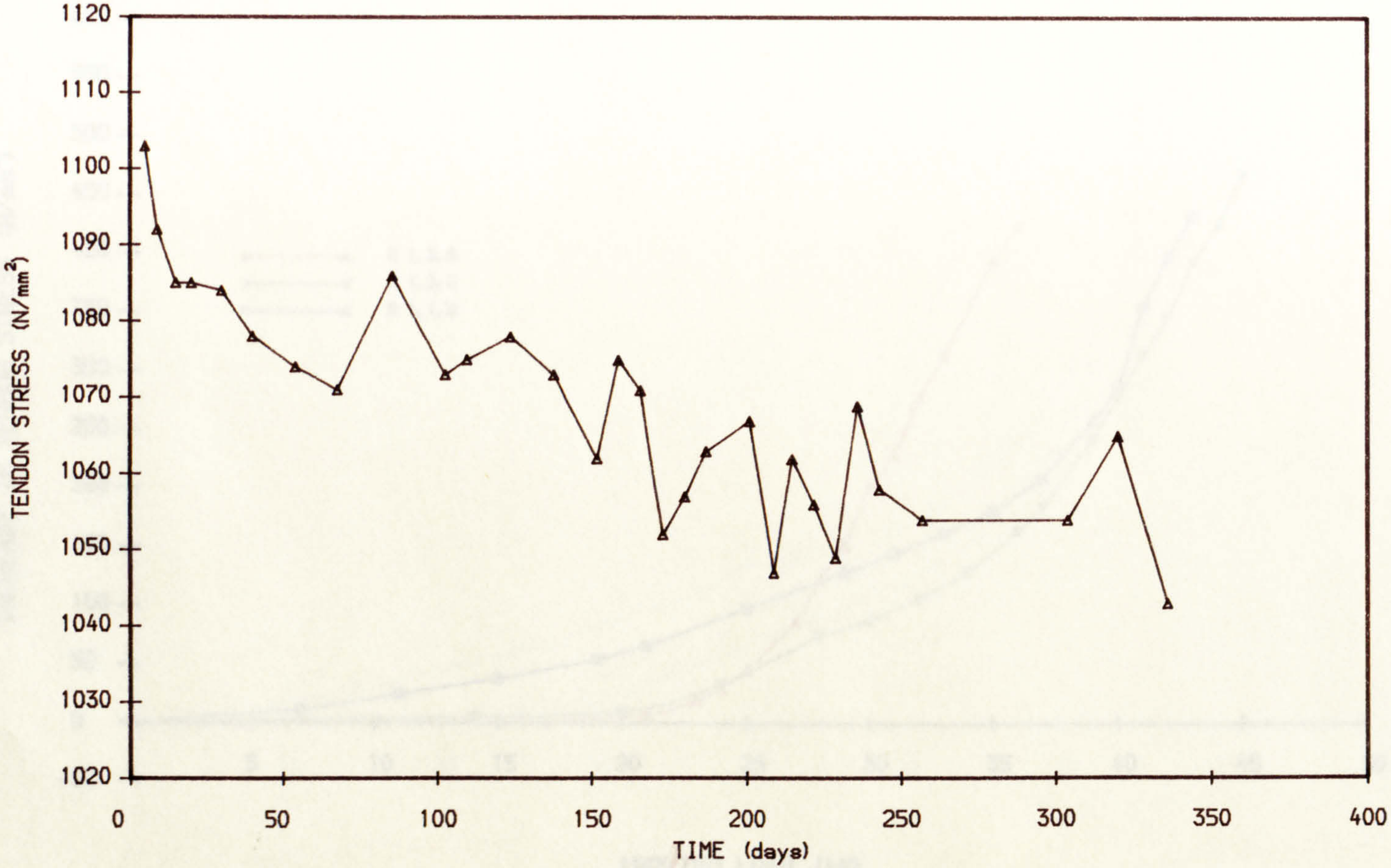

FIG. 6. 8a INCREASE IN TENDON STRESS IN FINAL LOADING (BEAM SERIES 1)

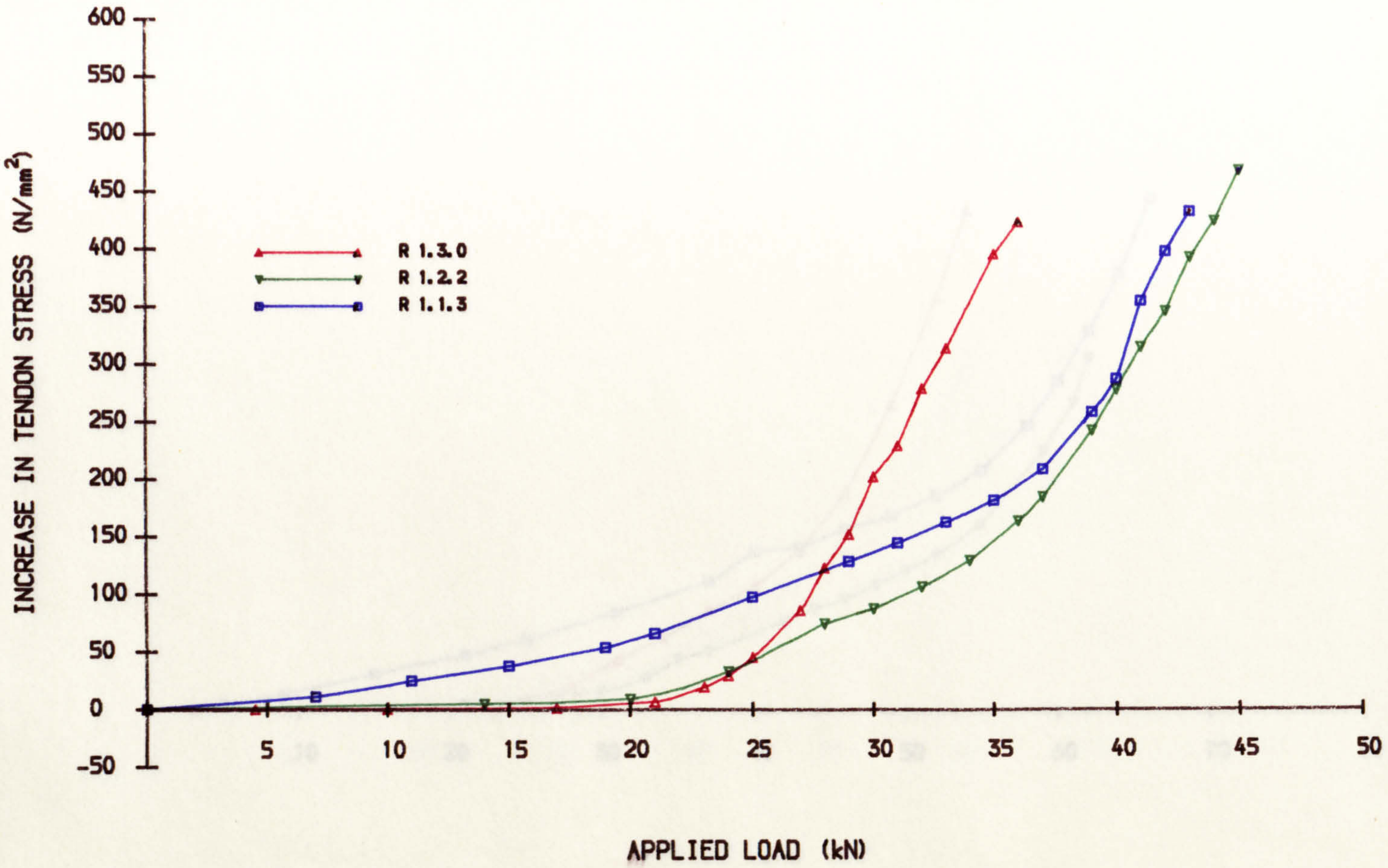

FIG. 6.8b INCREASE IN TENDON STRESS IN FINAL LOADING (BEAM SERIES 2)

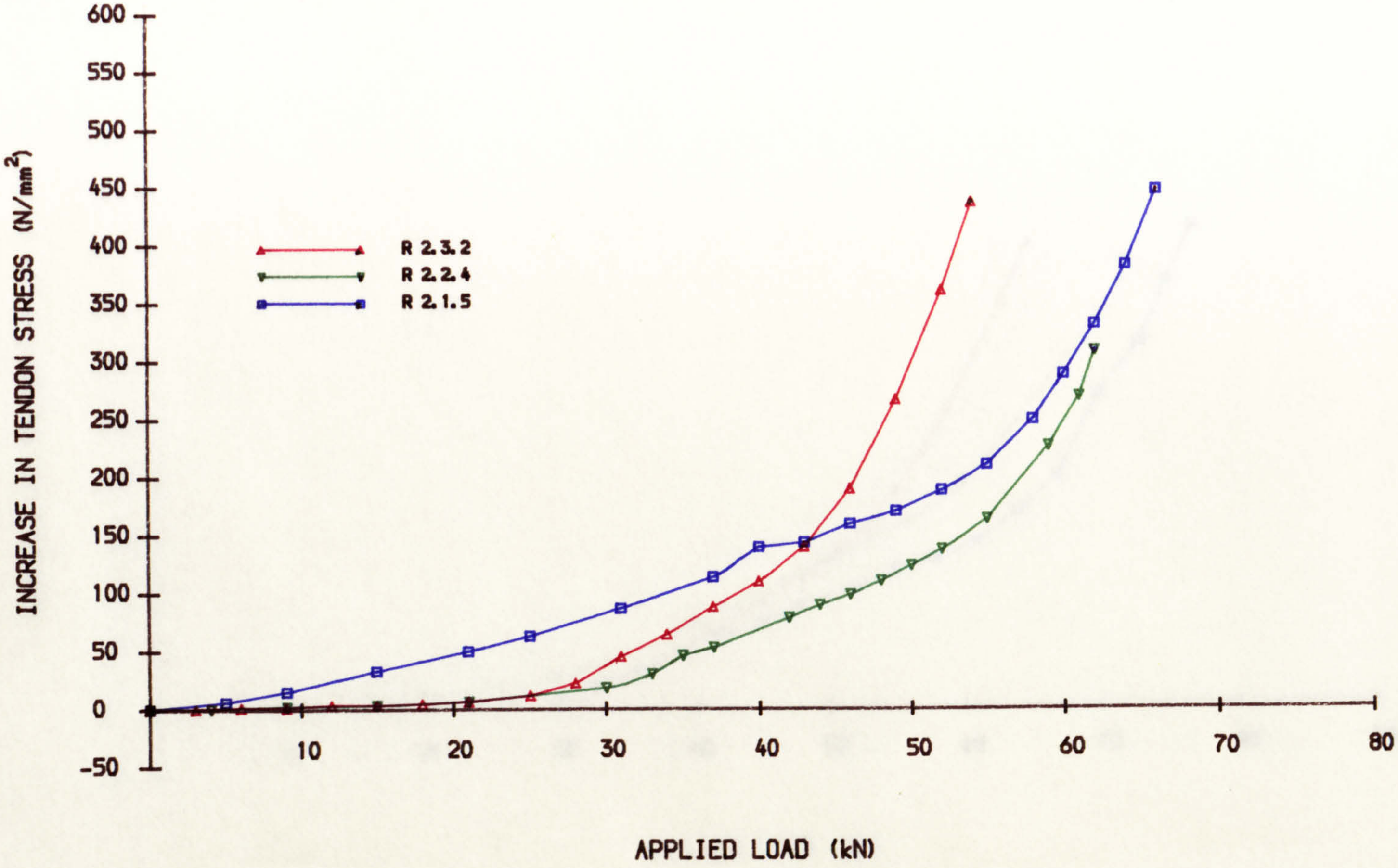

FIG. 6.8c INCREASE IN TENDON STRESS IN FINAL LOADING (BEAM SERIES 3)

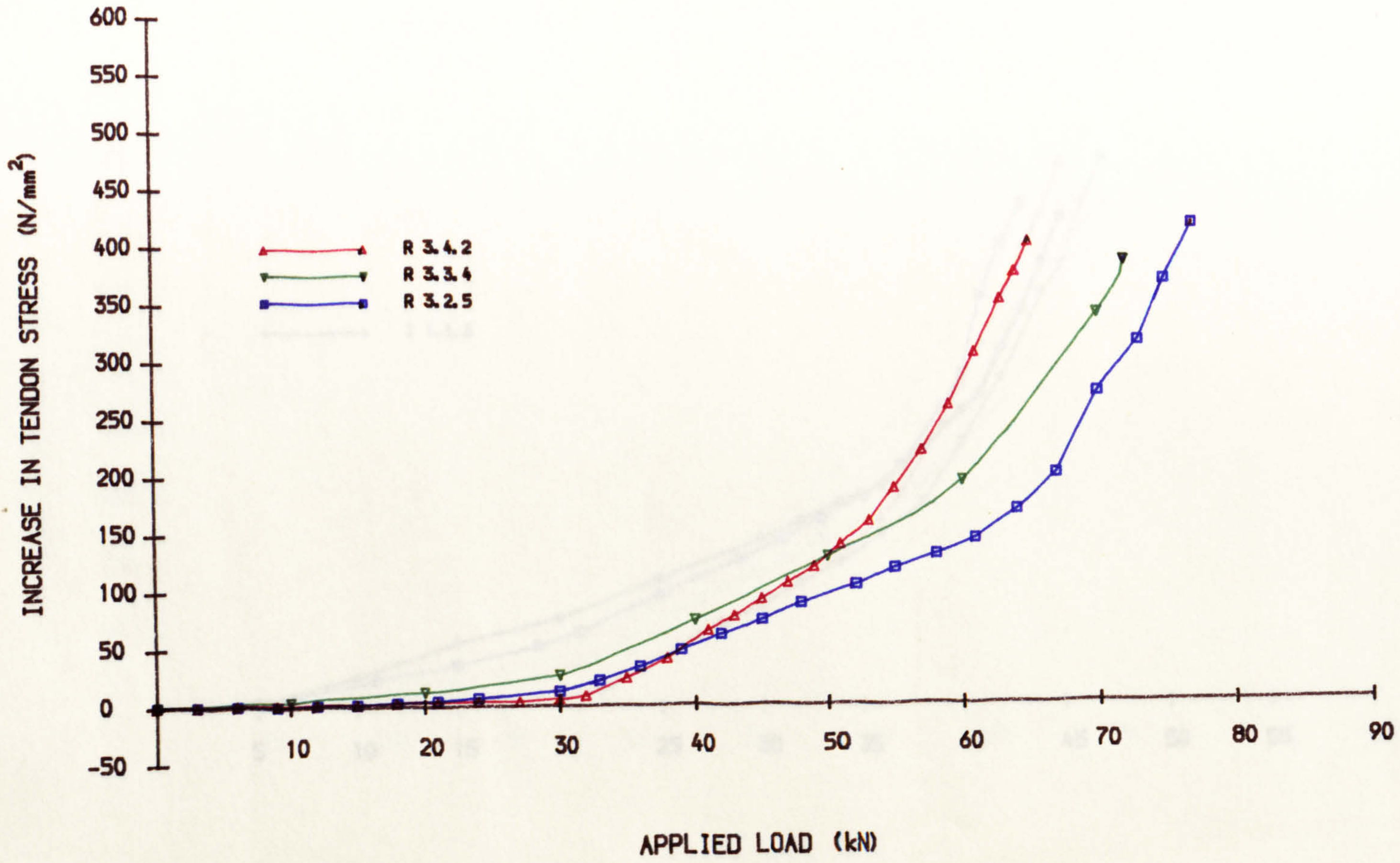

FIG. 6. 8d INCREASE IN TENDON STRESS IN FINAL LOADING (DIFFENENT CROSS-SECTION)

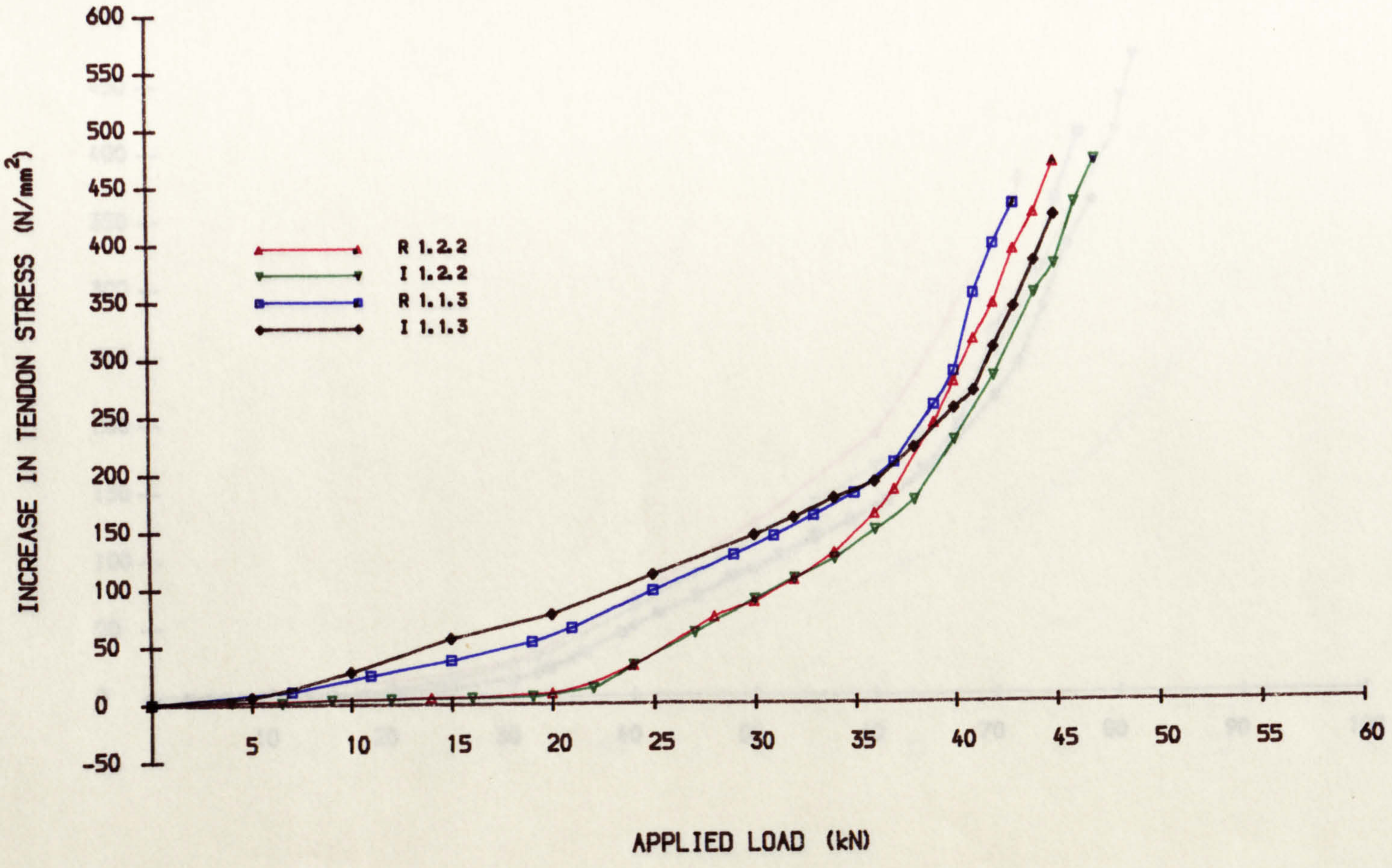

FIG. 6.8e INCREASE IN TENDON STRESS IN FINAL LOADING (DIFFERENT CROSS-SECTION)

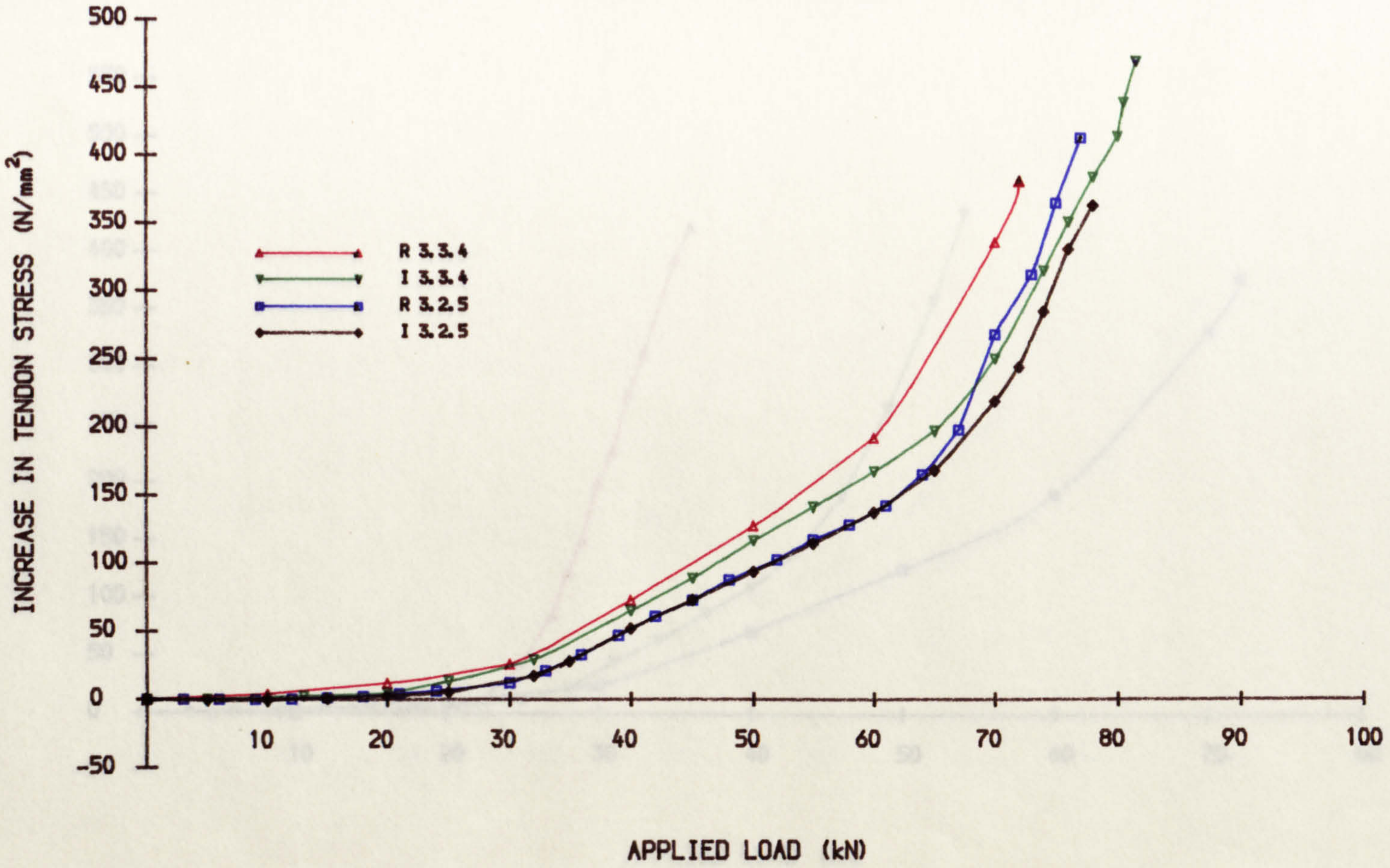

FIG. 6.8f INCREASE IN TENDON STRESS IN FINAL LOADING (SAME LEVEL OF PRESTRESS)

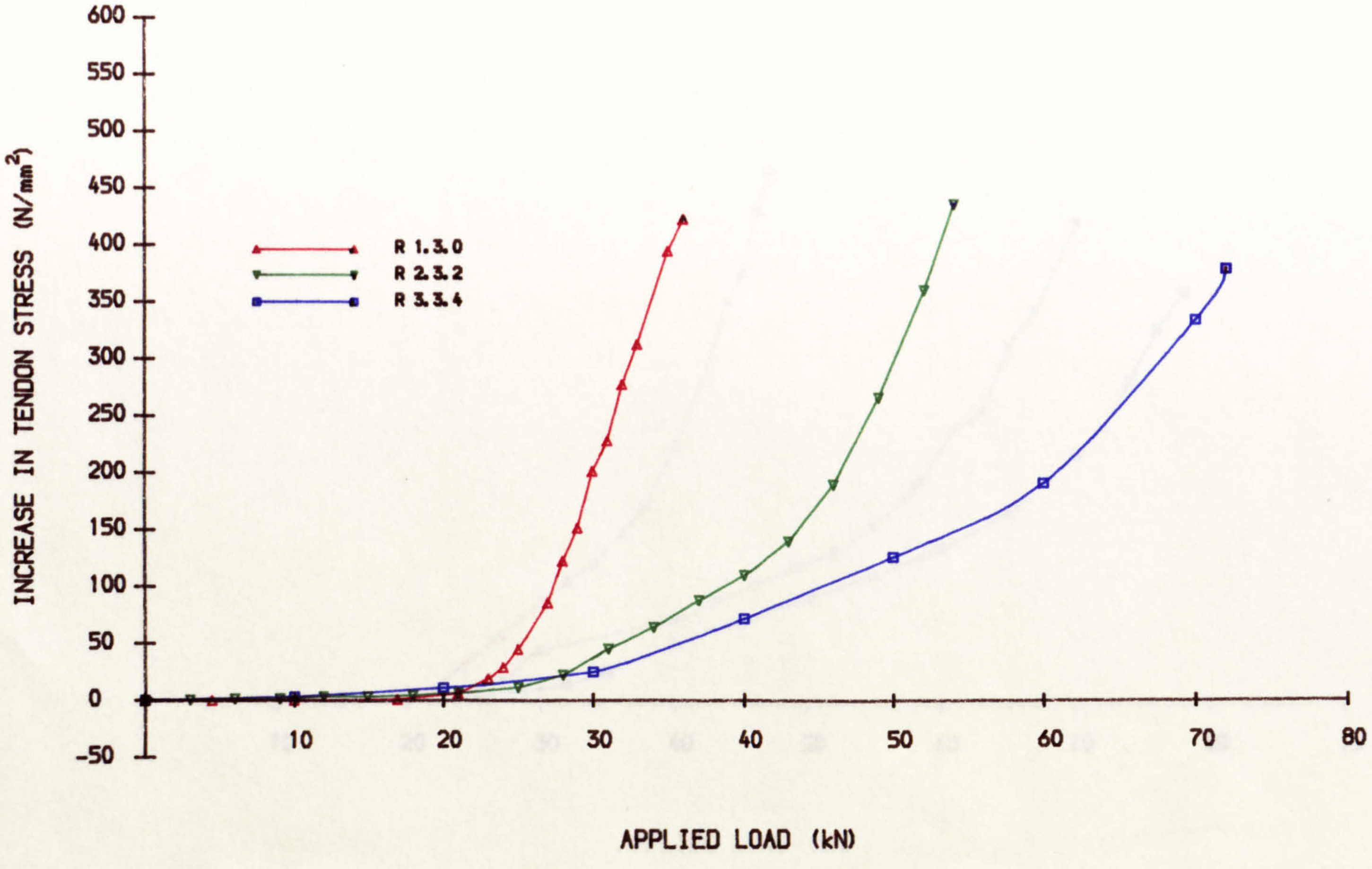

FIG. 6.8g INCREASE IN TENDON STRESS IN FINAL LOADING (SAME LEVEL OF PRESTRES)

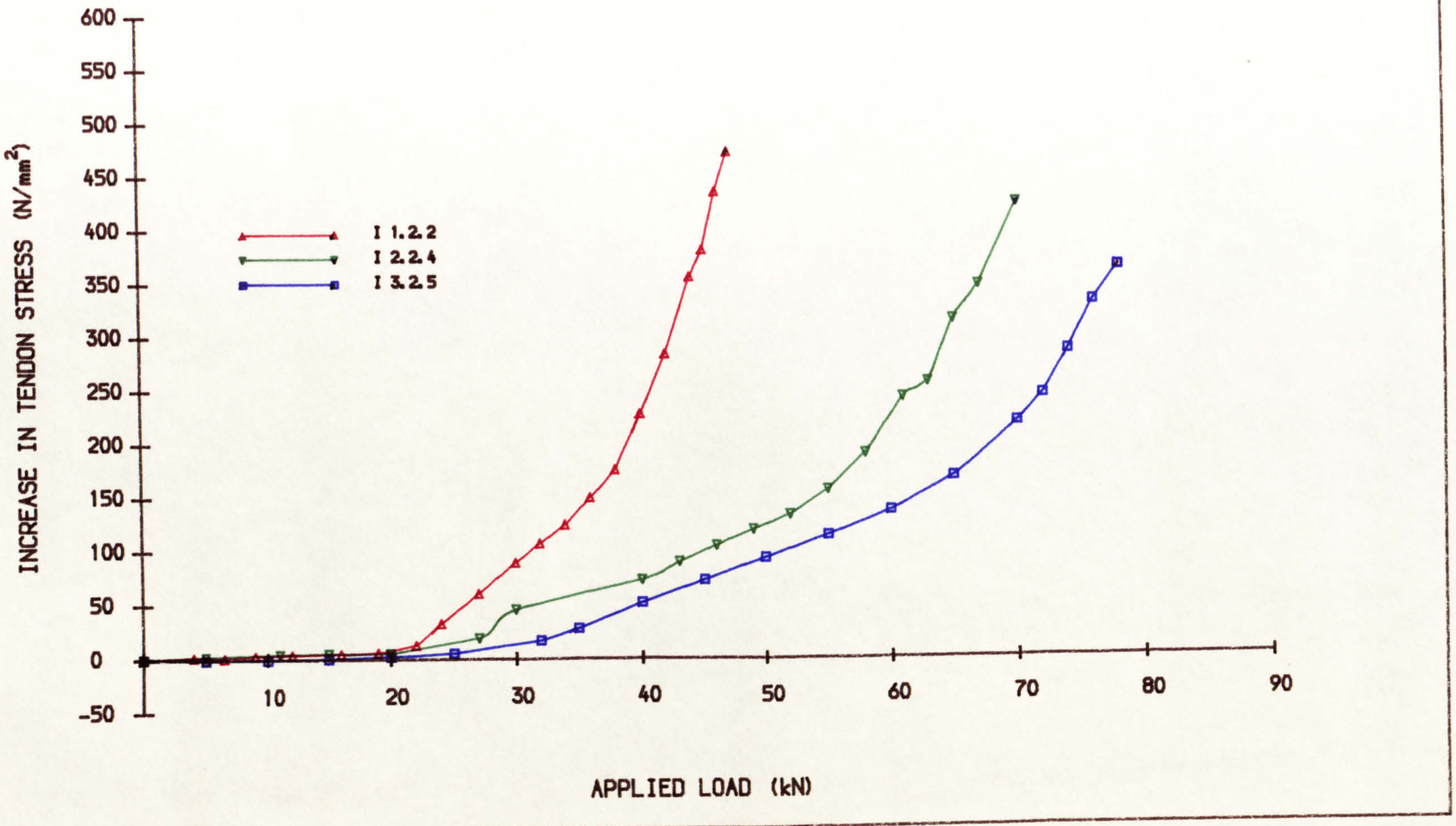

FIG. 6.9a TENDON STRESS MEASURED AT CENTRE AND SUPPORT (R1.3.0)

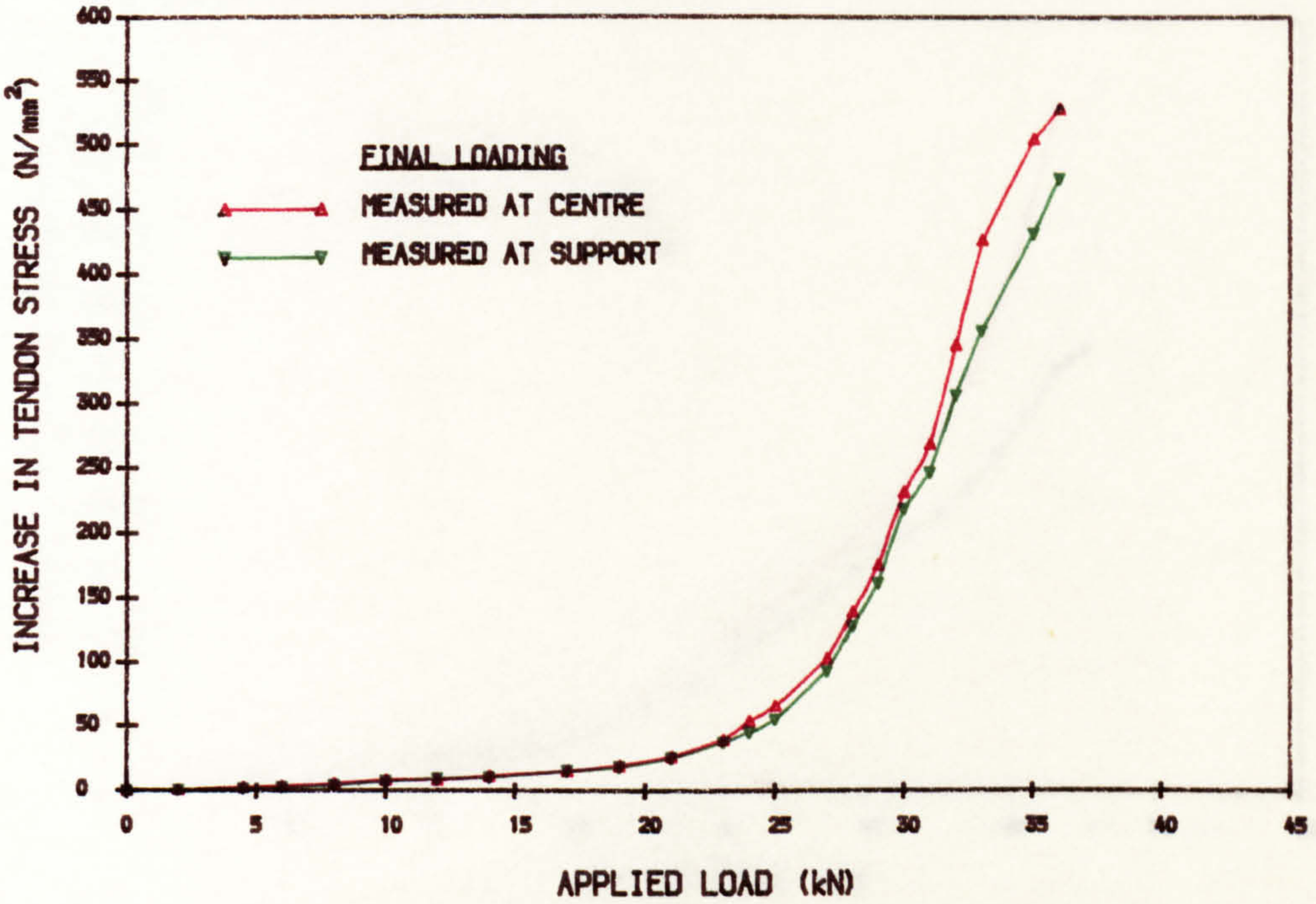

FIG. 6.9b TENDON STRESS MEASURED AT CENTRE AND SUPPORT (R2.1.5)

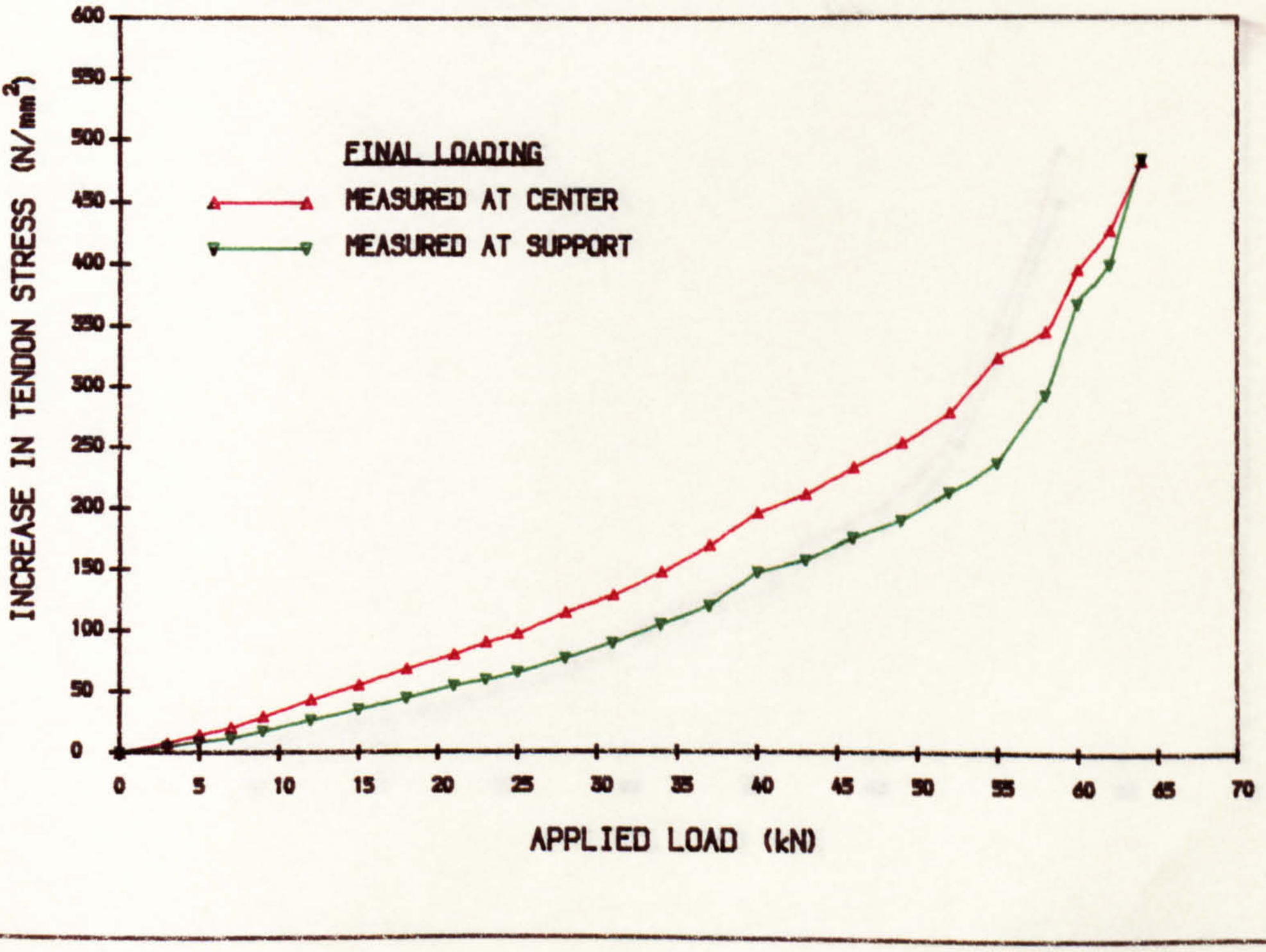

FIG. 6.9c TENDON STRESS MEASURED AT CENTRE AND SUPPORT (R3.4.2)

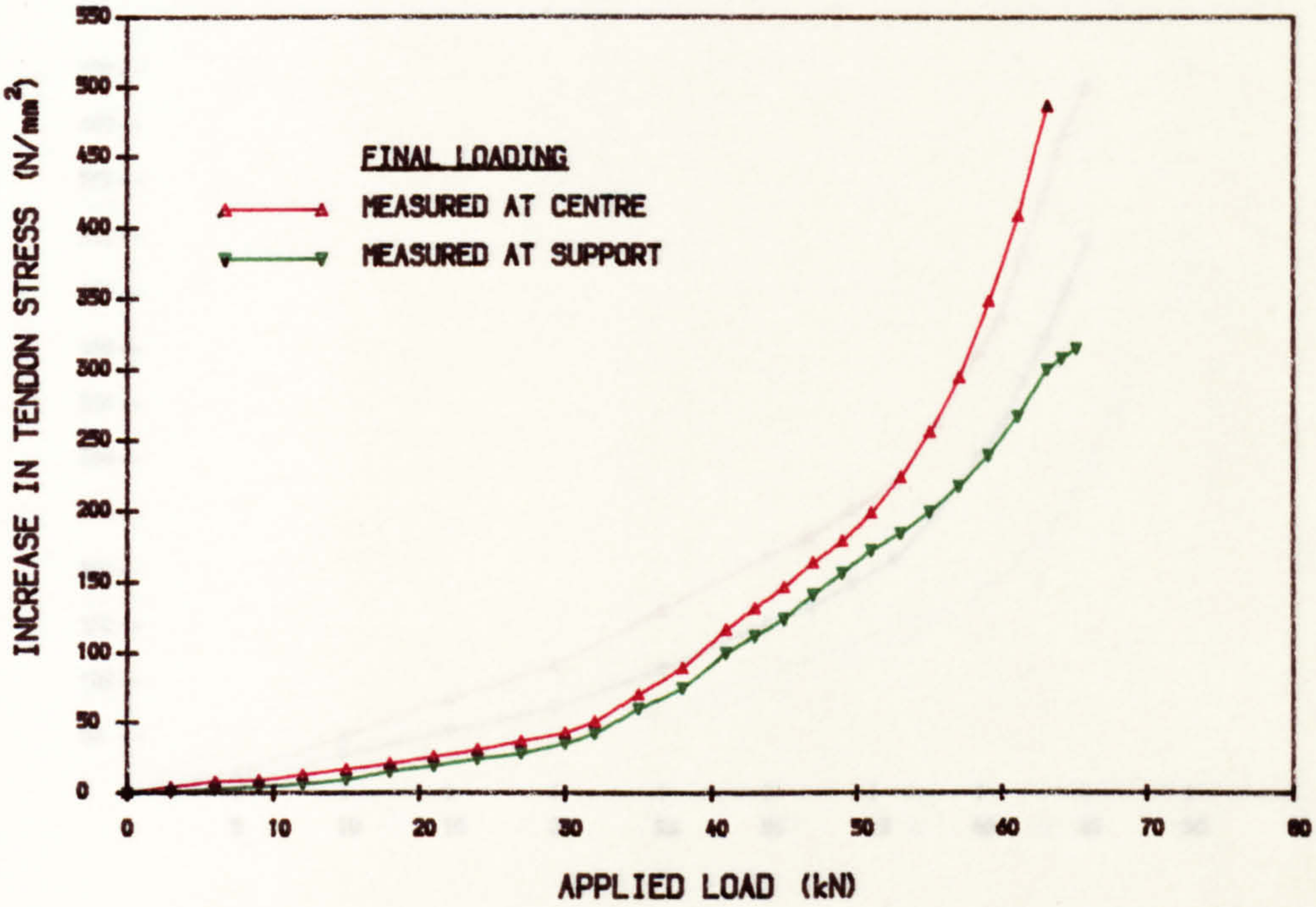

FIG. 6.9d TENDON STRESS MEASURED AT CENTRE AND SUPPORT (R3.2.5)

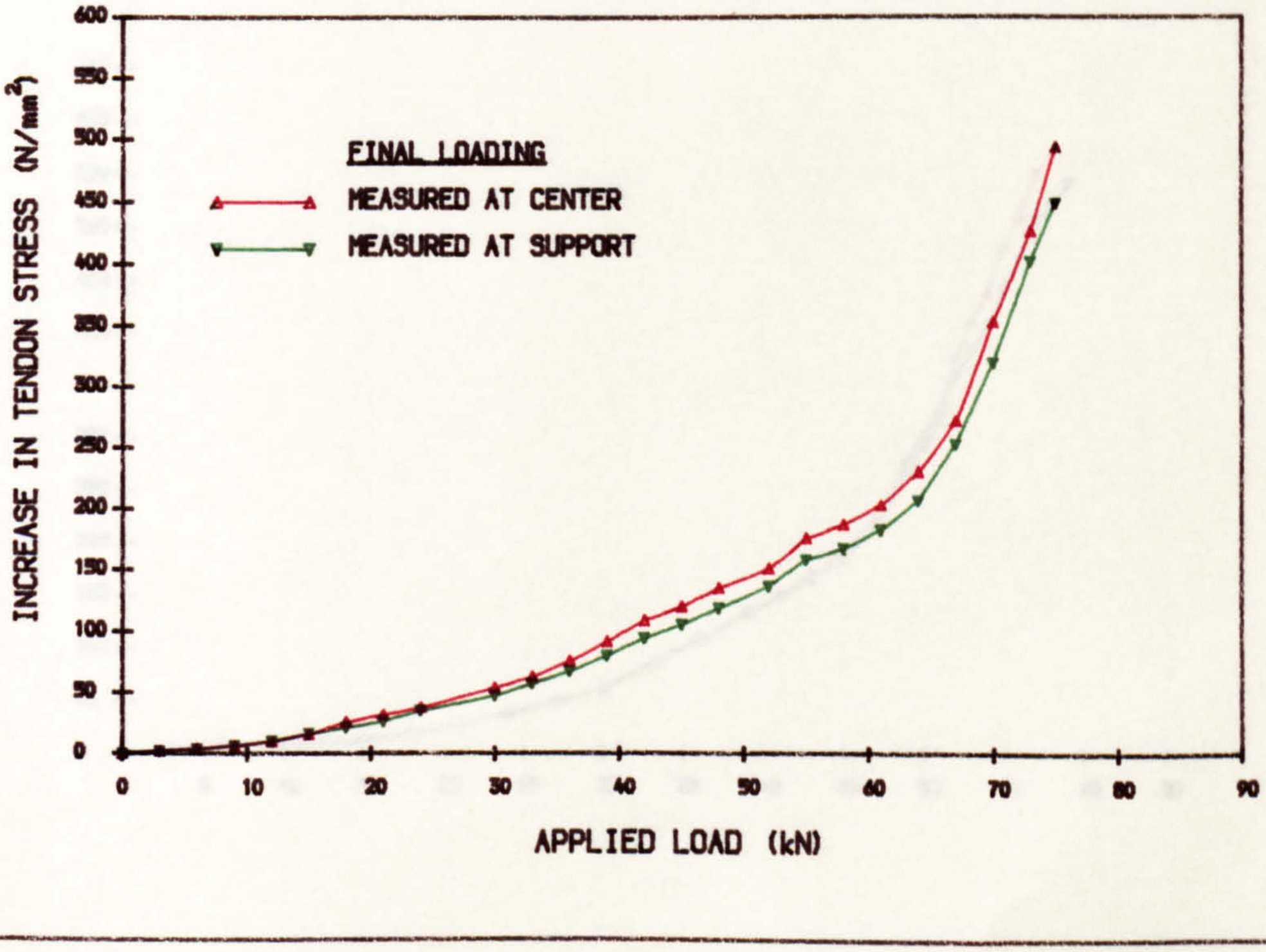

FIG. 6.9e TENDON STRESS MEASURED AT CENTRE AND SUPPORT (I1.1.3)

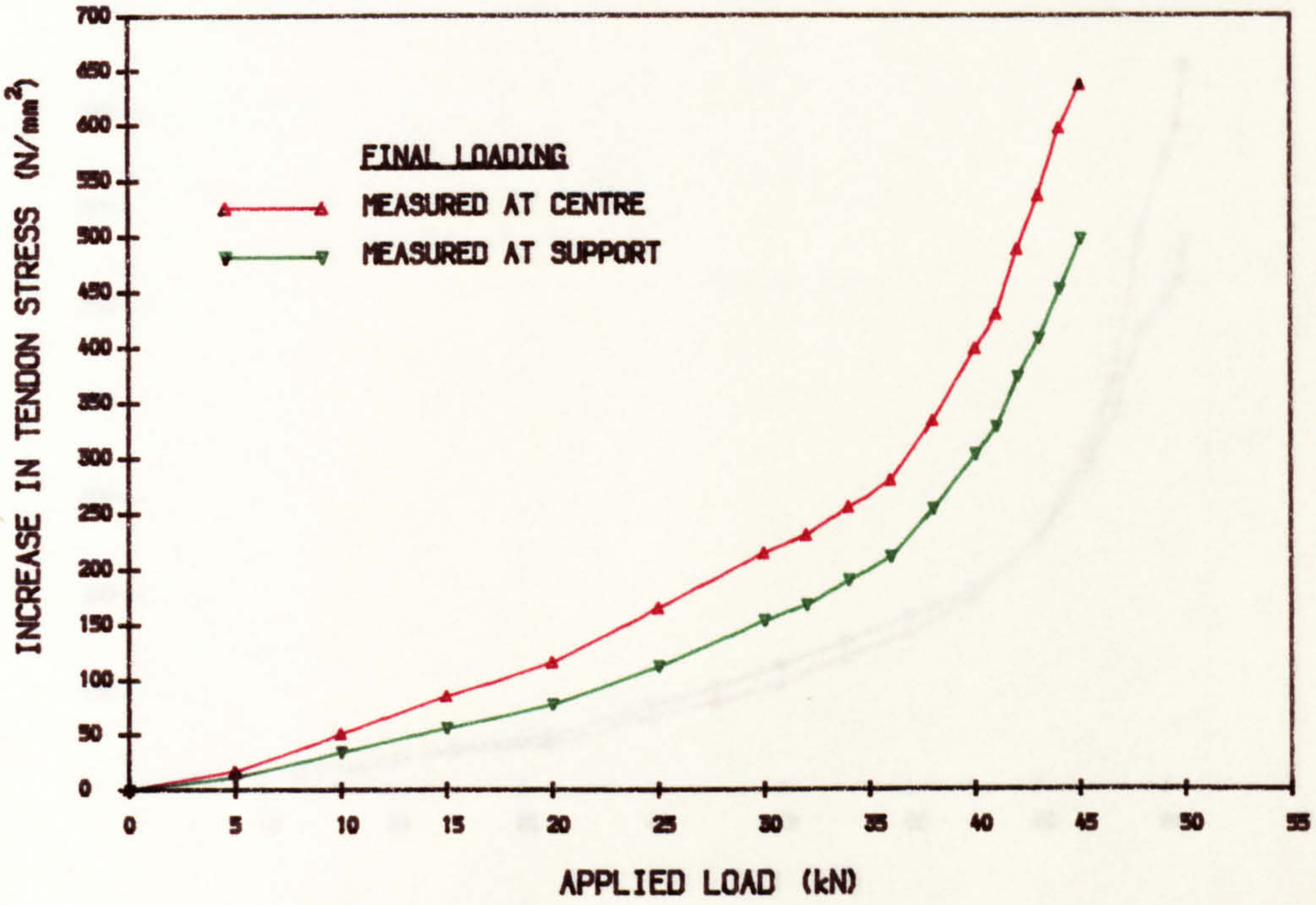

FIG. 6.9f TENDON STRESS MEASURED AT CENTRE AND SUPPORT (I2.3.2)

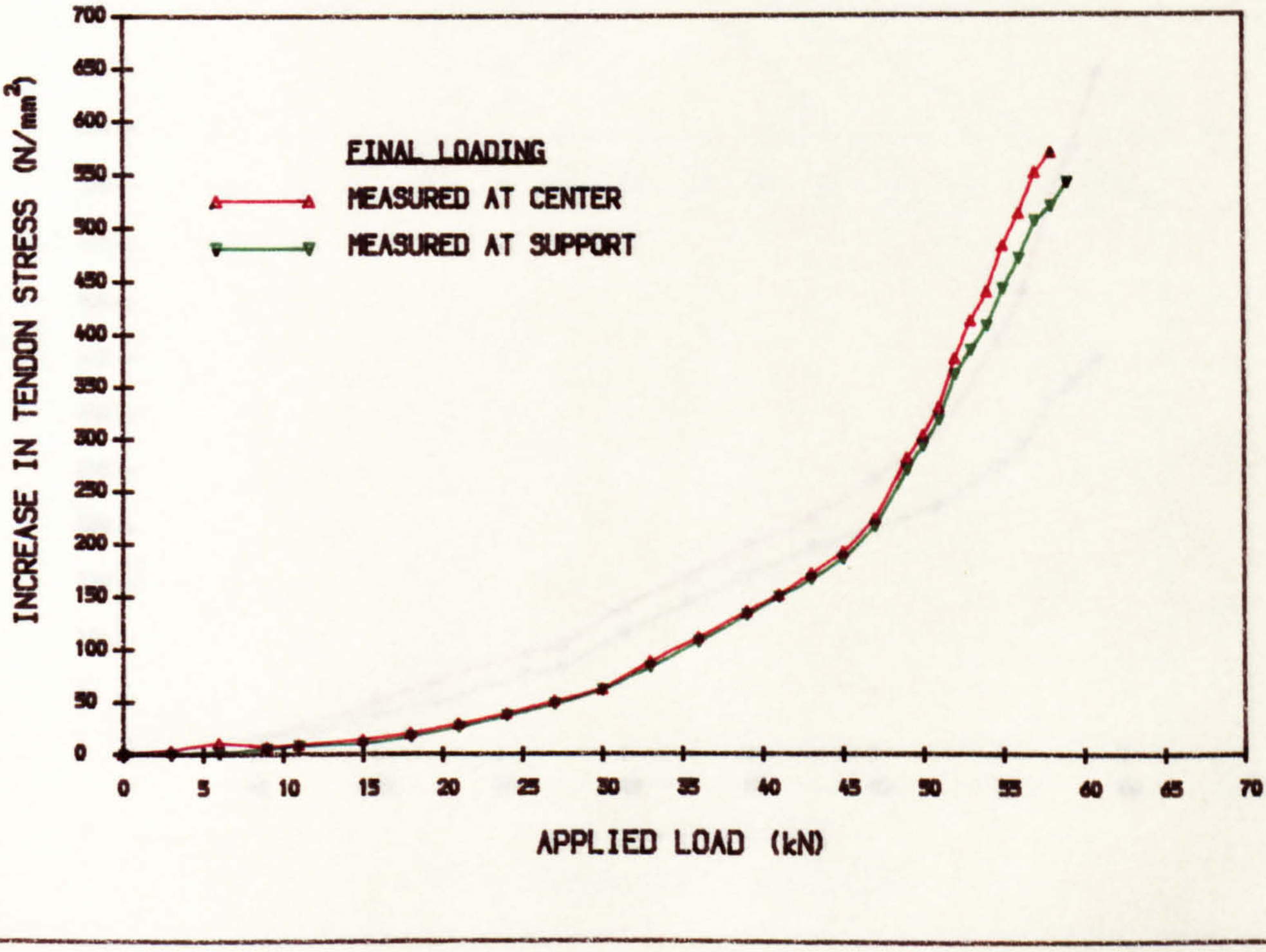

FIG. 6.9g TENDON STRESS MEASURED AT CENTRE AND SUPPORT (I3.3.4)

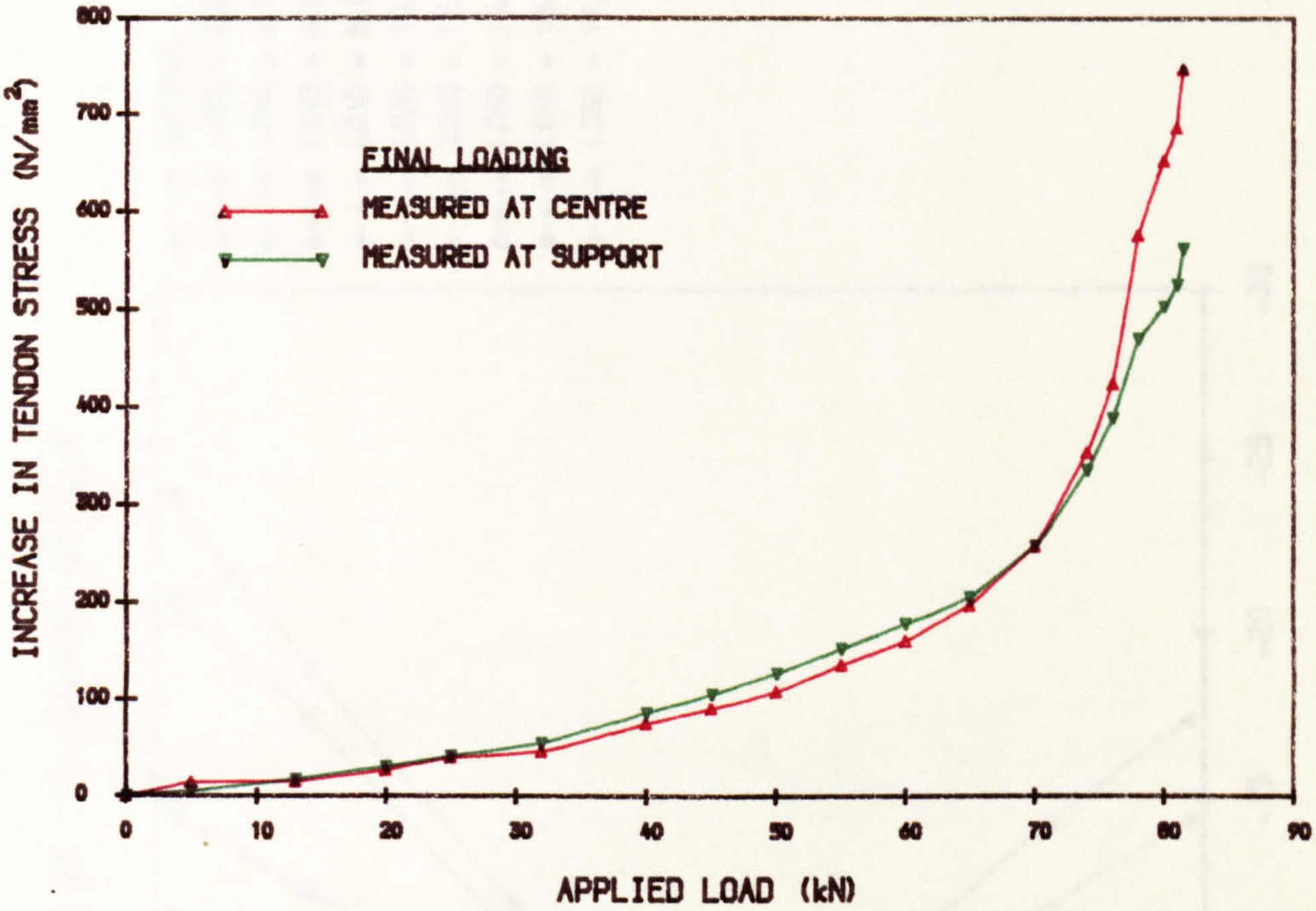

FIG. 6.9h TENDON STRESS MEASURED AT CENTRE AND SUPPORT (I3.2.5)

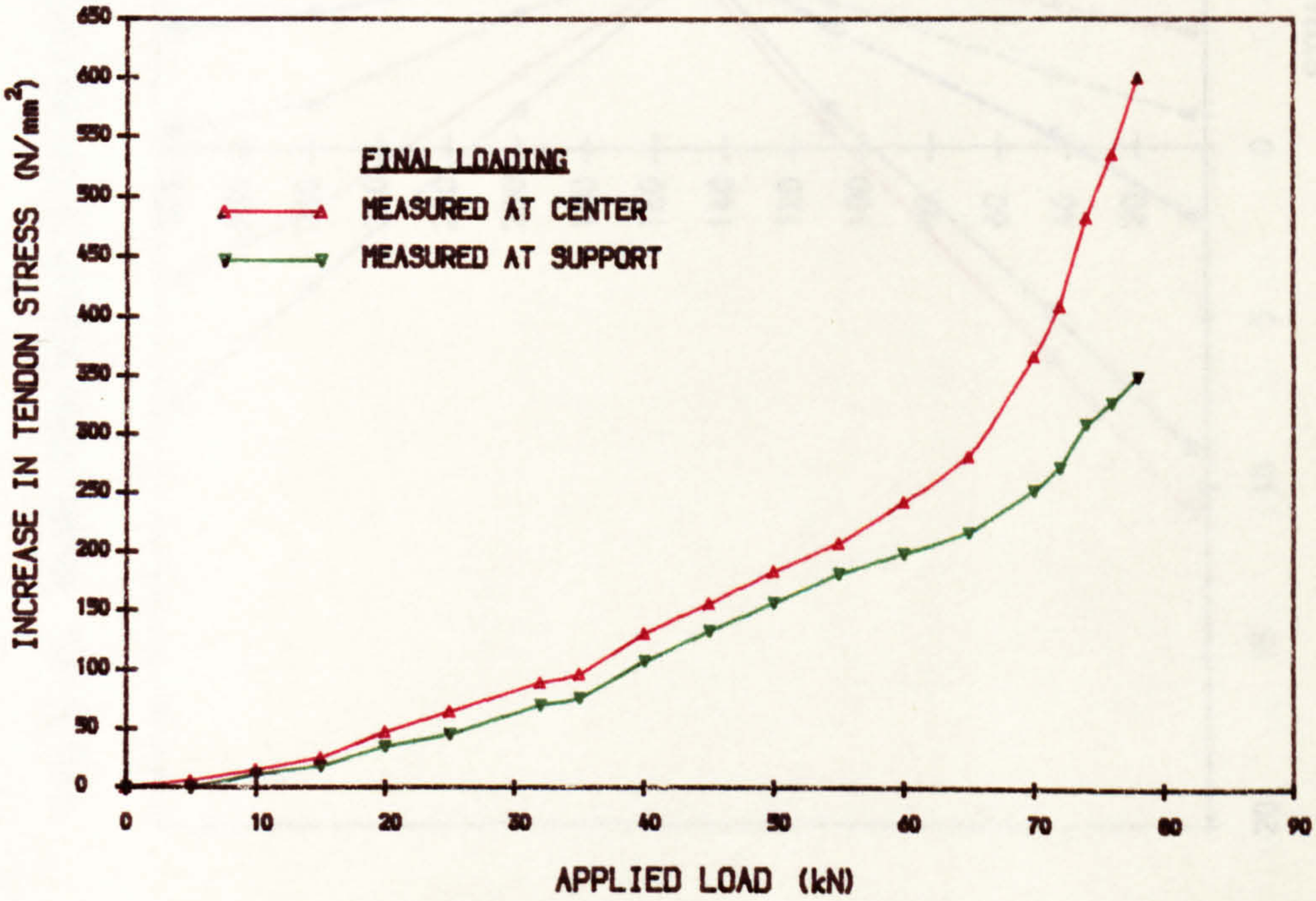

FIG. 6.10a SHORT-TERM STRAIN DISTRIBUTION AT MID SPAN IN 1ST LOADING (R1.3.0)

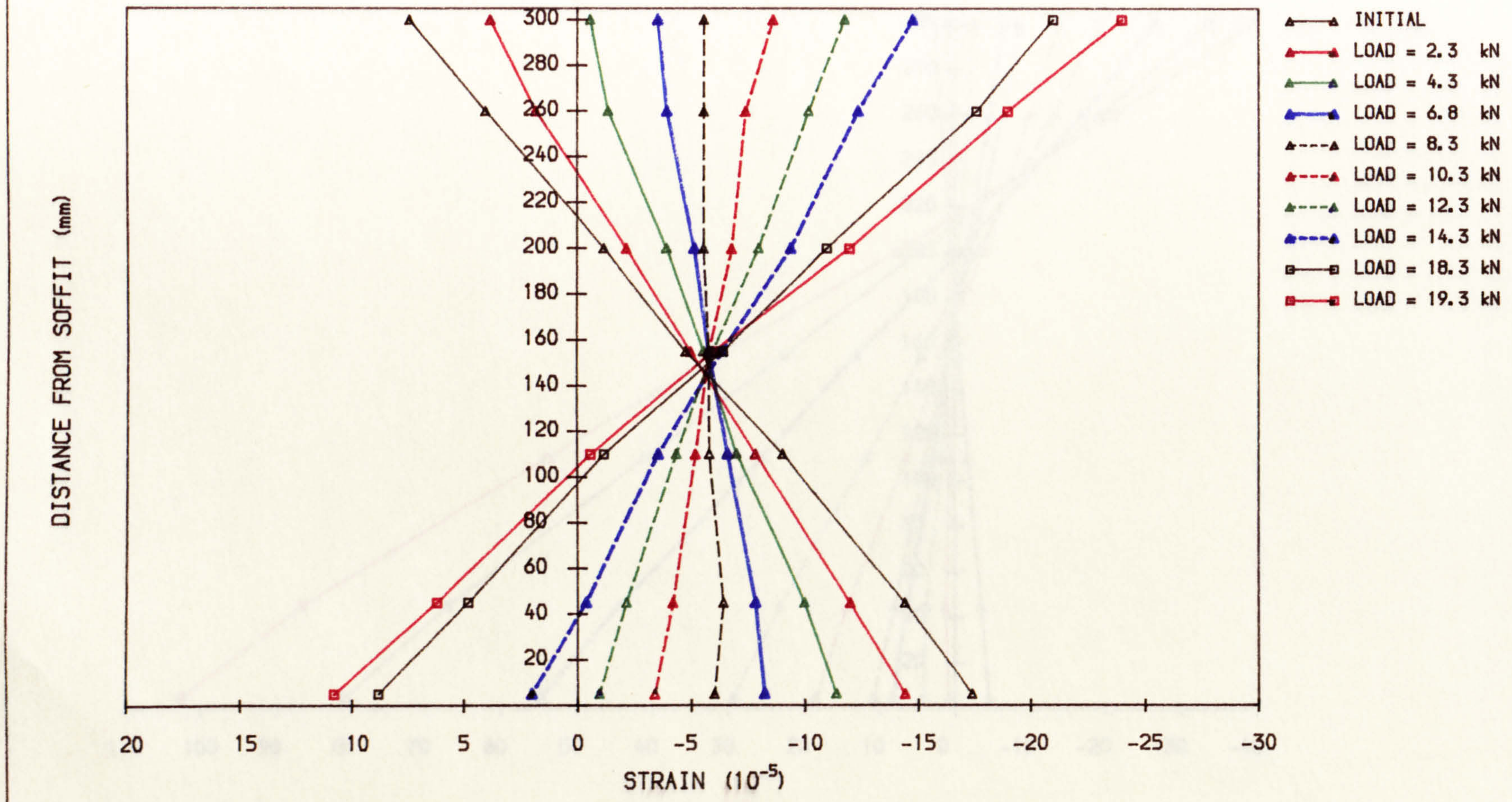

FIG. 6.10b SHORT-TERM STRAIN DISTRIBUTION AT MID SPAN IN 1ST LOADING (R1.1.3)

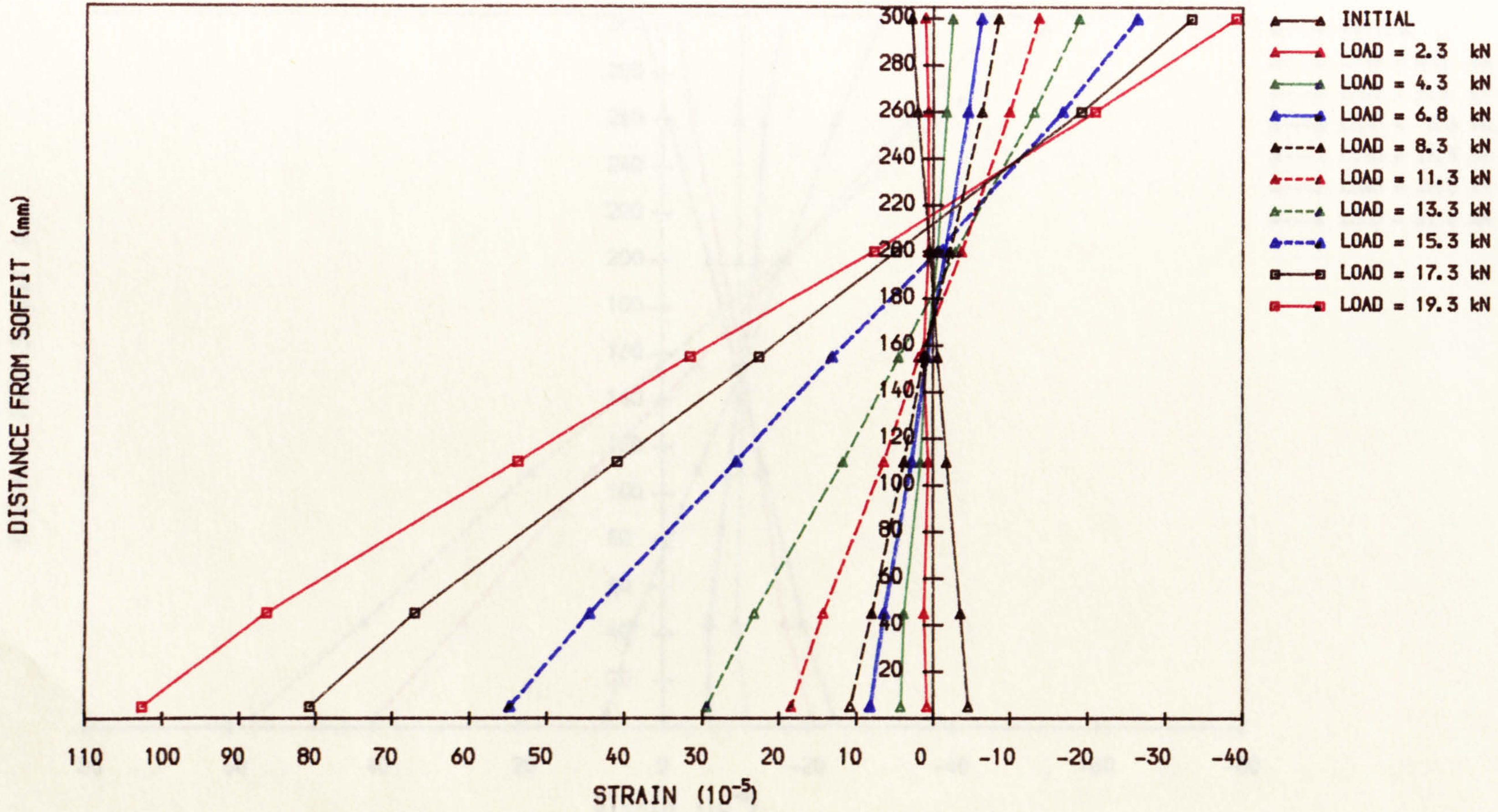

FIG. 6.10c SHORT-TERM STRAIN DISTRIBUTION AT MIDSPAN IN 1ST LOADING (R3.3.4)

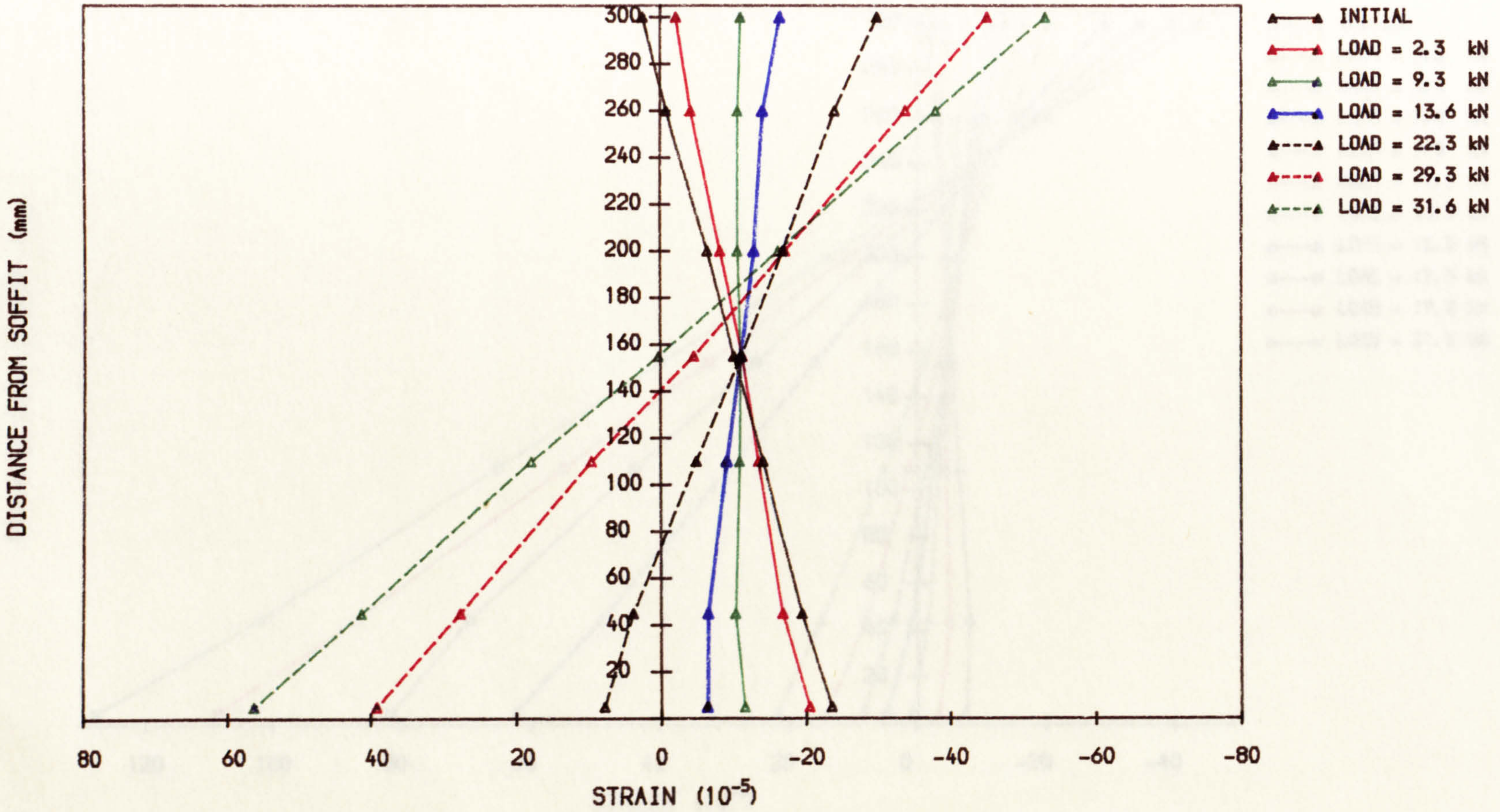

FIG. 6.10d SHORT-TERM STRAIN DISTRIBUTION AT MIDSPAN IN 1ST LOADING (I1.1.3)

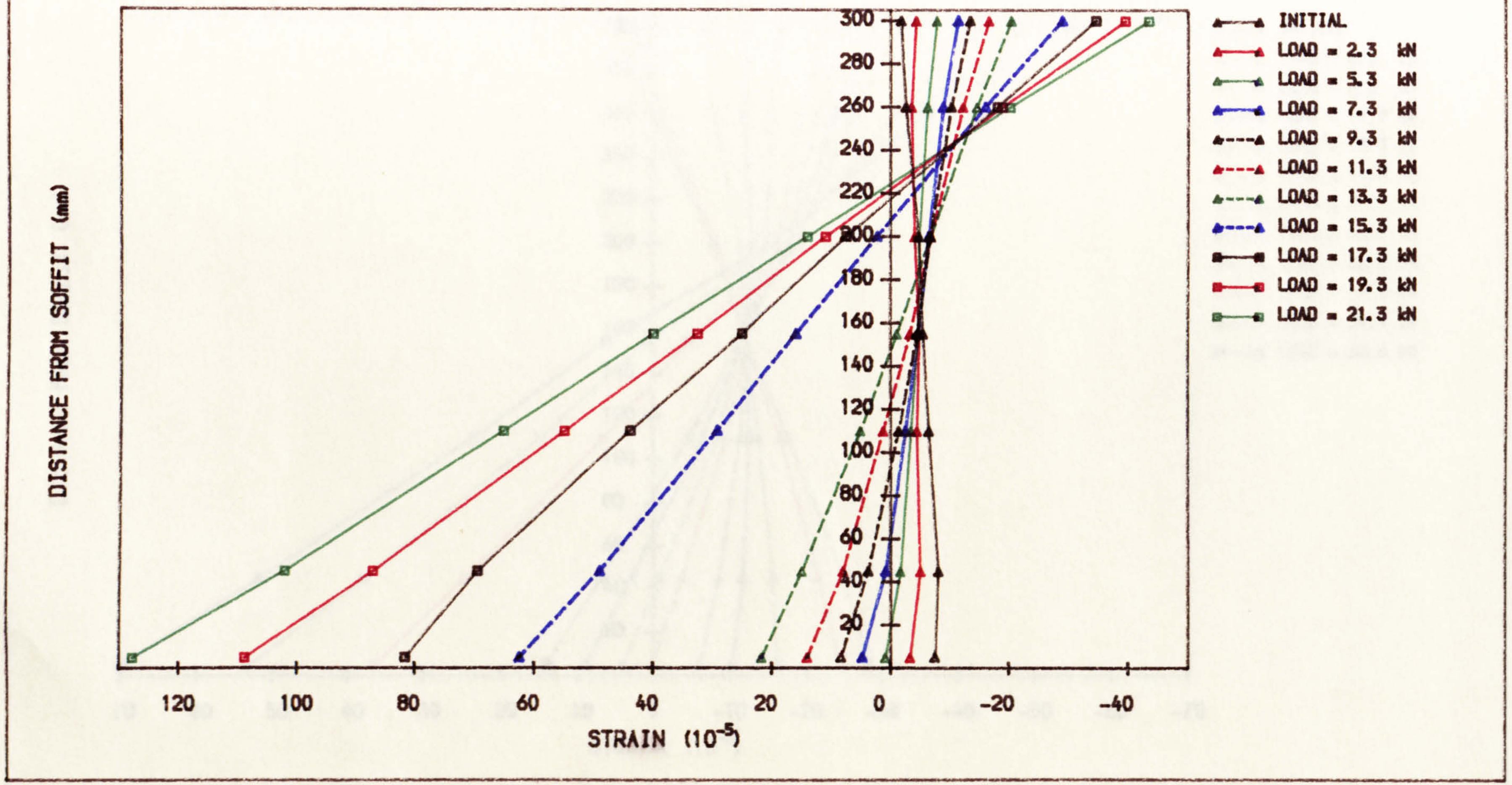

FIG. 6.10e SHORT-TERM STRAIN DISTRIBUTION AT MID SPAN IN 1ST LOADING (I3.3.4)

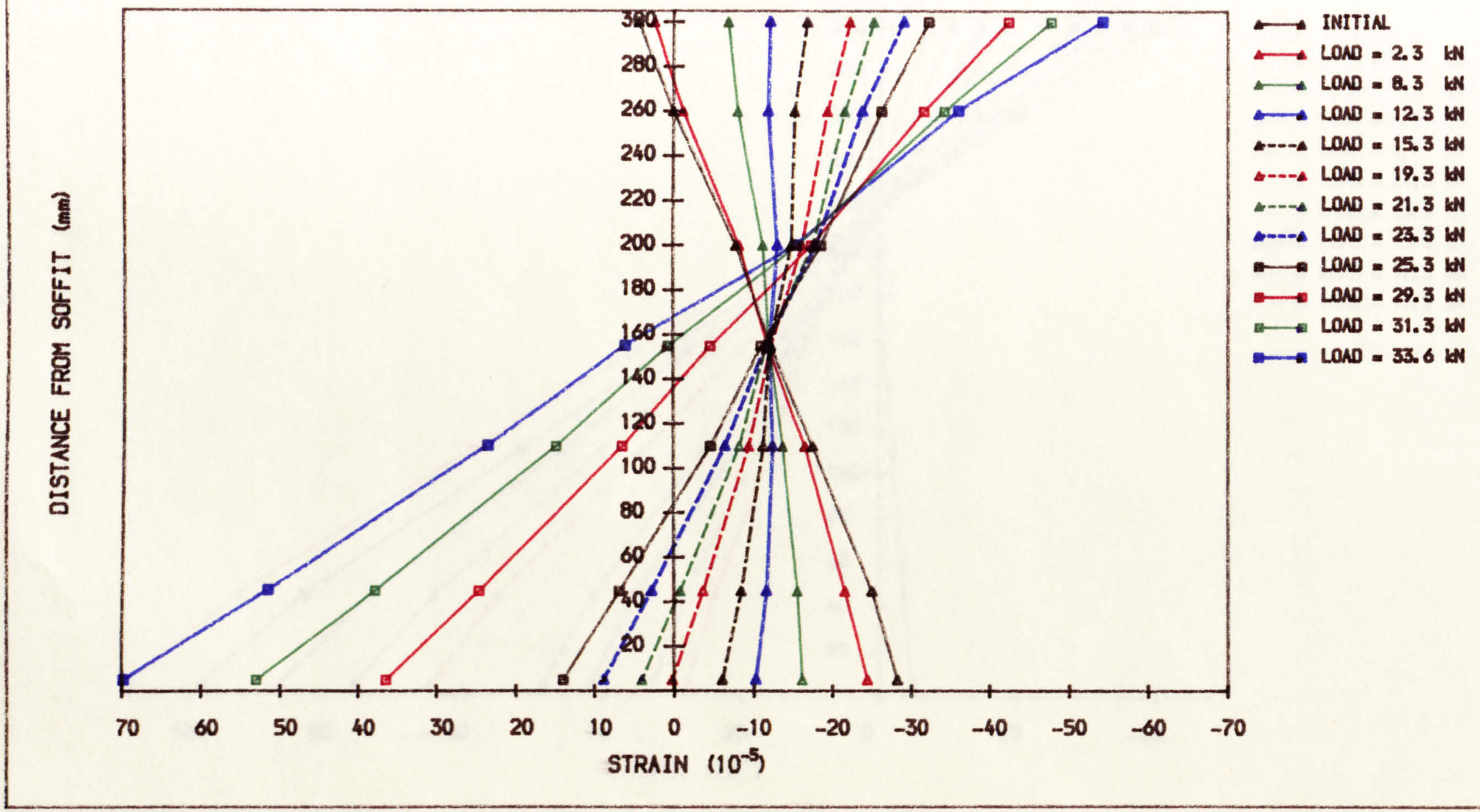

FIG. 6.10f SHORT-TERM STRAIN DISTRIBUTION AT MID SPAN IN 2ND LOADING (R1.1.3)

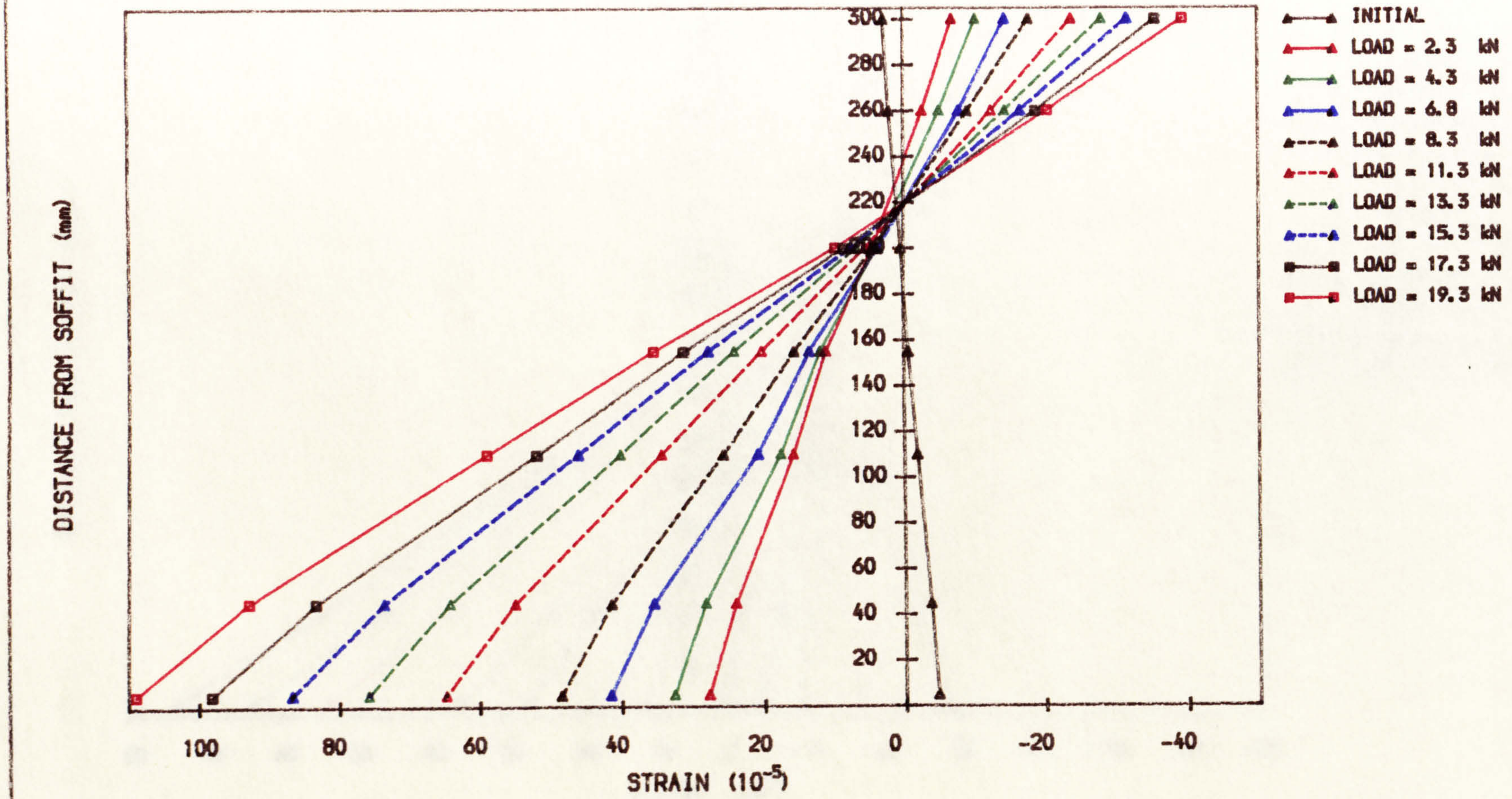

FIG. 6.10g SHORT-TERM STRAIN DISTRIBUTION AT MID SPAN IN 2ND LOADING (I3.3.4)

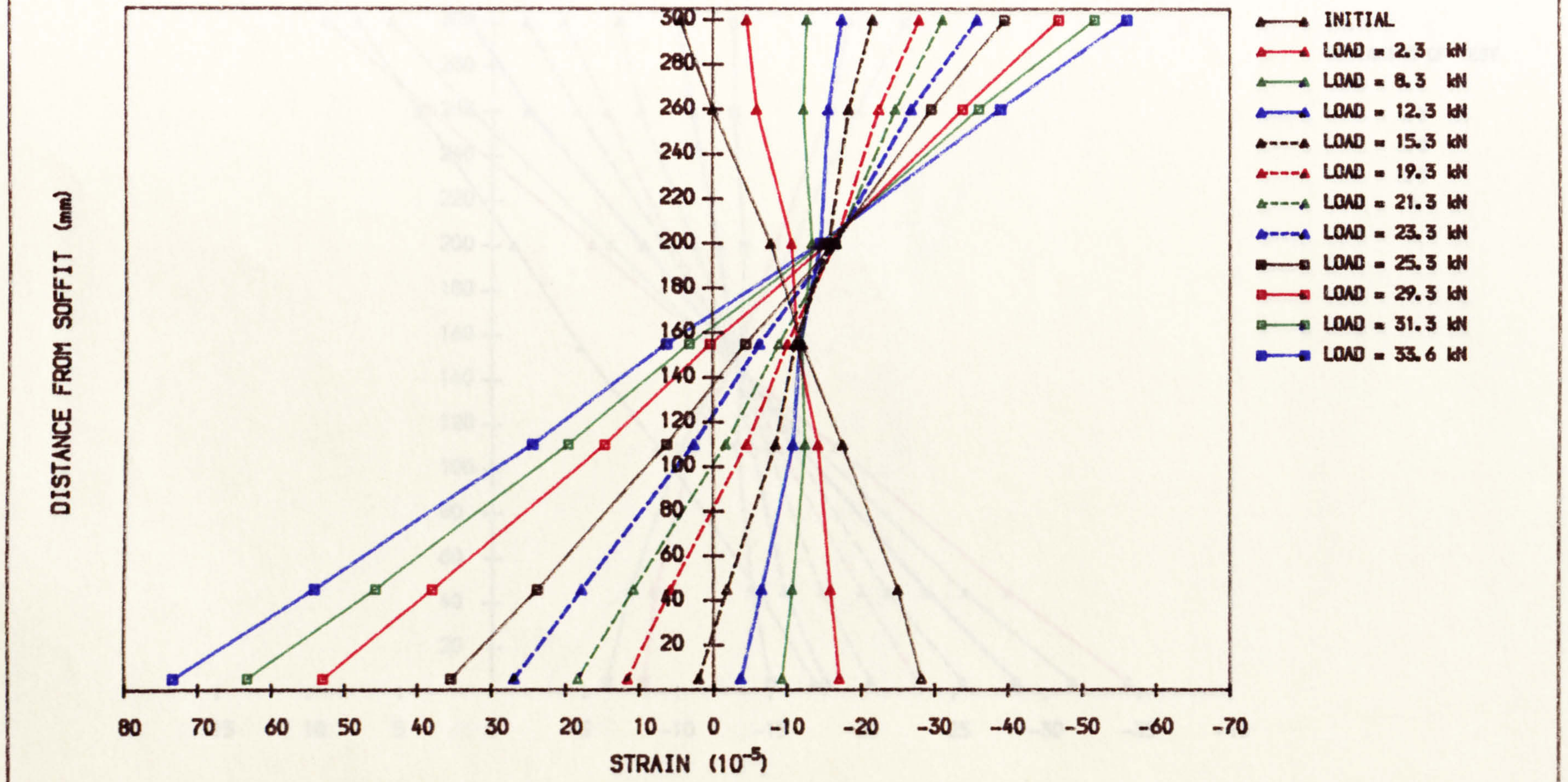

FIG. 6.11a TOTAL STRAIN DISTRIBUTION AT MID SPAN IN 1ST LOADING (R1.3.0)

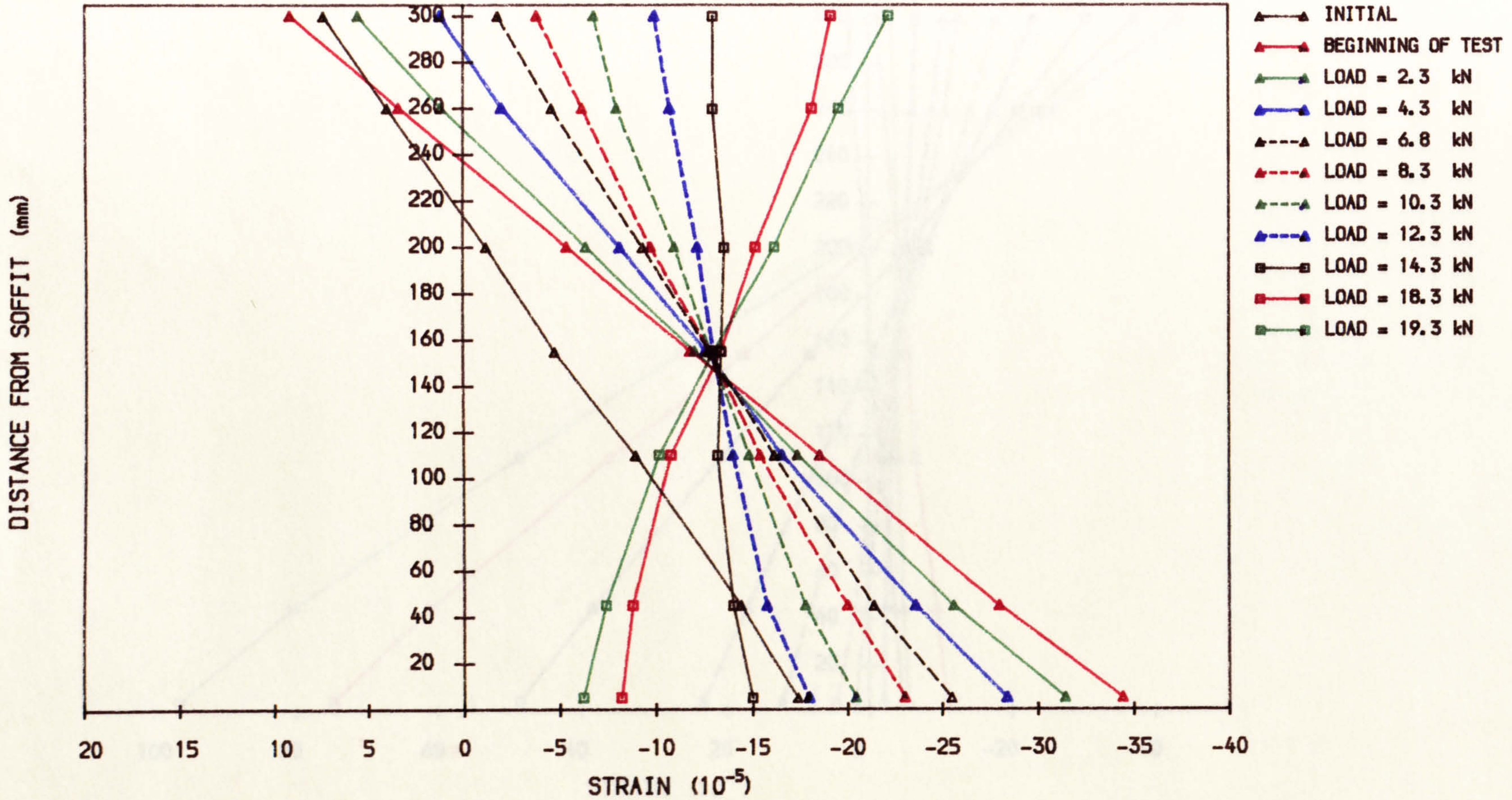

FIG. 6.11b TOTAL STRAIN DISTRIBUTION AT MID SPAN IN 1ST LOADING (R1.1.3)

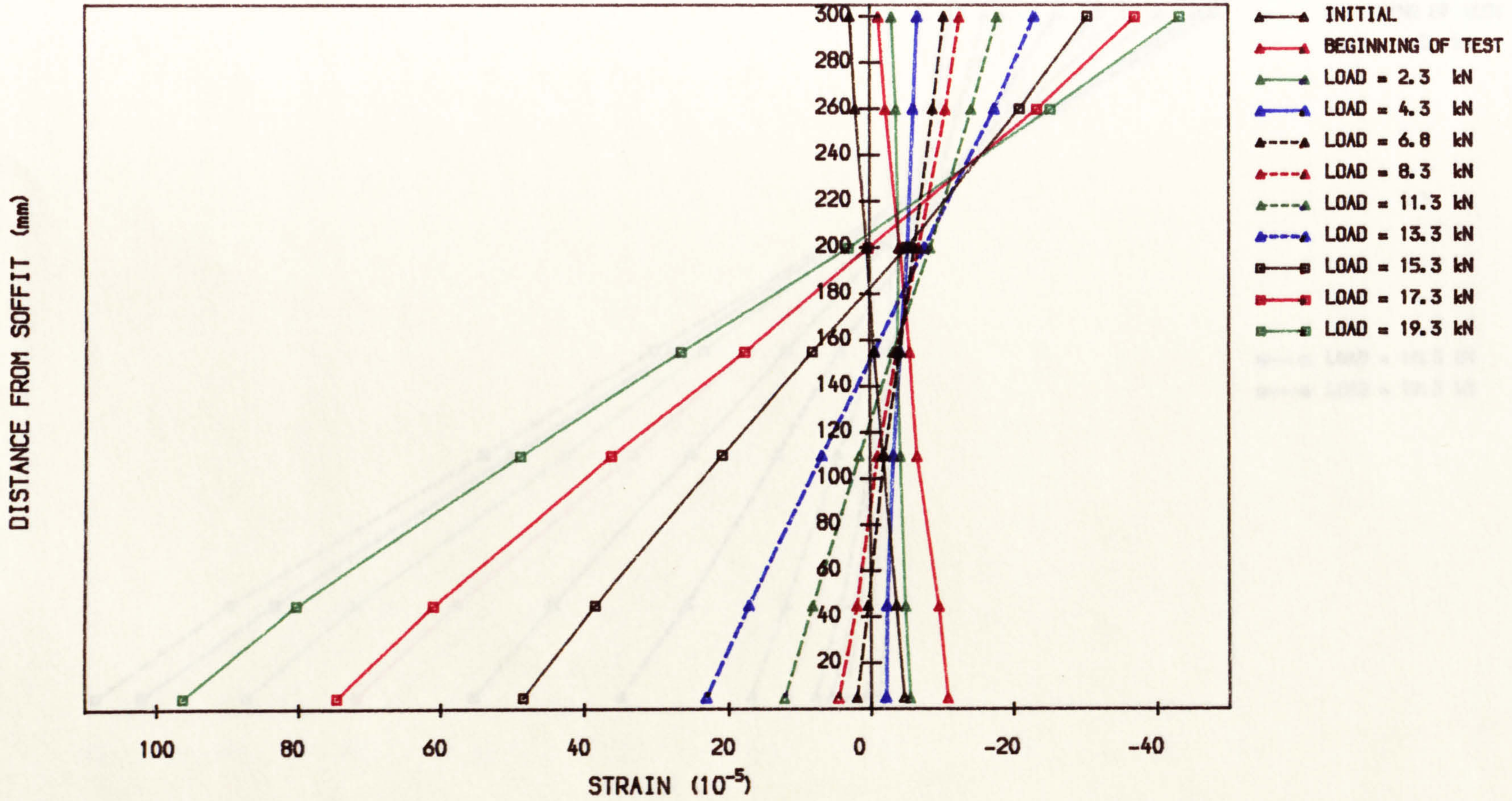

FIG. 6.11c TOTAL STRAIN DISTRIBUTION AT MID SPAN IN 1ST LOADING (R1.0.5)

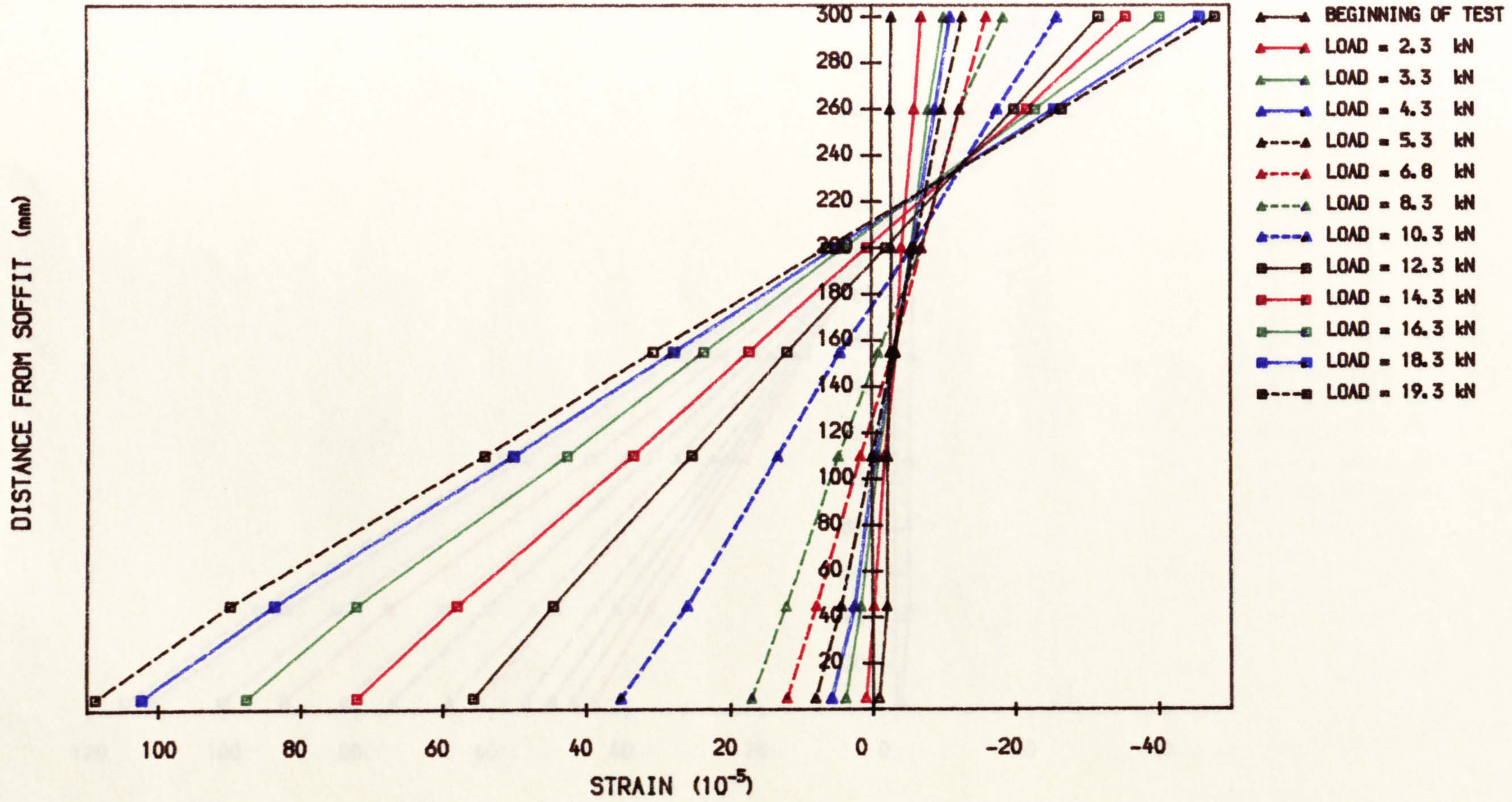

FIG. 6.11d TOTAL STRAIN DISTRIBUTION AT MIDSPAN IN 2ND LOADING (R1.0.5)

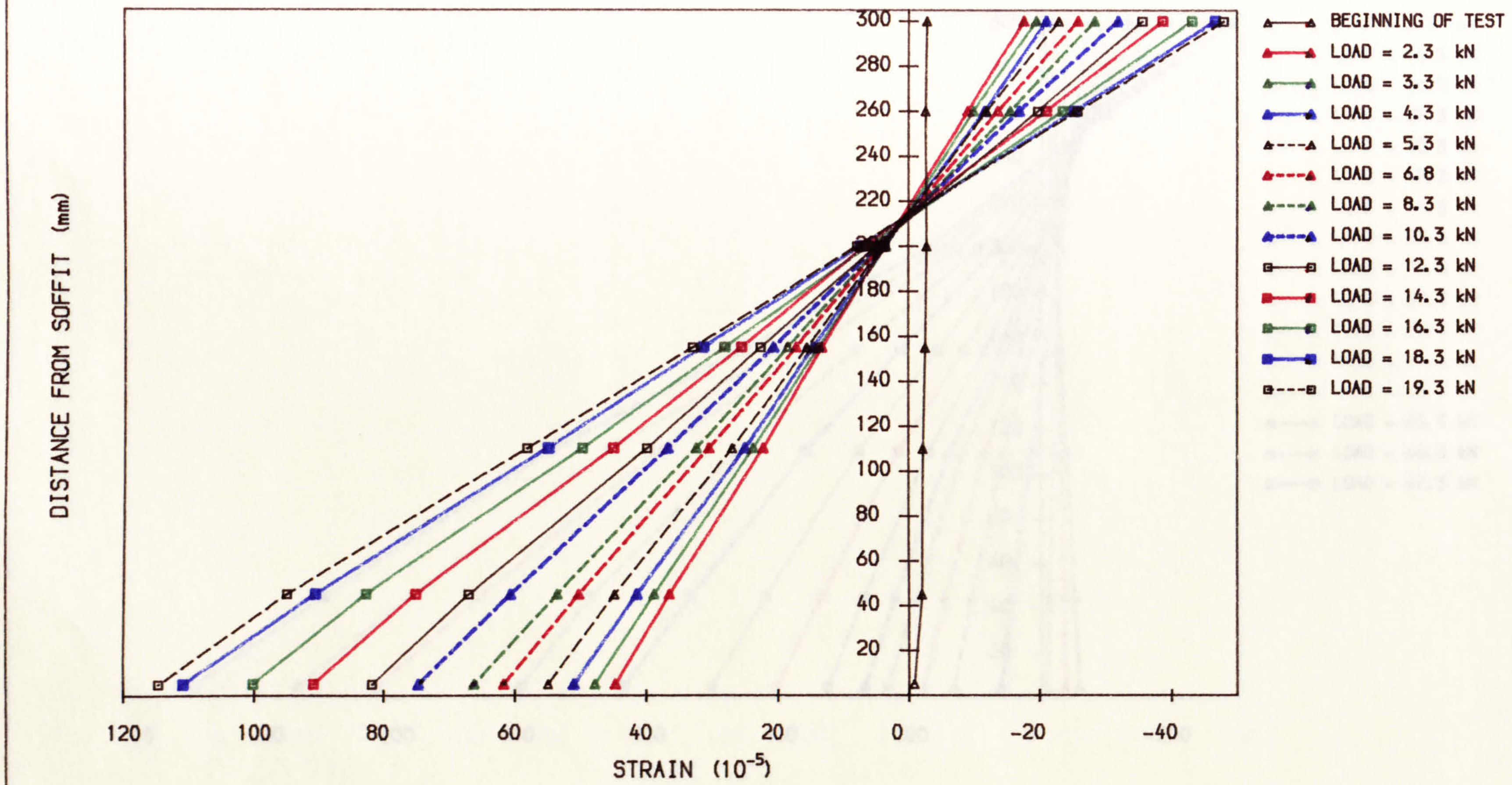

FIG. 6.11e TOTAL STRAIN DISTRIBUTION AT MID SPAN IN FINAL LOADING (R3.4.2)

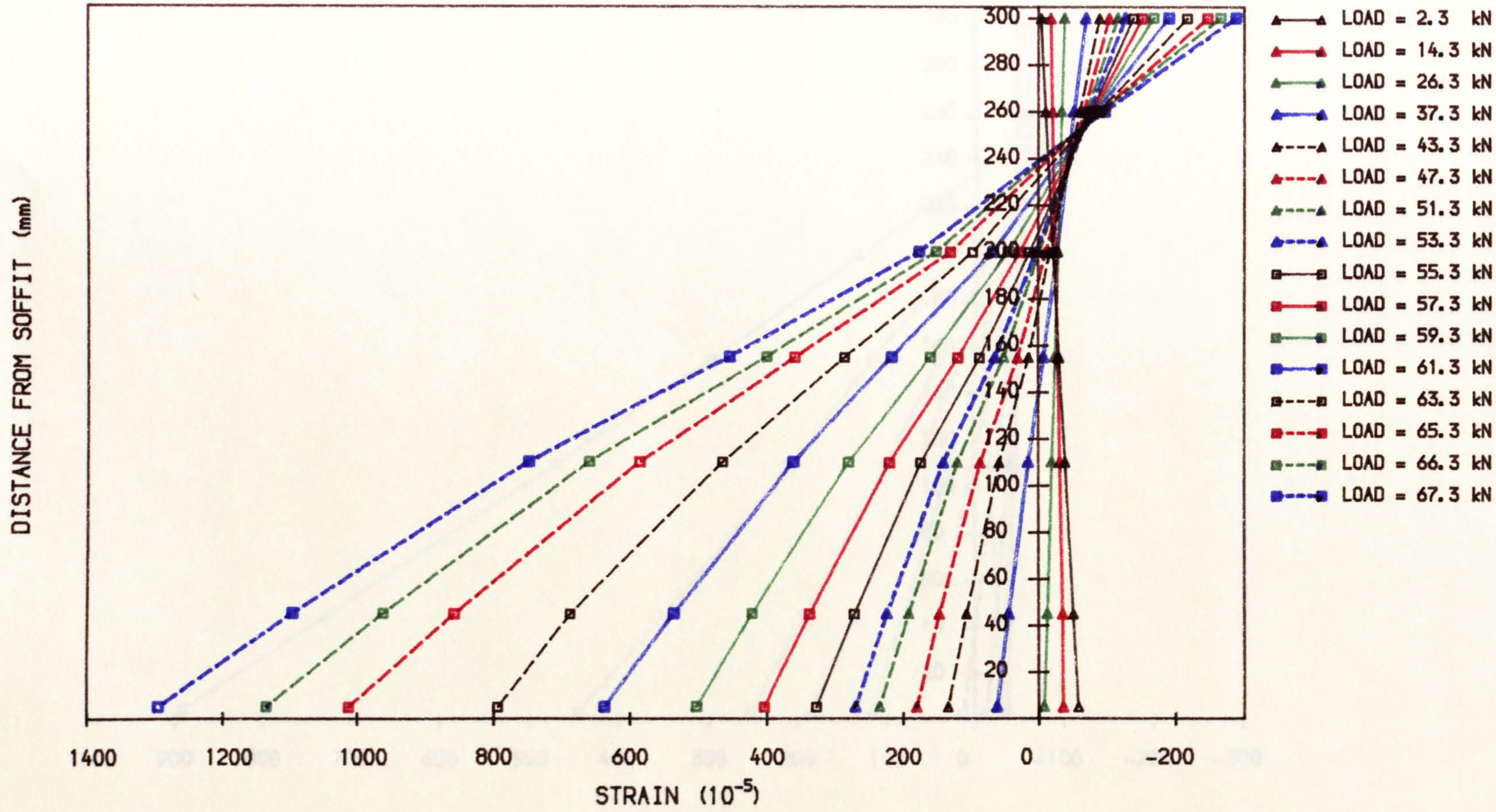

FIG. 6.11f TOTAL STRAIN DISTRIBUTION AT MID SPAN IN FINAL LOADING (I3.3.4)

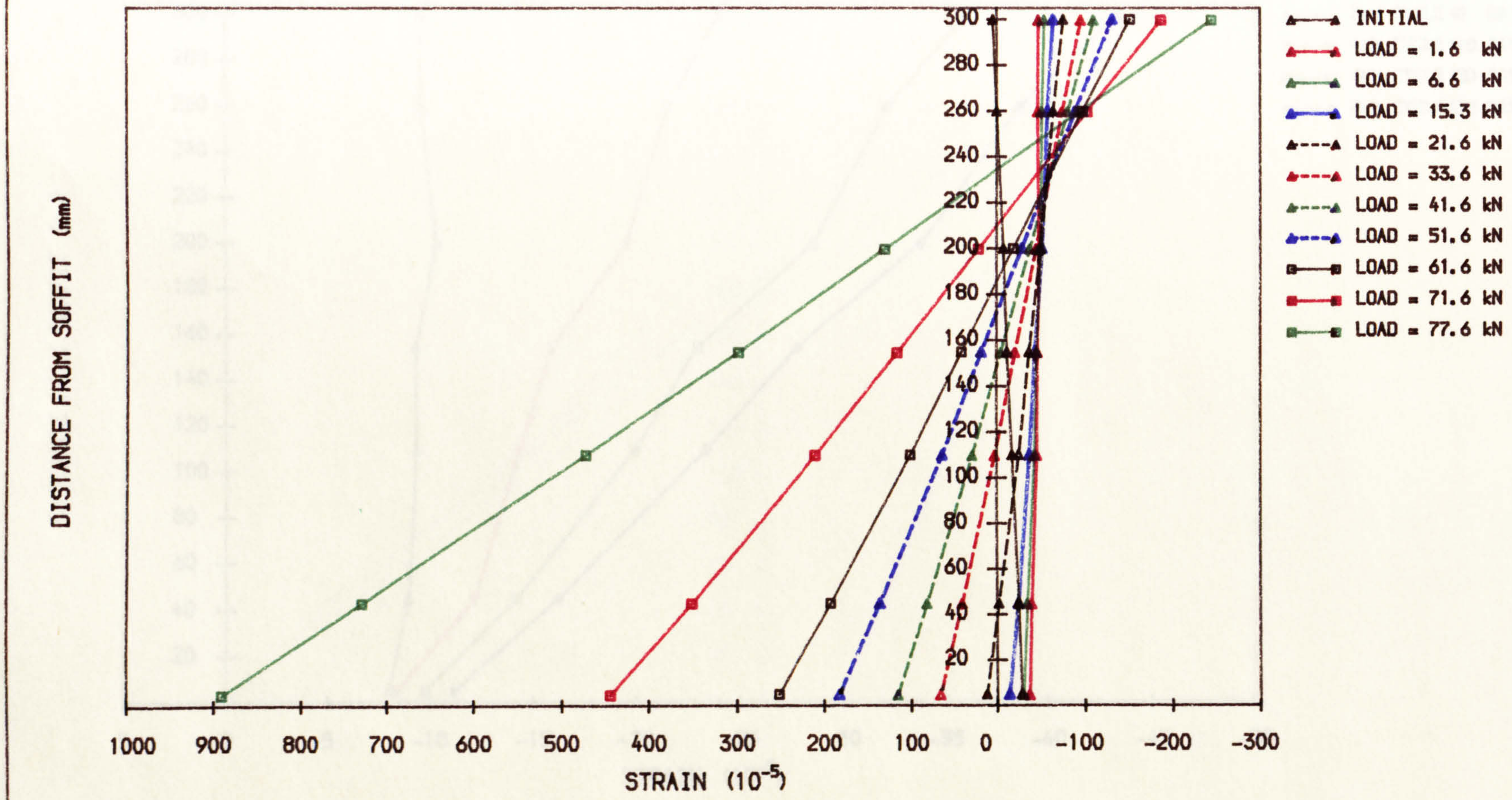

FIG. 6. 12a TOTAL STRAIN AT CENTRE AT HALF-SERVICE LOAD (R1. 2. 2)

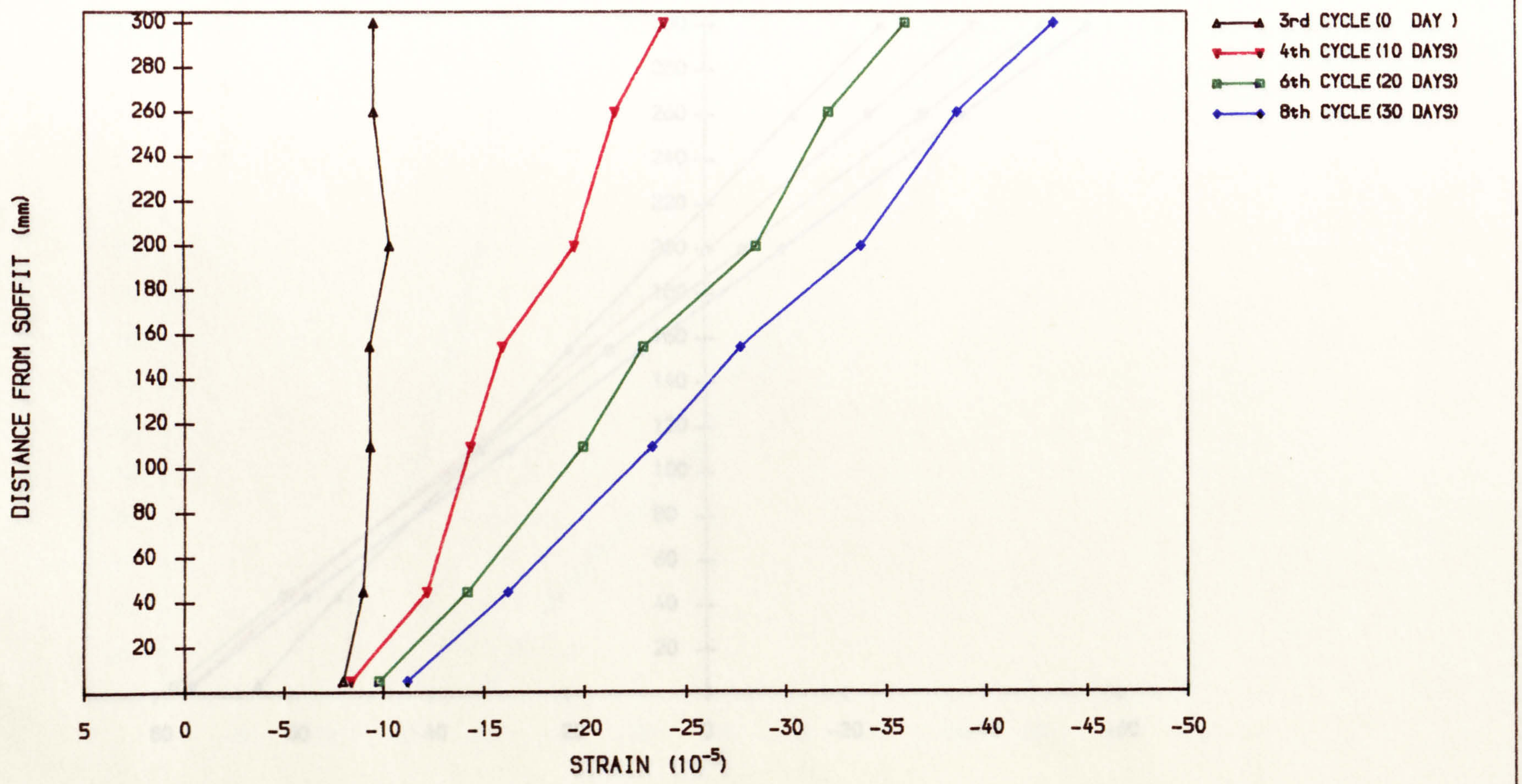

FIG. 6.12b TOTAL STRAIN AT CENTRE AT HALF-SERVICE LOAD (R1.0.5)

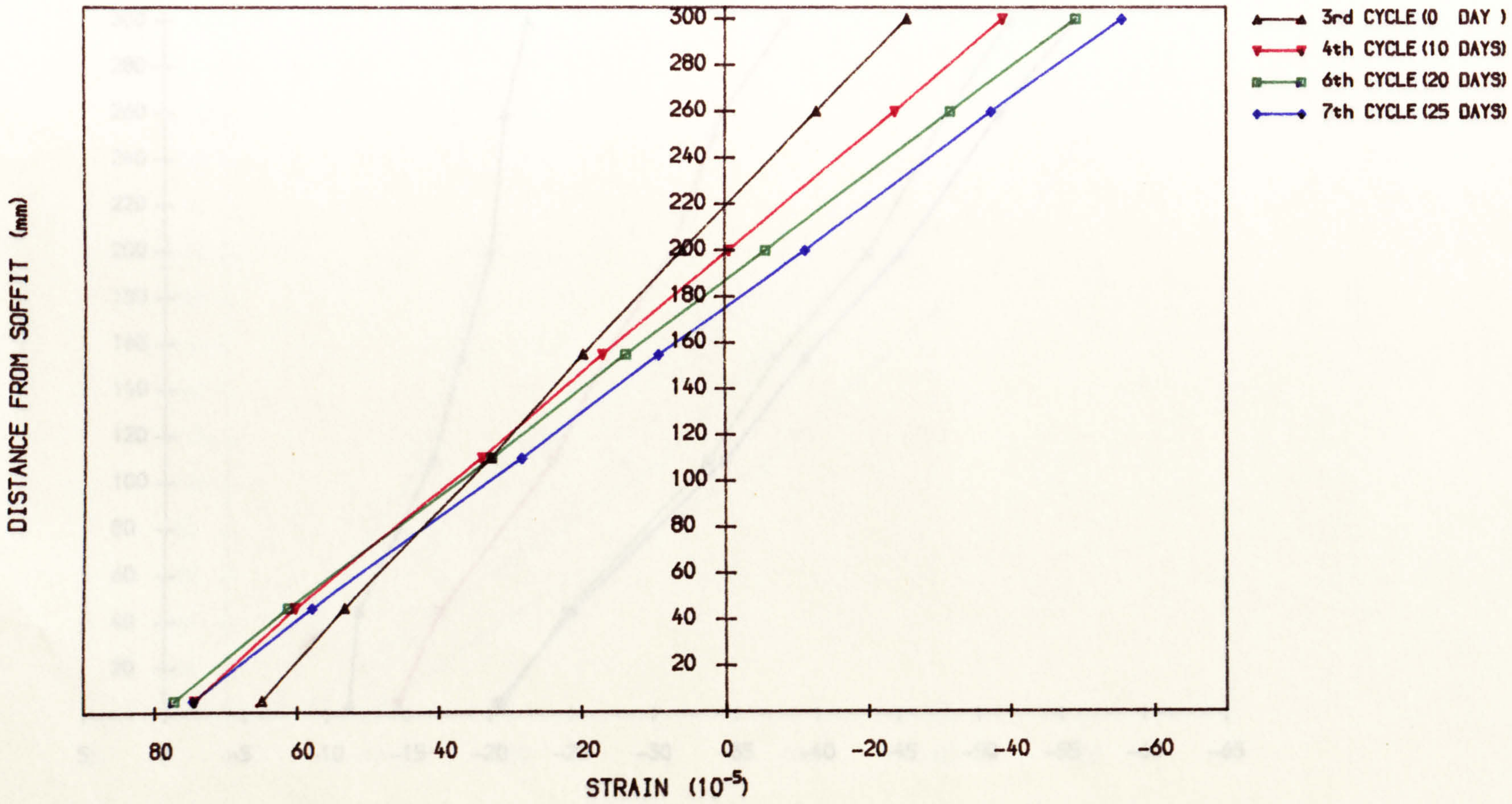

FIG. 6.12c TOTAL STRAIN AT CENTRE AT HALF-SERVICE LOAD (I1.2.2)

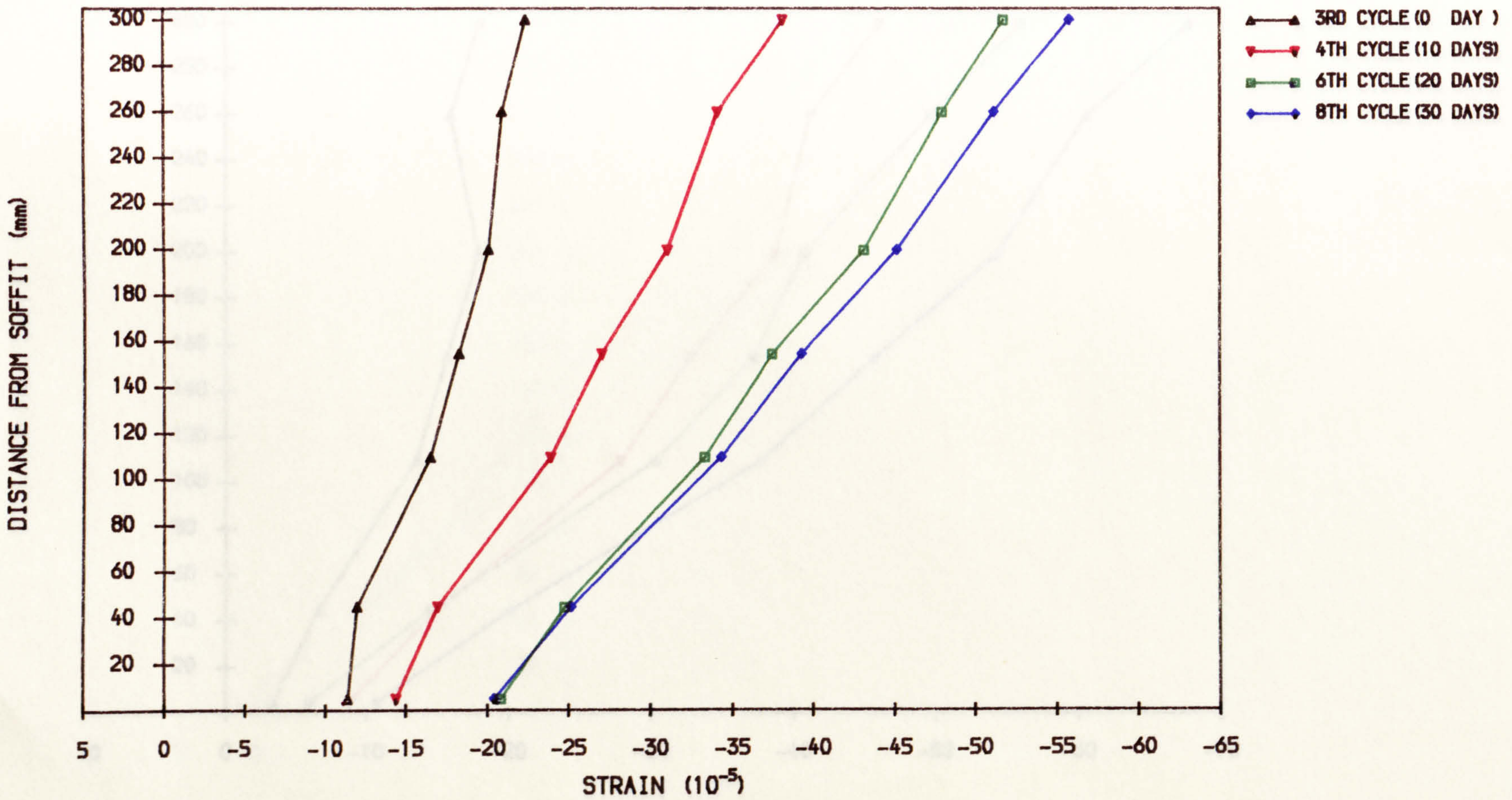

FIG. 6.12d TOTAL STRAIN AT CENTRE AT HALF-SERVICE LOAD (I3.3.4)

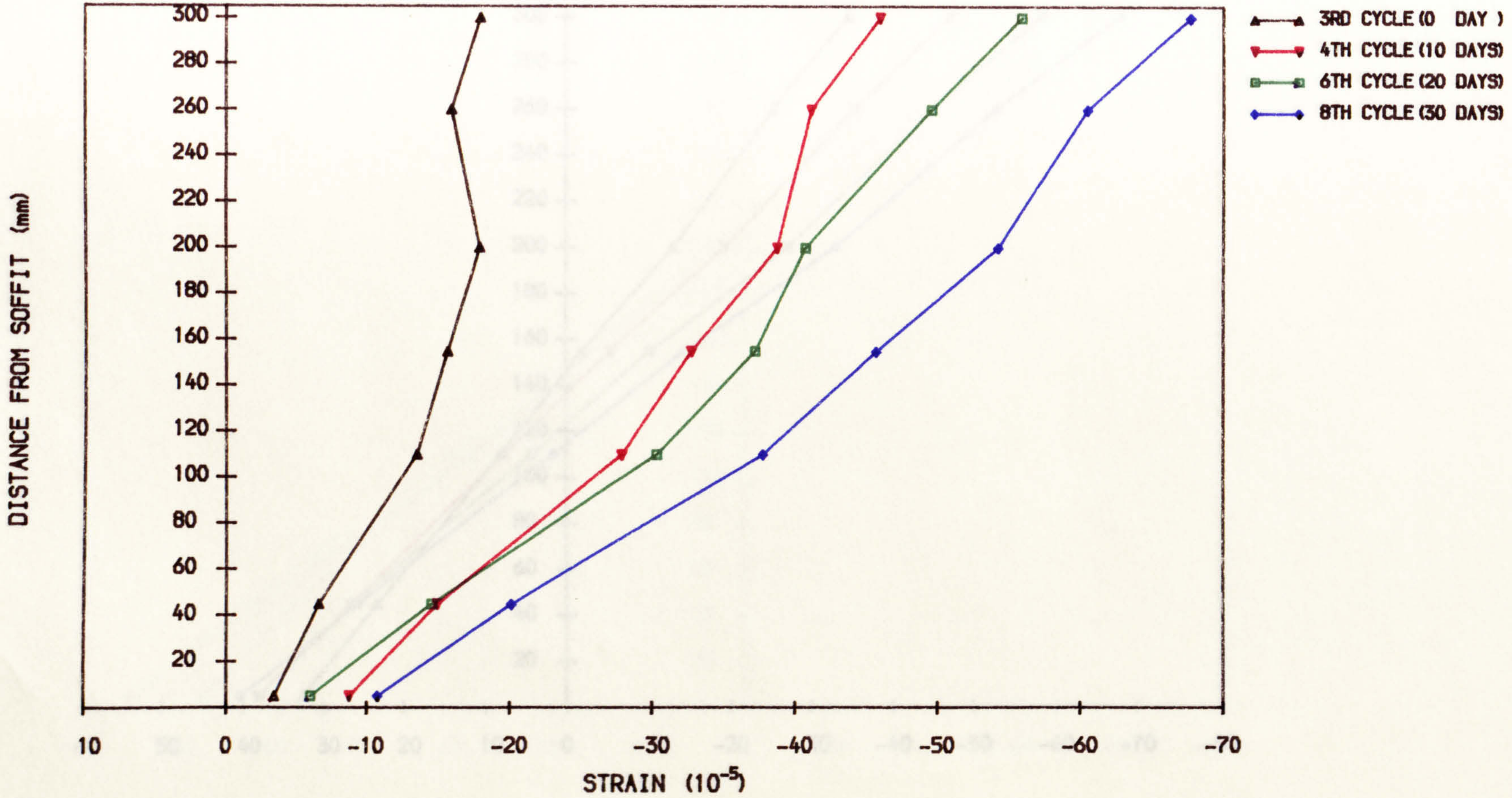

FIG. 6.13a TOTAL STRAIN AT CENTRE AT SERVICE LOAD (R1.2.2)

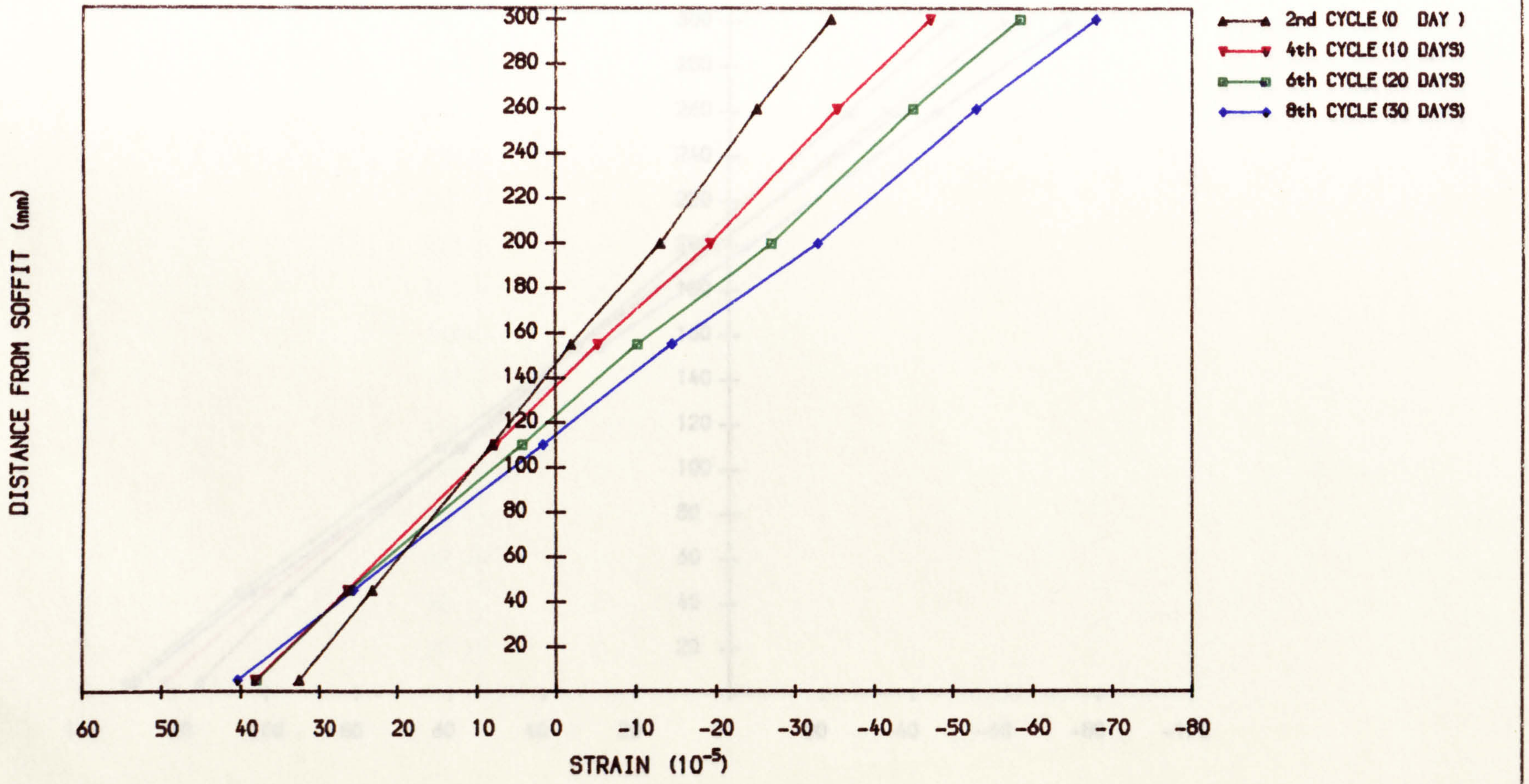

FIG. 6. 13b TOTAL STRAIN AT CENTRE AT SERVICE LOAD (R1. 0. 5)

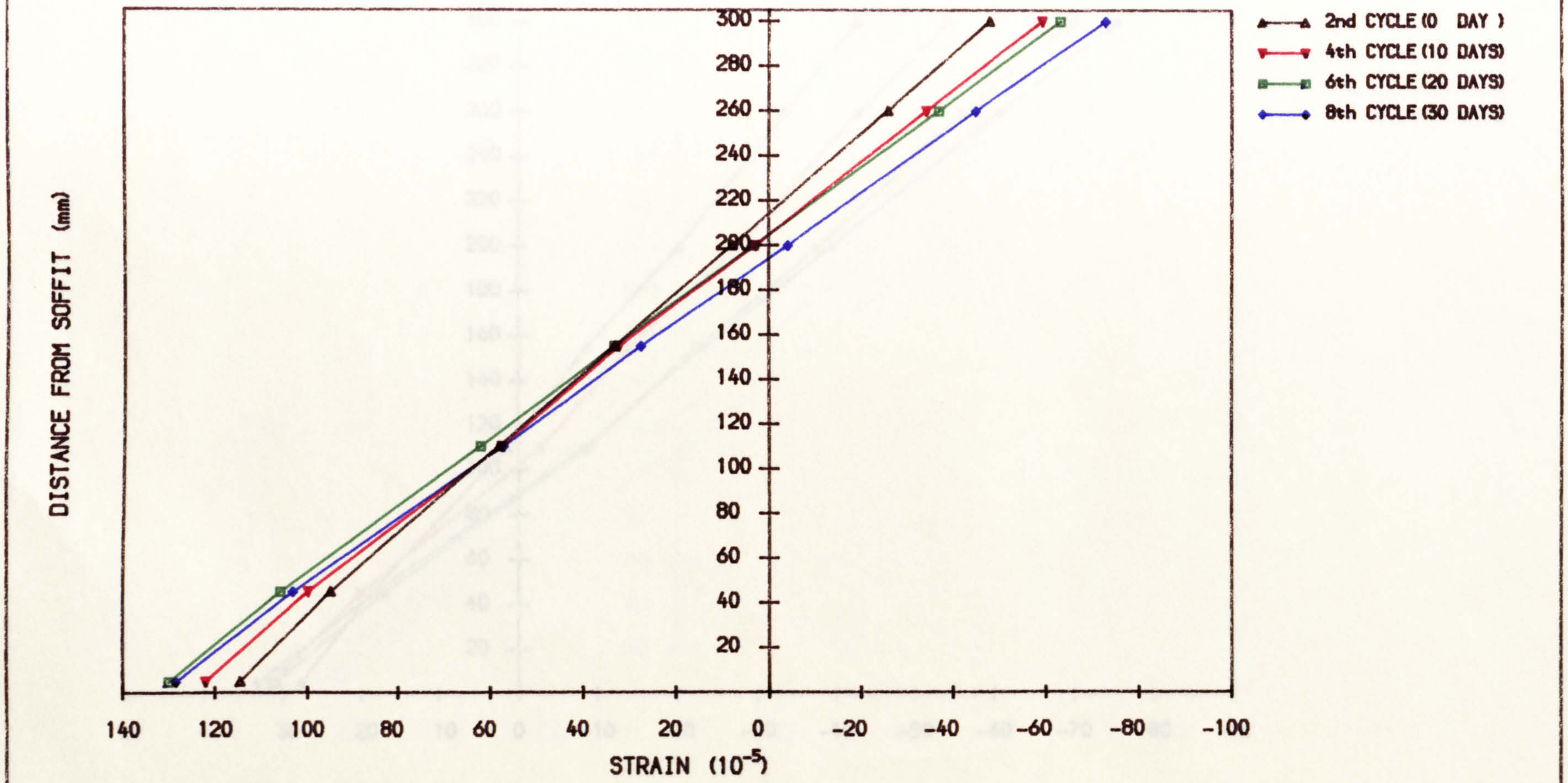

FIG. 6.13c TOTAL STRAIN AT CENTRE AT SERVICE LOAD (I1.2.2)

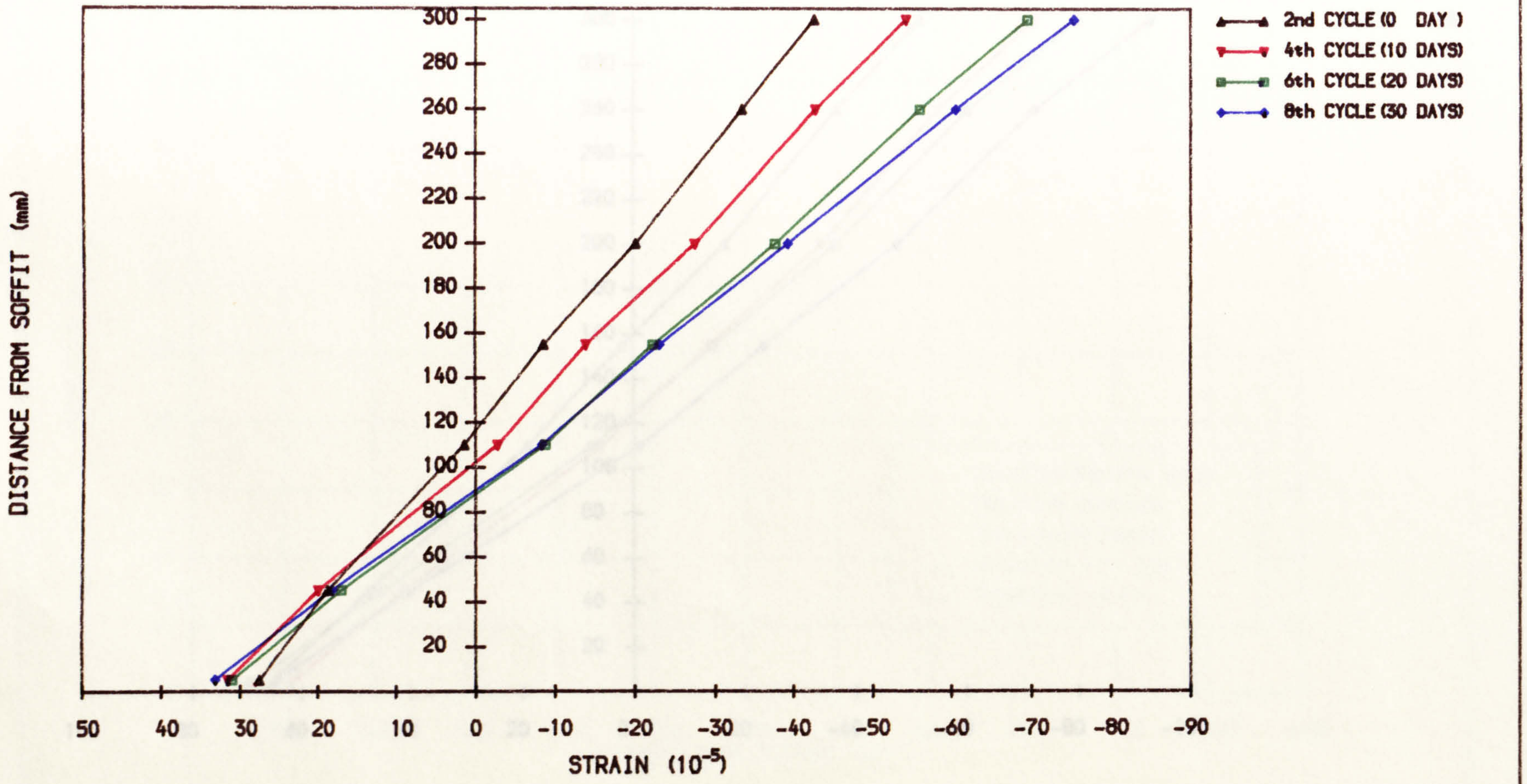

FIG. 6.13d TOTAL STRAIN AT CENTRE AT SERVICE LOAD (I3.3.4)

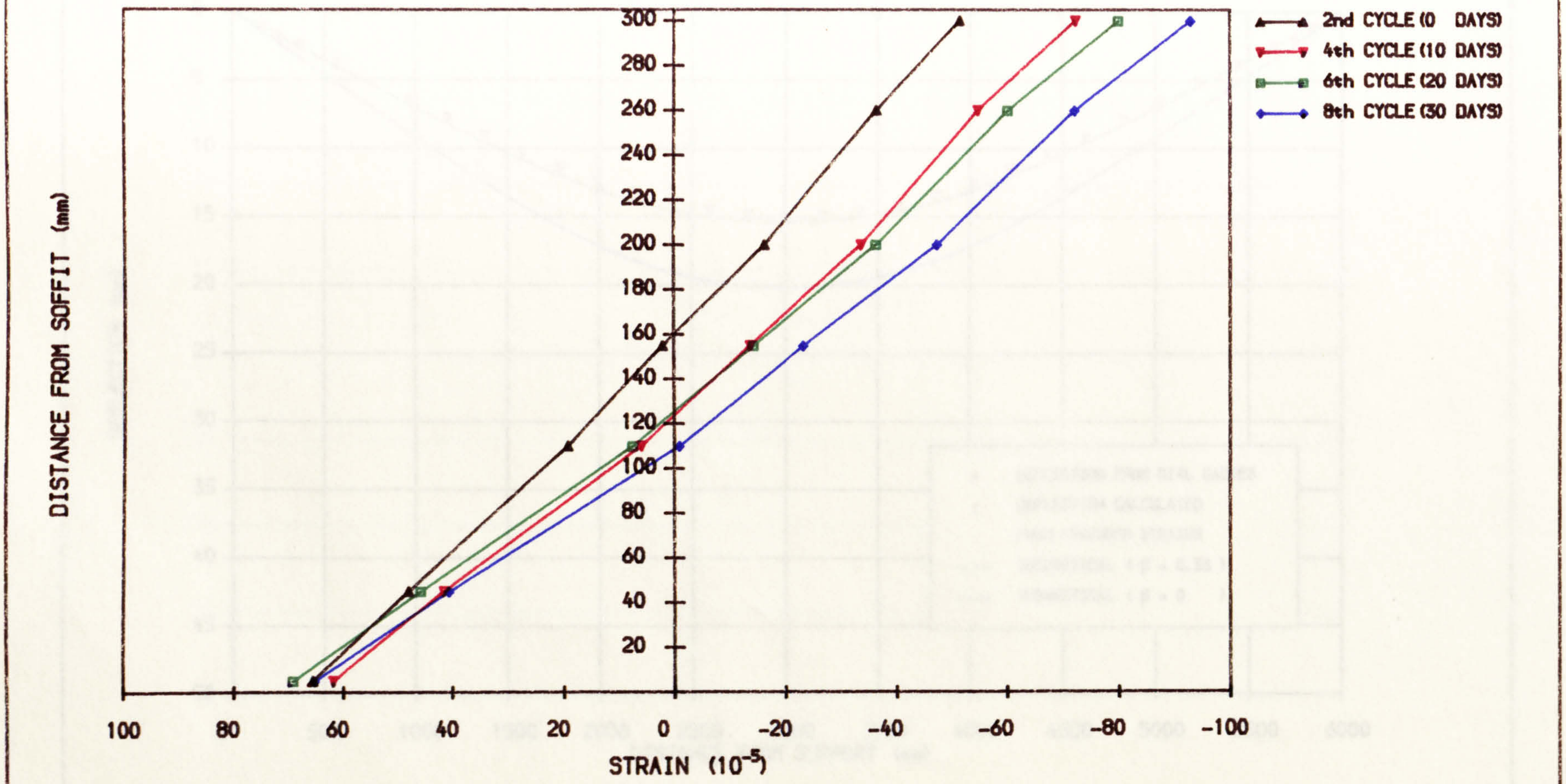

FIG. 6.14a THEORETICAL AND EXPERIMENTAL DEFLECTED PROFILE AT SERVICE LOAD IN 1ST LOADING (BEAM R1.1.3)

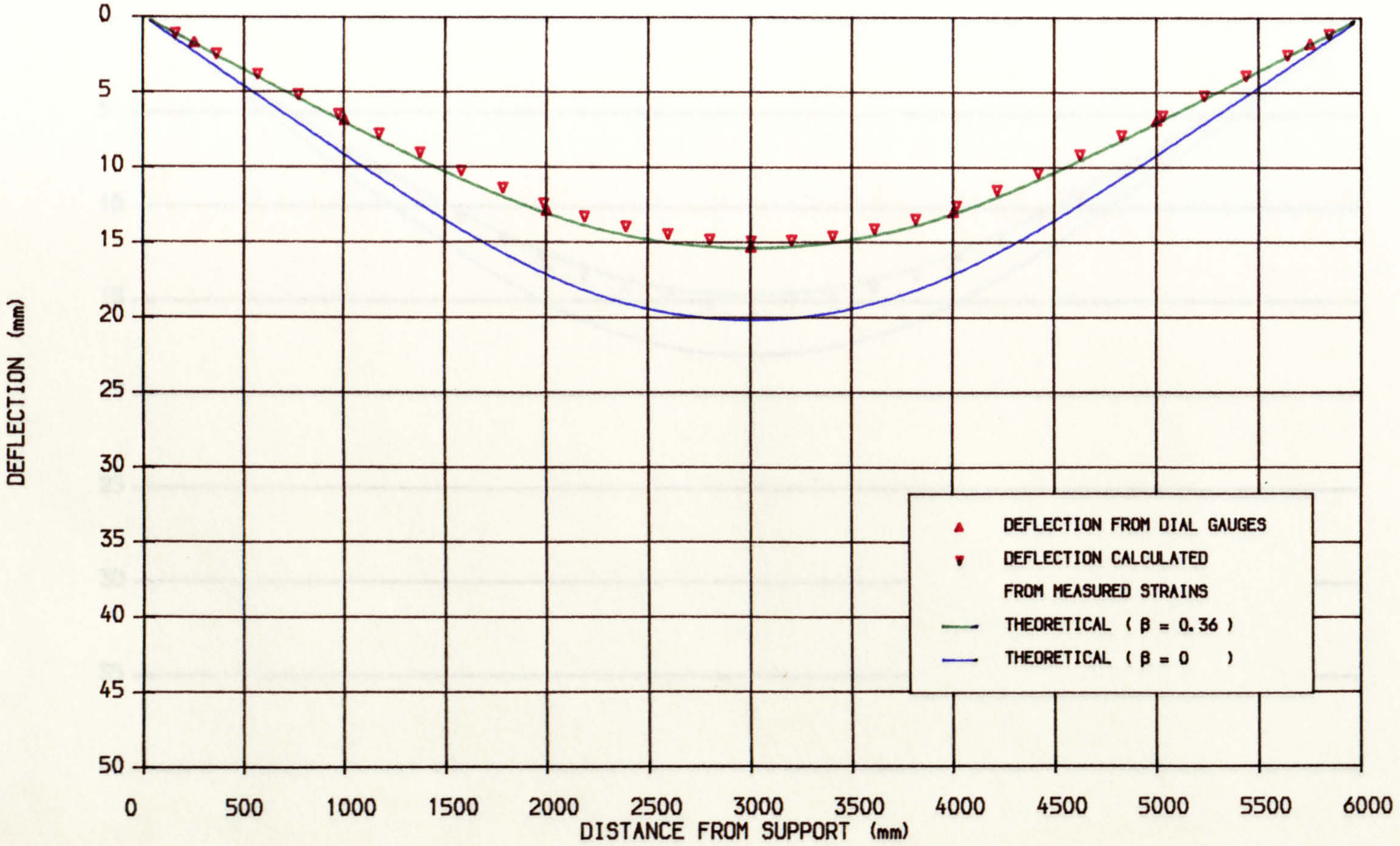

FIG. 6.14b THEORETICAL AND EXPERIMENTAL DEFLECTED PROFILE AT SERVICE LOAD
1ST LOADING (BEAM R2.2.4)

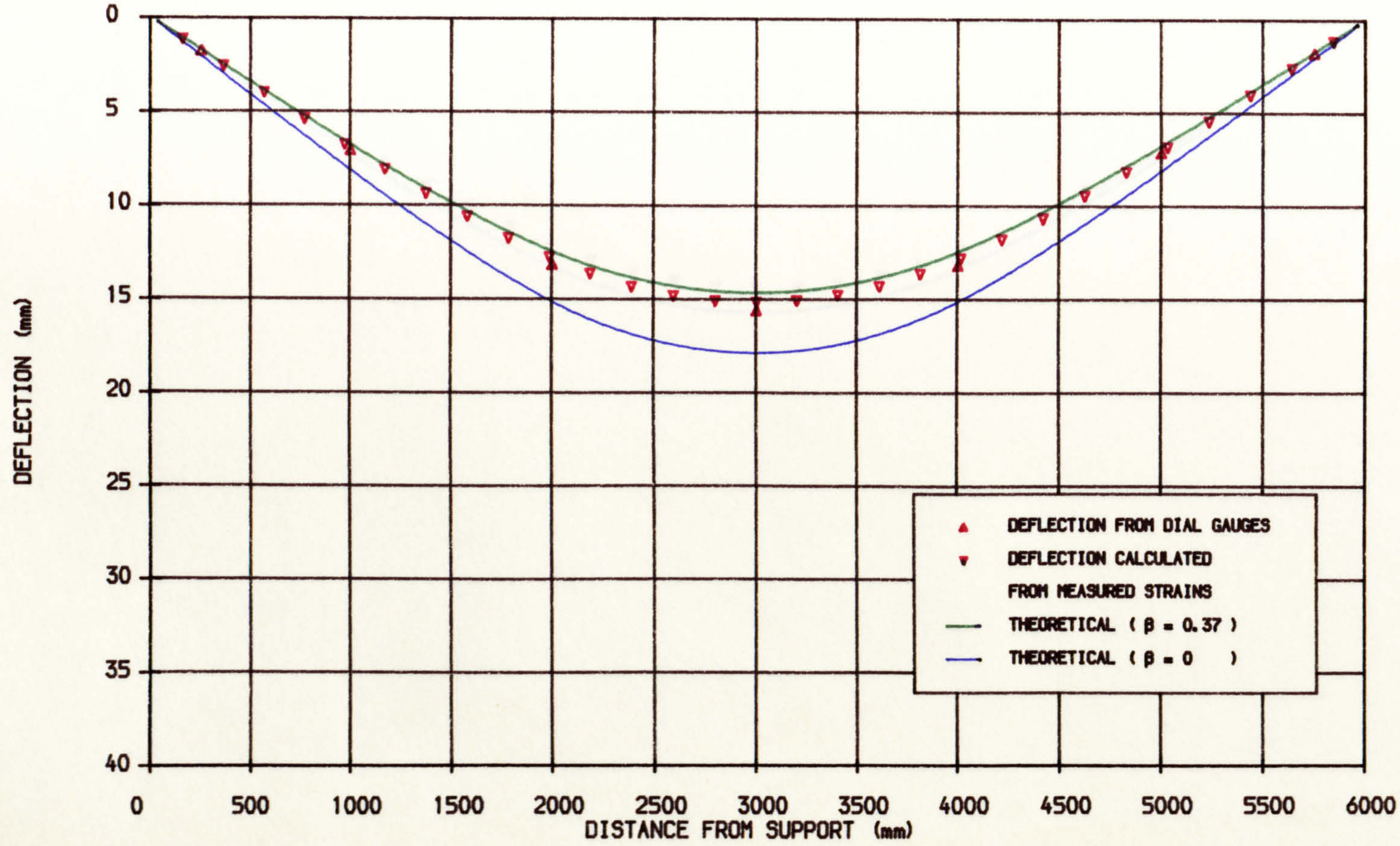

FIG. 6.14c THEORETICAL AND EXPERIMENTAL DEFLECTED PROFILE AT SERVICE LOAD IN 1ST LOADING (BEAM R3.3.4)

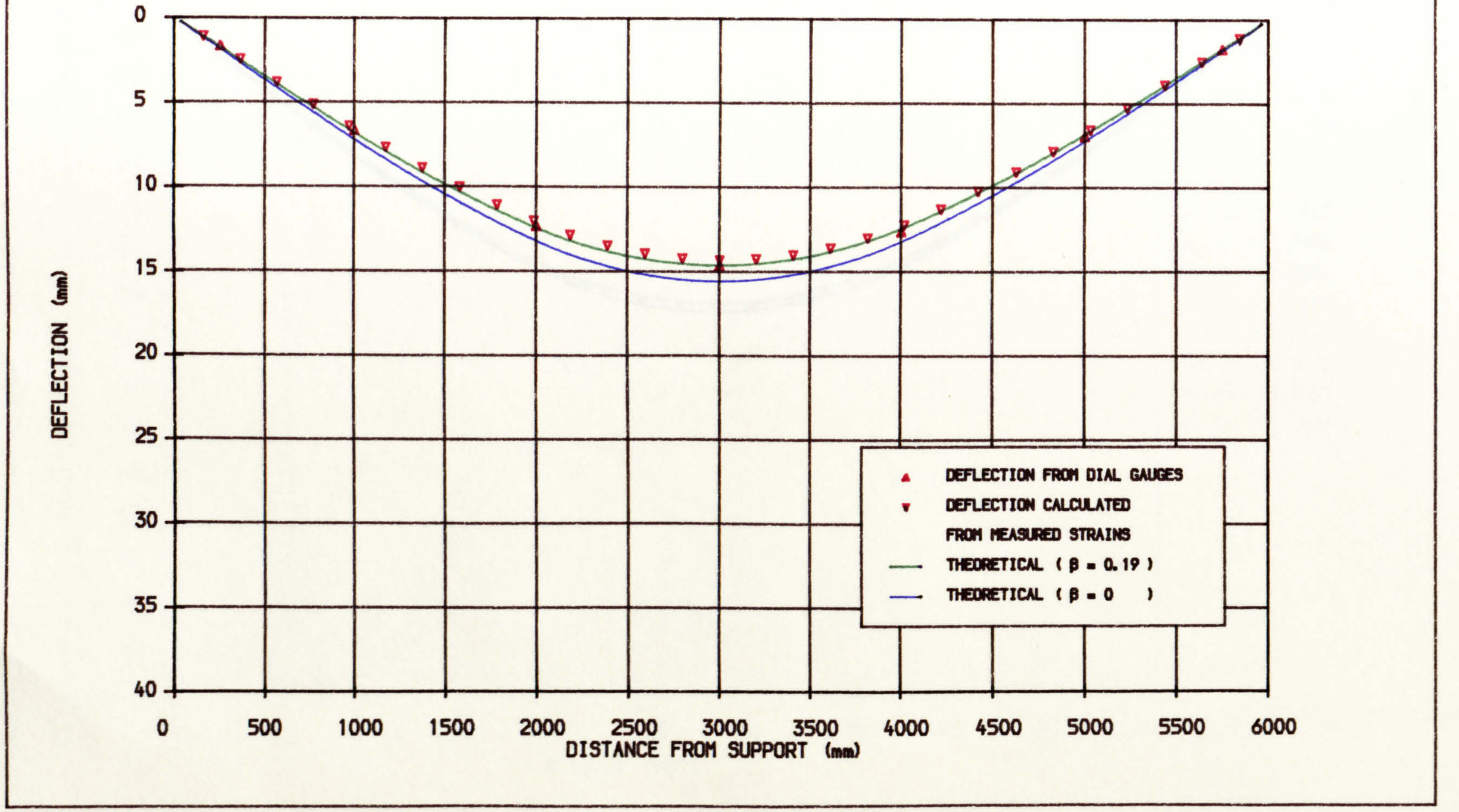

FIG. 6.14d THEORETICAL AND EXPERIMENTAL DEFLECTED PROFILE AT SERVICE LOAD IN 1ST LOADING (BEAM I3.3.4)

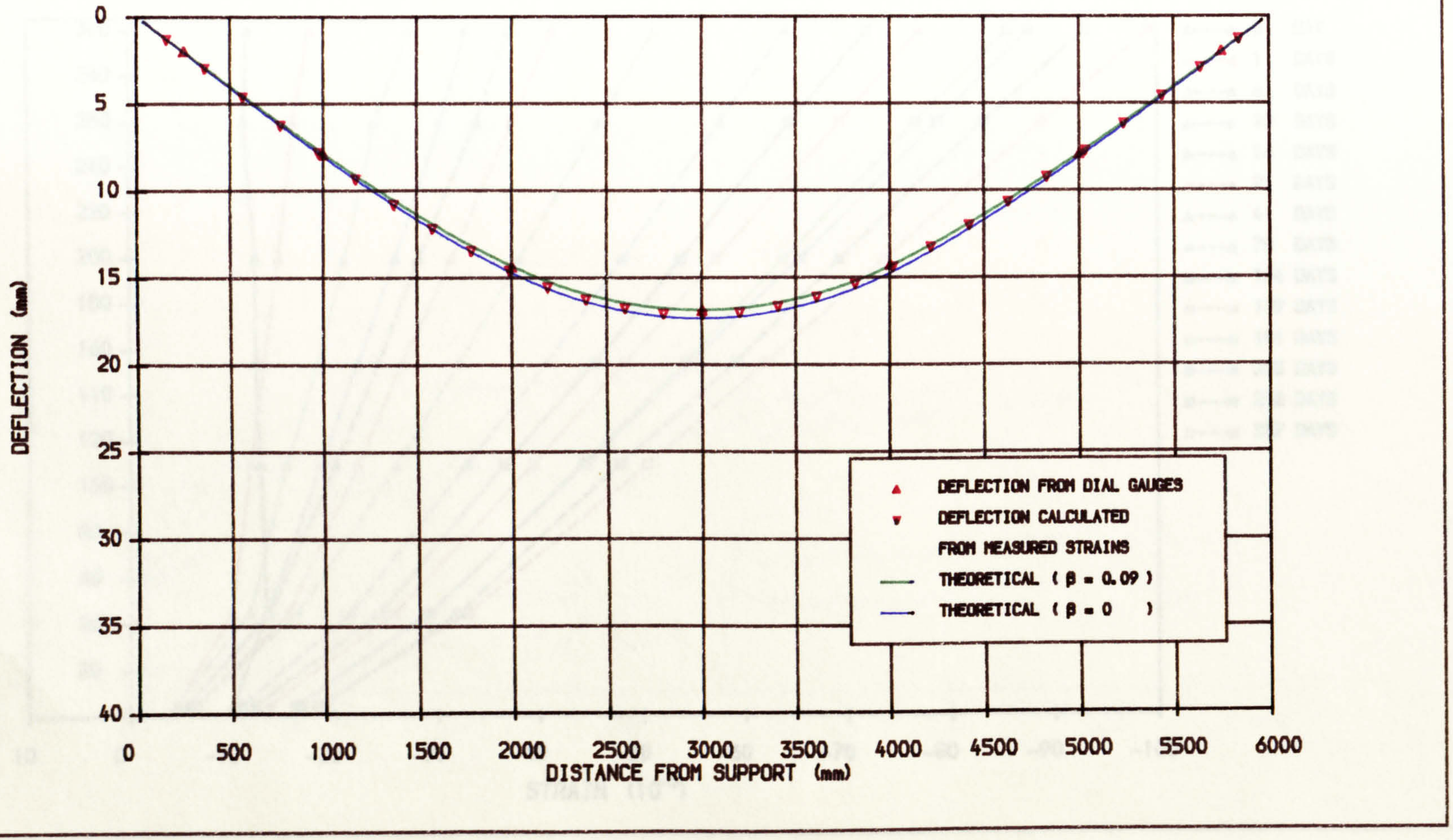

FIG. 6.15a TOTAL STRAIN DISTRIBUTION AT CENTRE AT HALF-SERVICE LOAD (R3.3.4)

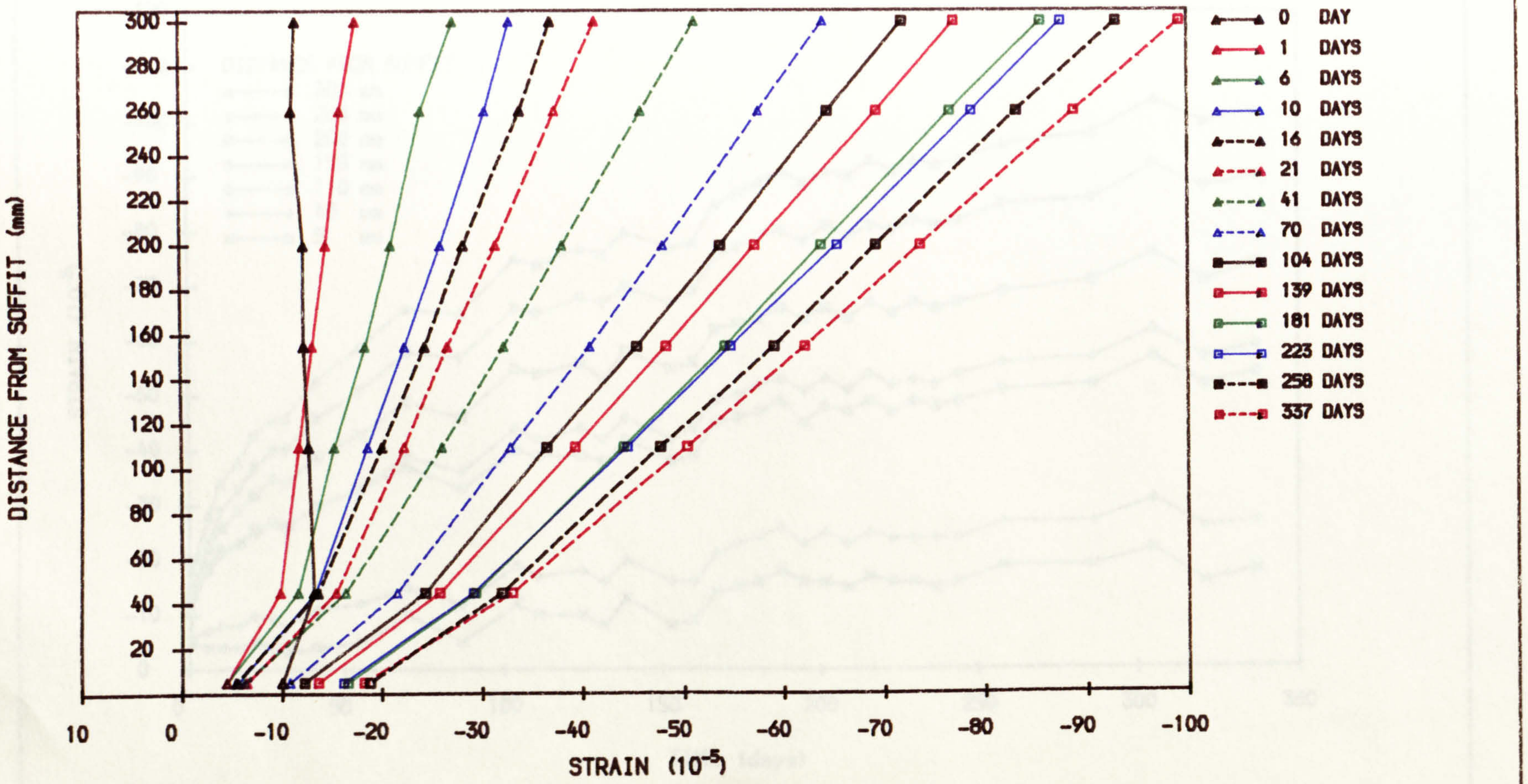

FIG. 6.15b LONG-TERM STRAIN DEFORMATION AT HALF-SERVICE LOAD (BEAM R3.3.4)

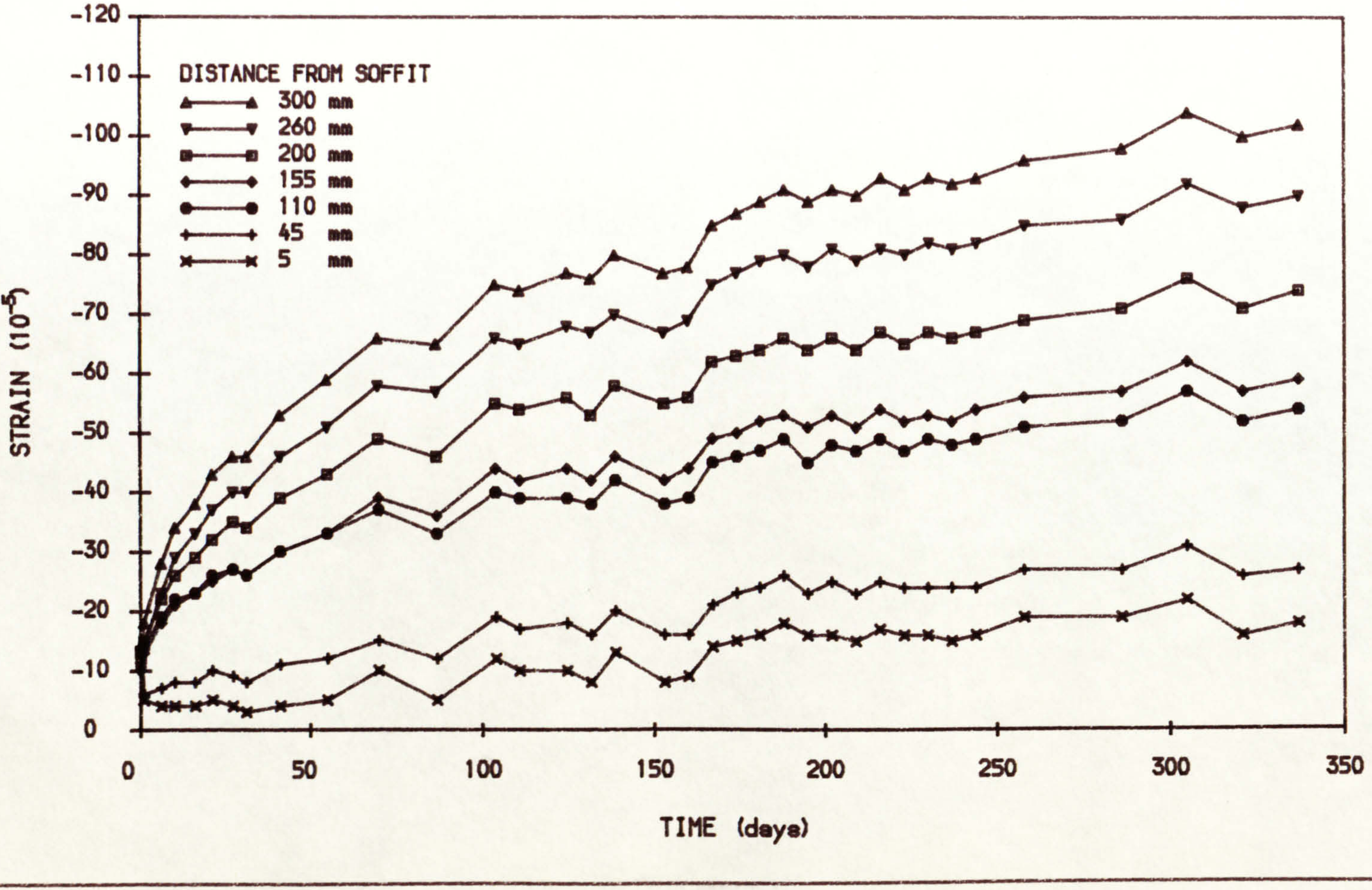

FIG. 6.16a LONGITUDINAL STRAIN AND CURVATURE DISTRIBUTION AT MIDSPAN IN 1ST LOADING (BEAM R2.3.2)

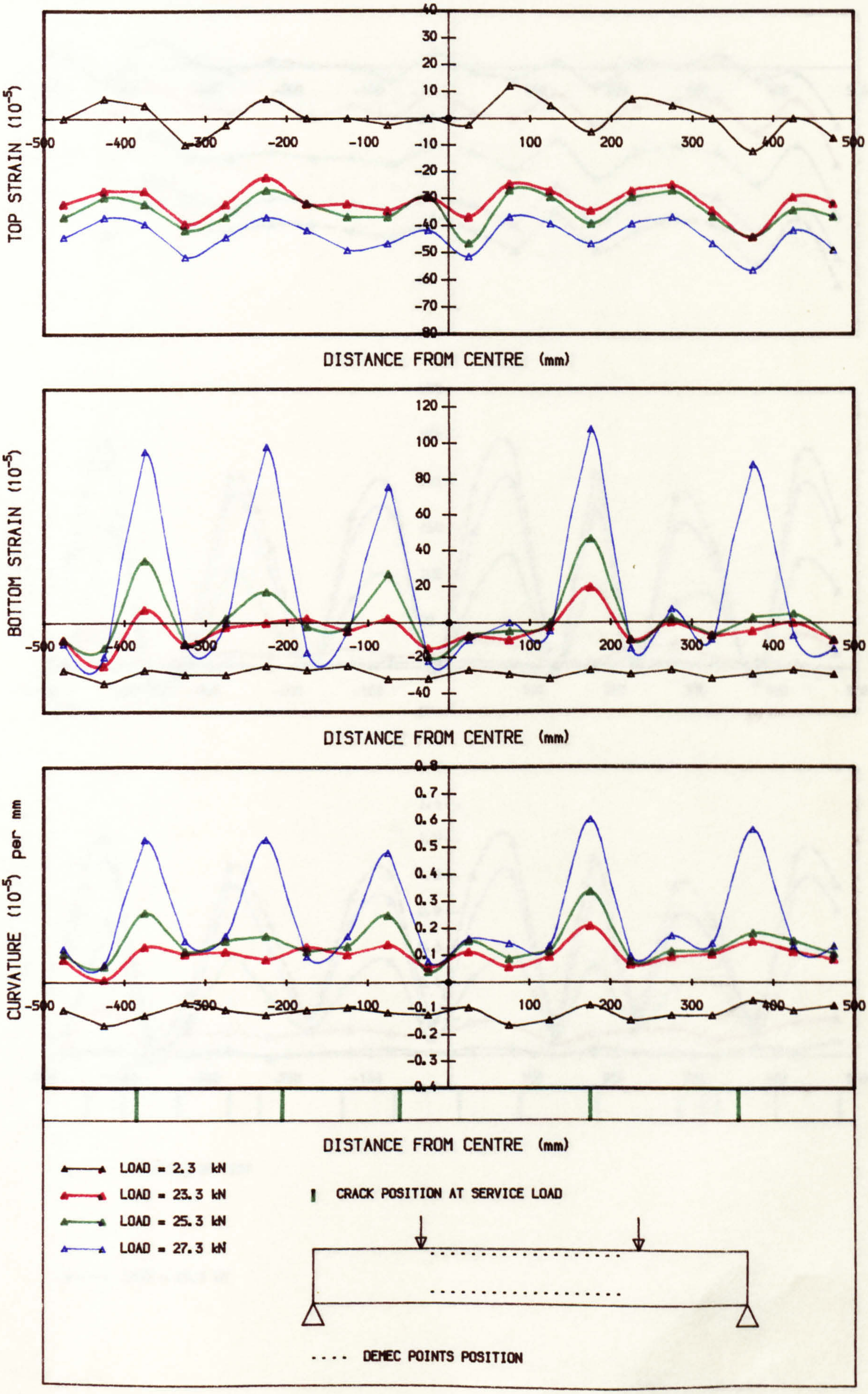

FIG. 6.16b LONGITUDINAL STRAIN AND CURVATURE DISTRIBUTION AT MIDSPAN IN 1ST LOADING (BEAM R2.0.7)

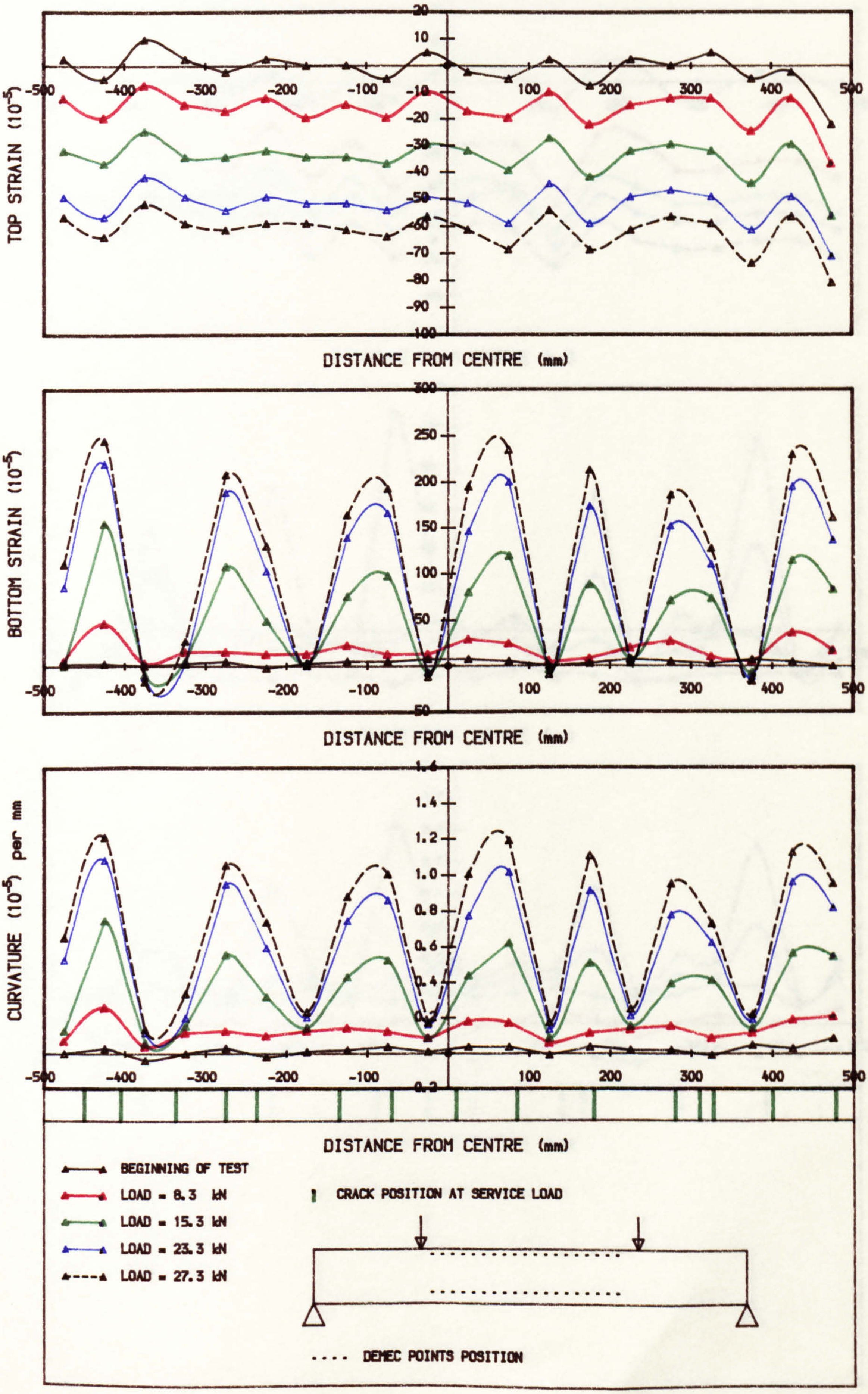

FIG. 6.16c LONGITUDINAL STRAIN AND CURVATURE DISTRIBUTION AT MIDSPAN IN 1ST LOADING (BEAM I1.2.2)

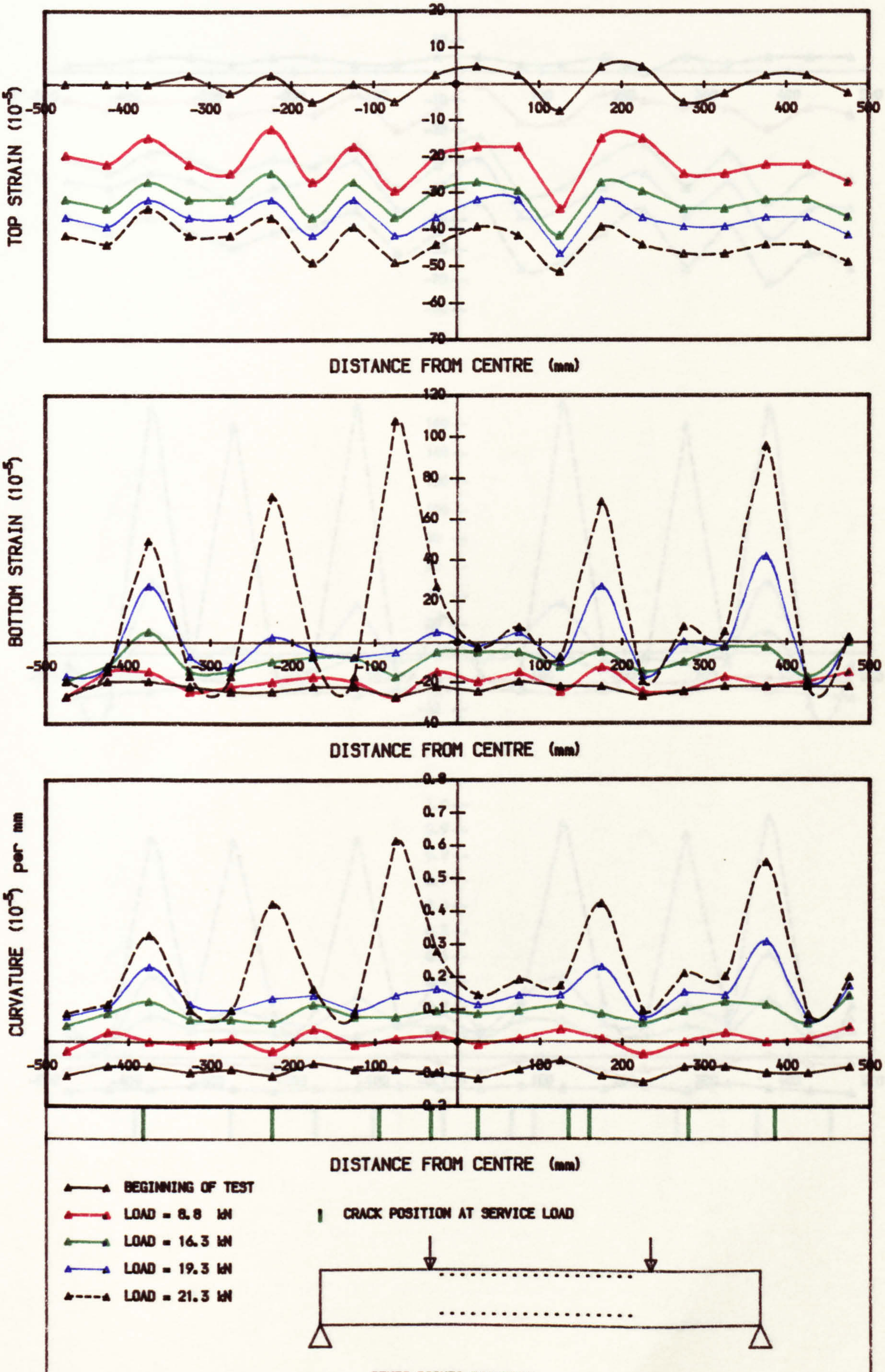

FIG. 6.16d LONGITUDINAL STRAIN AND CURVATURE DISTRIBUTION AT MIDSPAN IN 1ST LOADING (BEAM I2.3.2)

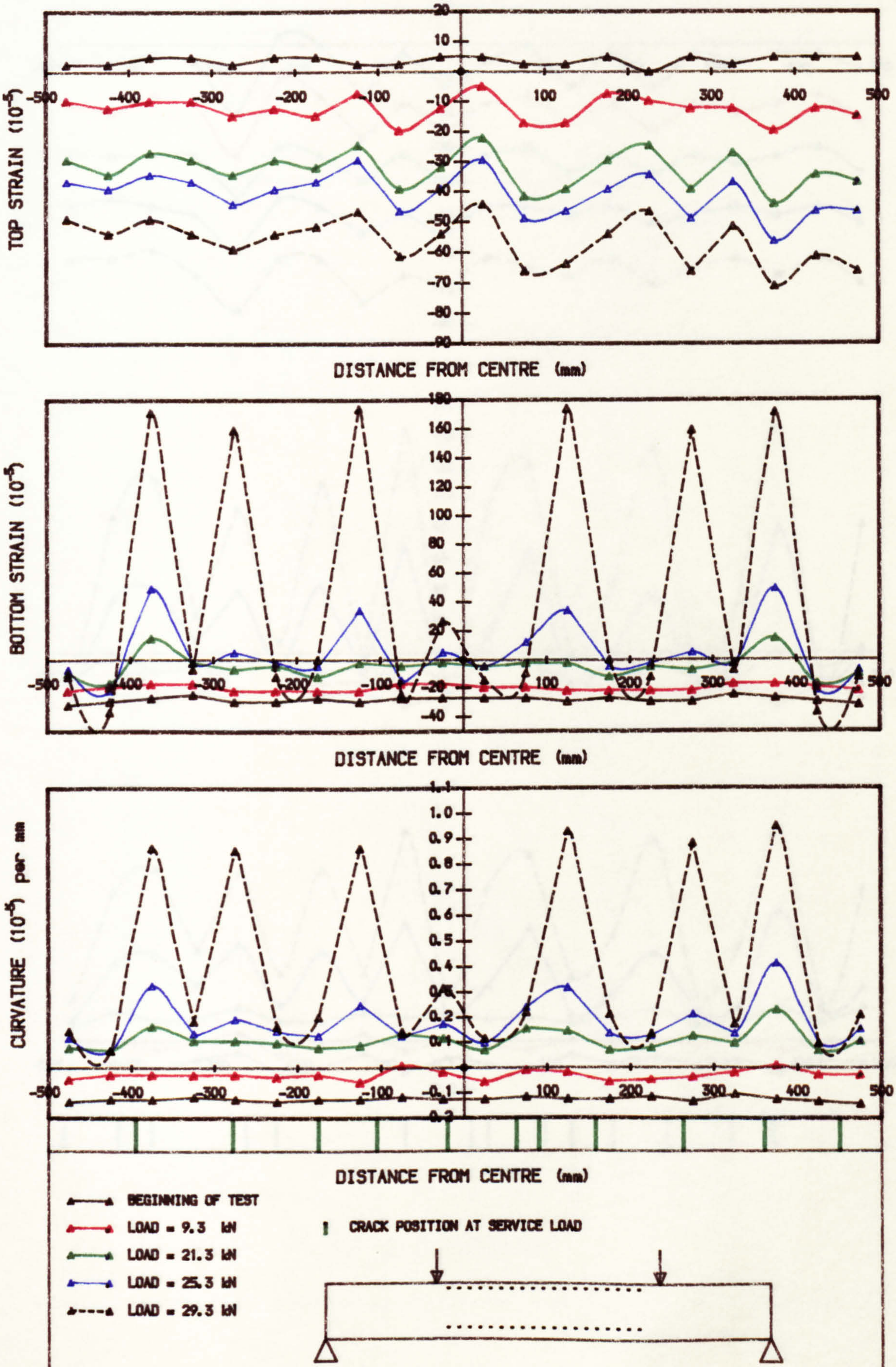

FIG. 6.16e LONGITUDINAL STRAIN AND CURVATURE DISTRIBUTION AT MIDSPAN IN 1ST LOADING (BEAM I2.2.4)

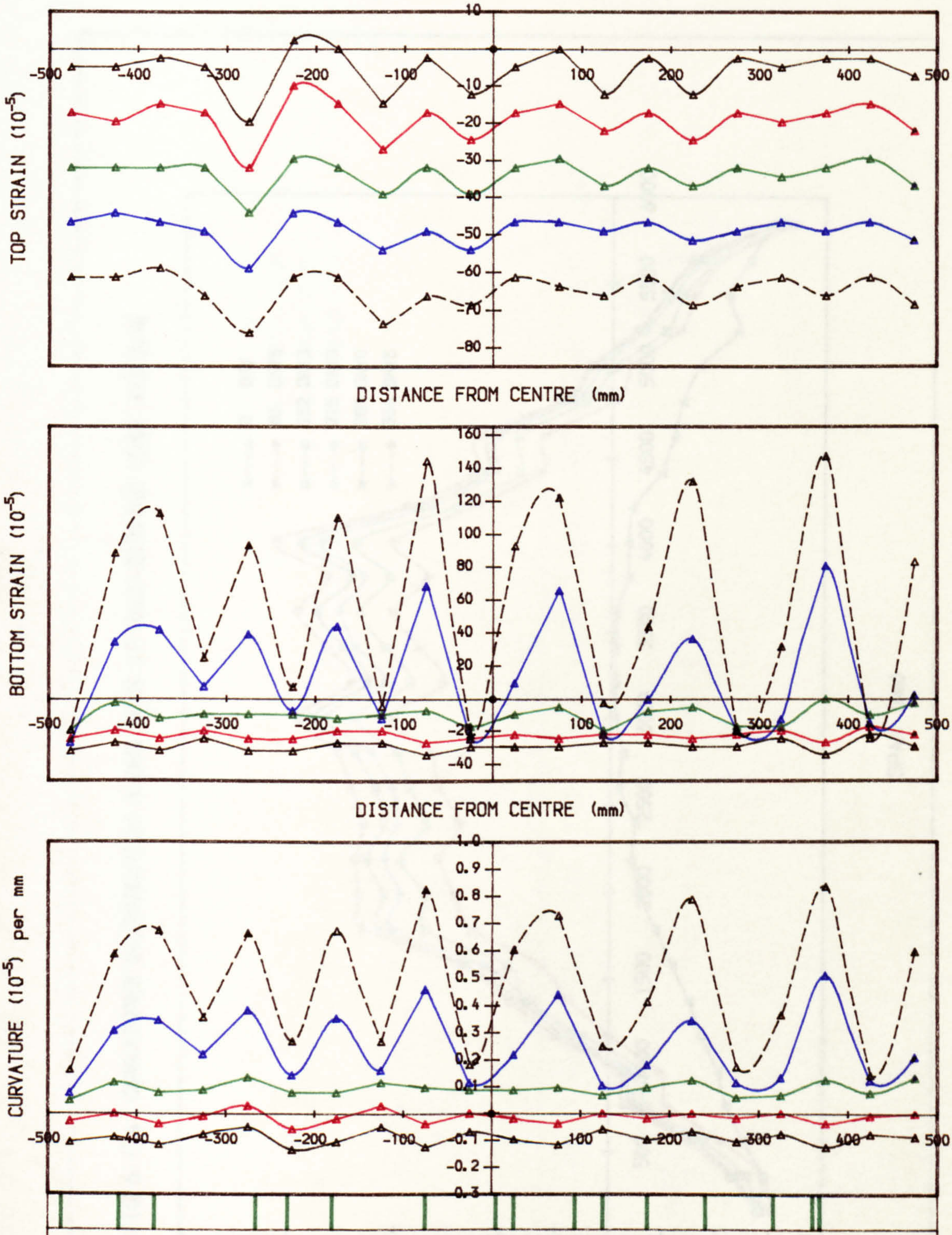

FIG. 6.17a CURVATURES DISTRIBUTION ALONG SPAN AT HALF-SERVICE LOAD (R3.3.4)

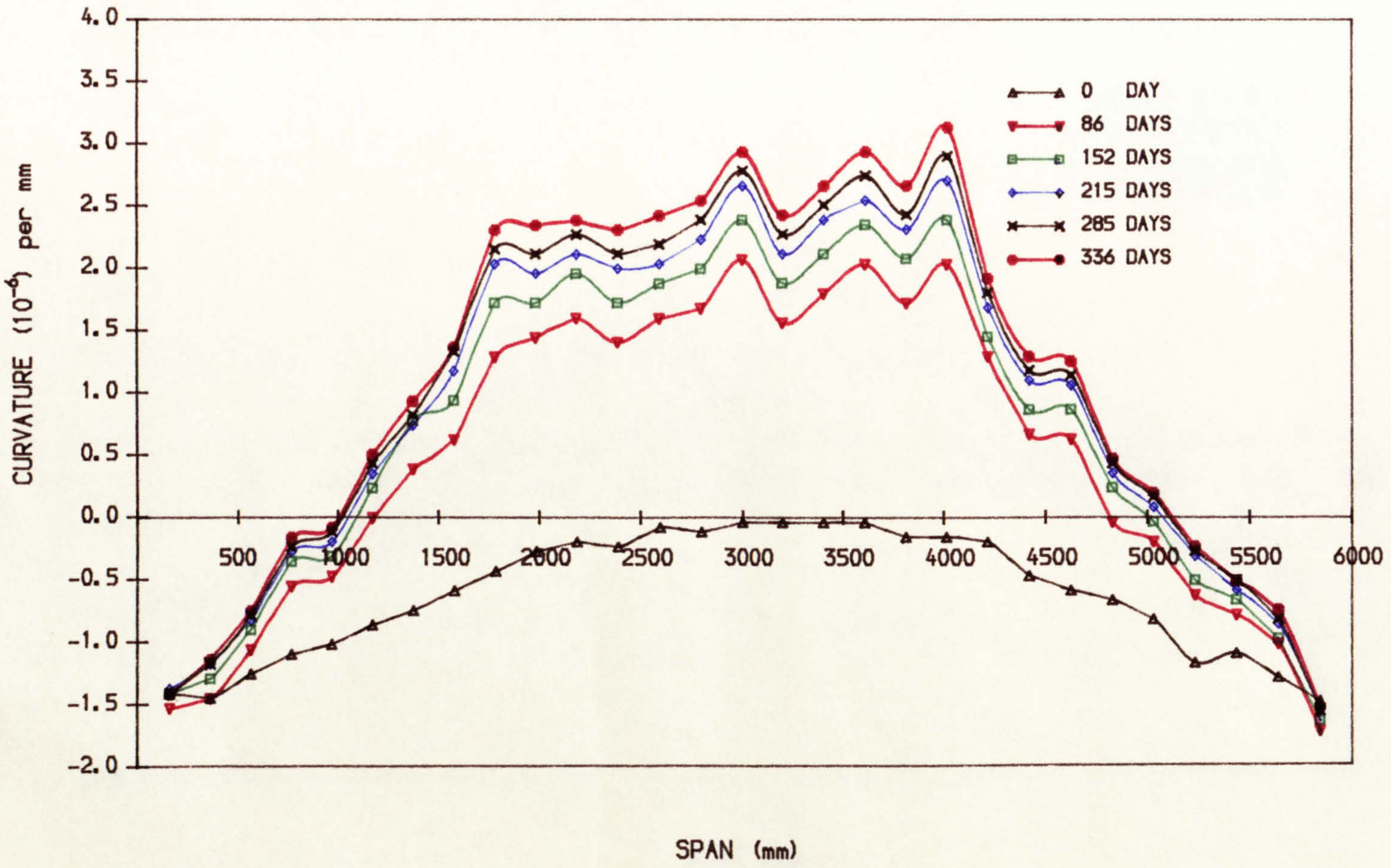

FIG. 6.17b CURVATURES DISTRIBUTION ALONG SPAN AT HALF-SERVICE LOAD (R1.2.2)

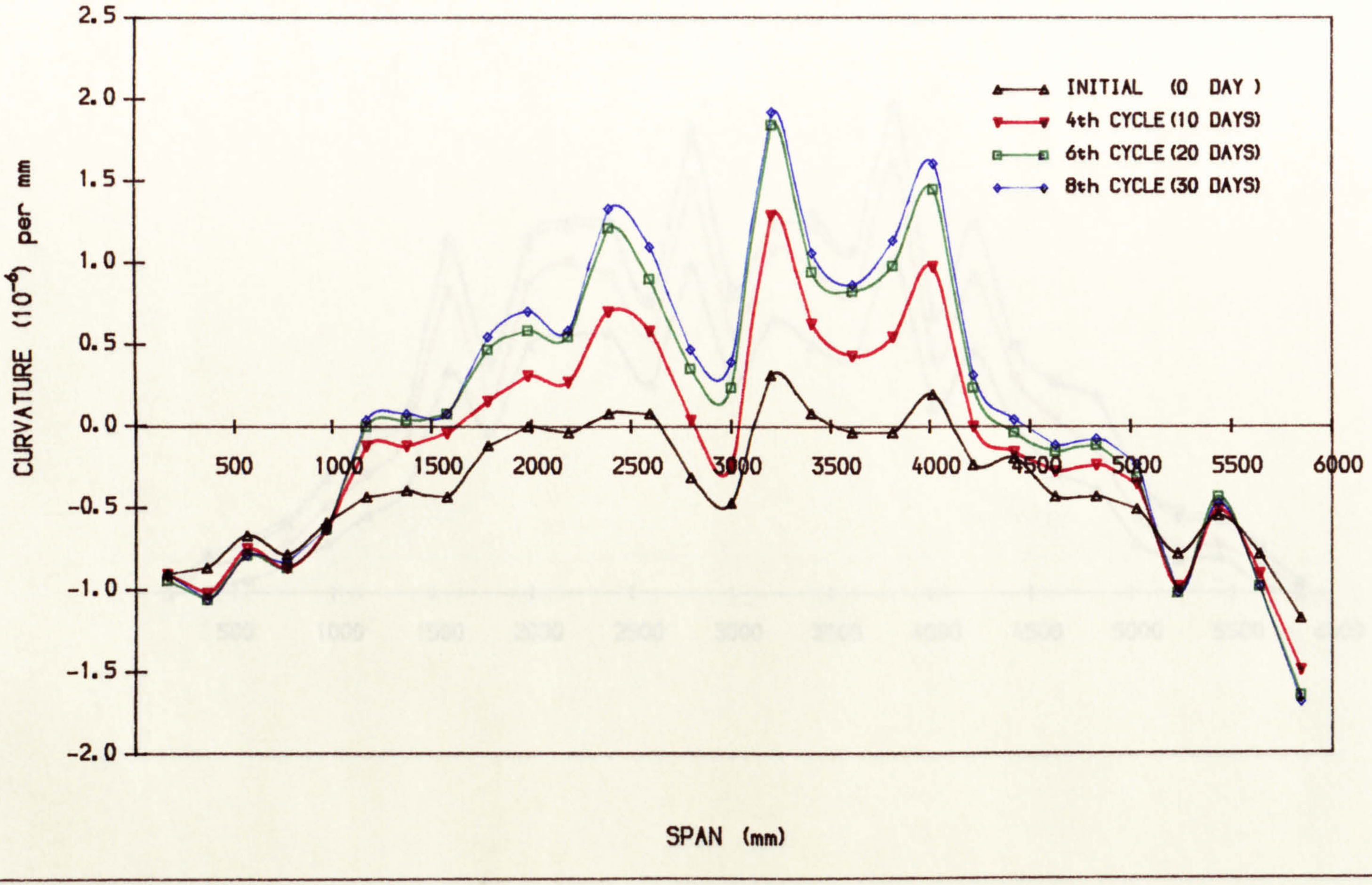

FIG. 6.17c CURVATURES DISTRIBUTION ALONG SPAN AT HALF-SERVICE LOAD (R1.0.5)

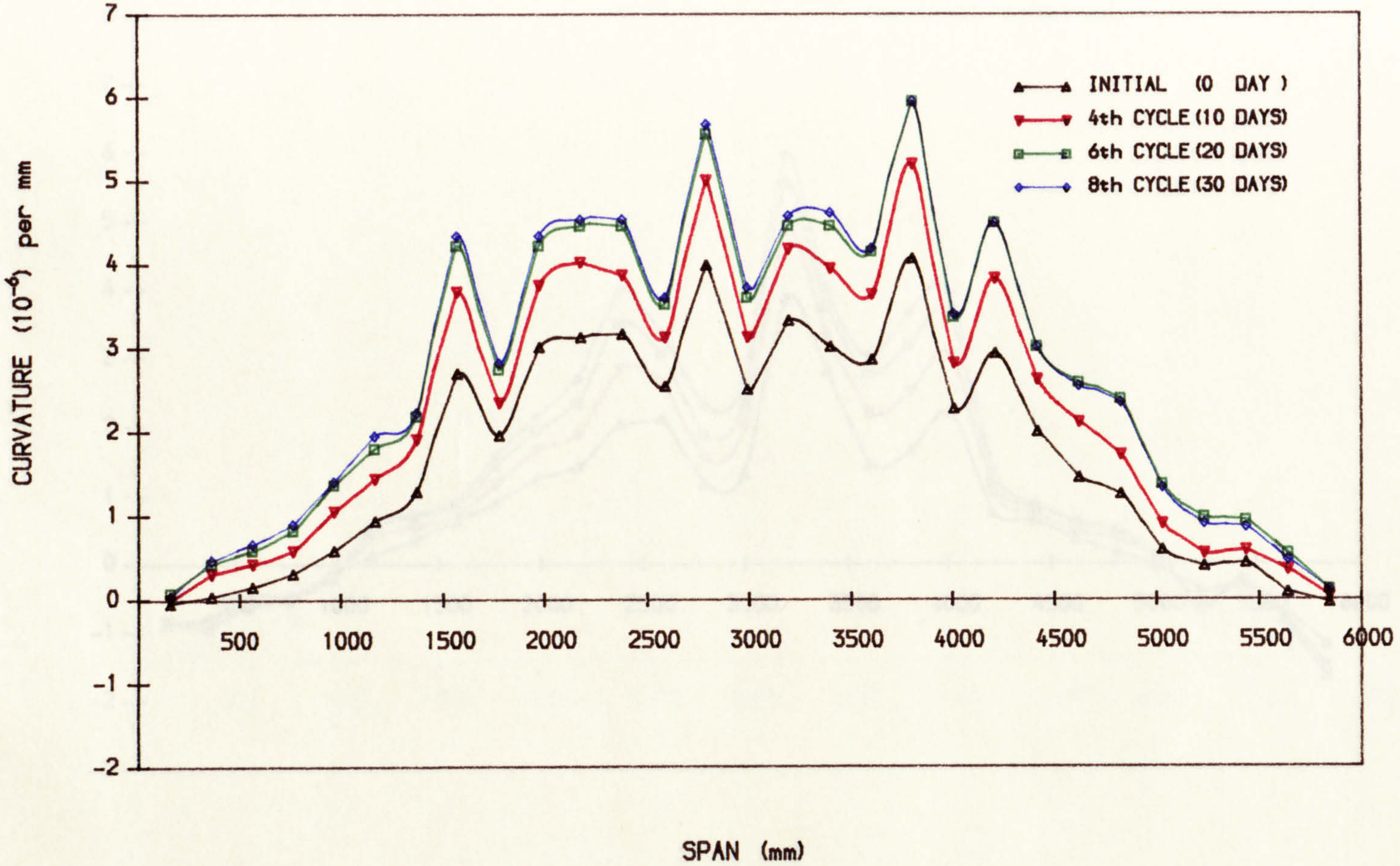

FIG. 6.17d CURVATURES DISTRIBUTION ALONG SPAN AT SERVICE LOAD (R1.2.2)

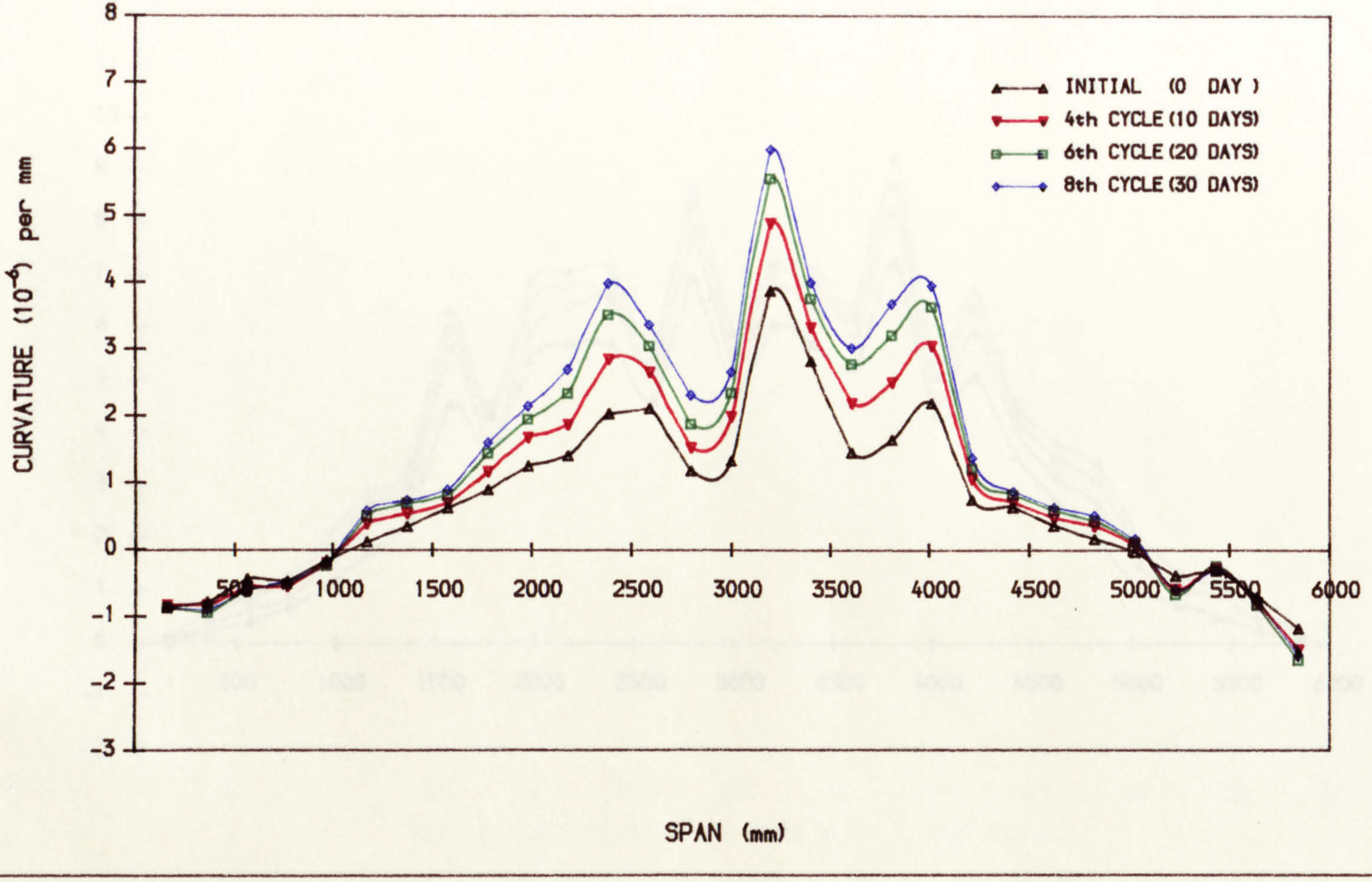

FIG. 6.17e CURVATURES DISTRIBUTION ALONG SPAN AT SERVICE LOAD (R1.0.5)

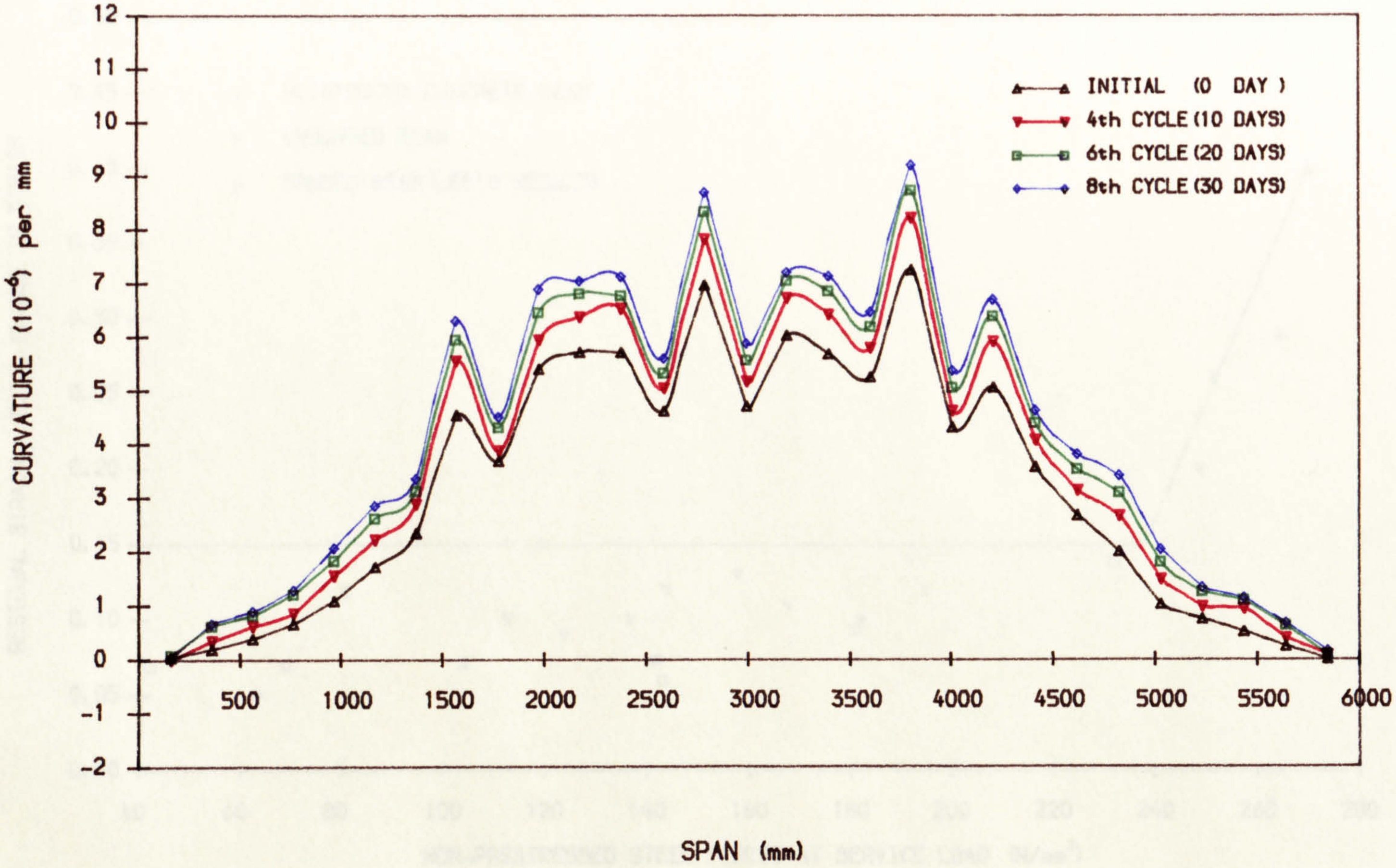

FIG. 6.18a RATIO OF RESIDUAL BOTTOM STRAIN (AFTER 1ST CYCLE) vs. STEEL STRESS

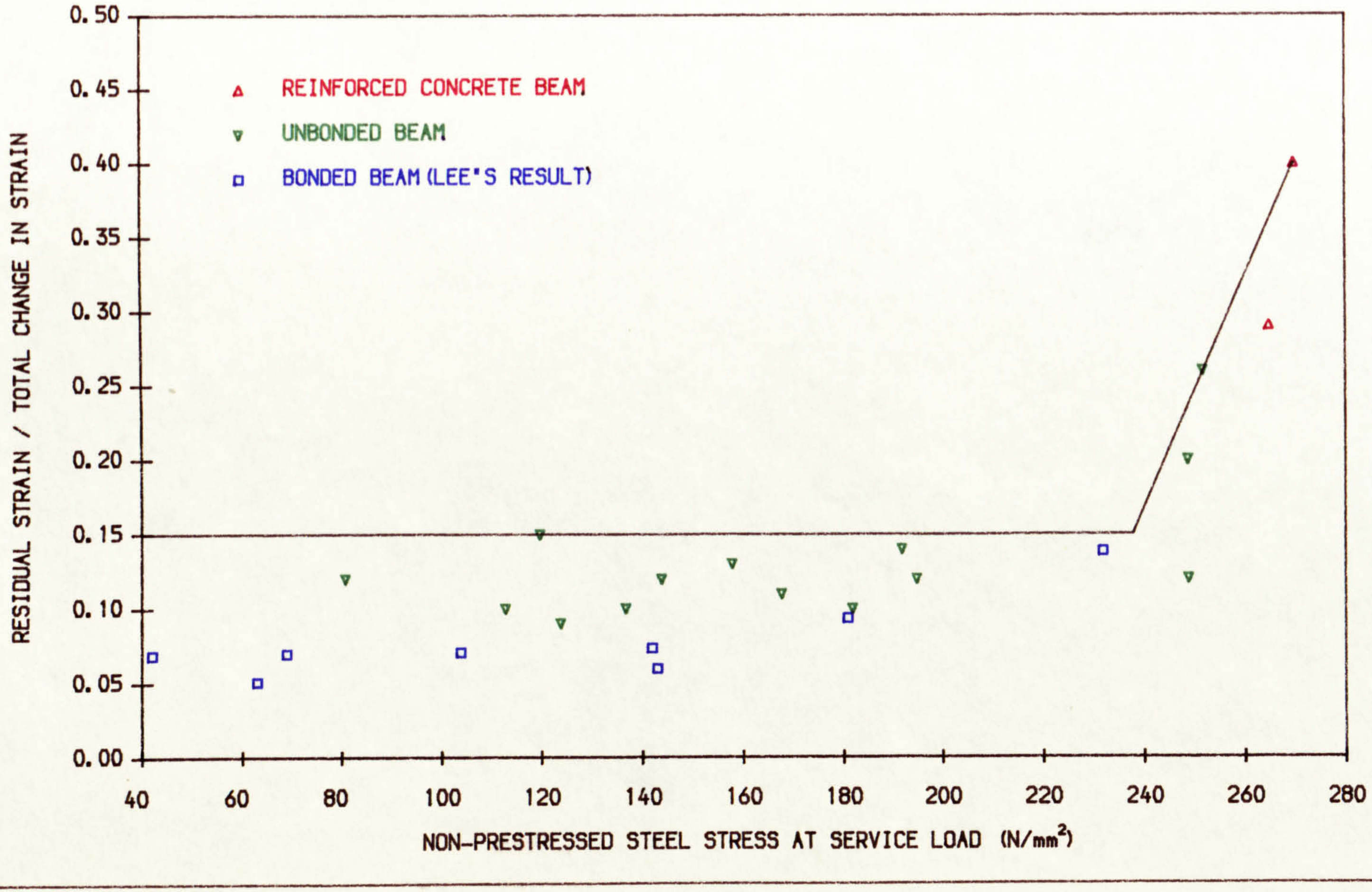

FIG. 6.18b RESIDUAL DEFLECTION AFTER 1ST CYCLE vs. PRESTRESS

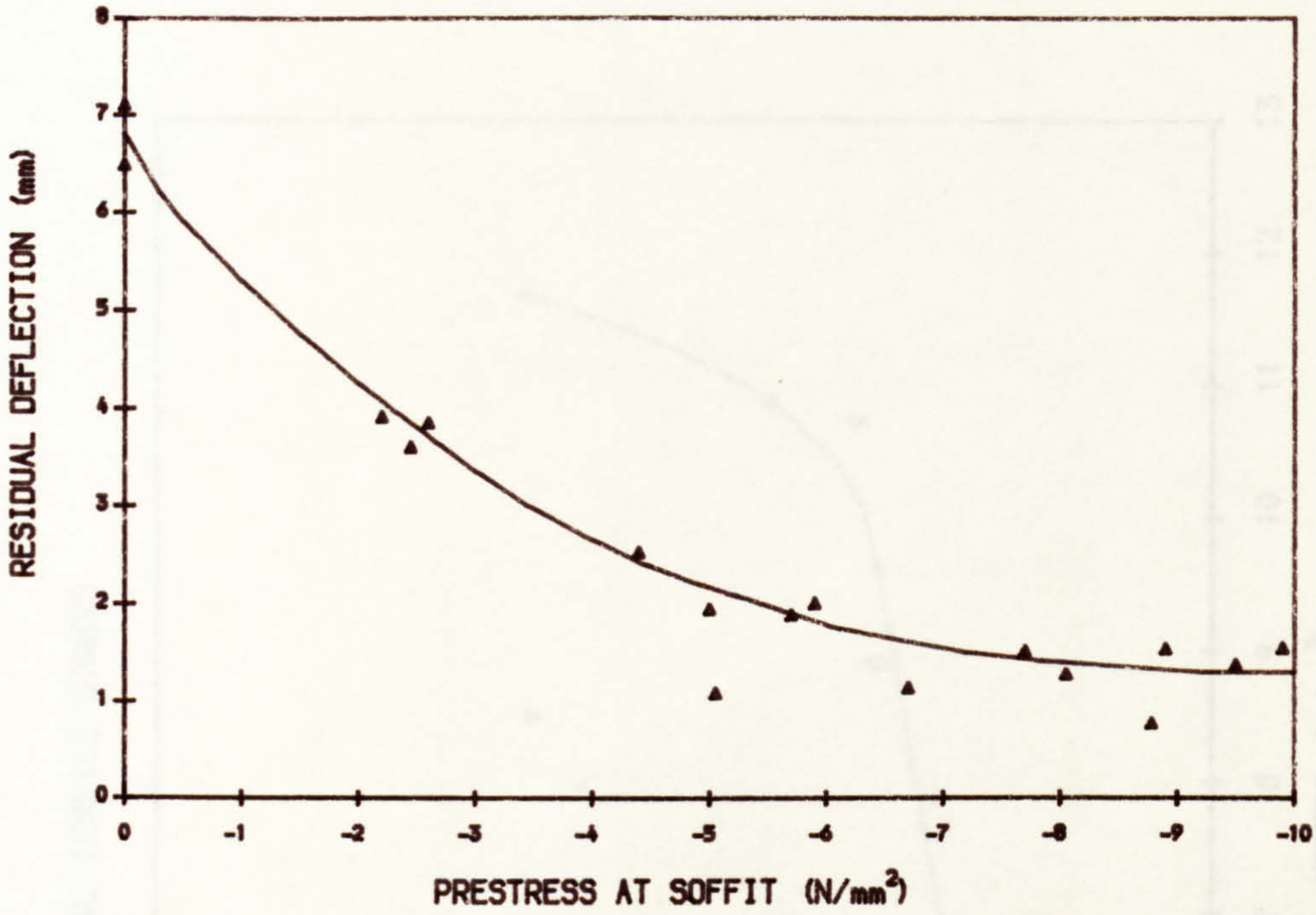

FIG. 6.18c ADD. RESIDUAL DEFLECTION AFTER 2ND CYCLE vs. PRESTRESS

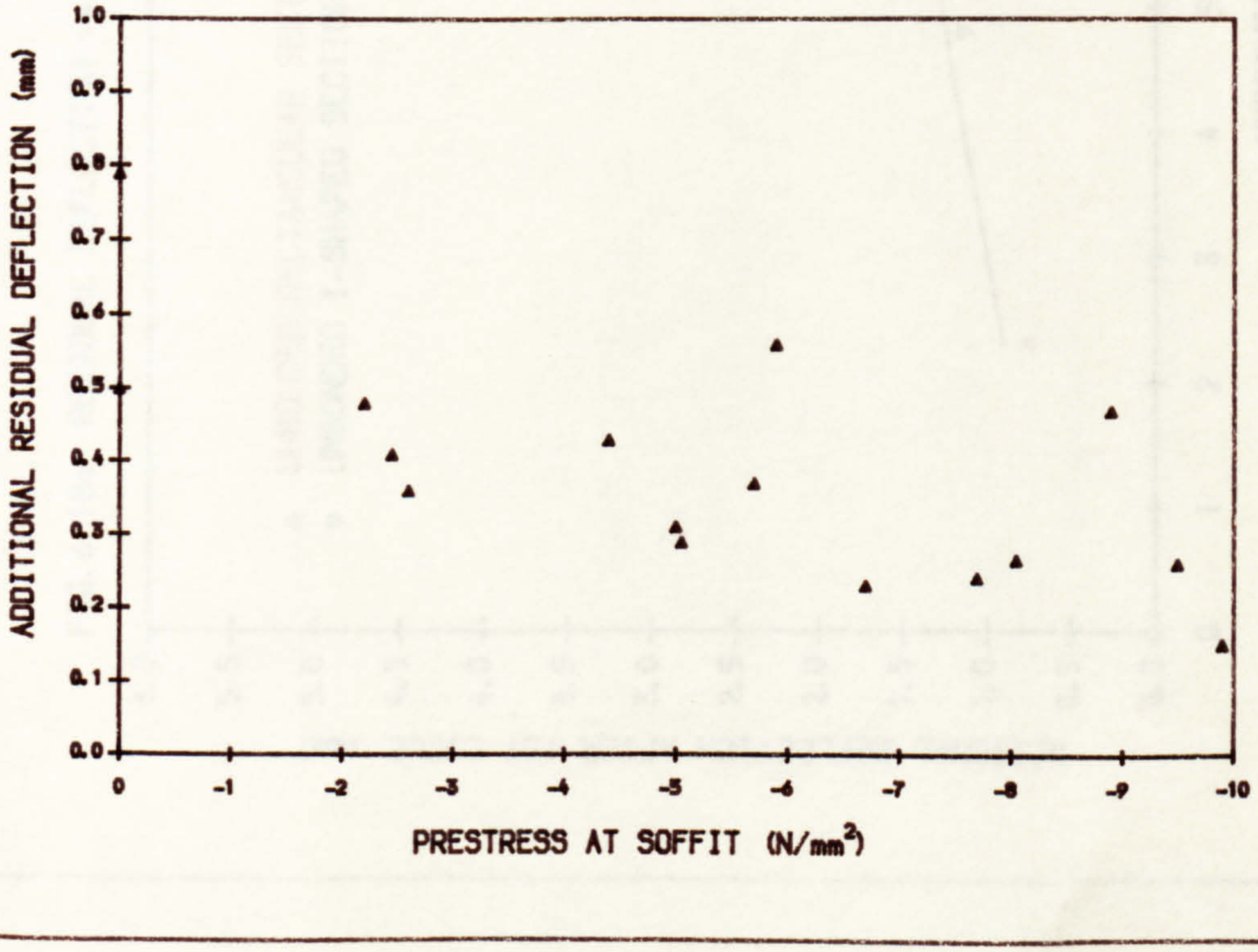

FIG. 6.18d RESIDUAL DEFLECTION vs. HYPOTHETICAL TENSILE STRESS

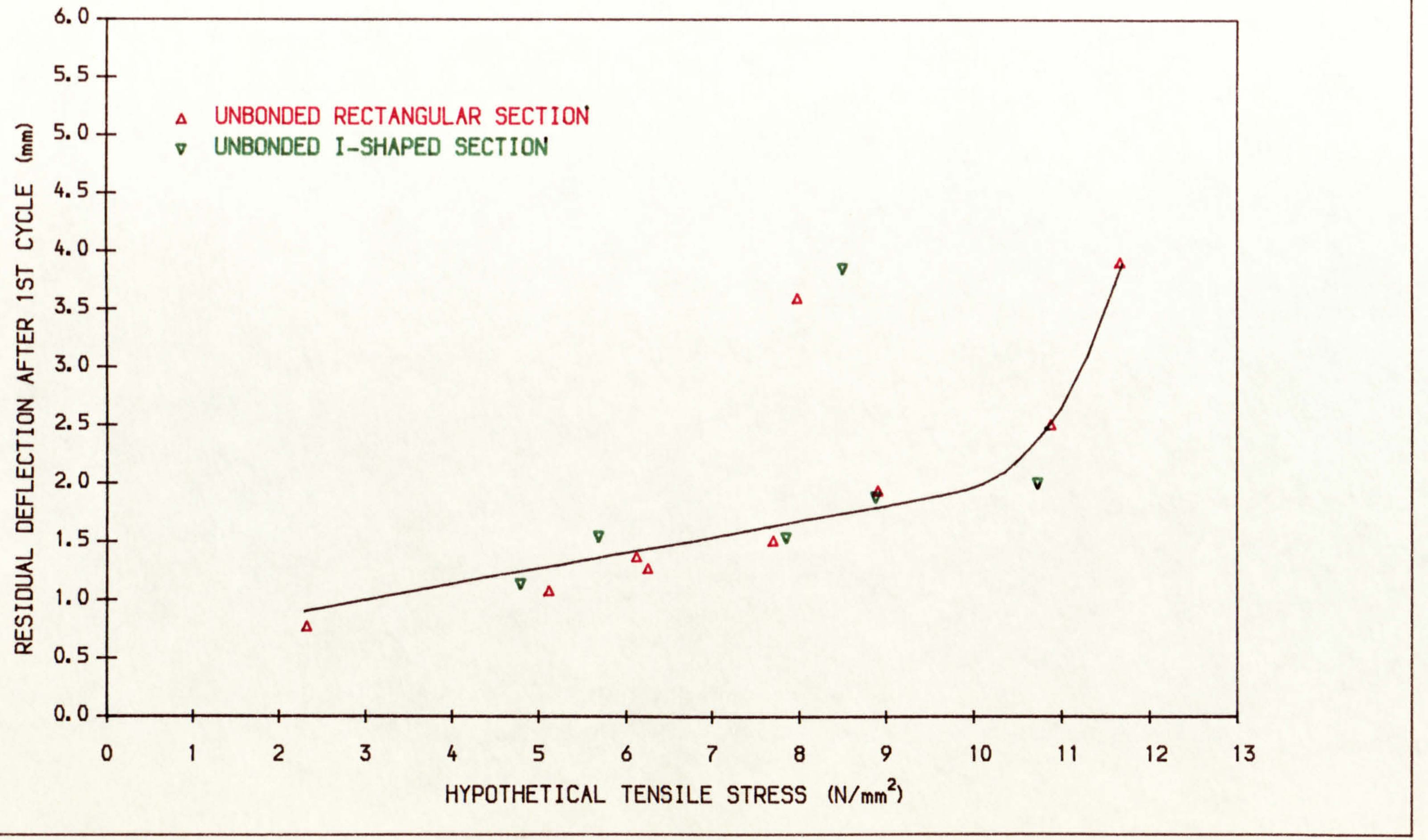

FIG. 6.19a DEFLECTION-TIME RELATIONSHIP (BEAM R1.2.2)

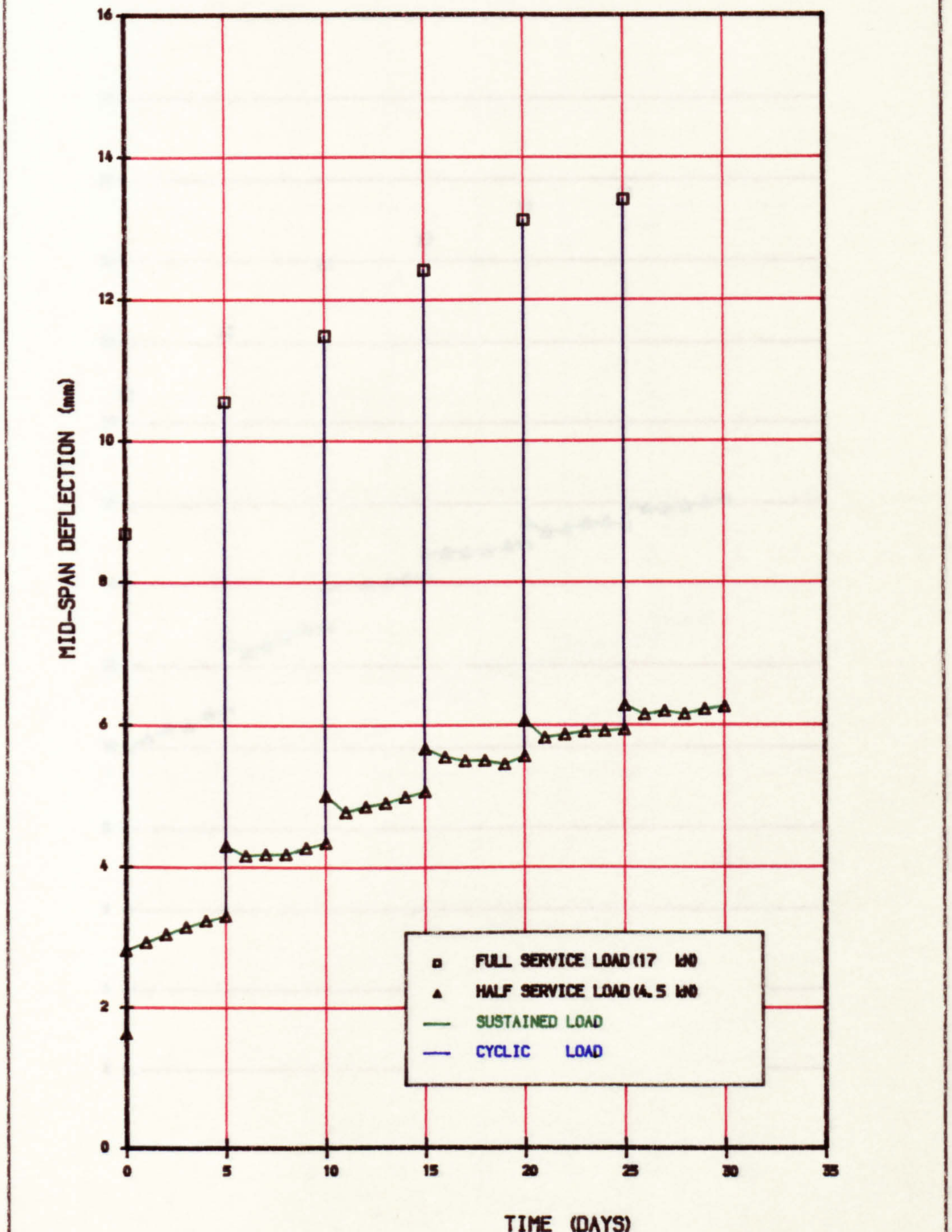

FIG. 6.19b DEFLECTION-TIME RELATIONSHIP (BEAM R1.0.5)

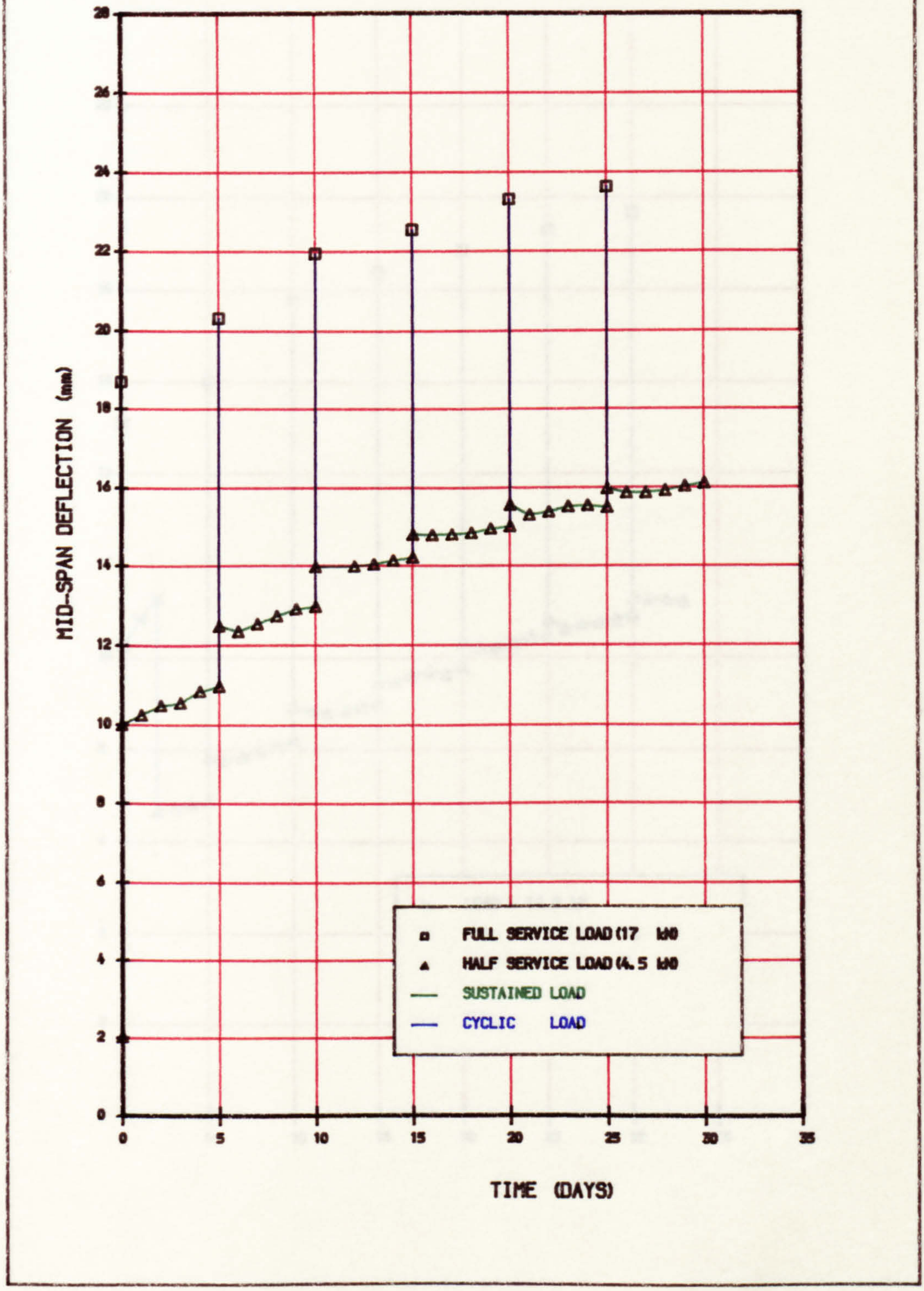

FIG. 6.19c DEFLECTION-TIME RELATIONSHIP (BEAM R2.2.4)

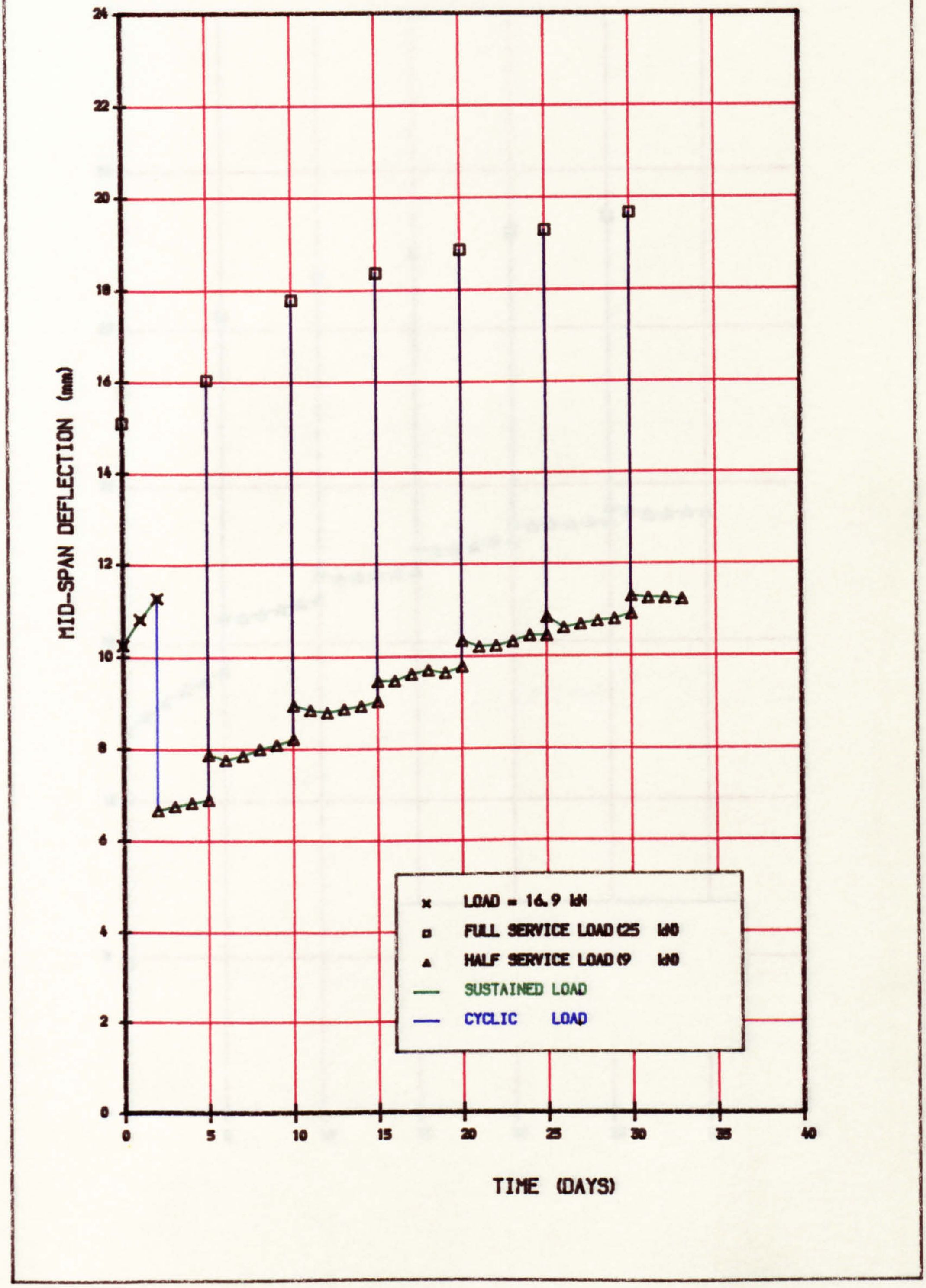

FIG. 6.19d DEFLECTION-TIME RELATIONSHIP (BEAM R2.0.7)

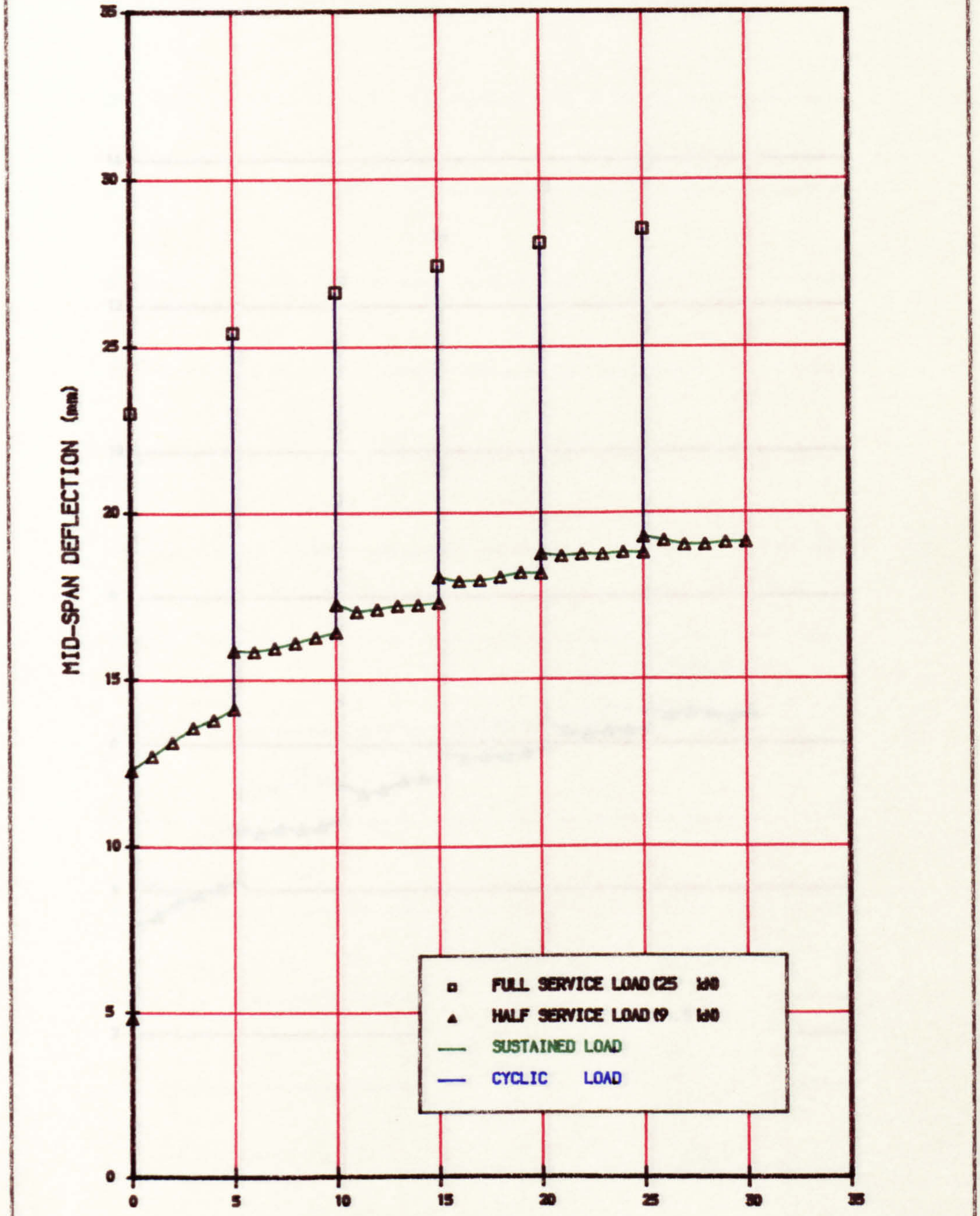

FIG. 6.19e DEFLECTION-TIME RELATIONSHIP (BEAM I1.2.2)

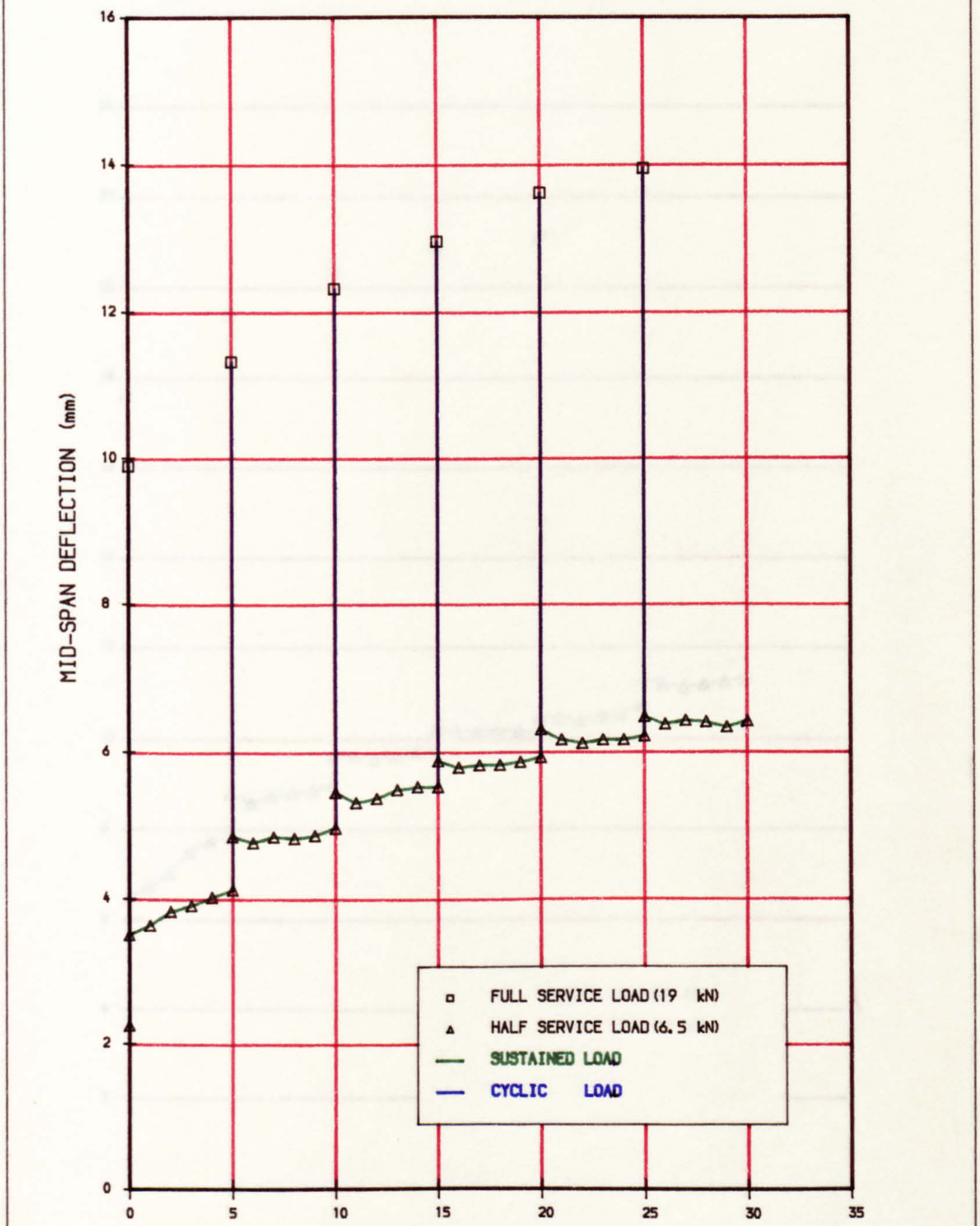

FIG. 6.19f DEFLECTION-TIME RELATIONSHIP (BEAM I2.2.4)

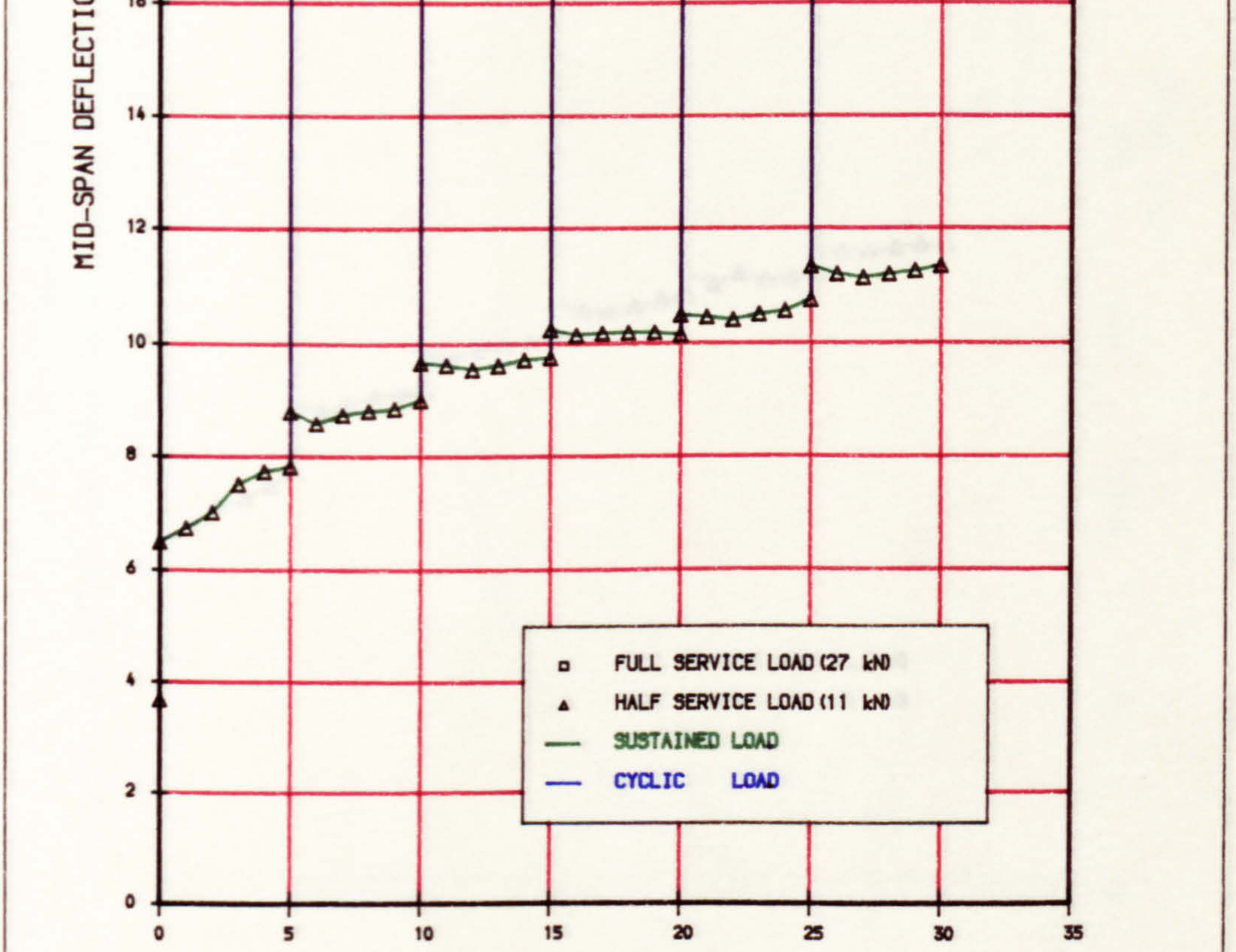

FIG. 6.19g DEFLECTION-TIME RELATIONSHIP (BEAM I3.3.4)

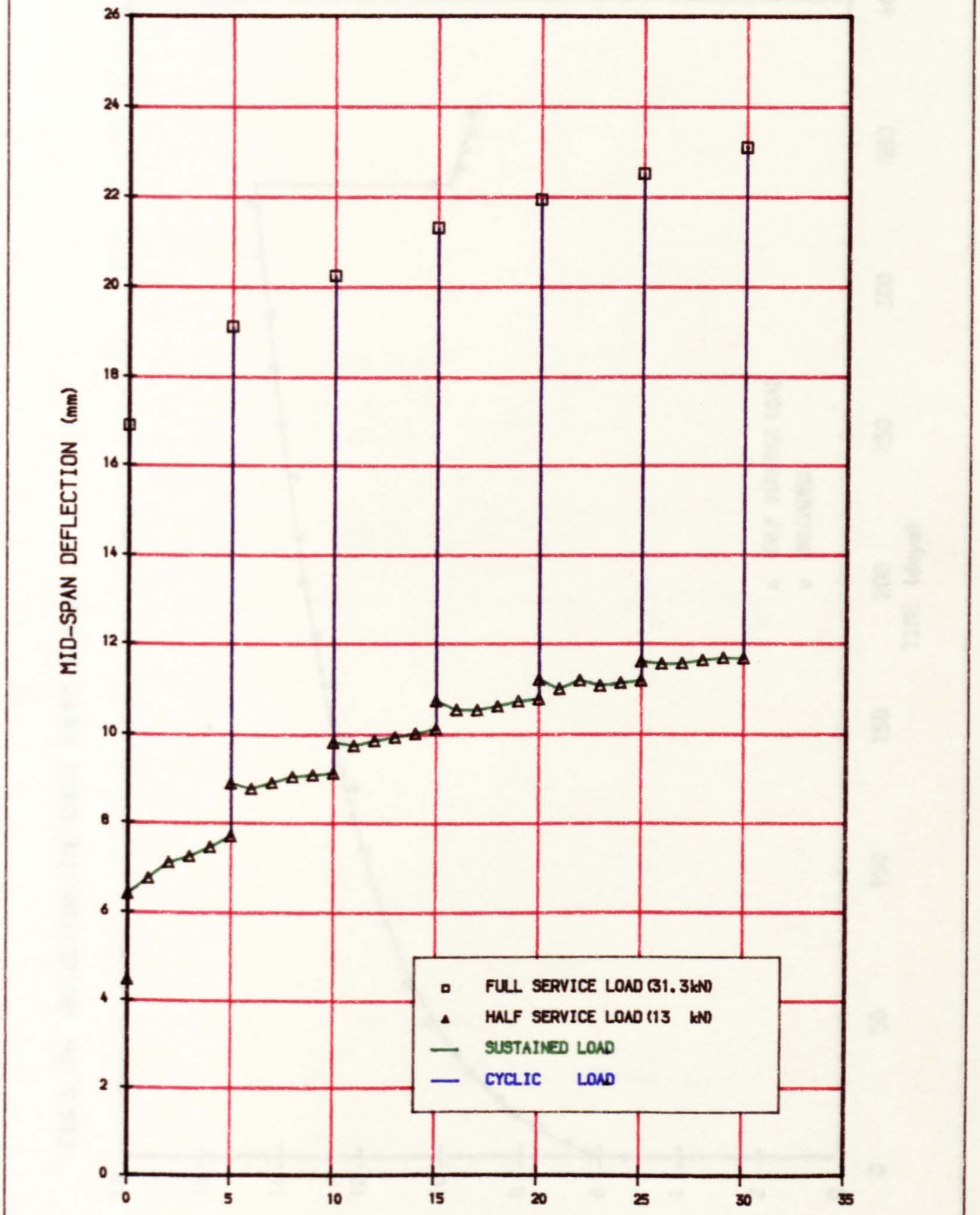

FIG. 6.19h DEFLECTION-TIME CURVE (BEAM R3.3.4)

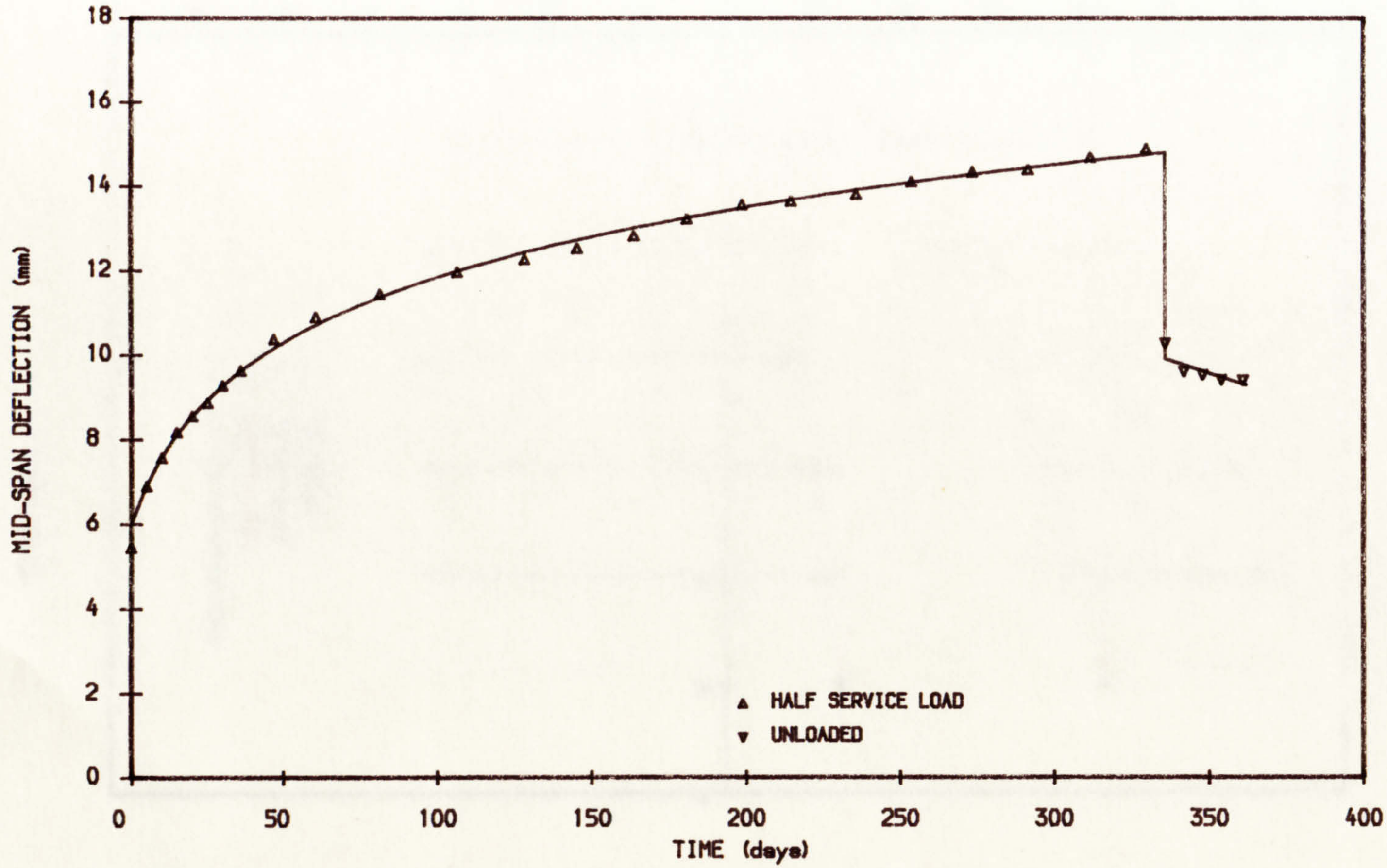

FIG. 6.20a CONCRETE STRAIN-TIME RELATIONSHIP (R1.2.2)

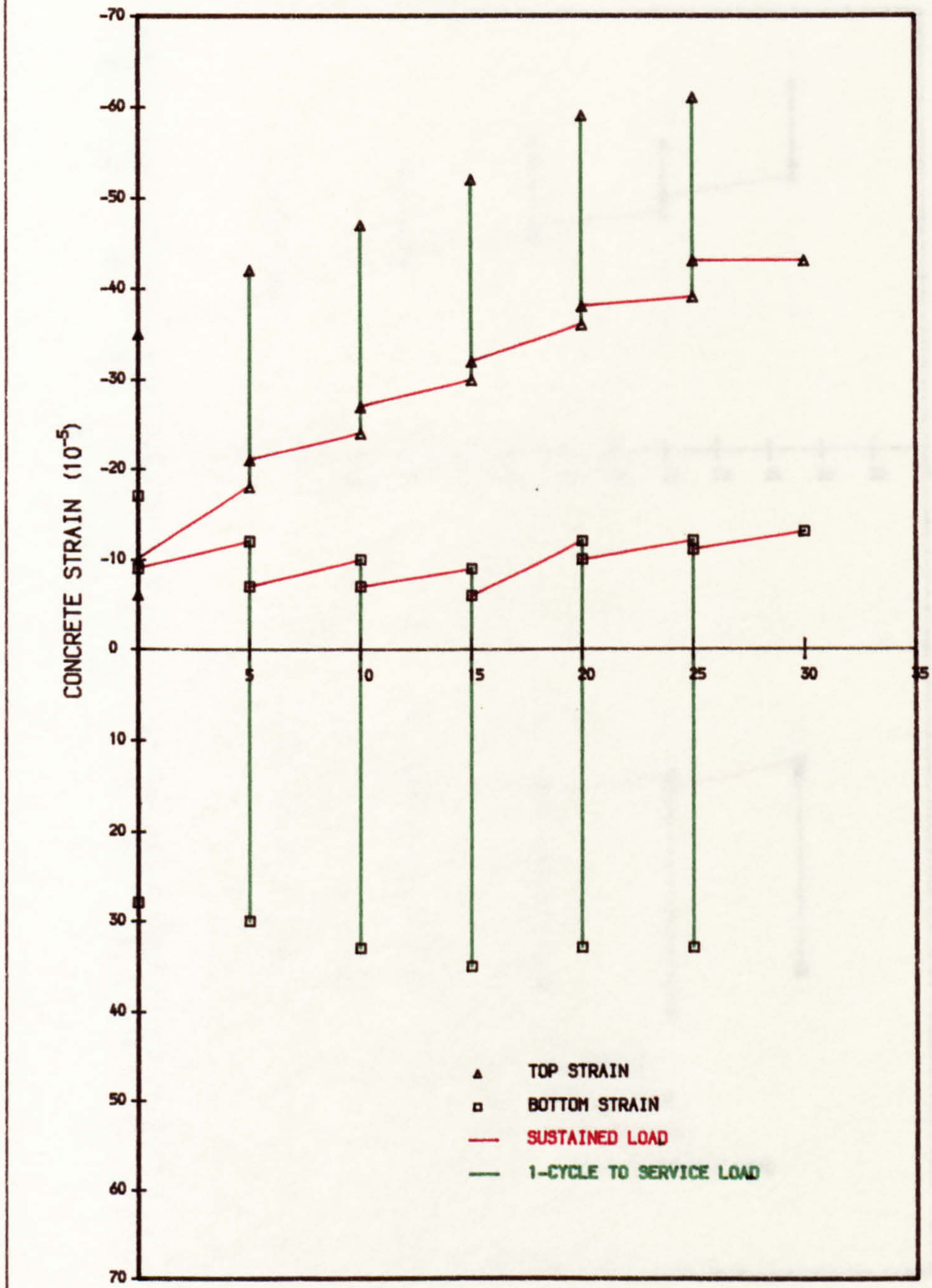

FIG. 6.20b CONCRETE STRAIN-TIME RELATIONSHIP (R1.0.5)

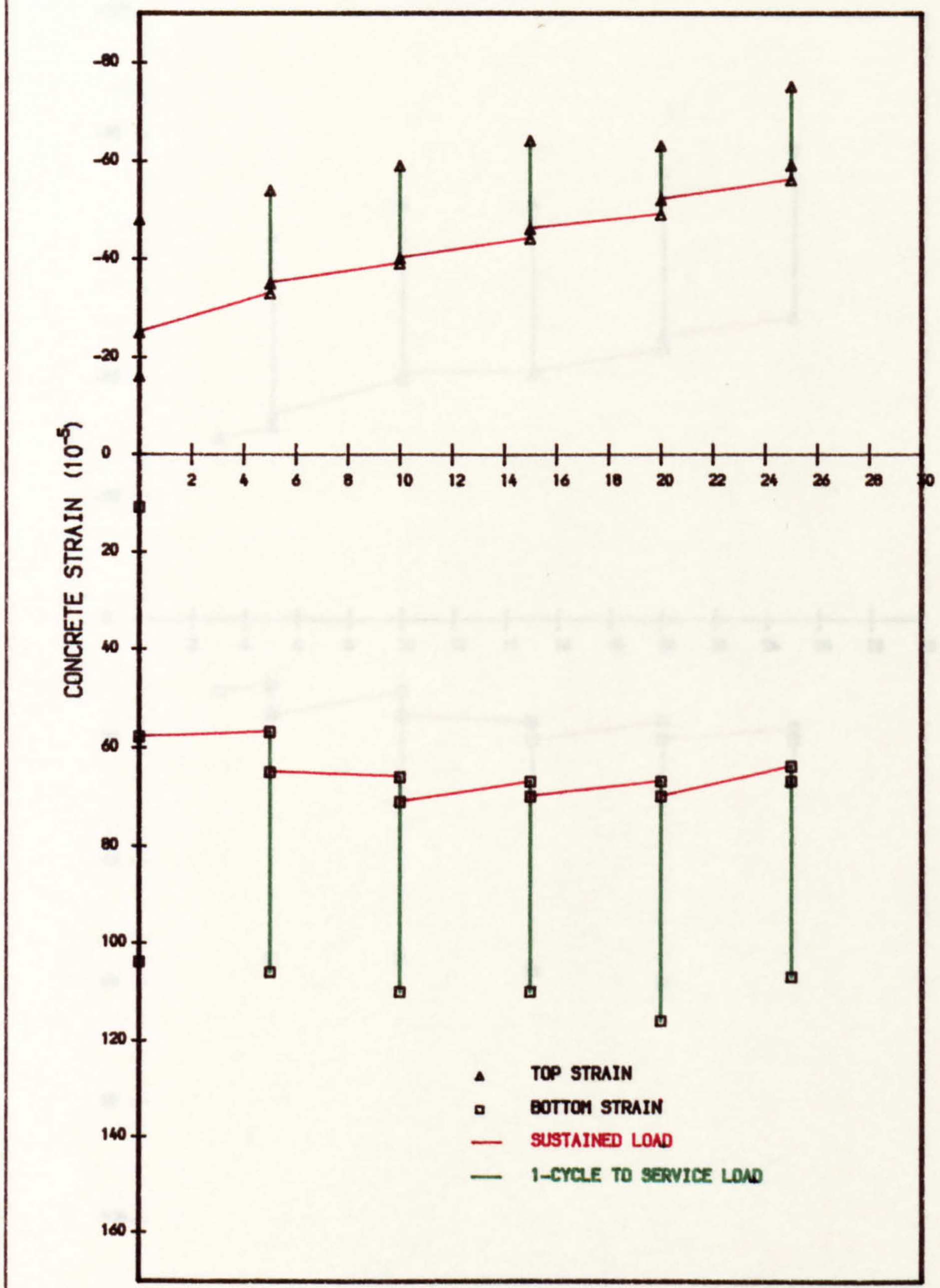

FIG. 6.20c CONCRETE STRAIN-TIME RELATIONSHIP (R2.2.4)

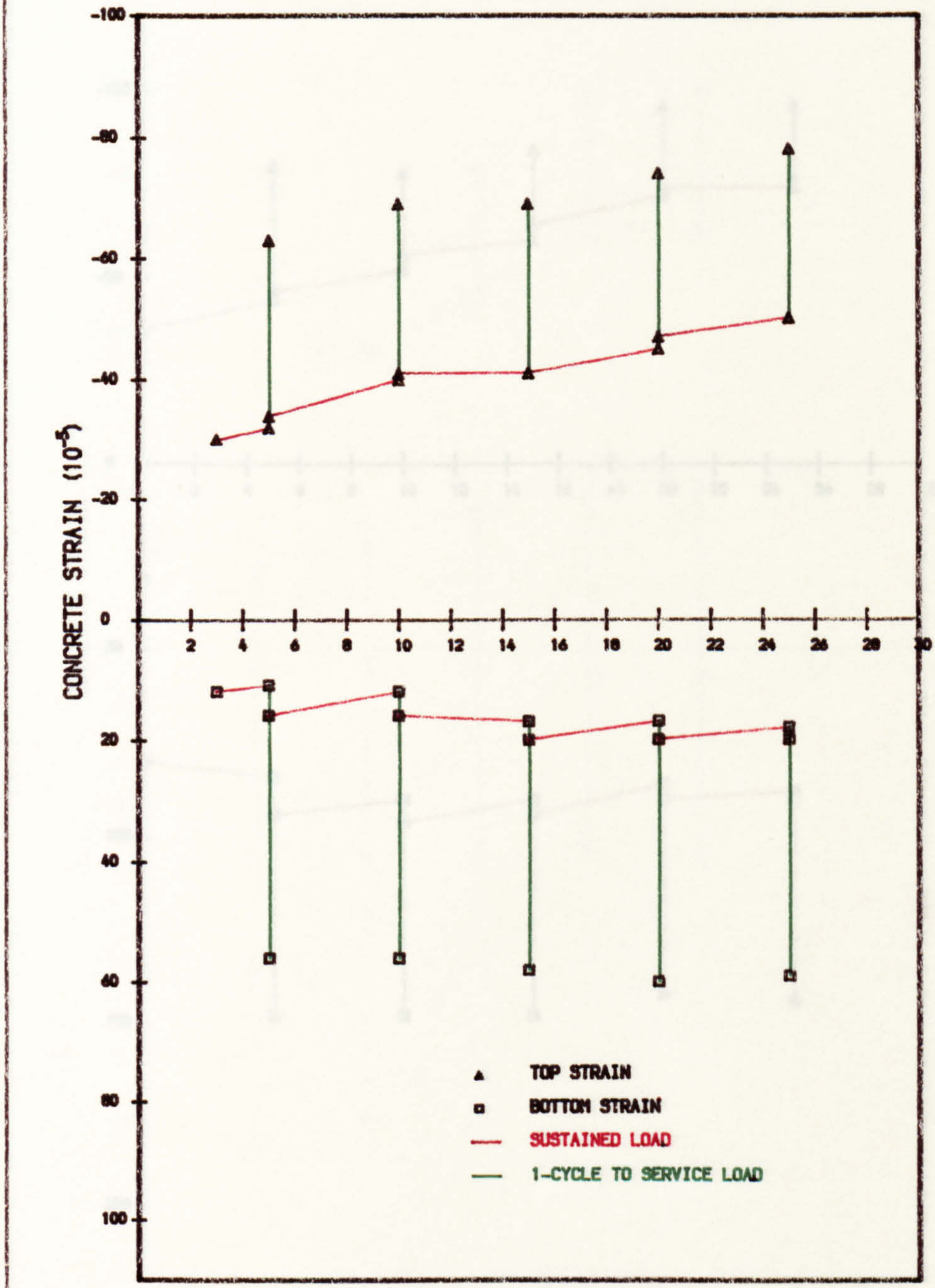

FIG. 6.20d CONCRETE STRAIN-TIME RELATIONSHIP (R2.0.7)

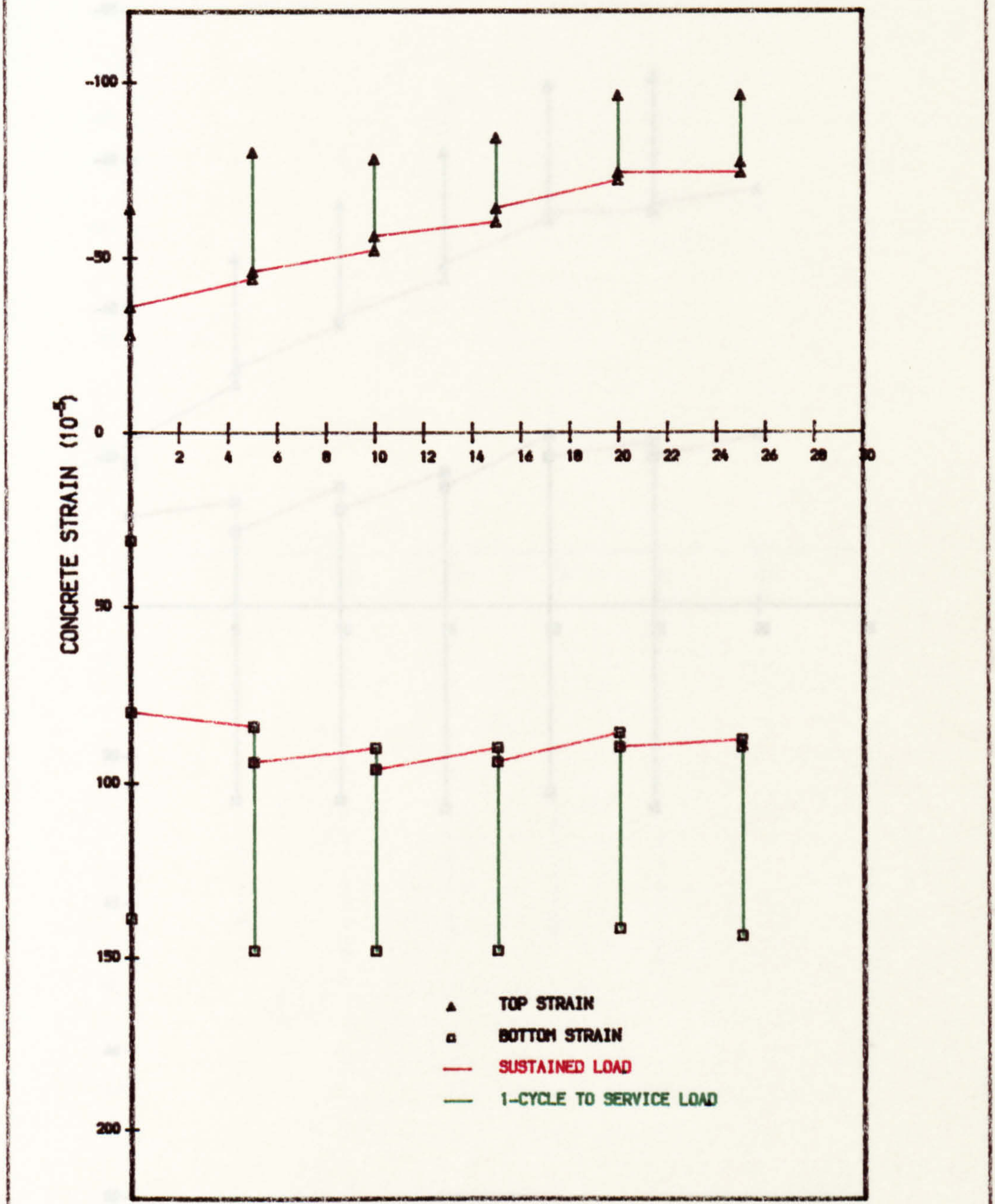

FIG. 6.20e CONCRETE STRAIN-TIME RELATIONSHIP (I1.2.2)

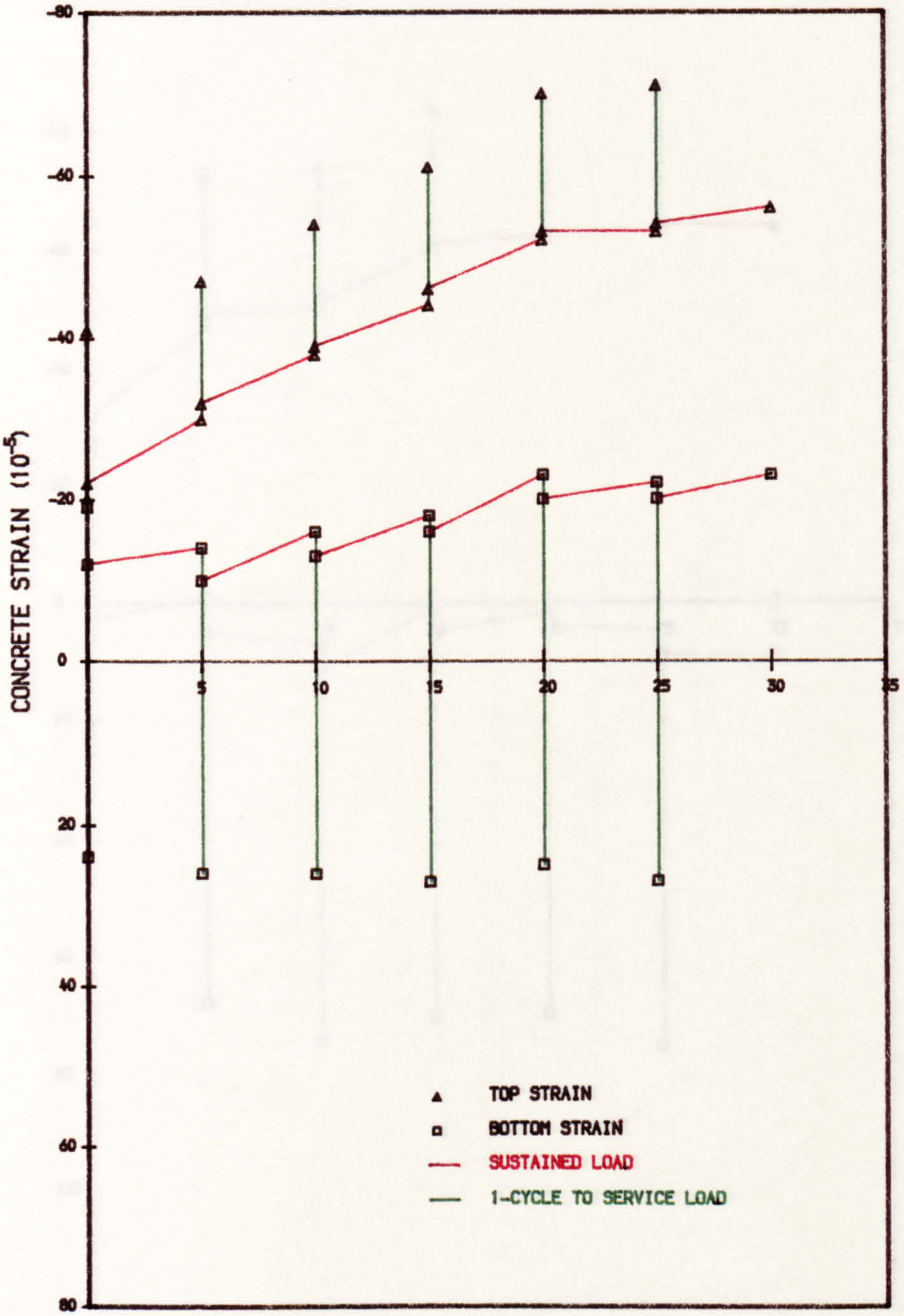

FIG. 6.20f CONCRETE STRAIN-TIME RELATIONSHIP (I2.2.4)

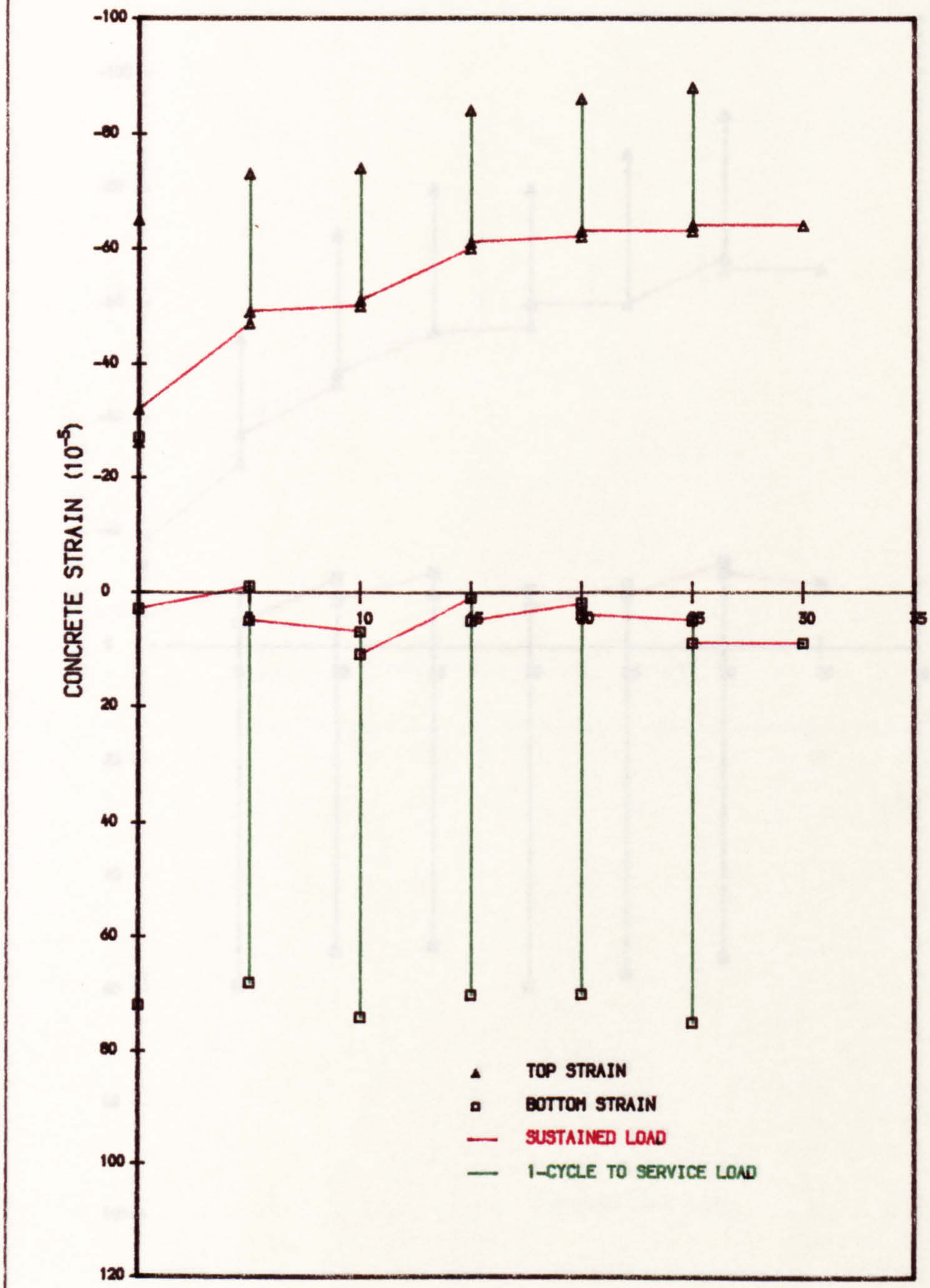

FIG. 6.20h CONCRETE STRAIN-TIME RELATIONSHIP (S1.3.5)
RESULT OBTAINED FROM LEE'S TEST

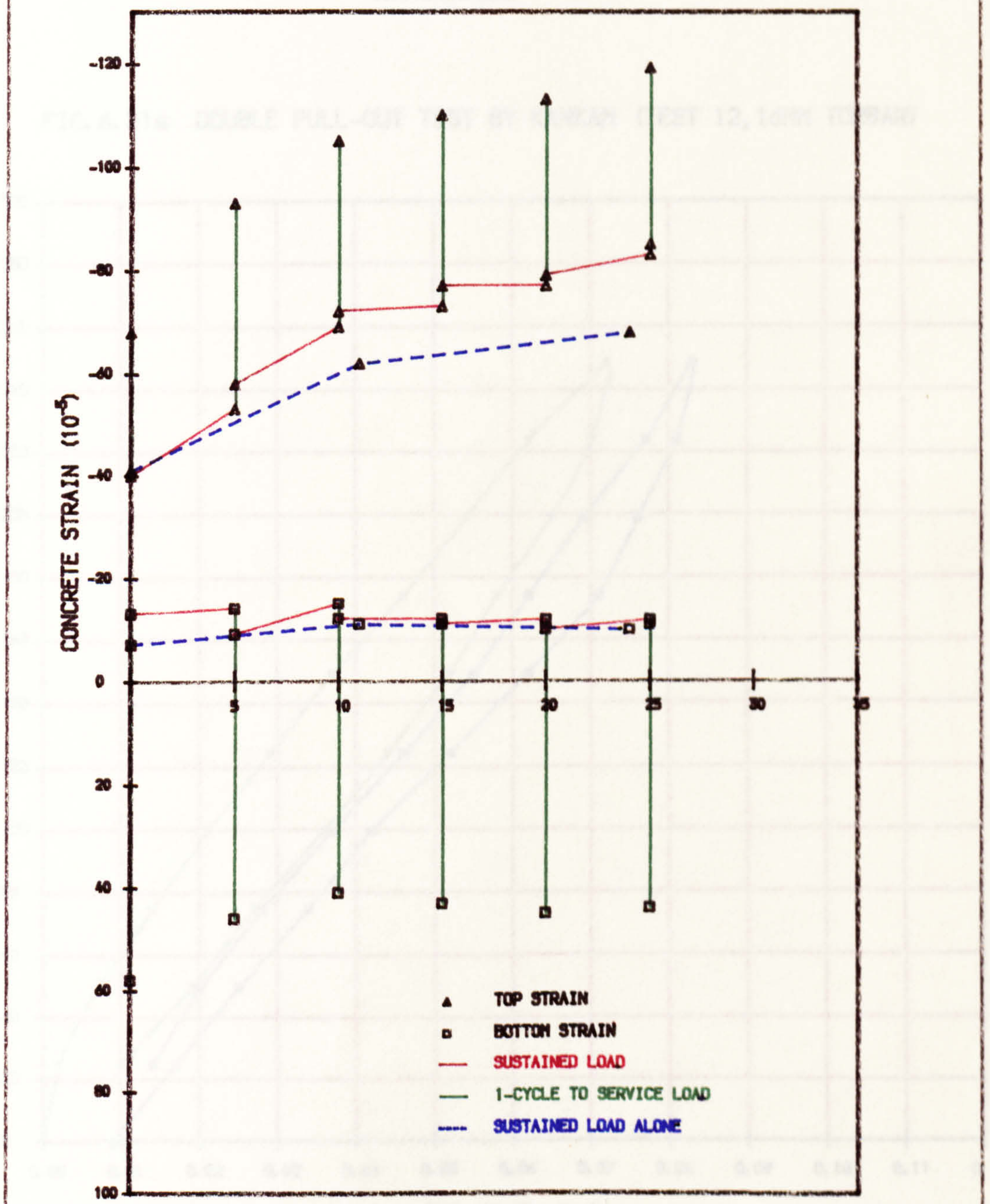

FIG. 6.20g CONCRETE STRAIN-TIME RELATIONSHIP (I3.3.4)

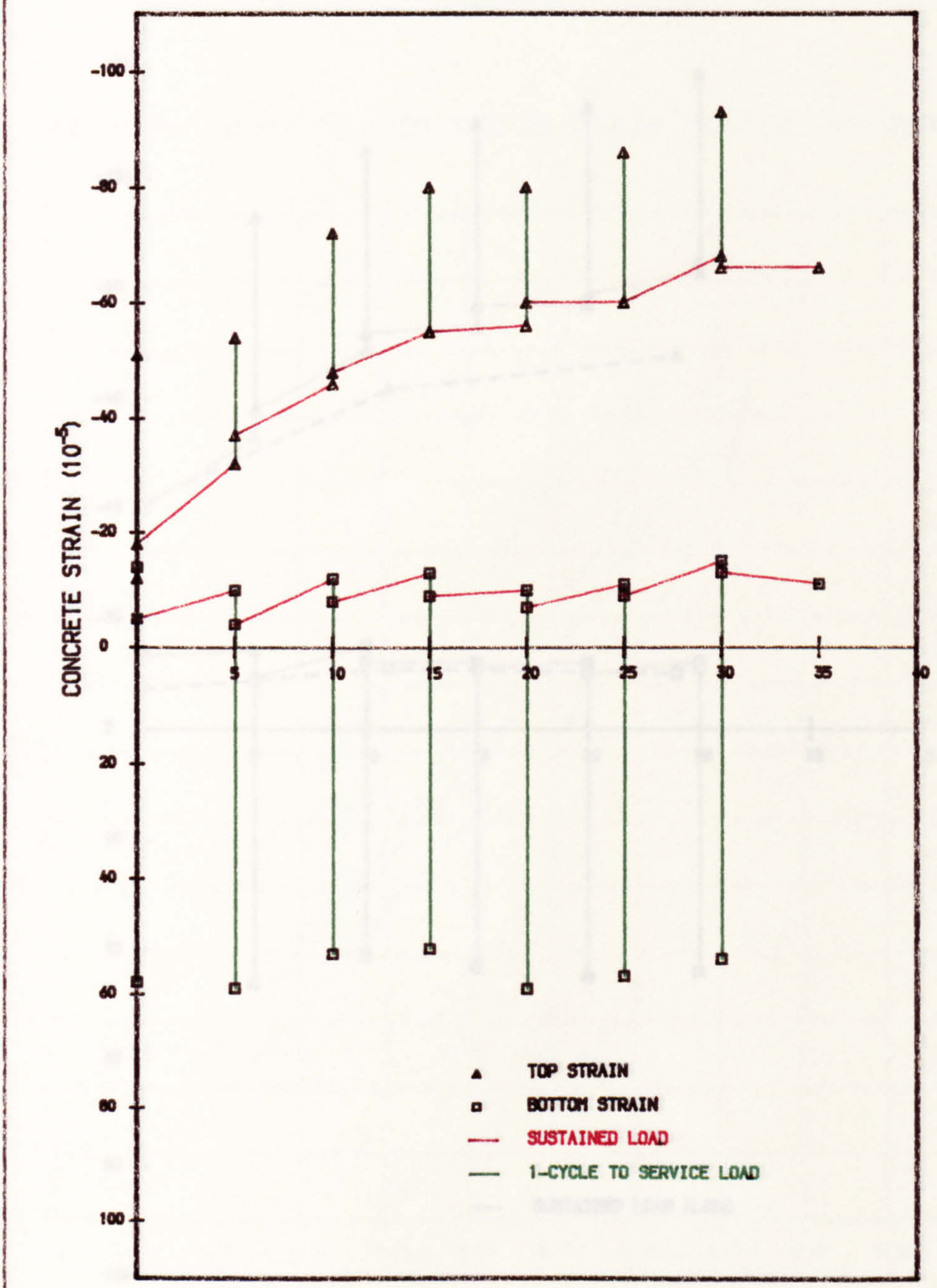

FIG. 6.21a DOUBLE PULL-OUT TEST BY KANKAM (TEST 12, 16MM TORBAR)

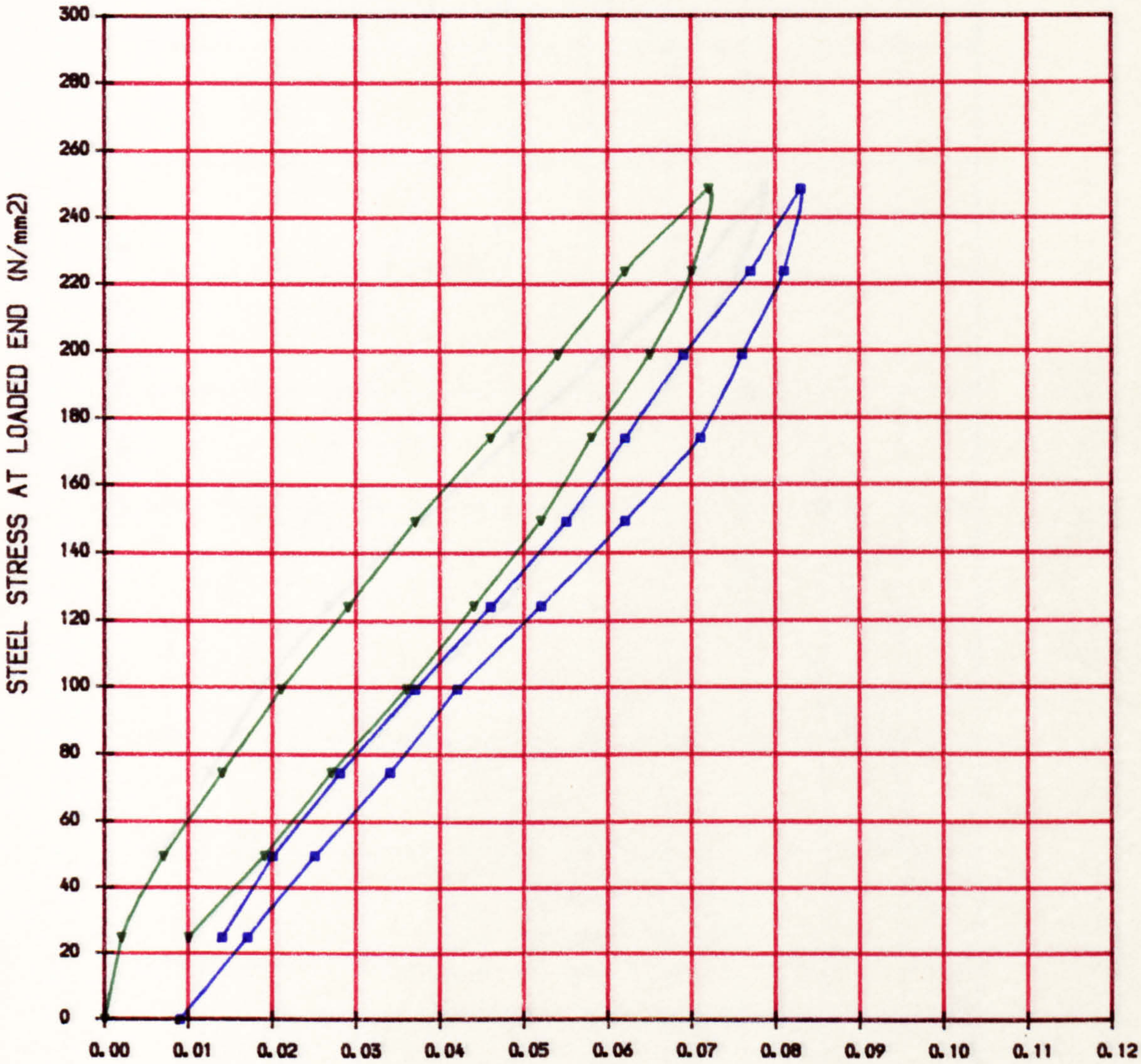

FIG. 6.21b DOUBLE PULL-OUT TEST BY KANKAM (TEST 13, 16MM TORBAR)

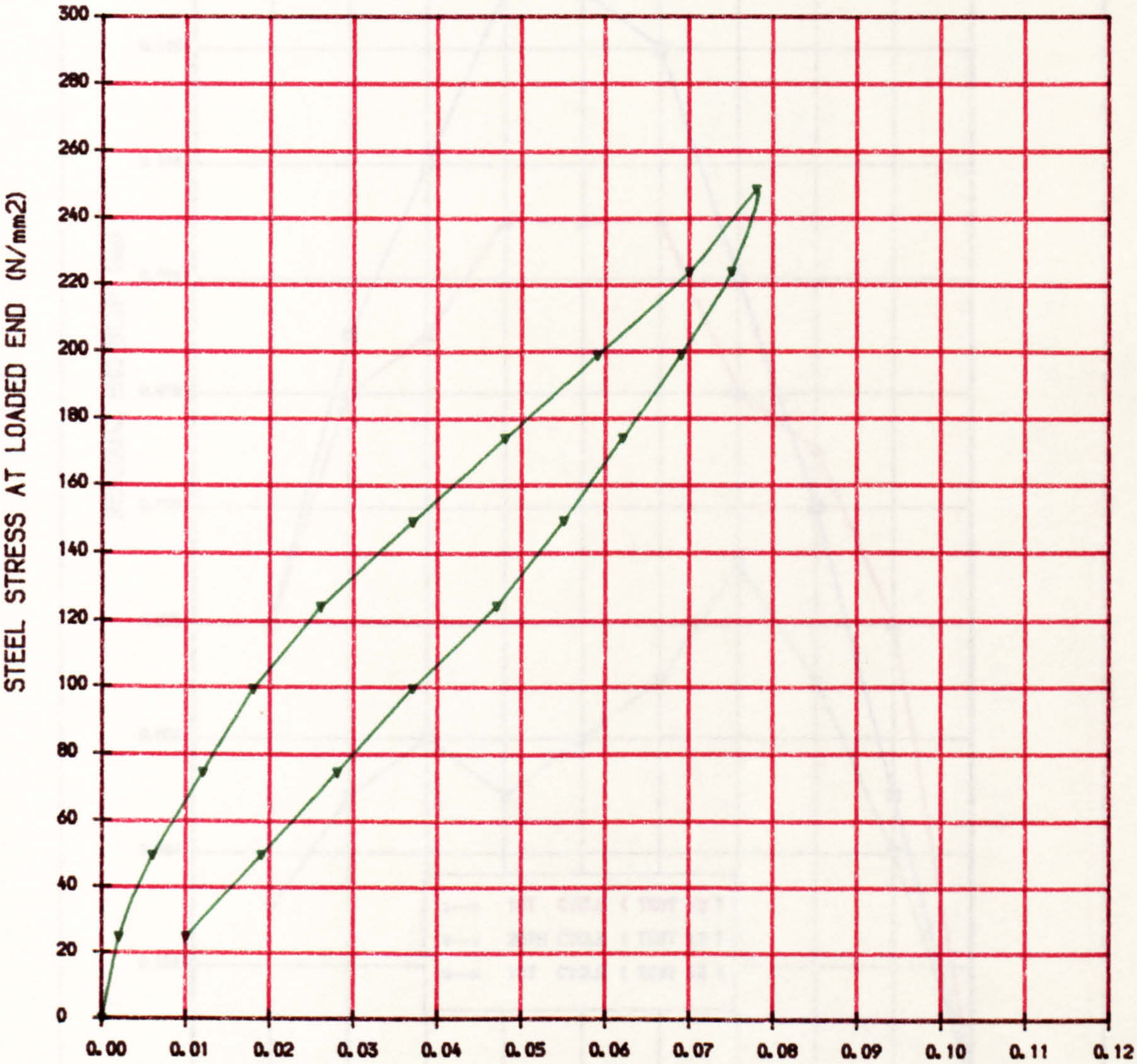

FIG. 6.21c RESIDUAL SLIP DURING DESCENDING LOAD IN DOUBLE PULL-OUT TEST BY KANKAM

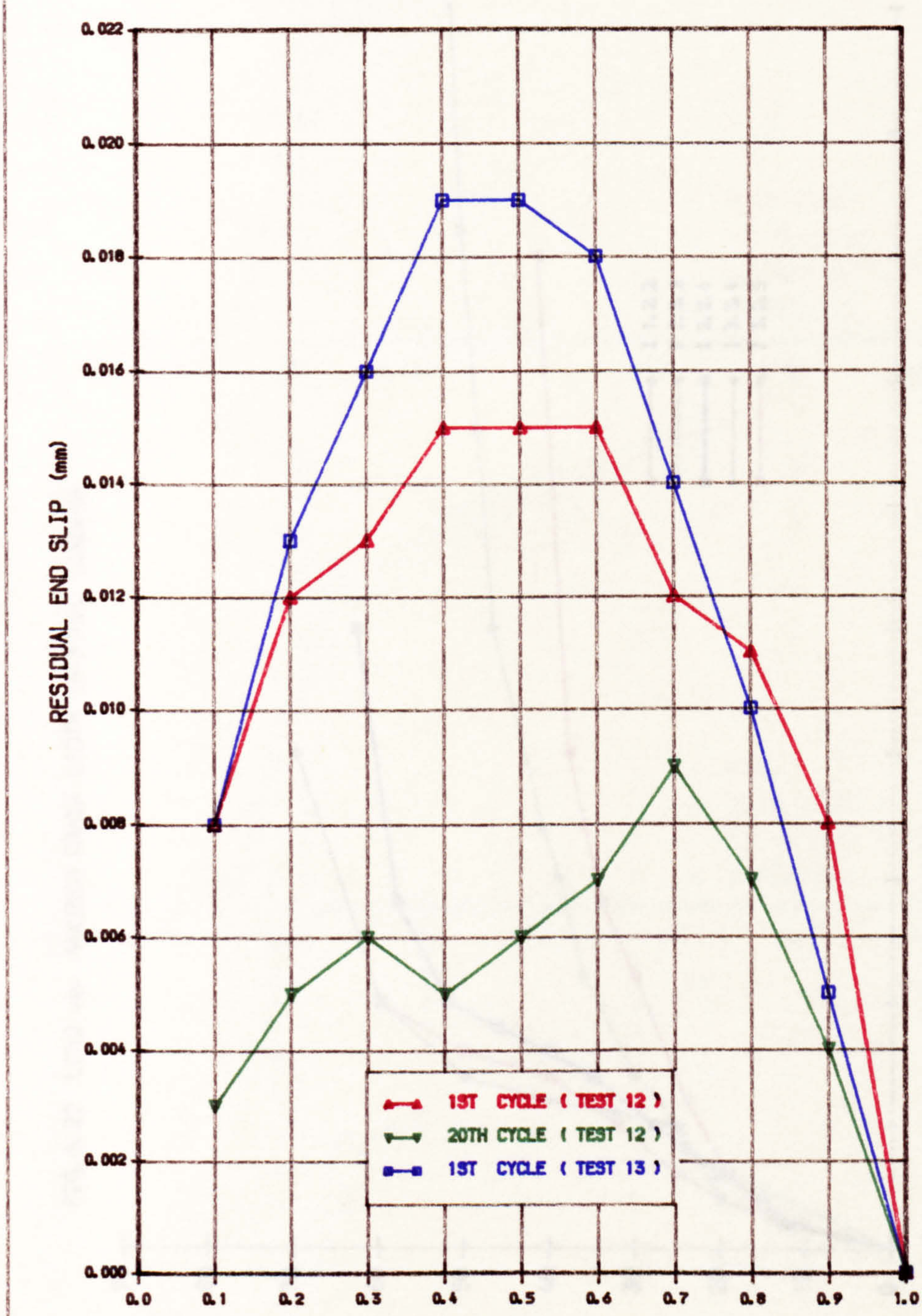

MAX. LOAD AT LOADED END IS EQUIVALENT TO 250 N/mm2

FIG. 6.22 LOAD vs. MAXIMUM CRACK WIDTH IN FINAL LOADING

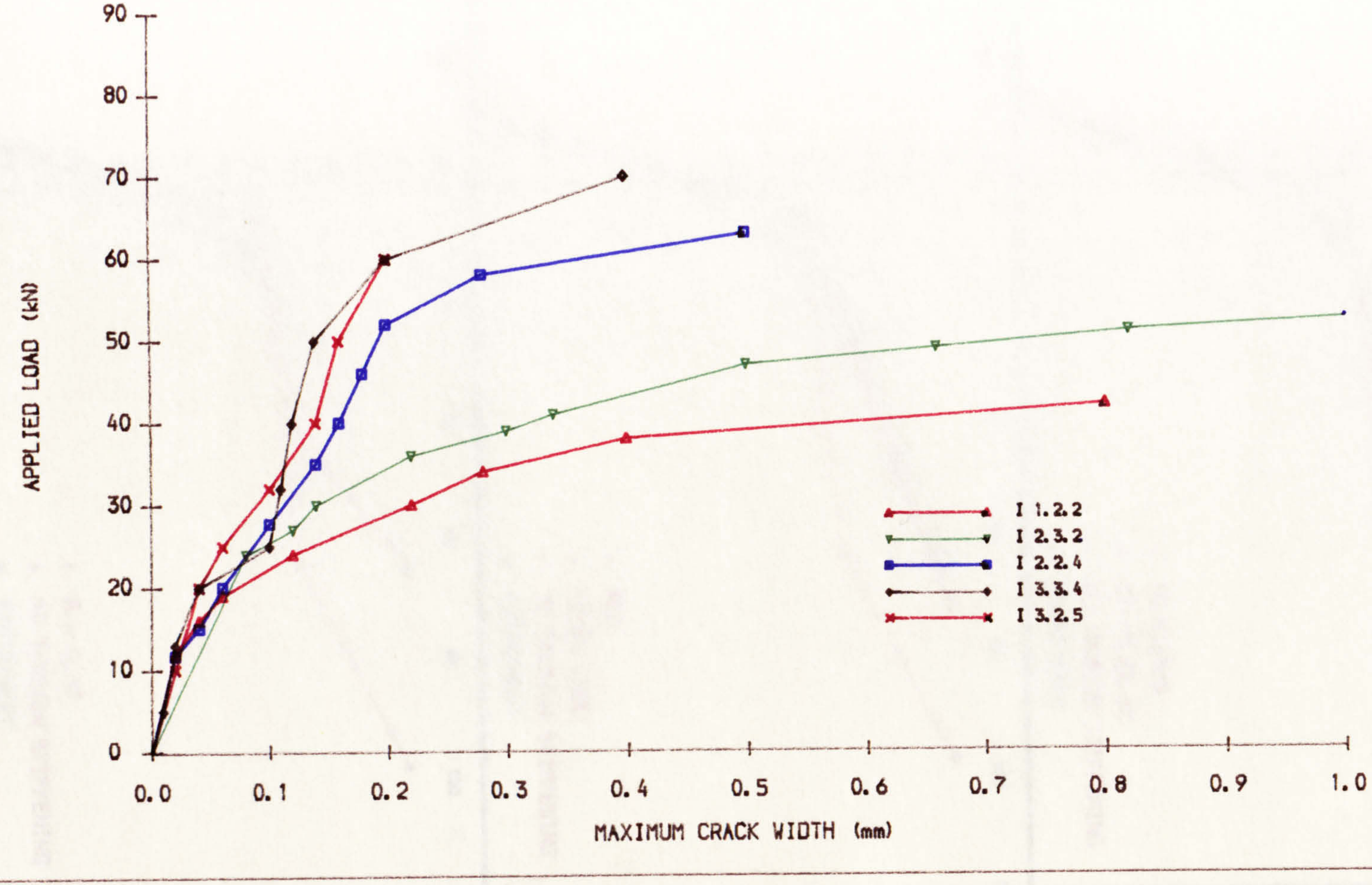

FIG. 6.23a LOAD vs NON-PRESTRESSED STEEL STRAIN IN 1ST LOADING , R2.2.4

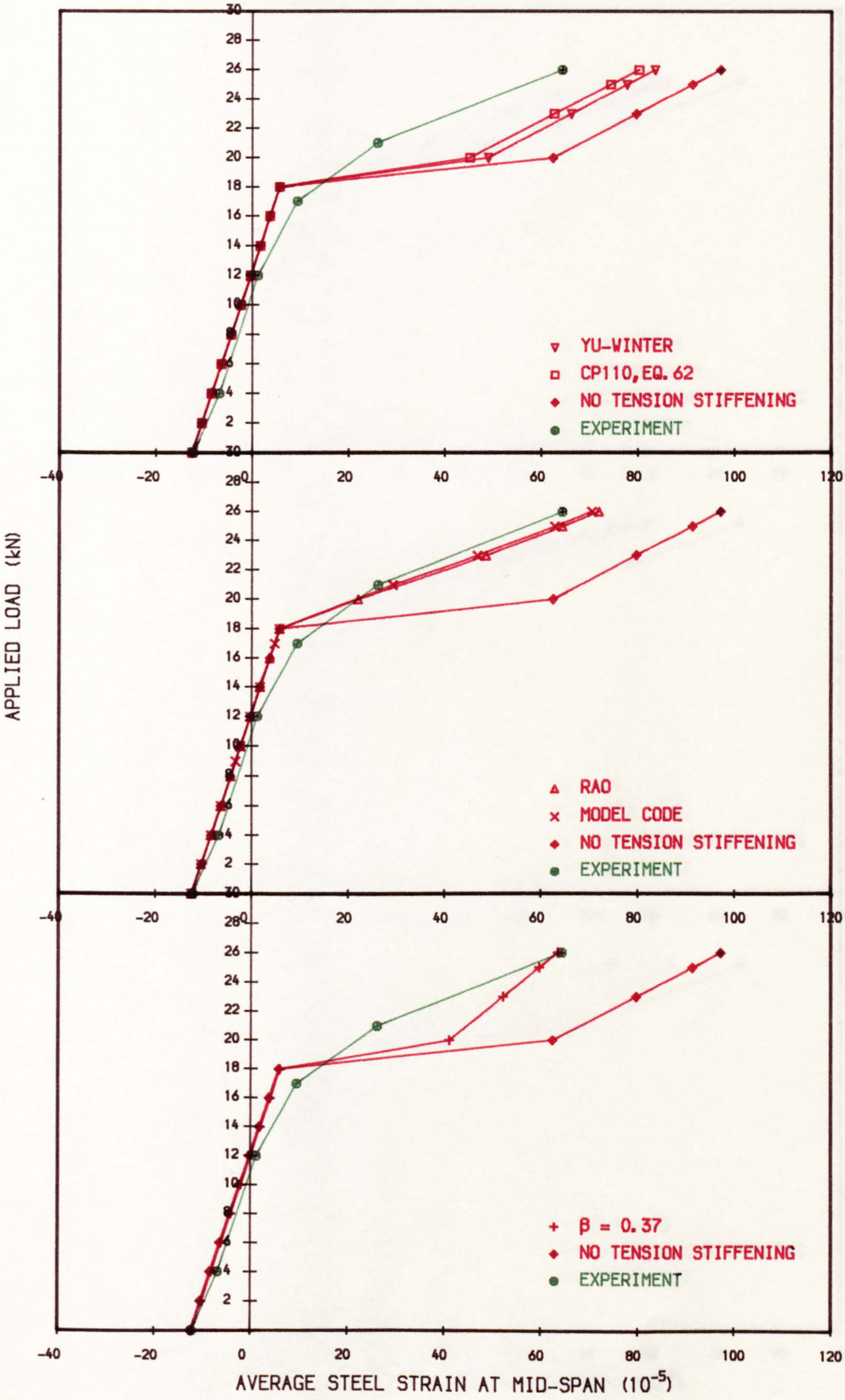

FIG. 6.23b LOAD vs NON-PRESTRESSED STEEL STRAIN IN 1ST LOADING , R3.3.4

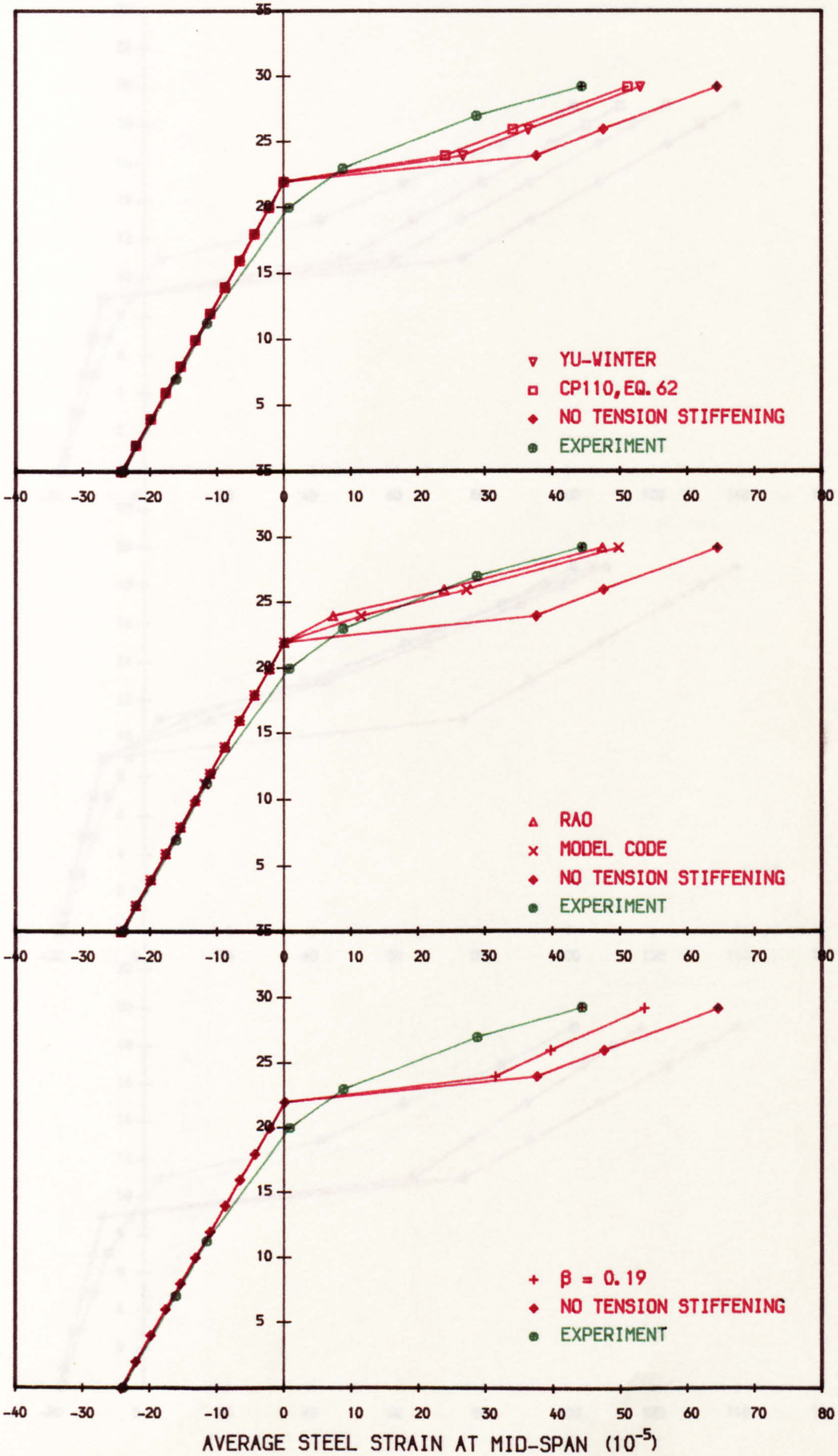

FIG. 6.23c LOAD vs NON-PRESTRESSED STEEL STRAIN IN 1ST LOADING , I1.1.3

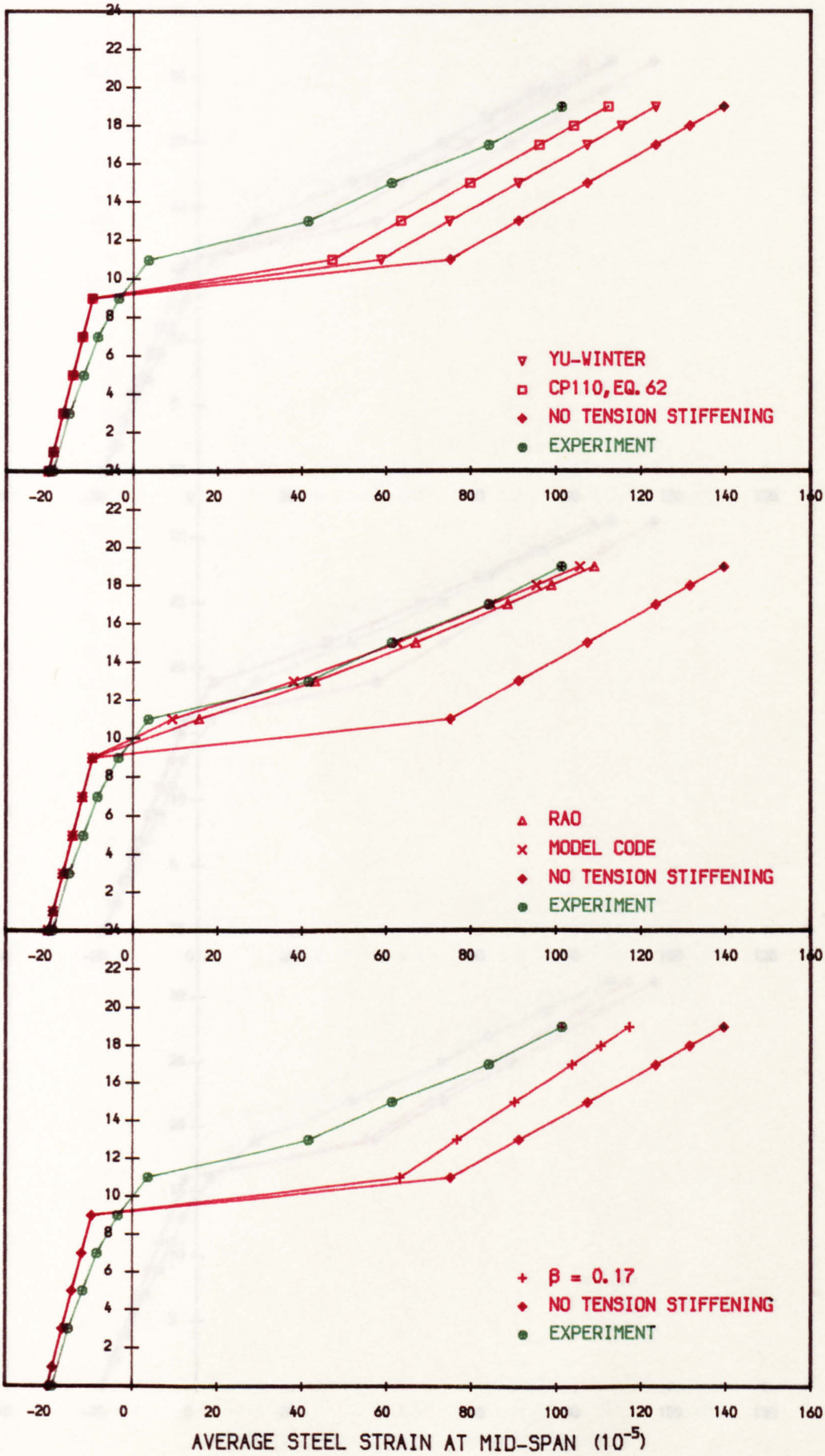

FIG. 6.23d LOAD vs NON-PRESTRESSED STEEL STRAIN IN 1ST LOADING , I3.2.5

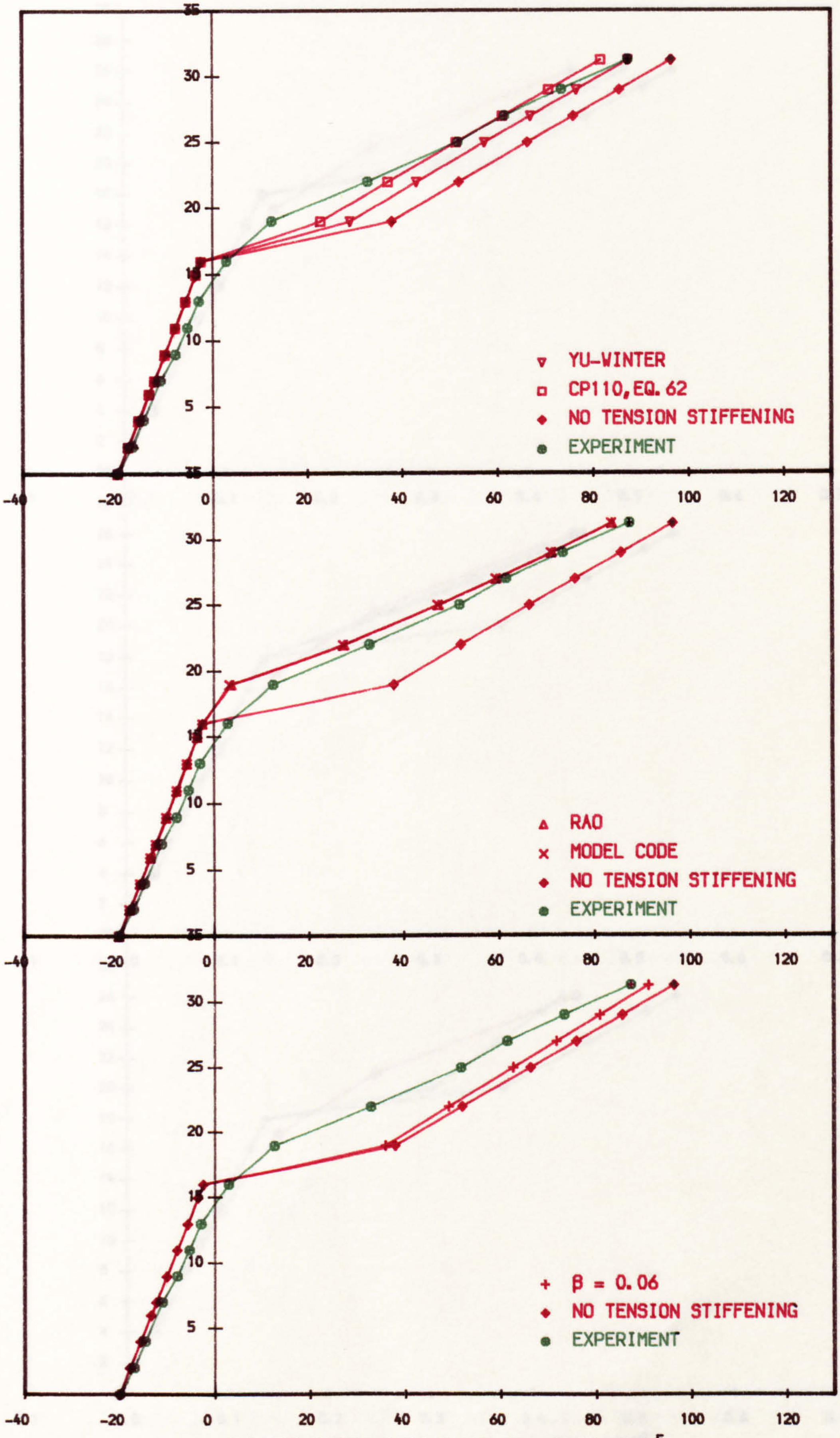

FIG. 6.24a LOAD vs AVERAGE CURVATURE IN 1ST LOADING , R2.2.4

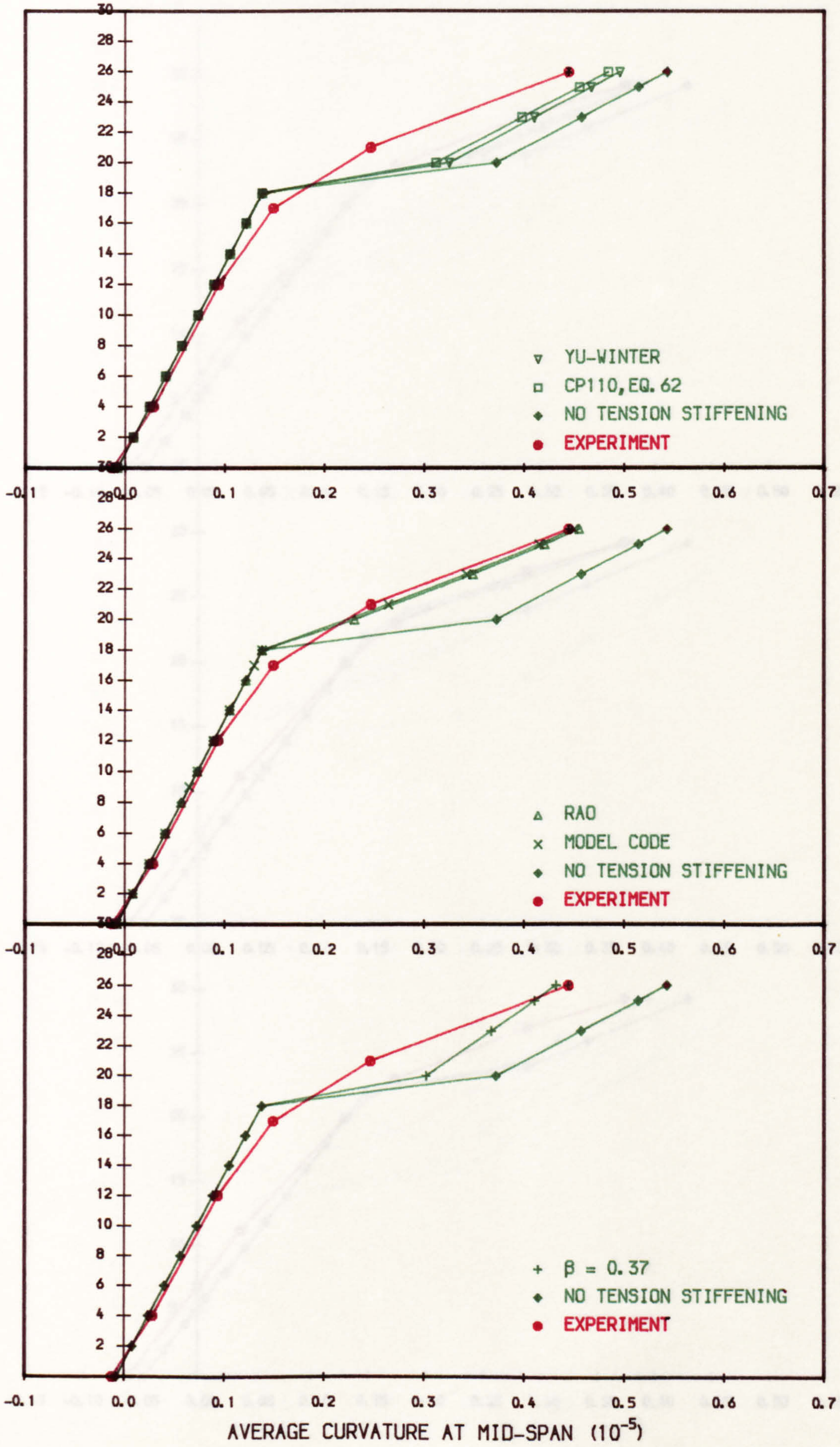

FIG. 6.24b LOAD vs AVERAGE CURVATURE IN 1ST LOADING , R3.3.4

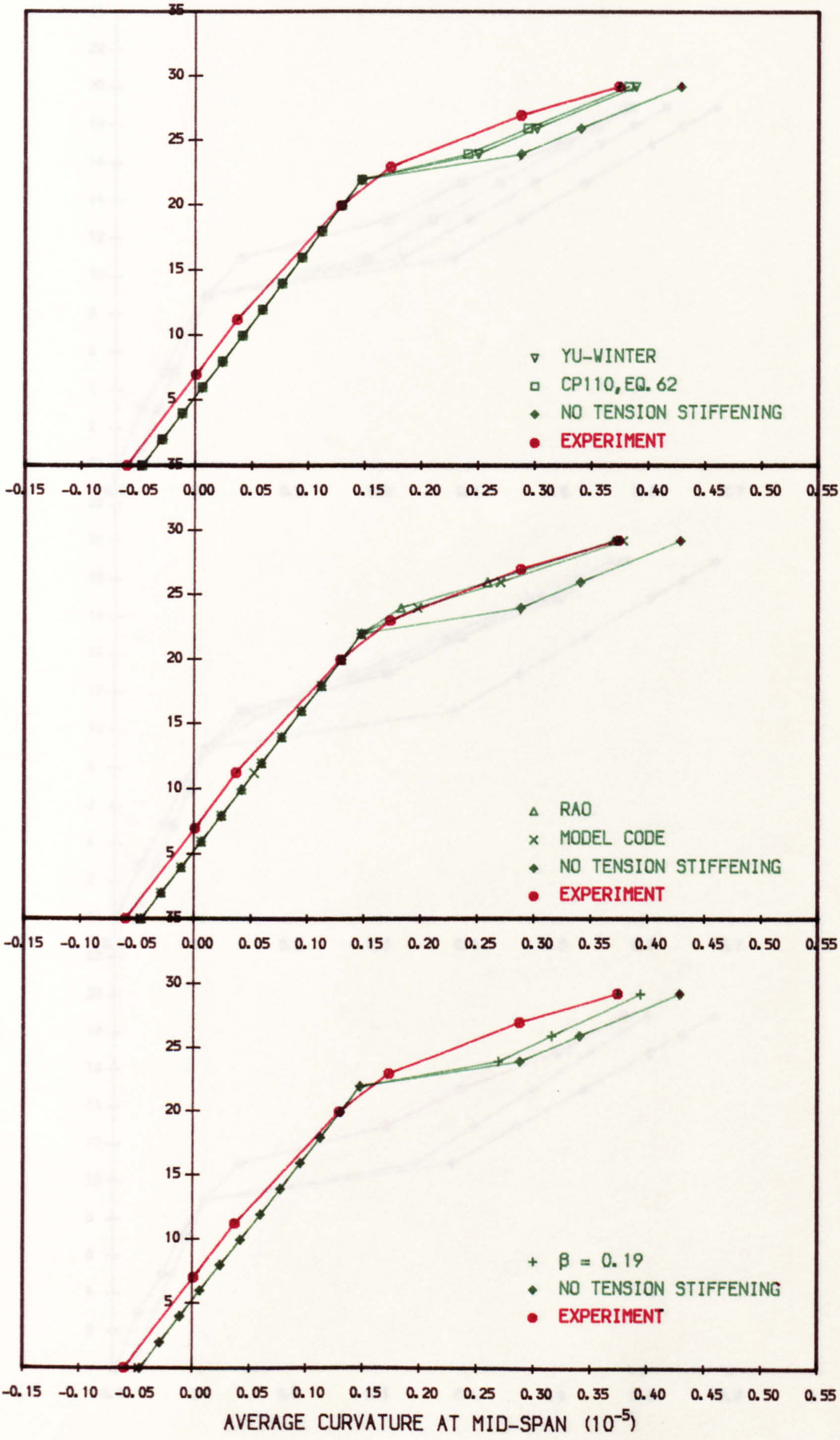

FIG. 6.24c LOAD vs AVERAGE CURVATURE IN 1ST LOADING , I1.1.3

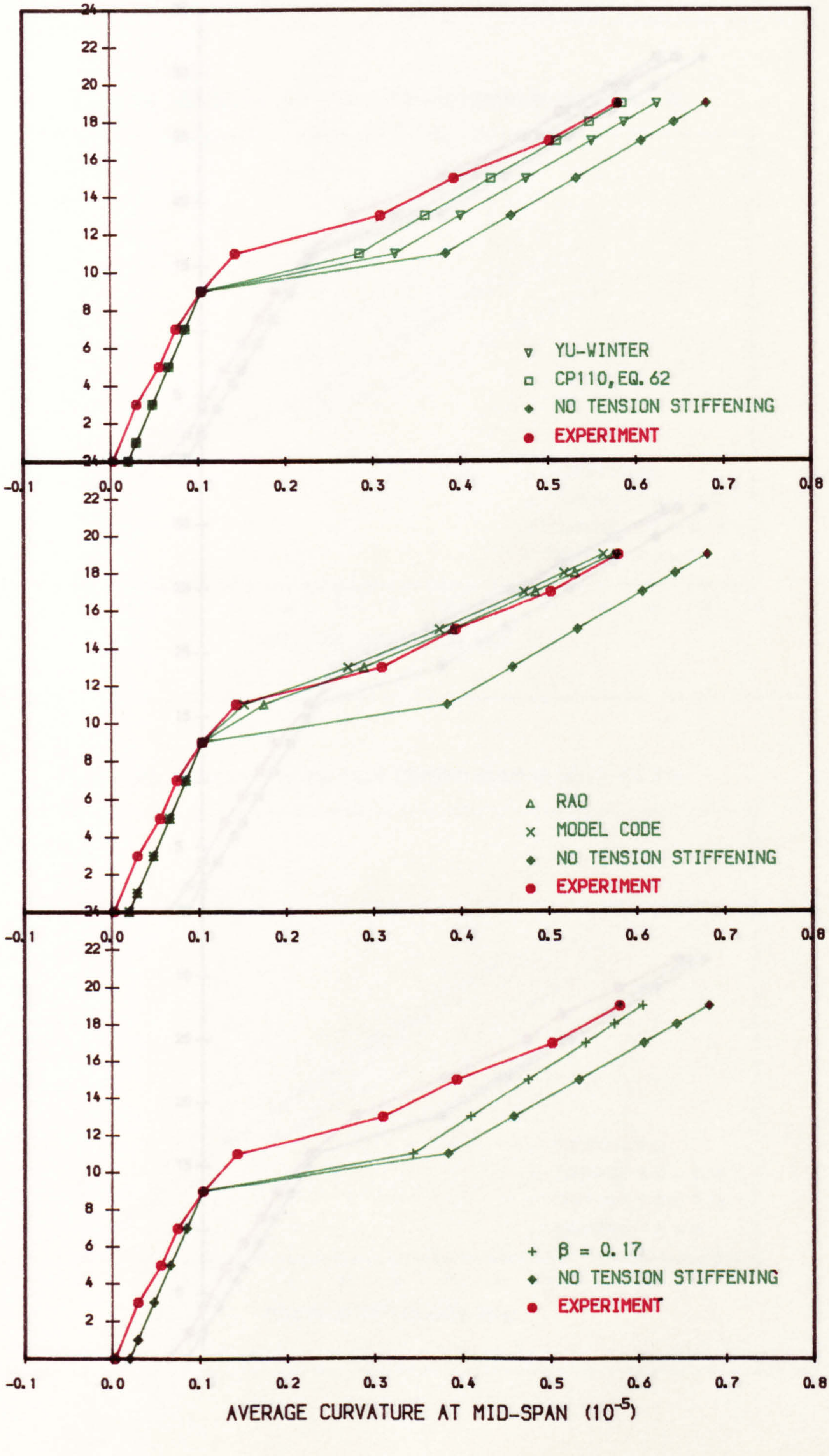

FIG. 6.24d LOAD vs AVERAGE CURVATURE IN 1ST LOADING , I3.2.5

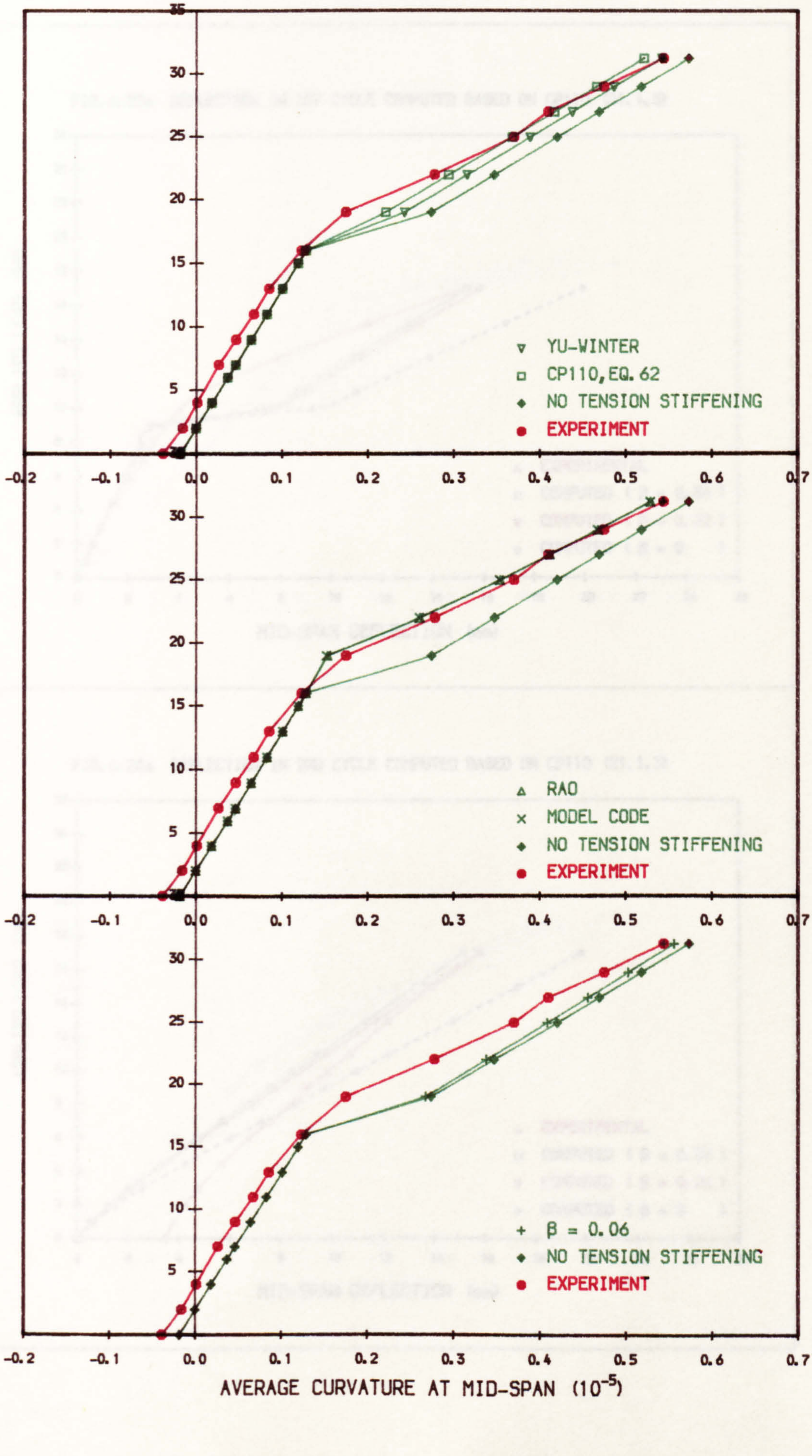

FIG. 6.25a DEFLECTION IN 1ST CYCLE COMPUTED BASED ON CP110 (R1.1.3)

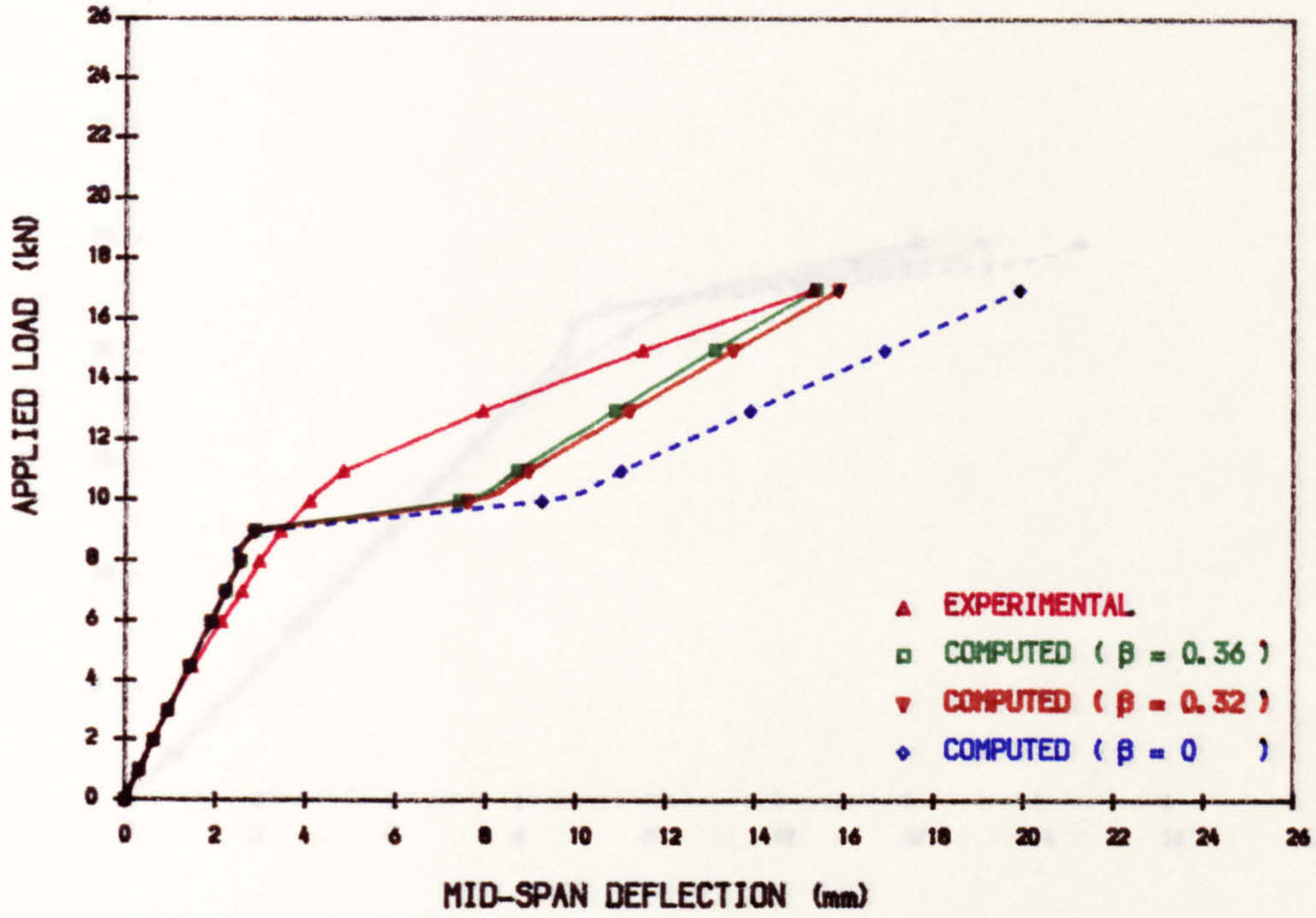

FIG. 6.26a DEFLECTION IN 2ND CYCLE COMPUTED BASED ON CP110 (R1.1.3)

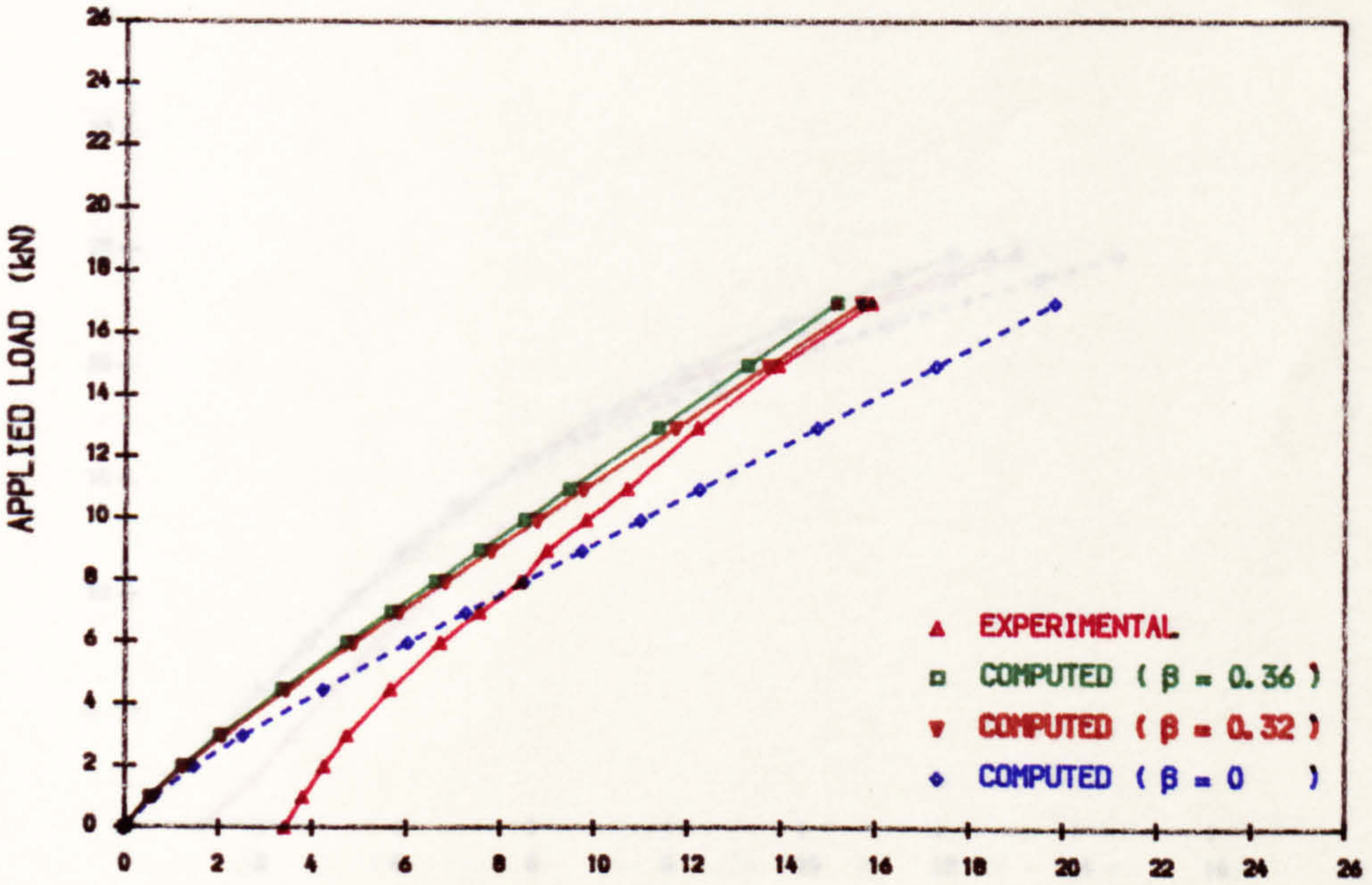

FIG. 6.25b DEFLECTION IN 1ST CYCLE COMPUTED BASED ON CP110 (R2.3.2)

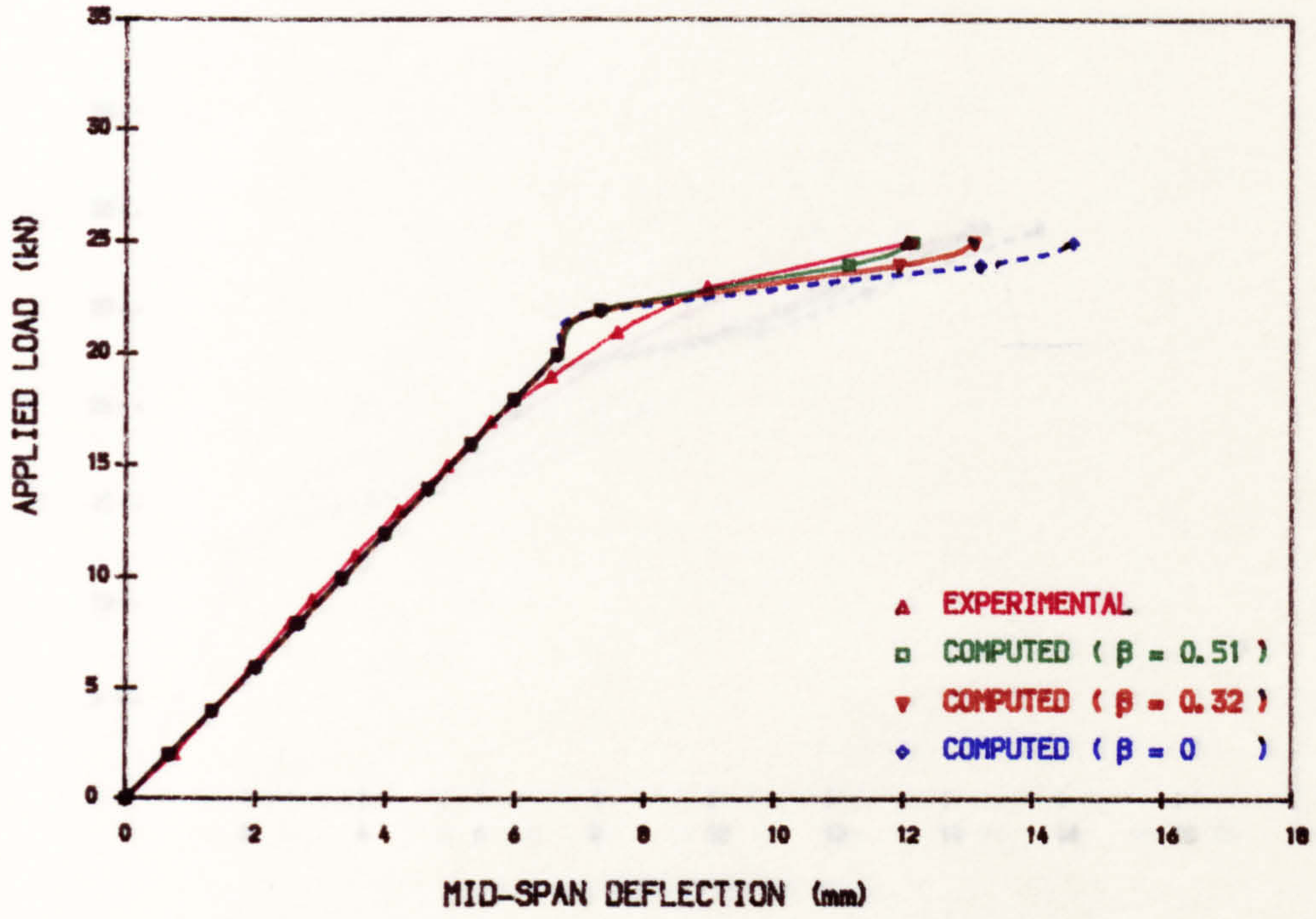

FIG. 6.26b DEFLECTION IN 2ND CYCLE COMPUTED BASED ON CP110 (R2.3.2)

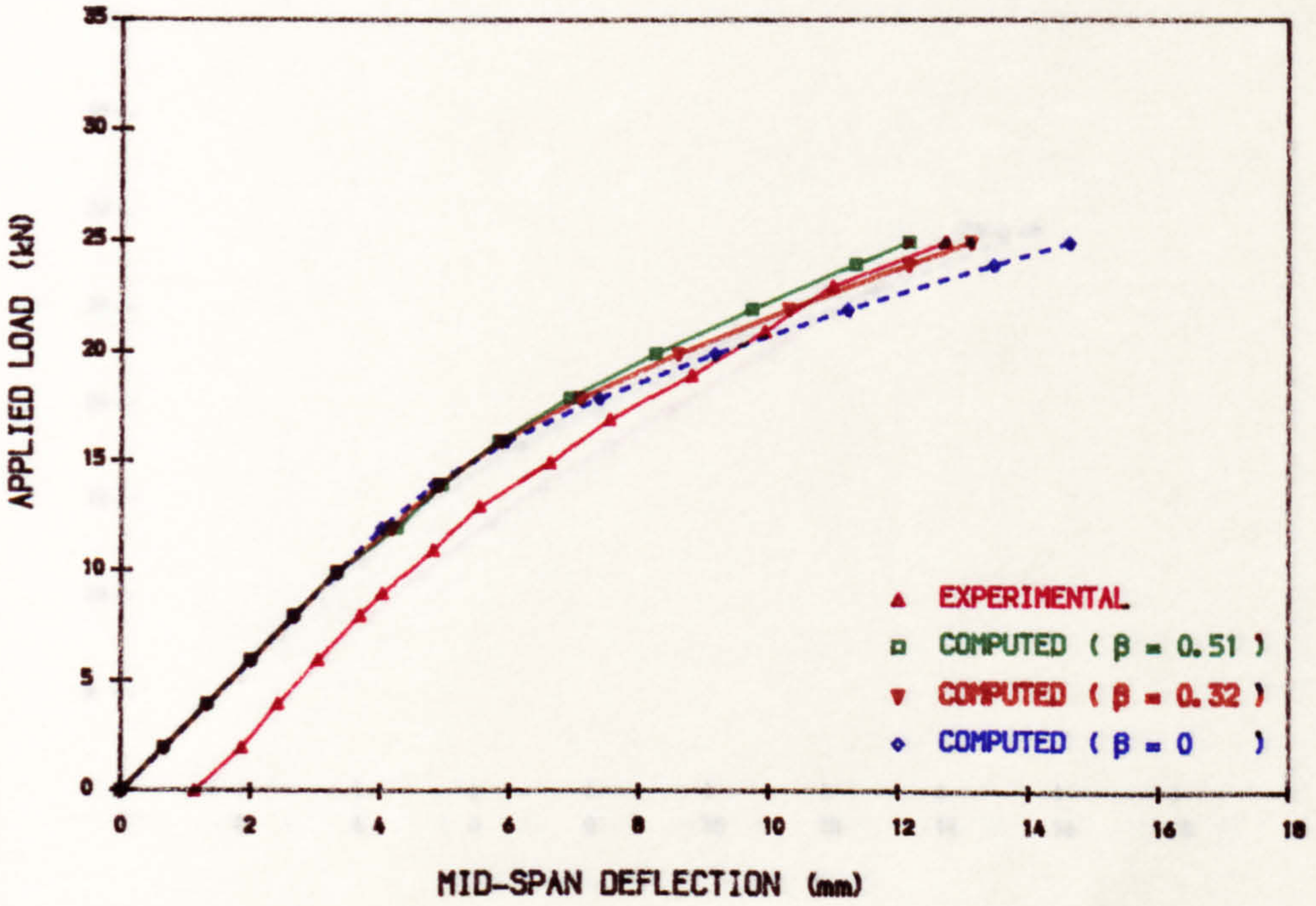

FIG. 6.25c DEFLECTION IN 1ST CYCLE COMPUTED BASED ON CP110 (R3.3.4)

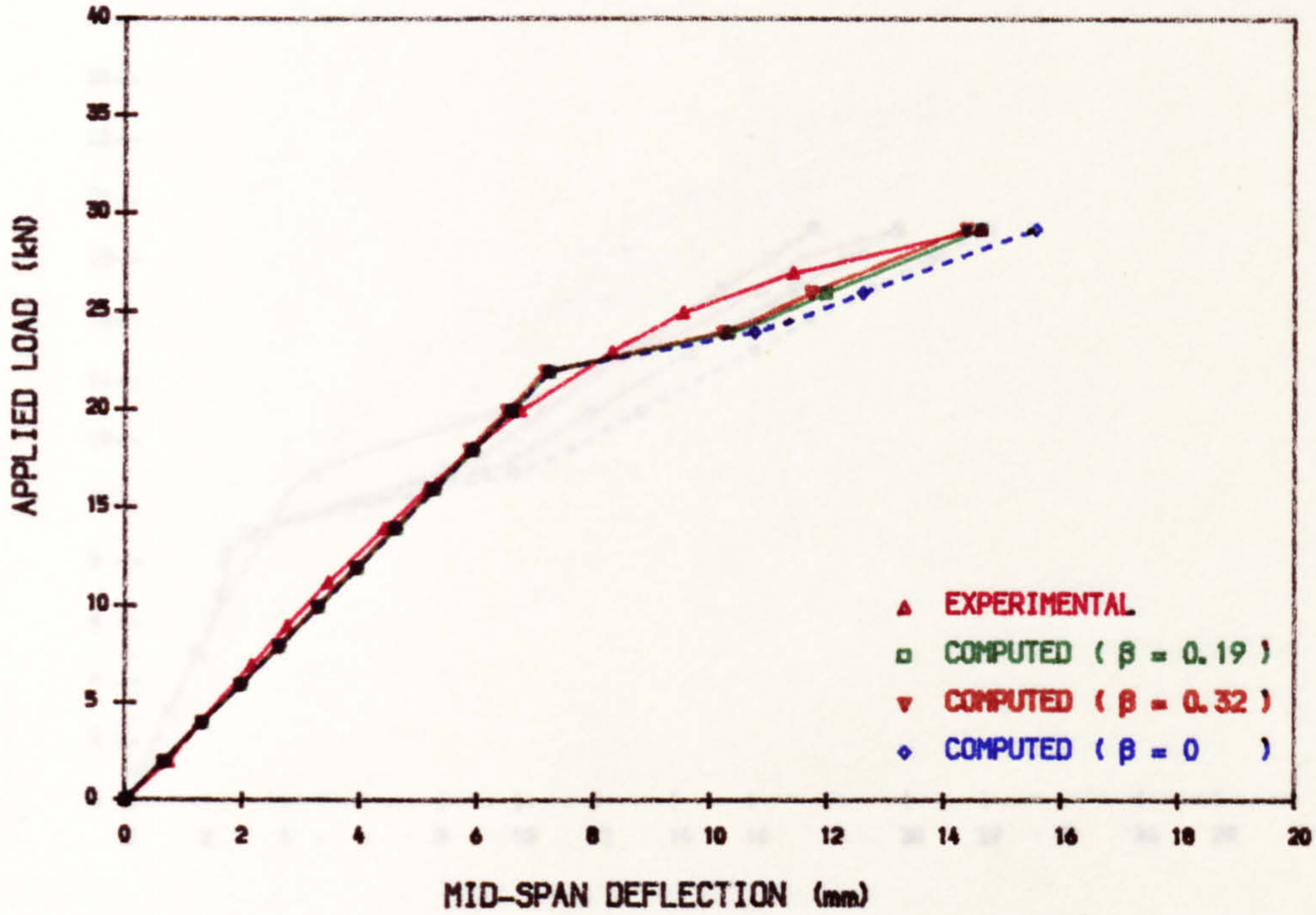

FIG. 6.26c DEFLECTION IN 2ND CYCLE COMPUTED BASED ON CP110 (R3.3.4)

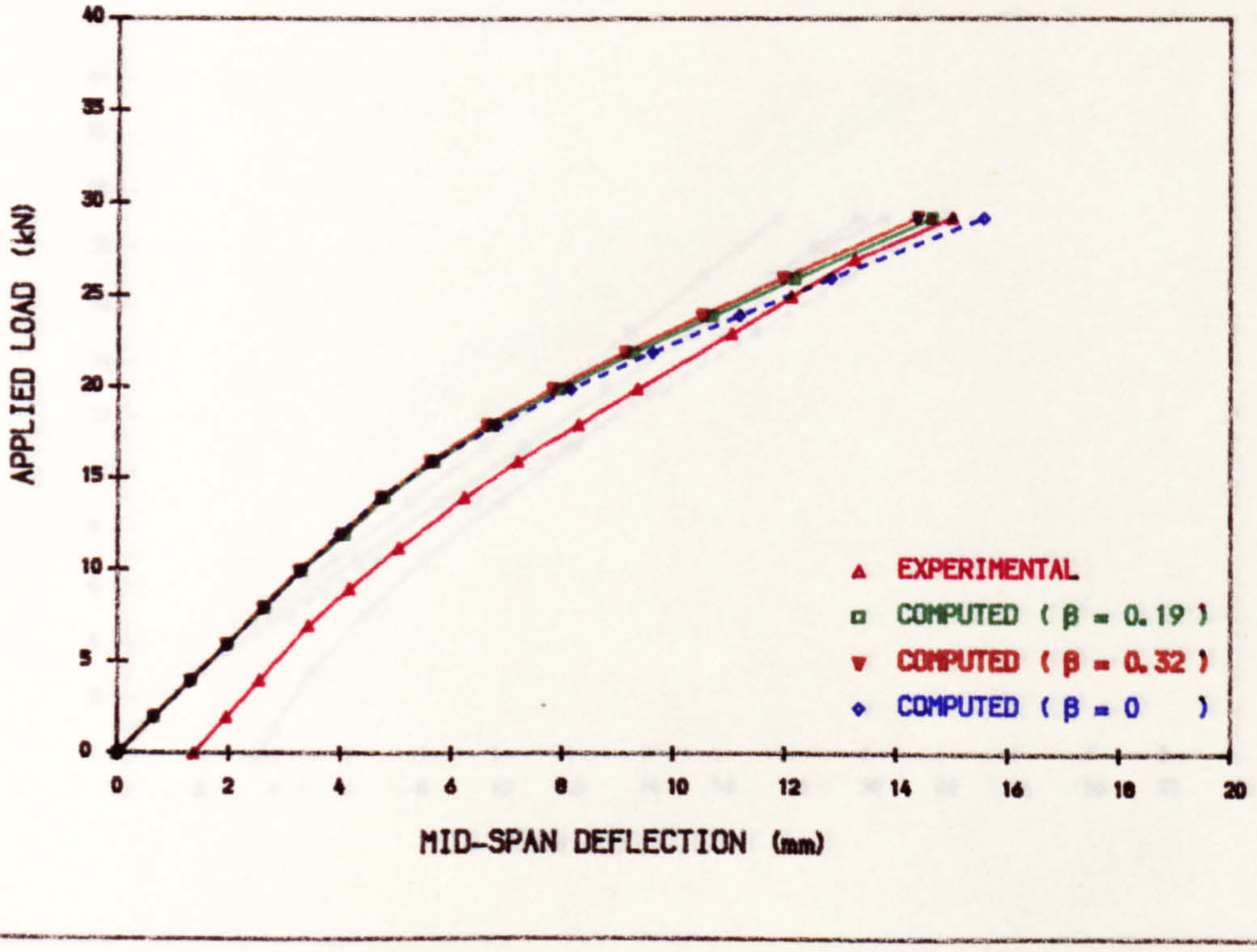

FIG. 6.25d DEFLECTION IN 1ST CYCLE COMPUTED BASED ON CP110 (I1.1.3)

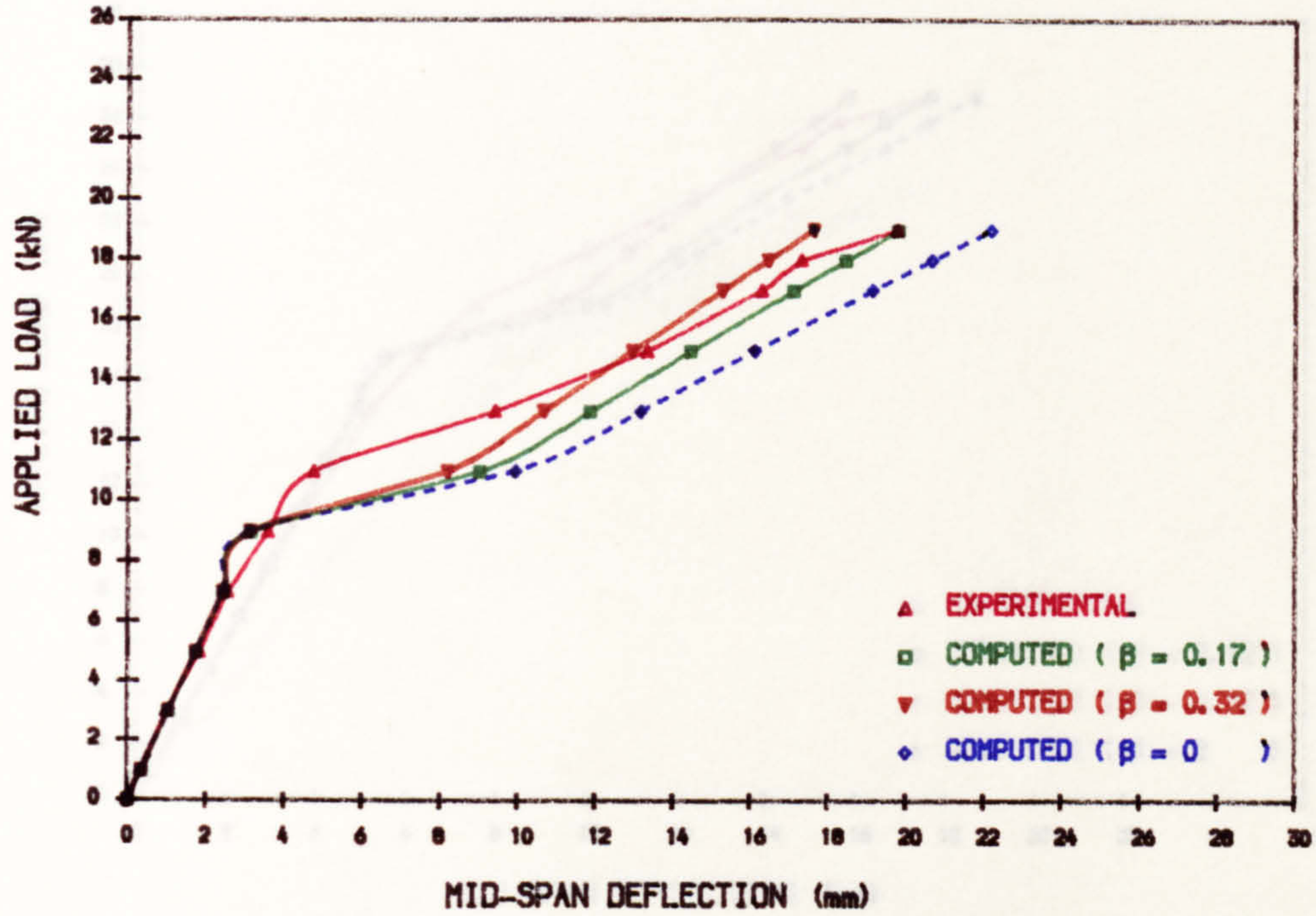

FIG. 6.26d DEFLECTION IN 2ND CYCLE COMPUTED BASED ON CP110 (I1.1.3)

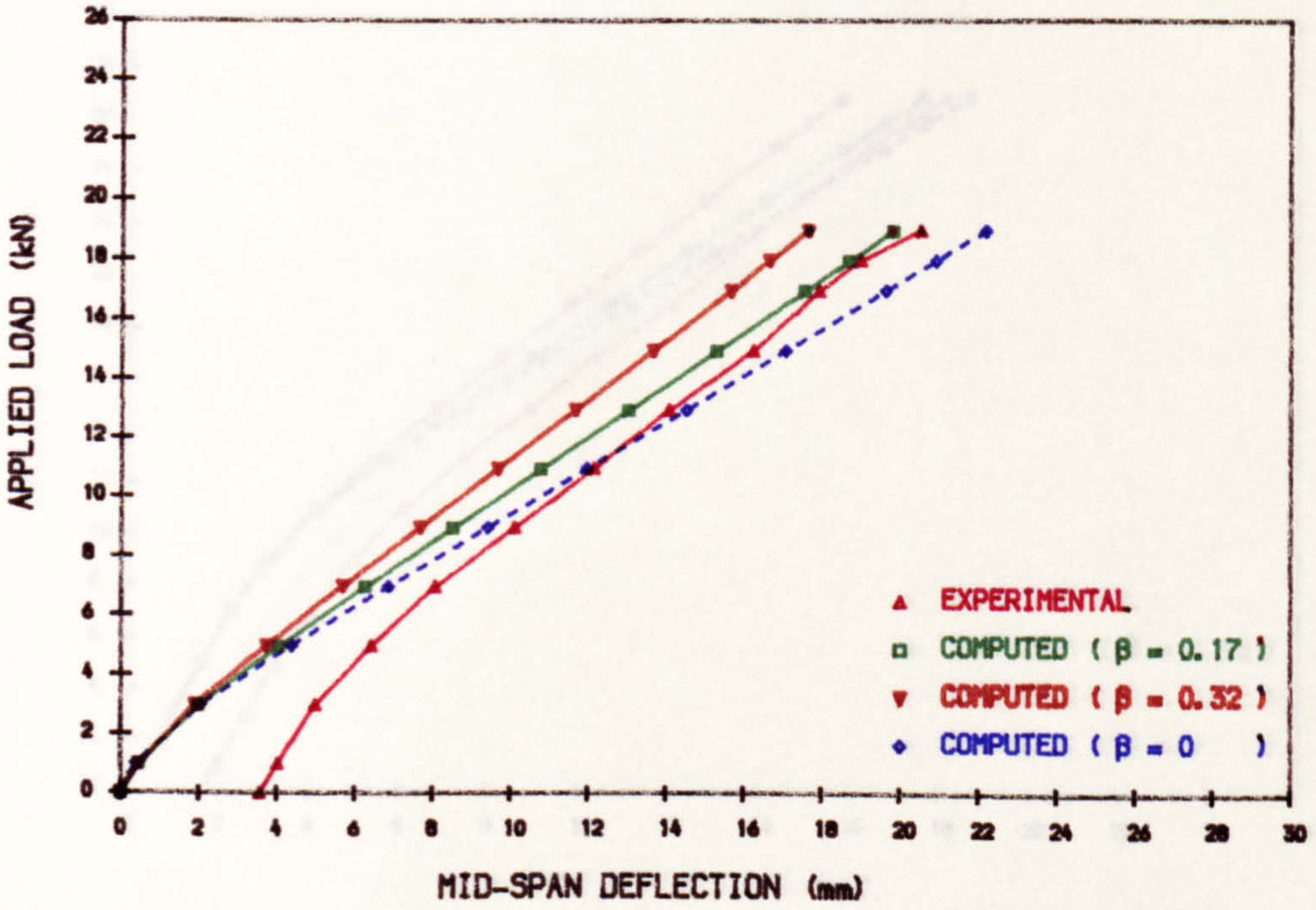

FIG. 6.25e DEFLECTION IN 1ST CYCLE COMPUTED BASED ON CP110 (I2.2.4)

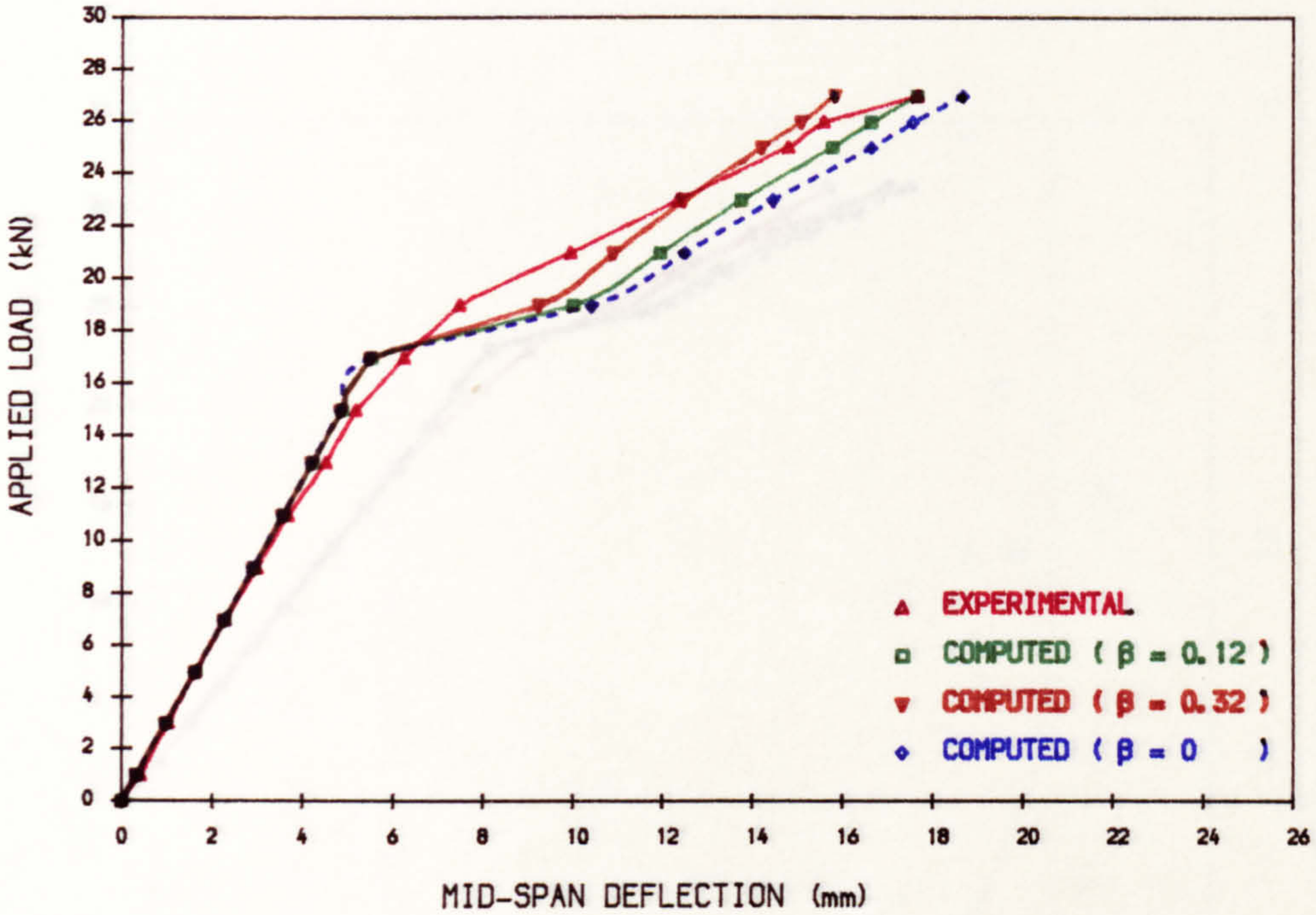

FIG. 6.26e DEFLECTION IN 2ND CYCLE COMPUTED BASED ON CP110 (I2.2.4)

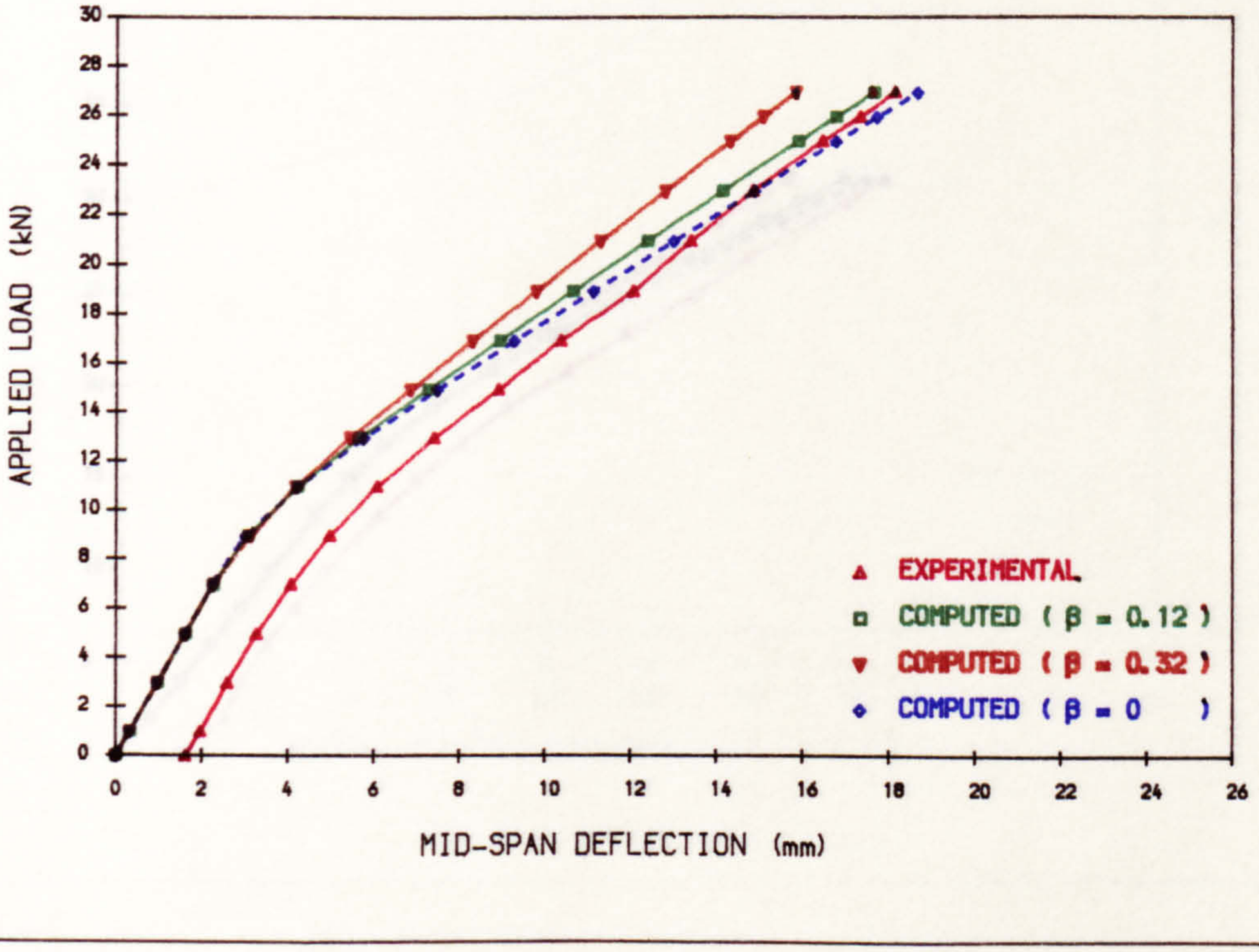

FIG. 6.25f DEFLECTION IN 1ST CYCLE COMPUTED BASED ON CP110 (I3.3.4)

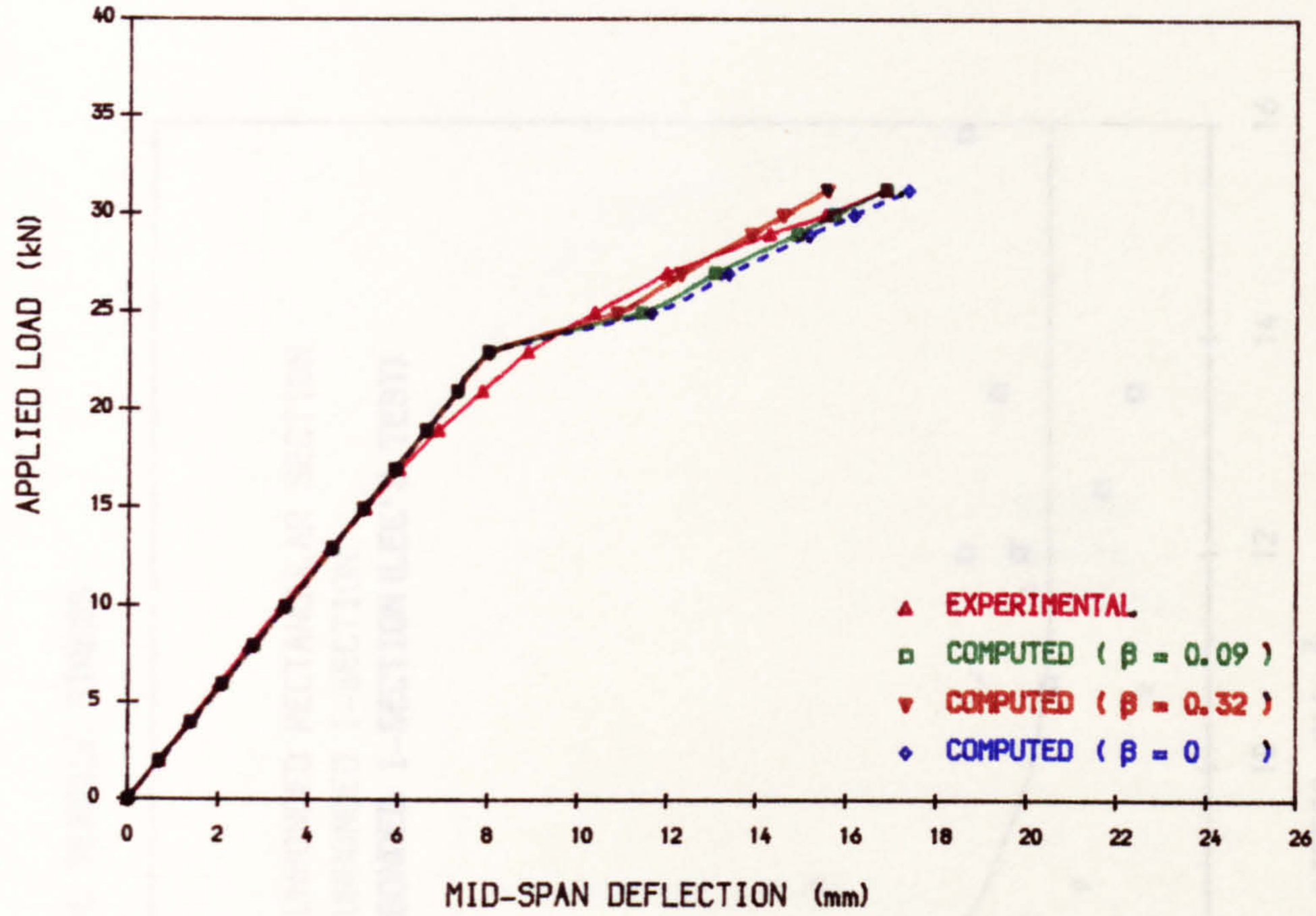

FIG. 6.26f DEFLECTION IN 2ND CYCLE COMPUTED BASED ON CP110 (I3.3.4)

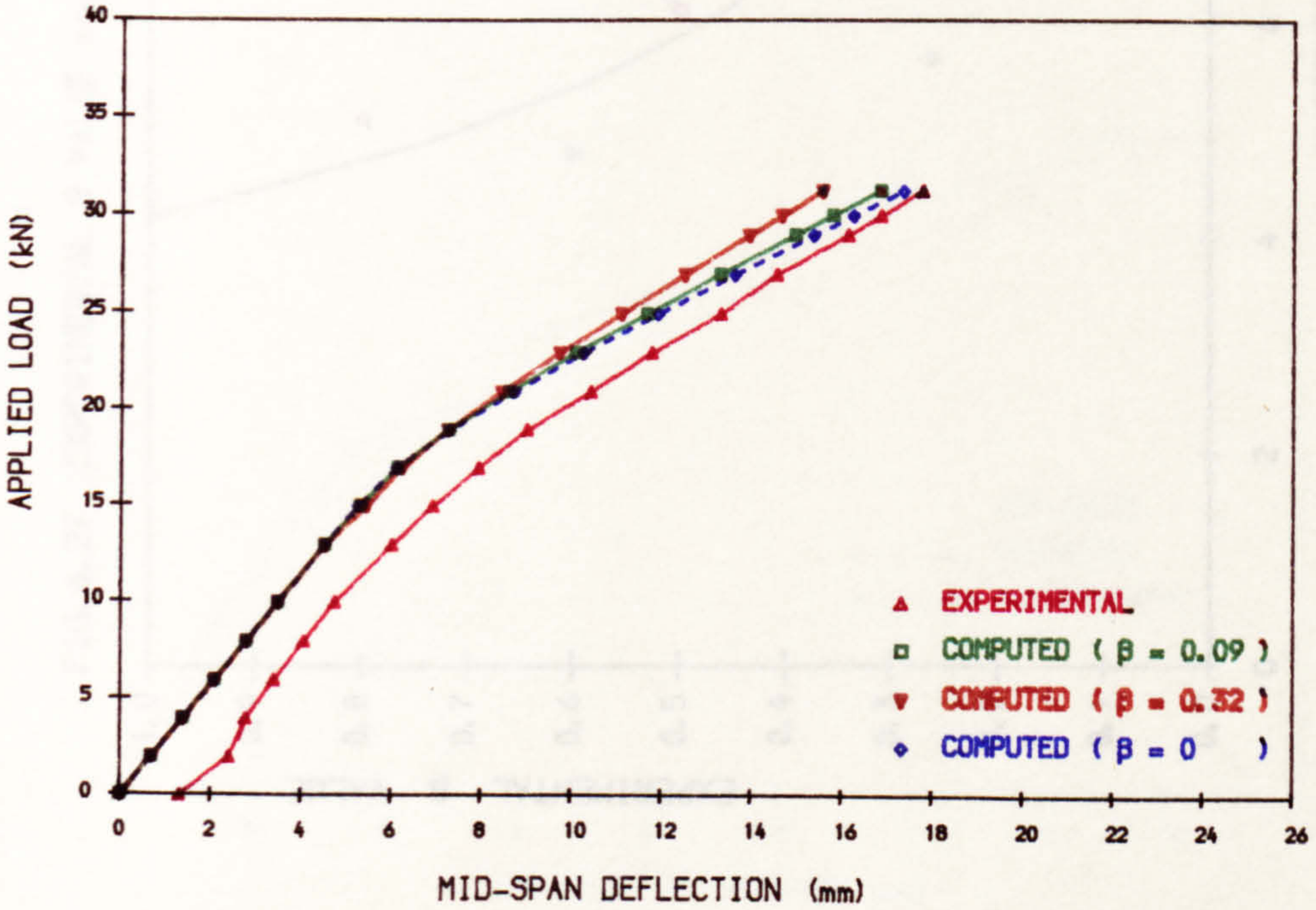

FIG. 6.27 EXPERIMENTAL β VALUE vs. HYPOTHETICAL TENSILE STRESS

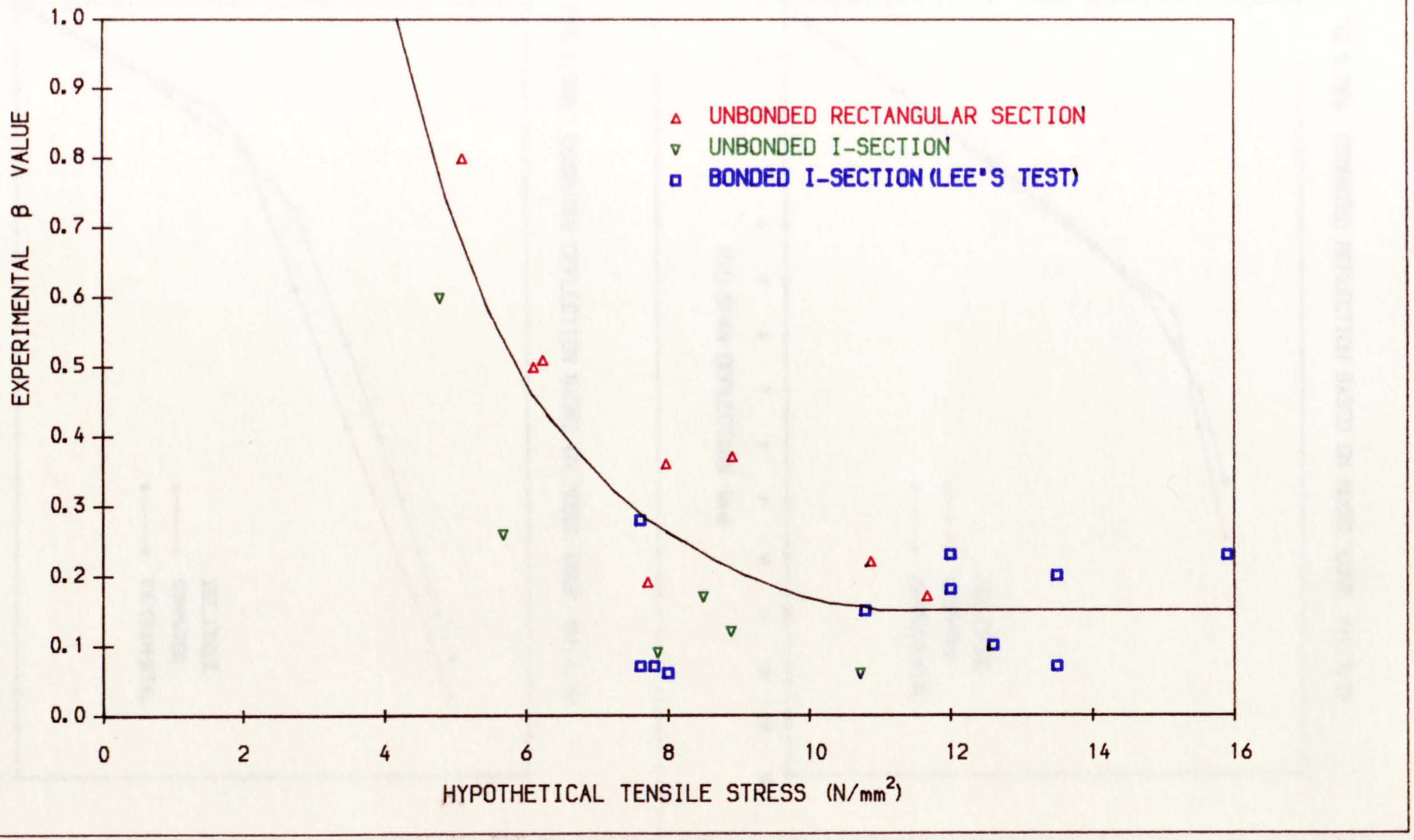

FIG. 6.28a COMPUTED DEFLECTION BASED ON MODEL CODE (R1.2.2)

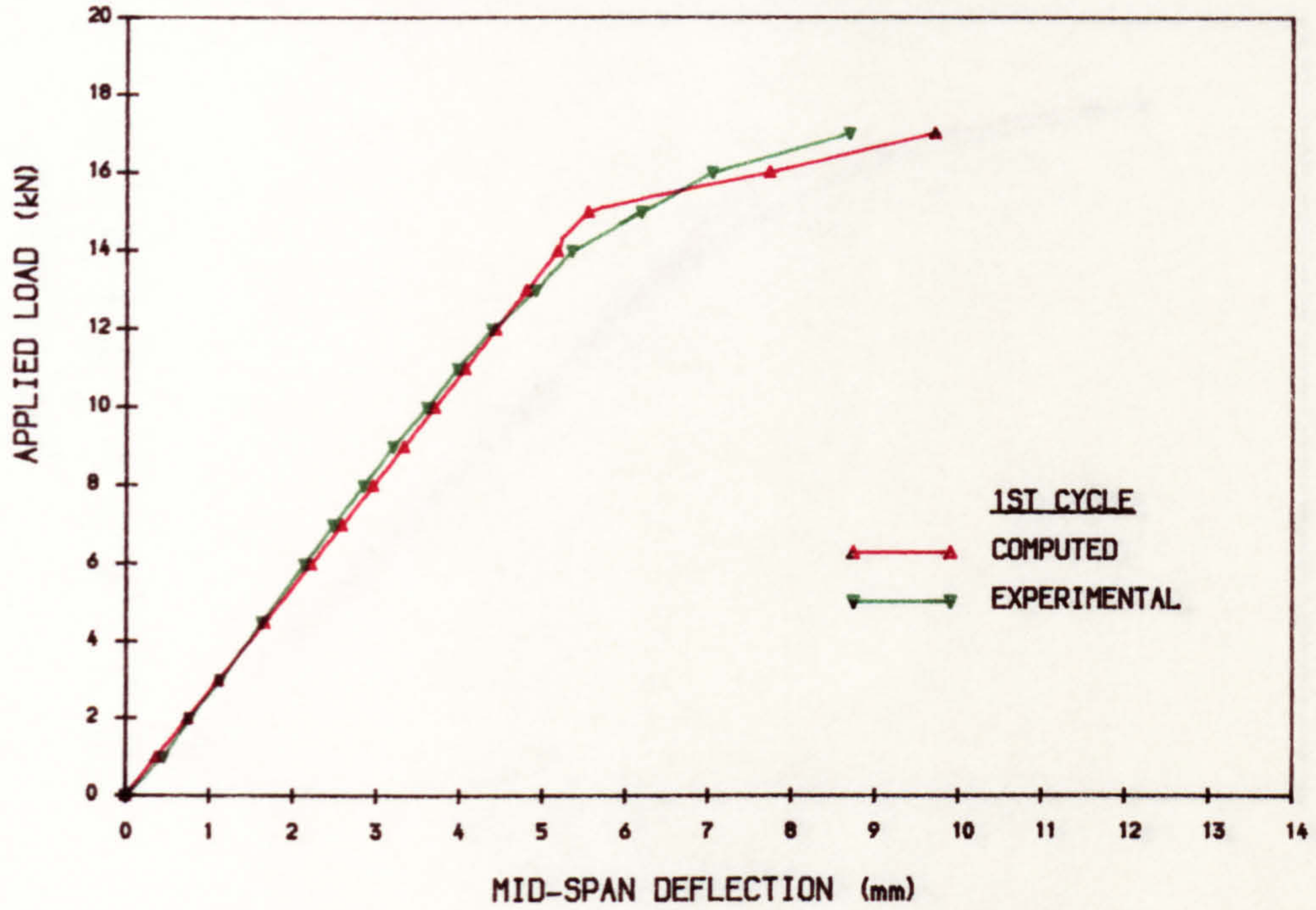

FIG. 6.28b COMPUTED DEFLECTION BASED ON MODEL CODE (R1.1.3)

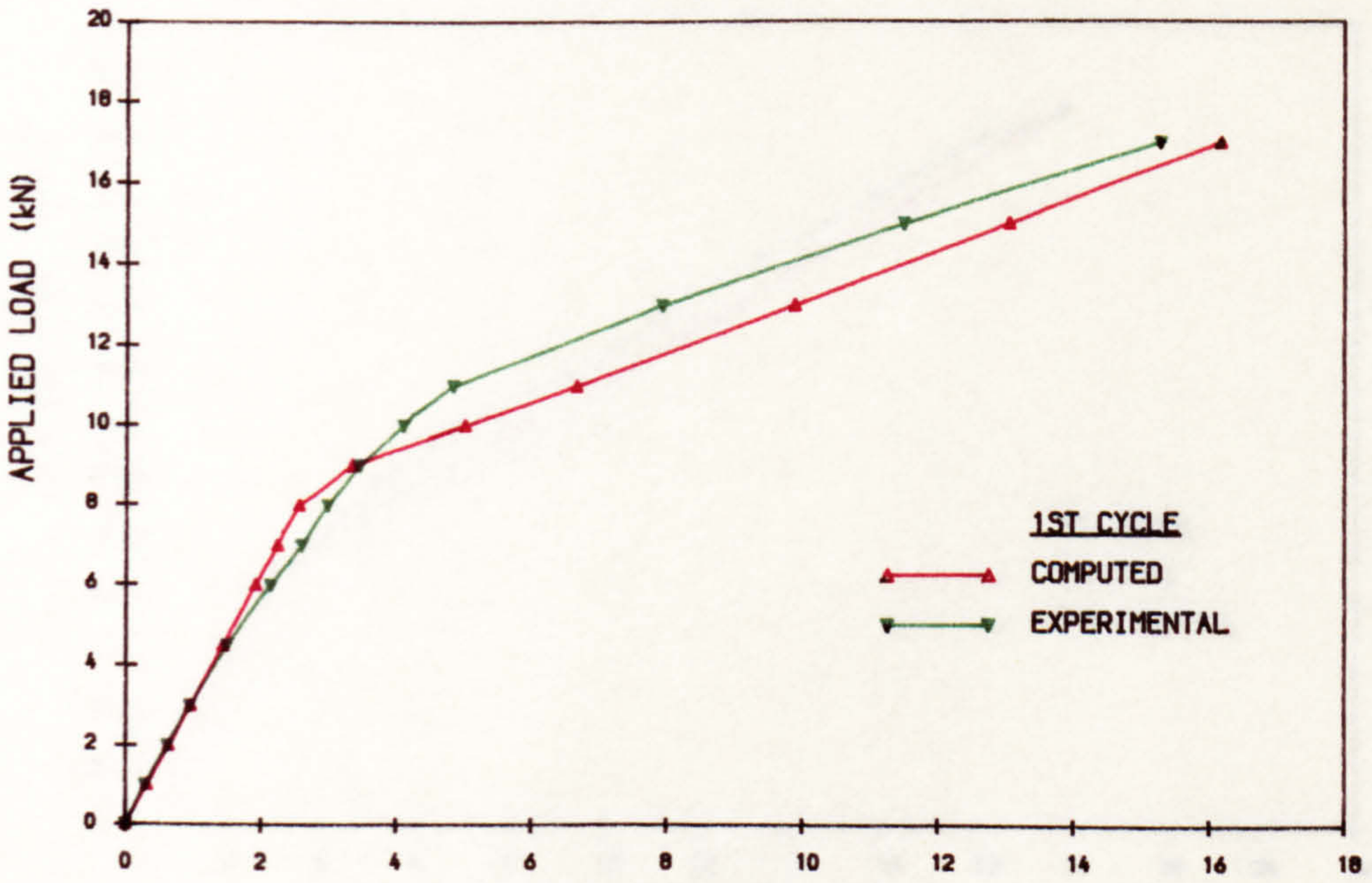

FIG. 6.28c COMPUTED DEFLECTION BASED ON MODEL CODE (R2.3.2)

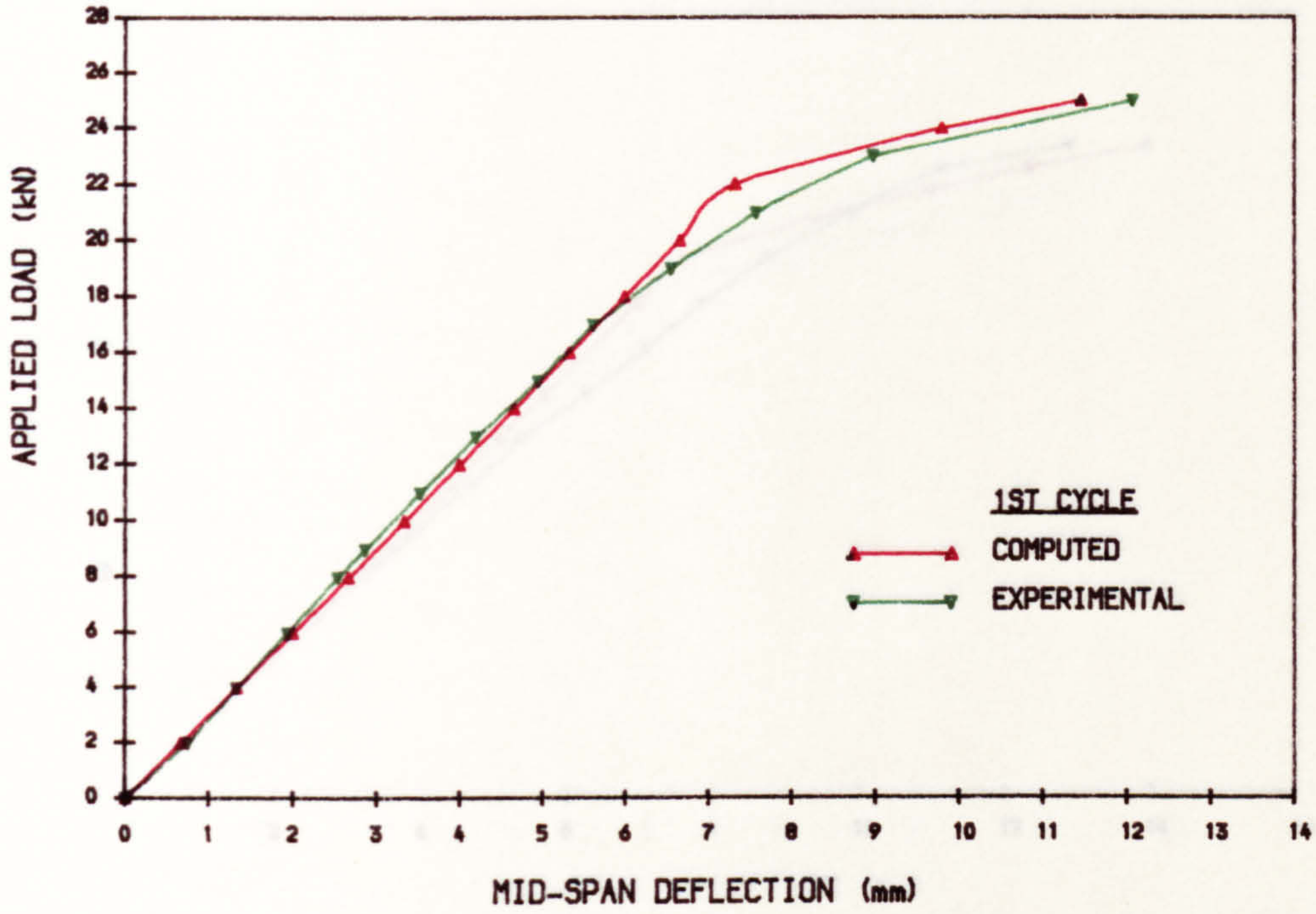

FIG. 6.28d COMPUTED DEFLECTION BASED ON MODEL CODE (R2.1.5)

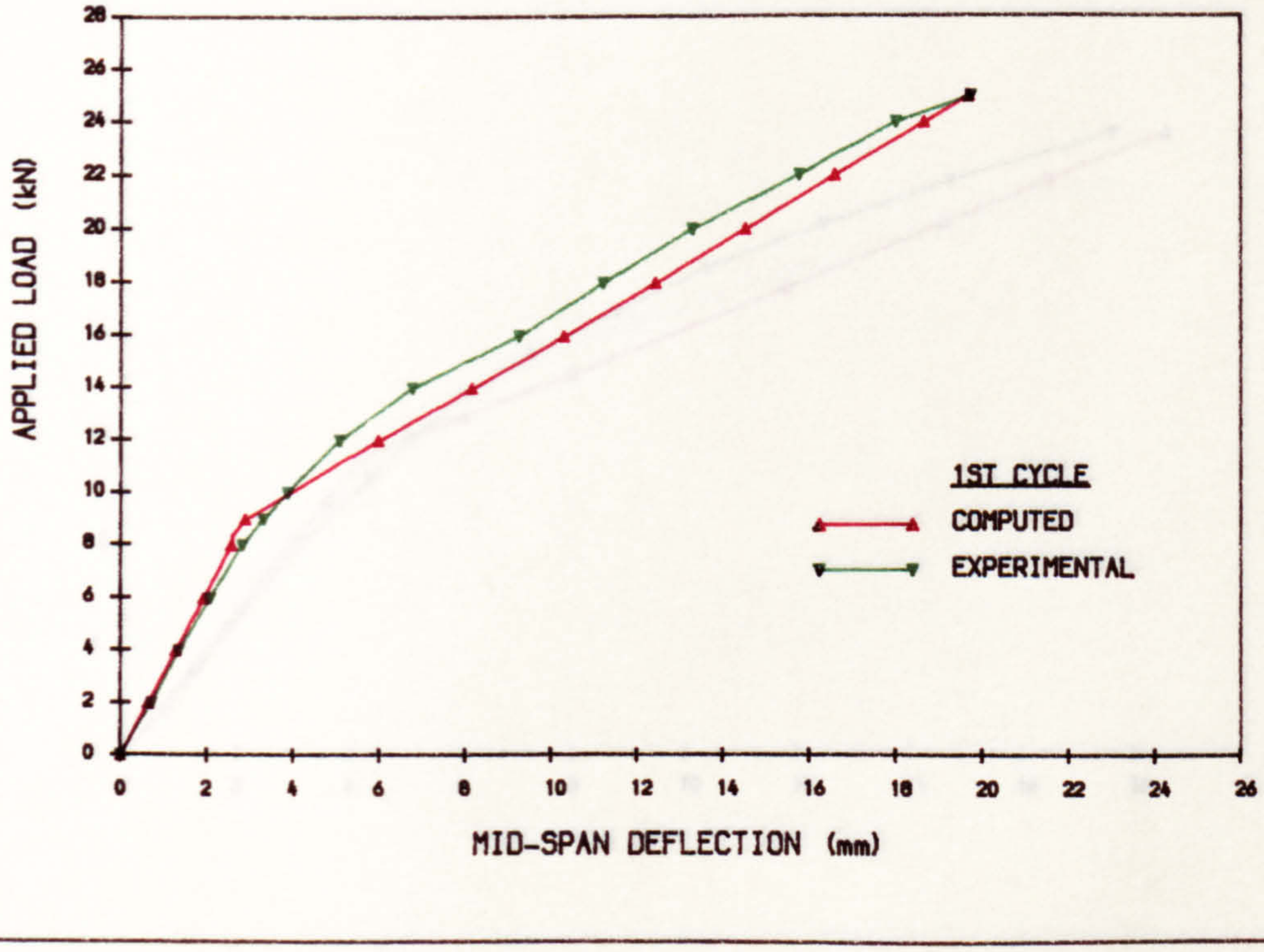

FIG. 6.28e COMPUTED DEFLECTION BASED ON MODEL CODE (R3.4.2)

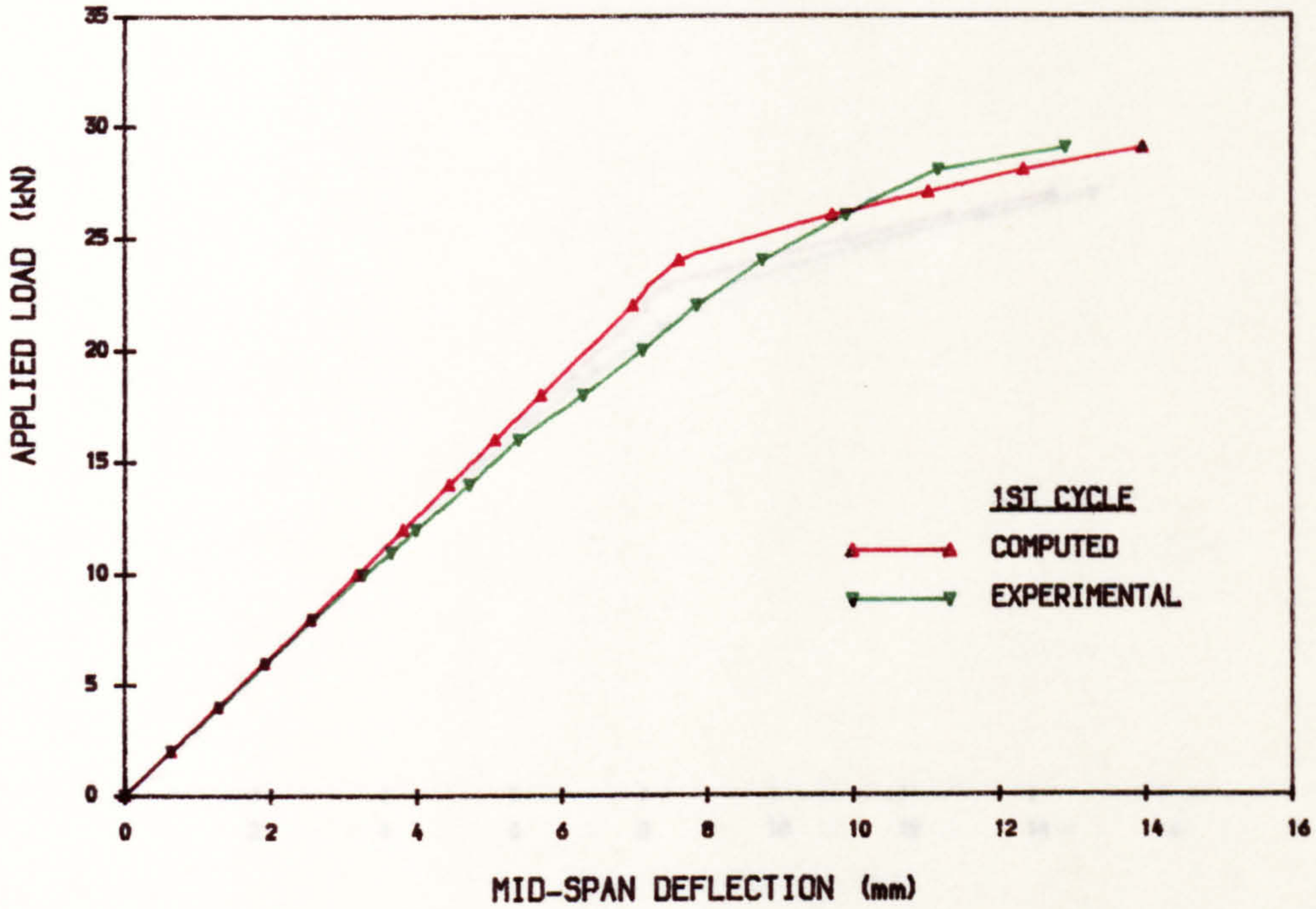

FIG. 6.28f COMPUTED DEFLECTION BASED ON MODEL CODE (R3.2.5)

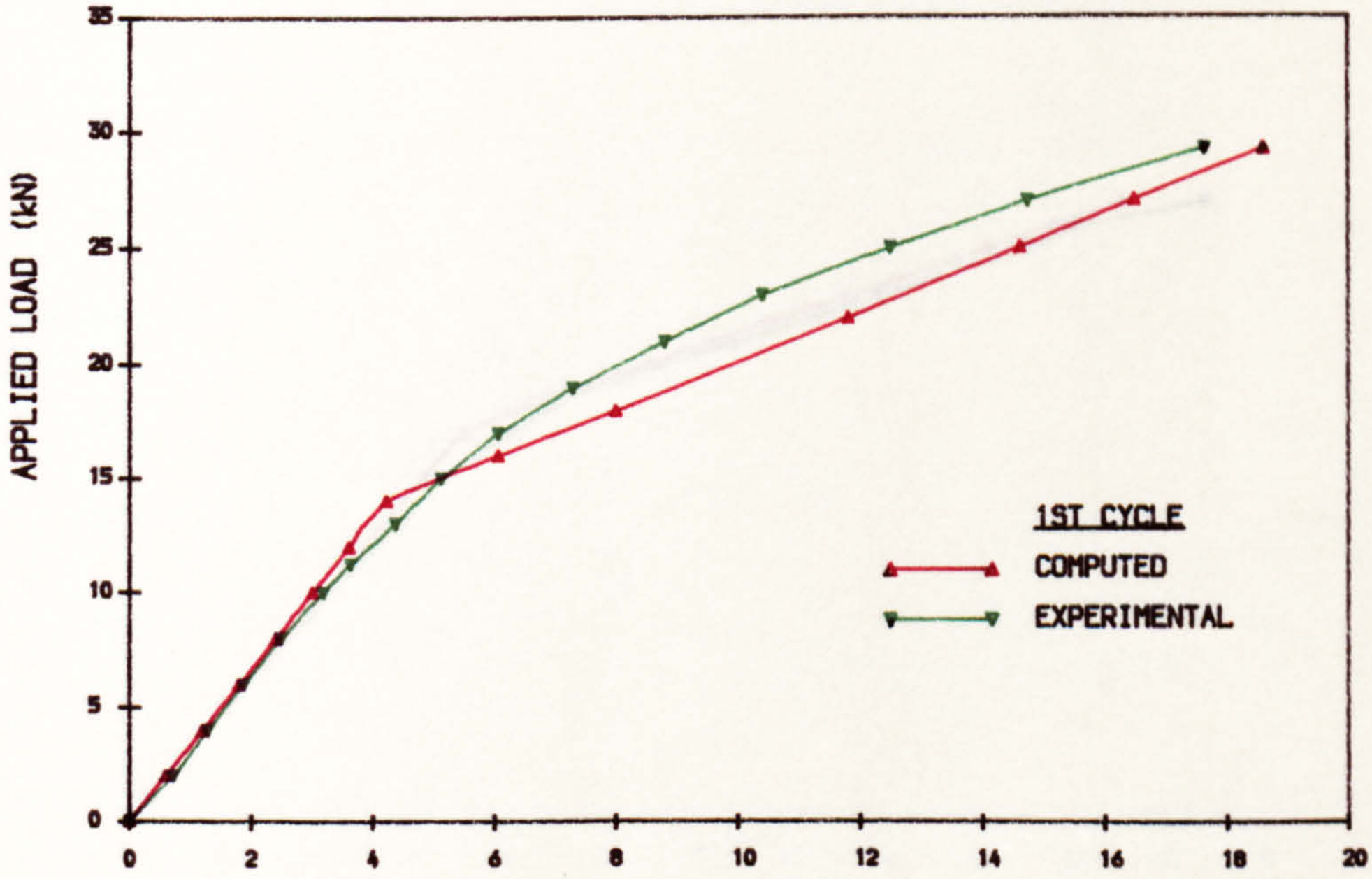

FIG. 6.28g COMPUTED DEFLECTION BASED ON MODEL CODE (I2.3.2)

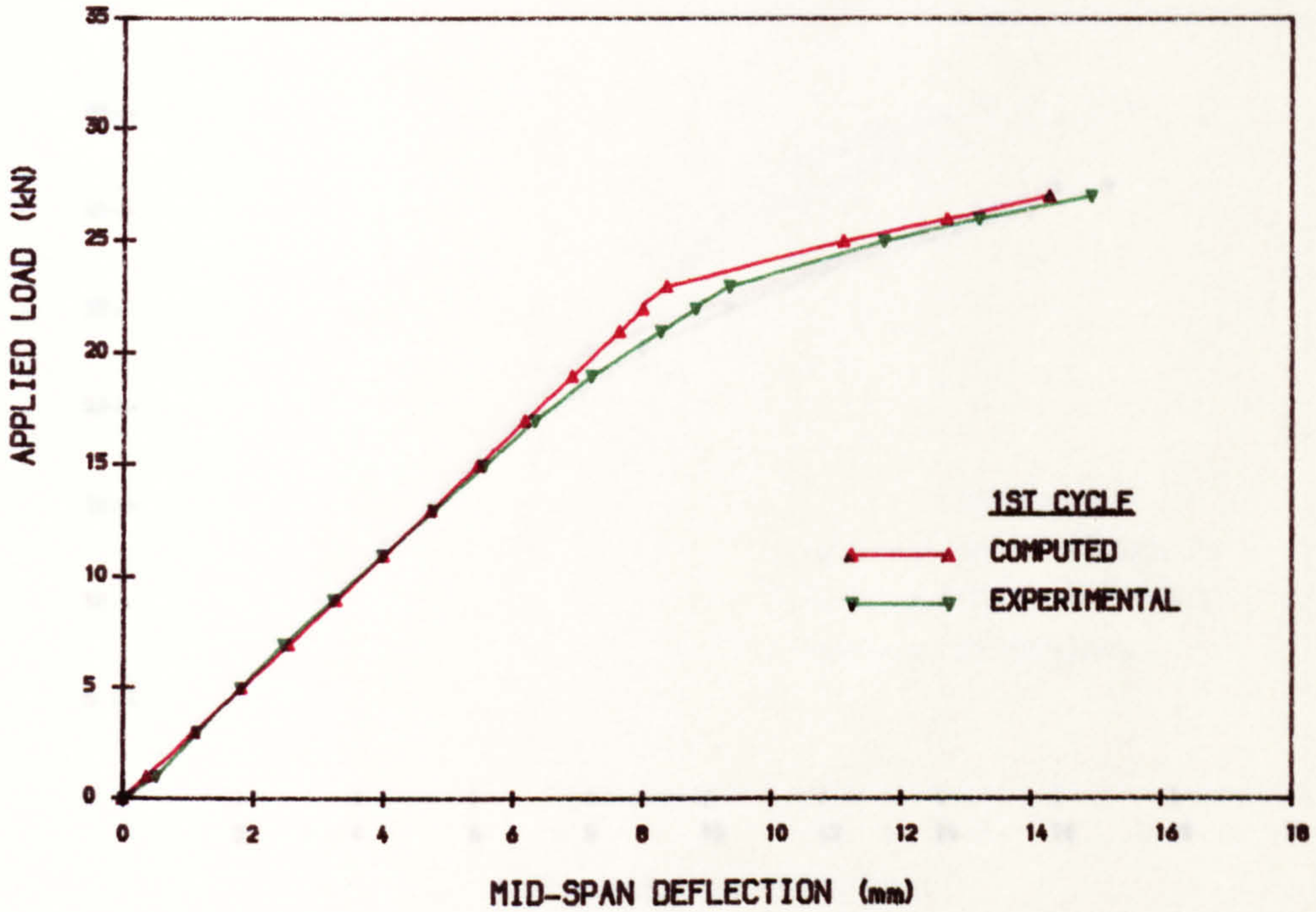

FIG. 6.28h COMPUTED DEFLECTION BASED ON MODEL CODE (I2.2.4)

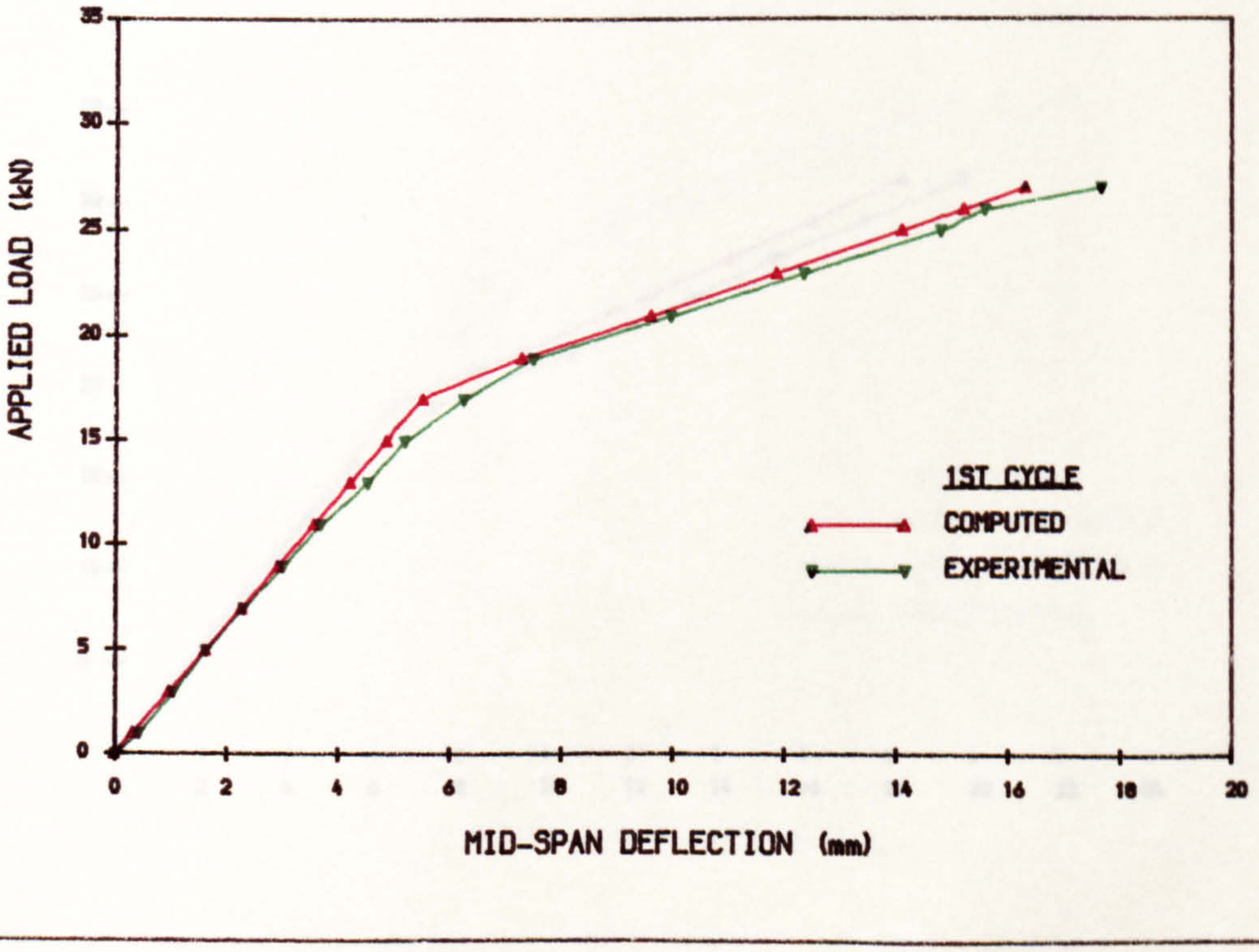

FIG. 6.28I COMPUTED DEFLECTION BASED ON MODEL CODE (I3.3.4)

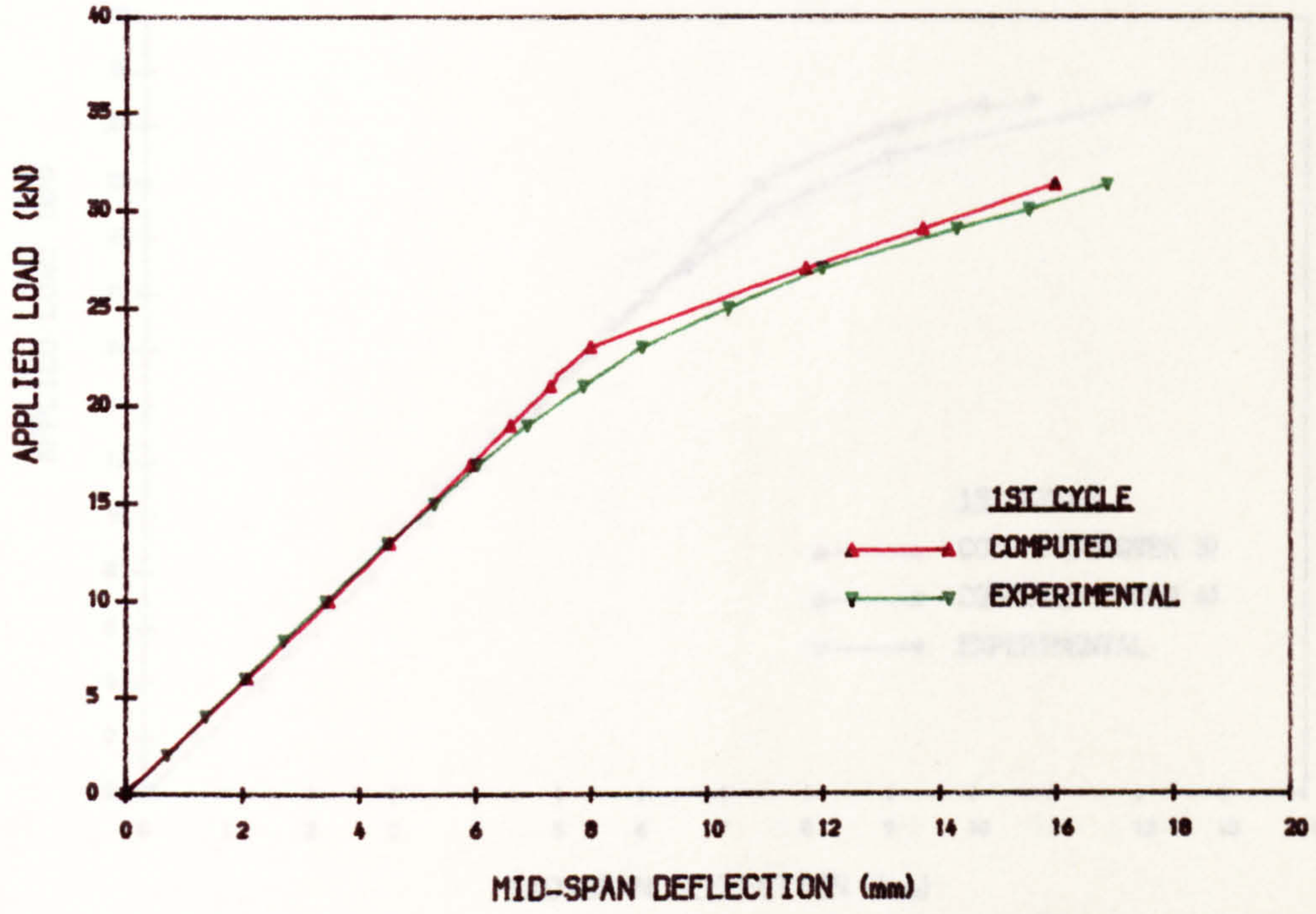

FIG. 6.28J COMPUTED DEFLECTION BASED ON MODEL CODE (I3.2.5)

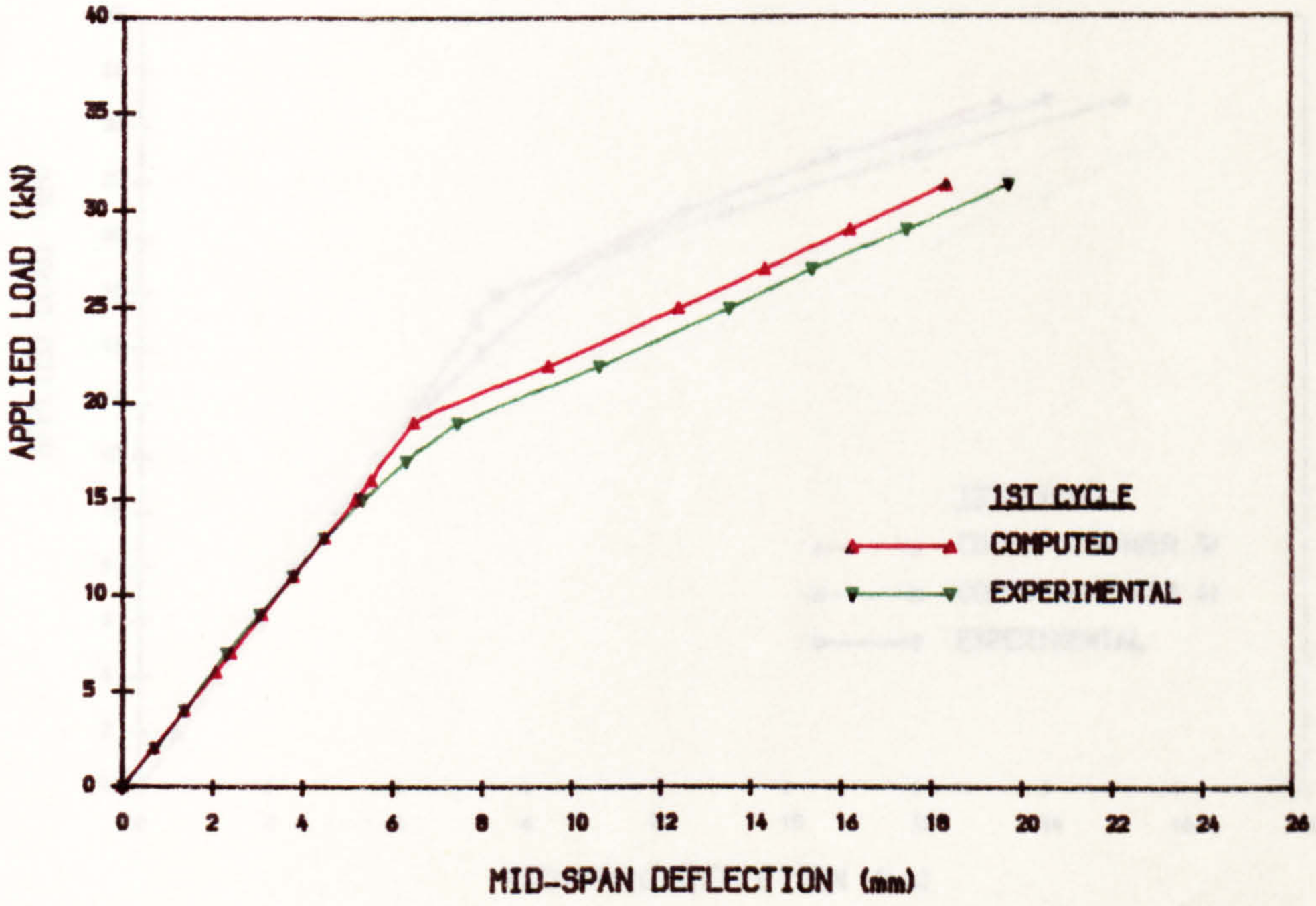

FIG. 6.29a COMPUTED DEFLECTION BASED ON ACI CODE (R2.3.2)

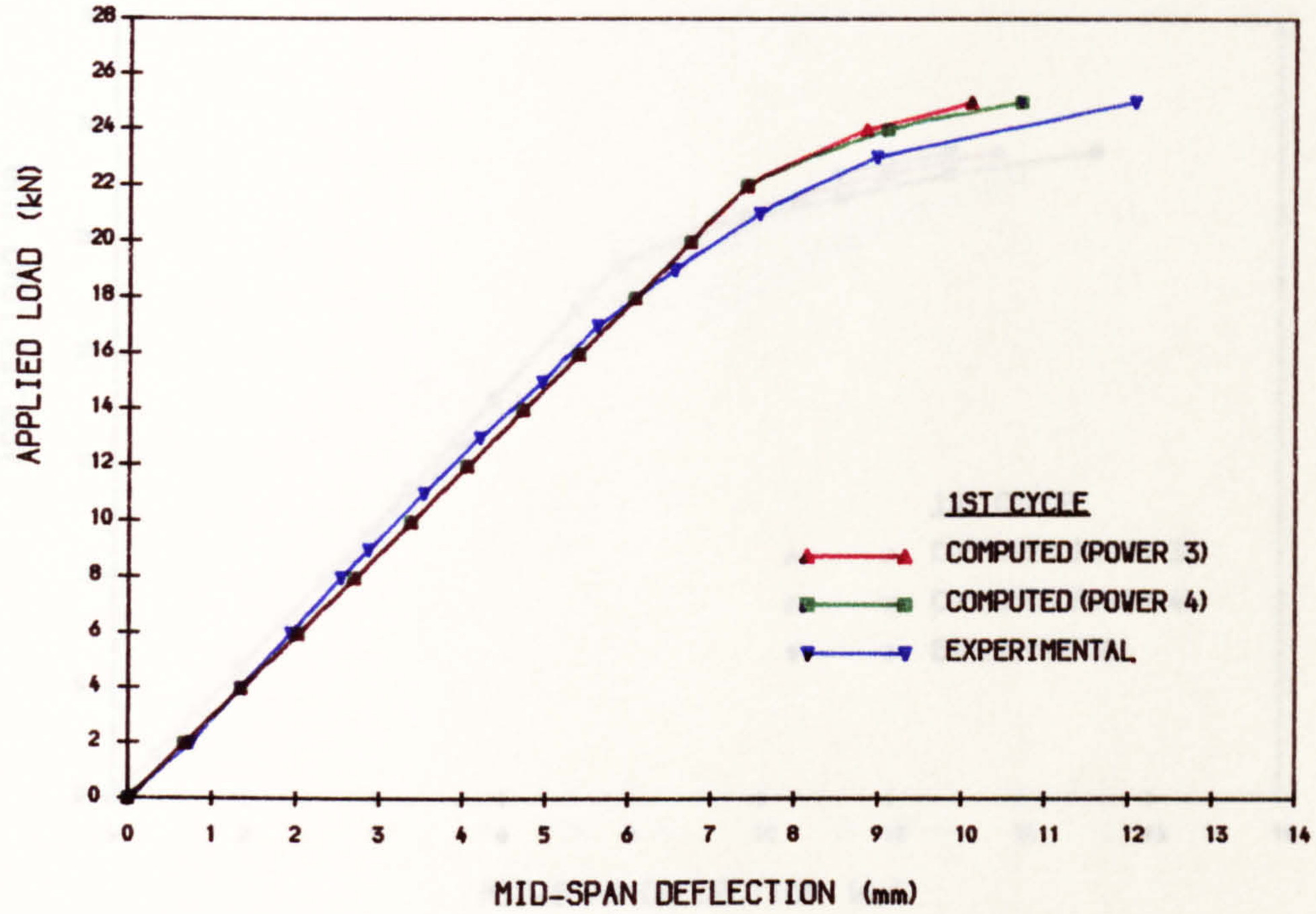

FIG. 6.29b COMPUTED DEFLECTION BASED ON ACI CODE (R2.2.4)

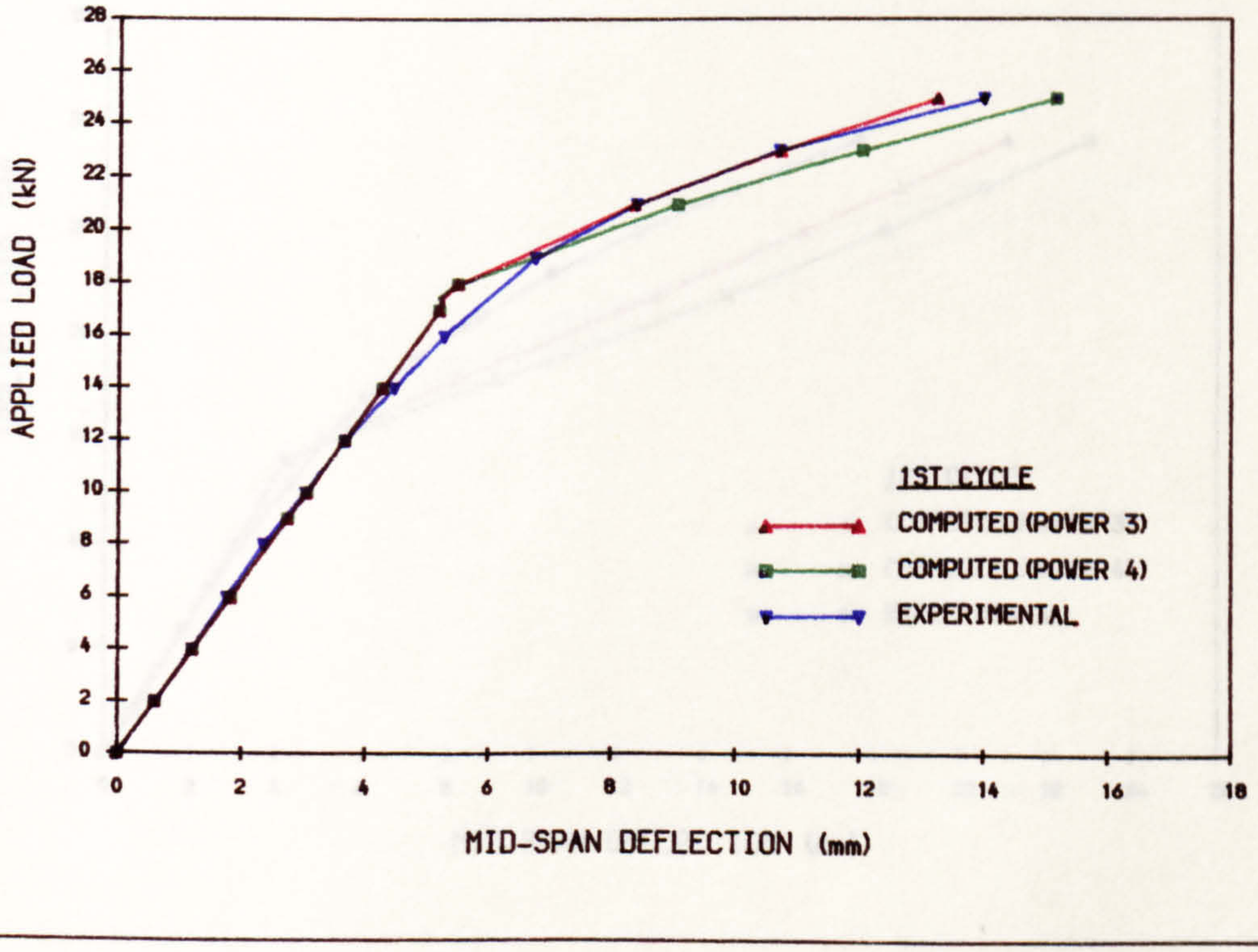

FIG. 6.29c COMPUTED DEFLECTION BASED ON ACI CODE (R3.4.2)

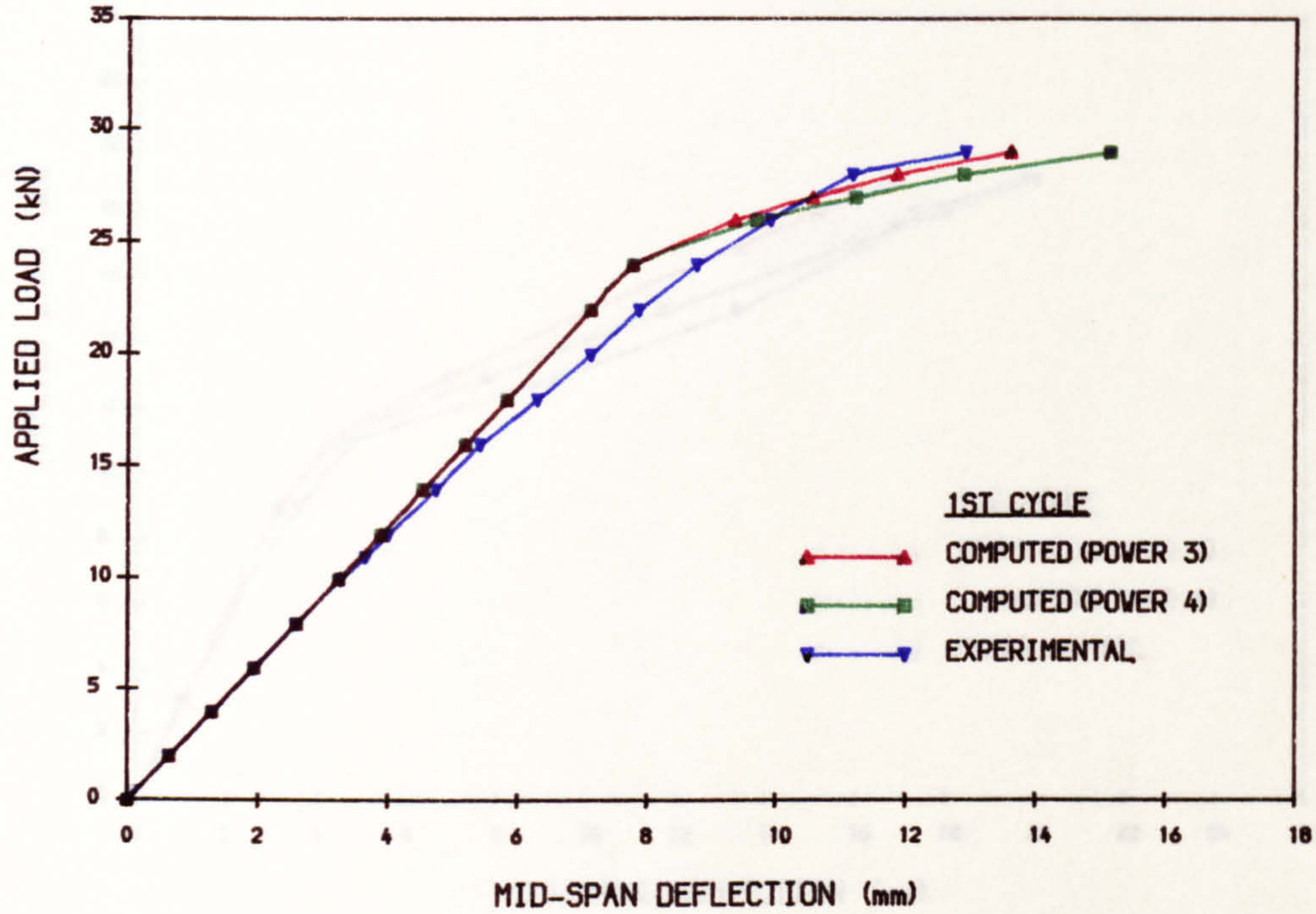

FIG. 6.29d COMPUTED DEFLECTION BASED ON ACI CODE (R3.2.5)

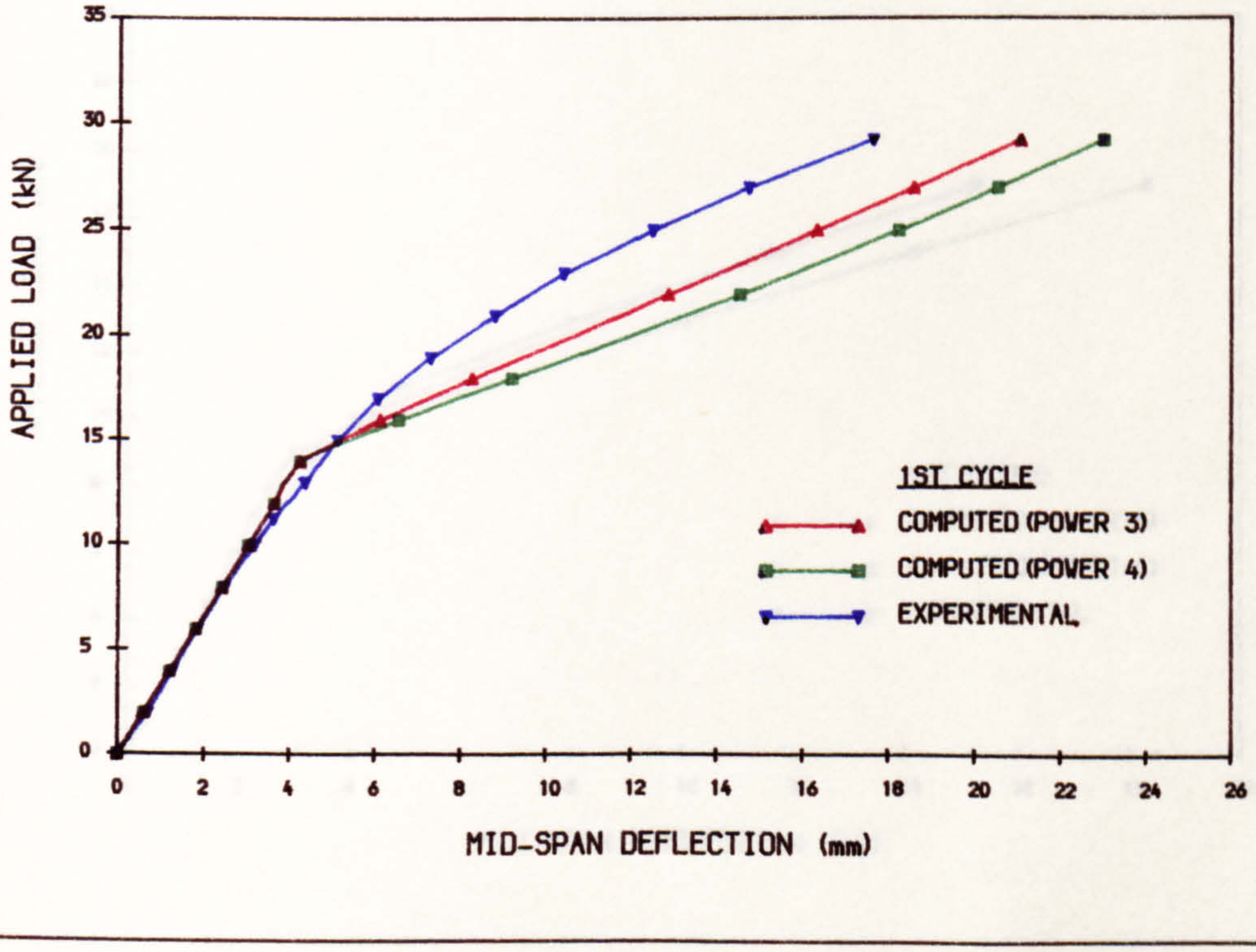

FIG. 6.29e COMPUTED DEFLECTION BASED ON ACI CODE (I1.1.3)

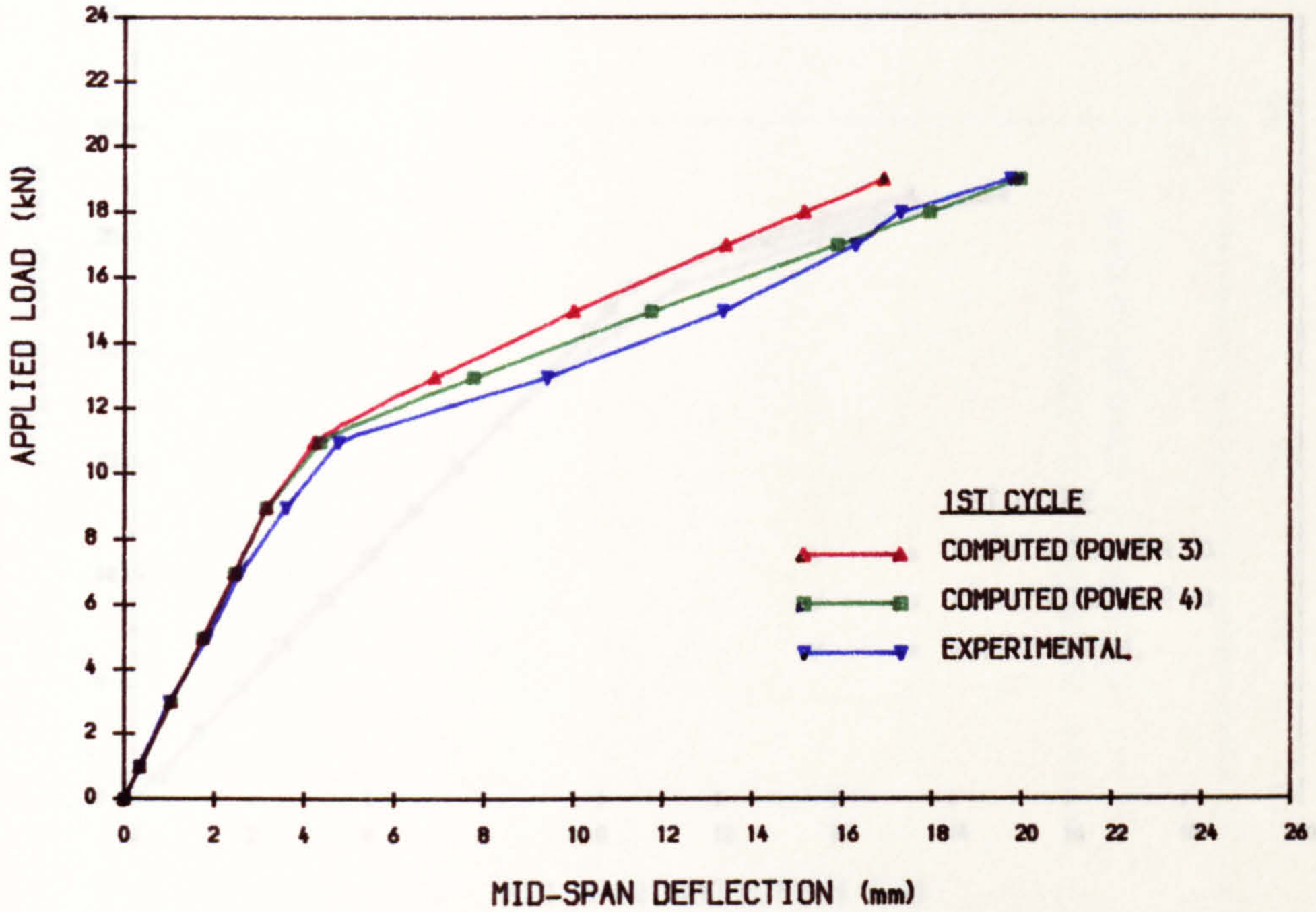

FIG. 6.29f COMPUTED DEFLECTION BASED ON ACI CODE (R1.1.3)

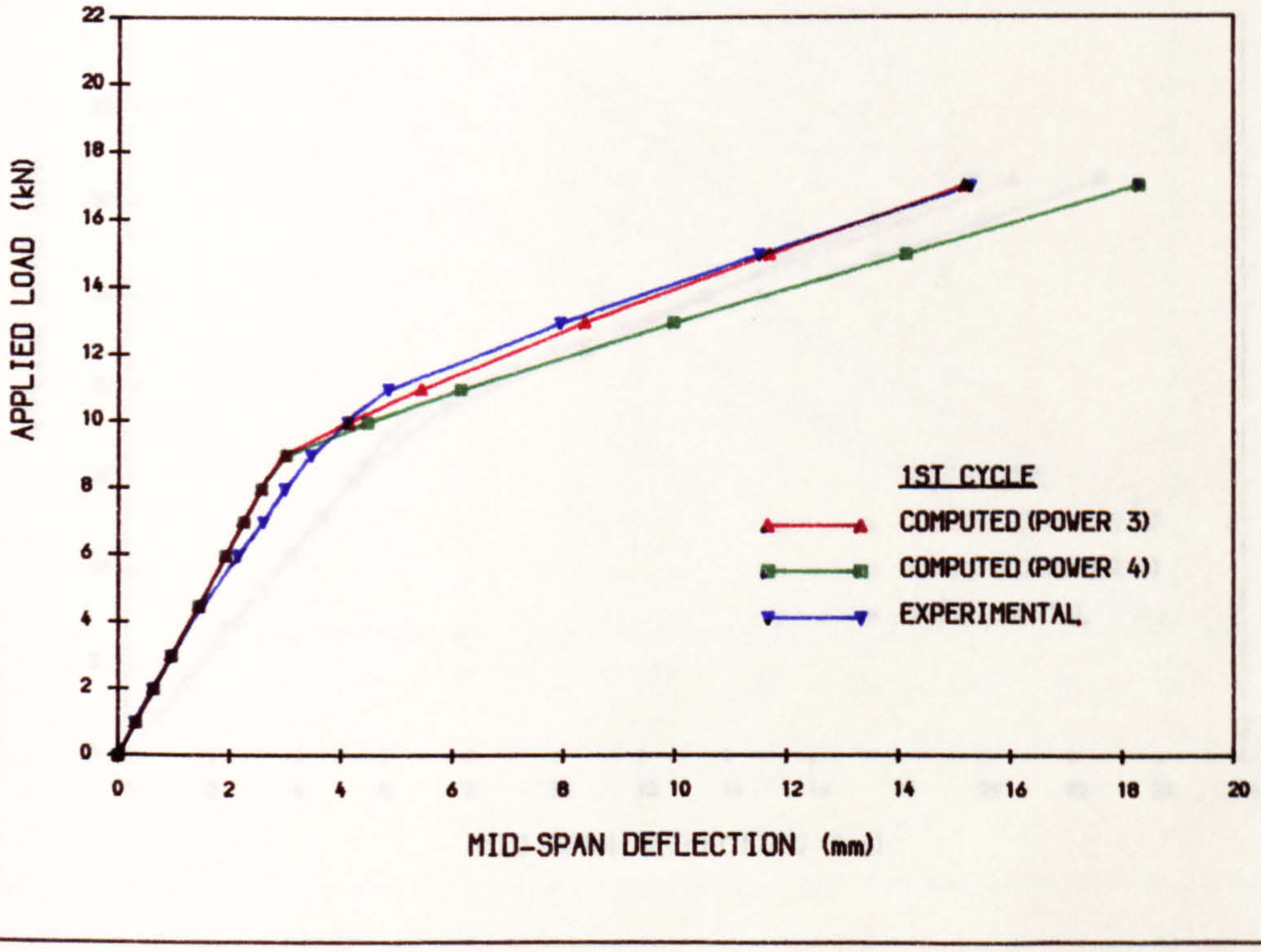

FIG. 6.29g COMPUTED DEFLECTION BASED ON ACI CODE (I2.3.2)

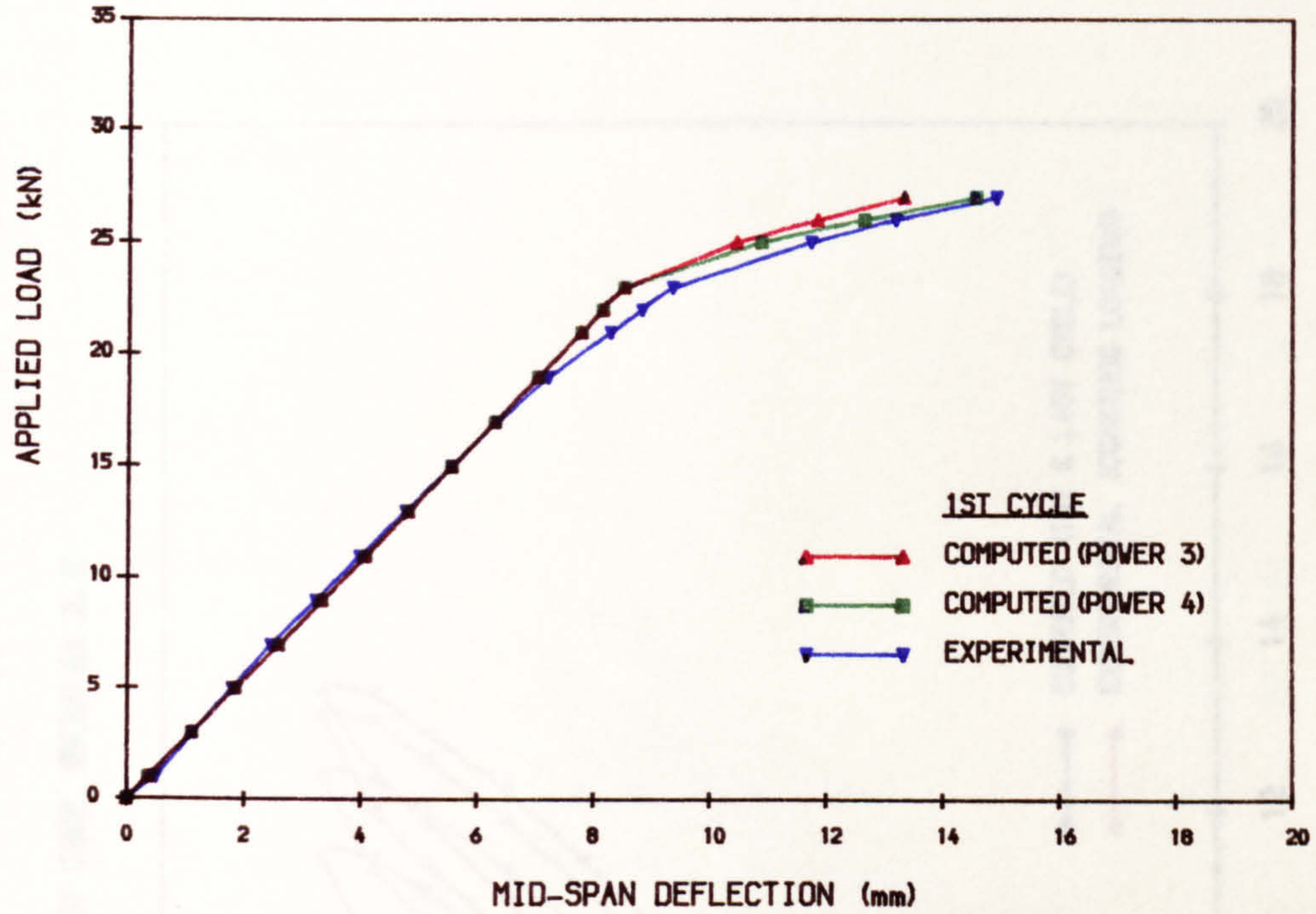

FIG. 6.29h COMPUTED DEFLECTION BASED ON ACI CODE (I3.2.5)

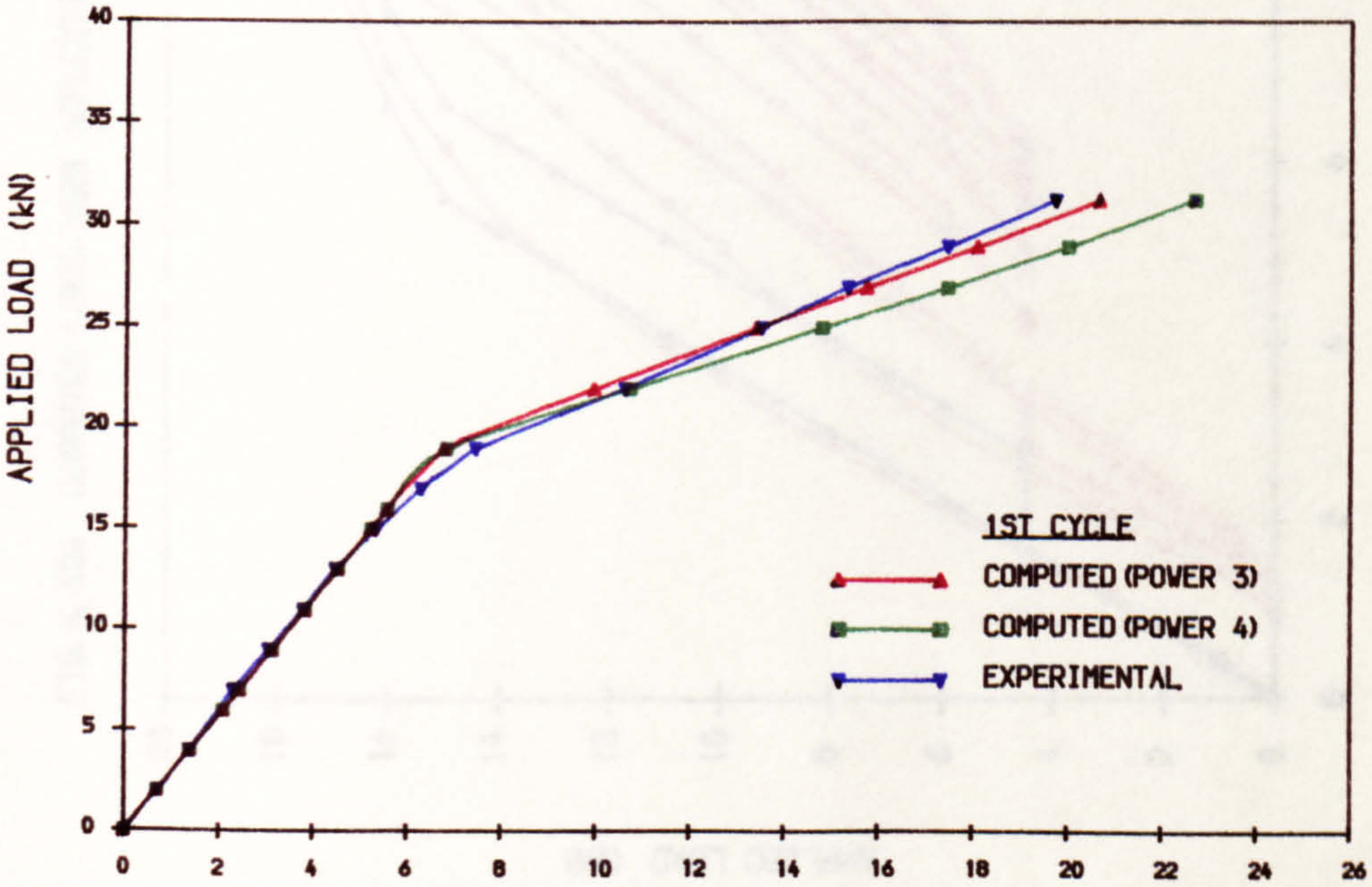

FIG. 6.30a COMPUTED LONG-TERM DEFLECTION BASED ON ACI CODE (BEAM R1.2.2)

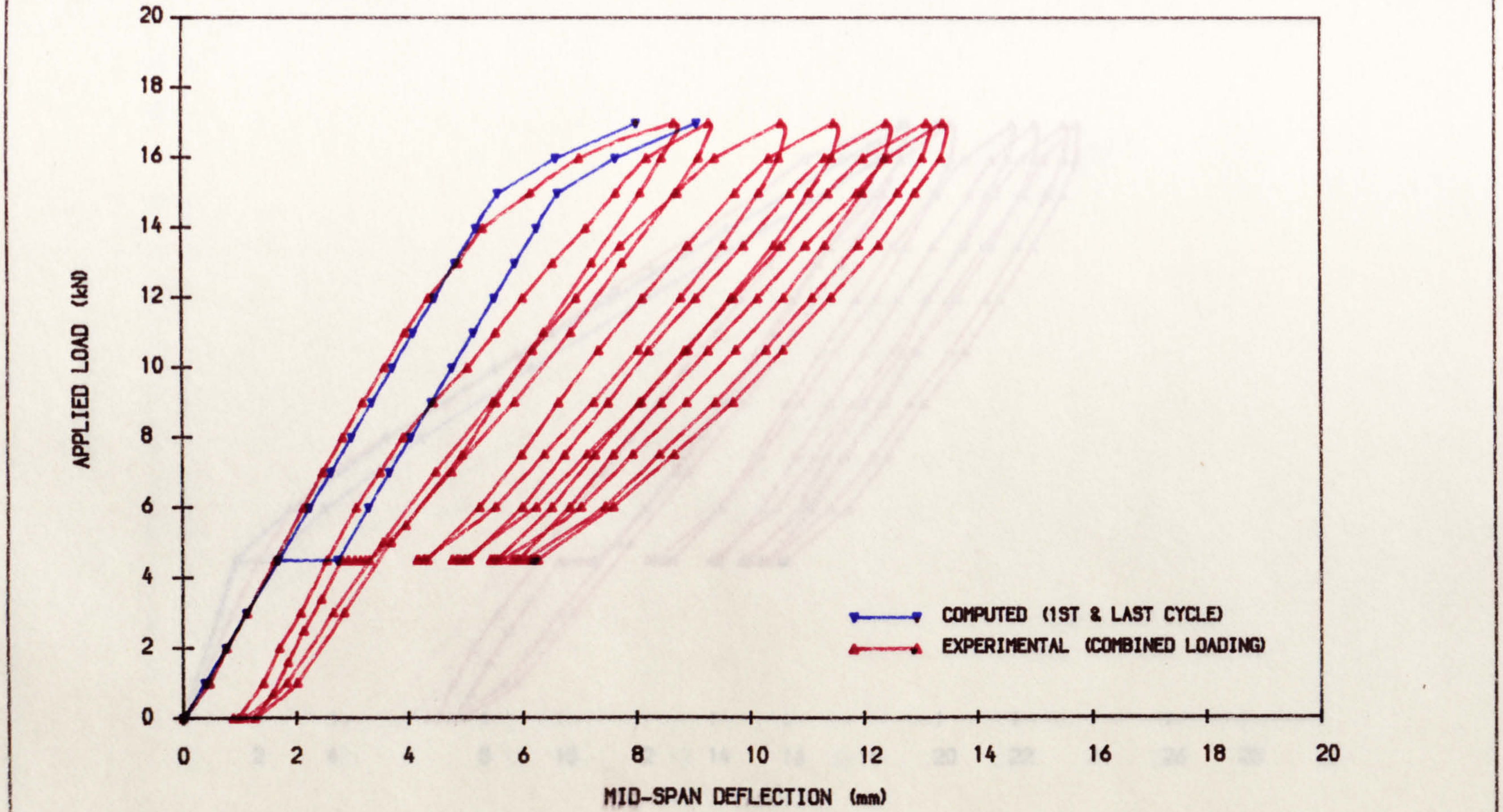

FIG. 6.30b COMPUTED LONG-TERM DEFLECTION BASED ON ACI CODE (BEAM R1.0.5)

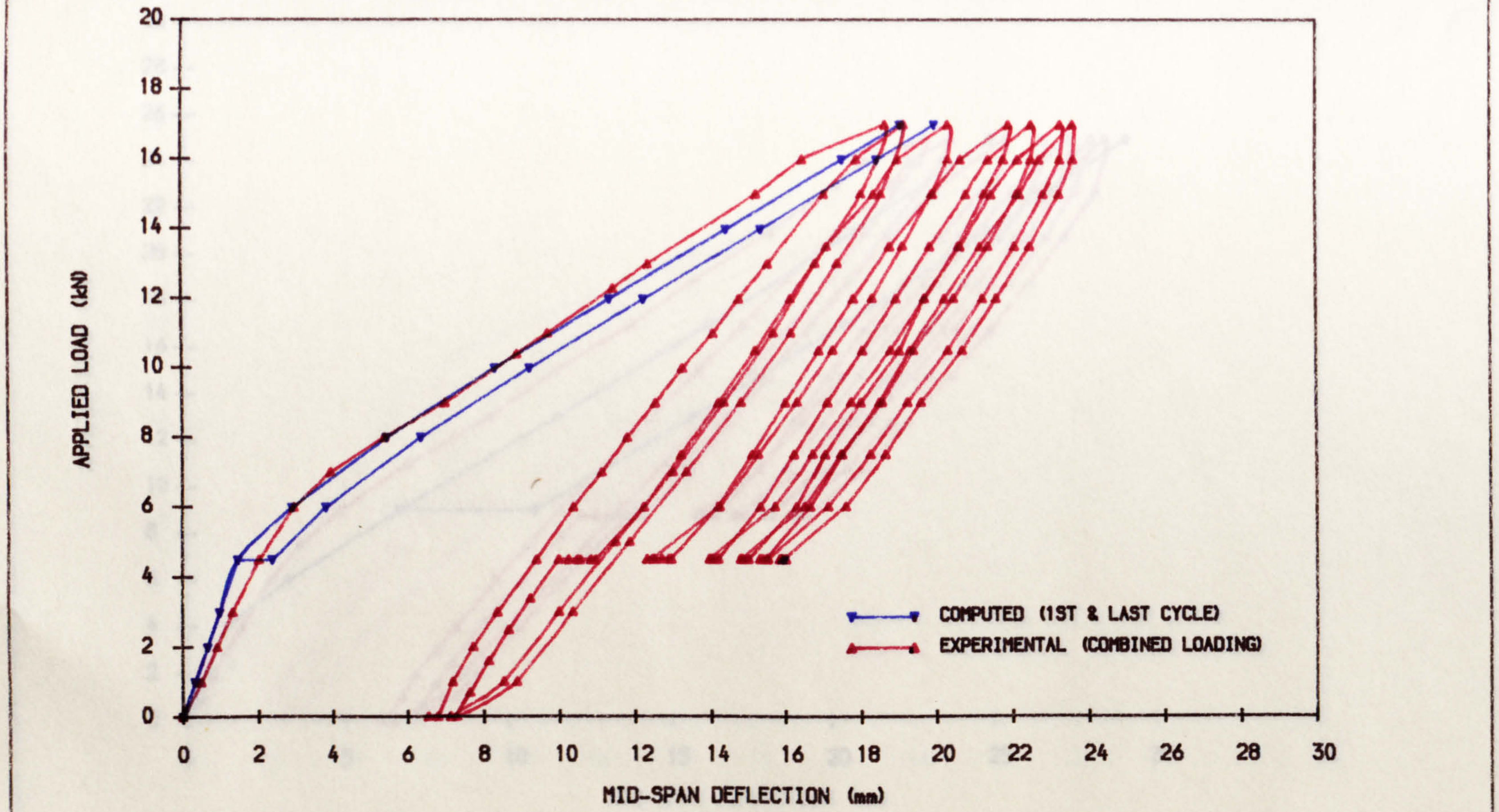

FIG. 6.30c COMPUTED LONG-TERM DEFLECTION BASED ON ACI CODE (BEAM R2.0.7)

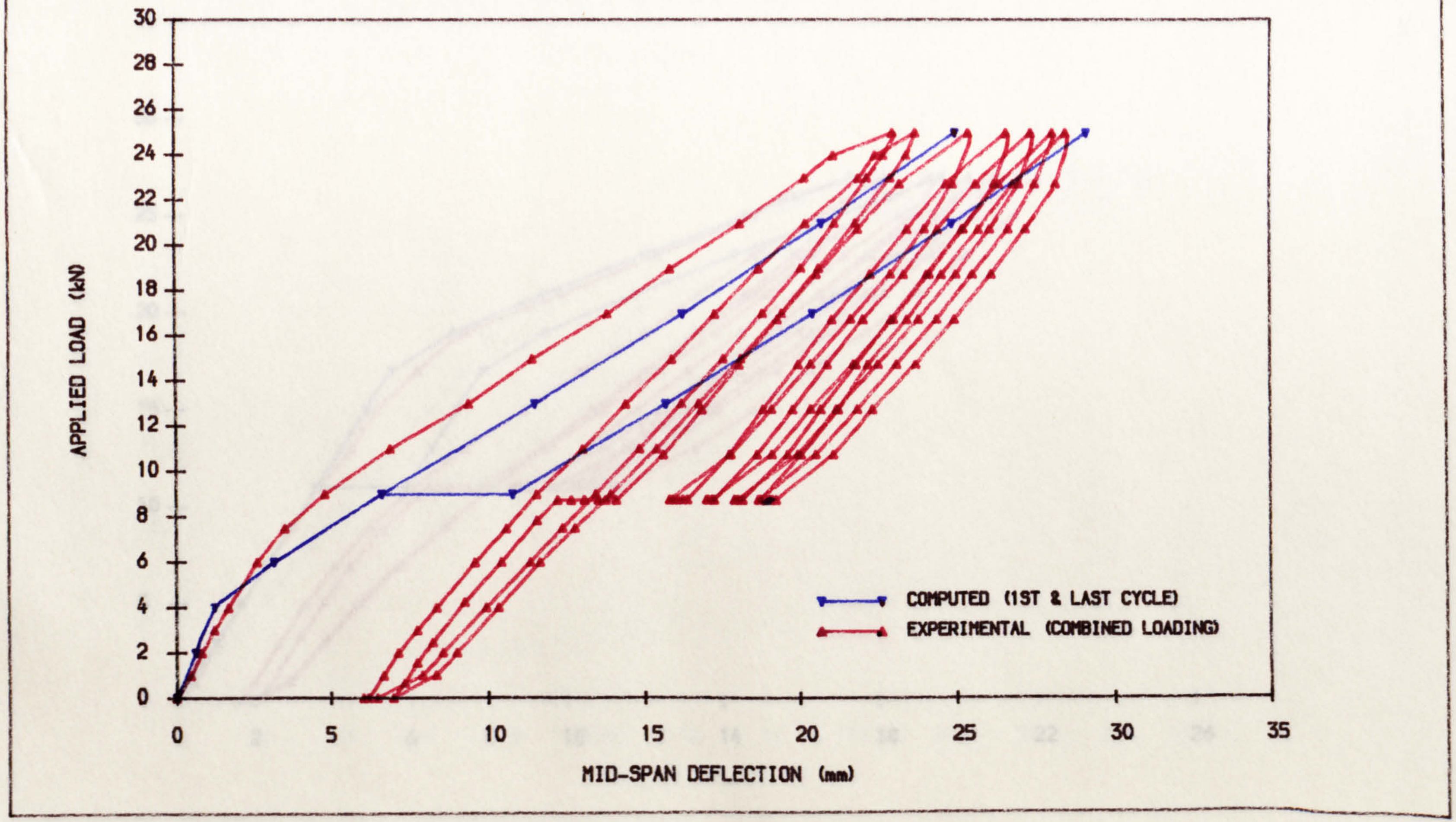

FIG. 6.30d COMPUTED LONG-TERM DEFLECTION BASED ON ACI CODE (BEAM I2.2.4)

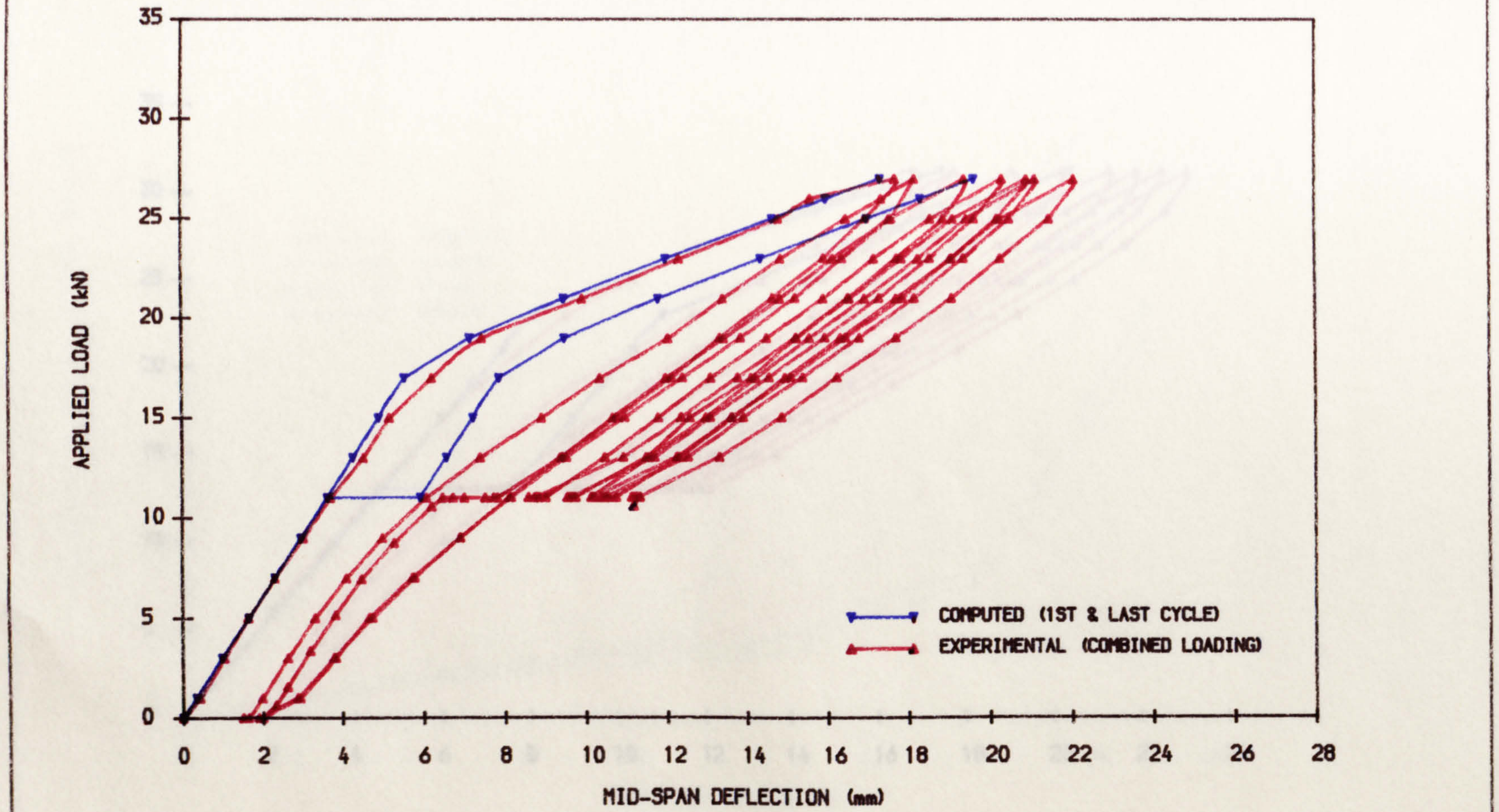

FIG. 6.30e COMPUTED LONG-TERM DEFLECTION BASED ON ACI CODE (BEAM I3.3.4)

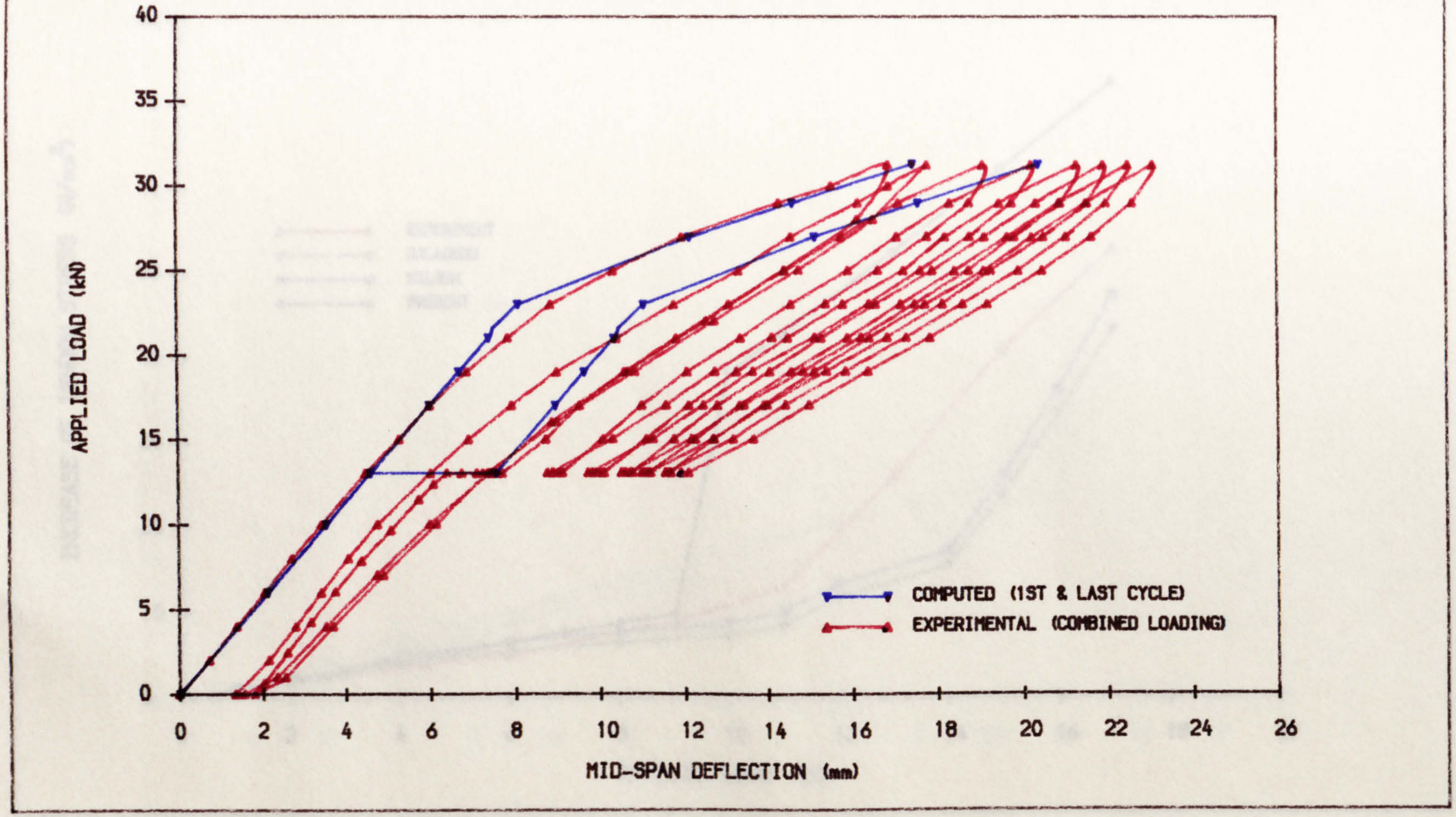

FIG. 6.31a INCREASE IN TENDON STRESS IN 1ST LOADING (BEAM R1.1.3)

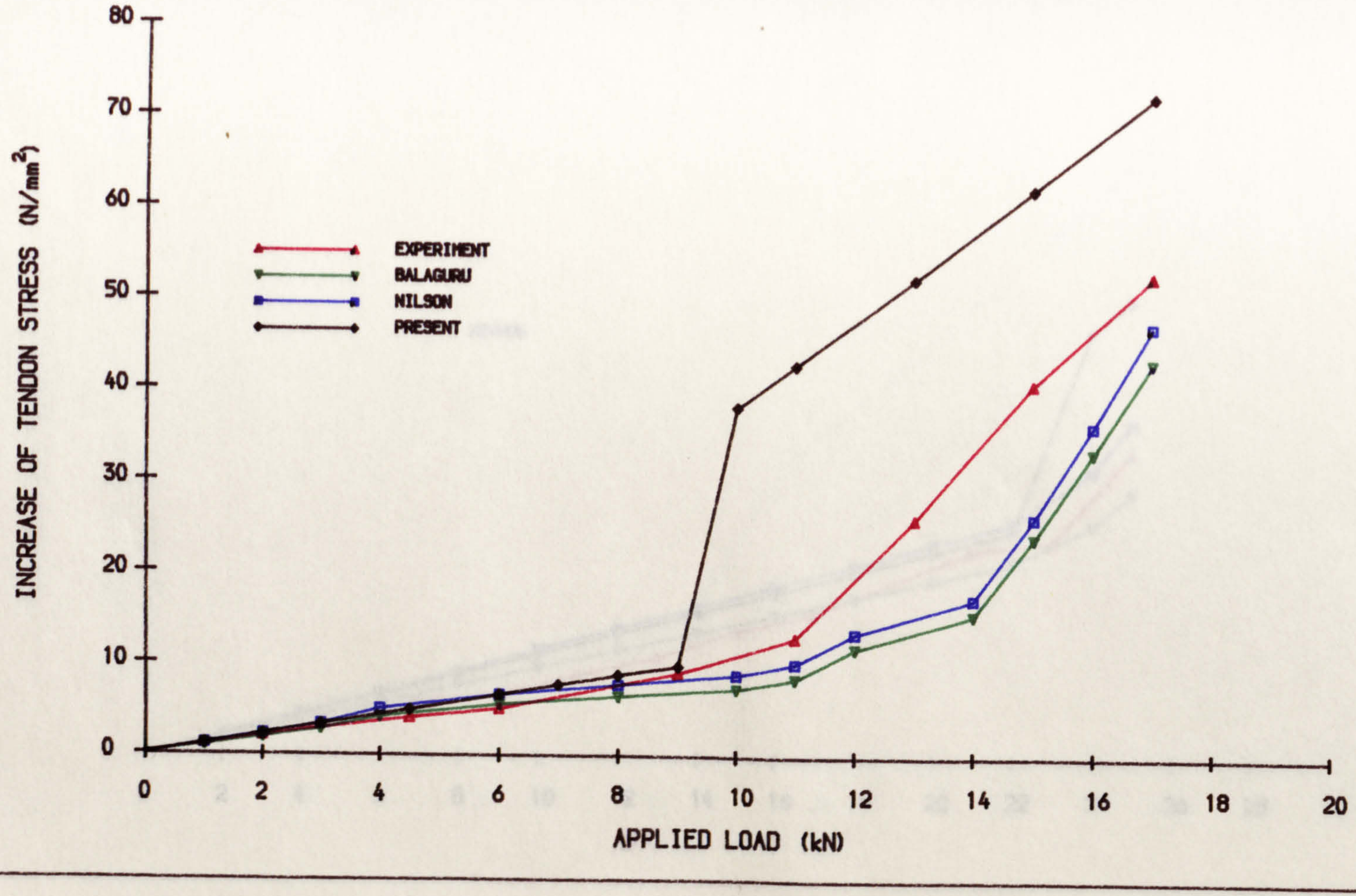

FIG. 6.31b INCREASE IN TENDON STRESS IN 1ST LOADING (BEAM R2.3.2)

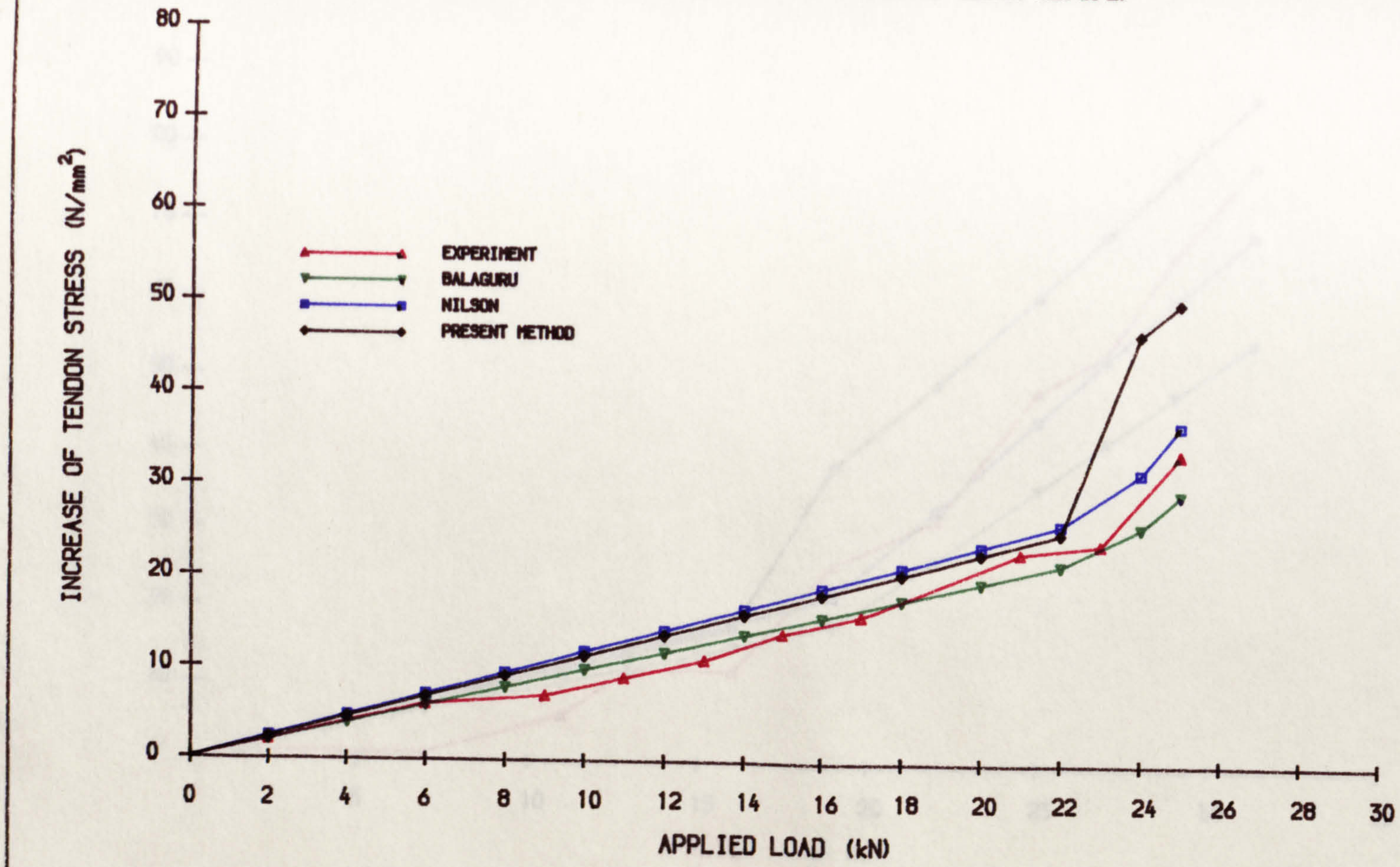

FIG. 6.31c INCREASE OF TENDON STRESS IN 1ST LOADING (BEAM I3.2.5)

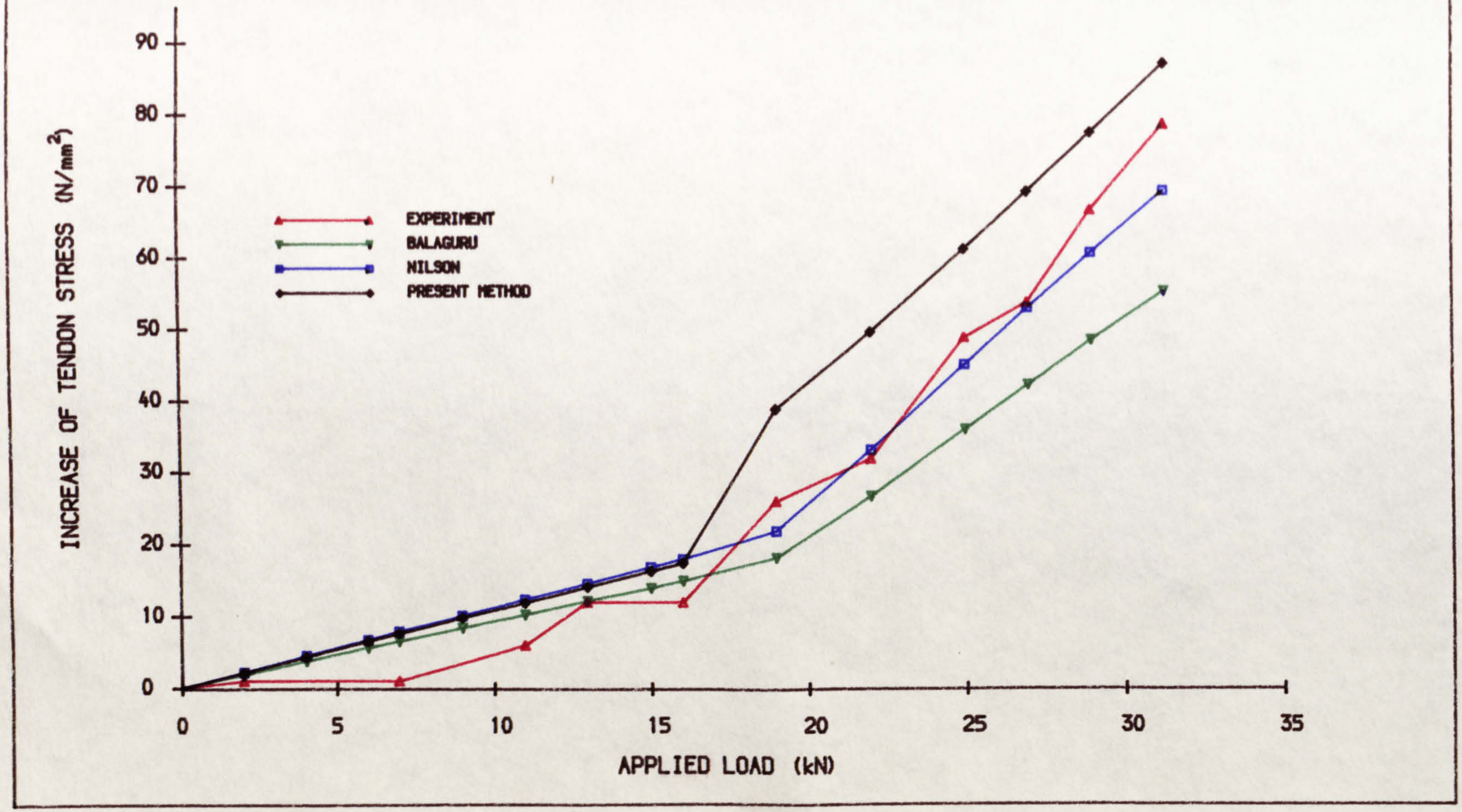

```
C MMMMMMMMMMMMMMMMMMMMMMMMMMMMMMMMMMMMMMMMMMMMMMMMMMMMMMMMMMMMMMMM
C MMMMMMMMM                                                 MMMM
C MMMMMMMMM   Programme to calculate the short-term deflections   MMMM
C MMMMMMMMM   and steel stresses of a partially prestressed con-  MMMM
C MMMMMMMMM   crete beam with unbonded tendons in the first and   MMMM
C MMMMMMMMM   second cycle of loading. The loading pattern is     MMMM
C MMMMMMMMM   symmetrical two points loading.                     MMMM
C MMMMMMMMM                                                 MMMM
C MMMMMMMMMMMMMMMMMMMMMMMMMMMMMMMMMMMMMMMMMMMMMMMMMMMMMMMMMMMMMMMM
C
      CHARACTER*4 INOP
      DIMENSION BMCRF(100),ARSF(100),FRACF(100),CAM(100),
     *          DEFXF(100),DLLF(100),DEFCF(100),DACF(100),
     *          BMCRS(100),ARSS(100),FRACS(100),
     *          DEFXS(100),DLLS(100),DEFCS(100),DACS(100),
     *          CURF(100),CURJCF(100),CURS(100),CURJCS(100),
     *          DEFXD(100),DDL(100),ARSD(100),CURD(100),
     *          DEFLLF(100),RSLLF(100),CURLLF(100),
     *          DEFLLS(100),RSLLS(100),CURLLS(100)
C
      COMMON /SECTN/  A,SMA,YINF,RG,E,RL
      COMMON /DIMAR/  HF,HB,HT,BW,BB,BT,AP,AS
      COMMON /LEVMAT/ EC,ES,DP,DS,ALPHA,TSE
      COMMON /LENGTH/ SLV,SLT,SL1(100),SLC
      COMMON /STRAIN/ ECPE,ECRE,ECTE,ECBE
      COMMON /FORCE/  PE,RE
      COMMON /MOMTF/  BMAMF,BMAF(100)
      COMMON /MOMTS/  BMAMS,BMAS(100)
      COMMON /RATIO/  H1,H2,H3,H4,H5,B1,B2,D1,D2,POS,S1,S2,BETA
C
      NSEC= 0
9     WRITE(6,13)
 13   FORMAT(' 1) 1ST  ',2X,'FIRST CYCLE OF LOADING')
      WRITE(6,14)
 14   FORMAT(' 2) 1STF ',2X,'FURTHER INCREMENT IN FIRST CYLCE OF',
     *       ' LOADING')
      WRITE(6,15)
 15   FORMAT(' 3) 2ND  ',2X,'SECOND CYCLE OF LOADING')
      WRITE(6,16)
 16   FORMAT(' 4) END  ',2X,'NO MORE COMPUTATION',/)
      WRITE(6,17)
 17   FORMAT(' <<< SELECT ONE OPTION FROM THE ABOVE INDEX >>>')
C
      READ(5,18,ERR=10)INOP
 18   FORMAT(A4)
      GOTO 20
C
 10   WRITE(6,19)
 19   FORMAT(' <<< INPUT ERROR, RESTART THE PROCEDURE >>>')
      GOTO 9
C
 20   IF( INOP .EQ. '1ST' )GOTO 21
      IF( INOP .EQ. '1STF' )GOTO 22
      IF( INOP .EQ. '2ND' )GOTO 23
      IF( INOP .EQ. 'END' )GOTO 24
```

```
      GOTO 10
C
 21   WRITE(6,25)
 25   FORMAT(' <<< INPUT DATA TO THE PROGRAMME IN THE ORDER',
     *       ' AS SHOWN >>>',/)
      WRITE(6,27)
 27   FORMAT(' Bt  Bb  Bw  Hf  Hb  Ht  dp  ds  (in mm.)')
      READ(5,*,ERR=10)BT,BB,BW,HF,HB,HT,DP,DS
      WRITE(6,28)
 28   FORMAT(' Ap  As  Aduct  (in mm2')
      READ(5,*,ERR=10)AP,AS,ADC
      WRITE(6,30)
 30   FORMAT(' EC  ES  FPE  FRE  FCT  FCTS (IN N/mm2)')
      READ(5,*,ERR=10)EC,ES,FPE,FRE,FCTA,TSE
      WRITE(6,31)
 31   FORMAT(' EFFECTIVE SPAN , VARYING MOMENT SPAN LENGTH (in mm.)')
      READ(5,*,ERR=10)SLT,SLV
      WRITE(6,32)
 32   FORMAT(' WHAT IS THE MOMENT AT SERVICE LOAD ?( in Nmm.)')
      READ(5,*)BMSER
      WRITE(6,33)
 33   FORMAT(' DIVIDE THE BEAM INTO "NP" NO. OF ELEMENTS. " BETA"')
      READ(5,*,ERR=10)NP,BETA
 221  WRITE(6,222)
 222  FORMAT(' WHAT IS THE DEAD LOAD (exclude self-wt.) ? (in N.)')
      READ(5,*)SBW
 22   WRITE(6,34)
  34  FORMAT(' WHAT IS THE APPLIED LIVE LOAD ? (in N.)')
      READ(5,*,ERR=10)ALF
C
      IF( INOP .EQ. '1STF' )GOTO 37
C
      PE= FPE*AP
      RE= FRE*AS
      H1= HF/HT
      H2= HB/HT
      H3= 1-H2
      H4= 3-2*HF/HT
      H5= 2*H2+1
      D1= DP/HT
      D2= DS/HT
      B1= (BT-BW)/BT
      B2= (BB-BW)/BT
      BETA= 1-BETA
      ALPHA= ES/EC
      POS= 6*ALPHA*AS/(BT*HT)
      SLC= SLT-(2*SLV)
      C6= (SLV+SLC)/SLT
      NH= (NP+1)/2
C*************************************************************
C  Calculate the section properties
C*************************************************************
      CALL SECT ( ACTA,ADC,IBON )
C
      YSUP= HT-YINF
```

```
      YSUP1= HT-YINF1
C*************************************************************
C  Calculate the concrete stresses and the effective prestrain
C*************************************************************
      FYINE= -PE*(1+E*YINF/RG)/A+RE*(-RL*YINF/RG-1)/A
      FSUPE= PE*(-1+E*YSUP/RG)/A+RE*( RL*YSUP/RG-1)/A
      FYINS= -PE*(1+E*YINF/RG)/A+BMSER*YINF/(RG*A)
      FYINH= -PE*(1+E*YINF/RG)/A+BMSER*YINF/(RG*A*2.0)
      FSUPS= PE*(-1+E*YSUP/RG)/A-BMSER*YINF/(RG*A)
      FSUPH= PE*(-1+E*YSUP/RG)/A-BMSER*YINF/(RG*A*2.0)
      ECBE= FYINE/EC
      ECTE= FSUPE/EC
      ECPE= (ECBE-ECTE)*DP/HT+ECTE
      ECRE= (ECBE-ECTE)*DS/HT+ECTE
C
      DEL= SLT/NP
      C1= ALPHA*AP*(1+E**2/RG)/A
C*************************************************************
C  Calcualte the deflection due to dead load in the first cycle
C*************************************************************
      CCC= (0.75*SLV/SLT-(SLV/SLT)**3)*32
      BSW= (ACTA*23.6E-6*SLT*5)/CCC
      DLOAD= SBW+BSW
      BMAMF= DLOAD*SLV/2
C
      DO 3721 I=1,NH
      SL1(I)= DEL/2+DEL*(I-1)
      IF ( SL1(I) .GE. SLV )THEN
      BMAF(I)= BMAMF
      GOTO 3721
      END IF
      BMAF(I)= BMAMF*SL1(I)/SLV
 3721 CONTINUE
C
      CALL FIRST( C1,C6,NP,NH,FCTA,
     *            PCRJF,RCRJF,ECPCJF,ECRCJF,EPTCD,
     *            BMCRF,DEFCF,DEFXD,CAM,DDL,DACF,
     *            FPACF,ATSD,FRACF,ARSD,TSF,SLJF,FFMF,CURD,
     *            CURJCF,FCTMD,BSW,ECRCCF )
C*************************************************************
C  Calculate the deflection due to total load in the first cycle
C*************************************************************
 37   BMAMF= (DLOAD+ALF)*SLV/2
      DO 371 I= 1,NH,1
      IF( SL1(I) .GE. SLV )THEN
      BMAF(I)= BMAMF
      GOTO 371
      END IF
      BMAF(I)= BMAMF*SL1(I)/SLV
371   CONTINUE
      CALL FIRST ( C1,C6,NP,NH,FCTA,
     *             PCRJF,RCRJF,ECPCJF,ECRCJF,EPTCF,
     *             BMCRF,DEFCF,DEFXF,CAM,DLLF,DACF,
     *             FPACF,ATSF,FRACF,ARSF,TSF,SLJF,FFMF,CURF,CURJCF,
     *             FCTMF,BSW,ECRCCF )
```

```
C
      BMAMFK= BMAMF/1.0E+06
      ALFK= ALF/1.0E+03
      TSLLF= ATSF-ATSD
      DO 362 I=1,NP
      DEFLLF(I)= DLLF(I)-DDL(I)
      RSLLF(I)= ARSF(I)-ARSD(I)
      CURLLF(I)= CURF(I)-CURD(I)
 362  CONTINUE
C*************************************************************************
C  Print out results for the first cycle
C*************************************************************************
      WRITE(7,35)
 35   FORMAT(1H1,T6,'FIRST CYCLE OF LOADING',/5X,'------------',
     *       '------------',/)
      WRITE(7,351)
 351  FORMAT(1HO,' I) AT THE CRACKED SECTION :--')
C
      WRITE(7,352)BMAMFK,ALFK
 352  FORMAT(1HO,T6,'MAXIMUM MOMENT',7X,'= ',F9.4,2X,'kNm.',
     *          /5X,'LIVE LOAD  (LL)       = ',F9.4,2X,'kN.')
C
      WRITE(7,353)ATSF,TSLLF,FCTMF
 353  FORMAT(1H ,T6,'ACTUAL TENDON STRESS = ',F6.1,5X,'N/sq.mm.',
     *          /5X,'TENDON STRESS (LL)   = ',F6.1,5X,'N/sq.mm.',
     *          /5X,'TOP CONCRETE STRESS  = ',F6.2,5X,'N/sq.mm.')
C
      WRITE(7,354)FPACF
 354  FORMAT(1H ,T6,'INCREASE IN TENDON    = ',F6.1,5X,'N/sq.mm.',/5X,
     *          'STRESS AFTER CRACK"G')
C
      WRITE(7,355)TSF,FFMF,SLJF
 355  FORMAT(1H ,T6,'X/Ht',17X,'= ',F5.3,/5X,'STRAIN FACTOR',
     *       8X,'= ',E8.3,/5X,'LAST CRACK FROM END  = ',F6.0,
     *       5X,'mm.',/)
C
      WRITE(7,356)
 356  FORMAT(1H ,'II) AT SECTIONS ALONG THE BEAM :--')
C
 397  WRITE(7,357)
 357  FORMAT(1HO,T6,'SECTION',4X,'CRACKING',6X,'N.P.S.STRESS',20X,
     *          'DEFLECTION (in mm.) DUE TO:-'
     *           ,16X,'CURVATURE DUE TO :-',/7X,'Lx',6X,
     *          'MOMEMT,Mcr',4X,'ACTUAL',3X,'AFTER',8X,'CAMBER',3X,
     *          'CAMBER &',3X,' LL+DL',6X,'AT',9X,'AFTER',
     *           7X,'LL+DL & ',5X,'AT')
C
      WRITE(7,358)
 358  FORMAT(1H ,T38,'CRACKING',15X,'LL+DL ',14X,'CRACKING',5X,
     *           'CRACKING',5X,'CAMBER',4X,
     *           'CRACKING',/6X,'(mm)',7X,'(Nmm)',9X,'(N/sq.mm.)',/1X,
     *       '----------------------------------------------------',
     *       '----------------------------------------------------',
     *       '-------------------------------',/)
C
```

```
      IF( INOP .EQ. '2ND' )GOTO 398
C
      WRITE(7,359)(I,SL1(I),BMCRF(I),ARSF(I),FRACF(I),CAM(I),DEFXF(I),
     *             DLLF(I),DEFCF(I),DACF(I),CURF(I),CURJCF(I),I= 1,NH)
      WRITE(12,238)BMCRF(NH)
 238  FORMAT(2X,F18.2)
 359  FORMAT(1H ,I2,') ',F5.0,4X,F9.0,5X,F6.1,3X,F6.1,6X,F8.3,
     *       2X,F8.3,3X,F8.3,3X,F8.3,3X,F8.3,3X,E11.4,3X,E11.4)
C
      WRITE(7,3591)
 3591 FORMAT(1HO,T6,'SECTION',4X,'N.P.S.STRESS',4X,'DEFLECTION',4X,
     *       'CURVATURE',/7X,'Lx',9X,'[L.LOAD]',7X,'[L.LOAD]',5X,
     *       '[L.LOAD]',/6X,'(mm)',7X,'(N/sq.mm.)',9X,'(mm)',8X,
     *       '(1/mm)',/1X,'-----------------------------',
     *                    '-----------------------------',/)
C
      WRITE(7,3592)(I,SL1(I),RSLLF(I),DEFLLF(I),CURLLF(I),I=1,NH)
 3592 FORMAT(1H ,I2,') ',F5.0,8X,F6.1,9X,F8.3,6X,E11.4)
C
 360  FORMAT(5X,F16.6,4X,F16.6)
C
      WRITE(8,361)BMAMFK,ALFK,ATSF,ARSF(NH),TSF,FFMF,FCTMF
 361  FORMAT(1X,F8.4,2X,F8.4,2X,F9.3,2X,F9.3,2X,F8.5,2X,F8.5,2X,F8.4)
C
      WRITE(10,3601)ALFK,TSLLF,RSLLF(NH)
      WRITE(13,360)DEFLLF(NH),ALFK
      WRITE(20,9100)ALFK,ECRCCF,CURF(NH)
 9100 FORMAT(F5.2,5X,E18.5,5X,E18.5)
 3601 FORMAT(1X,F8.3,2X,F6.1,2X,F8.3)
C
 41   GOTO 9
C
C*************************************************************************
C  Calculate the deflection due to dead load in the second cycle
C*************************************************************************
 23   WRITE(6,38)
 38   FORMAT(' WHAT IS THE APPLIED LIVE LOAD ? (in N.)')
      READ(5,*,ERR=10)ALS
C
      IF( NSEC .EQ. 2 )GOTO 3812
      BMAMS= DLOAD*SLV/2
      DO 3811 I=1,NH
      IF( SL1(I) .GE. SLV )THEN
      BMAS(I)= BMAMS
      GOTO 3811
      END IF
      BMAS(I)= BMAMS*SL1(I)/SLV
 3811 CONTINUE
C
      CALL SECOND ( PCRJF,RCRJF,ECPCJF,ECRCJF,EPTCF,
     *              PCRJS,RCRJS,ECPCJS,ECRCJS,EPTCD,
     *              C1,C6,NP,NH,FCTA,
     *              BMCRS,DEFCS,DEFXD,CAM,DDL,DACS,
     *              FPACS,ATSD,FRACS,ARSD,TSS,SLJS,
     *              SLJF,BMAMF,FFMS,CURD,CURJCS,FCTMD,BSW )
```

```
C*************************************************************************
C  Calculate the deflection due to total load in the second cycle
C*************************************************************************
 3812 BMAMS= (DLOAD+ALS)*SLV/2
      DO 381 I= 1,NH
      IF( SL1(I) .GE. SLV )THEN
      BMAS(I)= BMAMS
      GOTO 381
      END IF
      BMAS(I)= BMAMS*SL1(I)/SLV
 381  CONTINUE
C
 3817 CRACK= SLT/2.0
      IF( SLJF .EQ. SLV .OR. SLBF .EQ. CRACK )THEN
      WRITE(6,382)
 382  FORMAT(' <<< BEAM REMAIN UNCRACKED IN FIRST CYCLE OF LOADING',
     *       /4X,'SELECT OPTION "1ST" OR "1STF" INSTEAD >>>',/)
      GOTO 9
      END IF
C
      CALL SECOND ( PCRJF,RCRJF,ECPCJF,ECRCJF,EPTCF,
     *              PCRJS,RCRJS,ECPCJS,ECRCJS,EPTCS,
     *              C1,C6,NP,NH,FCTA,
     *              BMCRS,DEFCS,DEFXS,CAM,DLLS,DACS,
     *              FPACS,ATSS,FRACS,ARSS,TSS,SLJS,
     *              SLJF,BMAMF,FFMS,CURS,CURJCS,FCTMS,BSW )
C
      BMAMSK= BMAMS/1.0E+06
      ALSK= ALS/1.0E+03
      TSLLS= ATSS-ATSD
      DO 3901 I= 1,NP
      DEFLLS(I)= DLLS(I)-DDL(I)
      RSLLS(I)= ARSS(I)-ARSD(I)
      CURLLS(I)= CURS(I)-CURD(I)
 3901 CONTINUE
C
C*************************************************************************
C  Print out results for the second cycle of loading
C*************************************************************************
      WRITE(7,39)
 39   FORMAT(1H1,T6,'SECOND CYCLE OF LOADING',
     *       /5X,'-----------------------',/)
      WRITE(7,391)
 391  FORMAT(1HO,' I) AT THE CRACKED SECTION :--')
C
      WRITE(7,392)BMAMSK,ALSK
 392  FORMAT(1HO,T6,'MAXIMUM MOMENT',7X,'= ',F9.4,2X,'kNm.',
     *       /5X,'LIVE LOAD  (LL)       = ',F9.4,2X,'kN.')
C
      WRITE(7,393)ATSS,TSLLS,FCTMS
 393  FORMAT(1H ,T6,'ACTUAL TENDON STRESS = ',F6.1,5X,'N/sq.mm.',
     *       /5X,'TENDON STRESS (LL)   = ',F6.1,5X,'N/sq.mm.',
     *       /5X,'TOP CONCRETE STRESS  = ',F6.2,5X,'N/sq.mm.')
C
      WRITE(7,394)FPACS
```

```
 394  FORMAT(1H ,T6,'INCREASE IN TENDON    = ',F6.1,5X,'N/sq.mm.',/5X,
     *           'STRESS AFTER CRACK"G')
C
      WRITE(7,395)TSS,FFMS,SLJS
 395  FORMAT(1H ,T6,'X/Ht',17X,'= ',F5.3,/5X,'STRAIN FACTOR',8X,
     *       '= ',E8.3,/5X,'LAST CRACK FROM END  = ',F6.0,5X,
     *       'mm.',/)
C
      WRITE(7,396)
 396  FORMAT(1H ,'II) AT SECTIONS ALONG THE BEAM :--')
C
      GOTO 397
C
 398  WRITE(7,399)(I,SL1(I),BMCRS(I),ARSS(I),FRACS(I),CAM(I),DEFXS(I),
     *              DLLS(I),DEFCS(I),DACS(I),CURS(I),CURJCS(I),I= 1,NH)
      WRITE(12,238)BMCRS(NH)
 399  FORMAT(1H ,I2,') ',F5.0,4X,F9.0,5X,F6.1,3X,F6.1,6X,F8.3,
     *              2X,F8.3,3X,F8.3,3X,F8.3,3X,F8.3,3X,E11.4,3X,E11.4)
C
      WRITE(7,3591)
      WRITE(7,3592)(I,SL1(I),RSLLS(I),DEFLLS(I),CURLLS(I),I= 1,NH)
      WRITE(10,3601)ALSK,TSLLS,RSLLS(NH)
      WRITE(13,360)DEFLLS(NH),ALSK
      WRITE(8,361)BMAMSK,ALSK,ATSS,ARSS(NH),TSS,FFMS,FCTMS
C
      IF( SLJS .LT. SLJF )THEN
      SLJF= SLJS
      BMAMF= BMAMS
      PCRJF= PCRJS
      RCRJF= RCRJS
      ECPCJF= ECPCJS
      ECRCJF= ECRCJS
      EPTCF= EPTCS
      END IF
C
 40   NSEC= 2
      GOTO 9
C
 24   WRITE(11,360)(SL1(I),DEFLLF(I),I=1,NP)
      WRITE(11,360)(SL1(I),DEFLLS(I),I=1,NP)
 433  STOP
      END
C
C SSSSSSSSSSSSSSSSSSSSSSSSSSSSSSSSSSSSSSSSSSSSSSSSSSSSSSSSSSSSSSSSSSSSSSS
C SSSSSSSSS   Subprogramme to calculate the deflected profile and
C SSSSSSSSS   steel stresses along the beam in the first cycle of
C SSSSSSSSS   loading.
C SSSSSSSSSSSSSSSSSSSSSSSSSSSSSSSSSSSSSSSSSSSSSSSSSSSSSSSSSSSSSSSSSSSSSSS
C
      SUBROUTINE FIRST ( C1,C6,NP,NH,FCTA,
     *                   PCRJF,RCRJF,ECPCJF,ECRCJF,EPTCF,
     *                   BMCRF,DEFCF,DEFXF,CAM,DLLF,DACF,
     *                   FPACF,ATSF,FRACF,ARSF,TSF,SLJF,FFMF,
     *                   CURF,CURJCF,FCTMF,DLOAD,ECRAVE )
C
```

```
      COMMON /SECTN/  A,SMA,YINF,RG,E,RL
      COMMON /DIMAR/  HF,HB,HT,BW,BB,BT,AP,AS
      COMMON /LEVMAT/ EC,ES,DP,DS,ALPHA,TSE
      COMMON /LENGTH/ SLV,SLT,SL1(100),SLC
      COMMON /STRAIN/ ECPE,ECRE,ECTE,ECBE
      COMMON /FORCE/  PE,RE
      COMMON /MOMTF/  BMAMF,BMAF(100)
      COMMON /RATIO/  H1,H2,H3,H4,H5,B1,B2,D1,D2,POS,S1,S2,BETA
C
      DIMENSION  FRACF(100),FRF(100),ARSF(100),CURF(100),
     *           CURJCF(100),CURCAM(100),BMCRF(100),
     *           CAM(100),DLLF(100),DACF(100),DEFCF(100),DEFXF(100),
     *           PCRF(100),RCRF(100),ECPCF(100),ECRCF(100),EPF(100)
C
      REAL*8  COZ(3),REZ(3),AR(4),TOL
C
      S1= (BB*HT**2-(BB-BW)*(HT-HB)**2+(BT-BW)*HF**2)/(2*HT)
      S2= (BT*HT**2-(BT-BW)*(HT-HF)**2+(BB-BW)*HB**2)/(2*HT)
C
      ECREX= ECRE
      ECPEX= ECPE
      ECPE=ABS(ECPE)
      ECRE=ABS(ECRE)
C**********************************************************************
C  To analyse the critical section while it is at the point of cracking
C  i.e. under cracking moment, BMCRMF.
C**********************************************************************
C
      FJMFD=999.0
      FJMF=1.0
C
      DO 918 K=1,50
      FJMF0=FJMF
      FCCRMF= (PE+(ECPE+DP*FCTA/(EC*HT))*FJMF*AP*ES+
     1          RE+(ECRE+DS*FCTA/(EC*HT))*AS*ES+S1*FCTA)/
     2         (S2+(HT-DP)*FJMF*AP*ES/(EC*HT)+(HT-DS)*
     3          AS*ES/(EC*HT))
C
      FCCRMF=ABS(FCCRMF)
      CXM= (FCCRMF*HT)/(FCCRMF+FCTA)
      ECPCMF= (FCCRMF+FCTA)*(DP-CXM)/(EC*HT)
      ECRCMF= (FCCRMF+FCTA)*(DS-CXM)/(EC*HT)
      PCRMF= PE+(ECPE+ECPCMF)*FJMF*AP*ES
      RCRMF= RE+(ECRE+ECRCMF)*AS*ES
C
      FTCRM= FCTA*BB*(HT-CXM)/2-FCTA*(BB-BW)*(HT-CXM-HB)**2/
     *       (2*(HT-CXM))
      FCRMF= FCCRMF*BT*CXM/2-FCCRMF*(BT-BW)*(CXM-HF)**2/(2*CXM)
      CRM= CXM/HT
      ZCMF= HT*(CRM**2*(3-CRM)-B1*(CRM-H1)**2*(H4-CRM))/
     *      (3*CRM**2-3*B1*(CRM-H1)**2)
C
      ZTMF=HT*((1-CRM)**3-B2*(H3-CRM)**2*(H5-CRM))/(3*((1-CRM)**2-
     *     B2*(H3-CRM)**2))
      BMCRMF= FCRMF*ZCMF-PCRMF*(HT-DP)-RCRMF*(HT-DS)-FTCRM*ZTMF
```

```
      EPCRMF= (BMCRMF*E)*C6/(EC*SMA*(1+C1))
C
      FJMFN= EPCRMF/(ECPE+ECPCMF)
      FJMFD= ABS(FJMFN-FJMFO)
      IF (FJMFD .LT. 0.00001)GOTO 4
      FJMF= FJMFN
 918  CONTINUE
C*************************************************************
C  If the applied moment is less than the cracking moment of the
C  critical section, then use uncracked section theory.
C*************************************************************
C
  4   IF( BMAMF .LE. BMCRMF )THEN
      WRITE(6,31)
 31   FORMAT(' <<< Beam uncracked >>>')
C
      BMIL= DLOAD*SLV/2.0
      DO 993 I=1,NH
      EPOIL= BMIL*E*C6/(EC*SMA*(1+C1))
      IF(SL1(I).LT.SLV)THEN
      ECPIL= BMIL*SL1(I)*E/(SMA*EC*SLV)-EPOIL*C1
      ECRIL= BMIL*SL1(I)*RL/(SMA*EC*SLV)-EPOIL*ALPHA*AP*(1+E*RL/RG)/A
      ELSE IF(SL1(I).GE.SLV)THEN
      ECPIL= BMIL*E/(SMA*EC)-EPOIL*C1
      ECRIL= BMIL*RL/(SMA*EC)-EPOIL*ALPHA*AP*(1+E*RL/RG)/A
      END IF
C
      EPO= BMAMF*E*C6/(EC*SMA*(1+C1))
      ECP= BMAF(I)*E/(SMA*EC)-EPO*C1
      ECR= BMAF(I)*RL/(SMA*EC)-EPO*ALPHA*AP*(1+E*RL/RG)/A
      FPF= EPO*ES
      FPACF= 0.00
      FRACF(I)= 0.0
C
      ATSF= PE/AP+FPF-ECPIL*ES
      FRF(I)= 0.0
      ARSF(I)= 0.0
      IF( AS .EQ. 0.0 )GOTO 99
      FRF(I)= ECR*ES
      ARSF(I)= RE/AS+FRF(I)-ECRIL*ES
 99   FCT= ECTE*EC-BMAF(I)*(DP-E)/SMA+EPO*ES*AP*(E*(DP-E)/RG-1)/A
      FCTMF= FCT
C
      ECRA= ECREX+ECR
      ECRAVE= ARSF(I)/ES
      IF(AS.EQ.0.0)ECRAVE=ECRA
      CURF(I)= (ECRA-FCT/EC)/DS
      CONT= ECP-ECPIL
      IF(CONT .EQ. 0.00)THEN
      FFMF= 0.0
      GOTO 369
      END IF
      FFMF= (EPO-EPOIL)/(ECP-ECPIL)
 369  TSF= 0.0
      SLJF= SLV
```

```
      BMCRF(I)= 0.0
  993 CONTINUE
      GOTO 22
      END IF
C*************************************************************
C  If the critical section has cracked then use cracked section theory,
C  hence to determine the last cracked position from the support,SLJF,
C  and the average tendon stress along the beam.
C*************************************************************
C
      WRITE(6,1014)
 1014 FORMAT(' *** CRACKED ***')
      FFJF= 1.0
      FFMF= 1.0
      FFJFD= 999.0
      FFMFD= 999.0
C
      DO 321 J=1,50
      FFJF0= FFJF
      FFMF0= FFMF
      FCCRJF= (PE+(ECPE+DP*FCTA/(EC*HT))*FFJF*AP*ES+
     1          RE+(ECRE+DS*FCTA/(EC*HT))*AS*ES+S1*FCTA)/
     2          (S2+(HT-DP)*FFJF*AP*ES/(EC*HT)+(HT-DS)*AS
     3          *ES/(EC*HT))
C
      FCCRJF= ABS(FCCRJF)
      CXJ= (FCCRJF*HT)/(FCCRJF+FCTA)
      ECPCJF= (FCCRJF+FCTA)*(DP-CXJ)/(EC*HT)
      ECRCJF= (FCCRJF+FCTA)*(DS-CXJ)/(EC*HT)
      PCRJF= PE+(ECPE+ECPCJF)*FFJF*AP*ES
      RCRJF= RE+(ECRE+ECRCJF)*AS*ES
C
      FTCRJ= FCTA*BB*(HT-CXJ)/2-FCTA*(BB-BW)*(HT-CXJ-HB)**2/
     *       (2*(HT-CXJ))
      FCRJF= FCCRJF*BT*CXJ/2-FCCRJF*(BT-BW)*(CXJ-HF)**2/(2*CXJ)
      CRJ=CXJ/HT
      ZCJF= HT*(CRJ**2*(3-CRJ)-B1*(CRJ-H1)**2*(H4-CRJ))/(3*CRJ
     *      **2-3*B1*(CRJ-H1)**2)
C
      ZTJF= HT*((1-CRJ)**3-B2*(H3-CRJ)**2*(H5-CRJ))/(3*((1-CRJ)**2-
     *      B2*(H3-CRJ)**2))
      BMCRJF= FCRJF*ZCJF-PCRJF*(HT-DP)-RCRJF*(HT-DS)-FTCRJ*ZTJF
C
      SLJF= BMCRJF*SLV/BMAMF
C
      C3= PCRMF+RCRMF-ECPCMF*FFMF*AP*ES-ECRCMF*AS*ES
      C4= (PCRMF-ECPCMF*FFMF*AP*ES)*(HT-DP)+(RCRMF-ECRCMF
     *    *AS*ES)*(HT-DS)
      C5= (BMAMF+C4)/HT
      POP= (6*ALPHA*AP*FFMF)/(BT*HT)
C*************************************************************
C  Use NAG Routine to solve the cubic equation of neutral axis of the
C  section under maximum moment and determine the concrete stress at
C  the top , the non-prestressed steel stress and curvature.
C*************************************************************
```

```
C
      B1G= B1
      N= 0
 8    N=N+1
      W1= C3*(B1-1)
      W2= C3*(3-B1*H4-2*B1*H1)-C5*(3-3*B1)
      W3= C3*(2*B1*H1*H4+B1*H1**2+POP*(1-D1)+POS*(1-D2))-
     *    C5*(6*B1*H1+POP+POS)
      W4= -C3*(B1*H1**2*H4+D1*POP*(1-D1)+D2*POS*(1-D2))+
     *    C5*(3*B1*H1**2+D1*POP+D2*POS)
C
      N9= 4
      AR(1)= W1
      AR(2)= W2
      AR(3)= W3
      AR(4)= W4
      N91=N9-1
      TOL=1.0*10.0**(-11.0)
      IFAIA=0
C
      CALL CO2AEF ( AR,N9,REZ,COZ,TOL,IFAIA )
C
      IF( N .GT. 1 )GOTO 44
C
C     Is N.A. within the web ?
C
      DO 30 M=1,N91
      IF( COZ(M) .NE. 0.00 )GOTO 30
      IF( REZ(M) .LE. H3 .AND. REZ(M) .GT. H1 )GOTO 50
 30   CONTINUE
C
C     Is N.A. within the Top Flange ?
C
      DO 34 M=1,N91
      IF( COZ(M) .NE. 0.00 )GOTO 34
      IF( REZ(M) .LE. H1 .AND. REZ(M) .GE. 0.00 )GOTO 40
 34   CONTINUE
C
      KKK= 1001
      GOTO 60
C
C     If N.A. within the Top Flange, then
C
 40   B1= 0.0
      GOTO 8
 44   DO 46 M= 1,N91
      IF( COZ(M) .NE. 0.00 )GOTO 46
      IF( REZ(M) .LE. H1 .AND. REZ(M) .GE. 0.00 )GOTO 50
 46   CONTINUE
C
      KKK= 1002
      GOTO 60
C
 50   TSF= REZ(M)
      FCTMF= C3*6*TSF/(BT*HT)/(3*TSF**2-3*B1*(TSF-H1)**2-POP*
```

```
     *       (D1-TSF)-POS*(D2-TSF))
      B1= B1G
C
 250  ECBF= FCTMF*(1/TSF-1)/EC
      X= TSF*HT
      ECPMF= ABS(FCTMF)*(DP-X)/(EC*X)
      ECRMF= ABS(FCTMF)*(DS-X)/(EC*X)
      ECPUF= BMCRJF*E/((2*EC*SMA)*(1+C1))
      ECPCVF= ((ECPMF+ECPCJF)/2+TSE*(1/BETA-1)/EC)*BETA+ECPE
C
      ECPCCF= (ECPMF+TSE*(1/BETA-1)/EC)*BETA+ECPE
      EPTCF= (2*SLJF*ECPUF+(SLV-SLJF)*2*ECPCVF+SLC*ECPCCF)/SLT
      FPACF= (EPTCF-EPCRMF)*ES
      FPF= EPTCF*ES
      ATSF= PE/AP+FPF
      FRMF= 0.0
      FRACMF= 0.0
      ARSMF= 0.0
C
      IF( AS .EQ. 0.0 )THEN
      ECRAVE= (ECPCCF-ECPE)*(DS-X)/(DP-X)
      GOTO 123
      END IF
      FRMF= (ECRMF+ECRE)*ES
      FRACMF= (ECRMF-ECRCMF)*ES
      ARSMF= RE/AS+FRMF
      ECRAVE= (ECPCCF-ECPE)*(DS-X)/(DP-X)
 123  CURMF= (FCTMF+(ECPMF*EC-TSE)*BETA+TSE)/(EC*DP)
C
      FCTMF= -FCTMF
      FFJFN= EPTCF/(ECPE+ECPCJF)
      FFMFN= (EPTCF-EPCRMF)/(ECPMF-ECPCMF)
      FFJF= FFJFN
      FFMF= FFMFN
      FFJFD= ABS(FFJFN-FFJFO)
      FFMFD= ABS(FFMFN-FFMFO)
C
      IF( FFJFD .LT. 0.00001 .AND. FFMFD .LT. 0.00001 )GOTO 278
 321  CONTINUE
C*************************************************************
C  Compute the curvatures of other sections along the beam and
C  calculate the deflection by integration of curvature.
C*************************************************************
C
 278  CALL CRBMF ( PCRMF,RCRMF,ECPCMF,ECRCMF,BMCRMF,FCCRMF,EPCRMF,SLJF,
     *             PCRF,RCRF,ECPCF,ECRCF,BMCRF,EPF,
     *             NH,C1,C6,FCTA )
C
      DO 1000 I= 1,NH
      FFCF= 1.0
C*************************************************************
C      If the section being considered is within the constant
C      moment zone OR within the varying moment zone but remains
C      uncracked, then :---
C*************************************************************
```

```
      IF( SL1(I) .GE. SLV )THEN
      CURF(I)= CURMF
      ARSF(I)= ARSMF
      FRACF(I)= FRACMF
      FRF(I)= FRMF
      GOTO 1000
C
      ELSE IF( SL1(I) .LE. SLJF )THEN
      FRACF(I)= 0.00
      FRF(I)= 0.0
      ARSF(I)= 0.0
      ECRF= BMAF(I)*RL/(SMA*EC)-EPTCF*ALPHA*AP*(1+E*RL/RG)/A
      IF( AS .EQ. 0.00 )GOTO 7
C
      FRF(I)= ECRF*ES
      ARSF(I)= RE/AS+FRF(I)
 7    FCT= ECTE*EC-BMAF(I)*(DP-E)/SMA+EPTCF*ES*AP*(E*(DP-E)/RG-1)/A
      ECRA= ECREX+ECRF
      CURF(I)= (ECRA-FCT/EC)/DS
      GOTO 1000
      END IF
C*************************************************************
C     If the section being considered is within the varying
C     moment zone but has cracked, then use cracked section theory.
C*************************************************************
C
      FFCFD= 999.0
C
      DO 144 J= 1,50
      FFCFO= FFCF
      C3= PCRF(I)+RCRF(I)-ECPCF(I)*FFCF*AP*ES-ECRCF(I)*AS*ES
      C4= (PCRF(I)-ECPCF(I)*FFCF*AP*ES)*(HT-DP)+(RCRF(I)-
     *     ECRCF(I)*AS*ES)*(HT-DS)
      C5= (BMAF(I)+C4)/HT
      POP= (6*ALPHA*AP*FFCF)/(HT*BT)
C*************************************************************
C     Use NAG Routine to solve the cubic equation of Neutral Axis
C     of the section considered.
C*************************************************************
      KK= 0
 9    KK= KK+1
      W1= C3*(B1-1)
      W2= C3*(3-B1*H4-2*B1*H1)-C5*(3-3*B1)
      W3= C3*(2*B1*H4*H1+B1*H1**2+POP*(1-D1)+POS*(1-D2))-
     *     C5*(6*B1*H1+POP+POS)
C
      W4= -C3*(B1*H1**2*H4+D1*POP*(1-D1)+D2*POS*(1-D2))+
     *      C5*(3*B1*H1**2+D1*POP+D2*POS)
C
      AR(1)= W1
      AR(2)= W2
      AR(3)= W3
      AR(4)= W4
      IFAIB= 0
      N9= 4
```

```
      N91= N9-1
      TOL= 1.0*10.0**(-11)
C
      CALL CO2AEF ( AR,N9,REZ,COZ,TOL,IFAI8 )
C
      IF( KK .GT. 1 )GOTO 84
C
C     Is N.A. within the web ?
C
      DO 85 M= 1,N91
      IF( COZ(M) .NE. 0.00 )GOTO 85
      IF( REZ(M) .LE. H3 .AND. REZ(M) .GT. H1 )GOTO 90
 85   CONTINUE
C
C     Is N.A. within the Top Flange ?
C
      DO 86 M= 1,N91
      IF( COZ(M) .NE. 0.00 )GOTO 86
      IF( REZ(M) .LE. H1 .AND. REZ(M) .GE. 0.00 )GOTO 87
 86   CONTINUE
C
      KKK= 1003
      GOTO 60
C
C     If N.A. within the Top Flange, then
C
 87   B1= 0.0
      GOTO 9
 84   DO 96 M= 1,N91
      IF( COZ(M) .NE. 0.00 )GOTO 96
      IF( REZ(M) .LE. H1 .AND. REZ(M) .GE. 0.00 )GOTO 90
 96   CONTINUE
C
      KKK= 1004
      GOTO 60
C
 90   TS= REZ(M)
      FCTTF= C3*TS*6/(BT*HT)/(3*TS**2-3*B1*(TS-H1)**2-POP*
     *          (D1-TS)-POS*(D2-TS))
      B1=B1G
C
      ECBF= FCTTF*(1/TS-1)/EC
      X= TS*HT
      ECPF= ABS(FCTTF)*(DP-X)/(EC*X)
      ECRF= ABS(FCTTF)*(DS-X)/(EC*X)
      FRACF(I)= 0.00
      FRF(I)= 0.00
      ARSF(I)= 0.00
C
      IF( AS .EQ. 0.00 )GOTO 149
      FRACF(I)= (ECRF-ECRCF(I))*ES
      FRF(I)= (ECRF+ECRE)*ES
      ARSF(I)= RE/AS+FRF(I)
 149  CURF(I)= (FCTTF+(ECPF*EC-TSE)*BETA+TSE)/(EC*DP)
      FFCFN= (EPTCF-EPF(I))/(ECPF-ECPCF(I))
```

```
      FFCFD= ABS(FFCFN-FFCF0)
C
      IF( FFCFD .LT. 0.00001 )GOTO 1000
      FFCF=FFCFN
 144  CONTINUE
C
      KKK= 1005
 60   WRITE(6,70)KKK,I
      WRITE(7,70)KKK,I
 70   FORMAT(T3,'ERROR IN SUBROUINE FIRST, ERROR NO.:--',I4,2X,I2)
      GOTO 1001
C
 1000 CONTINUE
 22   EPJF= BMCRMF*E*C6/(EC*SMA*(1+C1))
      DO 323 KP= 1,NH
      IF( SL1(KP) .GE. SLV )THEN
      BMCF= BMCRMF
      GOTO 322
      END IF
      BMCF= BMCRMF*SL1(KP)/SLV
 322  ECTCR= ECTE-BMCF*(DP-E)/(SMA*EC)+EPJF*ALPHA*AP*(
     *        E*(DP-E)/RG-1)/A
      ECBCR= ECBE+BMCF*YINF/(SMA*EC)-EPJF*ALPHA*AP*(1+
     *        E*YINF/RG)/A
      CURJCF(KP)= (ECBCR-ECTCR)/HT
 323  CONTINUE
      DO 3231  I=1,NH
 3231 CURCAM(I)= (ECBE-ECTE)/HT
C
      CALL DEFL ( CURJCF,NP,DEFCF )
C
      CALL DEFL ( CURF,NP,DEFXF )
C
      CALL DEFL ( CURCAM,NP,CAM )
C
      DO 716 I= 1,NP
      DLLF(I)= DEFXF(I)-CAM(I)
      IF( BMAMF .LE. BMCRMF )THEN
      DACF(I)= 0.00
      GOTO 716
      END IF
      DACF(I)= DEFXF(I)-DEFCF(I)
 716  CONTINUE
      ECRE= ECREX
      ECPE= ECPEX
C
 1001 RETURN
      END
C SSSSSSSSSSSSSSSSSSSSSSSSSSSSSSSSSSSSSSSSSSSSSSSSSSSSSSSSSSSSSSSSSSSSSSS
C SSSSSSSSS   Subprogramme to compute the cracking moment along the
C SSSSSSSSS   beam which takes into account of the tensile srength
C SSSSSSSSS   of concrete before cracking. The steel stresses and
C SSSSSSSSS   curvatures in a particular section under corresponding
C SSSSSSSSS   cracking moment can also be obtained.
C SSSSSSSSSSSSSSSSSSSSSSSSSSSSSSSSSSSSSSSSSSSSSSSSSSSSSSSSSSSSSSSSSSSSSSS
```

```
C
      SUBROUTINE CRBMF ( PCRMF,RCRMF,ECPCMF,ECRCMF,BMCRMF,FCCRMF,
     *                   EPCRMF,SLJF,
     *                   PCRF,RCRF,ECPCF,ECRCF,BMCRF,EPF,
     *                   NH,C1,C6,FCTA )
C
      COMMON /SECTN/   A,SMA,YINF,RG,E,RL
      COMMON /DIMAR/   HF,HB,HT,BW,BB,BT,AP,AS
      COMMON /LEVMAT/  EC,ES,DP,DS,ALPHA,TSE
      COMMON /LENGTH/  SLV,SLT,SL1(100),SLC
      COMMON /STRAIN/  ECPE,ECRE,ECTE,ECBE
      COMMON /FORCE/   PE,RE
      COMMON /RATIO/   H1,H2,H3,H4,H5,B1,B2,D1,D2,POS,S1,S2,BETA
C
      DIMENSION ECPCF(100),ECRCF(100),PCRF(100),RCRF(100),
     *          BMCRF(100),FCCRF(100),EPF(100)
      REAL*8 COZ(3),REZ(3),AR(4),TOL
C*********************************************************************
C  Use iteration process to compute the cracking moment at a
C  particular section, say SLI(I).
C*********************************************************************
C
      DO 1 I= 1,NH
      FJF= 1.0
      FMF= 1.0
      FJFD= 999.0
      FMFD= 999.0
      DO 2 J=1,50
      FJF0=FJF
      FMF0=FMF
C*********************************************************************
C     If the section being considered is within the constant moment
C     zone, then :---
C*********************************************************************
C
      IF( SL1(I) .GE. SLV )THEN
      ECPCF(I)= ECPCMF
      ECRCF(I)= ECRCMF
      PCRF(I)= PCRMF
      RCRF(I)= RCRMF
      BMCRF(I)= BMCRMF
      FCCRF(I)= FCCRMF
      EPF(I)= EPCRMF
      GOTO 1
C*********************************************************************
C     OR if the section being considered is uncracked i.e.
C     SL1(I) .LE. SLJF , then the computation of cracking
C     moment of that particular section does not required.
C*********************************************************************
      ELSE IF( SL1(I) .LE. SLJF )THEN
      ECPCF(I)= 0.0
      ECRCF(I)= 0.0
      PCRF(I)= 0.0
      RCRF(I)= 0.0
      BMCRF(I)= 0.0
```

```
      FCCRF(I)= 0.0
      EPF(I)= 0.0
      GOTO 1
      END IF
C*************************************************************
C     If the section being considered has cracked but within the
C     varying moment zone, the cracking moment can be calculated
C     as follows:---
C*************************************************************
      FCCRF(I)= (PE+(ECPE+DP*FCTA/(EC*HT))*FJF*AP*ES+
     1           RE+(ECRE+DS*FCTA/(EC*HT))*AS*ES+S1*FCTA)/
     2          (S2+(HT-DP)*FJF*AP*ES/(EC*HT)+(HT-DS)*AS*
     3           ES/(EC*HT))
C
      FCCRF(I)= ABS(FCCRF(I))
      CX= (FCCRF(I)*HT)/(FCCRF(I)+FCTA)
      ECPCF(I)= (FCCRF(I)+FCTA)*(DP-CX)/(EC*HT)
      ECRCF(I)= (FCCRF(I)+FCTA)*(DS-CX)/(EC*HT)
      PCRF(I)= PE+(ECPE+ECPCF(I))*FJF*AP*ES
      RCRF(I)= RE+(ECRE+ECRCF(I))*AS*ES
C
      FTCRF= FCTA*BB*(HT-CX)/2-FCTA*(BB-BW)*(HT-CX-HB)**2/
     *       (2*(HT-CX))
      FCRF= FCCRF(I)*BT*CX/2-FCCRF(I)*(BT-BW)*(CX-HF)**2/(2*CX)
      CR=CX/HT
      ZCF= HT*(CR**2*(3-CR)-B1*(CR-H1)**2*(H4-CR))/(3*CR**2-
     *     3*B1*(CR-H1)**2)
      ZTF= HT*((1-CR)**3-B2*(H3-CR)**2*(H5-CR))/(3*((1-CR)**2-B2*
     *     (H3-CR)**2))
      BMCRF(I)= FCRF*ZCF-PCRF(I)*(HT-DP)-RCRF(I)*(HT-DS)-
     *          FTCRF*ZTF
      BMAX= BMCRF(I)*SLV/SL1(I)
C*************************************************************
C     Cracked section theory involves solving the cubic equation
C     of Neutral Axis of that particular section hence to compute
C     the change in tendon strain. The cubic equation is solved
C     by NAG Routine.
C*************************************************************
C
      C3= PCRMF+RCRMF-ECPCMF*FMF*AP*ES-ECRCMF*AS*ES
      C4= (PCRMF-ECPCMF*FMF*AP*ES)*(HT-DP)+(RCRMF-ECRCMF*AS*ES
     *    )*(HT-DS)
      C5= (BMAX+C4)/HT
      POP= (6*ALPHA*AP*FMF)/(BT*HT)
C
      B1F= B1
      N= 0
 8    N= N+1
      W1= C3*(B1-1)
      W2= C3*(3-B1*H4-2*B1*H1)-C5*(3-3*B1)
      W3= C3*(2*B1*H1*H4+B1*H1**2+POP*(1-D1)+POS*(1-D2))-
     *    C5*(6*B1*H1+POP+POS)
C
      W4= -C3*(B1*H1**2*H4+D1*POP*(1-D1)+D2*POS*(1-D2))+
     *     C5*(3*B1*H1**2+D1*POP+D2*POS)
```

```
C
      N9=4
      AR(1)= W1
      AR(2)= W2
      AR(3)= W3
      AR(4)= W4
      N91= N9-1
      TOL= 1.0*10.0**(-11.0)
      IFAIC= 0
C
      CALL CO2AEF ( AR,N9,REZ,COZ,TOL,IFAIC )
C
      IF( N .GT. 1 )GOTO 44
C
C     Is N.A. within the web ?
      DO 30 M= 1,N91
      IF( COZ(M) .NE. 0.00 )GOTO 30
      IF( REZ(M) .LE. H3 .AND. REZ(M) .GT. H1 )GOTO 50
 30   CONTINUE
C
C     Is N.A. within the Top Flange ?
      DO 34 M= 1,N91
      IF( COZ(M) .NE. 0.00 )GOTO 34
      IF( REZ(M) .LE. H1 .AND. REZ(M) .GE. 0.00 )GOTO 40
 34   CONTINUE
C
      KKK= 1001
      GOTO 60
C
C     If N.A. is within the Top Flange, then :--
 40   B1= 0.0
      GOTO 8
C
 44   DO 46 M= 1,N91
      IF( COZ(M) .NE. 0.0 )GOTO 46
      IF( REZ(M) .LE. H1 .AND. REZ(M) .GE. 0.00 )GOTO 50
 46   CONTINUE
C
      KKK= 1002
      GOTO 60
C
 50   TS= REZ(M)
      FCTF= C3*6*TS/(BT*HT)/(3*TS**2-3*B1*(TS-H1)**2-POP*
     *       (D1-TS)-POS*(D2-TS))
      B1= B1F
      ECB= FCTF*(1/TS-1)/EC
      X= TS*HT
C
      ECPM= FCTF*(DP-X)/(EC*X)
      ECRM= FCTF*(DS-X)/(EC*X)
      ECPU= BMCRF(I)*E/(2*EC*SMA*(1+C1))
      ECPCV= ((ECPM+ECPCF(I))/2+TSE*(1/BETA-1)/EC)*BETA+ECPE
      ECPCC= (ECPM+TSE*(1/BETA-1)/EC)*BETA+ECPE
      EPF(I)= (2*SL1(I)*ECPU+(SLV-SL1(I))*ECPCV*2+SLC*ECPCC)/SLT
C
```

```
      FJFN= EPF(I)/(ECPE+ECPCF(I))
      FMFN= (EPF(I)-EPCRMF)/(ECPM-ECPCMF)
C
      FJFD= ABS(FJFN-FJFO)
      FMFD= ABS(FMFN-FMFO)
      IF( FJFD .LT. 0.00001 .AND. FMFD .LT. 0.00001 )GOTO 1
      FJF= FJFN
      FMF= FMFN
 2    CONTINUE
C
      GOTO 1
C
 60   WRITE(6,70)KKK,I
      WRITE(7,70)KKK,I
 70   FORMAT(T3,'ERROR IN SUBROUTINE CRBMF, ERROR NO.:--',I4,2X,I2)
      GOTO 4
C
 1    CONTINUE
 4    RETURN
      END
C SSSSSSSSSSSSSSSSSSSSSSSSSSSSSSSSSSSSSSSSSSSSSSSSSSSSSSSSSSSSSSSSSSSSSSSSSSS:
C SSSSSSSSS   Subprogramme to evaluate the Section Properties of
C SSSSSSSSS   the beam.
C SSSSSSSSSSSSSSSSSSSSSSSSSSSSSSSSSSSSSSSSSSSSSSSSSSSSSSSSSSSSSSSSSSSSSSSSSSS:
C
C
      SUBROUTINE SECT ( ACTA,ADC,IBON )
C
      CHARACTER*4 IBON
      COMMON /SECTN/  AALS,STIFFN,YMALS,RAGYAL,E2,RL2
      COMMON /LEVMAT/ EC,ES,DP,DS,ALPHA,TSE
      COMMON /DIMAR/  HF,HB,HT,BW,BB,BT,AP,AS
C*************************************************************************
C     Blank concrete section.
C*************************************************************************
C
      A1=BT*HF
      A2=BB*HB
      A3=(HT-HF-HB)*BW
      AB=A1+A2+A3
      ACTA=AB-ADC
C
      AY1=A1*(HT-HF/2)
      AY2=A2*(HB/2)
      AY3=A3*(HB+(HT-HF-HB)/2)
      AYS=AY1+AY2+AY3
C
      AYS1=A1*(HT-HF/2)**2
      AYS2=A2*(HB/2)**2
      AYS3=A3*(HB+(HT-HF-HB)/2)**2
      AYSS=AYS1+AYS2+AYS3
C
      SMA1=BT*HF**3/12
      SMA2=BB*HB**3/12
      SMA3=BW*(HT-HF-HB)**3/12
```

```
      SMAS=SMA1+SMA2+SMA3
C
      YM=AYS/AB
      GROSSI=SMAS+AYSS-AB*YM**2
      RAGY=GROSSI/AB
      ALPHA= ES/EC
C*************************************************************
C     Effective section properties which take into account of
C     Non-prestressed steel stiffness.
C*************************************************************
      AYALS= AYS+AS*(HT-DS)*(ALPHA-1.0)-ADC*(HT-DP)
      AY2ALS= AYSS+AS*(HT-DS)**2*(ALPHA-1.0)-ADC*(HT-DP)**2
C
      AALS=AB+AS*(ALPHA-1)-ADC
 1    YMALS=AYALS/AALS
      STIFFN=SMAS+AY2ALS-AALS*YMALS**2
      RAGYAL=STIFFN/AALS
C
      E2=YMALS-(HT-DP)
      RL2=YMALS-(HT-DS)
      RETURN
      END
C SSSSSSSSSSSSSSSSSSSSSSSSSSSSSSSSSSSSSSSSSSSSSSSSSSSSSSSSSSSSSSS
C SSSSSSSSS   Subprogramme to calculate the deflections along
C SSSSSSSSS   the span by moment area method.
C SSSSSSSSSSSSSSSSSSSSSSSSSSSSSSSSSSSSSSSSSSSSSSSSSSSSSSSSSSSSSSSS
C
      SUBROUTINE DEFL ( CUR,NP,DEFX )
C
      DIMENSION CUR(100),AA(100),BS(100),DEFX(100)
      COMMON /LENGTH/ SLV,SLT,SL1(100),SLC
C
      NH=(NP+1)/2
      DELL= SLT/NP
      DO 444 J=1,NP,1
      SL1(J)= DELL/2+DELL*(J-1)
      N=0
      XL=SL1(J)
      DO 777 I=1,NP,1
      IF( I .GT. NH )THEN
      N=N+1
      SL1(I)=DELL/2+DELL*(I-1)
      KS=I-2*N
      CUR(I)=CUR(KS)
      END IF
C
      IF( SL1(I) .GE. XL )THEN
      BS(I)=0.00
      GO TO 666
      END IF
      BS(I)=DELL*CUR(I)*(XL-SL1(I))
666   AA(I)=DELL*CUR(I)*(SLT-SL1(I))/SLT
C
777   CONTINUE
      B=0.0
```

```
      RA=0.0
      DO 555 I=1,NP,1
      RA=AA(I)+RA
      B=BS(I)+B
555   CONTINUE
C
      DEFX(J)=RA*XL-B
444   CONTINUE
      RETURN
      END
C SSSSSSSSSSSSSSSSSSSSSSSSSSSSSSSSSSSSSSSSSSSSSSSSSSSSSSSSSSSSSSSSSSSSSSS
C SSSSSSSSSS  Subprogramme to compute the deflections and corresponding
C SSSSSSSSSS  steel stresses along the beam in the second cycle of
C SSSSSSSSSS  loading.
C SSSSSSSSSSSSSSSSSSSSSSSSSSSSSSSSSSSSSSSSSSSSSSSSSSSSSSSSSSSSSSSSSSSSSSS
C
      SUBROUTINE SECOND ( PCRAS,RCRAS,ECPCAS,ECRCAS,EPCRAS,
     *                    PCRJS,RCRJS,ECPCJS,ECRCJS,EPTCS,
     *                    C1,C6,NP,NH,FCTA,
     *                    BMCRS,DEFCS,DEFXS,CAM,DLLS,DACS,
     *                    FPACS,ATSS,FRACS,ARSS,TSS,SLJS,
     *                    SLJF,BMAMF,FFMS,CURS,CURJCS,FCT,DLOAD )
C
      COMMON /SECTN/   A,SMA,YINF,RG,E,RL
      COMMON /DIMAR/   HF,HB,HT,BW,BB,BT,AP,AS
      COMMON /LEVMAT/ EC,ES,DP,DS,ALPHA,TSE
      COMMON /LENGTH/ SLV,SLT,SL1(100),SLC
      COMMON /STRAIN/ ECPE,ECRE,ECTE,ECBE
      COMMON /FORCE/   PE,RE
      COMMON /MOMTS/   BMAMS,BMAS(100)
      COMMON /RATIO/   H1,H2,H3,H4,H5,B1,B2,D1,D2,POS,S1,S2,BETA
C
      DIMENSION FRACS(100),FRS(100),ARSS(100),CURS(100),
     *          CURJCS(100),CURCAM(100),BMCRS(100),
     *          CAM(100),DLLS(100),DACS(100),DEFCS(100),DEFXS(100),
     *          PCRS(100),RCRS(100),ECPCS(100),ECRCS(100),EPS(100)
C
      REAL*8 COZ(3),REZ(3),AR(4),TOL
C
      ECREX= ECRE
      ECPEX= ECPE
      ECPE= ABS(ECPE)
      ECRE= ABS(ECRE)
C**************************************************************
C  Analyse the critical section. It is assumed that the cracks will
C  be opened if the applied moment is greater than the decompression
C  moment.
C**************************************************************
C
      FJMSD= 999.0
      FJMS= 1.0
      CK= 2/EC/(BT*HT**2-(BT-BW)*(HT-HF)**2+(BB-BW)*HB**2)
      ZC= 2*HT*(1-B1*(1-H1)**3+B2*H2**3)/(3*(1-B1*(1-H1)**2
     *     +B2*H2**2))
C
```

```
      DO 991 K=1,50
      FJMSO= FJMS
      FCRMS= (PE+RE+FJMS*ECPE*AP*ES+ECRE*AS*ES)/(1+CK*ES*
     *       (FJMS*(HT-DP)*AP+(HT-DS)*AS))
      FCCRMS= FCRMS*CK*EC*HT
         ECPCMS= CK*FCRMS*(HT-DP)
      ECRCMS= CK*FCRMS*(HT-DS)
      PCRMS= PE+(ECPE-ECPCMS)*FJMS*AP*ES
      RCRMS= RE+(ECRE-ECRCMS)*AS*ES
      BMCRMS= FCRMS*ZC-PCRMS*(HT-DP)-RCRMS*(HT-DS)
      EPCRMS= (BMCRMS*E)*C6/(EC*SMA*(1+C1))
C
      FJMSN= EPCRMS/(ECPE-ECPCMS)
      FJMSD= ABS(FJMSN-FJMSO)
      IF( FJMSD .LT. 0.00001 )GO TO 919
      FJMS= FJMSN
 991  CONTINUE
C*****************************************************************
C     If the applied moment is less than the decompression moment
C     of the critical section, then use uncracked section theory.
C*****************************************************************
C
 919  IF( BMAMS .LE. BMCRMS )THEN
      WRITE(6,70)
 70   FORMAT(' <<< CRACKS REMAIN CLOSE >>>')
C
      BMIL= DLOAD*SLV/2.0
      DO 997 I= 1,NH
      EPOIL= BMIL*E*C6/(EC*SMA*(1+C1))
      IF(SL1(I).LT.SLV)THEN
      ECPIL= BMIL*SL1(I)*E/(SMA*EC*SLV)-EPOIL*C1
      ECRIL= BMIL*SL1(I)*RL/(SMA*EC*SLV)-EPOIL*ALPHA*AP*(1+E*RL/RG)/A
      ELSE IF( SL1(I).GE.SLV)THEN
      ECPIL= BMIL*E/(SMA*EC)-EPOIL*C1
      ECRIL= BMIL*RL/(SMA*EC)-EPOIL*ALPHA*AP*(1+E*RL/RG)/A
      END IF
C
      EPO= BMAMS*E*C6/(EC*SMA*(1+C1))
      ECP= BMAS(I)*E/(SMA*EC)-EPO*C1
      ECR= BMAS(I)*RL/(SMA*EC)-EPO*ALPHA*AP*(1+E*RL/RG)/A
      FPS= EPO*ES
      ATSS= PE/AP+FPS-ECPIL*ES
      FPACS= 0.00
      FRS(I)= 0.00
      FRACS(I)= 0.00
      ARSS(I)= 0.00
      IF( AS .EQ. 0.00 )GO TO 99
      FRS(I)= ECR*ES
      ARSS(I)= RE/AS+FRS(I)-ECRIL*ES
C
 99   FCT= ECTE*EC-BMAS(I)*(DP-E)/SMA+EPO*ES*AP
     *     *(E*(DP-E)/RG-1)/A
C
      ECRA= ECREX+ECR
      CURS(I)= (ECRA-FCT/EC)/DS
```

```
      TSS= 0.0
      SLJS= SLV
      CONT= ECP-ECPIL
      IF(CONT.EQ.0.00)THEN
      FFMS=0.0
      GOTO 3344
      END IF
      FFMS= (EPO-EPOIL)/(ECP-ECPIL)
 3344 BMCRS(I)= 0.0
C
 997  CONTINUE
      GO TO 27
      END IF
C**********************************************************************
C     If the applied moment is greater than the decompression moment,
C     cracks start to reopen. Three different situations will be en-
C     countered.
C     1 )  Some cracks reopen.
C     2 )  All the cracks reopen but no new cracks are formed.
C     3 ))  New cracks are formed.
C**********************************************************************
C
      WRITE(6,1014)
 1014 FORMAT(' *** CRACK REOPEN ***')
      I= 0
      L8= 0
      L9= 0
C
      IF( BMAMS .GT. BMAMF )L9= 1
      IF( L9 .NE. 1 )GOTO 275
      FFAS= 1.0
      FFASD= 999.0
C
  275 FFJS= 1.0
      FFMS= 1.0
      FFJSD= 999.0
      FFMSD= 999.0
      DO 321 J=1,100
      FFJSO= FFJS
      FFMSO= FFMS
C
      IF( L8 .EQ. 1 )GOTO 274
C
      IF( L9 .NE. 1 )GOTO 271
      FFASO= FFAS
      FCCRJS= (PE+(ECPE+DP*FCTA/(EC*HT))*FFJS*AP*ES+
     *        RE+(ECRE+DS*FCTA/(EC*HT))*AS*ES+S1*FCTA)/
     *        (S2+(HT-DP)*FFJS*AP*ES/(EC*HT)+(HT-DS)*AS
     *        *ES/(EC*HT))
C
      FCCRJS= ABS(FCCRJS)
      CXJ= (FCCRJS*HT)/(FCCRJS+FCTA)
      ECPCJS= (FCCRJS+FCTA)*(DP-CXJ)/(EC*HT)
      ECRCJS= (FCCRJS+FCTA)*(DS-CXJ)/(EC*HT)
      PCRJS= PE+(ECPE+ECPCJS)*FFJS*AP*ES
```

```
      RCRJS= RE+(ECRE+ECRCJS)*AS*ES
C
      FTCRJ= FCTA*BB*(HT-CXJ)/2-FCTA*(BB-BW)*(HT-CXJ-HB)**2/
     *       (2*(HT-CXJ))
      FCRJS= FCCRJS*BT*CXJ/2-FCCRJS*(BT-BW)*(CXJ-HF)**2/(2*CXJ)
      CRJ= CXJ/HT
      ZCJS= HT*(CRJ**2*(3-CRJ)-B1*(CRJ-H1)**2*(H4-CRJ))/(3*CRJ**
     *      2-3*B1*(CRJ-H1)**2)
      ZTJS= HT*((1-CRJ)**3-B2*(H3-CRJ)**2*(H5-CRJ))/(3*((1-CRJ)**2-
     *      B2*(H3-CRJ)**2))
C
      BMCRJS= FCRJS*ZCJS-PCRJS*(HT-DP)-RCRJS*(HT-DS)-FTCRJ*ZTJS
      GOTO 268
C
  271 FCRJS= (PE+RE+FFJS*ECPE*AP*ES+ECRE*AS*ES)/(1+CK*ES*(FFJS*(HT-
     *       DP)*AP+(HT-DS)*AS))
      FCCRJS= CK*FCRJS*EC*HT
      ECPCJS= CK*FCRJS*(HT-DP)
      ECRCJS= CK*FCRJS*(HT-DS)
      PCRJS= PE+(ECPE-ECPCJS)*FFJS*AP*ES
      RCRJS= RE+(ECRE-ECRCJS)*AS*ES
      BMCRJS= FCRJS*ZC-PCRJS*(HT-DP)-RCRJS*(HT-DS)
C
  268 SLJS= BMCRJS*SLV/BMAMS
      IF( SLJS .GT. SLV )SLJS= SLV
C
  274 C3= FCRMS+FFMS*ECPCMS*AP*ES+ECRCMS*AS*ES
      C4= (PCRMS+FFMS*ECPCMS*AP*ES)*(HT-DP)+(RCRMS+ECRCMS*AS*ES)*(HT-DS
      C5= (BMAMS+C4)/HT
C
      POP= (6*ALPHA*AP*FFMS)/(BT*HT)
C*************************************************************
C     Solve the cubic equation of Neutral Axis by NAG Routine,
C     for the section in the constant moment region i.e. under BMAX
C*************************************************************
      LL= 0
      IF( L9 .NE. 1 )GOTO 269
  270 LL= LL+1
C
  269 B2K= B2
      B1K= B1
C
      B2= 0.0
      N= 0
    8 N= N+1
C
      W1= C3*(B1-1-B2)
C
      W2= C3*(3-B1*H4-2*B1*H1+B2*H5+2*B2*H3)-C5*3*(1-B1+B2)
C
      W3= C3*(2*B1*H1*H4+B1*H1**2-2*B2*H3*H5-B2*H3**2+POP*
     *   (1-D1)+POS*(1-D2))-C5*(6*B1*H1-6*B2*H3+POP+POS)
C
      W4= C3*(B2*H3**2*H5-B1*H1**2*H4-D1*POP*(1-D1)-D2*POS*
     *    (1-D2))-C5*(3*B2*H3**2-3*B1*H1**2-D1*POP-D2*POS)
```

```
C
C       W1(X/HT)**3 + W2(X/HT)**2 + W3(X/HT) + W4 = 0.0
C
        N9= 4
        AR(1)= W1
        AR(2)= W2
        AR(3)= W3
        AR(4)= W4
        N91= N9-1
C
        TOL= 1.0*10.0**(-11.0)
        IFAID= 0
C
        CALL CO2AEF ( AR,N9,REZ,COZ,TOL,IFAID )
C
        IF ( N .GT. 1 ) GOTO 44
        I9= 0
        I8= 0
C
C       Is N.A. within the Web ?
C
        DO 30 M= 1,N91,1
        IF ( COZ(M) .NE. 0.0000 )GOTO 30
        IF ( REZ(M) .LE. H3 .AND. REZ(M) .GT. H1 )GOTO 50
 30     CONTINUE
C
C       Is N.A. Within the Top Flange ?
C
        DO 34 M= 1,N91
        IF ( COZ(M) .NE. 0.0000 )GOTO 34
        IF ( REZ(M) .LT. H1 .AND. REZ(M) .GE. 0.0000 )GOTO 40
 34     CONTINUE
C
C       Is N.A. within the Bottom Flange ?
C
        DO 36 M= 1,N91
        IF ( COZ(M) .NE. 0.0000 )GOTO 36
        IF ( REZ(M) .GT. H3  )GOTO 42
 36     CONTINUE
C
        KKK= 1001
        GOTO 60
C
C       If N.A. within the Top Flange
C
 40     B1= 0.0
        I8= 1
        GOTO 8
C
C       If N.A. within the Bottom Flange
C
 42     B1= B1K
        B2= B2K
        I9= 1
        GOTO 8
```

```
C
 44    IF ( I9 .EQ. 1 )GOTO 52
       DO 46 M= 1,N91
       IF ( COZ(M) .NE. 0.0000 )GOTO 46
       IF ( REZ(M) .LE. H1 .AND. REZ(M) .GT. 0.0000 )GOTO 50
 46    CONTINUE
C
       KKK= 1002
       GOTO 60
C
 52    DO 48 M= 1,N91
       IF ( COZ(M) .NE. 0.0000 )GOTO 48
       IF ( REZ(M) .GT. H3 .AND. REZ(M) .LT. 1.00 )GOTO 50
 48    CONTINUE
C
       KKK= 1003
       GOTO 60
C
 50    IF( LL .EQ. 2 )THEN
       TS3= REZ(M)
       FCT3= C3*6*TS3/(BT*HT)/(3*TS3**2-3*B1*(TS3-H1)**2+3*
      *       B2*(TS3-1+H2)**2-POP*(D1-TS3)-POS*(D2-TS3))
       X3= TS3*HT
       ECP3= FCT3*(DP-X3)/(EC*X3)
       B1= B1K
       B2= B2K
C
       ECPUS3= BMCRJS*E/(2*EC*SMA*(1+C1))
       EC31= ECPE+((ECP3+ECPCJS)/2+TSE*(1/BETA-1)/EC)*BETA
       EC32= ECPE+((ECPM+ECP3)/2+TSE*(1/BETA-1)/EC)*BETA
       ECPCCS= ECPE+(ECPM+TSE*(1/BETA-1)/EC)*BETA
       SS1= SLJF-SLJS
       SS2= SLV-SLJF
       EPTCS= (2*SLJS*ECPUS3+2*SS1*EC31+2*SS2*EC32+
      *       SLC*ECPCCS)/SLT
C
       FFJSN= EPTCS/(ECPE+ECPCJS)
       FFMSN= (EPTCS-EPCRMS)/(ECPM+ECPCMS)
       FFASN= (EPTCS-EPCRAS)/(ECP3-ECPCAS)
C
       FFJSD= ABS(FFJSN-FFJSO)
       FFMSD= ABS(FFMSN-FFMSO)
       FFASD= ABS(FFASN-FFASO)
C
       IF( FFJSD .LT. 0.00001 .AND. FFMSD .LT. 0.00001 )GOTO 267
       FFJS= FFJSN
       FFMS= FFMSN
       FFAS= FFASN
       GOTO 321
C
 267   IF( FFASD .LT. 0.00001 )GOTO 279
       FFJS= FFJSN
       FFMS= FFMSN
       FFAS= FFASN
       GOTO 321
```

```
      END IF
C
      TSS= REZ(M)
      FCT= C3*6*TSS/(BT*HT)/(3*TSS**2-3*B1*(TSS-H1)**2+3*B2*(TSS-1+H2)
     *     **2-POP*(D1-TSS)-POS*(D2-TSS))
C
      B1= B1K
      B2= B2K
C
250   ECB= FCT*(1/TSS-1)/EC
      X= TSS*HT
      ECPM= FCT*(DP-X)/(EC*X)
      ECRM= FCT*(DS-X)/(EC*X)
C
      IF( L8 .EQ. 1 )THEN
      BMAS2= BMAMS*SLJF/SLV
      ECPUS2= BMAS2*E/(2*EC*SMA*(1+C1))
      ECPAS2= (BMAS2*E/(SMA*EC)-ECPE*(FFJS*C1+1))/(1+FFJS*C1)
      ECVS2= ECPE+((ECPAS2+ECPM)/2+TSE*(1/BETA-1)/EC)*BETA
C
      ECCS2= ECPE+(ECPM+TSE*(1/BETA-1)/EC)*BETA
      EPTCS= (2*SLJF*ECPUS2+2*(SLV-SLJF)*ECVS2+SLC*ECCS2)/SLT
      FFJSN= EPTCS/(ECPE+ECPAS2)
      FFMSN= (EPTCS-EPCRMS)/(ECPM+ECPCMS)
      GOTO 273
      END IF
C
      IF( LL .EQ. 1 )THEN
      C3= PCRAS+RCRAS-FFAS*ECPCAS*AP*ES-ECRCAS*AS*ES
      C4= (PCRAS-FFAS*ECPCAS*AP*ES)*(HT-DP)+(RCRAS-ECRCAS*AS*
     *     ES)*(HT-DS)
      BMAS3= BMAMS*SLJF/SLV
C
      C5= (BMAS3+C4)/HT
      POP= (6*ALPHA*AP*FFAS)/(BT*HT)
      GOTO 270
      END IF
C
C
      ECPUS= BMCRJS*E/((2*EC*SMA)*(1+C1))
      ECPCVS= (ECPM/2+TSE*(1/BETA-1)/EC)*BETA+ECPE
      EPCRMS= (BMCRMS*E)*C6/(EC*SMA*(1+C1))
      ECPCCS= (ECPM+TSE*(1/BETA-1)/EC)*BETA+ECPE
      EPTCS= (2*SLJS*ECPUS+(SLV-SLJS)*2*ECPCVS+SLC*ECPCCS)/SLT
C
      FFJSN= EPTCS/(ECPE-ECPCJS)
      FFMSN= (EPTCS-EPCRMS)/(ECPM+ECPCMS)
C
 273  FFJSD= ABS(FFJSN-FFJSO)
      FFMSD= ABS(FFMSN-FFMSO)
C
      IF( FFMSN .GT. 1.00 )THEN
      FFMSN= 1.00
      FFMSD= 0.0000001
      END IF
```

```
      IF( FFJSD .LT. 0.00001 .AND. FFMSD .LT. 0.00001 )GOTO 278
      FFJS= FFJSN
      FFMS= FFMSN
  321 CONTINUE
C
      KKK= 1008
      GOTO 60
C
  278 IF( L8 .EQ. 1 )GOTO 279
C
C     Is it only some cracks reopen ?
C
      IF( SLJS .GE. SLJF )GOTO 279
C
C     Is it all cracks reopen but no new cracks formed ?
C
      IF( SLJS .LT. SLJF .AND. BMAMS .LE. BMAMF )GOTO 277
C
      KKK= 1004
      GOTO 60
C
C     If case (2) happen, then :---
C
  277 L8= 1
      SLJS= SLJF
      GOTO 275
C
  279 FPS= EPTCS*ES
      FPACS= (EPTCS-EPCRMS)*ES
      ATSS= PE/AP+FPS
      FRMS= 0.0
      ARSMS= 0.0
      FRACMS= 0.0
      IF( AS .EQ. 0.0 )GOTO 123
C
      FRMS= (ECRM+ECRE)*ES
      FRACMS= (ECRM+ECRCMS)*ES
      ARSMS= RE/AS+FRMS
  123 CURMS= (FCT+(ECPM*EC-TSE)*BETA+TSE)/(EC*DP)
      FCT= -FCT
C
C*****************************************************************
C  Compute the curvatures of other sections along the beam, hence to
C  calculate the deflections by integration of curvature.
C*****************************************************************
C
      CALL CRBMS ( PCRMS,RCRMS,FCRMS,ECPCMS,ECRCMS,BMCRMS,FCCRMS,
     *             EPCRMS,SLJF,SLJS,
     *             PCRS,RCRS,ECPCS,ECRCS,BMCRS,EPS,
     *             PCRAS,RCRAS,ECPCAS,ECRCAS,EPCRAS,
     *             ZC,CK,NH,C1,C6,FCTA )
C
      DO 1000 I= 1,NH
      FFCS= 1.0
      JJ= 0
```

```
C*************************************************************************
C     If the section being considered is within the constant
C     moment region .OR. within the varying moment zone but
C     remains uncracked, then :---
C*************************************************************************
C
      IF( SL1(I) .GE. SLV )THEN
      CURS(I)= CURMS
      ARSS(I)= ARSMS
      FRACS(I)= FRACMS
      FRS(I)= FRMS
      GOTO 1000
C
      ELSE IF( SL1(I) .LE. SLJS )THEN
      FRACS(I)= 0.00
      FRS(I)= 0.00
      ARSS(I)= 0.00
      ECRS= BMAS(I)*RL/(SMA*EC)-EPTCS*ALPHA*AP*(1+E*RL/RG)/A
C
      IF( AS .EQ. 0.00 )GOTO 7
      FRS(I)= ECRS*ES
      ARSS(I)= RE/AS+FRS(I)
 7    FCTO= ECTE*EC-BMAS(I)*(DP-E)/SMA+EPTCS*ES*AP*(E*(DP-E)/
     *      RG-1)/A
      ECRO= ECREX+ECRS
      CURS(I)= (ECRO-FCTO/EC)/DS
      GOTO 1000
      END IF
C*************************************************************************
C     If the section being considered is within the varying moment
C     zone but has been cracked. Therefore use cracked section theory.
C*************************************************************************
      FFCSD= 999.0
      DO 144 J= 1,100
      FFCSO= FFCS
C
      IF( SL1(I) .GT. SLJS .AND. SL1(I) .LE. SLJF )THEN
      C3= PCRS(I)+RCRS(I)-ECPCS(I)*AP*ES*FFCS-ECRCS(I)*AS*ES
      C4= (PCRS(I)-ECPCS(I)*AP*ES*FFCS)*(HT-DP)+(RCRS(I)-
     *    ECRCS(I)*AS*ES)*(HT-DS)
      JJ= 1
      GOTO 266
      END IF
C
      C3= PCRS(I)+RCRS(I)+ECPCS(I)*AP*ES*FFCS+ECRCS(I)*AS*ES
      C4= (PCRS(I)+ECPCS(I)*AP*ES*FFCS)*(HT-DP)+(RCRS(I)+
     *    ECRCS(I)*AS*ES)*(HT-DS)
C
 266  C5= (BMAS(I)+C4)/HT
      POP= (6*ALPHA*AP*FFCS)/(BT*HT)
C*************************************************************************
C     Use NAG Routine to solve the cubic equation of neutral axis
C     of that particular section.
C*************************************************************************
C
```

```
      B1G= B1
      B2G= B2
      B2= 0.0
      KK= 0
 9    KK= KK+1
C
      W1= C3*(B1-1-B2)
      W2= C3*(3-B1*H4-2*B1*H1+B2*H5+2*B2*H3)-C5*3*(1-B1+B2)
C
      W3= C3*(2*B1*H1*H4+B1*H1**2-2*B2*H3*H5-B2*H3**2+POP*
     *    (1-D1)+POS*(1-D2))-C5*(6*B1*H1-6*B2*H3+POP+POS)
C
      W4= C3*(B2*H3**2*H5-B1*H1**2*H4-D1*POP*(1-D1)-D2*POS*
     *    (1-D2))-C5*(3*B2*H3**2-3*B1*H1**2-D1*POP-D2*POS)
C
      AR(1)= W1
      AR(2)= W2
      AR(3)= W3
      AR(4)= W4
      IFAIE= 0
      N9= 4
      N91= N9-1
      TOL= 1.0*10.0**(-11.0)
C
      CALL CO2AEF ( AR,N9,REZ,COZ,TOL,IFAIE )
C
      IF( KK .GT. 1 )GOTO 10
      M9= 0
      M8= 0
C
C     Is N.A. within the Web ?
C
      DO 11 M= 1,N91
      IF( COZ(M) .NE. 0.00 )GOTO 11
      IF( REZ(M) .LE. H3 .AND. REZ(M) .GT. H1 )GOTO 12
 11   CONTINUE
C
C     Is N.A. within the Top Flange ?
C
      DO 13 M= 1,N91
      IF( COZ(M) .NE. 0.00 )GOTO 13
      IF( REZ(M) .LT. H1 .AND. REZ(M) .GE. 0.00 )GOTO 14
 13   CONTINUE
C
C     Is N.A. within the Bottom Flange ?
C
      DO 16 M= 1,N91
      IF( COZ(M) .NE. 0.00 )GOTO 16
      IF( REZ(M) .GT. H3 )GOTO 17
 16   CONTINUE
C
      KKK= 1005
      GOTO 60
C
C     If N.A. within the Top Flange, then:--
```

```
C
 14   B1= 0.0
      M8= 1
      GOTO 9
C
C     If N.A. within the Bottom Flange, then:--
C
 17   B1= B1G
      B2= B2G
      M9= 1
      GOTO 9
C
 10   IF( M9 .EQ. 1 )GOTO 18
      DO 19 M= 1,N91
      IF( COZ(M) .NE. 0.00 )GOTO 19
      IF( REZ(M) .LE. H1 .AND. REZ(M) .GT. 0.00 )GOTO 12
 19   CONTINUE
C
      KKK= 1006
      GOTO 60
C
 18   DO 20 M= 1,N91
      IF( COZ(M) .NE. 0.00 )GOTO 20
      IF( REZ(M) .GT. H3 .AND. REZ(M) .LE. 1.00 )GOTO 12
 20   CONTINUE
C
      KKK= 1007
      GOTO 60
C
 12   TS= REZ(M)
      FCTTS= C3*TS*6/(BT*HT)/(3*TS**2-3*B1*(TS-H1)**2+3*B2*
     *       (TS-1+H2)**2-POP*(D1-TS)-POS*(D2-TS))
      B1= B1G
      B2= B2G
      ECBS= FCTTS*(1/TS-1)/EC
      X= TS*HT
      ECPS= ABS(FCTTS)*(DP-X)/(EC*X)
      ECRS= ABS(FCTTS)*(DS-X)/(EC*X)
C
      FRACS(I)= 0.00
      FRS(I)= 0.00
      ARSS(I)= 0.00
      IF( AS .EQ. 0.00 )GOTO 21
C
      IF( JJ .NE. 1 )GOTO 29
      FRACS(I)= (ECRS-ECRCS(I))*ES
      GOTO 28
 29   FRACS(I)= (ECRS+ECRCS(I))*ES
 28   FRS(I)= (ECRS+ECRE)*ES
      ARSS(I)= RE/AS+FRS(I)
 21   CURS(I)= (FCTTS+(ECPS*EC-TSE)*BETA+TSE)/(EC*DP)
C
      IF( JJ .NE. 1 )GOTO 22
      FFCSN= (EPTCS-EPS(I))/(ECPS-ECPCS(I))
      GOTO 23
```

```
 22    FFCSN= (EPTCS-EPS(I))/(ECPS+ECPCS(I))
 23    FFCSD= ABS(FFCSN-FFCSO)
C
       IF( FFCSD .LT. 0.00001 )GOTO 1000
       FFCS= FFCSN
 144   CONTINUE
C
       GOTO 1000
 60    WRITE(6,71)KKK,I
       WRITE(7,71)KKK,I
 71    FORMAT(T3,'ERROR IN SUBROUTINE SECOND, ERROR NO.:--',I4,2X,I2)
C
       GOTO 1001
 1000  CONTINUE
C
 27    EPJS= BMCRMS*E*C6/(EC*SMA*(1+C1))
       DO 24 KP= 1,NH
       IF( SL1(KP) .GE. SLV )THEN
       BMCS= BMCRMS
       GOTO 25
       END IF
       BMCS= BMCRMS*SL1(KP)/SLV
C
 25    ECTCR= ECTE-BMCS*(DP-E)/(SMA*EC)+EPJS*ALPHA*AP*(E*(DP-E)/RG-1)/A
       ECBCR= ECBE+BMCS*YINF/(SMA*EC)-EPJS*ALPHA*AP*(1+E*YINF/RG)/A
       CURJCS(KP)= (ECBCR-ECTCR)/HT
 24    CONTINUE
       DO 2411 I=1,NH
 2411  CURCAM(I)= (ECBE-ECTE)/HT
C
       CALL DEFL ( CURJCS,NP,DEFCS )
C
       CALL DEFL ( CURS,NP,DEFXS )
C
       CALL DEFL ( CURCAM,NP,CAM )
C
       DO 26 I= 1,NP
       DLLS(I)= DEFXS(I)-CAM(I)
       IF( BMAMS .LE. BMCRMS )THEN
       DACS(I)= 0.00
       GOTO 26
       END IF
       DACS(I)= DEFXS(I)-DEFCS(I)
 26    CONTINUE
C
       ECRE= ECREX
       ECPE= ECPEX
 1001  RETURN
       END
C SSSSSSSSSSSSSSSSSSSSSSSSSSSSSSSSSSSSSSSSSSSSSSSSSSSSSSSSSSSSSSSSSSSSSSSSSS
C SSSSSSSSSS   Subprogramme to compute the variation of decompression
C SSSSSSSSSS   moments along the beam hence to calculate the steel
C SSSSSSSSSS   stress and curvature under respective decompression
C SSSSSSSSSS   moment.
C SSSSSSSSSSSSSSSSSSSSSSSSSSSSSSSSSSSSSSSSSSSSSSSSSSSSSSSSSSSSSSSSSSSSSSSSSS
```

```
C
      SUBROUTINE CRBMS ( PCRMS,RCRMS,FCRMS,ECPCMS,ECRCMS,BMCRMS,FCCRMS,
     *                   EPCRMS,SLJF,SLJS,
     *                   PCRS,RCRS,ECPCS,ECRCS,BMCRS,EPS,
     *                   PCRAS,RCRAS,ECPCAS,ECRCAS,EPCRAS,
     *                   ZC,CK,NH,C1,C6,FCTA )
C
      COMMON /SECTN/   A,SMA,YINF,RG,E,RL
      COMMON /DIMAR/   HF,HB,HT,BW,BB,BT,AP,AS
      COMMON /LEVMAT/ EC,ES,DP,DS,ALPHA,TSE
      COMMON /LENGTH/ SLV,SLT,SL1(100),SLC
      COMMON /STRAIN/ ECPE,ECRE,ECTE,ECBE
      COMMON /FORCE/   PE,RE
      COMMON /RATIO/   H1,H2,H3,H4,H5,B1,B2,D1,D2,POS,S1,S2,BETA
C
      DIMENSION ECPCS(100),ECRCS(100),PCRS(100),RCRS(100),
     *          BMCRS(100),FCCRS(100),EPS(100)
C
      REAL*8 COZ(3),REZ(3),AR(4),TOL
C
C*************************************************************
C     Use iteration process to compute the decompression moment at a
C     particular section, say SL1(I).
C*************************************************************
       DO 1 I= 1,NH
C*************************************************************
C     If the section being considered is within the constant moment
C     zone .OR. within the varying moment zone but remain uncracked,
C     then:---
C*************************************************************
C
       IF( SL1(I) .GE. SLV )THEN
       ECPCS(I)= ECPCMS
       ECRCS(I)= ECRCMS
       PCRS(I)= PCRMS
       RCRS(I)= RCRMS
       BMCRS(I)= BMCRMS
       FCCRS(I)= FCCRMS
       EPS(I)= EPCRMS
       GOTO 1
       ELSE IF( SL1(I) .LE. SLJS )THEN
       ECRCS(I)= 0.00
       ECPCS(I)= 0.00
       PCRS(I)= 0.00
       RCRS(I)= 0.00
       BMCRS(I)= 0.00
       FCCRS(I)= 0.00
       EPS(I)= 0.00
       GOTO 1
       END IF
C*************************************************************
C     If the section being considered has been cracked but within
C     the varying moment zone, the cracking moment can be calculated
C     as follows :--
C*************************************************************
```

```
C
      L9= 0
      L8= 0
      L7= 0
C
      IF( SLJS .LT. SLJF )L7= 1
      IF( SL1(I) .LE. SLJF .AND. SL1(I) .GT. SLJS )L8= 1
      IF( L7 .EQ. 1 .AND. L8 .EQ. 1 )L9= 1
C
      IF( L9 .NE. 1 )GOTO 275
      FAS= 1.0
      FASD= 999.0
C
 275  FJS= 1.0
      FMS= 1.0
      FJSD= 999.0
      FMSD= 999.0
      DO 321 J=1,100
      FJSO= FJS
      FMSO= FMS
C
      IF( L9 .NE. 1 )GOTO 271
      FASO= FAS
      FCCRS(I)= (PE+(ECPE+DP*FCTA/(EC*HT))*FJS*AP*ES+
     *          RE+(ECRE+DS*FCTA/(EC*HT))*AS*ES+S1*FCTA)/
     *          (S2+(HT-DP)*FJS*AP*ES/(EC*HT)+(HT-DS)*AS
     *          *ES/(EC*HT))
C
      FCCRS(I)= ABS(FCCRS(I))
      CX= (FCCRS(I)*HT)/(FCCRS(I)+FCTA)
      ECPCS(I)= (FCCRS(I)+FCTA)*(DP-CX)/(EC*HT)
      ECRCS(I)= (FCCRS(I)+FCTA)*(DS-CX)/(EC*HT)
      PCRS(I)= PE+(ECPE+ECPCS(I))*FJS*AP*ES
      RCRS(I)= RE+(ECRE+ECRCS(I))*AS*ES
C
      FTCRS= FCTA*BB*(HT-CX)/2-FCTA*(BB-BW)*(HT-CX-HB)**2/
     *        (2*(HT-CX))
      FCRS= FCCRS(I)*BT*CX/2-FCCRS(I)*(BT-BW)*(CX-HF)**2/(2*CX)
      CR= CX/HT
      ZCS= HT*(CR**2*(3-CR)-B1*(CR-H1)**2*(H4-CR))/(3*CR**
     *      2-3*B1*(CR-H1)**2)
      ZTS= HT*((1-CR)**3-B2*(H3-CR)**2*(H5-CR))/(3*((1-CR)**2-
     *      B2*(H3-CR)**2))
C
      BMCRS(I)= FCRS*ZCS-PCRS(I)*(HT-DP)-RCRS(I)*(HT-DS)-FTCRS*ZTS
      GOTO 268
C
 271  FCRS= (PE+RE+FJS*ECPE*AP*ES+ECRE*AS*ES)/(1+CK*ES*(FJS*(HT-
     *       DP)*AP+(HT-DS)*AS))
      FCCRS(I)= CK*FCRS*EC*HT
      ECPCS(I)= CK*FCRS*(HT-DP)
      ECRCS(I)= CK*FCRS*(HT-DS)
      PCRS(I)= PE+(ECPE-ECPCS(I))*FJS*AP*ES
      RCRS(I)= RE+(ECRE-ECRCS(I))*AS*ES
      BMCRS(I)= FCRS*ZC-PCRS(I)*(HT-DP)-RCRS(I)*(HT-DS)
```

```
C
 268  BMAX= BMCRS(I)*SLV/SL1(I)
C
C
 274  C3= FCRMS+FMS*ECPCMS*AP*ES+ECRCMS*AS*ES
      C4= (PCRMS+FMS*ECPCMS*AP*ES)*(HT-DP)+(RCRMS+ECRCMS*AS*ES)*(HT-DS)
      C5= (BMAX+C4)/HT
C
      POP= (6*ALPHA*AP*FMS)/(BT*HT)
C*************************************************************
C     Solve the cubic equation of Neutral Axis by NAG Routine.
C*************************************************************
      LL= 0
      IF( L9 .NE. 1 )GOTO 269
 270  LL= LL+1
 269  B2K= B2
      B1K= B1
      B2= 0.0
      N= 0
 8    N= N+1
C
      W1= C3*(B1-1-B2)
      W2= C3*(3-B1*H4-2*B1*H1+B2*H5+2*B2*H3)-C5*3*(1-B1+B2)
      W3= C3*(2*B1*H1*H4+B1*H1**2-2*B2*H3*H5-B2*H3**2+POP*
     *    (1-D1)+POS*(1-D2))-C5*(6*B1*H1-6*B2*H3+POP+POS)
      W4= C3*(B2*H3**2*H5-B1*H1**2*H4-D1*POP*(1-D1)-D2*POS*
     *    (1-D2))-C5*(3*B2*H3**2-3*B1*H1**2-D1*POP-D2*POS)
C
C     W1(X/HT)**3 + W2(X/HT)**2 + W3(X/HT) + W4 = 0.0
C
      N9= 4
      AR(1)= W1
      AR(2)= W2
      AR(3)= W3
      AR(4)= W4
      N91= N9-1
C
      TOL= 1.0*10.0**(-11.0)
      IFAIF= 0
C
      CALL CO2AEF ( AR,N9,REZ,COZ,TOL,IFAIF )
C
      IF ( N .GT. 1 ) GOTO 44
      I9= 0
      I8= 0
C
C     Is N.A. within the Web ?
C
      DO 30 M= 1,N91,1
      IF ( COZ(M) .NE. 0.0000 )GOTO 30
      IF ( REZ(M) .LE. H3 .AND. REZ(M) .GT. H1 )GOTO 50
 30   CONTINUE
C
C     Is N.A. Within the Top Flange ?
C
```

```
      DO 34 M= 1,N91
      IF ( COZ(M) .NE. 0.0000 )GOTO 34
      IF ( REZ(M) .LT. H1 .AND. REZ(M) .GE. 0.0000 )GOTO 40
 34   CONTINUE
C
C     Is N.A. within the Bottom Flange ?
C
      DO 36 M= 1,N91
      IF ( COZ(M) .NE. 0.0000 )GOTO 36
      IF ( REZ(M) .GT. H3  )GOTO 42
 36   CONTINUE
C
      KKK= 1001
      GOTO 60
C
C     If N.A. within the Top Flange
C
 40   B1= 0.0
      I8= 1
      GOTO 8
C
C     If N.A. within the Bottom Flange
C
 42   B1= B1K
      B2= B2K
      I9= 1
      GOTO 8
C
 44   IF ( I9 .EQ. 1 )GOTO 52
      DO 46 M= 1,N91
      IF ( COZ(M) .NE. 0.0000 )GOTO 46
      IF ( REZ(M) .LE. H1 .AND. REZ(M) .GT. 0.0000 )GOTO 50
 46   CONTINUE
C
      KKK= 1002
      GOTO 60
C
 52   DO 48 M= 1,N91
      IF ( COZ(M) .NE. 0.0000 )GOTO 48
      IF ( REZ(M) .GT. H3 .AND. REZ(M) .LE. 1.00 )GOTO 50
 48   CONTINUE
C
      KKK= 1003
      GOTO 60
C
 50   IF( LL .EQ. 2 )THEN
      TS3= REZ(M)
      FCT3= C3*6*TS3/(BT*HT)/(3*TS3**2-3*B1*(TS3-H1)**2+3*
     *       B2*(TS3-1+H2)**2-POP*(D1-TS3)-POS*(D2-TS3))
      X3= TS3*HT
      ECP3= FCT3*(DP-X3)/(EC*X3)
      B1= B1K
      B2= B2K
C
      ECPUS3= BMCRS(I)*E/(2*EC*SMA*(1+C1))
```

```
      EC31= ECPE+((ECP3+ECPCS(I))/2+TSE*(1/BETA-1)/EC)*BETA
      EC32= ECPE+((ECPM+ECP3)/2+TSE*(1/BETA-1)/EC)*BETA
      ECPCCS= ECPE+(ECPM+TSE*(1/BETA-1)/EC)*BETA
      SS1= SLJF-SL1(I)
      SS2= SLV-SLJF
      EPS(I)= (2*SL1(I)*ECPUS3+2*SS1*EC31+2*SS2*EC32+
     *        SLC*ECPCCS)/SLT
C
      FJSN= EPS(I)/(ECPE+ECPCS(I))
      FMSN= (EPS(I)-EPCRMS)/(ECPM+ECPCMS)
      FASN= (EPS(I)-EPCRAS)/(ECP3-ECPCAS)
C
      FJSD= ABS(FJSN-FJSO)
      FMSD= ABS(FMSN-FMSO)
      FASD= ABS(FASN-FASO)
C
      IF( FJSD .LT. 0.00001 .AND. FMSD .LT. 0.00001 )GOTO 267
      FJS= FJSN
      FMS= FMSN
      FAS= FASN
      GOTO 321
C
 267  IF( FASD .LT. 0.00001 )GOTO 1
      FJS= FJSN
      FMS= FMSN
      FAS= FASN
      GOTO 321
      END IF
C
      TSS= REZ(M)
      FCT= C3*6*TSS/(BT*HT)/(3*TSS**2-3*B1*(TSS-H1)**2+3*B2*(TSS-1+H2)
     *     **2-POP*(D1-TSS)-POS*(D2-TSS))
C
      B1= B1K
      B2= B2K
C
250   ECB= FCT*(1/TSS-1)/EC
      X= TSS*HT
      ECPM= FCT*(DP-X)/(EC*X)
      ECRM= FCT*(DS-X)/(EC*X)
C
      IF( LL .EQ. 1 )THEN
      C3= PCRAS+RCRAS-FAS*ECPCAS*AP*ES-ECRCAS*AS*ES
      C4= (PCRAS-FAS*ECPCAS*AP*ES)*(HT-DP)+(RCRAS-ECRCAS*AS*
     *    ES)*(HT-DS)
      BMAS3= BMAX*SLJF/SLV
C
      C5= (BMAS3+C4)/HT
      POP= (6*ALPHA*AP*FAS)/(BT*HT)
      GOTO 270
      END IF
C
C
      ECPUS= BMCRS(I)*E/((2*EC*SMA)*(1+C1))
      ECPCVS= (ECPM/2+TSE*(1/BETA-1)/EC)*BETA+ECPE
```

```
      EPCRMS= (BMCRMS*E)*C6/(EC*SMA*(1+C1))
      ECPCCS= (ECPM+TSE*(1/BETA-1)/EC)*BETA+ECPE
      EPS(I)= (2*SL1(I)*ECPUS+(SLV-SL1(I))*2*ECPCVS+SLC*ECPCCS)/SLT
C
      FJSN= EPS(I)/(ECPE-ECPCS(I))
      FMSN= (EPS(I)-EPCRMS)/(ECPM+ECPCMS)
C
 273  FJSD= ABS(FJSN-FJSO)
      FMSD= ABS(FMSN-FMSO)
C
      IF( FMSN .GT. 1.00 )THEN
      FMSN= 1.00
      FMSD= 0.00000001
      END IF
C
      IF( FJSD .LT. 0.00001 .AND. FMSD .LT. 0.00001 )GOTO 1
      FJS= FJSN
      FMS= FMSN
 321  CONTINUE
C
      KKK= 1004
C
 60   WRITE(6,70)KKK,I
      WRITE(7,70)KKK,I
 70   FORMAT(T3,'ERROR IN SUBROUTINE CRBMS,ERROR NO.:--',I4,2X,I2)
      GOTO 4
C
 1    CONTINUE
 4    RETURN
      END
```